frontiers | Research Topics

NHERI 2015-2025: a decade of discovery in natural hazards engineering

Edited by
Cheryl Ann Blain, Julio Alfonso Ramirez, David Richard Johnson, Navid Jafari, Qin Chen, Jack Cadigan and Rebecca Napolitano

Published in
Frontiers in Built Environment

FRONTIERS EBOOK COPYRIGHT STATEMENT

The copyright in the text of individual articles in this ebook is the property of their respective authors or their respective institutions or funders. The copyright in graphics and images within each article may be subject to copyright of other parties. In both cases this is subject to a license granted to Frontiers.

The compilation of articles constituting this ebook is the property of Frontiers.

Each article within this ebook, and the ebook itself, are published under the most recent version of the Creative Commons CC-BY licence. The version current at the date of publication of this ebook is CC-BY 4.0. If the CC-BY licence is updated, the licence granted by Frontiers is automatically updated to the new version.

When exercising any right under the CC-BY licence, Frontiers must be attributed as the original publisher of the article or ebook, as applicable.

Authors have the responsibility of ensuring that any graphics or other materials which are the property of others may be included in the CC-BY licence, but this should be checked before relying on the CC-BY licence to reproduce those materials. Any copyright notices relating to those materials must be complied with.

Copyright and source acknowledgement notices may not be removed and must be displayed in any copy, derivative work or partial copy which includes the elements in question.

All copyright, and all rights therein, are protected by national and international copyright laws. The above represents a summary only. For further information please read Frontiers' Conditions for Website Use and Copyright Statement, and the applicable CC-BY licence.

ISSN 1664-8714
ISBN 978-2-8325-6939-9
DOI 10.3389/978-2-8325-6939-9

Generative AI statement
Any alternative text (Alt text) provided alongside figures in the articles in this ebook has been generated by Frontiers with the support of artificial intelligence and reasonable efforts have been made to ensure accuracy, including review by the authors wherever possible. If you identify any issues, please contact us.

About Frontiers

Frontiers is more than just an open access publisher of scholarly articles: it is a pioneering approach to the world of academia, radically improving the way scholarly research is managed. The grand vision of Frontiers is a world where all people have an equal opportunity to seek, share and generate knowledge. Frontiers provides immediate and permanent online open access to all its publications, but this alone is not enough to realize our grand goals.

Frontiers journal series

The Frontiers journal series is a multi-tier and interdisciplinary set of open-access, online journals, promising a paradigm shift from the current review, selection and dissemination processes in academic publishing. All Frontiers journals are driven by researchers for researchers; therefore, they constitute a service to the scholarly community. At the same time, the *Frontiers journal series* operates on a revolutionary invention, the tiered publishing system, initially addressing specific communities of scholars, and gradually climbing up to broader public understanding, thus serving the interests of the lay society, too.

Dedication to quality

Each Frontiers article is a landmark of the highest quality, thanks to genuinely collaborative interactions between authors and review editors, who include some of the world's best academicians. Research must be certified by peers before entering a stream of knowledge that may eventually reach the public - and shape society; therefore, Frontiers only applies the most rigorous and unbiased reviews. Frontiers revolutionizes research publishing by freely delivering the most outstanding research, evaluated with no bias from both the academic and social point of view. By applying the most advanced information technologies, Frontiers is catapulting scholarly publishing into a new generation.

What are Frontiers Research Topics?

Frontiers Research Topics are very popular trademarks of the *Frontiers journals series*: they are collections of at least ten articles, all centered on a particular subject. With their unique mix of varied contributions from Original Research to Review Articles, Frontiers Research Topics unify the most influential researchers, the latest key findings and historical advances in a hot research area.

Find out more on how to host your own Frontiers Research Topic or contribute to one as an author by contacting the Frontiers editorial office: frontiersin.org/about/contact

NHERI 2015-2025: a decade of discovery in natural hazards engineering

Topic editors

Cheryl Ann Blain — Naval Research Laboratory, United States
Julio Alfonso Ramirez — Purdue University, United States
David Richard Johnson — Purdue University, United States
Navid Jafari — Louisiana State University, United States
Qin Chen — Northeastern University, United States
Jack Cadigan — Engineer Research and Development Center (ERDC), United States
Rebecca Napolitano — The Pennsylvania State University (PSU), United States

Citation

Blain, C. A., Ramirez, J. A., Johnson, D. R., Jafari, N., Chen, Q., Cadigan, J., Napolitano, R., eds. (2025). *NHERI 2015-2025: a decade of discovery in natural hazards engineering*. Lausanne: Frontiers Media SA.
doi: 10.3389/978-2-8325-6939-9

Table of contents

05 Editorial: NHERI 2015–2025: a decade of discovery in natural hazards engineering
Cheryl Ann Blain, Julio Ramirez, Jack Cadigan, Rebecca Napolitano, Navid Jafari, David Johnson and Qin Chen

08 Automated extraction and summarization of wind disaster data using deep learning models, with extended applications to seismic events
Huy Pham and Monica Arul

32 NHERI@UTexas experimental facility with large-scale mobile shakers for field studies: a decade of discovery in natural hazards engineering
Kenneth H. Stokoe, Sungmoon Hwang, Brady R. Cox, Patricia M. Clayton and Robert B. Gilbert

46 NHERI education and community outreach: longitudinal, educational outcomes of a coordinated, distributed network
Robin Nelson, Karina I. Vielma and JoAnn Browning

57 An ethnographic case study of undergraduate researchers in natural hazards engineering
Amina Meselhe, Karina I. Vielma, Daleen Torres Burgos and Tyler Rodrigues

68 Wind load impact on tall building facades: damage observations during severe wind events and wind tunnel testing
Omar Metwally, Haitham A. Ibrahim, Amal Elawady, Ioannis Zisis and Arindam Gan Chowdhury

89 Recent developments and discoveries in natural hazards mitigation research at the NHERI Lehigh Experimental Facility
Liang Cao, Thomas M. Marullo, James Michael Ricles, Richard Sause, Claudia Reis and Joseph Saunders

110 Multi-degree of freedom shake table testing of large-scale structural and geotechnical systems with NHERI-UCSD LHPOST6
John S. McCartney, Lelli Van Den Einde, Machel Morrison, Alessandro Palermo, Koorosh Lotfizadeh, Chin-Ta Lai and Joel P. Conte

134 Successful coordination of the distributed network, Natural Hazards Engineering Research Infrastructure
Cheryl Ann Blain, Julio A. Ramirez, Billy L. Edge, William Holmes, Marti LaChance, Robin Nelson, Ian Robertson and Dan Zehner

146 A unified framework for post-disaster hazard and structural assessment data collection across hazards and infrastructure typologies
Mohammad S. Alam, Tracy Kijewski-Correa, David B. Roueche, Khalid M. Mosalam, David O. Prevatt and Ian Robertson

170 A decade of DesignSafe: enabling open science in natural hazards
Ellen M. Rathje, Krishna Kumar, Maria Esteva, Scott J. Brandenberg, Tim Cockerill, Clint Dawson, Jamie E. Padgett, Jean-Paul Pinelli and Dan Stanzione

182 An open-source simulation platform to support and foster research collaboration in natural hazards engineering
Adam Zsarnóczay, Gregory G. Deierlein, Frank McKenna, Matthew Schoettler, Sang-Ri Yi, Barbaros Cetiner, Aakash Bangalore Satish, Jinyan Zhao, Justin Bonus, Abiy F. Melaku, Sina Naeimi, Pedro Arduino, Rachel Davidson, Catherine Gorle, Sanjay Govindjee, Ahsan Kareem, Tracy L. Kijewski-Correa, Laura N. Lowes, Michael Motley, Seymour M. J. Spence, Ertugrul Taciroglu, Alexandros A. Taflanidis and Matthew DeJong

208 NHERI centrifuge facility: systems-scale hypergravity modeling in engineering and scientific research
Jason T. DeJong, Daniel W. Wilson, Alejandro Martinez, Katerina Ziotopoulou, Soo-Min Ham and Ross W. Boulanger

frontiers | Frontiers in Built Environment

TYPE Editorial
PUBLISHED 22 September 2025
DOI 10.3389/fbuil.2025.1694676

Check for updates

OPEN ACCESS

EDITED AND REVIEWED BY
Barbara Zanuttigh,
University of Bologna, Italy

*CORRESPONDENCE
Cheryl Ann Blain,
cheryl.a.blain.civ@us.navy.mil

RECEIVED 28 August 2025
ACCEPTED 09 September 2025
PUBLISHED 22 September 2025

CITATION
Blain CA, Ramirez J, Cadigan J, Napolitano R, Jafari N, Johnson D and Chen Q (2025) Editorial: NHERI 2015–2025: a decade of discovery in natural hazards engineering. *Front. Built Environ.* 11:1694676. doi: 10.3389/fbuil.2025.1694676

COPYRIGHT
© 2025 Blain, Ramirez, Cadigan, Napolitano, Jafari, Johnson and Chen. This is an open-access article distributed under the terms of the Creative Commons Attribution License (CC BY). The use, distribution or reproduction in other forums is permitted, provided the original author(s) and the copyright owner(s) are credited and that the original publication in this journal is cited, in accordance with accepted academic practice. No use, distribution or reproduction is permitted which does not comply with these terms.

Editorial: NHERI 2015–2025: a decade of discovery in natural hazards engineering

Cheryl Ann Blain[1]*, Julio Ramirez[2], Jack Cadigan[3], Rebecca Napolitano[4], Navid Jafari[5], David Johnson[6] and Qin Chen[7]

[1]U.S. Naval Research Laboratory, Washington, DC, United States, [2]Lyles School of Civil and Construction Engineering, Purdue University, West Lafayette, IN, United States, [3]Engineering Research and Development Laboratory (ERDC), Vicksburg, MS, United States, [4]Department of Architectural Engineering, Penn State University, University Park, PA, United States, [5]Department of Civil and Environmental Engineering, Louisiana State University, Baton Rouge, LA, United States, [6]Edwardson School of Industrial Engineering and Political Science, Purdue University, West Lafayette, IN, United States, [7]Civil and Environmental Engineering and Marine and Environmental Sciences, Northeastern University, Boston, MA, United States

KEYWORDS

NHERI, natural hazard engineering research infrastructure, natural hazard engineering, distributed research network, extreme event research

Editorial on the Research Topic
NHERI 2015–2025: a decade of discovery in natural hazards engineering

Natural hazards such as earthquakes, windstorms, tsunamis and storm surge are all occurring with increased frequency and intensity. These events often cause significant disruptions to our built environment consisting of buildings, roads, bridges, parks, streets, and systems that provide transportation, water, power, and more, bringing to the forefront our need for resilient solutions. In the United States alone from 2015–2024, there have been 13 earthquakes of magnitude 6.4 or greater resulting in 2 deaths, 134 injuries, 250 houses destroyed, and 1937 homes damaged. The total cost of these events was 6.1 billion dollars (NGDC/WDS, 2025). Internationally earthquakes pose an even greater threat with deaths counted in the thousands, e.g., Nepal, 2015; Indonesia, 2018; Haiti, 2021; Turkey, 2023; Myanmar, 2025. Over the last 5 years (2020–2024), there were just 16 days on average between U.S. billion-dollar disaster events compared to 82 days in the 1980s. Billion-dollar severe storm events including tornadoes, hail and high winds have caused on average $37.9 billion in damage, while hurricanes are the costliest hazard type since 1980, with an average cost of $23.0 billion per event (NOAA, 2025). Furthermore, the U.S. has been impacted by landfalling category 4 or 5 hurricanes in six of the last 8 years (i.e., Harvey, Irma, Maria, Michael, Laura, Ida, Ian, Helene), which is the highest frequency on record (AOML, 2025).

In response to the increasing threat of natural hazards, the National Science Foundation funded the Natural Hazards Engineering Research Infrastructure (NHERI) starting in 2015. NHERI is a national, 12-component, distributed network of institutions focused on research that both mitigates damage and increases resilience from natural hazards such as hurricanes and other extreme windstorms, storm surge, tsunami waves, and earthquakes (see Figure 1 in Blain et al. this Research Topic). After almost a decade of operations, the Research Topic "*NHERI 2015–2025: A Decade of Discovery in Natural Hazards Engineering*" examines

how the NHERI network has changed the way people practice and conduct research in natural hazards engineering. This capstone Research Topic expands upon early advances (Ramirez et al., 2020; Blain and Ramirez, 2023) and emphasizes the NHERI network's lasting impact—specific ways that NHERI has innovated engineering research and practice that leads to resilience of the built environment in the face of natural hazards that are ever more frequent and destructive.

Five state-of-the-art, experimental facilities that tackle hazards from wind and earthquakes are highlighted in this Research Topic. Stokoe et al. describe advances in seismic subsurface imaging and *in-situ* characterization of liquefaction, among other things, using large-scale, one-of-a-kind, mobile field shakers and associated instrumentation. DeJong et al. detail how hypergravity experiments conducted with unique, world-class geotechnical centrifuges provide a new approach to explore the motion of multiphase media such as soil-foundation-structure interactions. The value of the tallest ever shake of a full-scale building structure, a ten-story mass timber building equipped with nonstructural components conducted by the outdoor shake table (LHPOST), is illustrated in McCartney et al. Metwally et al. discuss the value of integrating a downburst simulator with hurricane winds generated by the "Wall of Wind" to understand the complex interactions between wind forces and urban environments. Lastly, Cao et al. portray how directional structural testing in real-time using a cyber-physical simulation technique can be extended to include multi-physics (soil-foundation-structure interactions and fluid-soil-structure interactions) and multi-hazard (wind and earthquake) applications.

Other important components of the NHERI network whose impact is included in this Research Topic include DesignSafe, the leading and accredited cyberinfrastructure for engineering and social science research related to natural hazards. Rathje et al. share the vast capabilities and resources of the DesignSafe cyberinfrastructure that enable sophisticated simulations and data-driven workflows that accelerates natural hazards engineering research across the network. Within NHERI is a social sciences hub, CONVERGE, that connects seven Extreme Events Research/Reconnaissance (EER) networks. Innovations that unify and streamline the acquisition of post-event reconnaissance data is conveyed by Alam et al. Pham and Arul provide an example of DesignSafe data re-use. At the SimCenter, an open-source, modular framework detailed by Zsarnoczay et al. integrates performance-based engineering methodologies with regional scale assessments to enable multi-hazard, multi-scale simulations; key contributions include improved inventory generation, damage simulation, and recovery analysis, with applications extending across multiple hazard domains. Finally, activities of the Network Coordination Office (NCO), detailed by Blain et al., engage all facilities within NHERI through centralized governance, communication, and education activities that unite the natural hazards research community and amplify NHERI's impact. The components and impact of the extremely successful pipeline for engineering education designed and executed by the NCO are described by Nelson et al. and Meselhe et al. presents a case study of student authors' experience participating in one such program, the NSF NHERI Research Experience for Undergraduates (REU).

While NHERI's first decade is certainly marked by its groundbreaking experiments, the articles in this Research Topic not only archive continued advancement of knowledge and innovations aimed at mitigating the harmful impacts of natural hazards, but also reveal its defining legacy in the creation of a fully integrated research ecosystem. This Research Topic of papers demonstrates that weaving together physical testing, cyberinfrastructure, advanced simulation, and a coordinated community, NHERI has not only established a new paradigm for natural hazards engineering but continually raises the bar for what is possible in the field, laying the groundwork for the discoveries of the decade to come.

Author contributions

CB: Conceptualization, Writing – original draft, Writing – review and editing. JR: Funding acquisition, Project administration, Writing – review and editing. JC: Writing – review and editing. RN: Writing – review and editing. NJ: Writing – review and editing. DJ: Writing – review and editing. QC: Writing – review and editing.

Funding

The author(s) declare that financial support was received for the research and/or publication of this article. The programs and research are based upon work supported by the U.S. National Science Foundation under the Natural Hazards Engineering Research Infrastructure Network Coordination Office Award No. 2129782. Distribution Statement A. Approved for public release: distribution is unlimited.

Conflict of interest

The authors declare that the research was conducted in the absence of any commercial or financial relationships that could be construed as a potential conflict of interest.

Generative AI statement

The author(s) declare that no Generative AI was used in the creation of this manuscript.

Any alternative text (alt text) provided alongside figures in this article has been generated by Frontiers with the support of artificial intelligence and reasonable efforts have been made to ensure accuracy, including review by the authors wherever possible. If you identify any issues, please contact us.

Publisher's note

All claims expressed in this article are solely those of the authors and do not necessarily represent those of their affiliated organizations, or those of the publisher, the editors and the reviewers. Any product that may be evaluated in this article, or claim that may be made by its manufacturer, is not guaranteed or endorsed by the publisher.

References

AOML, Atlantic Oceanographic and Meteorological Laboratory, Hurricane Research Division, NOAA (2025). Continental United States hurricane impacts/landfalls, 1851–2023. Available online at: https://www.aoml.noaa.gov/hrd/hurdat/All_U.S._Hurricanes.html.

Blain, C. A., and Ramirez, J. A. (2023). Editorial: technology transfer from the natural hazards engineering research infrastructure (NHERI). *Front. Built Environ. Sec. Earthq. Eng.* 9. doi:10.3389/fbuil.2023.1269036

National Geophysical Data Center/World Data Service (NGDC/WDS) (2025). *NCEI/WDS global significant earthquake database*. NOAA National Centers for Environmental Information: Silver Spring, United States. doi:10.7289/V5TD9V7K

NOAA National Centers for Environmental Information (NCEI) U.S (2025). Billion-dollar weather and climate disasters. Available online at: https://www.ncei.noaa.gov/access/billions/(Accessed 17 June, 2025).

Ramirez, J., Blain, C., Bobet, A., Browning, J., Edge, B., LaChance, M., et al. (2020). NHERI impact 2020, multi-hazard research to make a more resilient nation. *DesignSafe-CI*. doi:10.17603/ds2-1f7x-9a52

frontiers | Frontiers in Built Environment

TYPE Original Research
PUBLISHED 12 December 2024
DOI 10.3389/fbuil.2024.1485388

Check for updates

OPEN ACCESS

EDITED BY
Cheryl Ann Blain,
Naval Research Laboratory, United States

REVIEWED BY
Kurtis Robert Gurley,
University of Florida, United States
Guangzhao Chen,
Florida International University, United States

*CORRESPONDENCE
Huy Pham,
phamanhuy@vt.edu

RECEIVED 23 August 2024
ACCEPTED 06 November 2024
PUBLISHED 12 December 2024

CITATION
Pham H and Arul M (2024) Automated extraction and summarization of wind disaster data using deep learning models, with extended applications to seismic events. *Front. Built Environ.* 10:1485388. doi: 10.3389/fbuil.2024.1485388

COPYRIGHT
© 2024 Pham and Arul. This is an open-access article distributed under the terms of the Creative Commons Attribution License (CC BY). The use, distribution or reproduction in other forums is permitted, provided the original author(s) and the copyright owner(s) are credited and that the original publication in this journal is cited, in accordance with accepted academic practice. No use, distribution or reproduction is permitted which does not comply with these terms.

Automated extraction and summarization of wind disaster data using deep learning models, with extended applications to seismic events

Huy Pham* and Monica Arul

Wind and Society Laboratory, Department of Civil and Environmental Engineering, Virginia Tech, Blacksburg, VA, United States

The United States experiences more extreme wind events than any other country due to its diverse climate and geographical features. While these events pose significant threats to society, they generate substantial data that can support researchers and disaster managers in resilience planning. This research leverages such data to develop a framework that automates the extraction and summarization of structural and community damage information from reconnaissance reports. The framework utilizes the large Bidirectional and Auto-Regressive Transformers model (BART-large), a deep learning model fine-tuned on the Multi-Genre Natural Language Inference (MNLI) and Cable News Network (CNN) Daily Mail datasets for these tasks. Specifically, the BART-large MNLI model employs zero-shot text classification to identify sentences containing relevant impact information based on user-defined keywords, minimizing the need for fine-tuning the model on wind damage-related datasets. Subsequently, the BART-large CNN model generates comprehensive summaries from these sentences, detailing structural and community damage. The performance of the framework is assessed using reconnaissance reports published by the Structural Extreme Events Reconnaissance (StEER), part of the Natural Hazards Engineering Research Infrastructure (NHERI) network. Particularly, the initial evaluation is conducted with the 2022 Hurricane Ian report. This is followed by a verification of the BART-large MNLI model's capability to extract impact sentences, utilizing the 2023 Hurricane Otis report. Finally, the versatility of the framework is illustrated through an extended application to the 2023 Türkiye earthquake sequences report, highlighting its adaptability across diverse disaster contexts.

KEYWORDS

wind disaster and resilience, structural damage, community damage, zero-shot text classification, text mining

1 Introduction

Statistics from the United States spanning from 1980 to July 2024 indicate that tropical cyclones and severe storms are the most frequent and costly natural disasters, with damages totaling $1,912.5B (69.3% of the total cost) (NCEI, 2024). Notable hurricanes such as Katrina in 2005 ($200B), Harvey in 2017 ($158.8B), and Ian in 2022 ($118.5B) have

inflicted severe financial tolls. In comparison, severe storms like the two consecutive Midwest/Southeast Tornadoes in April and May 2011 ($14.3B and $12.6B), were less costly but posed significant challenges to disaster management due to their short forecast times.

Despite the substantial economic losses, these extreme wind events, and natural hazards in general, generate vast amounts of data that can aid researchers and disaster managers in mitigating their impacts. These datasets typically exhibit the defining characteristics of big data, known as the 3Vs (Laney, 2001): significant Volume, high Velocity reflected by rapid data generation across all disaster phases, and wide Variety, with data spanning various formats and sources like texts and images from social media and news outlets. Subsequently, three additional aspects—Veracity, Value, and Complexity—have become crucial, underscoring the importance of data quality, the utility of insights extracted from data, and the challenges of data management (Kaisler et al., 2013; Patgiri and Ahmed, 2016). To overcome the challenges presented by these 6Vs, machine learning (ML), a subset of artificial intelligence (AI) focused on developing algorithms that learn from data to make predictions, and deep learning (DL), a branch of ML that employs artificial neural networks to model complex patterns in ways mimicking human decision-making, have been widely utilized. These techniques are pivotal in analyzing big data from disasters, with key resources including real-time Twitter data and structured disaster response documentation such as humanitarian and reconnaissance reports.

Over the last decade, ML and DL algorithms have been increasingly used to extract disaster-related information from Twitter. Particularly, Ikonomakis et al. (2005) leveraged classical ML algorithms to collect disaster-related tweets. Verma et al. (2011) assessed the impact of linguistic features on text classification efficiency. Imran et al. (2013) trained the Naïve Bayesian (NB) model to extract the disaster response nuggets from the 2011 Joplin Tornado-related tweets. Addressing challenges in using hazard-related tweets for model training, Imran et al. (2016) published a multi-lingual, annotated corpus of 52 million tweets. Nguyen et al. (2017) employed Convolutional Neural Networks (CNN) to accelerate the extraction process, and Kersten et al. (2019) examined the robustness and transferability of CNNs across various hazards, utilizing real-time data streams. Finally, ALRashdi and O'Keefe (2019) compared crisis tweet extraction methods by using Bidirectional Long Short-Term Memory (Bi-LSTM) networks.

Twitter, with its diverse yet subjective and inconsistent content, underscores the necessity for more reliable information sources in disaster response. Additionally, the varying needs of different research groups highlight the importance of developing objective, systematic resources like humanitarian and reconnaissance reports. A recent study by Riezebos (2019) involved extracting sentences from humanitarian reports that detail the impacts of natural hazards. A Linear Support Vector Machine model, with an F1 score of around 0.8, was selected as the most effective. This study contributed to the Impact-Based Forecasting tool of the 510 initiative, backed by the Netherlands Red Cross, to assist disaster managers in predicting future disaster impacts.

While humanitarian documentation focuses on the needs and resources required for disaster response—primarily targeting aid organizations and government agencies—this study aims to extract the impacts of these disasters on infrastructure and community from reconnaissance reports. These include building damages, lifeline system failures, population displacement, and economic disturbance. It is crucial to include the communities in the framework as they are directly affected by these hazards. This approach aligns with the resilience definitions since the 2000s that integrate infrastructure and community into resilience frameworks (Koliou et al., 2020).

This research has two main objectives. The first objective is to identify impact sentences from wind disaster reconnaissance reports. This process involves analyzing a particular report to retrieve sentences that provide relevant damage information. The second objective is to generate comprehensive summaries from that reconnaissance report. These summaries serve two important purposes: First, they distill the key points of a report, allowing researchers to quickly grasp essential information from areas of interest. Second, if integrated into data repositories like Design Safe—a cyberinfrastructure for civil engineering—these summaries could enhance the querying system for disaster-related data. This improvement would allow users to perform more nuanced searches using user-defined keywords to automatically extract and summarize information from various reports. This purpose is in line with the decadal vision of the Natural Hazard Engineering Research Infrastructure (NHERI) Schneider and Kosters (2024), which aims to incorporate AI and advanced analytics tools into cyberinfrastructure to improve dataset querying.

Employing supervised and deep learning algorithms to extract impact information from reconnaissance reports presents challenges due to the sequential nature of the content. For instance, a Linear Support Vector Machine (LSVM) analyzes words or sequences independently without considering contextual relationships. Conversely, Long Short-Term Memory (LSTM) networks process data sequentially, allowing them to capture long-range textual dependencies. However, they demand considerable computational resources for large datasets, and their complex architecture requires a deeper understanding of implementation, making them more challenging to use than traditional ML models. Meanwhile, CNNs are proficient at extracting local features but lack the inherent design to comprehend long-range dependencies and sequential context, which are vital for effective natural language processing (NLP).

The Transformer architecture, a type of DL model, addressed these shortcomings through its self-attention mechanism (Vaswani et al., 2017). This mechanism allows each part of the sequence to attend to every other part directly, enabling the model to capture long-range dependencies, parallel data processing, and mitigate the vanishing gradient problem. In line with these advancements, the Transformers library emerged as an open-source platform, offering various pre-trained Transformer-based models (Wolf et al., 2020) for NLP applications.

One common method of leveraging pre-trained models for targeted tasks is fine-tuning. For example, Liu et al. (2021) built CrisisBERT upon the Bidirectional Encoder Representations from Transformers (BERT) (Devlin et al., 2019) to detect crisis-related content in tweets. Additionally, Alam et al. (2021) introduced CrisisBench, a benchmarking framework designed to evaluate the effectiveness of various DL and transformer architectures in disaster response applications. Another approach is zero-shot classification, which utilizes pre-trained models for tasks they were not originally trained to perform. In this vein, Yin et al. (2019) conducted

benchmarking that included an evaluation of model performance on Zero-Shot Text Classification (0SHOT-TC), using BERT models trained on three mainstream datasets. Facebook AI researchers (Lewis et al., 2020) extended this idea by fine-tuning the large version of the Bidirectional and Auto-Regressive Transformer (BART) model on the Multi-Genre Natural Language Inference (MNLI) dataset (Williams et al., 2018), creating BART-large MNLI model. Originally applied to BERT, this method employs pre-trained Natural Language Inference models as zero-shot sequence classifiers by which the input sequence serves as the premise, while the labels serve as hypotheses. The labels are assigned to the input sequence based on their likelihood of entailment and contradiction.

The selection of ML models for this research is driven by the 0SHOT-TC approach, chosen due to the limited availability of training datasets related to wind damage. Particularly, the BART-large MNLI model is used to extract impact sentences from wind disaster reconnaissance reports. Sentences from these reports are considered premises, and the model uses predefined keywords related to hazard damage as hypotheses to classify impact information. For summaries generation, the large version of the BART model, fine-tuned on the Cable News Network (CNN) Daily Mail dataset (BART-large CNN) (Hermann et al., 2015; See et al., 2017), is employed to generate comprehensive summaries from these impact sentences.

Building upon the advancements within the Transformer family, the fourth iteration of the Generative Pre-trained Transformer (GPT-4) (OpenAI, 2023a) excels in advanced text generation and comprehension, capable of handling a wide range of tasks such as content extraction and summarization without specific training datasets. An upgraded version, GPT-4O (O for Omni) (OpenAI, 2024), extends these capabilities to support human-computer interaction across multiple formats, processing and generating outputs in text, audio, images, and video. However, the application of these models in this research is limited due to their generative nature, which can produce inconsistent results from identical prompts. This inconsistency undermines the reliability required for accurate data synthesis, including but not limited to extracting data on wind damage from reconnaissance reports. To mitigate this issue, the OpenAI Red Teaming Network, comprising experts across various fields, has been formed to rigorously evaluate these models on domain-specific tasks (OpenAI, 2023b). Continued research is essential to assess their effectiveness in analyzing damage from extreme wind events and other natural hazards.

Essentially, this study aims to develop a framework for automatically extracting and summarizing structural and community damage information from wind disaster reconnaissance reports, utilizing the BART-large MNLI and BART-large CNN models. Organized into several sections, the paper starts with an overview of the available datasets, followed by a description of the methodology. Using keywords obtained from documents up to 2022, the framework is first evaluated with the 2022 Hurricane Ian report and then verified with the 2023 Hurricane Otis report, both provided by the Structural Extreme Events Reconnaissance (StEER), part of the NHERI network. To demonstrate the adaptability of the framework to other hazards, its application is extended to the 2023 Türkiye Earthquake report from StEER by simply modifying the keyword list. Subsequently, the paper introduces the implementation framework, assesses computational efficiency, discusses limitations and future works, and concludes with final remarks.

2 Overview of key data sources for disaster damage assessment

2.1 Key organizations for disaster damage assessment

This section first offers an overview of datasets released by various organizations, each producing reports that vary in format, content, and intended audience. Notably, the actual readership of these reports often extends beyond the intended audience, with diverse interests in the specific information presented. Despite the wealth of data available, effectively accessing it remains a significant challenge. The organizations are categorized as follows:

- **Government Emergency Management Agencies:** This includes the Federal Emergency Management Agency (FEMA), state-level emergency management agencies, and county emergency management offices.
- **Federal Scientific and Engineering Agencies:** Notable agencies are the U.S. Geological Survey (USGS), the National Oceanic and Atmospheric Administration (NOAA), and the U.S. Army Corps of Engineers (USACE).
- **Other Organizations:** Examples include the American Society of Civil Engineers (ASCE) and the Structural Extreme Events Reconnaissance (StEER).

Although resources provided by these entities are publicly available, this overview prioritizes damage reports from FEMA and StEER, as they focus more on collecting and analyzing structural and community damage. Between these two, StEER is preferred for its rapid publication cycle and more manageable report lengths. Typically, StEER reports are published within 2 months, significantly faster than FEMA's Mitigation Assessment Team (MAT) reports, which can take over a year to publish due to additional focus on building code recommendations. This rapid update cycle and targeted focus on damage assessment are well-aligned with the research objectives, which include extracting and summarizing impact information from reconnaissance reports. Furthermore, StEER reports generally range from 40 to 150 pages, making them more suitable for the summary generation processes in this study (Section 3.4), compared to MAT reports, which span between 200 and 400 pages and may require multiple summaries to cover detailed aspects of infrastructure and community damage thoroughly. The following sections will delve into the background, purpose, outputs, and archiving practices of StEER, detailing their contributions to disaster data collection and analysis.

StEER Network was established in 2018 as part of the Natural Hazards Engineering Research Infrastructure (NHERI) CONVERGE node (Peek et al., 2020), funded by the National Science Foundation. It conducts post-disaster reconnaissance on natural hazards that have significant potential for generating new knowledge (Kijewski-Correa et al., 2021). The level of response by StEER can vary from 1 to 3, as illustrated in Figure 1, involving key groups such as Virtual Assessment Structural Teams (VAST),

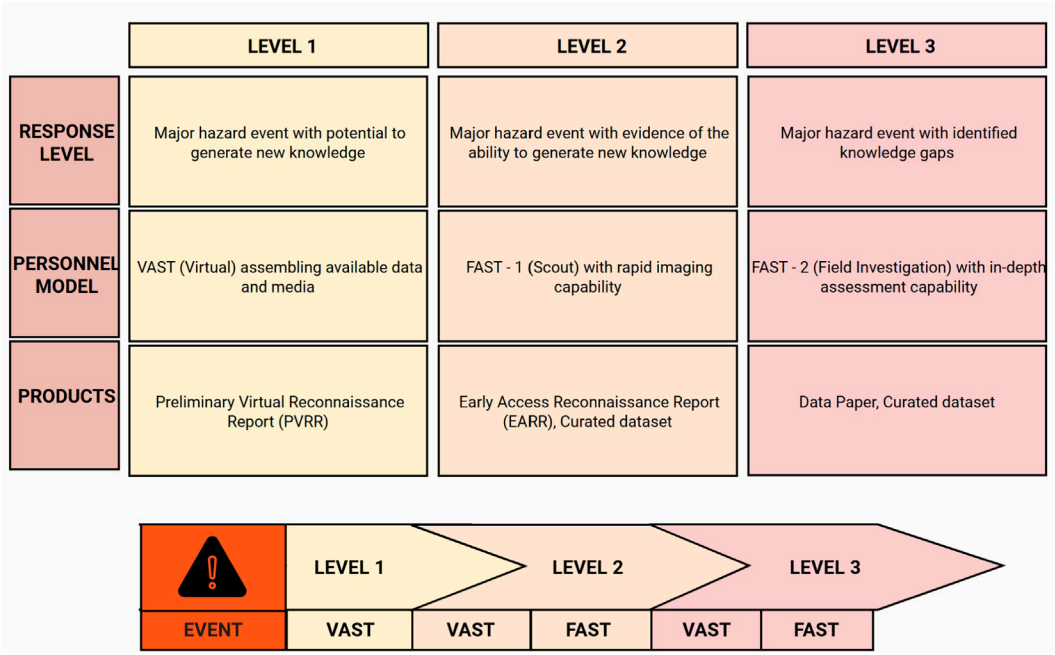

FIGURE 1
StEER Tiered Response Phasing Model (Source: StEER Network).

Field Assessment Structural Teams (FAST), Response Coordination, and Data Librarians. Their outputs include Preliminary Virtual Reconnaissance Reports (PVRR), Early Access Reconnaissance Reports (EARR), curated datasets, and journal papers, providing insights into hazard characteristics, local building codes, building and infrastructure performance, geotechnical performance, coastal protective systems performance, and recommended response strategies.

Decisions on team engagement and product delivery are driven by the Activation and Escalation Criteria, which consider the severity of the hazard, the level of infrastructure exposure, and the practicability of mounting a response. All published reports are archived in the Data Depot at DesignSafe—a cyberinfrastructure platform dedicated to managing extensive data from natural hazards engineering research (Pinelli et al., 2020). Its web interface enables users to manage data through browsing, uploading, downloading, sharing, curating, and publishing (Rathje et al., 2017).

2.2 Datasets for framework assessment

This study utilizes recent PVRR reports from both hurricane and seismic events. These reports synthesize and provide commentary on hazard characteristics, local building codes, building and infrastructure performance, geotechnical conditions, and recommended response strategies. The hurricane reports are initially used to evaluate and verify the performance of the framework. The seismic report is then utilized to demonstrate its versatility of when applied to other hazards. Table 1 provides an overview of each report, including the number of pages, the number of post-processed sentences, and the total number of words.

3 Methodology

Figure 2 presents a framework for automatic extraction and summarization of impact information from damage reports, focusing on structural and community damage from extreme wind events. It includes five main steps: data preprocessing, data labeling, extracting impact sentences, analyzing the results, and generating comprehensive summaries. Each step plays a crucial role in processing reconnaissance documents into informative impact summaries.

3.1 Step 1: Data preprocessing

The least error-prone process to retrieve text from damage reports stored in Portable Document Format (PDF) is outlined here. Initially, the typical document structure is considered to determine the level of granularity for text extraction. Figure 3 shows that the structure contains sections, paragraphs, sentences, words (unigrams, bigrams, etc.), and individual characters. Qualitatively, words and single characters would be insufficient to represent impact information, thus resulting in under-specification. In contrast, for sections and paragraphs, non-impact data can be intertwined with impact data, leading to over-specification. Sentences strike a balance between these two extremes; therefore, the data is extracted in the form of sentences. Due to the challenges posed by PDFs in preserving exact text positions, such as non-structured text and unclear boundaries between tables and paragraphs, it is beneficial to convert PDFs into a more editable format like.docx. This can be done using advanced PDF editing and conversion software.

TABLE 1 Dataset overview.

No.	Event	Year	Number of pages	Number of sentences (post-processing)	Number of words (post-processing)
1	Hurricane Ian	2022	45	254	6,279
2	Hurricane Otis	2023	40	276	5,965
3	Türkiye Earthquake	2022	144	779	18,496

After conversion, the document becomes more accessible for processing with Python preprocessing code to extract sentences efficiently.

3.2 Step 2: Data labeling

Before labeling impact sentences, it is important to establish the definition of impact sentence. In this context, impact refers to structural and community damages caused by a specific event, such as wind. Structural damage pertains to impacts on the physical infrastructure such as buildings and bridges, while community damage includes societal effects like loss of lives and livelihoods. A sentence is classified as an impact sentence if its content relates to keywords associated with damage caused by the hazard. This keyword-based classification method is informed by the BART-large MNLI model, as described in Section 3.3.1. For example, sentences containing keywords related to structural damage—categorized by building types, components, or damage terms—are classified as structural impact sentences. The creation of the list of keywords for both structural and community damage is provided in Table 2 in Section 3.3.2.

The entire dataset was manually annotated by the authors using the reports outlined in Section 2.2. This dataset is then used to evaluate the ability of the framework to identify impact sentences. Examples of this process, particularly for Hurricane Ian's PVRR, are presented in Section 4.2.

3.3 Step 3: Extracting impact sentences

The classification of impact sentences utilizes a keyword-based approach with the large **B**idirectional **A**uto-**R**egressive **T**ransformer fine-tuned on the **M**ulti-Genre **N**atural **L**anguage **I**nference dataset (BART-large MNLI). Specifically, sentences containing relevant keywords to either structural or community damage are labeled as impact, whereas unrelated sentences are marked as non-impact. The large scale of the model and its diverse training allow it to handle topics like wind disaster impacts without requiring additional fine-tuning on specialized datasets for wind damage, which are typically scarce.

3.3.1 Overview of BART model

BART (Lewis et al., 2020) is a denoising autoencoder designed for sequence-to-sequence models, which excels at various NLP downstream tasks involving sequence classification, token classification, sequence generation, and machine translation. It integrates the bidirectional encoder from BERT (Devlin et al., 2019) and the autoregressive decoder from GPT (Radford et al., 2018) within the Transformer architecture (Vaswani et al., 2017). The model is trained on text corrupted by masking spans of content to reconstruct the original sequences. Such training makes the model adept at understanding and correcting distortions in the input. Figure 4 provides a visual representation of the BART architecture. Specifically, the bidirectional encoder processes each sequence from both directions to grasp the overall context, which is then passed to the autoregressive decoder to regenerate the input sequence. To enhance training efficiency, BART incorporates the Gaussian Error Linear Unit (GeLU) activation function, which allows for the passage of small negative gradients (Hendrycks and Gimpel, 2016). Additionally, it initializes the training weights following a normal distribution of zero mean and standard deviation of 0.02, facilitating more effective training convergence.

The model is available in two sizes: the base model with 6 encoder and decoder layers totaling 140 M parameters, and the large variant with 12 of each, consisting of 400 M parameters. This increased capacity enables BART to capture more complex patterns and nuances in the data, potentially improving performance. However, higher computational resources are required for training and implementation.

BART has been adapted for sequence classification tasks, specifically for Zero-Shot Text Classification (0SHOT-TC), based on a method outlined in Yin et al. (2019). This method involves training models to perform Natural Language Inference on entailment datasets for 0SHOT-TC. Specifically, the model was fine-tuned on the **M**ulti **N**omial **L**anguage **I**nference (MNLI) dataset (Williams et al., 2018), which contains roughly 433 k sentence pairs from diverse genres. Each pair includes a premise and a hypothesis, with the pairs labeled as entailment, neutrality, or contradiction depending on the relationship between the two. This extensive and diverse dataset enables BART to classify text by assessing its compatibility with labels across these three dimensions.

3.3.2 Implementation of BART-large MNLI for extracting impact sectences

This research implements the BART-large MNLI model using sentences extracted from reconnaissance reports as premises and predefined keywords related to wind disasters as hypotheses. These keywords are systematically categorized and derived from sources such as StEER reports (published before 2023), FEMA

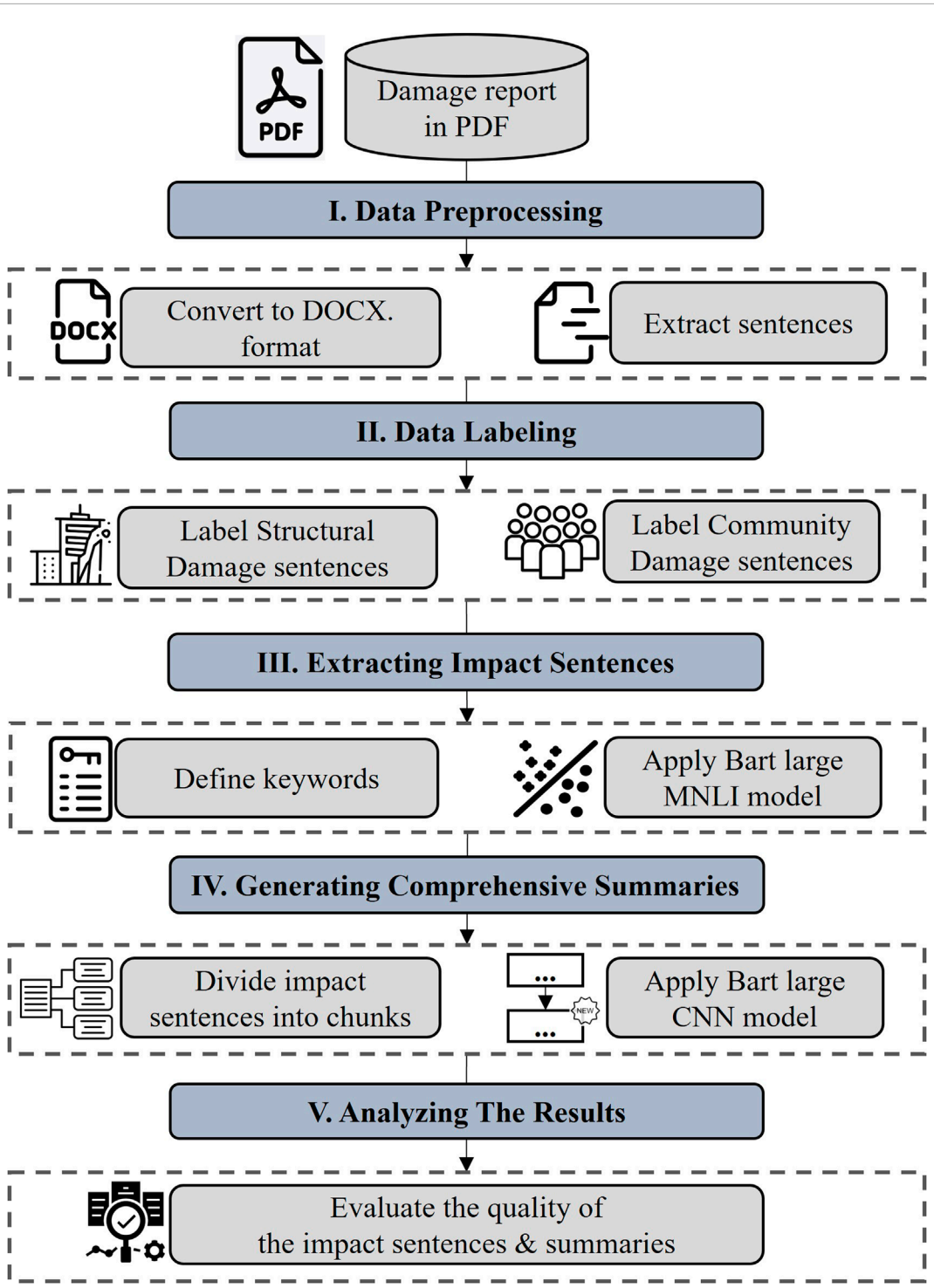

FIGURE 2
Overall procedure for extracting disaster impact data.

technical documents (prior to 2023), and ASCE 7-22. The initial list of keywords is selected based on their frequency in these documents, and closely related keywords are grouped and generalized according to the authors' expertise. The focus is primarily on structural damage, encompassing elements such as building types, components, other forms of infrastructure, and relevant structural terms. To enhance model accuracy, the term damage is appended to keywords related to building types, components, and infrastructure, ensuring that the model accurately identifies sentences discussing damage rather than merely describing structures. Owing to the primary focus of reconnaissance reports on building performance, keywords pertaining to community damage are grouped into a single category. Additionally, keywords that describe the extent of hazards are

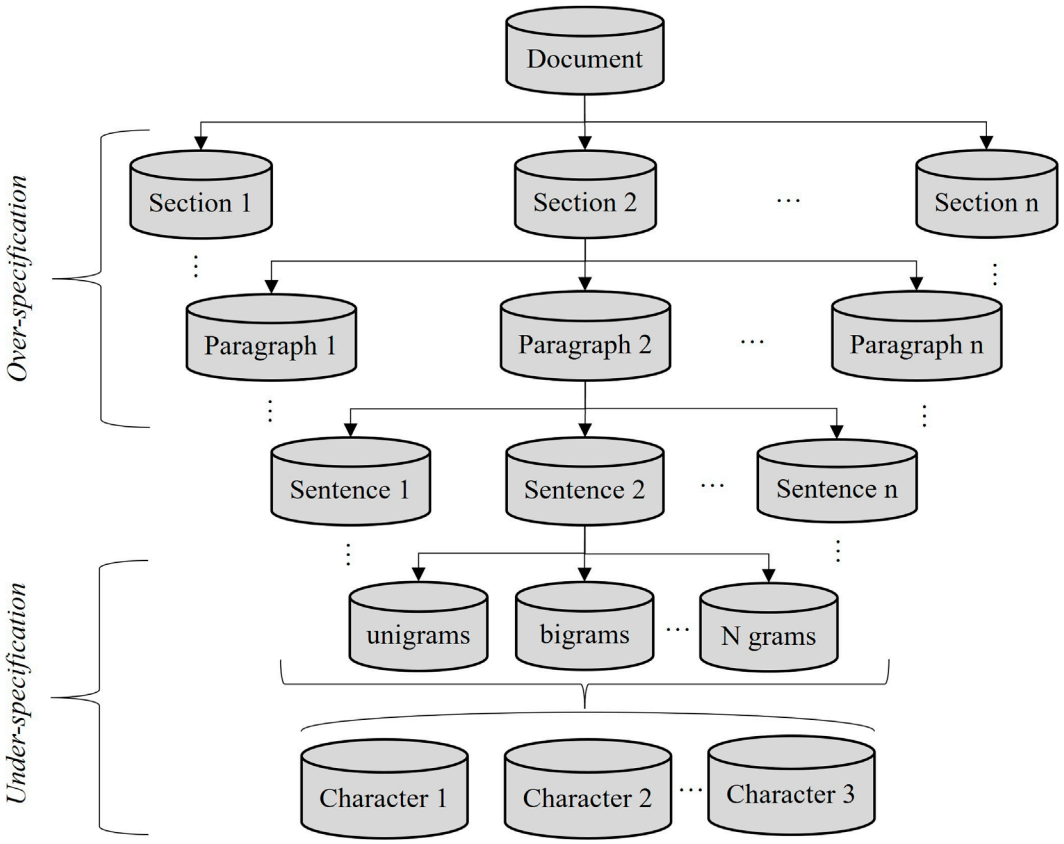

FIGURE 3
General document structure.

TABLE 2 Keywords related to wind disaster impacts.

Categories	Keywords
Building types	Family housing damage, school damage, mobile home damage, manufactured home damage, commercial facility damage, hospital damage, religious infrastructure damage, historical building damage, industrial facility damage, agricultural infrastructure damage, fire station damage, police station damage, parking damage, critical facility damage, shelter damage
Building components	Roof damage, secondary water resistance damage, roof deck damage, roof-wall connection damage, toenail damage, hurricane strap damage, shutter damage, roof cover damage, shingle damage, built-up roofing damage, single-ply membrane damage, wall damage, roof frame damage, wood truss damage, open web steel joist damage, joist spacing, window damage, tie-downs damage, foundation anchorage damage, door damage, glazing damage, cladding damage
Other infrastructure	Airport damage, port damage, bridge damage, road damage, causeway damage, pavement damage, seawall damage, levee damage, water tank damage, power plant damage, offshore structure damage
Structure-related terms	Structural behavior, structural damage, structural failure mechanisms, building resilience, structural connection damage, building interior damage, building exterior damage, building envelope damage, building damage, lateral force resisting systems, undamaged infrastructure
Terrestrial damages	Erosion, washout, wind-borne debris, scour, tree-related damage
Community damages	Fatalities, economic loss, power outage, healthcare disruption, agricultural damage, uninsured loss, telecommunication system disruption, transportation disruption, utility outage, water outage, service loss, supply halt, injuries, temporary medical facility, transaction suspension
Non-impact terms	Storm tracking, building code, research support

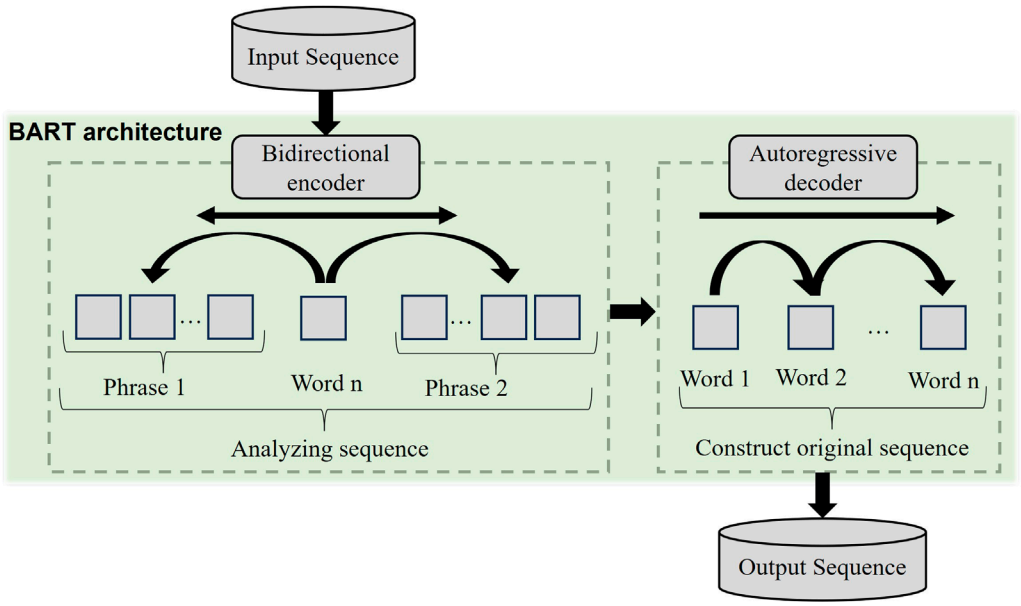

FIGURE 4
Schematic of BART architecture.

included in the terrestrial damage category. A separate list of keywords indicative of non-impact sentences is also compiled to help exclude irrelevant sentences. Table 2 presents the keywords used for identifying the impacts of wind disasters, following the categories mentioned.

BART, as a Transformer architecture variant, is integrated into the Hugging Face Transformers library (Wolf et al., 2020), providing a standardized framework for implementation. The end-to-end implementation for BART-large MNLI, illustrated in Figure 5, begins by dividing the dataset into smaller batches to manage the computational demands of the model, which has approximately 407 million parameters. This pipeline consists of three main stages: encoding, model processing, and decoding. During the encoding stage, raw text is converted into a format that the model can process. Each sentence within a batch is paired with relevant keywords to form sentence pairs. Subsequently, each of them undergoes tokenization—the process of breaking down text into smaller units, called tokens, which can be as small as words or subwords. This step is crucial for capturing nuanced meanings, enabling the model to process language more effectively. The specific tokenizer from BART-large MNLI is used, following its tokenization scheme. Post-tokenization, each token is converted into a unique ID. This step is fundamental as the model operates on numerical data, with these IDs enabling it to process the text. It is important to note that sentence pairs vary in length and are thus tokenized independently. To stack them into a 2D tensor, techniques like padding zeros and truncation are applied. This standardization ensures uniform tensor lengths for each sentence pair. The resulting 2D tensor serves as the input to the model processing stage, representing the textual data in a structured, machine-readable format.

The BART-large MNLI model processes a 2D tensor of tokenized IDs, which is optimized for sequence classification tasks. Both the encoder and decoder receive this tensor as their input. The key output of the model is the final hidden state from the last token of the decoder, capturing comprehensive information from the sentence pairs. This hidden state is then fed into a multi-class linear classifier that generates logits, representing the raw class predictions of the model. These logits are structured into a 2D tensor with three columns, corresponding to contradiction, neutral, and entailment, and rows that align the sentence pairs.

In the decoding stage, the logits tensor undergoes softmax normalization across each row, converting it into a probability tensor where each row sums up to one. Given the focus on contradiction and entailment classes, the neutral column is removed before applying the softmax function. This modification ensures that only the pertinent scores are factored into the probability calculations. For a detailed analysis of the entailment class, a 1D tensor representing these probabilities is extracted and reshaped into a 2D format that aligns with the number of sentence pairs and labels. The process concludes with the selection of the maximum value from each row, pinpointing the highest entailment score for each sentence pair.

The pipeline processes each batch sequentially until all batches are completed. A baseline entailment score of 0.9 is set as a threshold which will be verified in Step 5, signifying that sentences with at least 90% compatibility with the labels are considered relevant. These selected sentences are categorized as impact sentences. Based on their alignment with specific keywords, they are further classified into either structural or community damage categories. Additionally, these sentences are restored to their original positions within their respective documents. This repositioning is crucial for generating comprehensive summaries in the subsequent step.

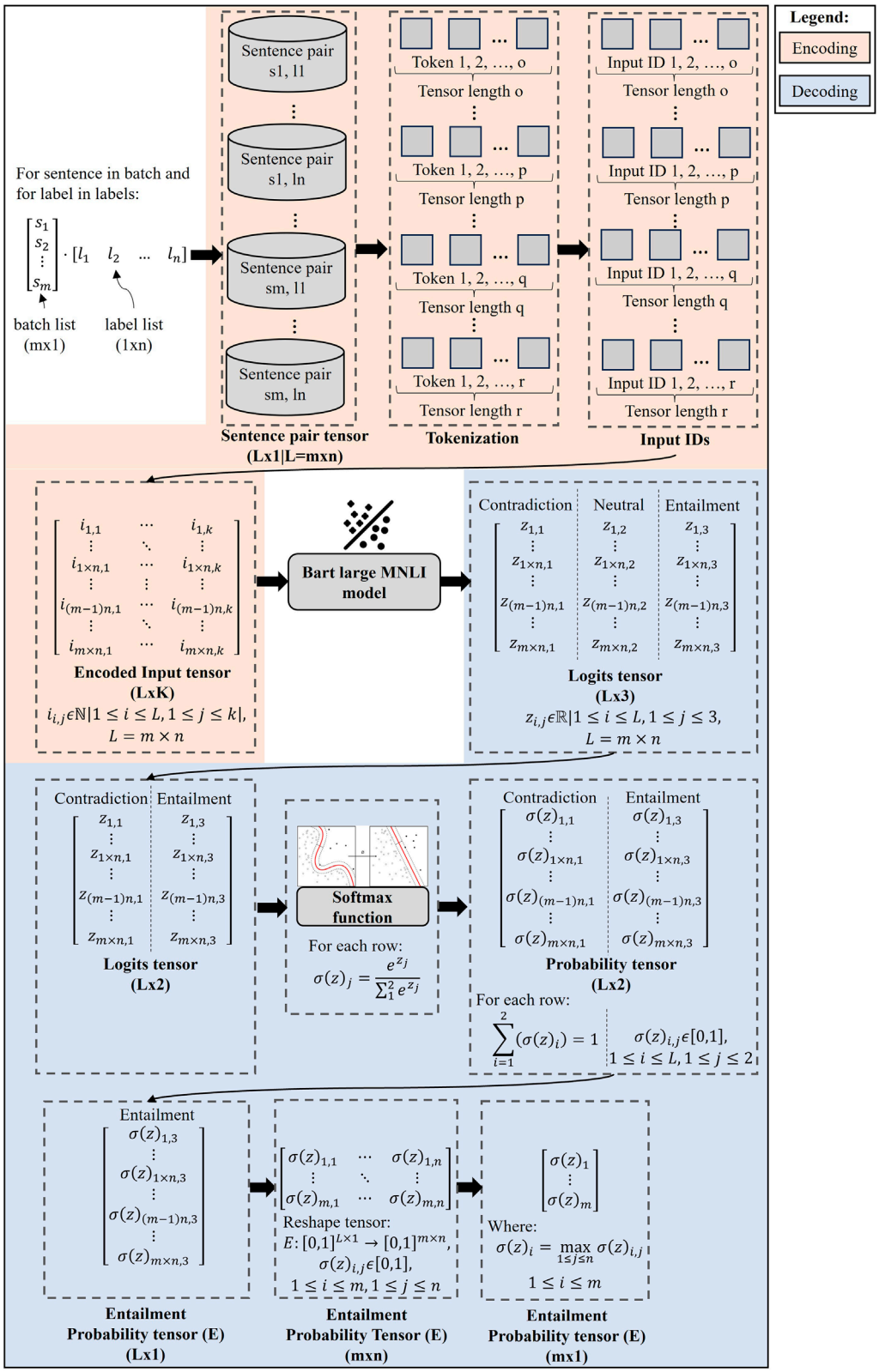

FIGURE 5
BART-large MNLI implementation pipeline.

BART-large MNLI brings two key advantages to this application. Firstly, it approaches the classification task through an inference-based method. Unlike traditional classification techniques that often rely on manual feature specification, the bidirectional encoder automatically captures features during training. This enables a more nuanced text analysis, allowing the model to discern underlying patterns and contexts beyond basic categorization. Secondly, the model has been fine-tuned on the extensive MNLI corpus which greatly boosts its inference capabilities, mitigating the need for fine-tuning the model with manually labeled wind-related impact sentences. This is particularly beneficial, as the model can be customized for different hazards, like seismic events, through modifying the keyword list.

3.4 Step 4: Generating comprehensive summaries

Following the identification of impact sentences, the subsequent step involves generating summaries for structural and community damage. This is accomplished by fine-tuning the BART model (BART-large CNN) for sequence generation tasks, specifically on the CNN Daily Mail dataset (Hermann et al., 2015; See et al., 2017). This dataset encompasses over 300 k news articles with accompanying summaries created by CNN and Daily Mail journalists, making it ideal for extractive and abstractive summarization. The substantial model size and the diverse content of the CNN dataset enable it to generate content on topics it has not seen during training, such as wind disaster impact. Consequently, this reduces the necessity for further fine-tuning on tailored datasets for wind damage summaries, which are not readily available.

Figure 6 outlines the BART-large CNN implementation pipeline, encompassing the encoding, model processing, and decoding stages. Unlike BART-large MNLI, which processes sentence pairs in a 2D tensor, BART-large CNN handles continuous text chunks, streamlining the input process. Particularly, during the encoding stage, each text chunk is tokenized according to the BART-large CNN tokenizer scheme, and the resulting tokens are converted into unique IDs. These IDs form the numerical input enabling the bidirectional encoder to process and interpret the text as cohesive sequences.

In addition to the processed data, several parameters critically influence the summary generation process of the autoregressive decoder. The max_length and min_length parameters define the upper and lower limits of the length of the summary in tokens. The do_sample parameter dictates the method by which the autoregressive decoder determines the next word. When set to True for stochastic mode, the model samples the next word from a probability distribution based on the context from the bidirectional encoder and the previously generated words, enhancing diversity but reducing predictability. Conversely, when set to False for deterministic mode, the model uses the probability distribution to determine the most likely next word, ensuring more predictable and stable outputs. The num_beams parameter in beam search determines the number of potential paths the model keeps simultaneously during text generation. Selecting an appropriate num_beams value balances the trade-off between the quality of the generated text and the computational demands. The early_stopping parameter is utilized to terminate processing once all text sequences are sufficiently generated, optimizing both sentence length and computational efficiency.

These parameters collectively guide the autoregressive decoder, which constructs a summary represented by a tensor of new IDs. In the decoding stage, which mirrors the encoding process, the output—a sequence of IDs—is transformed back into text. Specifically, it involves converting each ID into its corresponding token, where each token corresponds to a lexical unit as specified by the tokenization scheme. These tokens are subsequently detokenized to compile a comprehensive summary.

The pipeline is designed to simultaneously process all the impact sentences for each category—structural and community—but is constrained by a 1024-token limit for tokenized ID inputs. To circumvent this, another approach is employed where impact sentences are grouped into paragraphs without exceeding the token limit, allowing the pipeline to be applied multiple times. These paragraphs, organized based on their original placement in the report, are summarized by the BART-large CNN model, and the resulting summaries are concatenated. Given the extensive length of this combined summary, a recursive process illustrated in Figure 7 is employed to distill the content further. This process involves grouping impact paragraph summaries into larger chunks, each with a maximum of 1,024 tokens. Overlapping tokens are managed using a sliding window function to maintain coherence. The BART-large CNN model is sequentially utilized for each chunk, and if the combined summary exceeds the token limit, the process is iteratively refined. The final output consists of two distinct summaries, one for structural damage and another for community damage from wind disasters.

3.5 Step 5: Analyzing the results

This section assesses the performance of BART-large MNLI and BART-large CNN models. For the BART-large MNLI model, the focus is on the baseline entailment score set at 0.9, as discussed in Step 3. It involves comparing predicted impact sentences from Step 3 with those manually labeled in Step 2 to calculate four key metrics: accuracy, precision, recall, and F1 score. If these metrics yield positive results, this baseline entailment score can be applied to other wind damage reports. For the BART-large CNN model, summary quality is evaluated using the **R**ecall-**O**riented **U**nderstudy for **G**isting **E**valuation (ROUGE) score, which measures text overlap. An overview of these metrics is provided in the Supplementary Appendix.

4 Evaluation case: extracting impact information from Hurricane Ian report

The evaluation case is designed to assess the framework described in the previous section. As mentioned in Section 2, while several organizations offer relevant sources, StEER is chosen for its quick publication turnaround and concise report lengths. Accordingly, the StEER Hurricane Ian Preliminary Virtual

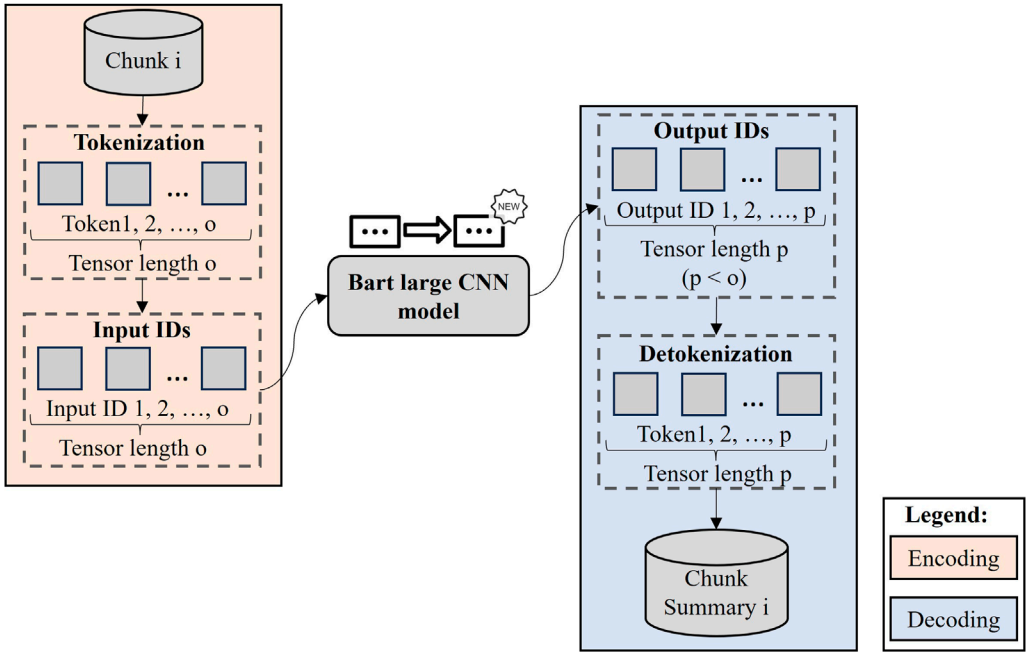

FIGURE 6
BART-large CNN implementation pipeline.

Reconnaissance Report (PVRR), published on 16 November 2022, is selected for this assessment.

4.1 Step 1: Data preprocessing

The report is initially converted from PDF to docx format to maintain the document structure. During this conversion, headings that do not contain damage information, such as preface, acknowledgment, and various appendices and administrative sections, are excluded. The document is then processed through a preprocessing script that extracts all remaining sentences, preparing them for subsequent analysis.

4.2 Step 2: Data labeling

Building upon the criteria for defining impact sentences, this section focuses on preparing the dataset used to assess the performance of the BART-large MNLI model. It includes examples from the dataset to demonstrate how sentences indicating structural and community damage are labeled. It also presents examples of sentences that, although not actually reflecting impact, might easily be misinterpreted as such. To enhance clarity, impact-related keywords are highlighted in italics.

- **Structural damage sentence example:** *Mobile/manufactured housing* and RV parks were the most susceptible to the damage as they lacked the *elevation* and *lateral force-resisting systems* necessary to resist any significant storm surge-induced loads.
- **Community impact sentence example:** Tragically, preliminary numbers available at the time of this report confirm that Ian has caused over 100 *fatalities* in Florida, the highest direct loss of life in any hurricane landfalling in Florida since the 1935 Labor Day hurricane.
- **Non-impact sentence examples:**

1. While the Florida Residential Code provides regulations and guidance for the construction of one and two-family dwellings, the Florida Building Code addresses all other permanent buildings and structures.
2. Lee County, the scene of the heaviest impacts, was under a Tropical Storm Warning by 5 p.m. EDT on Sept. 26th, and a Hurricane Warning by 8 a.m. EDT on Sept. 27th.
3. The first evacuation order for Lee County (Zone A) was issued at 7 a.m. EDT on Sept. 27th, approximately 32 h prior to landfall, and 13 h prior to the most likely time of the arrival of Tropical Storm force winds (> 39 mph) in the Ft. Myers region, as predicted by the National Hurricane Center.

The first sentence details structural components but is limited to code-specific information, lacking impact details. The second sentence, discussing tropical storm and hurricane warnings, i.e., hazard forecasting, similarly lacks details on infrastructure or community impact. The third sentence, mentioning the evacuation order, also does not directly address community impact, deviating from the emphasis of the research on direct effects.

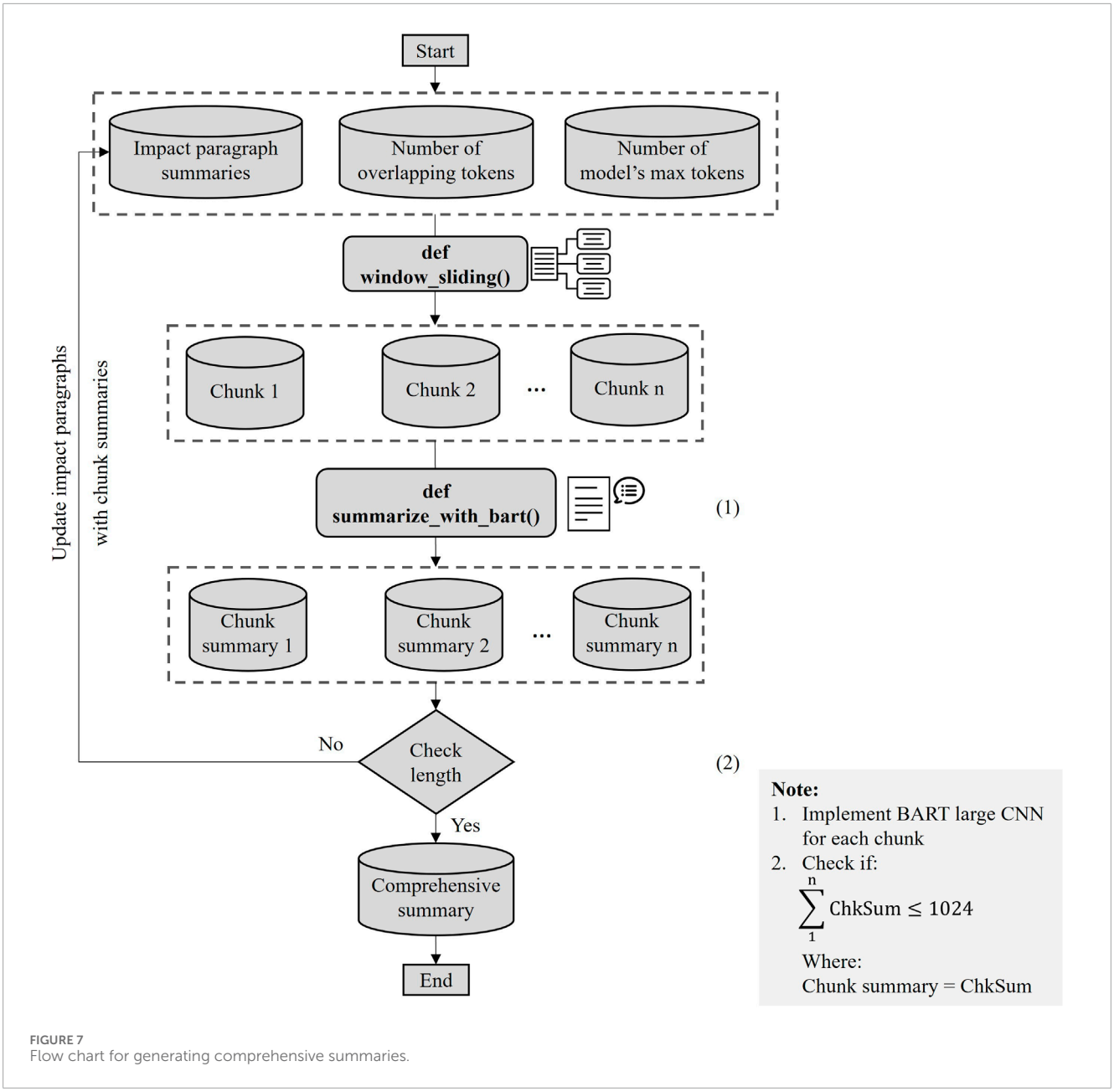

FIGURE 7
Flow chart for generating comprehensive summaries.

4.3 Step 3: Extracting impact sentences

The BART-large MNLI pipeline outlined in Figure 5 is followed to extract impact sentences. Due to the graphics processing unit (GPU) constraints, eight sentences are collectively processed in one batch. Each sentence is associated with 82 labels from Table 2, generating 82 distinct sentence-label pairs. These pairs are then tokenized to produce an encoded two-dimensional tensor, which serves as the input for the Bart-large MNLI model. The resulting logits tensor undergoes preprocessing and normalization via the softmax function, producing a probability tensor. From this tensor, the entailment tensor is extracted and reshaped into a 2D format, which allows for the selection of the highest entailment score for each sentence on a row-by-row basis, producing the final entailment scores.

Given the extensive number of sentences from the report, only the results from the impact examples in Step 2 are presented. Tables 3, 4 display the top five labels ranked by their highest entailment scores. The labels that best match the structural and community impact instances are mobile home damage and fatalities, respectively. It is important to note that sentences with a top entailment score below the assumed baseline of 0.9 are classified as non-impact.

4.4 Step 4: Generating comprehensive summaries

The BART-large CNN model is used to generate summaries for structural and community impacts, following a recursive approach

TABLE 3 Top five labels for structural damage example sentence.

Labels	Entailment score
Mobile home damage	0.987
Manufactured home damage	0.974
Structural damage	0.903
Shelter damage	0.874
Structural behavior	0.854

TABLE 4 Top five labels for community damage example sentence.

Labels	Entailment score
Fatalities	0.994
Storm tracking	0.654
Hurricane strap damage	0.531
Scour	0.470
Structural behavior	0.279

as detailed in Figure 7. The setup involves setting an overlap of 200 tokens and capping the maximum token count at 1,024 to create manageable text chunks. Key parameters for summary generation include setting num_beams to 4, which allows the model to simultaneously explore four potential paths. Additionally, early_stopping is enabled to prevent excessive processing, and do_sample is set to False, ensuring the model deterministically selects the most likely next word from the probability distribution for more consistent and stable outputs. These are the default settings of the model.

Initially, summaries are required to cover at least 80% of the length of the original impact paragraphs. These are then merged into larger text chunks, with subsequent summaries required to contain at least 40% of the total tokens from these chunks, ensuring the final outputs are concise yet substantial. The maximum length of the summaries corresponds to the number of tokens in the chunks prior to generating the summaries. The completed summaries for both structural and community impacts are provided below.

Structural impact summary: Unlike Hurricane Charley (2004), water more so than wind was the impetus behind the disaster that unfolded. Many buildings were completely washed away, and others were left to deal with significant scours and eroded foundations. The west coast of Florida and the Ft. Myers area are the most heavily impacted regions. Seawall collapses were reported along the Atlantic coastline of Florida at Daytona Beach Shores. A levee in Hidden River in Sarasota County, FL, was also breached, causing severe localized flooding (Clowe, 2022). According to the National Levee Database, the Hidden River levee is a 1.98-mile embankment levee along the Myakka River. The surge impacted regions with high population densities housed in both elevated and on-grade residential structures. These include mobile and manufactured home parks, along hundreds of miles of canals and coastal frontage in Cape Coral, Fort. Myers, and nearby barrier islands. It should be noted that 2 injuries and damage at the Florida Atlantic University Campus were reported as a result of the 130-mph estimated peak wind speed. The community has 700,000 solar panels, which continuously provided electricity for 2,000 households throughout Hurricane Ian's passage. These solar panels showed good structural performance with no damage. Single-family housing performance was variable, with exposure hazard being the driver of structural failures. Mobile/manufactured housing (MH) and RV parks were the most susceptible to damage. Wind damage was primarily limited to the building envelopes in site-built homes. More severe damage was observed in some mobile/manufactured home parks in Fort Myers, FL. Several multi-family units in Delray Beach, FL suffered structural damage from wind, surge, or flooding on inland flooding on MH, or MH parks. The most common pattern of failure was the severe coastal erosion near the causeways and roads that led to the scouring or washout of pavements and causeways. The Sanibel Causeway consists of three bridges (A, B, C) and two islands (Causeway Island Park A, B) as shown in Fig. CS.5. Many structures built at ground level, primarily those exposed to wave action, were completely washed away. Power infrastructure was more critically damaged in southwest Florida near the landfall area, causing power outages for several days. Roof cover loss and flooding were frequently observed in churches, but no reports of structural damage have been found. Damage appears to be somewhat more frequent in Port Charlotte than in Cape Coral and Ft. Myers. Only isolated reports of wind damage to the building envelope have been reported in the inland communities. In contrast to past major hurricanes like Hurricane Katrina, there was almost no damage to bridge superstructures. Extreme coastal erosion near transportation infrastructure led to scours and different damage levels to roads and pavements. The Sanibel Island causeway was washed out. The iconic pier was extensively damaged, and floating docks were twisted at Fort Myers. Damage to port facilities was limited to piers and seawalls damaged by storm surge in Florida. A levee was in danger of failing in the Hidden River area, threatening more extensive flooding.

Community impact summary: The storm-related death toll from Hurricane Ian was 125 as of 10 November 2022. Death toll included 119 storm-related fatalities in Florida, five in North Carolina, and one in Virginia. Risk modelers estimated wind and coastal storm surge losses of $40-$74 billion. The majority of the deaths (57) were reported in Lee County, FL, and an estimated 60% were caused by drowning. The strong hurricane winds associated with Hurricane Ian caused widespread power outages in Florida. North Carolina had a power outage of more than 358,000 (Dean and Cataudella, 2022). The Federal Communications Commission (FCC) reported that cell service outages dropped from 65.0% to around 5.0%. The total number of wireline/cable users affected in Florida dropped from around 320,000 users to around 110,000. 642 patients evacuated from 6 healthcare facilities in Charlotte, Lee, Sarasota, Orange, and Volusia Counties. Hospitals in the impacted area suffered severe staffing shortages due to displaced workers. Telecommunications infrastructure primarily in southwest Florida was not functional following the storm due to loss of power, flooded generators, and in at least one case, the collapse of a cellular tower.

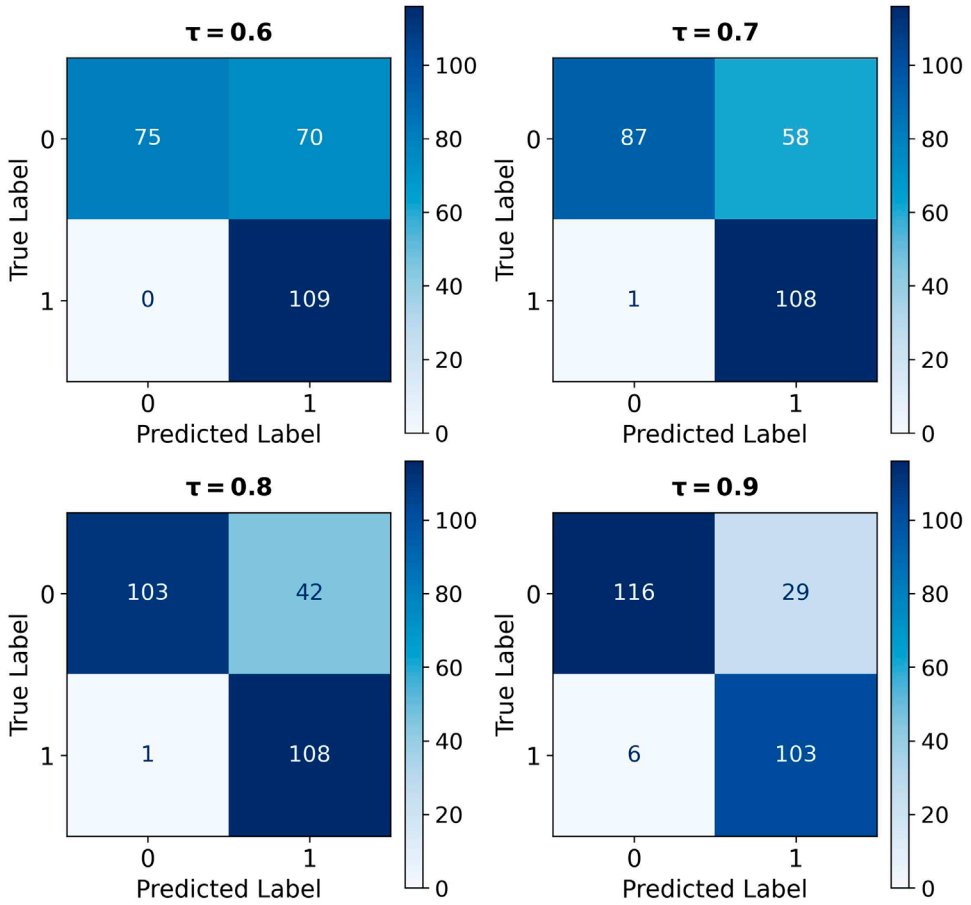

FIGURE 8
Confusion matrices at varied entailment thresholds (τ) - Hurricane Ian.

The coastal roads to port facilities and the access bridges were severely damaged. Isolated damage to power infrastructure caused several days of outages, notably downed power lines. The damage to agriculture was much larger, particularly for the citrus industry, due to wind damage to crops and the flooded access bridges of Sanibel Island. As such, Hurricane Ian will likely be one of the costliest landfalling hurricanes of all time in the US, claiming over 100 lives. It took almost 9 days to restore power in Lee, Charlotte, and De Soto counties in Florida. As of 3 October 2022, Florida had more than 80% of consumers without power.

4.5 Step 5: Analyzing the results

4.5.1 Performance evaluation of impact sentence extraction

The results from Step 3 show the entailment score ranging from 0 to 1 for each sentence, with higher scores indicating a better fit with the corresponding label. A threshold of 0.9 is set for identifying impact sentences, signifying only sentences with entailment scores of 0.9 or above are classified as impact. The effectiveness of this threshold is assessed by analyzing confusion matrices for four different thresholds: 0.6, 0.7, 0.8, and 0.9, as shown in Figure 8.

Figure 8 shows an inverse relationship between the True Positive (TP) and True Negative (TN) versus False Negative (FN) and False Positive (FP) pairs as the thresholds increase. Higher thresholds result in fewer FP (non-impact sentences mistakenly classified as impact sentences) and more TN (correctly classified non-impact sentences). However, they also lead to an increase in FN (impact sentences mistakenly classified as non-impact) and a decrease in TP (correctly classified impact sentences). In this context, FN is prioritized over FP, as misclassifying non-impact sentences is preferable to overlooking actual impact sentences.

While the trends offer some insights, they alone are insufficient to determine the optimal threshold. A more detailed quantitative analysis is necessary, incorporating Precision, Recall, and F1 Score metrics derived from the confusion matrix components. Observing these parameters in Figure 9; Table 5 shows that Precision increases with higher thresholds, while Recall slightly decreases. This narrowing gap between Precision and Recall improves the F1 scores, resulting in its upward trend. Notably, despite the declining trend, all Recall values exceed 0.9, indicating the capability of the BART-large MNLI model to identify impact sentences. Therefore, a threshold of 0.9 is selected for its robust F1 Score and Recall performance.

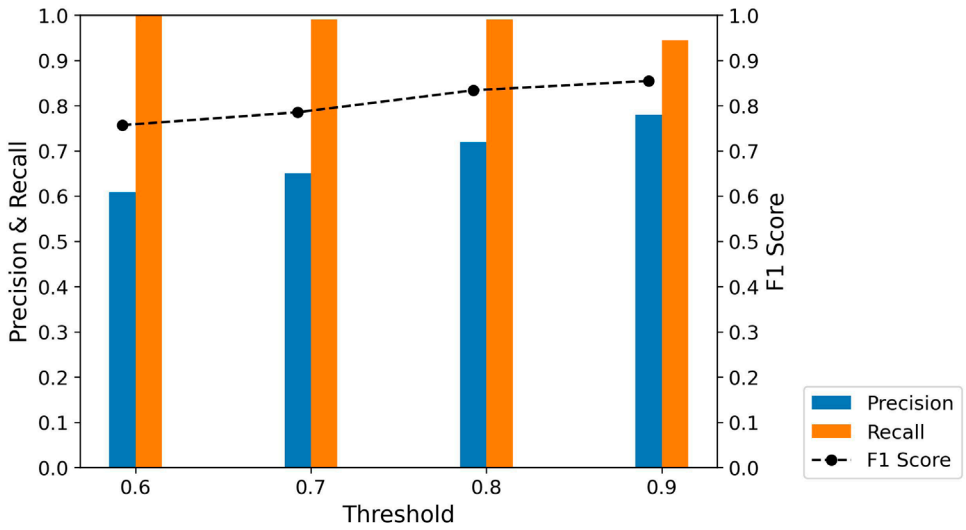

FIGURE 9
Precision, Recall, and F1 scores between different thresholds - Hurricane Ian.

TABLE 5 Performance metrics at different entailment thresholds—Hurricane Ian.

Threshold	Accuracy	Precision	Recall	F1 score
0.6	0.724	0.609	1.000	0.757
0.7	0.768	0.651	0.991	0.785
0.8	0.831	0.720	0.991	0.834
0.9	0.862	0.780	0.945	0.855

4.5.2 Performance evaluation of summary generation

The quality of generated summaries is typically assessed using the ROUGE score, which measures text overlap between a reference summary and the generated text. However, a significant challenge in this evaluation is the absence of human-generated reference summaries. Specifically, there is currently no available summary for the Hurricane Ian PVRR. While the authors could create their own summaries, this approach risks introducing bias due to their direct involvement in the impact sentence annotation process. Consequently, a summary evaluation using the ROUGE score has not been conducted.

5 Verification case: extracting impact information from Hurricane Otis report

The keyword list for wind disasters, shown in Table 2, is compiled from StEER and FEMA damage reports prior to 2023, including generalized keywords from the Hurricane Ian PVRR used in the evaluation case. To verify the capability of the BART-large MNLI model to extract impact sentences from documents not previously used in designing the keyword list, the Hurricane Otis PVRR report (Dang et al., 2024) is utilized. This approach ensures an unbiased verification of the model's performance on new data. Although the performance of the BART-large CNN model is not the focus of this verification, summaries generated by this model are provided for reference. All previously established parameters, such as the keyword list, the entailment threshold of 0.9, and the configuration settings for both the BART-large MNLI and CNN models, are maintained.

Similar to the Hurricane Ian evaluation, Figure 10 shows that as the threshold increases: TP and FP decrease, while TN and FN increase. These adjustments result in an inverse relationship between Precision and Recall, which contributes to an increase in F1 scores across thresholds, as detailed in Figure 11; Table 6. The upward F1 score trend, alongside the Recall score remaining above 0.9, verifies the decision to maintain a baseline threshold of 0.9.

Structural impact summary: Acapulco experienced significant damage, especially to residential and high-rise buildings along the coast. High winds dominated the structural responses, inducing failures to multiple glazing, cladding, and roof surfaces. About 120 hospitals and 33 schools in the region were reported as damaged due to the hurricane event. It was estimated that approximately 250,000 families have been left homeless because of Hurricane Otis, according to Mexico's President Andrés Manuel López Obrador (Rivera, 2023). The impact of blown-off roofs and walls led to widespread flooding inside houses. There was unprecedented damage to the building envelopes (e.g., glazing and cladding) of many structures due to wind loads, though the lateral force-resisting structural systems appeared to perform adequately. Some buildings experienced total exterior glazing loss over the full height of the building. Many buildings now display damaged roofs, loss of glaze, and failure of exterior wall cladding as a result. Rainwater caused significant geotechnical damage in elevated

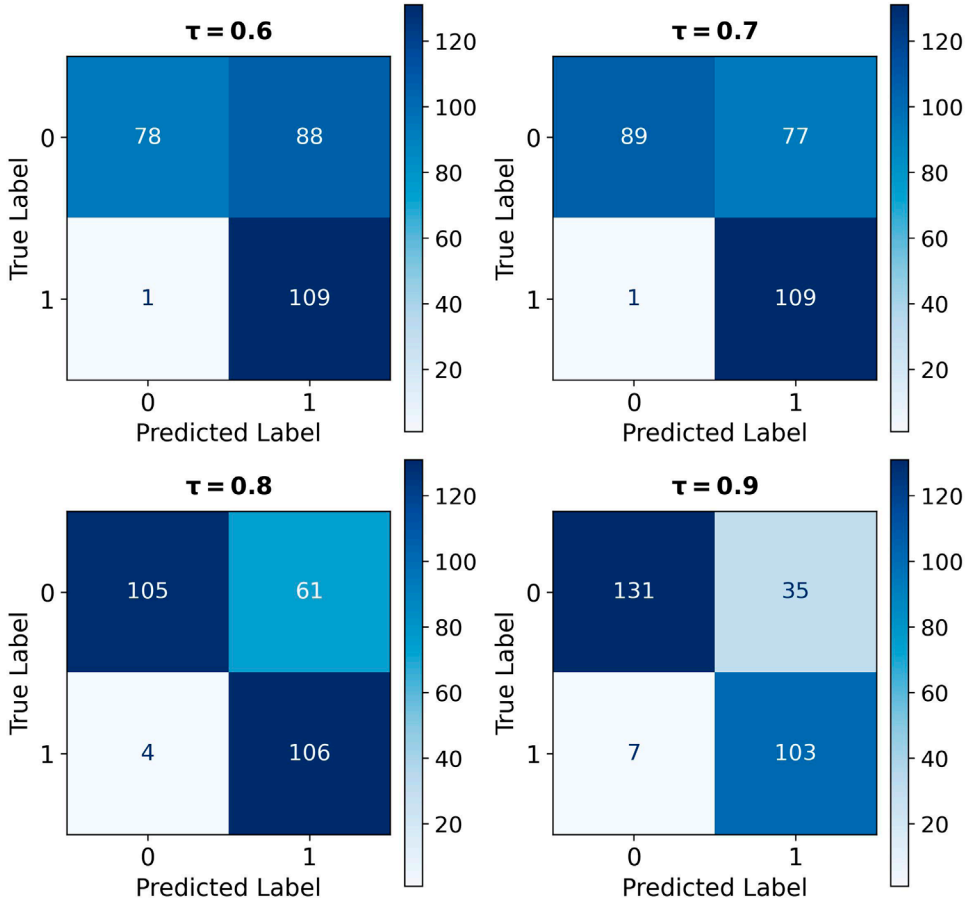

FIGURE 10
Confusion matrices at varied entailment thresholds (τ) - Hurricane Otis.

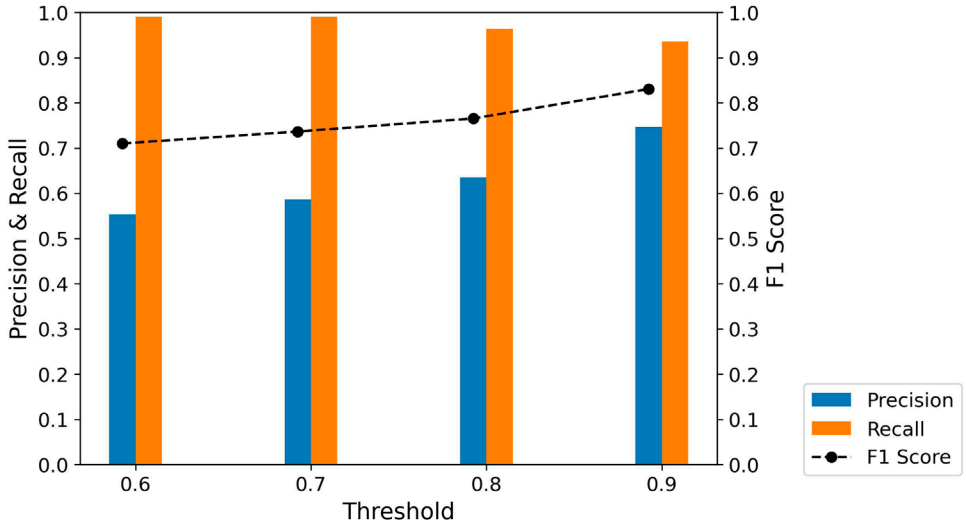

FIGURE 11
Precision, Recall, and F1 scores between different thresholds - Hurricane Otis.

TABLE 6 Performance metrics at different entailment thresholds—Hurricane Otis.

Threshold	Accuracy	Precision	Recall	F1 score
0.6	0.678	0.553	0.991	0.710
0.7	0.717	0.586	0.991	0.736
0.8	0.764	0.635	0.964	0.765
0.9	0.848	0.746	0.936	0.831

regions of Acapulco. The city's ports were forced to close during the hurricane, disrupting not only local trade and transportation but also the city's economic activities, which rely heavily on tourism. Early reports by CFE stated that the airport did not have electricity and it was not clear if the airport was closed or if it had been damaged by the hurricane. The Galerias Mall is one of the most severely damaged structures in the aftermath of Otis. Light-framed commercial properties along the coastline in Puerto Marqués Bay also showed evidence of damage from wind and breaking waves. The "stand-alone" tower appears to be intact, although the poles were severely damaged. Figure 6.2 presents a case where the edge of the road collapsed due to soil failure due to a slope failure. A clear eye and symmetric storm structure are visible, indicating Otis remained a powerful hurricane through landfall. Figure 4.4 shows three screenshots from a video of the damage caused to the Solar Ocean building. No widespread damage was reported, but video evidence showed strong winds blowing inside a hospital in Acapulco. Roof damage was observed in historical buildings. No significant damage has been reported in any of the hard coastal infrastructure (seawalls, port platforms, etc.). The failure of the exterior windows at the airport control tower resulted in water and wind damage to equipment and furniture in the tower. Water and sanitation systems were damaged, and the municipal water system was not operating due to power outages. If buildings are sufficiently damaged that they cannot receive power, the outage may never be restored. This scenario occurred in New Orleans, LA after Hurricane Katrina. Over 500,000 homes and businesses lost power—Water and sanitation systems were damaged. The Telemax power plant was restored. The re-establishment of high, medium, and low voltage poles continues for Avenida Costera Miguel Alaman, the City Center, Costa Azul, and Renacimiento. The following hospitals had their power restored by October 29: General, Military, Cancerology, and IMSS.

Community impact summary: Hurricane Otis left 45 people dead and 47 missing in Mexico. 80% of the hotels in Acapulco were damaged, and about 274,000 homes were destroyed in the region. The electric grid was severely affected, leaving 513,544 customers in the State of Guerrero without power. The government suspended electricity payments from November 2023 to February 2024 and called for the delivery of basic foods to the estimated 250,000 families impacted by the event. The financial implications of the hurricane's devastation are substantial. According to Enki Research, the cost of Hurricane Otis could potentially reach as high as $15 billion. It is unknown how much effect this had on air traffic control after the storm. As of November 7, locals reported that about 50 percent of the roads were accessible but with military restrictions. Only the military, aid vehicles, Mexican media, and people showing residency in Acapulco are allowed to enter under military escort. On the evening of November 2, CFE posted on X (formerly known as Twitter) that the electricity had been restored to the airport. The port was inoperable, and the airport was closed. Significant disruptions to the transportation system occurred due to several rockslides above the Chilpancingo-Acapulco highway. At the road level, floodwaters caused mudslides that resulted in partial or full collapse of road lanes. The main highway between Acapulco and Mexico City could not be accessed, which hampered electric power restoration. CFE reports 513,524 outages out of 1.4 million users in the state, which is 36.6% of the population. On October 30, CFE reported that 65% of outages had been restored. It also noted that the Telemax power plant for communications was restored (CFE, 2023). By October 31, CFE reported the restoration of 75% of outages for Guerrero. On November 2 the electricity was restored to Acapulco. On Nov. 3, CFE reported that the power service for the Raney water well was restored.

6 Illustration of framework versatility: extracting impact information from Türkiye earthquake report

This versatility of the framework is evaluated through its ability to adapt to various hazards, using the 2023 StEER Magnitude 7.8 Kahramanmaraş Türkiye Earthquake Sequence PVRR (Safiey et al., 2023). This adaptability is shown by modifying the keyword list, detailed in Table 7. In earthquake scenarios, keywords related to building components and structural terms are tailored to reflect the impact of seismic loads. Meanwhile, keywords for building types and community damage are kept consistent across various hazards due to their broad applicability. All other configuration settings for the BART-large MNLI and CNN models are also preserved.

The performance of the BART-large MNLI model in the Türkiye earthquake report (779 sentences) is comparable to its performance in the Hurricane Ian (254 sentences) and Hurricane Otis (276 sentences) reports. Figure 12 illustrates that increasing thresholds result in a decrease in TP and FP, but an increase in TN and FN. This creates a trade-off where Precision rises significantly, and Recall slightly declines, leading to an upward F1 score trend shown in Figure 13; Table 8. The combination of this trend and consistently high Recall above 0.9 supports maintaining a baseline threshold of 0.9 and highlights the applicability of the framework to different hazards. Besides, the lack of human-generated reference summaries limits the use of the ROUGE score to evaluate the performance of the BART-large CNN model in generating summaries.

Structural impact summary: The Dead Sea Fault (DSF) is a major transform fault that extends from the Red Sea to the southeast of Turkey. The mechanism and location of the earthquake are consistent with the DSF and the East Anatolian Fault (EAF). The earthquake was followed by many aftershocks, including several larger than magnitude 6 (one with Mw 6.6). As of 19 February 2023, the number of reported completely and partially collapsed

TABLE 7 Keywords related to seismic impacts.

Categories	Keywords
Building types	Family housing damage, school damage, mobile home damage, manufactured home damage, commercial facility damage, hospital damage, religious building damage, historical building damage, industrial facility damage, agricultural infrastructure damage, fire station damage, police station damage, parking damage, critical facility damage
Building components	Wall damage, column damage, slab damage, beam damage, footing damage, cladding damage, foundation damage, connector damage, floor damage, frame damage, diaphragm damage, coupling beam damage, brace damage, panel damage, ceiling damage, strut damage, stair damage, seismic base isolator
Other infrastructure	Airport damage, port damage, bridge damage, road damage, causeway damage, pavement damage, water tank damage, power plant damage
Structure-related terms	Structural behavior, structural damage, structural failure mechanisms, building resilience, structural connection damage, building interior damage, building exterior damage, building envelope damage, building damage, lateral force resisting systems, insufficient unbraced length, loss of load-path, insufficient building gap, insufficient anchorage length, ductile building, non-ductile building, plastic hinging, brittle failure, soft story, insufficient confinement, insufficient inelastic deformation, shear failure, crushing of unconfined concrete, bond failure, splice failure, compression bars buckle, sliding at base, insufficient seismic hoops, insufficient seismic hooks, cover spalling, drift failure, P-delta effect, structural irregularity, vertical irregularity, horizontal irregularity, overturning, accidental torsion, non-compliance seismic detailing, excessive lateral displacement, collapsed building, nonstructural damage, degradation, content damage, drift compatibility, good performance, undamaged infrastructure
Community damages	Fatalities, economic loss, power outage, healthcare disruption, injuries, agricultural damage, uninsured loss, telecommunication system disruption, transportation disruption, utility outage, water outage, service loss, supply halt, injuries, temporary medical facility, transaction suspended
Non-impact terms	Building code, research support, ground motion intensity

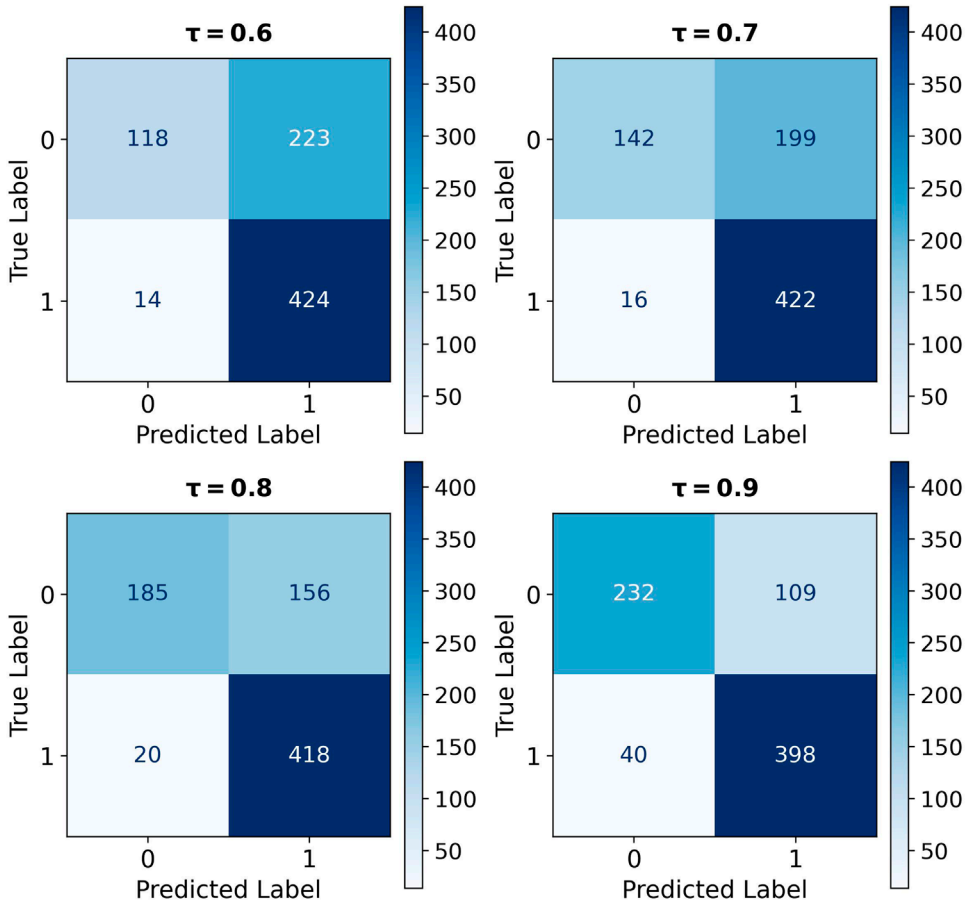

FIGURE 12
Confusion matrices at varied entailment thresholds (τ) - Türkiye Earthquake.

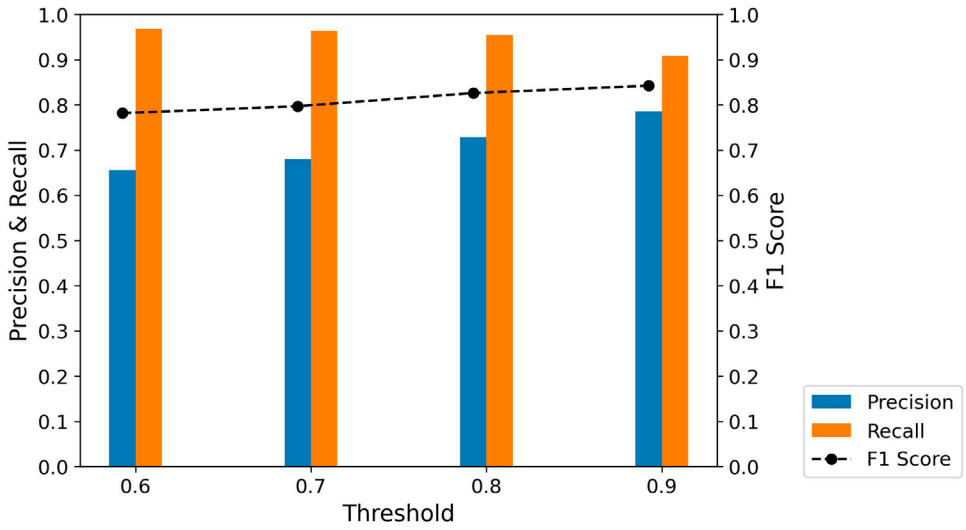

FIGURE 13
Precision, Recall, and F1 scores between different thresholds - Türkiye Earthquake.

TABLE 8 Performance metrics at different entailment thresholds—Türkiye Earthquake.

Threshold	Accuracy	Precision	Recall	F1 score
0.6	0.696	0.655	0.968	0.782
0.7	0.724	0.680	0.963	0.797
0.8	0.774	0.728	0.954	0.826
0.9	0.809	0.785	0.909	0.842

buildings was 28,362. 75,717 buildings and 306,563 dwellings were either collapsed or severely damaged. In Syria, more than 22,000 buildings were affected by the earthquakes with 2,850 of them partially/completely collapsed or severely damaged. Almost two-thirds of residential buildings in Gaziantep city are masonry. One-third is Reinforced Concrete (RC). The lessons learned from the 1999 Kocaeli and Duzce Earthquakes led to the implementation of earthquake engineering principles in the whole country. The observations from the recent Mw 6.1 Duzce Earthquake on 23 November 2022, showed the importance of taking action to reduce the number of buildings with seismic deficiencies. The majority of the buildings in the DuzCE region affected by this earthquake were new and constructed following the lessons learned in the 1999 Kocaeli Earthquake. The low level of damage observed during the 2022 Duzce Earthquake demonstrated the effectiveness of code-specified seismic design requirements on the newer buildings. The seismic design/provisions for existing non-reinforced masonry wall systems are made available in Appendix 1 of the Syrian. Code for the Syrian Base Code (TBSC) was published in 1996. These provisions were considered optional to adopt until 2008 and were not considered to be required to adopt. In addition to their stiffness, upper masonry walls, both at the exterior and interior, add considerable mass to the building, resulting in larger inertial forces during ground shaking. Infill walls in the first event could have led to a more common collapse of these structures during the second event. It is possible that the presence of soft stories is accompanied by low ductility. Many buildings in Syria that were damaged during the war are believed to have been rebuilt by individuals with low-quality materials. The heaviest damage and the most collapses occurred in 4 cities in Syria (Aleppo, Latakia, Idlib, and Hama) and 40 towns and villages in Northern Syria. In concrete buildings that experienced severe damage or partial or total collapse, some common deficiencies can be observed in the collapse photographs. Concrete quality/strength appears very low by visual inspection of texture and color. Thin columns can be seen in many damaged buildings. Many buildings had lightly reinforced column sections, with no or little transverse reinforcement, and potentially inadequate lap splices located immediately above the slabs. The absence of drop (projected) beams below the ribbed slab and flat plate systems creates a slab-column connection situation (no beam-column joints) which is known to perform poorly under severe earthquake shaking unless well reinforced. Government facilities play a key role during extreme events like earthquakes. The large displacement due to the directivity effects during these two events likely contributed to the collapse during these directivity events. This practice results in high-mass buildings which induce large seismic forces during ground shaking. There were 11 base-isolated hospitals within 7.8 km from the epicenter of the Mw8 earthquake. Most seismically protected buildings remained functional, but some buildings collapsed. All hospitals have curved surface slider (CSS) pendulum and triple-pendulum systems. The number of seismic isolators used in these hospitals is reported to be high. The Turkish health minister reported that on February 8, 77 field hospitals were set up across 10 regions. Two state hospitals were completely destroyed, one of the three private hospitals collapsed, and the City Hospital was damaged. The affected schools are mainly located in the urban area of TarFGtous (99), Aleppo (71), Lattakia (50), Hama

(27), and in the rural area of Idleb (1) World Health Organization (WHO) spokeswoman Harris mentioned impacts on healthcare in Türkiye and Syria as "huge long-term" issues. Road damage occurred throughout the impacted region due to the earthquake sequence. No damage was reported at the Akkuyu nuclear power plant (Figure 5.11). This nuclear plant is under construction. The Sultansuyu Dam in Malatya experienced significant longitudinal cracking at the crest due to a lateral spreading type failure. A lateral spreading-induced landslide was observed on the road between Adana and Gaziantep. The Banias refinery in Syria was partially damaged. The main damage to the refinery was to the concrete bases of equipment. The connectivity was not fully recovered as of 8 February 2023.

Community impact summary: As of 9 March 2023, the total death toll was reported to be 45,968 people in Türkiye and around 6,000 in Syria. More than 100,000 people were reported as injured. The number of fatalities estimated by PAGER for the Mw 7.8 event is shown in Figure 1.2. For the Mw 7.5 earthquake, economic losses are shown in Figures 1.3 and 1.4. Extreme Event Solutions at Verisk predicted that the economic losses and industry-insured losses due to the earthquake sequence will likely exceed $20 billion. In terms of economic loss, the ramifications could include the spoiling of food items requiring refrigeration. There is past evidence of the collapse of war-damaged residential buildings in Aleppo and consequential casualties (Reuters, 2023). There was one casualty in this historical neighborhood, which was known as a symbol of the region due to these old buildings. Hundreds of medical facilities were damaged, disrupting treatment capacities across large regions. It was delivering emergency healthcare assistance in a tent in the hospital garden (Müslüm, 2023). A relevant observation was the significant number of critical patients mobilized to the functional hospitals by helicopter as access was overwhelmed. On February 7, the Ministry of Health reported that injured people from Iskenderun were transferred to Mersin City Hospital in ambulances. Ninety-eight wounded patients were transferred on the day of the earthquake. About 11,780 citizen volunteers, who went to airports to go to the quake zone following an invitation from AFAD, were taken to Adana, Gaziantep, Adiyaman, and Urfa. The Capital Markets Board (SPK) announced that the Turkish Electronic Fund Trading Platform (TEFAS) transactions were suspended. Borsa İstanbul, the sole Turkish stock exchange, announced that all transactions would be halted for at least five business days. The entire network was destroyed during the war except for the two stations in Damascus and Tartus. There was an emergency stairway attached to the exterior of the building on each level of the Tarsus-Adana-Gaziantep Highway. Aftershocks have caused planes to be grounded at airports throughout the region. Roads were also closed due to inclement weather that occurred immediately after the earthquake sequence. Over 30 electrical substations were damaged causing power outages and blackouts reported in Antep, Hatay, and Kilis. Internet connectivity was lost in all cities impacted by the event in Türkiye. Deformation of the railway tracks was observed between Kahramanmaraş and Gaziantep. Phone lines were down in the southern provinces after the quake. Airports remained closed for a few days following the earthquake. Due to this, tanker loading operations were suspended for a day. But the leak was fixed, and the loading operations have resumed.

7 Implementation framework

The performance of the BART-large MNLI model is demonstrated through three use cases, achieving a Recall exceeding 0.9 and an F1 score above 0.8. These metrics confirm the capability of the model to automatically extract impact sentences, tailored to domain-specific keywords. These positive results facilitate the development of an implementation framework, which is built upon the foundational framework shown in Figure 2 and detailed in Figure 14. This framework consists of two main phases: Execution and Evaluation. The Execution phase processes damage reports and disaster-related keywords to generate comprehensive summaries. It encompasses three primary steps: Data Preprocessing, Extracting Impact Sentences, and Generating Comprehensive Summaries. An optional Evaluation phase is proposed to assess the output quality, incorporating Data Labeling and Analyzing The Results steps. For a detailed overview of the code, guidance, and specific examples, refer to the Impact Data Mining repository on GitHub.

8 Computational efficiency

The implementation framework in Figure 14 is optimized for the Google Colab environment where each step is executed via a separate Python file. Table 9 outlines these files, indicating the recommended computational resources and their estimated processing times for Hurricane Ian PVRR. For example, the files that execute the machine learning models require an A100 GPU and 40 GB of CPU RAM to handle parallel processing efficiently. The processing times for these tasks are approximately 101 s and 85 s, respectively. Thus, excluding time for input file preparation, executing all computational code for a 40-page damage report generally takes around 4 min.

9 Limitations, future works, and research implications

9.1 Limitations and future works

While the model is equipped with 407 million parameters and fine-tuned on the MNLI dataset to facilitate 0SHOT-TC—yielding positive results across three examples—the model may still misinterpret impact data. This issue stems from a lack of specific tuning for identifying structural and community damage information. To address this issue for the time being, incorporating more user-defined keywords could improve the performance of the model. However, for a viable solution, it is essential to develop a custom entailment corpus tailored to wind disasters, inspired by the format of the MNLI dataset, to enhance Natural Language Inference tasks related to disaster impacts.

In the summary generation task, the BART-large CNN model operates with default settings including a num_beams value of 4, a do_sample value set to False, and early_stopping option enabled as True. It also utilizes customized parameters such as a 200-token overlap threshold, a minimum length of 80% for initial summary output, 40% for subsequent summaries, and a maximum length

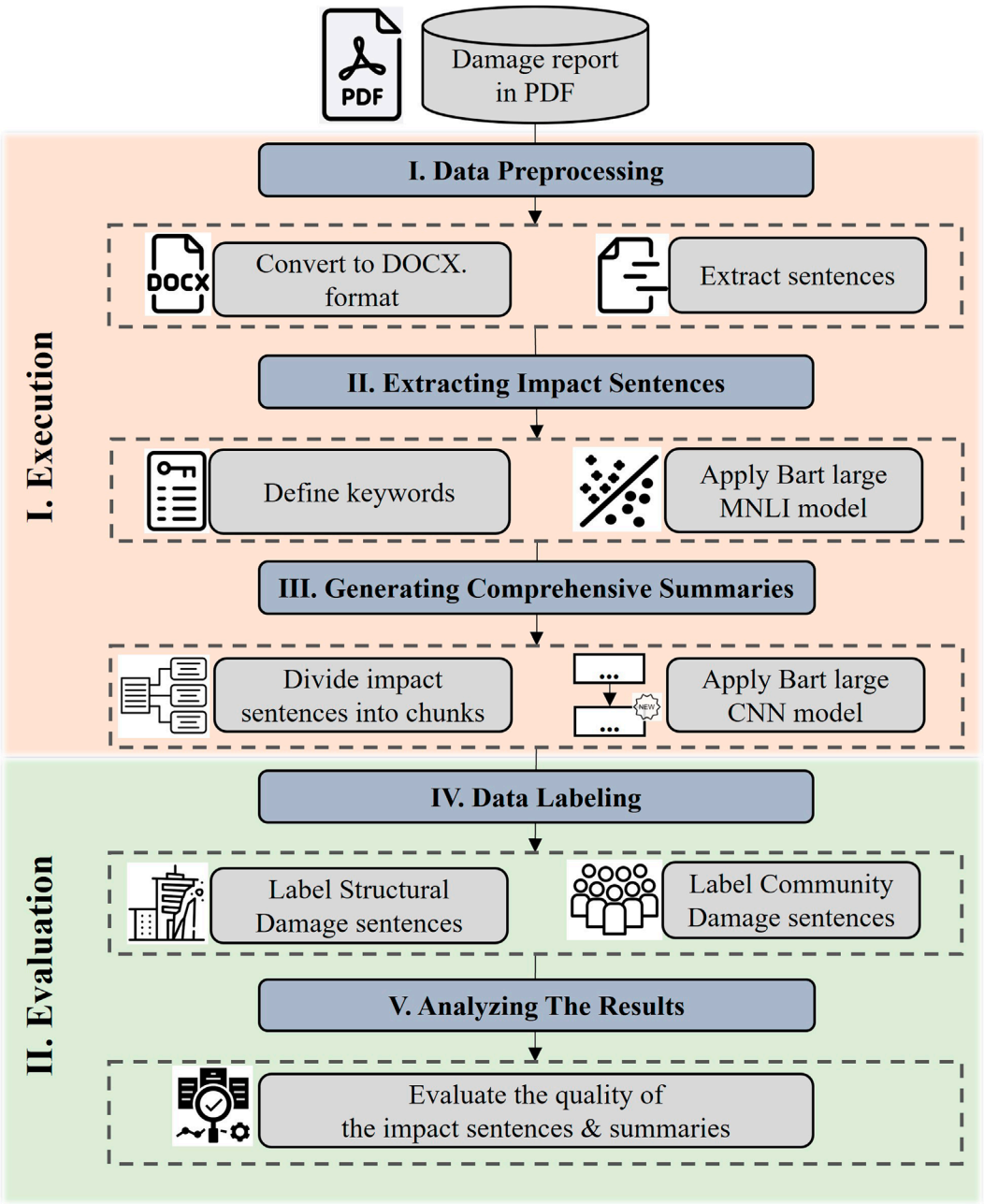

FIGURE 14
Implementation framework.

TABLE 9 General information of Python files.

Steps	File names (.ipynb)	GPU type	Duration (s)
Data preprocessing	1_preprocessing	None	30
Extracting impact sentences	2_extracting_impact_sentences	A100	101
Generating comprehensive summaries	3_generating_comprehensive_summaries	A100	85
Data labeling	4_data_labeling	None	—
Analyzing the results	5_analyzing_the_results	None	30

equivalent to the number of tokens in the chunk being considered. Establishing well-defined evaluation criteria is essential to optimize these settings. One approach is to incorporate human-generated summaries into the evaluation, enabling the use of metrics such as ROUGE. Future studies should also explore the capabilities of the BART-large CNN model in processing lengthy documents, like FEMA documentation that ranges from 200 to 400 pages, possibly by training the model to self-adjust the number of summaries to be generated based on the volume of the content.

Once the framework demonstrates proficiency in handling text, the next step is to develop it into a multi-modal system that can generate summaries from both text and images. Upon completion, the model would be integrated into a data repository designed to accept keywords and images as inputs, facilitating the automatic extraction and summarization of related content from various reports. Specifically, the model will function as a platform where users can interact by submitting queries in a chat-based format, with the model providing answers and suggesting additional relevant information. Its performance will also be improved by incorporating user feedback, helping to identify both the framework's strengths and areas for improvement. This approach aligns with the decadal vision of the NHERI network to incorporate AI and advanced analytics into cyberinfrastructure, improving data querying and disaster response strategies (Schneider and Kosters, 2024).

9.2 Implications and applications of research for disaster resilience

The fully developed model, once implemented as a platform, will serve a diverse range of users, including emergency managers, policymakers, insurance firms, and the natural hazard research community. However, its primary target audience is small to medium-sized communities, which often face systemic disadvantages in building resilience and managing preparedness, mitigation, and recovery efforts. These challenges arise primarily from two factors.

First, there is a lack of centralized, structured, and accessible disaster data. In the U.S., organizations like FEMA, NOAA, USGS, and state/local emergency management agencies release vast amounts of information following natural disasters. This information, which includes situation reports, damage assessments, recovery plans, guidance documents, humanitarian assistance plans, reconnaissance reports, and resilience planning documents, is presented in disparate contexts, formats, and content. Each year, the volume of these documents grows significantly, yet there are insufficient mechanisms to harness the insights contained within this extensive body of free-text data. Currently, manual reading and interpretation of these documents are required to extract valuable insights, which is both time-consuming and inefficient.

Second, many small to medium-sized communities lack the capacity to develop comprehensive disaster management plans, such as Hazard Mitigation Plans. These plans often span long timeframes and may be complicated by compounding hazards during ongoing recovery, leaving communities vulnerable to further damage. Even large, well-resourced states such as Louisiana have faced significant challenges in managing multiple, consecutive disasters. Between 2020 and 2021, Louisiana experienced several disasters, including Hurricanes Laura, Delta, Zeta, and Ida, as well as a severe storm in May. While the state was assessing damage from the earlier hurricanes to secure $600 million in Community Development Block Grant Disaster Recovery funds (OCD, 2023), it had to account for damages from subsequent disasters simultaneously. As a result, Louisiana had to revise its Action Plan, extending the recovery timeline from 1 January 2023, to 31 July 2028. If a state with substantial resources struggles with these complexities, the challenge is even more overwhelming for smaller communities with limited capacities.

The fully developed model addresses these challenges by providing users with access to structured information from various sources and enabling interaction through a chat-based format, where the model answers questions and suggests additional relevant information. For well-prepared communities, the model acts as a support tool for data querying, extraction, and summarization. For less-prepared communities, it provides essential background information to help them get started. The model will then assist all users in assessing their current vulnerabilities and guide them in developing key documents, such as Hazard Mitigation Plans, to mitigate the disaster impact. Ultimately, by gradually enhancing the capacity of its users, the model empowers small to medium-sized communities to better prepare for and recover from natural hazards.

10 Conclusion

This research develops a framework that leverages BART-large MNLI and BART-large CNN models to extract structural and community damage information from wind disaster reconnaissance reports using user-defined keywords. Fine-tuning this DL model on the MNLI and CNN Daily Mail datasets enables it to perform 0SHOT-TC and summary generation, thereby mitigating the need for specialized training datasets related to wind hazard impacts. Initially, the BART-large MNLI model identifies impact information using user-defined keywords. Subsequently, the BART-large CNN model generates summaries from these identified sentences, helping users grasp the overall content quickly. The performance of this framework was first evaluated with the Hurricane Ian PVRR report, achieving an F1 score of 0.855 and a recall of 0.945. The capability of the BART-large MNLI model to extract impact sentences was further verified on the Hurricane Otis PVRR report, which was not used to derive the keyword list, resulting in an F1 score of 0.831 and a recall of 0.936. The versatility of the framework is illustrated in an extended application to the Türkiye earthquakes PVRR report. Adjustments to the keyword list are the only changes needed, with an F1 score of 0.842 and a recall of 0.909. Overall, the framework performs well across use cases, consistently achieving F1 scores above 0.8 and recall rates above 0.9. These positive outcomes have led to the development of an implementation framework, with instructions and Python code available in the Impact Data Mining repository on GitHub.

Future efforts will focus on improving the accuracy of the BART-large MNLI model by developing a dedicated corpus for wind disaster impacts. Further studies will also establish evaluation criteria to assess the quality of the generated summaries and enhance the capability of the BART-large CNN model to process lengthy documents. The next step will involve creating a multi-modal system

in a chat-based format that can interpret both text and images to improve querying capabilities. These advancements will support small to medium-sized communities in managing resilience across both pre- and post-hazard phases.

Data availability statement

The original contributions presented in the study are included in the article/Supplementary Material, further inquiries can be directed to the corresponding authors.

Author contributions

HP: Formal Analysis, Methodology, Visualization, Writing–original draft, Writing–review and editing. MA: Funding acquisition, Methodology, Project administration, Supervision, Writing–review and editing.

Funding

The author(s) declare that no financial support was received for the research, authorship, and/or publication of this article.

Acknowledgments

The authors acknowledge the reconnaissance reports provided by StEER and their teams, which have significantly contributed to this research. Furthermore, the authors recognize the assistance of ChatGPT-4 in enhancing the clarity and readability of the paper.

Conflict of interest

The authors declare that the research was conducted in the absence of any commercial or financial relationships that could be construed as a potential conflict of interest.

Publisher's note

All claims expressed in this article are solely those of the authors and do not necessarily represent those of their affiliated organizations, or those of the publisher, the editors and the reviewers. Any product that may be evaluated in this article, or claim that may be made by its manufacturer, is not guaranteed or endorsed by the publisher.

Supplementary material

The Supplementary Material for this article can be found online at: https://www.frontiersin.org/articles/10.3389/fbuil.2024.1485388/full#supplementary-material

References

Alam, F., Sajjad, H., Imran, M., and Ofli, F. (2021). "Crisisbench: benchmarking crisis-related social media datasets for humanitarian information processing," in Proceedings of the International AAAI Conference on Web and Social Media, 923–932. doi:10.1609/icwsm.v15i1.18115

Alrashdi, R., and O'Keefe, S. (2019). Deep learning and word embeddings for tweet classification for crisis response. arXiv Prepr. arXiv:1903.11024. doi:10.48550/arXiv.1903.11024

CFE (2023). *CFE personnel persevere and restore electricity to 65% of those affected by Hurricane Otis in Guerrerog*. https://www.cfe.mx/Pages/default.aspx.

Clowe, S. (2022). *Sarasota county community affected by levee break cleaning up afterHurricane Ian*. https://www.wtsp.com/article/news/local/sarasotacounty/sarasota-county-community-levee-break-cleaning-up-hurricane-ian/67-8c2a4ac4-94ee-4811-81cb-463509963953.

Dang, H., Alawode, K., Lahna, T., Roueche, D., Kalliontzis, D., Mostafa, K., et al. (2024). *Steer: hurricane otis preliminary virtual reconnaissance report (pvrr)*. doi:10.17603/DS2-MB7Z-XW74

Dean, K., and Cataudella, K. (2022). *358,000+ without power in NC as Post-Tropical Cyclone Ian moves inland*. https://www.newsobserver.com/news/weather/hurricane/article266608621.html.

Devlin, J., Chang, M.-W., Lee, K., and Toutanova, K. (2019). "BERT: pre-training of deep bidirectional transformers for language understanding," in Proceedings of the 2019 Conference of the North American Chapter of the Association for Computational Linguistics, (Volume 1: Long and Short Papers) (Minneapolis, Minnesota: Association for Computational Linguistics), 4171–4186. doi:10.18653/v1/N19-1423

Hendrycks, D., and Gimpel, K. (2016). Gaussian error linear units (gelus). arXiv Prepr. arXiv:1606.08415. doi:10.48550/arXiv.1606.08415

Hermann, K. M., Kocisky, T., Grefenstette, E., Espeholt, L., Kay, W., Suleyman, M., et al. (2015). "Teaching machines to read and comprehend," in *Advances in neural information processing systems*, 1693–1701.

Ikonomakis, M., Kotsiantis, S., and Tampakas, V. (2005). Text classification using machine learning techniques. *WSEAS Trans. Comput.* 4, 966–974.

Imran, M., Elbassuoni, S., Castillo, C., Diaz, F., and Meier, P. (2013). "Extracting information nuggets from disaster-related messages in social media," in Proceedings of the 10th International Conference on Information Systems for Crisis Response and Management (ISCRAM 2013), 791–800.

Imran, M., Mitra, P., and Castillo, C. (2016). "Twitter as a lifeline: human-annotated twitter corpora for nlp of crisis-related messages," in Proceedings of the Tenth International Conference on Language Resources and Evaluation (LREC'16), 1638–1643.

Kaisler, S., Armour, F., Espinosa, J. A., and Money, W. (2013). "Big data: issues and challenges moving forward," in 2013 46th Hawaii International Conference on System Sciences (IEEE), 995–1004.

Kersten, J., Kruspe, A., Wiegmann, M., and Klan, F. (2019). "Robust filtering of crisis-related tweets," in Proceedings of the 16th International Conference on Information Systems for Crisis Response and Management (ISCRAM 2019) (Valencia, Spanien: ISCRAM Association), 19–22.

Kijewski-Correa, T., Roueche, D. B., Mosalam, K. M., Prevatt, D. O., and Robertson, I. (2021). Steer: a community-centered approach to assessing the performance of the built environment after natural hazard events. *Front. Built Environ.* 7, 636197. doi:10.3389/fbuil.2021.636197

Koliou, M., van de Lindt, J. W., McAllister, T. P., Ellingwood, B. R., Dillard, M., and Cutler, H. (2020). State of the research in community resilience: progress and challenges. *Sustain. Resilient Infrastructure* 5, 131–151. doi:10.1080/23789689.2017.1418547

Laney, D. (2001). 3D data management: controlling data volume, velocity, and variety. *Tech. Rep.* META Group.

Lewis, M., Liu, Y., Goyal, N., Ghazvininejad, M., Mohamed, A., Levy, O., et al. (2020). "Bart: denoising sequence-to-sequence pre-training for natural language

generation, translation, and comprehension," in *Proceedings of the 58th annual meeting of the association for computational linguistics (ACL 2020)*, 1234–1245. doi:10.18653/v1/2020.acl-main.703

Liu, J., Singhal, T., Blessing, L. T., Wood, K. L., and Lim, K. H. (2021). "Crisisbert: a robust transformer for crisis classification and contextual crisis embedding," in Proceedings of the 32nd ACM Conference on Hypertext and Social Media, 133–141. doi:10.1145/3465336.3475117

Müslüm, E. (2023). *AKP deputy visiting the earthquake zone: state hospital is in an unusable condition.* https://www.sozcu.com.tr/deprem-bolgesine-giden-akpli-vekil-devlet-hastanesi-girilemez-halde-wp7583416 (Accessed November 27, 2024).

NCEI (2024). U.s. billion-dollar weather and climate disasters. doi:10.25921/stkw-7w73

Nguyen, D., Al Mannai, K. A., Joty, S., Sajjad, H., Imran, M., and Mitra, P. (2017). "Robust classification of crisis-related data on social networks using convolutional neural networks," in Proceedings of the International AAAI Conference on Web and Social Media, 632–635.

OCD (2023). Action plan amendment: response to the 2020-21 storms (apa 3). Available at: https://cdn2.assets-servd.host/utopian-bustard/production/2020-21-Storms-APA-3-8.29.23.pdf?dm=1694459353.

OpenAI (2023a). GPT-4 technical report. *Tech. Rep.*, OpenAI. doi:10.48550/arXiv.2303.08774

OpenAI (2023b). Openai red teaming network. Available at: https://openai.com/index/red-teaming-network/.

OpenAI (2024). Hello gpt-4o. Available at: https://openai.com/index/hello-gpt-4o/.

Patgiri, R., and Ahmed, A. (2016). "Big data: the v's of the game changer paradigm," in 2016 IEEE 18th International Conference on High-Performance Computing and Communications; IEEE 14th International Conference on Smart City; IEEE 2nd International Conference on Data Science and Systems (HPCC/SmartCity/DSS), 17–24. doi:10.1109/hpcc-smartcity-dss.2016.0014

Peek, L., Tobin, J., Adams, R. M., Wu, H., and Mathews, M. C. (2020). A framework for convergence research in the hazards and disaster field: the natural hazards engineering research infrastructure converge facility. *Front. Built Environ.* 6, 110. doi:10.3389/fbuil.2020.00110

Pinelli, J.-P., Esteva, M., Rathje, E. M., Roueche, D., Brandenberg, S. J., Mosqueda, G., et al. (2020). Disaster risk management through the designsafe cyberinfrastructure. *Int. J. Disaster Risk Sci.* 11, 719–734. doi:10.1007/s13753-020-00320-8

Radford, A., Narasimhan, K., Salimans, T., and Sutskever, I. (2018). *Improving language understanding by generative pre-training*.

Rathje, E. M., Dawson, C., Padgett, J. E., Pinelli, J.-P., Stanzione, D., Adair, A., et al. (2017). Designsafe: new cyberinfrastructure for natural hazards engineering. *Nat. Hazards Rev.* 18, 06017001. doi:10.1061/(asce)nh.1527-6996.0000246

Reuters (2023). *Thirteen killed after building collapses in Syria's Aleppo, state media report*. https://www.reuters.com/world/middle-east/thirteen-killed-after-building-collapses-syrias-aleppo-state-media-2023-01-22/.

Riezebos, A. (2019). *Finding impact data in humanitarian documents*. M.S. thesis, Leiden University. M.S. thesis.

Rivera, S. (2023). *Family displaced by Hurricane Otis is first to move into new housing*. https://www.yahoo.com/news/family-displaced-hurricane-otis-first-202314211.html.

Safiey, A., Roueche, D., Huallpa, L. A. M., Hassan, W., Reis, C., Sorosh, S., et al. (2023). *Steer: 2023 mw 7.8 kahramanmaras, Turkiye earthquake sequence preliminary virtual reconnaissance report (pvrr) media repository*. doi:10.17603/DS2-MM04-XQ43

Schneider, N., and Kosters, J. (2024). U.S. National science foundation natural hazards engineering research infrastructure (NHERI) decadal visioning study 2026-2035. *Tech. Rep.*, NHERI. doi:10.17603/DS2-AFZA-M544

See, A., Liu, P. J., and Manning, C. D. (2017). "Get to the point: summarization with pointer-generator networks," in *Proceedings of the 55th annual meeting of the association for computational linguistics (volume 1: long papers)* (Vancouver, Canada: Association for Computational Linguistics), 1073–1083. doi:10.18653/v1/P17-1099

Vaswani, A., Shazeer, N., Parmar, N., Uszkoreit, J., Jones, L., Gomez, A. N., et al. (2017). "Attention is all you need," in *Advances in neural information processing systems*, 5998–6008.

Verma, S., Vieweg, S., Corvey, W., Palen, L., Martin, J., Palmer, M., et al. (2011). "Natural language processing to the rescue? extracting "situational awareness" tweets during mass emergency," in Proceedings of the Fifth International Conference on Weblogs and Social Media (ICWSM 2011), 385–392. doi:10.1609/icwsm.v5i1.14119

Williams, A., Nangia, N., and Bowman, S. (2018). "A broad-coverage challenge corpus for sentence understanding through inference," in Proceedings of the 2018 Conference of the North American Chapter of the Association for Computational Linguistics: Human Language Technologies, (Volume 1: Long Papers) (New Orleans, Louisiana: Association for Computational Linguistics), 1112–1122. doi:10.18653/v1/N18-1101

Wolf, T., Debut, L., Sanh, V., Chaumond, J., Delangue, C., Moi, A., et al. (2020). "Transformers: state-of-the-art natural language processing," in Proceedings of the 2020 Conference on Empirical Methods in Natural Language Processing: System Demonstrations (Association for Computational Linguistics), 38–45. doi:10.18653/v1/2020.emnlp-demos.6

Yin, W., Hay, J., and Roth, D. (2019). "Benchmarking zero-shot text classification: datasets, evaluation and entailment approach," in Proceedings of the 2019 Conference on Empirical Methods in Natural Language Processing (EMNLP 2019), 3914–3923. doi:10.18653/v1/D19-1404

frontiers | Frontiers in Built Environment

TYPE Original Research
PUBLISHED 07 January 2025
DOI 10.3389/fbuil.2024.1524030

Check for updates

OPEN ACCESS

EDITED BY
Jack Cadigan,
Engineer Research and Development Center (ERDC), United States

REVIEWED BY
Filippo Gatti,
Université Paris-Saclay, France
Liangjie Qi,
Xi'an University of Architecture and Technology, China

*CORRESPONDENCE
Kenneth H. Stokoe,
k.stokoe@mail.utexas.edu
Sungmoon Hwang,
sungmoon@utexas.edu

RECEIVED 06 November 2024
ACCEPTED 04 December 2024
PUBLISHED 07 January 2025

CITATION
Stokoe KH, Hwang S, Cox BR, Clayton PM and Gilbert RB (2025) NHERI@UTexas experimental facility with large-scale mobile shakers for field studies: a decade of discovery in natural hazards engineering. *Front. Built Environ.* 10:1524030. doi: 10.3389/fbuil.2024.1524030

COPYRIGHT
© 2025 Stokoe, Hwang, Cox, Clayton and Gilbert. This is an open-access article distributed under the terms of the Creative Commons Attribution License (CC BY). The use, distribution or reproduction in other forums is permitted, provided the original author(s) and the copyright owner(s) are credited and that the original publication in this journal is cited, in accordance with accepted academic practice. No use, distribution or reproduction is permitted which does not comply with these terms.

NHERI@UTexas experimental facility with large-scale mobile shakers for field studies: a decade of discovery in natural hazards engineering

Kenneth H. Stokoe[1]*, Sungmoon Hwang[1]*, Brady R. Cox[2], Patricia M. Clayton[3] and Robert B. Gilbert[1]

[1]Maseeh Department of Civil, Architectural and Environmental Engineering, University of Texas at Austin, Austin, TX, United States, [2]Department of Civil and Environmental Engineering, Utah State University, Logan, UT, United States, [3]Department of Engineering, Wake Forest University, Winston-Salem, NC, United States

Introduction: Natural hazards present significant risks to infrastructure and communities, emphasizing the importance of advanced tools and methods to better understand and mitigate these challenges. The Natural Hazards Engineering Research Infrastructure (NHERI) experimental facility at the University of Texas (NHERI@UTexas), funded by the National Science Foundation (NSF), addresses this need by offering unique resources for large-scale field testing.

Methods: NHERI@UTexas contributes unique, large-scale, literally one-of-a-kind, mobile dynamic shakers and associated instrumentation to investigate seismic, cyclic, and static *in-situ* testing. These capabilities allow researchers to conduct experiments on actual infrastructure and geotechnical systems under real-world conditions, often impossible to accurately simulate in the laboratory.

Results: NHERI@UTexas has supported pioneering research in several areas, including: (1) enhanced 2D/3D geotechnical and seismic subsurface imaging, (2) *in-situ* characterization of liquefaction resistance and nonlinear dynamic soil behavior, (3) development of *in-situ* nondestructive soil-foundation-structure interaction (SFSI) methods, and (4) rapid geotechnical assessments following natural hazard events. These efforts have advanced the validation and calibration of numerical model and methodologies using full-scale experimental data.

Discussion: NHERI@UTexas enable researchers to gain new insights and drive innovations in advancing resilient and sustainable solutions for natural hazards problems.

KEYWORDS

NHERI@UTexas, large mobile shakers, *in-situ* seismic testing, subsurface imaging, liquefaction testing, soil-structure interaction

1 Introduction

=1The Natural Hazards Engineering Research Infrastructure (NHERI) is a nationwide, shared-use network of large-scale facilities dedicated to advancing natural hazards engineering research. The NHERI program is funded by the National Science Foundation (NSF) with goal of enhancing the resilience of the civil infrastructure and communities against earthquakes, windstorms, tsunamis, and other natural hazards. A key aspect of NHERI is its nationally distributed facilities, which provide state-of-the-art experimental, computational, and simulation tools to support diverse research needs. The NSF-supported facilities not only offer access to cutting-edge technology, but also provide comprehensive data management, enabling the collection, storage, and sharing of valuable research data. This wealth of resources, combined with collaboration opportunities across institutions, is made available to the broader research community, facilitating innovation and the development of effective solutions to mitigate the impact of natural hazards.

In alignment with this purpose, the NHERI@UTexas, Large-Scale Mobile Shakers facility, supported 20 shared-use projects and more than 25 non-shared-use projects from 2016 to 2024. Shared-use projects are funded by NSF which are typically led by researchers from other universities, often in collaboration with UT researchers, and focus on developing new testing techniques to achieve specific goals. Shared-use projects are typically funded by the Division of Civil, Mechanical, and Manufacturing Innovation (CMMI). However, NHERI@UTexas has recently expanded its scope to include efforts that advance the understanding of Earth's systems, allowing it to also secure funding from the Division of Earth Sciences (EAR). Over the past 5 years, about half of the shared-use projects have been supported by EAR funding. From designing field studies and developing sensors to conduct tests, uploading, and analyzing data, each project typically lasts between 1 to 3 years. Non-shared-use projects have not been supported by NSF and have typically been conducted by researchers at UT. These types of projects generally contribute to improving the sustainability and resilience of civil infrastructure against natural hazards, including nuclear power plants and, more recently, Small Modular Reactor (SMR) facilities. With rising concerns about global warming, nuclear energy is becoming a key zero-emission clean energy option. SMRs offer enhanced safety, flexibility, and cost advantages, which makes them a promising solution in the future of nuclear power generation. The NHERI@UTexas facility has been actively involved in researching soil stiffness profiles for earthquake response studies ranging in depth up to 450 m for both new and existing nuclear power plants and is recognized as a leader in this area. These types of projects often last about 6 months. In this article, the equipment capabilities at NHERI@UTexas are discussed, and key areas of investigation and example shared-use projects are presented. These examples showcase how NHERI@UTexas equipment contributes to advancements in various areas of research. More information about NHERI@UTexas and the NSF-supported NHERI program can be found at https://utexas.designsafe-ci.org/.

2 Overview of NHERI@UTexas

NHERI@UTexas provides unique large, mobile dynamic shakers and associated instrumentation for *in-situ* testing of civil infrastructure. These innovative field-testing methods can be used to evaluate the behavior of existing infrastructure as well as enhance the design of future infrastructure, which will contribute to the development of more resilient communities. While laboratory shake tables at both small and large scales provide valuable insights into dynamic infrastructure behavior, focusing on these methodologies exclusively, without the ability to test real structural and geotechnical systems under actual field conditions, would leave a significant gap in the transformative tools needed for the next frontier of natural hazards research.

The equipment available at the NHERI@UTexas experimental facility includes: (1) five large, hydraulically-controlled shakers mounted on mobile platforms (i.e., trucks) that can provide wide-band dynamic excitation sources for geotechnical and structural systems, (2) a tractor-trailer necessary to transport the four largest shakers, (3) a supply truck with resources for mobile shaker maintenance and refueling in the field, (4) an instrumentation van that houses data acquisition systems and power generators, (5) an air-conditioned instrumentation trailer that serves as a work space in the field, and (6) a wide array of field instrumentation, data acquisition systems, and various sensors for measuring vibrational motions and pore water pressures (Stokoe, et al., 2020).

The five mobile shakers, shown in Figure 1 and summarized in Table 1, are named (1) T-Rex, (2) Liquidator, (3) Raptor, (4) Rattler, and (5) Thumper. The force and frequency generation capabilities of these shakers are presented in Figure 2. The two heaviest shakers are T-Rex (29,000 kg) and Liquidator (32,800 kg). T-Rex (Figure 1A) can be used to generate large dynamic forces in any of three directions (vertical, horizontal in-line, and horizontal cross-line), and the shaking direction can be changed with a simple push of a button by the operator. The shaking system, mounted on an off-road, all-wheel-drive vehicle, can produce a maximum force output of around 267 kN in the vertical direction, and around 134 kN in each horizontal direction, as shown in Figures 2A, B, respectively. In addition to T-Rex's shaking capabilities, it can also be used to: (1) push cone penetrometers and other custom-made vibration and/or pressure-sensing instrumentation into the ground using a hydraulic ram located on the rear bumper of the vehicle (shown in Figure 3D), and (2) perform pull-over tests of large-scale structural models in the field using a hydraulically-operated winch on the front bumper of the vehicle. In total, T-Rex's capabilities make it unique in the world. Liquidator (Figure 1B) is a unique, custom-built shaker designed specifically for low-frequency, large-motion operation. To change the shaking direction from the vertical mode to the cross-line horizontal (shear) mode requires approximately two working days at the manufacturer's facilities in Tulsa, OK. The shaker can generate a maximum force output of approximately 89 kN in either mode down to a frequency of 1.3 Hz, as shown in Figure 2. However, a modified configuration where the entire off-road mobile platform is lifted off the ground and oscillates in the vertical mode allows Liquidator to generate maximum forces of

FIGURE 1
Photographs of the five mobile shakers and tractor-trailer rig available at NHERI@UTexas: **(A)** High-force, three-axis shaker called T-Rex, **(B)** Low-frequency, two-axis shaker called Liquidator, **(C)** Single-axis, vertical shaker called Raptor, **(D)** Single-axis, horizontal shaker called Rattler, **(E)** Urban, three-axis shaker called Thumper, and **(F)** Tractor-trailer rig, called the Big Rig, loaded with T-Rex (after Stokoe, et al., 2017).

TABLE 1 Key features of the five mobile shakers available at NHERI@UTexas

Shaker	Vehicle type	Shaking direction: Primary direction (transformable directions)	Max. Output: Primary direction (transformable directions)
T-Rex	Off-road vehicle	Vertical (Horizontal in-line and cross-line)	267 kN (134 kN)
Liquidator	Off-road vehicle	Vertical (Horizontal cross-line)	89 kN (89 kN)
Raptor	Highway legal	Vertical	120 kN
Rattler	Off-road vehicle	Horizontal cross-line	134 kN
Thumper	Highway legal	Vertical (Horizontal in-line and cross-line)	26.7 kN (26.7 kN)

89 kN down to a frequency of 0.7 Hz. Below 0.7 Hz, the force level decreases but is still substantial to about 0.3 Hz. This modification provides unique capabilities that can facilitate deeper (1 km or more) active-source subsurface imaging (Stokoe, et al., 2019). Like T-Rex, the Liquidator shaking system is also housed on an off-road vehicle with hydraulic penetrometer/instrumentation pushing capabilities mounted on the rear steel bumper of the vehicle and a winch with pull-over capabilities mounted on the front steel bumper. Use of these pull-over capacities are illustrated in field studies with 1/4-scale bridge bents by Stokoe, et al. (2017).

Raptor and Rattler provide intermediate-level force generation. Raptor (Figure 1C) is called a compression-wave (P-wave) shaker in the geophysical exploration community. The maximum vertical force output is about 120 kN, as shown in Figure 2A. Raptor is ideal for situations where Thumper's force output (discussed below) is not sufficient for the desired testing application and T-Rex's triaxial shaking capability and/or higher force output is not required. Rattler (Figure 1D) is a horizontal (shear-wave) vibrator mounted on an off-road vehicle. Rattler has a frequency-force response which is similar to T-Rex in the shear mode, as shown in Figure 2B. By having two

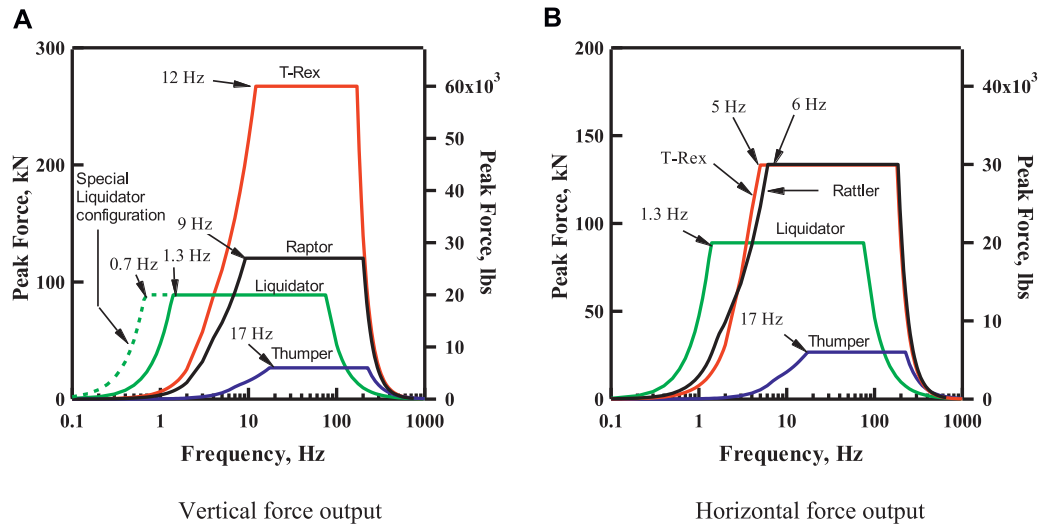

FIGURE 2
Theoretical force outputs of the five mobile shakers at NHERI@UTexas in the: **(A)** vertical mode and **(B)** horizontal mode (Stokoe, et al., 2017).

shear-wave vibrators (T-Rex and Rattler), this equipment can be used simultaneously with synchronized force outputs to generate a larger surface area of high shear strains. Thus, for *in-situ* liquefaction and nonlinear soil testing, soil beneath the two shakers, in which the instrumentation is placed, can be excited in a nearly plane-strain condition. T-Rex and Raptor can also be used in tandem to create similar conditions in the vertical direction. Since T-Rex, Liquidator, and Rattler are not street-legal, the 26-wheel, tractor-trailer rig, called the Big Rig and shown in Figure 1F, is generally used to transport them to the test site.

Thumper (shown in Figure 1E) is the smallest shaker and is mounted on a street-legal truck and has a moderate force output, making it ideal for testing in urban areas. The maximum force output of Thumper in the vertical or horizontal directions is about 27 kN, as shown in Figure 2. With around 2 hours of work in the field, Thumper's direction of shaking can be changed at the test site. It is important to note that hydraulic take-off connections are provided on T-Rex, Liquidator, and Thumper, which can be used to power other hydraulic equipment at the site. For example, these three vibroseis could be used at the test site to run linear hydraulic actuators for *in-situ*, pushover or pullout testing of superstructure and substructure subassemblages in the field (Stokoe, et al., 2017). Also, the hydraulic shakers mounted on the T-Rex, Liquidator, and Thumper vehicles can also be removed and mounted on a structure, while the hydraulics and electronics on the associated truck can be used to run the shaker. The selection of an appropriate mobile shaker depends primarily on the desired frequency range, sufficient force output, and shaking direction. For instance, if a researcher aims to image deeper areas with a wide range of sensor deployments, Liquidator is an optimal choice due to its ability to vibrate down to 0.7 Hz with a special configuration. On the other hand, if the goal is to study structural responses to different shaking directions, T-Rex is ideal, as it can switch shaking directions within seconds. Additional details regarding cost and operational support are available at https://utexas.designsafe-ci.org/.

NHERI@UTexas instrumentation and field support vehicles are shown in Figure 3. The supply truck, shown in Figure 3A, carries fuel and spare parts for the shaker trucks. Additionally, there is a customized Ford cargo van (shown in Figure 3B) and a 2.4 m by 4.8 m instrumentation trailer (shown in Figure 3A) that both provide an air-conditioned workspace, data acquisition systems, and electrical power. The NHERI@UTexas facility also has a significant amount of field instrumentation, including: (1) four primary data acquisition systems (discussed below), (2) 85, 1-Hz vertical geophones (Figure 3C), (3) 24, 1-Hz horizontal geophones, (4) 6 high-capacity dynamic load cells, (5) 18 triaxial MEMS accelerometers, (6) cone penetrometer test (CPT) equipment and seismic CPT equipment (Figure 3D), (7) 6 direct push crosshole sensors, (8) 10, 120-seconds and 10, 20-seconds Trillium Compact broadband seismometers (Figure 3F), (9) 100 SmartSolo IGU-16HR 3C nodal stations (Figure 3G), and (10) OptaSense ODH4 Distributed Acoustic Sensing (DAS) interrogator (Figure 3H).

The four main data acquisition systems are a 96-channel Data Physics spectrum analyzer system, a SmartSolo with integrated data acquisition system, 10 three-channel Nanometrics Taurus and 10 three-channel Nanometrics Centaur digitizers, and a DAS interrogator. The Data Physics system uses the SignalCal 730 software to generate input signals (sinusoidal, stepped-sine, white noise, frequency sweeps, *etc.*) that drive the mobile shakers and to record output signals from various sensors. The Data Physics system (shown in Figure 3E) consists of four dynamic signal analyzers, which have a total of 96 channels. The Data Physics analyzers can be set up as four separate units with different sampling rates, or they can be linked together as a single system. The Data Physics spectrum analyzers have the capacity to record data for hours of time at a high sampling rate up to 200 kHz. The Data Physics control software can also be used to perform real-time frequency domain calculations and display auto-power spectra, transfer functions, coherency, and phase plots to facilitate reviewing and analyzing data in the field.

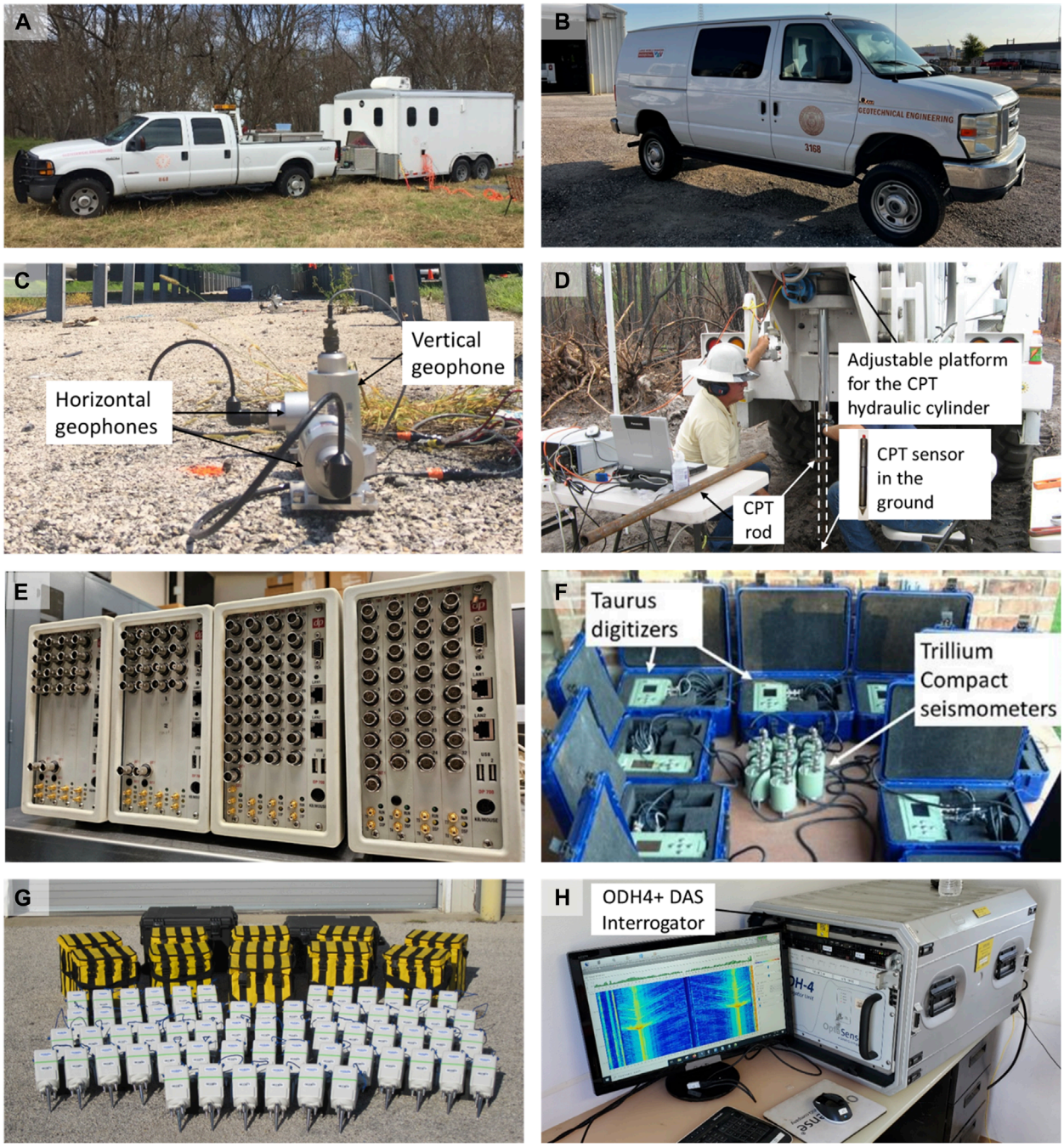

FIGURE 3
Photographs of the field supply truck, mobile instrumentation trailer and some associated instrumentation available at NHERI@UTexas: **(A)** Field supply truck and instrumentation trailer, **(B)** Customized Ford cargo van, **(C)** 1-Hz vertical geophones and cables, **(D)** Cone penetration test equipment, **(E)** Data Physics analyzers, **(F)** Trillium Compact Seismometers and Taurus Digitizers, **(G)** SmartSolo IGU-16HR 3C nodal stations, and **(H)** OptaSense ODH4 Distributed Acoustic Sensing (DAS) interrogator (after Stokoe, et al., 2017).

For field studies requiring a distributed sensor array, with sensors spaced hundreds of meters to a kilometer apart, such as in passive surface wave testing or topographic amplification studies, the SmartSolo, Taurus, and Centaur digitizers are suitable options, as shown in Figures 3F, G. The SmartSolo is a cost-effective, all-in-one nodal system that integrates the sensor, data logger, and battery, making it highly portable and easy to deploy. In contrast, while the Taurus and Centaur digitizers are less portable due to the need for external sensors, they offer a higher dynamic range, more flexibility in sensor choices, and greater versatility in sampling rates.

The OptaSense ODH4+ DAS Interrogator system, shown in Figure 3H, utilizes advanced fiber optic technology to detect vibrations over long distances. In a DAS system, laser pulses travel through the fiber optic cable, and any disturbances or acoustic

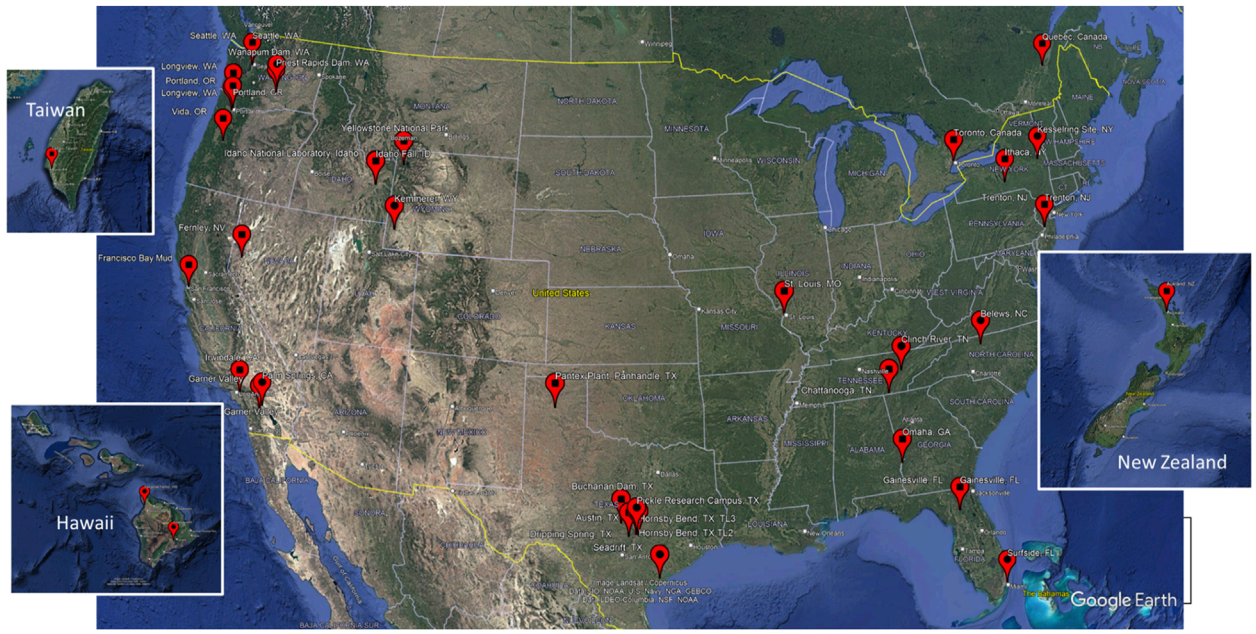

FIGURE 4
Project locations of NHERI@UTexas mobile shakers since 2015 (from Google Earth).

signals along the cable cause changes in the backscattered light, which are then recorded and analyzed. This effectively turns the fiber into thousands of individual sensors, capturing data at precise points along its length. The OptaSense ODH4+ DAS Interrogator can operate with various fiber types, including single-mode, multi-mode, and enhanced high-backscatter fibers, offering a sampling rate of up to 100 kHz and selectable gauge lengths from 2 to 32 m.

3 Establishing a test site near Austin, TX for validating methodologies or simulation models

The mobility features inherent in the NHERI@UTexas facility have enabled projects across a wide geographical range, both domestically and internationally. Domestically, the facility has supported projects around the United States, including Hawaii, as shown in Figure 4. Internationally, NHERI@UTexas has also conducted several projects in Taiwan, Canada, and New Zealand (See Figure 4). This mobility feature allows researchers to perform tests in complex and site-specific ground conditions or on permanent structures in various locations. For example, the T-Rex shaker was used to investigate the 3D magma structure of the Kilauea summit in Hawaii. Additionally, the facility has contributed to assessing liquefaction susceptibility at several sites in the states of Washington and Oregon, where liquefaction events have previously been recorded. The only drawback of an out-of-state Texas project is the cost of transporting the large shakers.

To support researchers in validating methodologies or simulation models using the large mobile shakers without high travel costs, NHERI@UTexas has established a local testing site, Hornsby Bend (HB), approximately 3.5 km north of the Austin-Bergstrom International Airport in Austin, Texas. The site is located away from buildings and infrastructure, making it optimal to conduct vibration-related testing. Additionally, the site is situated on an alluvial plain with relatively simple geology. CPT test results show the upper 8 m consist of sandy silt and clay, followed by 5 m of clayey sand or clayey gravel with sand, underlain by shale. Numerous tests have been performed at this site particularly near a fiber optic cable line equipped for Distributed Acoustic Sensing (DAS), as shown in Figure 5. In 2021, two types of fiber optic cables were installed, and subsequent data collected using DAS interrogators have been analyzed to assess the benefits of this emerging technology. Recent publications presenting these results are included in Abbas et al., 2024b, Yust et al., 2022b, and Yust et al., 2023. These studies demonstrate the efficacy of DAS in capturing high-resolution waveforms across long arrays. This capability not only enhances 2D and 3D subsurface imaging but also enables support to other applications, such as damping measurements. Extensive testing has been conducted at the HB site to compare DAS results with other methods, including thirteen CPTs, two triangular Microtremor Array Measurements (MAM), downhole seismic testing at two boreholes, and four direct push crosshole tests. Additionally, borehole logs are available for both boreholes, with P-wave reflection and electrical resistivity testing scheduled for November 2024. This comprehensive dataset is available through DesignSafe (Vantassel et al., 2022; Yust et al., 2022a) and provides an invaluable resource for researchers seeking diverse analytical opportunities, supported by robust ground-truth information.

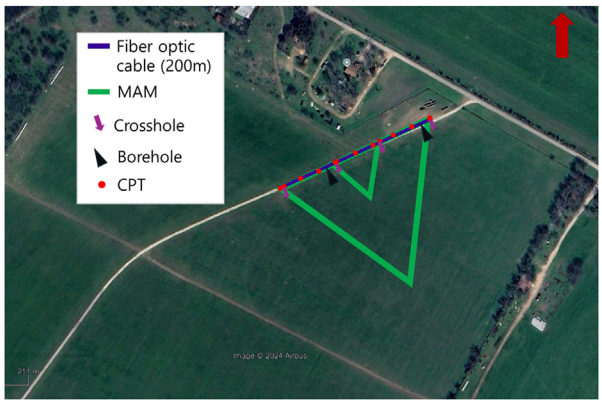

FIGURE 5
A satellite image of the Hornsby Bend (HB) site showing the various testing locations near the fiber optic cable line.

4 Key areas of investigation

The NHERI@UTexas facility is focused on four main challenges. These challenges are: (1) performing deeper, more accurate, higher resolution, 2D/3D subsurface geotechnical imaging through the use of cutting-edge equipment and analysis methods, (2) developing innovative testing techniques to propagate waves to greater depths for *in situ* characterization of the nonlinear dynamic response and liquefaction resistance of complex geomaterials, (3) developing rapid, *in-situ* methods for nondestructive structural evaluation and soil-foundation-structure interaction (SFSI) studies to better understand how structures respond to seismic and dynamic forces, and (4) conducting rapid investigation of geotechnical parameters at high-profile and natural hazard events for preventing secondary hazards and immediate risk assessment (after Stokoe et al., 2017). These challenges are substantial, yet the unique equipment resources at NHERI@UTexas are well-positioned to help researchers to address them. The progress achieved in each area over the past 10 years using NHERi@UTexas equipment is outlined, and advancements are described in the sections below.

4.1 Performing deeper, more accurate, higher resolution, 2D/3D subsurface imaging

The progress in non-invasive imaging has revolutionized healthcare, with technologies like X-rays, CAT scans, ultrasounds, and MRIs now an essential part of modern diagnostics. Despite ultrasound imaging only gaining popularity in the United States in the 1970s, it is now ubiquitous, with 3D color ultrasound imagery accessible in commercial settings. This trajectory suggests a promising parallel for subsurface imaging in civil engineering applications. Developing high-resolution, 3D images of the subsurface that include precise elastic properties, such as shear modulus, constrained modulus, and Poisson's ratio, could fundamentally change the approach to designing resilient and sustainable infrastructure. The NHERI@UTexas facility is already equipped with the advanced technology necessary to drive this development, marking a crucial step toward in making this vision a reality.

In addition to enhancing civil infrastructure and geotechnical systems, NHERI@UTexas also supports improved seismic imaging of natural topography, such as magma systems beneath volcanoes. This capability can provide vital information for understanding geological processes and assessing natural hazards. As these imaging techniques continue to progress, their potential applications in environmental monitoring and resource management will grow substantially, fostering a future where sophisticated subsurface imaging becomes as accessible and essential as ultrasound technology is today. Although many examples exist, the focus in this article is on two sites where advanced subsurface imaging enhanced engineering research and practice: one site demonstrates 2D/3D imaging of geotechnical systems, and the other site is focused on natural topography.

4.1.1 Continuous 2D/3D in-situ profiling for anomaly detection in newberry, Florida

The comprehensive experiments and projects conducted over the last 10 years at a dry retention pond in Newberry, Florida, a site known for its karst cavities and subsurface anomalies, illustrate significant advancements in 2D and 3D subsurface imaging techniques. This work demonstrates the continuous support from NHERI@UTexas, emphasizing the facility's commitment to enhancing our understanding of complex subsurface environments.

Tran and Hiltunen (2011) conducted surface wave testing at the Newberry site, but the study was confined to a smaller area and used less advanced equipment. The findings from the surface wave testing indicated that the subsurface is composed of medium-density fine sand and silt ranging in depth from 2 to 10 m overlying a highly variable limestone. Subsequently, Tran et al. (2013), Tran et al. (2020) applied full waveform inversion (FWI) techniques to detect subsurface anomalies. These studies utilized equipment from the NHERI@UTexas, including the uniaxial, small vibroseis called Thumper. In their 2013 study, Tran et al. employed 2D FWI and successfully identified an underground anomaly that was later confirmed to be a void through Standard-Penetration-Test (SPT) soundings. However, the predicted depth of the void was greater than its actual depth, which was attributed to the difference between the measured wavefield, and the assumed plane strain condition used in the 2D FWI. Building on this work, in 2020, Tran et al. expanded the FWI studies by exciting the ground at 65 locations within a 2D grid of 48 vertical geophones arranged in a 4 m × 12 m configuration, covering an area of 12 m × 36 m. The 3D FWI analysis resulted in a subsurface model identifying three voids, although only two of these were confirmed by SPT soundings. These earlier studies highlighted the challenges in accurately detecting and imaging subsurface anomalies using real field data, primarily due to limitations such as smaller spatial coverage, less dense spatial sampling, and the use of single-component sensors. While NHERI@UTexas supported the equipment, more advanced sources, such as the broadband T-Rex vibroseis shaker truck, were not utilized. Additionally, the presence of sinkholes of varying sizes and depths combine with some sinkholes filled with uncontrolled material, complicated the subsurface imaging efforts. These limitations highlighted the need for more comprehensive

and technologically advanced approaches to subsurface imaging, particularly in complex karst environments like the Newberry site.

Our current study builds on this previous work, representing a significant advancement in experimental design and data collection. Supported by the U.S. National Science Foundation (Grant Numbers CMMI-2120155, CMMI-1930697, and CMMI-2037900), this experiment combined an extensive 2D DAS fiber-optic cable network with a dense array of three-component nodal seismometers. This setup is shown in Figure 6 and includes approximately 2 km of DAS cable deployed in a zigzag pattern, creating 1920 horizontal component channels, complemented by 144 three-component nodal seismometers arranged in a 12 × 12 grid. This configuration provides unprecedented spatial resolution over the 75 m × 155 m experimental area. In the experiment, the powerful T-Rex vibroseis truck is utilized as the active source for these measurements, exciting the ground at 260 distinct locations in three directions. Additionally, impact sources were also employed at 286 locations within the instrumented area, resulting in a total of 367 source positions. The shot locations are categorized as "Shots Inside" (SI) and "Shots Outside" (SO), with the SO positions further divided into south (SOS), west (SOW), and north (SON) locations. This strategic arrangement provides excellent spatial coverage and enables a wide range of measurements, offering unique opportunities for developing and testing advanced subsurface anomaly detection and imaging techniques (Abbas et al., 2024a). The integration of high-density DAS technology with traditional seismometers, along with the use of both active and passive sources, represents a significant leap in geophysical imaging capabilities. This study addresses crucial needs in earthquake engineering, geohazard assessment, and infrastructure development, particularly in complex karst environments like Newberry, Florida. By providing open-access data through DesignSafe (Abbas et al., 2023), this experiment is contributing significantly to the broader scientific community, facilitating further research and development in geophysical imaging techniques and paving the way for more accurate and higher-resolution 2D/3D subsurface geotechnical imaging.

4.1.2 Imaging of structure and magma system beneath the summit of Kilauea Volcano

The Kīlauea volcano in Hawaii is one of the world's most active volcanoes and has attracted scientific interest for centuries. Despite extensive research on various aspects of the volcano, a definitive understanding of the size and configuration of Kīlauea's magmatic plumbing system remains elusive. Past estimates of the volumes of the magma system have varied significantly, ranging from 0.2 to 240 cubic kilometers (Decker, 1987; Denlinger, 1997; Fiske and Kinoshita, 1969; Pietruszka et al., 2015; Poland et al., 2014). These estimates have proposed differing storage systems, from disconnected dikes and sills to large subterranean bodies with established connections. The lack of size and configuration of the magmatic plumbing inhibits scientists' ability to predict the volume and duration of eruptions, resulting in extensive damage to the infrastructure and nearly destroying 2,000 properties in May 2018. In response to the challenges posed by the 2018 eruption, Congress allocated supplemental funding to the U.S. Geological Survey (USGS) for rebuilding the Hawaiian Volcano Observatory and enhancing research capabilities. USGS proposed a passive imaging experiment and, in collaboration with academic partners, secured additional NSF funding for active source seismic imaging through the NSF project titled "Collaborative Research: Active and Passive Seismic Imaging of the Three-Dimensional Structure and Magma System beneath the Summit of Kilauea Volcano" (Award Number, EAR-2218645/2218646).

This project on the Kilauea summit marks the largest and most complex field experiment ever conducted on an active volcano, with more seismic nodes and a larger active source component than previous studies at sites like Yellowstone and Mount St. Helens. Approximately 1,815 seismometers were deployed across Kīlauea's summit region, including areas affected by the 2018 caldera collapse. A central component of the experiment was the 34-ton triaxial vibroseis shaker truck called T-Rex supported by NEHRI@UTexas. In total, T-Rex shook at 396 locations around the summit of the Kilauea volcano. At 132 of these shot points, a 3-direction sweep was performed. At the rest of the 264 shot points, a one-direction sweep was performed. A photograph of T-Rex at a shot point on the summit of the Kilauea volcano is shown in Figure 7A. With data from both the T-Rex active source and natural seismicity recorded by the HVO and summit nodes, the researchers detected approximately 35,000 local earthquakes within 30 km of the center of Kīlauea, resulting in nearly 192 million waveforms for analysis. This extensive data set is enabling the creation of cross-sectional images of the volcano's internal structure, similar to CT scans in medical imaging as shown in Figure 7B (Denlinger and Flinders, 2024). These images will gradually reveal the configuration of magma system, offering new insights into how Kīlauea stores and transports magma, feeds distant lava flows, and collapses at the summit. These findings will not only enhance scientific understanding of Kīlauea's eruption mechanisms and magma storage but also provide valuable information for emergency managers, policymakers, and the public on the hazards posed by this evolving volcano system. Such insights are vital for informing future monitoring and response strategies, potentially minimizing the risks to nearby communities.

4.2 Characterizing the nonlinear dynamic response and liquefaction resistance of complex geomaterials *in situ*

Natural geotechnical materials, including soil and rock, play a critical role in the performance of our nation's infrastructure during earthquakes and other natural hazards, such as hurricanes and floods. For example, the devastating effects of soil liquefaction and site amplification have been observed in essentially every significant earthquake. Additionally, the impact of geotechnical materials during hurricanes and floods is significant, often governed by compacted soils that form levees, dams, and dikes, as well as the underlying natural materials. The poor performance of levees during hurricanes can lead to extensive inundation, as evidenced by the failure of levees surrounding New Orleans, Louisiana, during Hurricane Katrina in 2005. Furthermore, global warming compounds these risks, intensifying the frequency and severity of extreme weather events. Rising temperatures, increased precipitation, and higher sea levels increases the susceptibility of certain soils to liquefaction, posing even greater challenges for earthquake-prone and flood-impacted areas. Unfortunately,

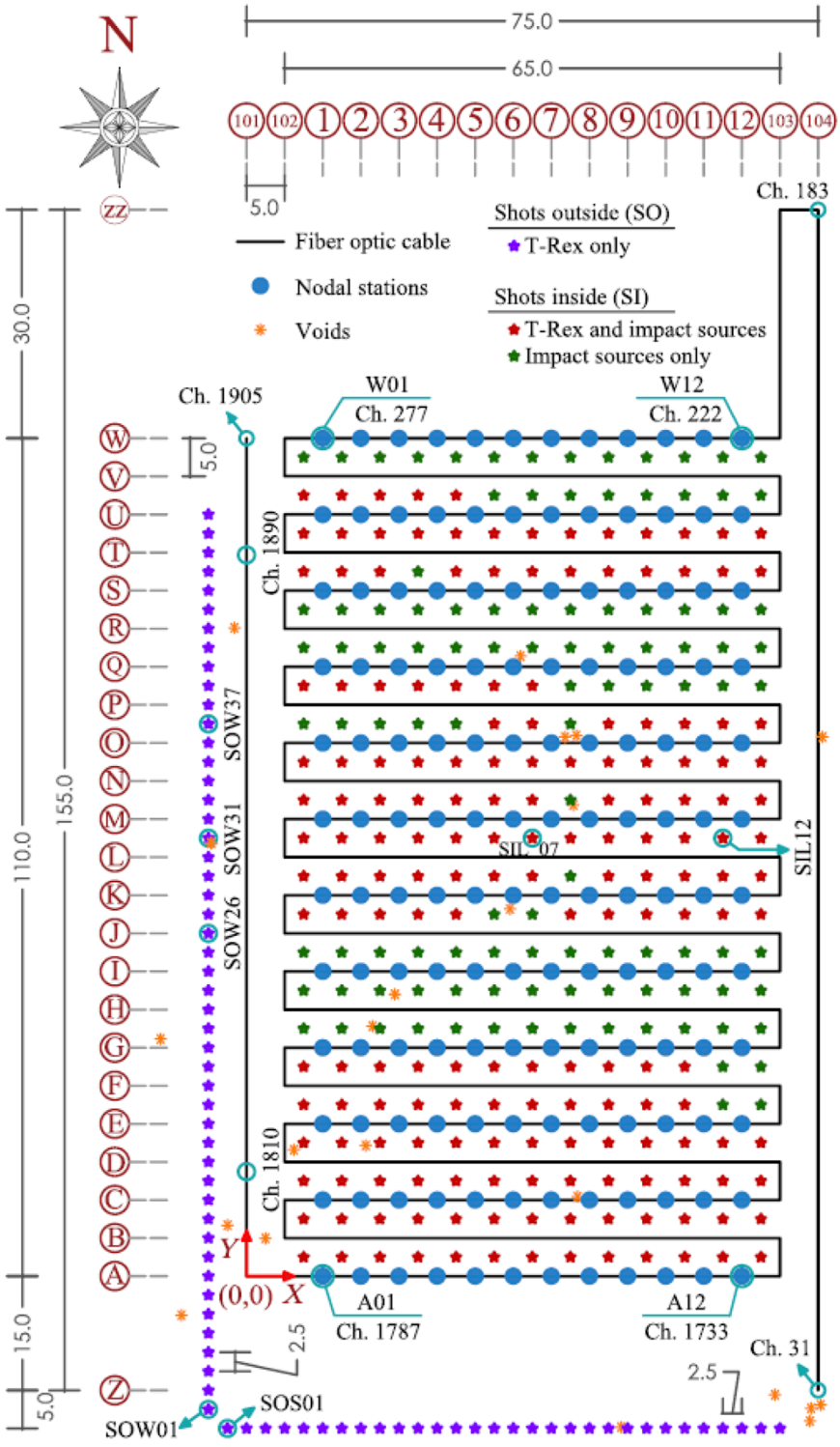

FIGURE 6
Schematic layout of the test site showing locations of the: 3C geophone nodal stations, fiber-optic cable, T-Rex and impact shots, and voids that are visible from the ground surface. The layout is comprehensive, including all the line numbers, letters, and dimensions in meters used to arrange the equipment (from Abbas et al., 2024a).

natural geotechnical materials are the least investigated, most variable, and least controlled of all materials that form part of the U.S. infrastructure inventory (Coduto et al., 2015). Therefore, a significant challenge to making our infrastructure resilient and sustainable is characterizing the nonlinear dynamic response and liquefaction resistance of complex geomaterials *in situ*.

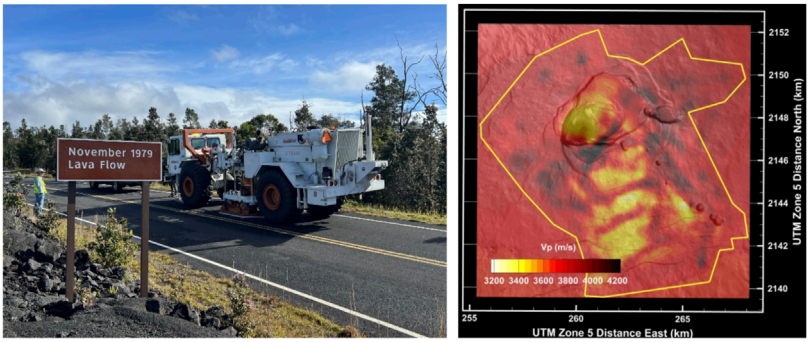

(a) T-Rex at a shot point on the summit of the Kilauea volcano

(b) An example tomographic slice below the Kīlauea volcano at sea level produced using both earthquakes and controlled seismic source data (Denlinger et al., 2024)

FIGURE 7
Seismic imaging of the three-dimensional structure and magma system beneath the summit of Kilauea volcano project: **(A)** T-Rex at a shot point on the summit of the Kilauea volcano. **(B)** An example tomographic slice below the Kīlauea volcano at sea level produced using both earthquakes and controlled seismic source data (Denlinger et al., 2024).

Nonlinear dynamic soil properties are required in predicting the response of geotechnical and structural systems during earthquakes and hurricanes. The key nonlinear properties include: (1) the variation of shear modulus (G) and material damping ratio in shear (D) with shear strain (γ), and (2) how these properties vary with soil type and number of cycles of loading. These properties are typically expressed as G-log γ and D-log γ relationships, as the shear strains induced during natural hazards can easily range over a factor of 1,000 (γ from below 0.001% to above 1.0%). Before the Network for Earthquake Engineering Simulation (NEES) and NHERI programs were funded by NSF, these dynamic soil properties could not be measured in the field due to the challenges of generating controlled, sinusoidal loading across a wide range of strains and number of loading cycles. Therefore, the field G-log γ and D-log γ relationships were empirically estimated by combining large-strain nonlinear measurements from small-scale dynamic laboratory testing of intact or reconstituted soil specimens with the limited, low-strain, field seismic testing that was available at that time.

4.2.1 *In situ* nonlinear measurement using a helical pile

Over the past 20 years, the NEES/NHERI@UTexas mobile shakers facility has pioneered and advanced a generalized, staged-loading approach to measuring the *in-situ* G-log γ and pore-water pressure-log γ relationships. This form of *in situ* parametric testing is essential for both understanding the limitations of empirical methods and for testing geotechnical materials that cannot be easily or cost-effectively assessed in the laboratory. The latest technique developed by NHERI@UTexas involves installing a helical pile to a depth of the target liquefiable soil layer, as shown in Figure 8A. One of the four vibroseises shown in Figure 1 and capable of controlled shaking in the vertical direction is positioned on top of the helical pile. Vertical waveforms generated by the vibroseis propagate directly into the soil at the desired testing depth. This approach overcomes limitations of conventional *in-situ* liquefaction testing, where the vibroseis excitation occurs at the ground surface. In traditional methods, rapid attenuation of cyclic strain with depth restricts the effective testing zone to approximately 2 m. With this new enhanced technique using the helical pile, cyclic strains at any depth can be achieved at levels of 0.3%–0.4%.

Two NSF-funded projects are utilizing this pioneering liquefaction testing technique to measure nonlinear dynamic soil properties *in situ*. The first project, titled "RAPID/Collaborative Research: Investigating the Liquefaction Susceptibility of Calcareous Sand in Hawaii with an Enhanced NHERI@UTexas Large Mobile Shaker" (Award Numbers CMMI-2317659/2317660), focuses on studying the cyclic behavior of calcareous soils at the Kawaihae Harbor. Initial results indicate differences between field and laboratory data, likely due to limited resources on remote islands. For example, the low-capacity skid steer required for installing the helical pile may inadvertently disturb the soil. The second project, titled "Engineering Research Center for Bio-mediated and Bio-inspired Geotechnics" (Award Number EEC-1449501), examines the nonlinear properties of soils treated using the Microbially-Induced Desaturation (MID) method. Here, the nonlinear field measurements obtained from the testing pad are consistent with laboratory results, as shown in Figure 8B. The results from a depth of 2.95 m demonstrate the effectiveness of this enhanced testing technique, surpassing the limitations of conventional methods. The maximum strain level achieved at this depth reached 0.4%, a significant improvement in capturing *in situ* nonlinear soil behavior. These promising findings build upon the initial research conducted in Hawaii, which included improvements such as sensor array modifications, vibroseis adjustments, sensor recalibration, and crosshole sensor installations to ensure high-quality data. Insights from these projects have contributed valuable knowledge for evaluating and mitigating earthquake hazards in liquefaction-prone areas.

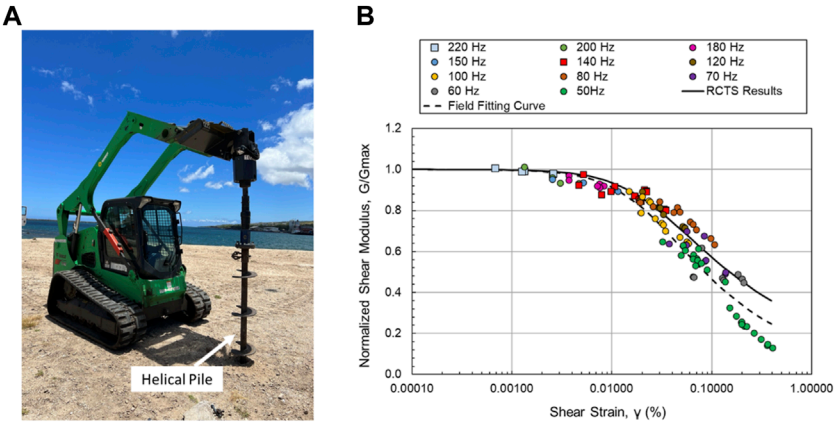

Helical pile installation using skid steer

Nonlinear field measurement compared with laboratory result

FIGURE 8
Nonlinear field measurements using the helical pile: **(A)** Helical pile installation using a skid steer and **(B)** Comparison of normalized shear modulus *versus* shear-strain relationship from field and laboratory tests.

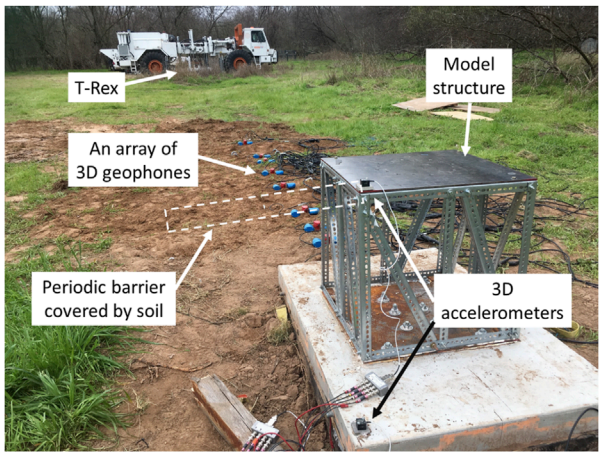

FIGURE 9
A photograph of T-Rex used as a vibrational source in passive isolation tests with a model structure accompanied by arrays of 3D geophones and 3D accelerometers.

4.3 Developing rapid, *in situ* methods for nondestructive structural evaluation and soil-foundation-structure interaction (SFSI) studies

The NHERI@UTexas facility also offers equipment uniquely capable of conducting *in-situ* testing on structural engineering systems. Unlike the vast majority of structural engineering experimental research that comprises quasi-static, pseudo-dynamic, or shake table tests to characterize structural performance under idealized boundary conditions, NHERI@UTexas's equipment enables the examination of complex soil-foundation-structure interaction (SFSI) behaviors in real-world settings. Traditional experimental research on SFSI often involves on small-scale models (scaled 1:30 to 1:100) tested in uniform soil containers on shake tables or in centrifuges, which may not accurately represent construction materials, methods, or varied soil conditions. While scaled laboratory studies are valuable, NHERI@UTexas facilitates a wide range in field testing that incorporates a range of soil environments, offering a realistic approach to understanding SFSI in full-scale infrastructure. The NHERI@UTexas shakers enable multiple testing approaches, including indirect excitation of the structure by shaking the surrounding soil, direct excitation by placing the shaker mechanism on or attaching it directly to the structure, and quasi-static testing methods *in situ*. Originally designed for geotechnical applications, the shakers generate maximum force outputs at relatively high frequencies, which may limit their ability to induce nonlinear or damaging responses in large-scale structures. For testing where nonlinear behavior is essential, smaller-scale structural specimens can be designed to align with force and frequency capacities of the mobile shakers.

4.3.1 Seismic isolation of embedded foundations using periodic barriers

An NSF-funded project titled "Collaborative Research: Seismic Isolation of Embedded Foundations using Periodic Barriers to Create Resilient Structures" (Award Number CMMI-1761597) is an example of using the mobile shakers for direct and indirect dynamic testing of a soil-foundation-structure system in the field. The aim of this research effort is to develop a periodic barrier capable of effectively attenuating incoming seismic waves. The project goals include: (1) deriving the analytical solution of the Rayleigh-wave frequency band gap of periodic metamaterial, (2) conducting passive isolation tests and active isolation tests to evaluate the performance of the barriers, and (3) establishing a finite element model for a comprehensive parametric study of periodic barriers. Field testing is being performed to examine the feasibility of the periodic barrier

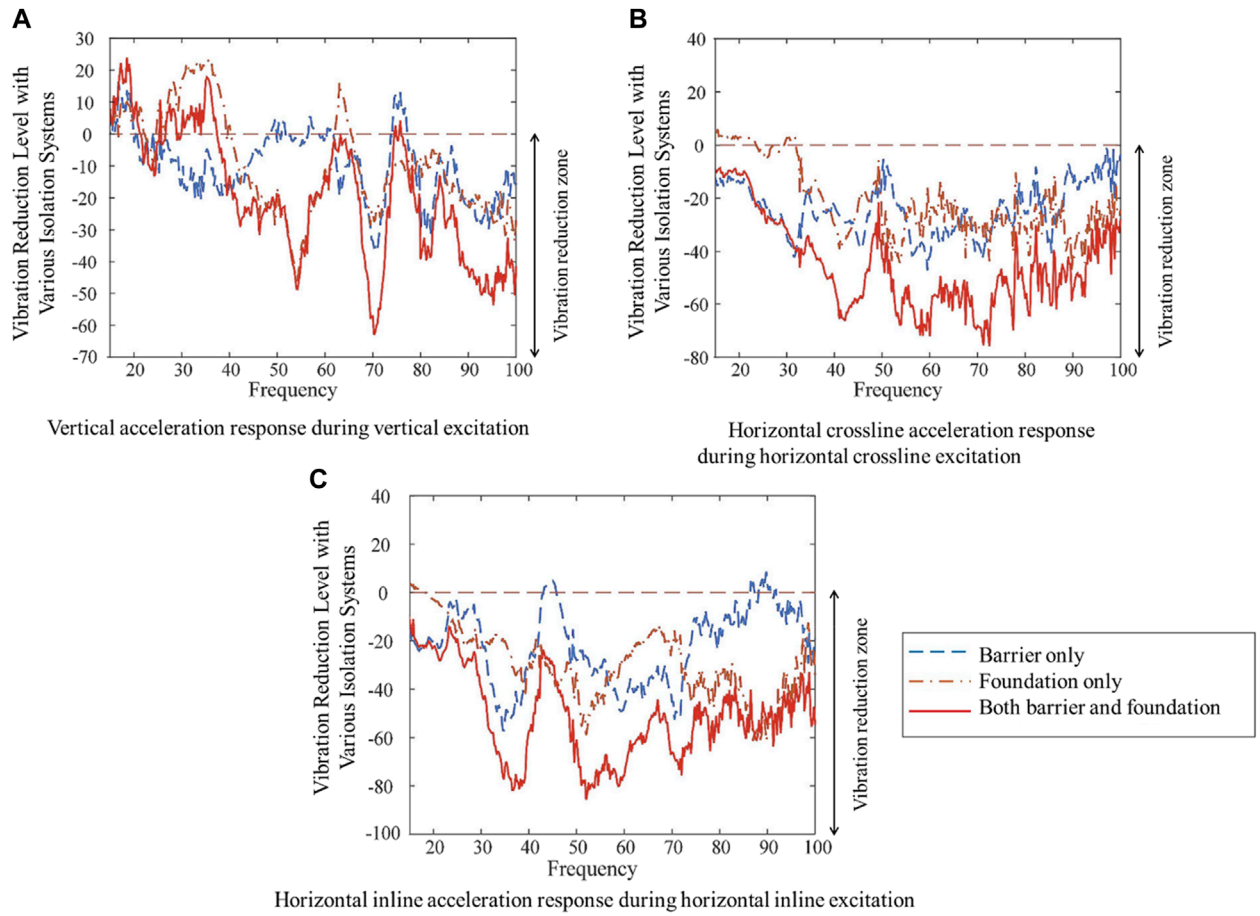

FIGURE 10
Vibration reduction level of the wave isolation system composed of the periodic barrier and periodic foundation obtained from seismic excitation tests in all three directions generated by T-Rex (Zhang et al., 2022). **(A)** Vertical acceleration response during vertical excitation. **(B)** Horizontal crossline acceleration response during horizontal crossline excitation. **(C)** Horizontal inline acceleration response during horizontal inline excitation.

for seismic isolation, facilitated by NHERI@UTexas's state-of-the-art equipment. The T-Rex mobile shaker is being used to provide surface wave excitation in three directions—vertical, horizontal crossline, and horizontal inline—while an array of surface sensors from NHERI@UTexas are being used to record real-time ground and structural responses as shown in Figure 9. Effectiveness of the periodic foundation and the periodic barriers were determined based on the motions recorded with these sensors.

Key findings from this study (Zhang et al., 2022; Wang et al., 2022; Huang et al., 2020; Huang et al., 2021) demonstrate the vibration mitigation potential of periodic barriers and foundations, as well as the impact of various excitation methods and directions of motion on the screening performance. In Figure 10, the results of the field tests with T-Rex show significant vibration reduction across multiple frequencies and directions, which ambient vibrations alone would not reveal. The advanced excitation capabilities of T-Rex provided a comprehensive view of the total system, revealing the broad frequency-band gaps achieved by combining periodic barriers and foundations. Numerical simulations, primarily using 2D finite element models, showed good agreement with the field experiments, validating their use in predicting and optimizing the barrier performance. While these test programs successfully demonstrated the effectiveness of metamaterial-based isolation systems for both active and passive vibration mitigation, further *in-situ* field testing of complex systems is necessary to better address research needs related to broadband vibration control and optimization of barrier-foundation systems for various applications.

4.4 Rapid field investigation of geotechnical parameters at high-profile and natural hazard events

The mobile capability of the NHERI@UTexas facility can be leveraged to rapidly investigate geotechnical parameters after devastating natural or man-made hazards. An example of this rapid field response is the investigation of the Champlain Towers South collapse, a project funded by NIST through the NSF NHERI program. In collaboration with Utah State University, NHERI@UTexas utilized an urban vibroseis called, Thumper, to assess the foundation and surrounding soil conditions with minimal disturbance to the site. Given the high-profile nature of the

Champlain Towers South investigation, data publication is restricted at this time.

5 Summary

The specialized, mobile field equipment available at the NHERI@UTexas facility for dynamically and cyclically loading the natural and built environments is discussed in this article and examples are presented. This facility offers researchers worldwide access, under the NSF NHERI shared-use policy, to five large, hydraulically controlled shakers, a tractor-trailer for transporting the largest shakers, field-support vehicles, and an extensive array of field instrumentation and sensors. The NHERI@UTexas facility targets four main challenges: (1) performing deeper, more accurate, higher resolution 2D/3D subsurface geotechnical imaging, (2) characterizing the nonlinear dynamic response and liquefaction resistance of complex geomaterials *in situ*, (3) developing *in-situ* methods to perform nondestructive soil-foundation-structure interaction (SFSI) studies, and (4) rapid investigation of geotechnical parameters at high-profile and natural hazard events (after Stokoe et al., 2017). In this article, examples of how this unique equipment has been applied to support the goals of numerous researchers and also outlines the enhancements made to expand field testing capabilities.

Data availability statement

The original contributions presented in the study are included in the article/supplementary material, further inquiries can be directed to the corresponding authors.

Author contributions

KS: Writing–original draft, Writing–review and editing, Funding acquisition, Project administration, Resources, Supervision. SH: Data curation, Formal Analysis, Project administration, Validation, Visualization, Writing–original draft, Writing–review and editing. BC: Data curation, Methodology, Project administration, Writing–original draft, Writing–review and editing. PC: Methodology, Writing–original draft, Writing–review and editing. RG: Methodology, Writing–original draft, Writing–review and editing.

Funding

The author(s) declare that financial support was received for the research, authorship, and/or publication of this article. The U.S. National Science Foundation financially supports the development and operation of the NHERI@UTexas Equipment Sites under grant CMMI-2037900. The research projects included in this paper were funded by grants CMMI-2120155, CMMI-1930697, CMMI-2100889, EAR-2218645/2218646, CMMI-2317659/2317660, EEC-1449501, and CMMI-1761597.

Acknowledgments

The authors would like to thank the U. S. National Science Foundation for the financial support to develop and operate the NHERI@UTexas Equipment Sites under grant CMMI-2037900. The authors also would like to thank the following researchers who utilized the NHERI@UTexas equipment facility including Drs. Arash Khosravifar, Armin Stuedlein, Diane Moug, Clinton Wood, Edward Kavazanjian, Khiem Tran, Roger Denlinger, Jyotsna Sharma, Leon van Paassen, Susan Bilek, Joel Johnson, Daniel Cadol, Danica Roth, and Nenad Gucunski. Special thanks also go to the graduate students and staff members at the University of Texas at Austin who assisted in the field work, including Drs. Benchen Zhang, Julia Roberts, Gunwoong Kim, Reihaneh Hosseini, Zhongze Xu, Farnyuh Menq, Jihwan Lee, Chenghao Bai, Cecil Hoffpauir, Andrew Valentine, Elido Ruiz, and Robert Kent.

Conflict of interest

The authors declare that the research was conducted in the absence of any commercial or financial relationships that could be construed as a potential conflict of interest.

Generative AI statement

The author(s) declare that Gen AI was used in the creation of this manuscript.

Publisher's note

All claims expressed in this article are solely those of the authors and do not necessarily represent those of their affiliated organizations, or those of the publisher, the editors and the reviewers. Any product that may be evaluated in this article, or claim that may be made by its manufacturer, is not guaranteed or endorsed by the publisher.

References

Abbas, A., Cox, B. R., Tran, K. T., Corey, I., and Dawadi, N. (2024a). An open-access data set of active-source and passive-wavefield DAS and nodal seismometer measurements at the Newberry Florida site. *Seismol. Res. Lett.* 95, 1082–1098. doi:10.1785/0220230216

Abbas, A., Cox, B. R., Tran, K. T., Corey, I., Dawadi, N., and Menq, F. (2023). Active-source and passive-wavefield DAS and nodal station measurements at the Newberry Florida site. *DesignSafe-CI*. doi:10.17603/ds2-50eh-7v93

Abbas, A., Cox, B. R., Tran, K. T., Kumar, K., and Crocker, J. (2024b). Emerging technologies and advanced analyses for non-invasive near-surface site characterization. Soils and Rock. *Int. J. Geotechnical Environ. Eng.* doi:10.28927/SR.2024.006923

Coduto, D. P., Kitch, W. A., and Yeung, M. R. (2015). *Foundation design: principles and practices*. 3rd Edition. Upper Saddle River, NJ: Prentice Hall.

Decker, R. W. (1987). "Dynamics of Hawaiian volcanoes: an overview," in *Volcanism in Hawaii: papers to commemorate the 75th anniversary of the founding of the Hawaiian Volcano Observatory* (Reston, VA: U.S. Geol. Surv. Prof. Pap.), 1350, 997–1018.

Denlinger, R., O'Connell, D. R. H., Lin, G., Roecker, S., and Bennington, N. (2024). An unprecedented experiment to map Kilauea's summit magma system. *Eos* 105. doi:10.1029/2024EO240392

Denlinger, R. P. (1997). A dynamic balance between magma supply and eruption rate at Kilauea volcano, Hawaii. *J. Geophys. Res.* 102 (18), 18091–18100. doi:10.1029/97JB01071

Denlinger, R. P., and Flinders, A. (2024). Density structure of Kīlauea volcano: implications for magma storage and transport. *Geophys. J. Int.* 237 (1), 1339–1352. doi:10.1093/gji/ggae101

Fiske, R. S., and Kinoshita, W. T. (1969). Inflation of Kīlauea volcano prior to its 1967-1968 eruption: vertical and horizontal deformation give clues regarding the structure of an active Hawaiian volcano. *Science* 165, 341–349. doi:10.1126/science.165.3891.341

Huang, H. W., Wang, J., Zhao, C., and Mo, Y. L. (2020). Two-dimensional finite-element simulation of periodic barriers. *J. Eng. Mech.* 165, 147. doi:10.1061/(asce)em.1943-7889.0001891

Huang, H. W., Zhang, B., Wang, J., Menq, F. Y., Nakshatrala, K. B., Mo, Y. L., et al. (2021). Experimental study on wave isolation performance of periodic barriers. *Soil Dyn. Earthquake Eng.* 144, 106602. doi:10.1016/j.soildyn.2021.106602

Pietruszka, A. J., Heaton, D. E., Marske, J. P., and Garcia, M. O. (2015). Two magma bodies beneath the summit of Kīlauea Volcano unveiled by isotopically distinct melt deliveries from the mantle. *Earth Planet. Sci. Lett.* 413, 90–100. doi:10.1016/j.epsl.2014.12.040

Poland, M. P., Miklius, A., and Montgomery-Brown, E. K. (2014). "Magma supply, storage, and transport at shield-stage Hawaiian volcanoes," in *Characteristics of Hawaiian volcanoes* (Reston, VA: U.S. Geol. Surv. Prof. Pap.), 1801, 179–234. doi:10.3133/pp18015

Stokoe, K. H., Cox, B., Clayton, P., and Menq, F. (2017). *NHERI@UTEXAS experimental facility: large-scale mobile shakers for natural-hazards field studies*. Santiago: Chile: 16th World Conference on Earthquake.

Stokoe, K. H., Hwang, S., Cox, B. R., Menq, F., Roberts, J., and Park, K. (2019). "Field studies of the natural and built environments using large mobile shakers," in *7th international conference on earthquake geotechnical engineering (7 ICEGE)* (Roma: Italy), 17–20.

Stokoe, K. H., Menq, F., Zhang, B., and Kim, G. (2020). "Field assessment of microbially-induced carbonate precipitation (MICP) and microbially-induced desaturation and precipitation (MIDP) methods," in *Geotechnical engineering report GR20-01, geotechnical engineering center* (Austin, TX: the University of Texas at Austin).

Tran, K. T., and Hiltunen, D. R. (2011). Inversion of first-arrival time using simulated annealing. *J. Environ. Eng. Geophys* 16, 25–35. doi:10.2113/JEEG16.1.25

Tran, K. T., McVay, M., Faraone, M., and Horhota, D. (2013). Sinkhole detection using 2D full seismic waveform tomography. *Geophysics* 78 (5), R175–R183. doi:10.1190/geo2013-0063.1

Tran, K. T., Nguyen, T. D., Hiltunen, D. R., Stokoe, K. H., and Menq, F. (2020). 3D full-waveform inversion in time-frequency domain: field data application. *J. Appl. Geophys.* 178, 104078. doi:10.1016/j.jappgeo.2020.104078

Vantassel, J. P., Cox, B. R., Hubbard, P. G., Yust, M. B. S., and Menq, F. (2022). "Active-source, near-surface, surface-wave measurements using distributed acoustic sensing (DAS) and traditional geophones," in *Characterization of the NHERI@UTexas Hornsby Bend test site [version 2]. DesignSafe-CI*. doi:10.17603/ds2-bz52-ep82

Wang, J., Huang, H. W., Zhang, B., Menq, F.-Y., Nakshatrala, K. B., Mo, Y. L., et al. (2022). Active isolation tests of metamaterial-based barriers and foundation. *Eng. Struct.* 260, 114253. doi:10.1016/j.engstruct.2022.114253

Yust, M. B. S., Cox, B. R., Menq, F., Hubbard, P. G., and Vantassel, J. P. (2022a). "Active-source, near-surface, surface-wave measurements using distributed acoustic sensing (DAS), cone penetration testing (CPT), and downhole (DH) testing," in *Characterization of the NHERI@UTexas Hornsby Bend test site [version 2]. DesignSafe-CI*. doi:10.17603/ds2-6ap5-sk09

Yust, M. B. S., Cox, B. R., Vantassel, J. P., Hubbard, P. G., Boehm, C., and Krischer, L. (2022b). DAS for 2D MASW imaging: a case study on the benefits of flexible sub-array processing. *arXiv* 2210, 14261. doi:10.48550/arXiv.2210.1426

Yust, M. B. S., Cox, B. R., Vantassel, J. P., Hubbard, P. G., Boehm, C., and Krischer, L. (2023). Near-surface 2D imaging via FWI of DAS data: an examination on the impacts of FWI starting model. *Geosciences* 13 (3), 63. doi:10.3390/geosciences1303 0063

Zhang, B., Huang, H. W., Menq, F.-Y., Wang, J., Nakshatrala, K. B., Stokoe, K. H., et al. (2022). Field experimental investigation on broadband vibration mitigation using metamaterial-based barrier-foundation system. *Soil Dyn. Earthq. Eng.* 155, 107167. doi:10.1016/j.soildyn.2022.107167

frontiers | Frontiers in Built Environment

TYPE Original Research
PUBLISHED 23 January 2025
DOI 10.3389/fbuil.2025.1512507

Check for updates

OPEN ACCESS

EDITED BY
Jack Cadigan,
Engineer Research and Development Center (ERDC), United States

REVIEWED BY
Jasmine Bekkaye,
Louisiana State University, United States
Julie Paprocki,
University of New Hampshire, United States
Richard Johansen,
Engineer Research and Development Center (ERDC), United States

*CORRESPONDENCE
Robin Nelson,
robin.nelson@utsa.edu

RECEIVED 16 October 2024
ACCEPTED 03 January 2025
PUBLISHED 23 January 2025

CITATION
Nelson R, Vielma KI and Browning J (2025) NHERI education and community outreach: longitudinal, educational outcomes of a coordinated, distributed network.
Front. Built Environ. 11:1512507.
doi: 10.3389/fbuil.2025.1512507

COPYRIGHT
© 2025 Nelson, Vielma and Browning. This is an open-access article distributed under the terms of the Creative Commons Attribution License (CC BY). The use, distribution or reproduction in other forums is permitted, provided the original author(s) and the copyright owner(s) are credited and that the original publication in this journal is cited, in accordance with accepted academic practice. No use, distribution or reproduction is permitted which does not comply with these terms.

NHERI education and community outreach: longitudinal, educational outcomes of a coordinated, distributed network

Robin Nelson[1]*, Karina I. Vielma[2,3] and JoAnn Browning[1]

[1]Department of Civil and Environmental Engineering, Natural Hazards Engineering Research Infrastructure (NHERI), University of Texas at San Antonio, San Antonio, TX, United States, [2]Engineering Education Program, Department of Biomedical Engineering and Chemical Engineering, Natural Hazards Engineering Research Infrastructure (NHERI), University of Texas at San Antonio, San Antonio, TX, United States, [3]Engineering Education Program, Department of Interdisciplinary Learning and Teaching, Natural Hazards Engineering Research Infrastructure (NHERI), University of Texas at San Antonio, San Antonio, TX, United States

The U.S. National Science Foundation (NSF) Natural Hazards Engineering Research Infrastructure (NHERI) Network Coordination Office (NCO) Education and Community Outreach (ECO) led coordinated efforts to promote educational activities along various pathways for students and educators targeted at broadening participation in and awareness of natural hazards engineering research through the Research Experiences for Undergraduates (REU) Summer Program, the Graduate Student Council (GSC), and the Summer Institute for Early Career Researchers and K-12 Educators. NHERI connects a diverse group of undergraduate and graduate students, faculty and K-12 educators, and researchers interested in mitigating the effects of natural hazards through these flagship educational programs. After 6 years of implementing these integrated educational activities, longitudinal outcomes and impacts for both students and faculty have been collected and are reported in this paper. Embedded in this report are several best practices used in educational outreach for recruitment, mentoring, and engagement of diverse participants that have been evaluated and enhanced through assessment and in collaboration with the larger NHERI network. Throughout 6 years of leading education activities, these practices have also helped create an intentional focus on challenge areas and informed the evolution of interdisciplinary pathways for natural hazards engineering research.

KEYWORDS

broadening participation, educational impacts, NHERI, REU, early-career faculty, NSF

1 Introduction

As a diverse science, technology, engineering, and math (STEM) workforce continues to be a critical area for improvement within the United States (National Academies of Science, Engineering and Medicine, 2016), the U.S. National Science Foundation (NSF) Natural Hazards Engineering Research Infrastructure (NHERI) Network Communication Office (NCO) Education Community Outreach (ECO), or NHERI ECO for short, developed inclusive pathways to support members of underrepresented groups (URGs) in pursuit of STEM careers. These URGs include women and historically marginalized racial and ethnic

participants (American Society for Engineering Education, 2022). As part of a large, distributed network of natural hazards engineering research and experimental facilities across twelve universities and thirteen components, the NHERI ECO developed educational programming to prepare and support future natural hazards engineers and researchers. These programs are developed, executed, and assessed in collaboration with these network components. In collaboration with educational experts, educational activities are also designed using evidence-based practices. These practices are adapted to focus on engaging the various targeted audiences that the NHERI ECO aims to reach. This paper presents the NHERI ECO programming as a whole and its impact on broadening participation for URG within the STEM workforce and specifically, the natural hazards engineering research community.

2 NSF NHERI NCO ECO programs

The NHERI ECO programs are organized and orchestrated collaboratively between the NHERI ECO and the ECO Committee. The ECO Committee is composed of representatives from each of the NHERI components (See Figure 1 for details) and is chaired by a member of the NHERI ECO responsible for the education activities. The ECO Committee meets monthly to strategically organize network-wide education and outreach activities. NHERI facility representatives who serve on the ECO Committee also play an essential role in communicating between their sites, other NHERI facilities, and the NCO. Working together, NHERI ECO launched two flagship educational programs in 2017, the NSF NHERI Research Experiences for Undergraduates (REU) Summer Program and the NSF NHERI Summer Institute for Early-Career Researchers and K-12 Educators. Both programs were developed to illuminate pathways for members of underrepresented groups (URGs) in STEM and provide necessary training, career development, resource awareness, and support. In 2020, educational programs were adapted to regulations resulting from the COVID-19 pandemic. In 2021, the virtual graduate student program, known as the NSF NHERI Graduate Student Council (GSC), was added in response to community input to create a continuous STEM workforce pathway to natural hazards engineering and research linking the two previous programs.

2.1 NSF NHERI REU summer program

The REU Summer Program is a hybrid (virtual and in-person) program and coordinated effort across the NHERI network sites that engages up to thirty-three, funded undergraduate students of all classes (freshman-senior) in natural hazards engineering research. Undergraduate researchers often participate in their first hands-on research project during the summer program and experience a research-based curriculum designed to introduce students to the rhetoric of scholarly writing in their specific disciplines through a scaffolded weekly approach tailored to their experience. Over the ten-week summer program, participants are mentored in person by experienced NHERI faculty and staff as they conduct research at one of the NHERI research and experimental facilities. Students are also guided and purposefully mentored by the NHERI ECO Program Coordinator and Education Specialist in weekly virtual research meetings and personal check-ins as they create their research posters, presentations, and papers. In weekly virtual meetings, they also build community with their peers across the NHERI sites by sharing their experiences and problem-solving challenges. The program ends with an in-person culminating event, the NSF NHERI REU Symposium, hosted at one of the NHERI components that provides participants an opportunity to share research and network with their peers. The REU program offers research and career training, a network of mentors, and socializing in the engineering and research community that prepares participants for future careers in STEM, specifically in natural hazard mitigation.

2.2 NSF NHERI graduate student council

In response to an observed need to bridge the undergraduate experience with the needs of early career faculty, NHERI ECO also developed a program that supports graduate students through the GSC which was launched in October of 2021 as a student-led virtual organization. Designed to connect like-minded graduate students from around the world, the GSC invites graduate students interested in mitigating natural hazards to connect with peers and prominent researchers from NHERI and beyond. The group is committed to offering learning opportunities and career development programs to graduate students without registration fees. Beyond building community, the organization offers graduate students leadership opportunities, workshops, mini-conferences, general monthly meetings with speakers from the natural hazard community, and various funding opportunities. GSC members also mentor REU students, serve on panels, and lead presentations that benefit and engage undergraduate researchers interested in natural hazards engineering. The GSC has become an integral piece of the education pathways within NHERI, supporting and preparing the next-generation of the STEM workforce.

2.3 NSF NHERI summer institute for early career faculty

Finally, the NHERI ECO engages early-career faculty and researchers in preparation to successfully begin and continue their academic and research careers. The Summer Institute for Early Career Researchers is a three-day intensive workshop focused on introducing NSF grant writing, presenting NHERI resources (i.e., experimental facilities, NSF NHERI Science Plan, NSF NHERI Technology Transfer Committee, DEI/Broader Impacts), and building community through networking that supports twenty funded early career faculty, five GSC members, and five K-12 certified teachers as education consultants. NHERI faculty and staff from all eleven sites present information on experimental, simulation, reconnaissance, and cyberinfrastructure resources. Site representatives also mentor participants and help scaffold a grant writing experience with a series of workshops, speakers, and panels. The event ends with presentations from collaborative groups of early career faculty. They present a mock grant proposal created during the workshop to a panel of judges selected from the natural hazards engineering community. A top proposal is selected as the

FIGURE 1
Diagram of NSF NHERI distributed network.

winning team, and all interdisciplinary groups receive proposal feedback from accomplished NSF-funded researchers. This unique workshop offers information about NHERI experimental facilities, components, resources, and awareness to begin the proposal process in partnership with a NHERI site using the Science Plan, knowledge about NSF grant guidelines, and guidance from a Civil, Mechanical, and Manufacturing Innovation (CMMI) NSF Director, practice detailing broader impacts in an education plan with K-12 education consultants, and the opportunity to actively use this information and mentorship with peers to create a mock grant proposal.

3 Methodology

Using a longitudinal case study design (Singer and Willet, 2003; Yin, 2009), the NHERI ECO collected demographic application/registration data for each program, tracked longitudinal impact data, and analyzed changes in pre-program and post-program assessment surveys for participants funded through the REU and Summer Institute. All pre- and post-assessments used a Likert scale ranging from one (1), "Strongly disagree/Not at all," to five (5) "Strongly agree/A great deal."

The demographic information collected for each program included race/ethnicity, gender, first-generation college student status, home university's Carnegie classification (American Council on Education, 2024), geographic location, research experience, and major/career focus. Demographic and diversity data were collected for all three programs as seen in Table 1 (REU), Table 2 (NHERI GSC), and Table 3 (Summer Institute). Additionally, the demographic data were compared to national data from the American Society of Engineering Education (2022) to place the program in a national civil engineering context.

Further, longitudinal data were collected for the REU and Summer Institute participants through LinkedIn, Google Scholar, and/or NSF Award Search to track career progress after participation. This data specifically identified graduation date, discipline and level of degree attainment, and current employment status for past participants of both programs as well as the number of publications and amount of NSF funding awarded to Summer Institute alumni. In the future, NHERI GSC longitudinal data will be collected via a member graduate exit survey as well as with participant surveys.

The pre-program and post-program self-assessment data were collected for both REU and Summer Institute participants and analyzed using a paired sample t-test for its robustness against error to determine changes in research self-efficacy in participants using mean-difference (Fradette, et al., 2003; Rasch and Guiard, 2004; Wiedermann and von Eye, 2013). Bandura (2006) defined self-efficacy as an individual's confidence in their ability to perform

TABLE 1 NSF NHERI REU demographic breakdown [a]2017–2023.

Cohorts		2017 (n = 17)	2018 (n = 29)	2019 (n = 31)	2021 (n = 28)	2022 (n = 31)	2023 (n = 29)	Total ([b]*N* = 166)
Race	American Indian/ Alaskan Native	—	3%	—	—	—	—	1%
	Asian	29%	10%	13%	7%	—	27%	13%
	Black	18%	13%	7%	11%	18%	14%	13%
	Hispanic	12%	3%	29%	29%	18%	24%	19%
	Multiracial (At least one URG)	6%	16%	6%	21%	16%	14%	14%
	Native Hawaiian or Pacific Islander	—	3%	—	—	—	—	1%
	White	24%	52%	45%	32%	47%	21%	1%
	Not reported	11%	—	—	—	—	—	1%
Gender	Female	47%	52%	39%	50%	59%	69%	57%
	Male	53%	48%	61%	50%	41%	28%	42%
	Transgender non-conforming	—	—	—	—	—	3%	1%
First-Generation Status	First-Generation	41%	19%	19%	29%	19%	39%	27%
	Not First-Generation	47%	81%	78%	71%	81%	61%	72%
	Not reported	12%	—	3%	—	—	—	1%
Carnegie Classification	R1 University	65%	57%	71%	57%	65%	[c]52%	61%
	Non-R1 Universities	35%	43%	29%	43%	35%	[c]42%	39%

[a]NHERI did not host an REU program in 2020 due to the COVID-19 pandemic.
[b]Reflects one student who participated twice and one student who left the program without completing it.
[c]First year REU selection committee considered Carnegie Classification in selection process.

in a specific area. Further, Bandura (1977) argued that self-efficacy is most often developed through performance events that result in mastery, but may also be developed through observation, persuasion, and events that tax both mind and emotion. While all ECO programs endeavor to build research self-efficacy through such vicarious and performance events, the REU and Summer Institute collect pre- and post-program data to track research self-efficacy. Thus, after the survey data were collected from participants, questions that focused on research objectives (i.e., research reading, writing, presenting, preparation, and mentoring) were analyzed to identify the self-efficacy of participants after completing the NSF NHERI REU or Summer Institute programs [Table 4 (REU) and Table 5 (Summer Institute)].

In terms of the time of programming and intervention, each program is unique in its scope, aim, timeline, and funding, and thus, constitutes its own case study analysis. Between 2017 and 2023, selected REU students, funded by NSF, conducted research for 10 weeks during one summer of their undergraduate careers at one of the NHERI research and experimental facilities. Registered GSC members may elect to participate in monthly meetings, a mini-conference, and various workshops targeting graduate student members throughout the academic year (i.e., August-June). Five NHERI GSC members were selected each year to attend the Summer Institute as NSF-funded participants in 2022-2023. Also, between 2017 and 2023, NSF-funded Summer Institute early-career faculty participated in a three-day intensive workshop. The experience of each group of participants in the educational outreach efforts differed and was targeted to impact members' performance and vicarious experience positively, incorporating them into the natural hazards engineering research community.

TABLE 2 NSF NHERI GSC demographic breakdown[a] 2021–2023.

Cohorts[b]		2021 Y1 (n = 230)	2022 Y2 (n = 155)	Total (*N* = 385)
Race	American Indian/ Alaskan Native	0%	0%	0%
	Asian	30%	34%	32%
	Black	13%	12%	12%
	Hispanic	10%	5%	8%
	Multiracial (At least one URG)	3%	7%	4%
	Native Hawaiian or Pacific Islander	1%	1%	1%
	White	36%	30%	34%
	Not reported	7%	11%	9%
Gender	Female	38%	41%	39%
	Male	61%	57%	59%
	Not reported	1%	2%	1%
First-Generation Status	First-Generation	29%	44%	35%
	Not First-Generation	67%	52%	61%
	Not reported	4%	4%	4%
Geographic Diversity	Domestic (U.S. Citizen)	41%	40%	41%
	Domestic – Study within U.S.	41%	39%	40%
	Domestic – Study outside U.S.	2%	0%	1%
	International (not U.S. Citizen)	57%	59%	58%
	Int. – Study within U.S.	48%	46%	47%
	Int. – Study outside U.S.	8%	12%	10%
	Not reported	2%	1%	2%
Level of Degree	Doctoral Candidate	28%	22%	26%
	Doctoral Student	51%	51%	51%
	Master's (thesis)	12%	15%	13%
	Master's (coursework)	4%	8%	6%
	Other	5%	6%	4%
General Area of Study	Engineering/STEM	87%	87%	87%
	Social Science	13%	13%	13%

[a]NHERI launched the GSC in October 2021.
[b]Membership statistics are a snapshot of new membership added by year. Year 1 (Y1) 1 October 2021-31 July 2022; Year 2 (Y2) 1 August 2022-31 July 2023.

4 Program impact: broadening participation

One main objective of the NHERI ECO programs is to broaden participation of URGs in STEM with a specific focus on civil engineering and interdisciplinary hazards research. The NHERI ECO uses strategic recruitment, holistic application review, diversity, equity, and inclusion awareness and programming, and multiple program components aimed at supporting a diverse cohort of participants, i.e., skill building, mentoring, socialization,

10.3389/fbuil.2025.1512507

TABLE 3 NSF NHERI Summer Institute demographic breakdown[a] 2017–2023.

Cohorts		2017 (n = 18)	2018 (n = 21)	2019 (n = 20)	2021 (n = 18)	2022 (n = 22)	2023 (n = 30)	Total (*N* = 129)
Race	American Indian/ Alaskan Native	—	—	—	—	—	—	0% 0%
	Asian	22%	24%	55%	17%	27%	27%	29%
	Black	17%	—	5%	—	14%	7%	7%
	Hispanic	17%	5%	10%	11%	9%	13%	11%
	Multiracial (At least one URG)	6%	—	—	6%	9%	13%	6%
	Native Hawaiian or Pacific Islander	—	—	—	—	5%	—	1%
	White	22%	52%	30%	50%	32%	40%	38%
	Not reported	17%	19%	—	17%	5%	—	9%
Gender	Female	50%	52%	60%	56%	36%	43%	49%
	Male	50%	48%	40%	44%	64%	57%	51%
First-Generation Status	First-Generation	33%	38%	20%	28%	45%	43%	36%
	Not First-Generation	56%	57%	55%	72%	55%	57%	58%
	Not reported	11%	5%	25%	—	—	—	6%

[a]NHERI did not host a full in-person Summer Institute program in 2020 due to the COVID-19 pandemic.

TABLE 4 NSF NHERI REU research self-efficacy questions and results.

Question	Mean	SD	*t*	*df*	Sig.	Cohen's *d*
Q1: How much experience do you have engaging in real-world, hands-on engineering research?	1.62	1.29	15.62	154	0.000	1.26
Q3: How much experience do you have understanding the theory and concepts guiding a research project?	1.10	1.27	10.82	154	0.000	0.87
Q4: How much experience do you have understanding the relevance of research to your coursework?	0.88	1.35	8.16	154	0.000	0.66
Q5: How much experience do you have understanding what everyday research work is like?	1.70	1.23	17.18	154	0.000	1.38
Q7: How much experience do you have understanding research journal articles?	1.05	1.24	10.54	154	0.000	0.85
Q9: How much experience do you have understanding professional data and research presentations?	1.13	1.18	11.89	154	0.000	0.96
Q10: How much experience do you have writing scientific reports and publishable papers?	1.32	1.22	13.48	154	0.000	1.08
Q11: How much experience do you have preparing a scientific poster?	1.68	1.44	14.60	154	0.000	1.17
Q13: How much experience do you have explaining a research project to people outside the field?	1.41	1.38	12.73	154	0.000	1.02
Q20: How much experience do you have collaborating on a research project with an experienced faculty mentor?	1.57	1.61	12.08	154	0.000	0.97
Q22: How much experience do you have engaging in quality mentorship?	1.02	1.61	7.91	154	0.000	0.64

TABLE 5 NSF NHERI summer institute research self-efficacy questions and results.

Question	Mean	SD	*T*	*df*	Sig.	Cohen's *d*
Q1: How much experience do you have working with the natural hazards engineering community in general?	1.78	1.01	20	123	0.000	1.26
Q2: How much do you work with the natural hazards engineering community in your specialization (i.e., wind, coastal, earthquake, data, etc.)?	0.71	1.34	6	123	0.000	0.87
Q3: How much did you work with other natural hazards engineering professionals and researchers outside your specialization?	1.50	1.27	13	123	0.000	0.66
Q4: How much are you interested in collaborating with other natural hazards engineering professionals?	0.40	0.93	0.05	123	0.631	1.38
Q14: How much do you know about the NHERI community and their research work?	1.40	1.05	15	123	0.000	0.85
Q15: How much are you interested in learning more about the NHERI network, the research work, and resources?	−0.09	0.88	−1	123	0.266	0.96
Q10: How prepared do you feel writing a grant proposal that will supplement or extend your research?	0.90	1.10	9	123	0.000	1.08
Q11: How prepared do you feel working on research projects with other professionals/researchers outside your university?	0.59	1.18	6	123	0.000	1.17
Q17: How prepared do you feel working on research projects with other professionals/researchers outside your specialization?	0.516	1.18	5	123	0.000	1.02

supplemental learning, bridge programs, and funding (Palid et al., 2023), to reach this program objective. These programs also included methods to improve research self-efficacy through performance events, observation, and cognitive and emotional engagement (Bandura, 1977). These methods were intentionally selected to support participants since increased self-efficacy is known to predict STEM intentions which are also linked to persistence in STEM as well as supporting URG engagement (Estrada, et al., 2011).

The REU, GSC, and Summer Institute strategic recruitment methods include emailing individuals in departments and professors in ABET-accredited, Minority Serving Institutions (MSIs) and universities outside of Carnegie R1 institutions to reach underrepresented and underserved STEM populations and encourage application submissions and participation. This list includes emails for professors within civil engineering departments of MSIs and all NHERI components. In 2021, a social science list was also created to recruit participants for participation at the NSF NHERI CONVERGE Social Science Research Facility. CONVERGE supported REU participants in 2021 and 2023. This list was created with the help of CONVERGE representatives and included social scientists who focused on natural hazards and disaster resilience research. Finally, in 2024 the GSC began actively recruiting members from a small pilot group of international universities whose names were gathered from NCO and GSC leadership. Once the efforts are analyzed, the GSC may expand the international recruitment campaign.

The NHERI ECO and ECO Committee also trained the selection committee on the holistic review process. By 2023, this included consideration of seven diversity measures, along with other more traditional criteria, e.g., GPA, for recruitment and selection of ECO program participants. The seven demographic considerations included 1) race/ethnicity; 2) gender; 3) first-generation college student status; 4) geographic location; 5) home university Carnegie Classification; 6) previous research experience; and 7) native language. Initial considerations included the first four demographic items but were expanded to include all seven by the fall of 2022.

Beginning in the fall of 2022, NHERI ECO programming also consisted of diversity, equity, and inclusion workshops within the REU, GSC, Summer Institute, ECO Committee Meetings, NHERI-sponsored research summits, and multiple program components. The diversity, equity, and inclusion programming demonstrated NHERI's commitment to diverse cohorts and inclusive practices. These programs strengthened diverse representation across all flagship events and supported an understanding of the holistic review of applications and participation across the network. After conducting a literature review of 82 STEM intervention programs, Palid et al. (2023) argued that programs that used multiple components to support URGs "likely increase[d] participant success." Since persistence is often seen as a challenge within STEM fields, the NHERI ECO defines success as persistence in a STEM field or program whether in education or occupation. To support this definition of success, NHERI ECO programs offered all six program components identified in the review (i.e., mentoring, skill building, supplemental learning, socializing, bridge programs, and funding) across its programs to better support all participants. These components also support self-efficacy through the intentional use of performance events, observation/modeling opportunities, and cognitive and emotional engagement (Bandura, 1977).

4.1 REU summer program demographic data

Since 2017, NHERI ECO has hosted six REU cohorts, totaling 166 undergraduate research participants. Seventy-one percent of participants self-identified as civil engineering (i.e.,

civil engineering, civil and environmental engineering, and structural engineering) majors and other participants identified as 7% mechanical engineering, 5% architectural engineering, 4% environmental engineering, 3% computer science, 2% geology, 2% mathematics, 1% aerospace engineering, 1% anthropology, 1% biological systems engineering, 1% computer engineering, 1% electrical engineering, 1% engineering, 1% environmental analysis, 1% geotechnical engineering, 1% sociology, 1% urban planning. Each January, all REU cohort data is updated to provide a longitudinal view of participants' progress which begins a semester after completing the REU Summer Program. This paper provides a snapshot of the ongoing longitudinal data from participants from 2017–2023. Of the program alumni, 64% earned their undergraduate degrees, 34% remained in their undergraduate program, and 2% did not respond or found on LinkedIn. These participants were classified as having an unknown status. All accessible participants tracked longitudinally via LinkedIn, have completed or remained in STEM degree programs as of January 2024. Over a third of the REU alumni (35%) have pursued graduate degrees, and 8% were pursuing a doctoral degree in STEM at the time of publication.

Table 1 shares the demographic breakdown of the 166 undergraduate students who participated in the REU Summer Program. The impact of the REU program in broadening participation for URGs in civil engineering from 2017–2023 (except 2020 when no program was offered due to the COVID-19 pandemic) is reflected in its participant make-up, success, and self-efficacy.

The average percentage of students who identified as members of an underrepresented group in STEM, specifically civil engineering, from the REU program include 13.4% Black, 19.5% Hispanic, and 0.6% American Indian or Alaskan Native (AIAN). According to the American Society for Engineering Education (2022) national statistics of students enrolled in engineering programs, only 5.4% identify as Black, 15.8% as Hispanic, and 0.3% as AIAN; therefore, the REU program is increasing the participation percentages compared to the national average. The program aims to expand the representation across typical populations to provide a positive research experience for all participants. Similarly, while 57.3% of REU participants self-identified as women, only 24.2% of engineering undergraduate degrees and 35.6% of civil engineering undergraduate degrees were awarded to women nationally (American Society for Engineering Education, 2022).

Research has shown that diverse populations can provide better solutions to the problems society faces (Hong and Page, 2004), so it is also important to consider other areas of diversity when working to broaden participation. This includes first-generation students currently enrolled in a bachelor's program whose parents or guardians did not earn a four-year degree (RTI International, 2024); students who attend universities not categorized as Carnegie R1 institutions which may be less likely to offer undergraduate research opportunities; and geographic location.

While NHERI ECO tracks a number of diversity measures, it is more difficult to place these three categories into a larger context. For example, the Center for First-Generation Student Success 2018 report defines a first-generation student as an "undergraduate student whose parents do not have a bachelor's degree" (RTI International, 2024). Although this is the first-generation definition utilized by the NHERI ECO, the definition of first-generation varies by institution. Only 73% of universities define first-generation college students (Whitley, et al., 2018). According to the First-Gen Forward fact sheets produced by RTI International (2023), 54% of all undergraduate students in 2019–2020 identified as first-generation college students. But when looking specifically at engineering students approximately 3.9% of first-generation college students majored in engineering between 1992 and 2000 (Chen and Carroll, 2005). Of the 166 REU participants from 2017–2023, 27% identified as first-generation college students.

Geographic location is another criterion utilized in participant selection as it addresses underserved populations or areas. In 2017, the Established Program to Stimulate Competitive Research (EPSCoR) was created to fund research in 27 jurisdictions (i.e., states, territories, and commonwealths) that received less federal research funding (U.S. National Science Foundation, 2024). These specific geographic underserved locations receive targeted funding to encourage STEM workforce development and research. EPSCoR is also part of the NSF Broadening Participation Portfolio designed to expand STEM opportunities (NSF, n.d.). REU students from 2017–2023 originated from 37 U.S. states, territories, and the District of Columbia. Of the 166 REU participants, 23% attended school in an EPSCoR jurisdiction. By supporting students from EPSCoR, NHERI ECO continues NSF's work in building more pathways for students to pursue STEM careers.

Finally, as an NSF-funded program, ensuring funding is equitable across states and universities and the students supported is critical. This equitable distribution also helps to ensure diversity in thought. In 2023 the NHERI ECO began tracking and considering Carnegie Classification as part of the holistic selection process of REU applications. NSF encourages REU programs to support students from institutions that may not receive the same research opportunities. From 2017–2023, 39% of REU participants attended a university not categorized as Carnegie R1 (very high research activity as defined by the Carnegie classification system) (ACE, n.d.). Carnegie R1 research universities support robust research experiences for undergraduates that receive more funding (Jayabalan, et al., 2021). By including the Carnegie Classification as one of the seven categories included in the application review, NHERI hopes to further broaden STEM opportunities for students with fewer undergraduate research opportunities.

4.2 Graduate student council demographic data

The NHERI GSC was launched in October 2021 as a student-led organization to provide virtual programming and mentorship for a community of like-minded graduate students interested in natural hazards research. In the first 2 years of operation (1 October 2021 – 31 July 2023), the GSC registered 385 new members, and the demographic breakdown can be viewed in Table 2. Over half (58%) of the membership originated from countries other than the United States with 41 countries represented. Of the members who are not U.S. citizens, 11% percent are international students studying outside the United States. Doctoral students and candidates made up the largest sector of membership (77%), 19% were master's students, and 4% were listed as other—comprised of assistant professors,

post-doctoral scholars, and undergraduate students. Overall, the NCO-ECO team was pleased with this distribution of membership as it demonstrates pathways for master's students interested in pursuing research-related degrees and significant support for doctoral students seeking entrance into research positions.

Of the GSC members in the first two years, 12% identified as Black, and 8% identified as Hispanic. The GSC membership compares favorably to the national statistics of engineering doctoral degrees awarded which reported 3.9% Black and 7.5% Hispanic (American Society for Engineering Education, 2022). In addition, when NHERI GSC membership is compared to the national statistics of U.S. science and engineering faculty with 2.5% Black and 3.9% Hispanic (American Society for Engineering Education, 2022), the members show promise for broadening representation for future faculty positions and the next-generation STEM workforce. The graduate student organization reported that 39% of members identified as female compared to the 26.2% of females who were awarded engineering doctoral degrees and the 18.6% of females who were employed as science and engineering faculty (American Society for Engineering Education, 2022).

Thirty-five percent (35%) of GSC members identified as the first in their family to earn an undergraduate degree. However, many graduate schools or surveys use a different definition of first-generation college students. As mentioned earlier, all NHERI ECO programs define a first-generation individual as a student whose parents or guardians did not complete a four-year degree. One brief, *Understanding Career Pathways for Program Improvement*, using data from the Council of Graduate Schools, defined first-generation as a student who is the "first in their generation to earn a bachelor's degree and pursue a doctoral degree" (Mitic, 2022). The brief reported that 23% of engineering doctoral students identified as first-generation college students, which again demonstrates the diversity of the GSC.

Since the NHERI GSC accepts members from institutions around the world, its focus is on the number of countries represented rather than states. Members hail from 41 countries, and over half of the members reported citizenship outside the U.S. (58%). American Society for Engineering Education (2022) reported that 57% of the engineering doctoral program enrollment comes from countries other than the United States. Of the international members, 10% are enrolled in institutions outside the U.S. This includes members of the GSC leadership team who attend institutions in Hungary, Nepal, Nigeria, and Iran.

4.3 Summer institute demographic data

NHERI's Summer Institute has hosted six cohorts of participants, totaling 129 early career faculty and researchers from 40 U.S. states, territories, and the District of Columbia since 2017. The Summer Institute participants represented 13 EPSCoR jurisdictions with 22% of participants enrolled or employed at an institution within an EPSCoR jurisdiction. Pivoting from the in-person Summer Institute, a virtual-only program was held in 2020 due to the COVID-19 pandemic and was open to all members of the community for participation; because of this, no demographic data were available for 2020 Summer Institute participants. Demographic data from participants is identified in Table 3. Early career participants included senior-level graduate students, postdoctoral fellows, researchers, and assistant professors; individuals are tracked longitudinally through LinkedIn, Google Scholar, and NSF Award Search.

Of the Summer Institute alumni, 6.8% identified as Black, and 10.6% identified as Hispanic, compared to 2.5% Black and 3.9% Hispanic of U.S. science and engineering faculty (American Society for Engineering Education, 2022) or the 5% Black and 9% Hispanic for individuals above the age of 25 in engineering positions, according to the Pew Research Center (Fry, et al., 2021). Further, 49% of Summer Institute participants identified as women compared to 18.6% of science and engineering faculty (American Society for Engineering Education, 2022) or 15% of engineers and architects who identified as women (Fry, et al., 2021) Thirty-six percent (36%) of Summer Institute alumni also identified as the first in their family to complete a four-year degree.

Finally, of the Summer Institute participants, 35% of postdoctoral scholars and graduate students secured tenure-track positions, compared to the 12.8% of engineering doctoral graduates who Larson et al. (2013) calculated from 2011 ASEE data can secure a tenure-track faculty position based on the number of graduates and faculty members and the current rate of growth of engineering departments. Similarly, Roy, et al. (2024) expanded Larson et al. (2013) work to include ASEE data from 2006–2021 and found 12.4% of doctoral engineering graduates are likely to secure a tenure-track faculty position. At the time of publication, Summer Institute alumni amassed $39.7 million in NSF funding, published 2,392 articles, won seven prestigious NSF Faculty Early CAREER Awards, and obtained one NSF Graduate Researcher Fellowship Program Award after participating in the Summer Institute.

5 Program impacts

Besides bringing together a diverse group of participants, the NHERI REU and Summer Institute programs provided educational opportunities for them to expand their career experiences. Because the programs were intentionally designed to provide targeted learning outcomes for each audience, it was expected that shifts in learning metrics and research self-efficacy would be achieved. Below is a report of some of the highlights of the learning outcomes and educational impacts for six cohorts of the REU Summer Program and the Summer Institute from 2017–2023.

5.1 REU educational impacts on research self-efficacy

While research experiences supported by specific program components are shown to support members of URGs, self-efficacy has also been found to have a positive impact on URG's STEM outcomes (Palid, et al., 2023). Thus, the final NHERI REU table shares the pre- to post-assessed research self-efficacy of the 2017–2023 NHERI REU participants which were analyzed using a paired samples t-test in SPSS 27 (Table 4). The table compares the mean (*M*) and standard deviation (*SD*) of change in research self-efficacy. The longitudinal undergraduate participant data shows a statistically significant growth in research self-efficacy in each key area after a 10-week REU experience.

REU participants showed a statistically significant increase in self-efficacy in understanding theory and concepts (M = 1.10, SD = 1.27), $t(154) = 10.82$, $p < 0.0005$ $d = 0.87$, journal articles (M = 1.05, SD = 1.24) $t(154) = 10.54$, $p < 0.0005$, $d = 0.85$, professional data and research presentations (M = 1.13, SD = 1.18) $t(154) = 11.89$, $p < 0.0005$, $d = 0.96$, relevance of research to coursework (M = 0.88, SD = 1.35), $t(154) = 8.16$, $p < 0.0005$, $d = 0.66$, and what is involved in everyday research (M = 1.70, SD = 1.23), $t(154) = 17.18$, $p < 0.0005$, $d = 1.38$. Participants also demonstrated a statistically significant improvement in confidence in engaging in hands-on research (M = 1.62, SD = 1.29), $t(154) = 15.62$, $p < 0.0005$, $d = 1.26$, writing papers (M = 1.32, SD = 1.22), $t(154) = 13.48$, $p < 0.0005$, $d = 1.08$, creating and preparing posters (M = 1.68, SD = 1.44), $t(154) = 14.60$, $p < 0.0005$, $d = 1.17$, and discussing scientific concepts with those outside the field (M = 1.41, SD = 1.38), t(154) = 12.73, $p < 0.0005$, $d = 1.02$. Finally, the data also shows that participants experienced a statistically significant amount of quality mentorship (M = 1.02, SD = 1.61), $t(154) = 7.91$, $p < 0.0005$, $d = 0.64$ and mentor collaboration (M = 1.57, SD = 1.61), $t(154) = 12.08$, $p < 0.0005$, $d = 0.97$ during their research experience. The effect size of all results ranged from medium (0.50–0.79) to large effect size (0.80+) as shown in Cohen's d column in Table 4 (Cohen, 1988).

5.2 Summerns institute impacts on knowledge and research self-efficacy

Summer Institute participants' knowledge and self-efficacy show statistically significant improvement for all self-efficacy questions except Q4 and Q15. Pre- and post-assessment data demonstrate that participants developed additional experience working with the natural hazards engineering community in general (M = 1.78, SD = 1.01), $t(123) = 20$, $p < 0.0005$, $d = 1.26$, within their specialization (M = 0.71, SD = 1.34), $t(123) = 6$, $p < 0.0005$, $d = 0.87$, and outside their specialization (M = 1.50, SD = 1.27), $t(123) = 13$, $p < 0.0005$, $d = 0.66$. Although there was a mean increase between pre- and post-assessment, there was not a statistically significant change in participants' interest in collaborating with other natural hazards engineering professionals (M = 0.40, SD = 0.93), $t(123) = 0.05$, p = 0.631 $d = 1.38$, nor learning about the NHERI network, the research work, and resources (M = -0.09 SD = 0.88), $t(123) = -1$, $p = 0.266$, $d = 0.96$. Participants reported a statistically significant increase in knowledge about the NHERI network and its resources (M = 1.40, SD = 1.05) $t(123) = 15$, $p < 0.0005$, $d = 0.85$, feelings of preparedness to write a proposal supplementing or extending their research (M = 0.90, SD = 1.10), $t(123) = 9$, $p < 0.0005$, $d = 1.08$, with researchers outside their university (M = 0.59, SD = 1.18), t(123) = 6, $p < 0.0005$, $d = 1.17$, and with researchers outside their specialization (M = 0.51, SD = 1.18), $t(123) = 5$, $p < 0.0005$, $d = 1.02$. All questions' effect sizes also ranged from medium (0.50–0.79) to large effect sizes (0.80+) as shown in Table 5 under Cohen's d (Cohen, 1988).

6 Conclusion

The NHERI ECO, ECO Committee, and NHERI research and experimental facilities collaborated to identify pathways to broaden participation for underrepresented populations in STEM and natural hazards engineering research. The NHERI community used targeted recruitment efforts for participants at MSIs, holistic application review, diverse and inclusive training and programming, and multiple supportive program components (Palid et al., 2023) as well as intentional programming that included performance mastery and vicarious learning experience (Bandura, 1977) to engage the whole individual academically, personally, and socially. These focused activities helped to open various, diverse pathways that support undergraduates, graduate students, and early-career faculty and connect them with accomplished NHERI researchers and scholars. These pathways help broaden participation in STEM and natural hazards engineering research while expanding the interdisciplinary knowledge needed to effectively mitigate future natural hazards. The demographic, longitudinal, and pre-assessment and post-assessment data demonstrate the varied pathways that participants take within the natural hazard workforce. These data also provide the impact of knowledge gained through participation in established programs. The NHERI ECO, ECO Committee, and the NHERI research and experimental facilities worked to deliberately create a community supporting the next-generation of natural hazards researchers.

For engineering educators interested in preparing the next-generation of diverse workforce and faculty (American Society of Engineering Education and National Academy of Engineering, 2024), it is critical to enlist the expertise of equity-focused education and engineering education researchers. This can be done by collaborating with engineering education experts on program design, recruitment, holistic selection, implementation, and assessment, or by training to learn the many ways engineering education research can improve programs. During the formative stages of the REU and Summer Institute programs, lesson plans were created in partnership with education experts that included learning objectives, activities designed to engage participants, and assessments connected to the grant's goals and the established learning objectives. In this way, the focus of the education outreach activities was meaningful and targeted toward equity by design. These actions remain essential to creating pathways where people from all backgrounds feel welcomed and included. Their ideas and ways of problem-solving can lead to more innovations in the much-needed and evolving natural hazards engineering fields.

Data availability statement

The raw data supporting the conclusions of this article will be made available by the authors, without undue reservation.

Ethics statement

The studies involving humans were approved by the Shannon Marquess and Tammy Lopez, University of Texas at San Antonio. The studies were conducted in accordance with the local legislation and institutional requirements. The participants provided their written informed consent to participate in this study. Written informed consent was obtained from the individual(s) for the

publication of any potentially identifiable images or data included in this article.

Author contributions

RN: Formal Analysis, Investigation, Writing–original draft, Writing–review and editing. KV: Conceptualization, Supervision, Writing–original draft, Writing–review and editing. JB: Project administration, Supervision, Writing–review and editing.

Funding

The author(s) declare that financial support was received for the research, authorship, and/or publication of this article. The programs and research are based upon work supported by the U.S. National Science Foundation under the Natural Hazards Engineering Research Infrastructure Network Coordination Office Award No. 2129782.

Conflict of interest

The authors declare that the research was conducted in the absence of any commercial or financial relationships that could be construed as a potential conflict of interest.

Generative AI statement

The author(s) declare that no Generative AI was used in the creation of this manuscript.

Publisher's note

All claims expressed in this article are solely those of the authors and do not necessarily represent those of their affiliated organizations, or those of the publisher, the editors and the reviewers. Any product that may be evaluated in this article, or claim that may be made by its manufacturer, is not guaranteed or endorsed by the publisher.

References

American Council on Education (ACE) (2024). "Carnegie classification of institutions of higher education," in *Carnegie classification*. Available at: https://carnegieclassifications.acenet.edu (Accessed September 25, 2024).

American Society for Engineering Education (ASEE) (2022). Profiles of engineering and engineering technology. Available at: https://ira.asee.org/wp-content/uploads/2024/03/Engineering-and-Engineering-Technology-by-the-Numbers-cover-combined.pdf (Accessed May 10, 2024).

American Society of Engineering Education and National Academy of Engineering (ASEE and NAE) (2024). The inclusive engineering mindset. Available at: https://mindset.asee.org/wp-content/uploads/2024/09/The-Engineering-Mindset-Report.pdf (Accessed September 30, 2024).

Bandura, A. (1977). Self-efficacy: toward a unifying theory of behavioral change. *Psychol. Rev.* 84 (2), 191–215. doi:10.1037/0033-295X.84.2.191

Bandura, A. (2006). "Guide for constructing self-efficacy scales," in *Self-efficacy beliefs of adolescents*. Editors F. Pajares, and T. C. Urdan (Greenwich, CT: Information Age Publishing), 5, 307–337.1.

Chen, X., and Carroll, C. D. (2005). "First-generation students in postsecondary education: a look at their college transcripts," in *Nces 2005-171*. U.S. Department of Education, National Center for Education Statistics. Washington D.C.: U.S. Government Printing Office.

Cohen, J. W. (1988). *Statistical power analysis for the behavioral sciences*. 2nd Edn. Hillsdale, NJ: Lawrence Erlbaum Associates.

Estrada, M., Woodcock, A., Hernandez, P. R., and Schultz, P. W. (2011). Toward a model of social influence that explains minority student integration into the scientific community. *J. Educ. Psychcol.* 103 (1), 206–222. doi:10.1037/a0020743

Fradette, K., Keselman, H. J., Lix, L., Algina, J., and Wilcox, R. R. (2003). Conventional and robust paired and independent-samples t tests: type I error and power rates. *J. Mod. Appl. Stat. Methods* 2 (2), 481–496. doi:10.22237/jmasm/1067646120

Fry, R., Kennedy, B., and Funk, C. (2021). *STEM jobs see uneven progress in increasing gender, racial, and ethnic diversity*. Washington D.C.: Pew Research Center. Available at: https://www.pewresearch.org/social-trends/2021/04/01/stem-jobs-see-uneven-progress-in-increasing-gender-racial-and-ethnic-diversity/ (Accessed December 17, 2024).

Hong, L., and Page, S. E. (2004). Groups of diverse problem solvers can outperform groups of high-ability problem solvers. *Econ. Sci.* 101 (46), 16385–16389. doi:10.1073/pnas.0403723101

Jayabalan, M., Caballero, M. E., Cordero, A. D., White, B. M., Asalone, K. C., Moore, M. M., et al. (2021). Unrealized potential from smaller institutions: four strategies for advancing STEM diversity. *Cell* 184, 5845–5850. doi:10.1016/j.cell.2021.10.030

Larson, R. C., Ghaffarzadegan, N., and Xue, Y. (2013). Too many PhD graduates or too few academic job openings: the basic reproductive number R0 in academia. *Syst. Res. Behav. Sci.* 31, 745–750. doi:10.1002/sres.2210

Mitic, R. R. (2022). Insights into first-generation doctoral Students. *PhD career Pathw. A Proj. Counc. Graduate Sch.* Available at: https://cgsnet.org/wp-content/uploads/2022/03/CGS_CP_First-Gen-Doc-Students_ForWeb.pdf (Accessed September 29, 2024).

National Academies of Science, Engineering and Medicine (NASEM) (2016). *Barriers and opportunities for 2-Year and 4-Year STEM degrees: systematic change to support students' diverse pathways*. Washington, DC: The National Academies Press. doi:10.17226/21739

Palid, O., Cashdollar, S., Deangelo, S., Chu, C., and Bates, M. (2023). Inclusion in practice: a systematic review of diversity-focused STEM programming in the United States. *Int. J. STEM Educ.* 10, 2. doi:10.1186/s40594-022-00387-3

Rasch, D., and Guiard, V. (2004). The robustness of parametric statistical methods. *Psychol. Sci.* 46 (2), 175–208. doi:10.1073/pnas.0403723101

Roy, S., Velasco, B., and Edwards, M. A. (2024). Competition for engineering tenure-track faculty positions in the United States. *PNAS Nexus* 3 (5), pgae169. doi:10.1093/pnasnexus/pgae169

RTI International (2023). *First-generation college students in 2020: demographic characteristics and postsecondary enrollment*. Washington, DC: FirstGen Forward. Available at: https://firstgen.naspa.org/files/dmfile/15405_NASPA_FactSheet-01.pdf (Accessed December 11, 2024).

RTI International (2024). *First-generation college graduates after four years: experiences during the COVID-19 pandemic: 2020 to 2021*. Washington, DC: NASPA. Available at: https://firstgen.naspa.org/files/dmfile/15405_NASPA_FactSheet-041.pdf (Accessed December 11, 2024).

Singer, J. D., and Willet, J. B. (2003). *Applied longitudinal data analysis: modeling change and event occurrence*. Oxford University Press. doi:10.1093/acprof:oso/9780195152968.001.0001

U.S. National Science Foundation (2024). NSF established program to stimulate competitive research (EPSCoR). Available at: https://new.nsf.gov/funding/initiatives/epscor (Accessed December 11, 2024).

Whitley, S. E., Benson, G., and Wesaw, A. (2018). First-generation student success: a landscape analysis of programs and services at four-year institutions. *Cent. First-generation Student Success, NASPA–Student Aff. Adm. High. Educ. Entangled Solutions*. Available at: https://firstgen.naspa.org/files/dmfile/NASPA-First-generation-Student-Success-FULL-REPORT.pdf (Accessed December 11, 2024).

Wiedermann, W., and von Eye, A. (2013). Robustness and power of the parametric t-test and the nonparametric Wilcoxon test under non-independence of observations. *Psychol. Test. Assess. Mod.* 55 (1), 39–61.

Yin, R. K. (2009). *Case study research: design and methods*. Thousand Oaks, CA: Sage Publications, Inc.

frontiers | Frontiers in Built Environment

TYPE Original Research
PUBLISHED 17 February 2025
DOI 10.3389/fbuil.2025.1535761

Check for updates

OPEN ACCESS

EDITED BY
Rebecca Napolitano,
The Pennsylvania State University (PSU), United States

REVIEWED BY
Mihaela Kouteva-Guentcheva,
University of Architecture, Bulgaria
Amirali Najafi,
Texas A and M University, United States

*CORRESPONDENCE
Amina Meselhe,
meselhea@oregonstate.edu

RECEIVED 27 November 2024
ACCEPTED 20 January 2025
PUBLISHED 17 February 2025

CITATION
Meselhe A, Vielma KI, Burgos DT and Rodrigues T (2025) An ethnographic case study of undergraduate researchers in natural hazards engineering.
Front. Built Environ. 11:1535761.
doi: 10.3389/fbuil.2025.1535761

COPYRIGHT
© 2025 Meselhe, Vielma, Burgos and Rodrigues. This is an open-access article distributed under the terms of the Creative Commons Attribution License (CC BY). The use, distribution or reproduction in other forums is permitted, provided the original author(s) and the copyright owner(s) are credited and that the original publication in this journal is cited, in accordance with accepted academic practice. No use, distribution or reproduction is permitted which does not comply with these terms.

An ethnographic case study of undergraduate researchers in natural hazards engineering

Amina Meselhe[1]*, Karina I. Vielma[2,3,4,5], Daleen Torres Burgos[6] and Tyler Rodrigues[7]

[1]School of Civil and Construction Engineering, Oregon State University, Corvallis, OR, United States, [2]Department of Biomedical Engineering and Chemical Engineering, The University of Texas at San Antonio, San Antonio, TX, United States, [3]Department of Interdisciplinary Learning and Teaching, The University of Texas at San Antonio, San Antonio, TX, United States, [4]Klesse College of Engineering and Integrated Design, The University of Texas at San Antonio, San Antonio, TX, United States, [5]College of Education and Human Development, The University of Texas at San Antonio, San Antonio, TX, United States, [6]Department of Civil and Coastal Engineering, University of Florida, Gainesville, FL, United States, [7]Department of Civil and Environmental Engineering, University of California at Berkeley Alumni, Berkeley, CA, United States

Engineering education utilizes various methods to broaden participation in engineering disciplines. Quantitative studies show the demographics and contributing factors of successful engineering researchers within educational pathways. However, there is a need to report on the rich experiences of students who participate in programs designed to prepare undergraduate students to remain and succeed in engineering fields. The paper explores the process and impact of the National Science Foundation (NSF) funded Natural Hazards Engineering Research Infrastructure (NHERI) Research Experience for Undergraduates (REU) using qualitative measures. A humanizing model of the undergraduate researchers as holders of knowledge framed their 10 week research program and associated research opportunities, faculty mentoring, and incorporation into the community of the natural hazards field. The focus of this case study highlighted autoethnographic reflections of REU participants who continued as researchers at various academic institutions or in industry. Led by the students as co-authors, light is shed on their 1) individual professional and personal developments during the process, 2) relationships with peers and mentors, and 3) the career impacts following the experience. This collection of guided reflective responses provide insight into the experiences, merits, and challenges of the undergraduate researchers' (now graduate students) summer experience.

KEYWORDS

REU, NHERI, undergraduate research, engineering education, Social Cognitive Career Theory

1 Introduction

In 2021, twenty-eight (28) students participated in a Research Experience for Undergraduates (REU) Program at various United States universities, all connected by a common thread: National Science Foundation (NSF) funded facilities and leading natural hazard engineering researchers. The Natural Hazards Research Infrastructure (NHERI) is a collaborative network that joins these universities, pushing the boundaries of

different, interdisciplinary fields concerning hazards: earthquakes, windstorms, tsunamis, and more (e.g., water hazards, wildfires, extreme heat). Initiatives like the NSF NHERI REU Program facilitate the active participation of undergraduates in meaningful and engaging research by building on the student's formal education and connecting them with supportive mentors and peers (Sutterer et al., 2005). The outcomes of REU programs are students who have garnered skills in their respective fields (Sutterer et al., 2005) through the completion of projects of which students feel a commitment towards and sense of ownership, whether the idea was student or mentor-generated (Halstead, 1997). REU programs hereby contribute to the increased number of students who are interested in, apply to, and succeed within science, technology, engineering and mathematics (STEM) programs and careers (Petrella and Jung, 2008; Economy et al., 2013). Many quantitative studies show the demographics and contributing factors of successful engineering researchers within the educational pipeline. However, there is a need to report on the rich experiences of students who participate in intentional programs designed to prepare undergraduates to remain and succeed in engineering. This paper aims to investigate the formation process and career and personal impacts of the NSF-funded NHERI REU program by exploring a collection of guided autoethnographic reflections of REU participants. These provide insights into the experiences, merits, and challenges from the student participants, capturing qualitative data on the NHERI REU impact. Each of the participants shares their individual backgrounds that led to their application and participation in the REU experience and subsequently provide perspectives on their 1) individual professional and personal developments during the process, 2) personal and professional relationships fostered with peers and mentors, and 3) the impacts on their careers following the experience. Altogether, this work seeks to highlight the longitudinal potentialities created by participating in a NHERI REU Program, the advancements of scientific knowledge, and creation of effective researchers and engineers.

1.1 REU program

The Council on Undergraduate Research, CUR, defines undergraduate research as "a mentored investigation or creative inquiry conducted by undergraduates that seeks to make a scholarly or artistic contribution to knowledge" (CUR, 2025). Research provides an opportunity for students to engage with the application of scientific methods and expand the limits of knowledge on our world and its function (Halstead, 1997). Undergraduate research initiatives are mutually beneficial for all involved parties: the institutions, faculty mentors, students, and, because of their research, society as a whole (Petrella and Jung, 2008; Adebisi, 2022).

The benefits of undergraduate research extend beyond the academic environment (Adebisi, 2022), from the development of resilience in facing challenges, reinforcing the value of creating and advancing original and evidence-based knowledge to the increase in confidence and self-efficacy in research that results from tackling each of these (Petrella and Jung, 2008; Adebisi, 2022; Bandura, 1977; Vielma et al., 2024; Nelson, Vielma and Browning, 2023). The "products" of REU programs are the students (Sutterer et al., 2005) who then work in careers in industry or conduct research that is often influenced to some degree by their experiences. Students can be discouraged by negative experiences just as much as they can be encouraged by positive experiences. For this reason, it is vital to design programs that focus on providing the best possible experiences for students. By enabling and supporting underrepresented groups, the NHERI REU can and has supported diverse cohorts of students in an opportunity that largely impacts the students' scientific identity and assists in realizing their goals (Economy et al., 2013). Using Social Cognitive Career Theory (Lent et al., 1994), this paper examines the ways in which the NSF NHERI REU experience, combined with other important factors, impacted three students' career pathways.

1.2 NSF NHERI REU

The NSF NHERI REU program is a hybrid 10 week program that is hosted by the various NSF NHERI sites and the NHERI Education and Community Outreach (ECO). Each program participant works 40 h weeks composed of "graduate school and professional development workshops, research group meetings, networking, mentor evaluations, timesheets, reflections, research, and research writing," (NSF NHERI DesignSafe, 2025).

Funding for undergraduate research comes primarily from the National Science Foundations and is supplemented by various institutions, agencies, or other sources. The Natural Hazards Engineering Research Infrastructure (NHERI) is a network of NSF-funded facilities and researchers that focuses on investigating earthquakes, windstorms, tsunamis, and other hazards (e.g., water hazards, wildfires, extreme heat). The 2024 NHERI REU program was composed of experimental facilities within NHERI plus the RAPID Reconnaissance Center, the Simulation Center, the CONVERGE Facility, and Cyberinfrastructure teams. These research sites and the collegiate leaders are shown in Table 1.

Altogether, these multi-hazard and interdisciplinary research sites enable students to form their summer experience to develop a fundamental understanding of and contribution towards the mitigation and impacts of hazards on communities. Each university receives funding for three undergraduate student researchers to participate in the NHERI REU summer Program. The sites work together to distribute selected students to their first or second choice sites.

1.3 NSF NHERI REU demographics

The NSF NHERI REU combines the valuable components of quality undergraduate research with another tenant of the program to encourage individuals in gendered, racial, and ethnic underrepresented groups to persist in engineering fields and to improve the diversity of such career fields (Sutterer et al., 2005). This is done through targeted recruitment efforts at minority serving institutions, MSIs, and holistic selection approaches. The research sites communicate throughout the selection process, selecting students with skills and interests to successfully complete the research projects expected during the summer months.

Demographic data, included in Table 2 above, were collected on the NHERI REU program impact between 2017–2023, with

TABLE 1 National science foundation NHERI research sites and university.

NHERI research site	University
Wall of Wind (WOW)	Florida International University
Real-time Multi-Directional Natural Hazards Simulation Facility (RTMD)	Lehigh University
O. H. Hinsdale Wave Research Laboratory	Oregon State University
NHERI Simulation Center (SimCenter)	University of California, Berkeley
Center for Geotechnical Modeling (CGM)	University of California, Davis
Large High Performance Outdoor Shake Table (LHPOST)	University of California, San Diego
CONVERGE Facility	University of Colorado Boulder
Boundary Layer Wind Tunnel Experimental Facility	University of Florida
Large-Scale Mobile Shakers	University of Texas at Austin
NHERI Cyberinfrastructure and Data Management team	University of Texas at Austin in collaboration with the Texas Advance Computing Center (TACC)
Rapid Response Research Facility (RAPID)	University of Washington

6 cohorts represented, comprising a total of 164 participants. Just under 40% of the participants self-identified as White (n = 65), about 19% as Hispanic (n = 31), and closely represented were Multiracial, Black, and Asian students (n = 23, 21, 21 respectively). The remaining students were American Indian or Alaskan Native, Native Hawaiian or Other Pacific Islander, and None of the above/Wishing not to answer (n = 1 each). Altogether, nearly half of the students (47%) identified as members of underrepresented racial and ethnic groups in STEM. The demographic impact includes 58% of participants who self-identified as non-male, 27% who are first generation 4-year college students, and 37% who are from non-Research Tier One (R1) institutions according to the Carnegie Classification of Institutions of Higher Education (American Council on Education, 2025).

This paper presents a research study centered on student data from a collection of autoethnographic reflections by three former NSF NHERI REU participants who are referenced throughout the paper. First, the backgrounds of the students were explored to identify themes and motivations behind their desire to participate in the NHERI REU program. Then, using the Social Cognitive Career Theory, individual professional and personal experiences during the NSF REU Program were analyzed, followed by 2) relationships with peers and mentors, and 3) the career impacts following the experience. Comparisons were made between the students whose pathways after the REU Program took them to industry and students whose pathways following the REU took them into academic pathways.

2 Autoethnographic case study

The qualitative research was guided by the overarching research question, How do NHERI REU students experience the summer program activities during the formation of their careers? This case study explores how background and identity contributed to learning experiences, interests and career choices. Therefore, a research sub question was also explored: How did the research program experiences, coupled with background and contextual characteristics, contribute to the students' career pathways including interest development and career choices?

2.1 Theoretical frameworks

To engage these research questions, Figure 1 shows the Social Cognitive Career Theory in engineering (SCCT, Lent et al., 1994) that was employed to explore the experiences of students in the NHERI REU program. This theory emphasizes the various components that contribute to career formation. The theory also posits that personal inputs including social identities, along with the students' backgrounds, contribute to the ways in which they experience learning, which in turn impact self-efficacy–the belief that they can achieve their goals (Bandura, 1977), interests, expectations, and career choices. The theory also, importantly, highlights the ways in which contextual influences, in the form of support and barriers, impact students' career decisions. This study used SCCT to better understand the impacts of a program focused on supporting diverse students as they learned to conduct research in an academic setting and aiming to remove barriers for students underrepresented in engineering and research.

The program was also designed to use evidence-based educational supports such as guided practice in the research process, fostering a network of supportive mentors, and cultivating a community of learners and researchers within the natural hazards engineering and research fields. In these ways, the focused support elements also drew from various existing theoretical

10.3389/fbuil.2025.1535761

TABLE 2 Demographic data for participants to the NHERI REU summer program, 2017–2023.

	Demographic category	Number of participants	Percent (%)
Total Participants		164	100.0
	White	64	39.6
	Hispanic	31	18.9
	Multiracial	23	14.0
	Black	21	12.8
	Asian	21	12.8
	Other*	3	1.8
	Underrepresented in STEM**	77	47.0
	Non-male	95	58.0
	First-generation college students	44	27.0
	From non-R1 institutions	61	37.0

*Other includes American Indian or Alaskan Native, Native Hawaiian or Other Pacific Islander, and None of the above/Wish not to answer (n = 1 per category).
**Underrepresented in STEM, includes Hispanic, Black, Multiracial, and Other race categories.
Note: Percentages are rounded to one decimal place.

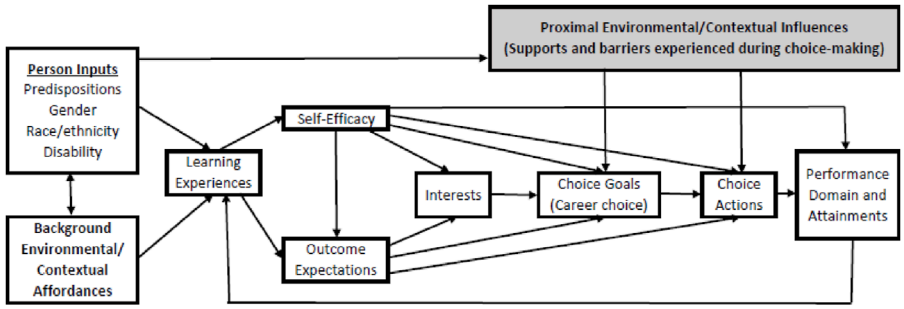

FIGURE 1
Social cognitive career theory (Lent et al., 1994).

frameworks in engineering education aimed at supporting and removing barriers for students in their formation as emerging researchers.

2.2 Methodology

The qualitative research is a case study (Yin, 2018) of volunteer research participants who were part of the 2021 NHERI REU summer Program. All the case study contributors participated during the same summer and were impacted by the systemic effects of the COVID-19 pandemic at the institutions where they conducted research. The case was therefore bounded by context and time as all undergraduate researchers participated during the 10 week research program during the same summer. Although each of the case study participants were part of different research projects at different institutions, they shared common experiences because of the pandemic as well as through organized virtual meetings with their peers and mentors. They also came together for an in-person research symposium with limited attendance at the end of the summer program to present their research and build stronger community bonds.

Because the data centers on the students' perspectives of their experiences in the REU program and their own interpretations and reflections on the impact of the program, this study is also autoethnographic in nature (Adams et al., 2021). The students' written autoethnographies were collected as data and shared from their point of view. These were the main sources of data used, and other artifacts produced during the REU program served as triangulation and validation tools.

TABLE 3 Student author demographic information and undergraduate area of study.

Name	Gender	Race and/or ethnicity	Undergraduate degree/Major	Area of work/Study
Amina	Female	Middle Eastern/Asian	Civil Engineering	Academia – PhD
Daleen	Female	Latina	Mechanical to Civil Engineering	Academia – PhD
Tyler	Male	Latino	Civil Engineering	Industry – MEng

2.3 Participants

The three case study participants volunteered to take part in the research study. They organized the data collection and data analysis strategies and responded to guiding autoethnographic questions. The demographics of the students are listed in Table 3 to share transparency about their unique experiences, intersectionalities, and potential differences in part due to their backgrounds, identities, and degree pathways. We recognize that students may have different experiences based on the theory of Social Cognitive Career Theory that emphasizes that "person inputs" such as social identity, including race and gender, impacts the way individuals navigate education.

All students were undergraduates enrolled in engineering degrees at the time of their participation in the NHERI REU Program. They attended different universities and were part of the same REU cohort. After their REU experience, they navigated different educational pathways. The data were collected at specific times during their careers where their positionality could impact their responses. Data were collected before, after, and during the NHERI REU Program, and reflective, autoethnographic responses were collected when they were far removed from the NHERI REU program. The study participants were in both academia and industry.

2.4 Data and data collection

Each of the authors were prompted to write individually about their REU experiences following a similar structure that focused on the following key points of interest: 1) individual professional and personal developments during the formation process, 2) relationships with peers and mentors, and 3) the career impacts following the REU experience. More broadly the questions used to outline the individual reflections were separated into background (or experiences prior to participating in the REU program), during (capturing experiences during the program), and following the REU experience(s) (post-program career journey). Table 4 details the prompting questions for each of the selected timeframes.

Using Social Cognitive Career Theory, the analyses of these reflections centered around the three key time points of interest with additional consideration of components identified in the literature and the challenges faced in the duration of the research experience. Comparisons can also be noted between the students whose pathways following the REU program took to industry and students whose pathways following the REU continued in academic spaces.

3 Results

Social Cognitive Career Theory points to the various ways in which background and identity can influence learning experiences, which impact self-efficacy and interests (Lent et al., 1994). While analyzing the autoethnographic responses, themes emerged between the students' responses. Concepts such as the influence and value of background motivations for scientific research, or more specifically interests, expressed as passions, for the research focus offered in the NHERI REU Program, reinforced students' short- and long-term career development and goals. Further the performance within the NSF REU Program was largely impacted by academic and formalized structures as well as personal and social relationships. Finally, the outcomes of this experience greatly impacted the career actions pursued by individuals by exposure to concepts and development of skills and expansion of networks within natural hazards engineering research.

3.1 Personal inputs and background

For the three study participants, the motivation to pursue academic studies in STEM related fields in their undergraduate degrees was associated with a measure of exposure to concepts requiring scientific solutions or curiosities explored using scientific structures (i.e., scientific method exploration of everyday observations). Participants cited a curiosity around ways the world functioned that may be solved or optimized through processes and techniques they derived or contributed to. The course work, although challenging, inspired academic achievement and a fascination with engineering frameworks. This was especially true of concentrated topics applied to infrastructure systems that people encountered and interacted with daily. Daleen stated:

> I create my own internal world of whatever the topic is and play with it by mentally "poking" and "prodding" it again and again with questions and what I like to call "thought experiments" until my curiosity is fed. At the end, I gain a better understanding of the subject, not unlike the creation of a narrative, a story that is exciting to share with others.

The challenging nature of solving engineering problems and the potential for their application have been a driving force in the areas of focus pursued by the participants within a wider umbrella of STEM fields. The specific background motivations that may have led the students specifically to the field of hazards engineering research, derived from identifying a direct relationship because of exposure to

TABLE 4 Prompting questions for individual author reflection.

Time frame (with respect to REU experience)	Questions
Background	Where were you studying? What were you studying? What were you considering for your post-graduate pathways? How does your personal background impact your career interests? (Why natural hazards? Why NHERI)?
During the Program	Where did you do your REU? Who were your mentors? Who did you work with? What was your research about? How did that work and structure feel? Specifically, what were the challenges? How did you develop personally and/or professionally? What were your relationships like with your peers and mentors?
After the Program	Where are you now? How has your participation in the NHERI REU program impacted your research trajectory/career trajectory/network?

natural hazards in their formative years. These periods of exposure to natural hazards, e.g., Hurricane Katrina (2005), Hurricane Maria (2017), M6.4 Earthquake in Puerto Rico (2020), Hurricane Laura (2021), and proximity to the physical, social, and environmental aftermath of the respective areas to such disasters largely reinforced the urgency and passions behind their scholastic and career pursuits. The authors cited feeling unsettled, helpless, or despair at both the immediate responses to and in the long-term recovery of systems that contributed to community resilience, whether their own or in proximity. These experiences were reflected in the choice goals and actions selected by authors and study participants: the pursuit of ways to prepare and mitigate before disasters and to address these gaps in knowledge that contribute to the damages and recovery afterwards. Importantly, these pursuits were not limited to a purely infrastructure focus but rather, required a holistic approach to community resilience. Amina stated,

> In a world of progress and wonder, I was able to see pockets left behind whether through manufactured or naturally driven events. This motivated me to explore a career centered around service to lessen the burdens of affected communities while improving the scientific foundations of discovery from the bottom up.

As the authors navigated their undergraduate careers motivated by these background experiences and predispositions, they often found themselves at a crossroads: the pursuit of either an industry and consulting or a research-centric internship. For these authors, the application of engineering skills was a key point of interest and could have been applied in either setting. Both provided invaluable experiences and opportunities for skill development. Through access of supportive influences proximal to the students (e.g., an author took a course taught by a visiting scholar who was a postdoctoral student at a NHERI site) and choice goals and actions (e.g., other authors looked for hazard specific research opportunities), the students selected to engage in the NSF-sponsored NHERI 10 week research experience, familiarizing themselves with the advancement of fundamental engineering theories and their applications in hazards research beyond the abstract and academic spheres.

Choice actions included submitting applications and required materials for consideration to participate in the NHERI REU Program. Each research contributor, prior to participating in the NHERI REU program, completed an application process that included faculty recommendations pertaining to their personal and professional characters as well as a suite of prompted questions and essays that reflected their interests in the program. These were coupled with selected site preferences which then were used to assign each student with a NHERI Site and an associated research team developed at their respective sites. Table 5 features the home universities, assigned NHERI sites, research teams, and project titles/outputs to provide a scope of the environments in which the students participated during their REU summer(s).

It is important to note that the student participants had the motivation and support to apply to the NHERI REU Program. By successfully submitting their application to participate, they were considered and then selected by their site to participate in the research project coinciding with their time at the NHERI site. Interests coupled with support systems contributed to their goals and actions, resulting in favorable outcomes for the participants.

3.2 Performance and experience

The output of the REU, such as the titled research projects in Table 5, do not necessarily reflect the entire scope of the intended project and project outcomes that were originally derived by the students or tasked by the Primary Investigators (PIs). The NHERI REU Program was designed to foster community through weekly research meetings and career development workshops. The program also aimed to increase research self-efficacy by providing meaningful research experiences and a scaffolded curriculum during the weekly research meetings. A final aim was to provide mentorship which intended to increase their social network and social capital within the natural hazards engineering research community. The following section focuses on these

10.3389/fbuil.2025.1535761

TABLE 5 Student author NHERI REU Project(s) site and Project(s) information.

Name	Home university	NHERI site	Research project title	Research team	Research outcome
Amina	Louisiana State University	University of Colorado Boulder, CONVERGE	Design-Level Events and Residential Construction Performance: Hurricane Laura Case Study	Tracy Kijewski-Correa Lori Peek Heather Champeau Jessica Austin	DesignSafe Data Depot publication #3234
Daleen	University of Puerto Rico - Mayaguez	Lehigh University, RTMD	Mitigation of Seismic Risk to Critical Building Contents via Rolling Pendulum Isolation Systems: Multi-Directional Hybrid Shake Table Tests	Phillip Harvey Liang Cao Esteban Vega Villalobos James Ricles	DesignSafe Data Depot publication #3227
		University of Florida, NHERI Boundary Layer Wind Tunnel	Higher-Order Turbulence and its Effects on Structural Loads and Response: A Study on Experimental Equivalence	Mariel Ojeda-Tuz Kurtis Gurley	DesignSafe Data Depot publication #3624
Tyler	University of California, Berkeley	Lehigh University, RTMD	Investigation of Semi-Active Controlled Friction Dampers for Seismic Hazard Mitigation	Liang Cao James Ricles	DesignSafe Data Depot publication #3246

targeted experiences of the students during their REU research projects and the individual professional and personal developments resulting from the research and other non-research activities (e.g., workshops).

The structural support provided by academic and social mentors or by peers provided an immediate sense of belonging in research work according to the students' autoethnographic data. There are some systemic supports provided by the NSF REU Program through weekly meetings with a designated NHERI ECO education specialist who facilitated the REU experience by providing individual guidance and larger group meetings. Herein, REU participants were provided the space and time to process the ongoing research experience and challenges and gauge the experiences of their peers not placed at the same NHERI experimental facility or site. The group meetings provided positive contributions to the individual performance of the participants with respect to the summer experience (e.g., learning technical writing and communication skills), career skills (e.g., diversity and ethics in engineering), and other means of professional advancement (e.g., industry panels and LinkedIn profile creation). Checkpoints for the research component of the REU provided additional opportunities for feedback and milestones for students to feel a sense of progress even when specific research advancements may have stalled or faced setbacks. These supports were important to highlight and normalize within research work.

The individual REU sites and research teams were some of the most integral components which the authors interfaced with. The frequency and nature of these interactions were central to the research outcomes of undergraduate students whose summer internships culminated in a paper and presentation showcased at a symposium of all REU participants at the end of their programs. These interactions were regulated to fit the needs of the participants with mentorship interchangeably in the form of graduate and/or faculty assistance. The authors noted consistent check-ins with both PIs and graduate student mentors as key cornerstones in their successes. The mentorship process was necessary for the introduction to concepts and research motivations which were often proposed by the PI as an original 10 week project or a contribution to an ongoing larger research project. Daleen stated, "Throughout the whole process, my mentors provided valuable guidance and helped me grow professionally, especially in academic writing." Mentors often aimed at preparing the participants for graduate studies and introduced them to components that they would face. Their co-sponsorship of the students' work and endorsements to the students' characters and abilities had unquantifiable benefits for students extrinsically (e.g., career trajectories, letters of recommendation) and intrinsically (e.g., research confidence). One author noted an instance of benign recognition by her research team and mentor as an engineer during their participation in the annual Natural Hazards Workshop as formative in their development. They herein felt more empowered to address critiques of their work, engage with field experts, participate in forums, and reinforce the value of collaborative work.

3.3 Challenges faced

Within Research Experiences for Undergraduate Programs, the expectation is to place students in existing research projects where they can make a significant contribution to the work. Because

students come into a project at different stages of the engineering research process, students have a variety of experiences, and their challenges differ from site to site. This was not any different for the NSF NHERI REU students. They faced challenges consistent with other REU programs, and because of this, support structures such as a network of mentors and individual check-in meetings were provided.

The authors noted challenges associated with participation in the program, many of which are associated with rigor of the project, tasks, and software, or feelings of inadequacy such as "imposter syndrome". The feelings of being underprepared or overworked can be expected when encountering a new experience with a short time for completion. Participants were encouraged and expected to interface with new techniques and programs which they may not have been privy to or interacted with during previous internships, research experiences, or classroom settings. The structure of the REU Program, while beneficial in providing a framework within which to operate, challenged the authors to create or redefine their time management skills.

The introduction to new topics in research and associate technical writing skills associated with preparing literature reviews and project reports posed additional challenges which one author cited as the motivation for pursuing a course-based master's program as opposed to a doctoral program. It is worth noting, however, that the technical skills and overall topics were of interest to the author and were credited in their pursuit of a graduate program. He stated:

> While I did find my research project to be interesting, … I did not particularly like writing a research paper. I did understand its importance … documenting and sharing the knowledge … , but it was not something I wanted to do….What I really enjoyed was the technical aspects of engineering, and I still loved to learn about more advanced ways of doing those things. And that was something I could do at the graduate level by taking graduate classes. That's when I decided that I would apply for graduate school, specifically for a course-based masters degree in structural engineering.

Through the various activities in the NHERI REU program, the students weighed their skills and interests and considered different pathways which required or prioritized specific products such as research publications. The student saw the importance of the academic and scholarly writing process and chose a graduate degree pathway that did not place as much importance on publications as products for educational success.

Overcoming and addressing these challenges was a testament to both the participants' personal abilities and, once again, the value of structural support. Where structural supports did not previously exist, the students created them. Regular interactions with peers, research mentors, and social mentors all contributed to successful outcomes of the summer research experiences. Despite facing steep learning curves and navigating unfamiliar environments (e.g., cultural and neurodevelopmental differences), the outcomes and attainments of the program remain overwhelmingly positive. Tyler noted the challenges and how these were faced during the REU Program:

> It was all overwhelming to be doing that for 40 h a week, day in and out for 2 months, especially towards the very end, when I had deadlines to get results and my code was outputting incorrect results. It was incredibly frustrating and I was on the verge of tears yet I knew that this is what I want to do […] I continually would meet with my graduate mentor, referred to the background knowledge of my dynamics and vibrations class, spent countless hours perfecting my code, all while being very patient with it, and learning to improve.

All participants faced obstacles like those mentioned by Tyler. The supports available through the program as well as their own interests and preparation helped them overcome the challenges. Those supports included having an education expert meet individually with each student weekly; the meetings were personalized to help each student address concerns, practice advocating for themselves at the sites, and strategizing writing sessions and timelines for deliverables. A network of peers was available to them at the site they were assigned to and across the NHERI REU network. Important to overcome the research challenges were Tyler's mentor, a graduate student, and background knowledge in the knowledge needed to address the research work.

Individual interests, background skills and knowledge, personal attributes, and support within the environment were essential to address obstacles. As Tyler mentioned, patience was also important, and an interest in research work and growth mindset (learning to improve) played a key role in the skills needed to overcome research challenges. The NHERI REU Program was designed to help students reflect on their challenges using a growth mindset. Although not mentioned directly in Tyler's reflective autoethnography, weekly reflective questions aided in reflexive thinking of strategies that can be used to overcome challenges. These reflections, coupled with individual meetings with the education specialist, may help to provide ideas and planned approaches to the challenges faced at the research site.

3.4 Outcomes and attainments

Built into the structure of the NHERI REU Program were weekly deliverables that scaffolded the final program outcomes and provided feedback and opportunities to foster research self-efficacy. The completion of the NSF REU Program was filled with both tangible and intangible outcomes with benefits that proliferated long after the summer experience. The authors noted personal developments within such an experience resulting from lessons learned on their own or imparted upon them by mentors and peers. The authors associated feelings of confidence, accomplishment, and contentment with the completion of their research projects and with having overcome the challenges they faced throughout their summer research projects. About this, Daleen stated, "Overall, I felt a sense of ownership to my contribution in the research and enjoyed having the space for my creativity." The publication of their work on an open-source platform such as DesignSafe gave additional value to their work that employed a sense of pride that was shared by their peers and others within the larger NHERI network.

Professional outcomes for the students were manifested differently based on each unique experience with the facilities, research teams, personal goals, and other factors. Generally, participants received exposure to and understanding that the scope of hazards research extends beyond any [one] discipline and is strengthened by those alternate perspectives. In fact, the authors were encouraged to implement these diverse perspectives and community-centered approaches in their careers. The applied nature of research completed in the NHERI REU program aided in visualizing the impacts of the research conducted by students and may inspire similarly motivated future research projects. "After months of being plunged into online learning, the work I conducted reinvigorated my interest in applied research and reinforced my hope to continue in a career fusing theory with real life implementation." This quote from Amina's authoethnographic responses illustrates how interests combined with authentic and meaningful experiences were able to fuel continuation of the research work and propel her towards applying for a doctoral program in natural hazards engineering research.

While REU experiences generally aim to develop research skills within students and encourage participation as researching graduate students, adjacent skills and opportunities were opened for the NHERI REU students who participated in this study. The NHERI network by nature is a broad collaborative network that spans multiple disciplines and geographies across the United States The authors noted that participation in this REU Program expanded their own networks and equipped them with skills and experiences that are useful in numerous contexts. "I was shocked at how much I was talking about this internship, and how useful it actually was at showcasing my skills as an engineer. Not only did NHERI assist me on my graduate school journey, but it also assisted me in the industry space." Tyler, through this comment, explained how the NHERI REU experience was brought into spaces with industry interviews and how connected the network was. Being part of the NHERI network helped Tyler in these ways.

Additionally, two studies have been conducted to show the overall research self-efficacy of participants in the NHERI REU program (Nelson et al., 2023; Vielma et al., 2024). Positive outcomes in these studies showed increases in research self-efficacy which can translate into career choices and actions to pursue graduate studies. Of the six NHERI REU cohorts to date of which the authors were a part of, 35% of students pursued STEM graduate degrees and 8% of all cohort participants pursued doctoral degrees. Two of the participants in this study, at the time of publication, were enrolled in doctoral programs, and all three research participants went on to graduate programs focused on natural hazards engineering research.

4 Discussion

The formation of engineers in the natural hazards engineering research fields remains an important educational task for mitigating the effects of natural hazards around the world as climates increase the intensity and frequency of disasters. This study qualitatively illustrates the experiences and outcomes of three engineering students who participated in the NHERI REU Program, sponsored by the National Science Foundation. Sustained efforts to broaden participation across engineering and scientific disciplines are fundamental to cultivating a multifaceted workforce capable of generating transformative approaches to contemporary and anticipated societal issues.

Social Cognitive Career Theory points to ways in which educators can support students as they design their career paths. Having supportive environments and helping students through barriers toward success remain an important part of their development, especially in engineering and research. Programs such as the NHERI REU Program are also designed with specific goals to address the educational challenges of broadening participation in engineering. This program specifically recruited participants from diverse backgrounds to engage in research. The program also provided support structures to aid in the challenges that research work affords through a network of experienced and caring mentors. Mentors addressed technical challenges as well as difficulties associated with social aspects of uncertainties in research experiences. Mentors and an educational specialist worked together to support students through individualized attention towards their specific needs. Career workshop activities targeted social and technical preparation for graduate school. The program also implemented a formatively evaluated curriculum that scaffolds the deliverables produced by the REU students. This curriculum introduces students to the rhetoric of academic writing. Having a system of support that intentionally assists all students in the program remains a critical component for positive outcomes.

As Tyler, Daleen, and Amina also shared, their background experiences contributed greatly to their interest and preparation in natural hazards engineering research. Helping students navigate their interests remains an essential component of their formation as young scholars. Having champions to dialogue with and reinforce students' interests and reflect on their future contributions with their careers also remains important piece of their narratives. Students in this study had the space to dream about how they could contribute to the world in ways important to them based on their personal experiences and were given the opportunities to prepare academically for this work prior to the NHERI REU experience. Increasing interest can contribute to resilience in challenging times throughout the students' academic and research journeys. Reminding students of their much-needed contribution to the field, through mentors and educators, can increase their retention in the field.

Like all research studies, this qualitative study has limitations. First, the students' experiences are unique. All the student authors in this work continued to complete some degree of graduate schooling (course-based masters or otherwise) and were making reflections of their summer experiences, which occurred in the Summers of 2021 or 2022. These summers and experiences were also historically affected by the height of the COVID-19 pandemic wherein some of the students were offered hybrid or fully virtual research experiences which may differ from traditional REU experiences that included a housing and relocation aspect.

While the professional outcomes of the REU can often be tracked and documented, the intangible, personal developments made

by students are greatly underrepresented. The autoethnographic case study highlights the experiences of the participants 3 years after they participated in the REU Program and documents the program impact on their career trajectories through the use of Social Cognitive Career Theory (SCCT). This case study centers around student authors who are the authentic holders of knowledge. They were asked to reflect on their REU summer(s) beginning with the background and motivations, then the duration of their experience and any challenges they may have faced, and finally the impact this program had on their career trajectory to date. The inspiration for their pursuit of a STEM career and specifically their REU summer participation were largely informed by personal outlooks and experiences with the natural, built, and social environments around them. The REU summer experience itself was largely found to be impacted by the structural support that was provided for or developed by the students and integral to overcoming personal and professional setbacks. Altogether, the NHERI REU experience and the network developed within the NHERI structure have longstanding positive impacts for participants in whatever career path they pursued.

Data availability statement

The datasets presented in this article are not readily available because Data is the autoethnography of each research participant and the data belongs to each participant. Requests to access the datasets should be directed to AM, meselhea@oregonstate.edu.

Ethics statement

Ethical approval was not required for the studies involving humans, because the authors are the research participants. The studies were conducted in accordance with the local legislation and institutional requirements. The participants provided their written informed consent to participate in this study. Written informed consent was obtained from the individual(s) for the publication of any potentially identifiable images or data included in this article.

Author contributions

AM: Conceptualization, Formal Analysis, Investigation, Methodology, Writing–original draft, Writing–review and editing. KV: Conceptualization, Formal Analysis, Methodology, Supervision, Writing–original draft, Writing–review and editing. DB: Conceptualization, Formal Analysis, Investigation, Writing–review and editing. TR: Formal Analysis, Investigation, Writing–review and editing.

Funding

The author(s) declare that financial support was received for the research, authorship, and/or publication of this article. This material is based upon work supported by the National Science Foundation under Grant No. 2129782.

Conflict of interest

The authors declare that the research was conducted in the absence of any commercial or financial relationships that could be construed as a potential conflict of interest.

Generative AI statement

The author(s) declare that no Generative AI was used in the creation of this manuscript.

Publisher's note

All claims expressed in this article are solely those of the authors and do not necessarily represent those of their affiliated organizations, or those of the publisher, the editors and the reviewers. Any product that may be evaluated in this article, or claim that may be made by its manufacturer, is not guaranteed or endorsed by the publisher.

Author disclaimer

Any opinions, findings, and conclusions or recommendations expressed in this material are those of the authors and do not necessarily reflect the views of the National Science Foundation.

References

Adams, T. E., Holman Jones, S., and Ellis, C. (2021). *Handbook of autoethnography*. New York: Routledge.

Adebisi, Y. A. (2022). Undergraduate students' involvement in research: values, benefits, barriers and recommendations. *Ann. Med. Surg.* 81, 104384. doi:10.1016/j.amsu.2022.104384

American Council on Education (2025). Carnegie classification of institutions on higher education. Available at: https://carnegieclassifications.acenet.edu/.

Bandura, A. (1977). Self-efficacy: toward a unifying theory of behavioral change. *Psychol. Rev.* 84 (2), 191–215. doi:10.1037//0033-295x.84.2.191

Council on Undergraduate Research (2025). What is undergraduate research? Available at: https://www.cur.org/about/what-is-undergraduate-research/.

Economy, D. R., Martin, J. P., and Kennedy, M. S. (2013). "Factors influencing participants' selection of individual REU sites," in *2013 IEEE frontiers in education conference*, 1257–1259. doi:10.1109/fie.2013.6685032

Halstead, J. A. (1997). What is undergraduate research? *J. Chem. Educ.* 74 (12), 1390–1391. doi:10.1021/ed074p1390

Lent, R. W., Brown, S. D., and Hackett, G. (1994). Toward a unifying social cognitive theory of career and academic interest, choice, and performance. *J. Vocat. Behav.* 45, 79–122. doi:10.1006/jvbe.1994.1027

Nelson, R., Vielma, K., and Browning, J. (2023). "Building research self-efficacy in undergraduate students through authentic research experiences," in *Paper presented at the 2023 American society for engineering education annual conference and exposition, Baltimore, MD.*

NSF NHERI DesignSafe (2025). NHERI research experiences for undergraduates summer program. *Nat. Hazards Eng. Res. Infrastructure*. Available at: https://www.designsafe-ci.org/learning-center/reu/.

Petrella, J. K., and Jung, A. P. (2008). Undergraduate research: importance, benefits, and challenges. *Int. J. Exerc. Sci.* 1 (3), 91–95. doi:10.70252/mxri7483

Sutterer, K., Brenny, and M., and Pirnia, J. D. (2005). Engineering REU sites: designing for appropriate and valuable summer educational experiences. *Am. Soc. Eng. Educ. Annu. Conf. and Expo.* doi:10.18260/1-2–15082

Vielma, K., Nelson, R., and Browning, J. (2024). "Examining the evolution of research self-efficacy in undergraduate students in the natural hazards engineering research infrastructure (NHERI)," in *Paper presented at the 2024 American society for engineering education annual conference and exposition, portland, OR.*

Yin, R. K. (2018). *Case study research and applications: design and methods*. 6th ed. Thousand Oaks, CA: SAGE Publications.

frontiers | Frontiers in Built Environment

TYPE Original Research
PUBLISHED 21 February 2025
DOI 10.3389/fbuil.2024.1514523

Check for updates

OPEN ACCESS

EDITED BY
David Richard Johnson,
Purdue University, United States

REVIEWED BY
David James Henderson,
James Cook University, Australia
Bo Li,
Beijing Jiaotong University, China

*CORRESPONDENCE
Amal Elawady,
aelawady@fiu.edu

RECEIVED 21 October 2024
ACCEPTED 31 December 2024
PUBLISHED 21 February 2025

CITATION
Metwally O, Ibrahim HA, Elawady A, Zisis I and Chowdhury AG (2025) Wind load impact on tall building facades: damage observations during severe wind events and wind tunnel testing.
Front. Built Environ. 10:1514523.
doi: 10.3389/fbuil.2024.1514523

COPYRIGHT
© 2025 Metwally, Ibrahim, Elawady, Zisis and Chowdhury. This is an open-access article distributed under the terms of the Creative Commons Attribution License (CC BY). The use, distribution or reproduction in other forums is permitted, provided the original author(s) and the copyright owner(s) are credited and that the original publication in this journal is cited, in accordance with accepted academic practice. No use, distribution or reproduction is permitted which does not comply with these terms.

Wind load impact on tall building facades: damage observations during severe wind events and wind tunnel testing

Omar Metwally[1], Haitham A. Ibrahim[1], Amal Elawady[1,2]*, Ioannis Zisis[1,2] and Arindam Gan Chowdhury[1,2]

[1]Department of Civil and Environmental Engineering, Florida International University, Miami, FL, United States, [2]Extreme Events Institute, Florida International University, Miami, FL, United States

As global urbanization accelerates, the construction of tall buildings has surged, becoming a defining feature of modern cityscapes. Tall buildings, while contributing to economic growth and urban development, face substantial risks from extreme wind events, such as hurricanes and downbursts. This study provides a comprehensive evaluation of the performance of tall building facades under severe wind conditions, with a focus on recent events that impacted the Gulf Coast of the United States, specifically in Houston, during May to July 2024, including a powerful derecho and Hurricane Beryl. Through extensive damage assessments of various tall buildings, this research highlights the different damages observed from these wind events, revealing critical vulnerabilities in tall building façades, particularly in relation to wind channeling effects in densely built urban areas. The observed damage patterns, including extensive glass breakage and façade failures, underscore the need for a reassessment of wind effects on tall buildings to better reflect the complex interactions between wind forces and urban environments. Additionally, by integrating real-world damage observations with wind tunnel simulations carried out at the NSF NHERI Wall of Wind Experimental Facility, this research offers valuable insights into the factors that may have influenced the observed damage. In this wind tunnel testing campaign, a series of aerodynamic testing of a tall building model under both atmospheric boundary layer and downburst winds were conducted. Additionally, interference effects are tested for both types of events. The preliminary findings have shown that downburst winds can have higher negative pressures compared to atmospheric boundary layer (ABL) which needs to be further studied including several downburst events to characterize the difference between both types of winds. Also, the results indicated the need to conduct a detailed interference study to compare ABL and downburst to properly include these effects for dense urban areas.

KEYWORDS

tall building aerodynamics, downburst winds, wind tunnel testing, damage observations, ABL wind

1 Introduction

In 2022, the world surpassed 2,000 buildings taller than 200 m (CTBUH, 2023). In 2023, a record was set for tall building completions with 177 buildings of 200 m or taller being completed (CTBUH, 2024). According to this data, the number and height of tall buildings have seen a significant rise over the past few decades making 200 m tall buildings now common in many metropolitan areas. As global cities continue to expand both in population and economic activity, the demand for vertical development has surged. Therefore, the increasing adoption of tall buildings in urban landscapes has become a defining feature of modern cities. These structures serve as vital business and residential hubs, contributing to economic growth and urban development.

Tall buildings, due to their height and structural complexity, are particularly vulnerable to wind loads. The susceptibility of these structures to damage can lead to significant economic losses, not only from direct damage but also from the disruption of business activities. These damages can be classified into several categories including human discomfort caused by large acceleration, interior damage due to high vibrations resulting in falling objects and damaged electrical appliances, and finally façade damage due to the wind-borne debris or the high wind pressure exceeding the design value (Cui and Caracoglia, 2020). Additionally, the recovery time for these buildings is a concern since the interruption of services can have a significant economic impact which should be taken into consideration in risk assessment models. For example, an earthquake in 2011 caused the displacement of 60% of the business in Christchurch's central business district (Molina Hutt et al., 2016). Moreover, debris from the failure of tall building façades during high intensity wind events can cause significant disruptions to transportation networks which includes road blockages, vehicle damage, and risks to pedestrians. Such observation was reported during the Dallas microburst in June 2019 where the travel time increased in certain highways by approximately 95% (INRIX, 2024).

Hurricanes and localized convective systems such as derecho and downbursts rank among the most formidable natural forces capable of inflicting severe damage on tall structures. Although both phenomena are marked as intense winds, they differ markedly in their origins and the characteristics of the wind forces they produce. Hurricanes, vast tropical cyclones formed over warm ocean waters, are distinguished by sustained high winds, heavy rainfall, storm surges, and waves. These systems can persist for days, affecting large geographical areas and often causing widespread devastation. In contrast, downbursts are intense, spatially and temporally localized downdrafts that create powerful straight-line winds near the ground, typically associated with thunderstorms. While convective winds can generate wind speeds comparable to hurricanes, their effects are confined to much smaller areas and occur over shorter periods. Understanding these differences is essential for evaluating their impact on tall buildings and for devising effective mitigation strategies.

The damage inflicted by extreme wind events varies considerably depending on the nature of the event. Hurricanes tend to have a broad impact, often causing significant damage to the glass and cladding of tall buildings. This was evident during Hurricane Katrina, when tall buildings in New Orleans, such as the Hyatt Regency Hotel and the Amoco Building, sustained substantial façade damage, particularly on the windward sides. This damage was primarily due to wind-borne debris, resulting in costly repairs and extended business interruptions (Kareem and Bashor, 2006). Similarly, typhoons in Japan, such as Maemi in 2003, have highlighted the vulnerability of tall buildings to wind-induced damage, with many structures experiencing significant damage to windowpanes due to intense wind pressures and flying debris (Tamura, 2009).

Another notable example of hurricane damage is the JP Morgan Chase Tower in Houston which sustained devastating damage to its facade during hurricane Ike in 2008. (Butler & Kareem, 2012) studied the damage observations on this building using computational fluid dynamics and wind tunnel testing and indicated that damage may have initiated by high pressures and increased by interference effects with surrounding buildings producing rotational flow which caused the wind-borne debris to contribute to the damage. Another extreme case of tall building damage during hurricanes is the Capital One tower in Lake Charles, Louisiana. This building sustained damage during Hurricane Rita in 2005, leading to repairs and upgrades. However, it was severely damaged again during Hurricanes Laura and Delta in 2020, ultimately leading to its demolition in September 2024 after nearly 4 years of closure (Malcolm, 2024).

In contrast to the widespread impacts of hurricanes, localized wind events like derechos, downbursts, and microbursts have been known to cause severe, concentrated damage. A notable example is the collapse of a 37-story building in Belém, Brazil, on 29 January 2011, which was attributed to a downburst (Loredo-Souza et al., 2019). Also, a downburst impacted Porto Alegre, Brazil, on 29 January 2016, with gust reaching around 42 m/s, causing cladding damage in several tall buildings despite not reaching the design wind speed (Loredo-Souza et al., 2019). The pattern of damage closely matched areas identified as high-pressure zones in previous wind tunnel tests, indicating the building's vulnerability to the intense, localized wind pressures of downbursts. In downtown Dallas, a microburst struck the area on 9 June 2019, causing windows damage to several tall buildings such as Fountain Place skyscraper on and the KPMG building (Krause, 2019).

These observations have documented a range of impacts on tall building, including both global and localized damage to façade elements highlighting the vulnerabilities of tall buildings to wind-induced forces. The types of damage observed often include the detachment or failure of façade panels, window breakage, and in some cases, damage to structural connections between the façade and the building's primary framework. Such damage not only compromises the structural integrity of the building but also poses significant safety risks to occupants and causes significant losses to the building's interior. Additionally, these events often result in direct and indirect economic losses due to repair costs and disruptions to business operations, respectively. Such consequences underscore the need for continuous improvement in wind load assessment methods and the design standards that guide the construction of tall buildings.

The accurate assessment of wind loads on tall buildings is critical for ensuring their safety and resilience. Various methodologies, including wind tunnel testing, field measurements, analytical

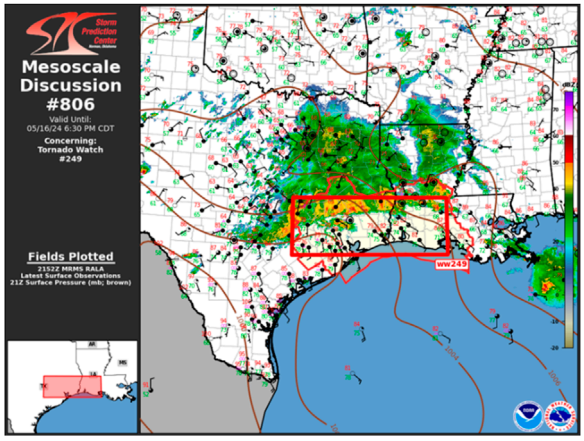

FIGURE 1
Map showing the formation of the Mesoscale Convective System (MCS) over Texas which evolved into a derecho (NOAA Storm Prediction Center, 2024).

FIGURE 3
Hurricane Beryl track (National Weather Service, 2024b).

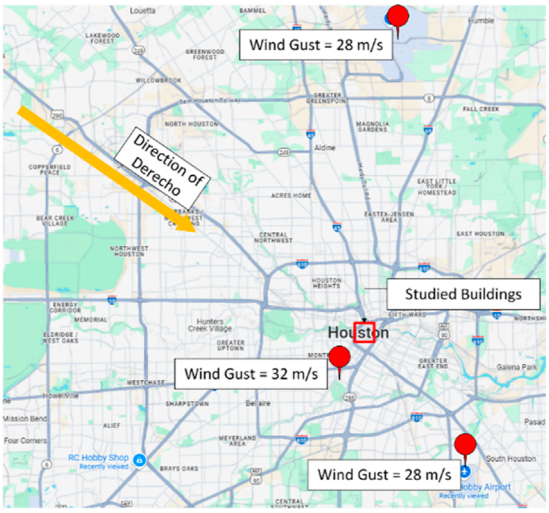

FIGURE 2
Map of the location of studied buildings along with gust speeds recorded by ASOS observation network during the derecho.

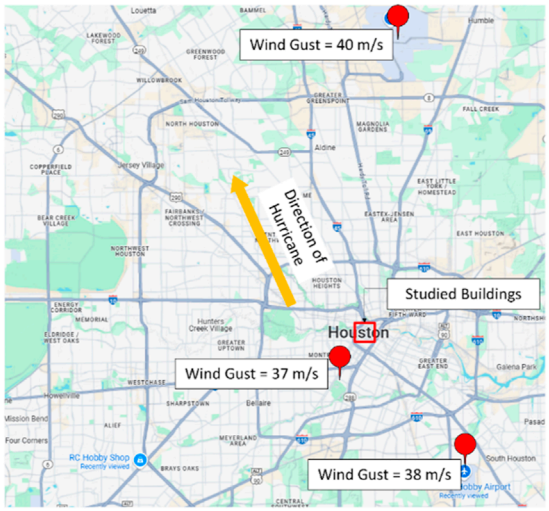

FIGURE 4
Map of the location of studied buildings along with gust speeds recorded by ASOS observation network during Hurricane Beryl.

methods and computational fluid dynamics (CFD) simulations, have been employed to evaluate these loads under different wind conditions. Wind tunnel testing has been instrumental in understanding how wind flows around tall buildings and the resulting pressure on their facades. Despite the intensive research done in characterizing wind loads on tall buildings under different atmospheric boundary layer (ABL) conditions, tall buildings are still experiencing damage. Additionally, not enough investigations have been carried out to characterize the differences in loading characteristics between ABL and convective localized storms such as downbursts.

Worth noting that failures in tall building facades may stem from a combination of factors beyond mere wind design criteria. Inadequate design decisions, such as considering the dynamics of the panels which can result in wind-induced vibrations. Material selection is equally critical employing materials with low thermal resistance or brittleness can lead to stress fractures and fatigue under dynamic wind conditions. Construction errors, including improper sealing, misaligned panels, and deficient anchoring, further compromise facade integrity. A notable example is the John Hancock Tower in Boston. In this building, the original glass panels failed due to several poor design choices as the panel exhibited thermal expansions resulting in stresses at the edge of the glass. Additionally, the reflective coating resulted in loss of bond in some parts of the lead tape to glass connection. These issues yielded some cracks which resulted in glass failure when subjected to wind buffeting necessitating the replacement of all windows (Schwartz and Gumpertz, 2004). Additionally, the poor performance of glass in façade panels can be an issue since the performance of glass can be affected by its brittle failure, duration of load and loss of strength (Kareem, 1986). Maintenance is also crucial to identify existing defects such as initial cracks and loosening of connections.

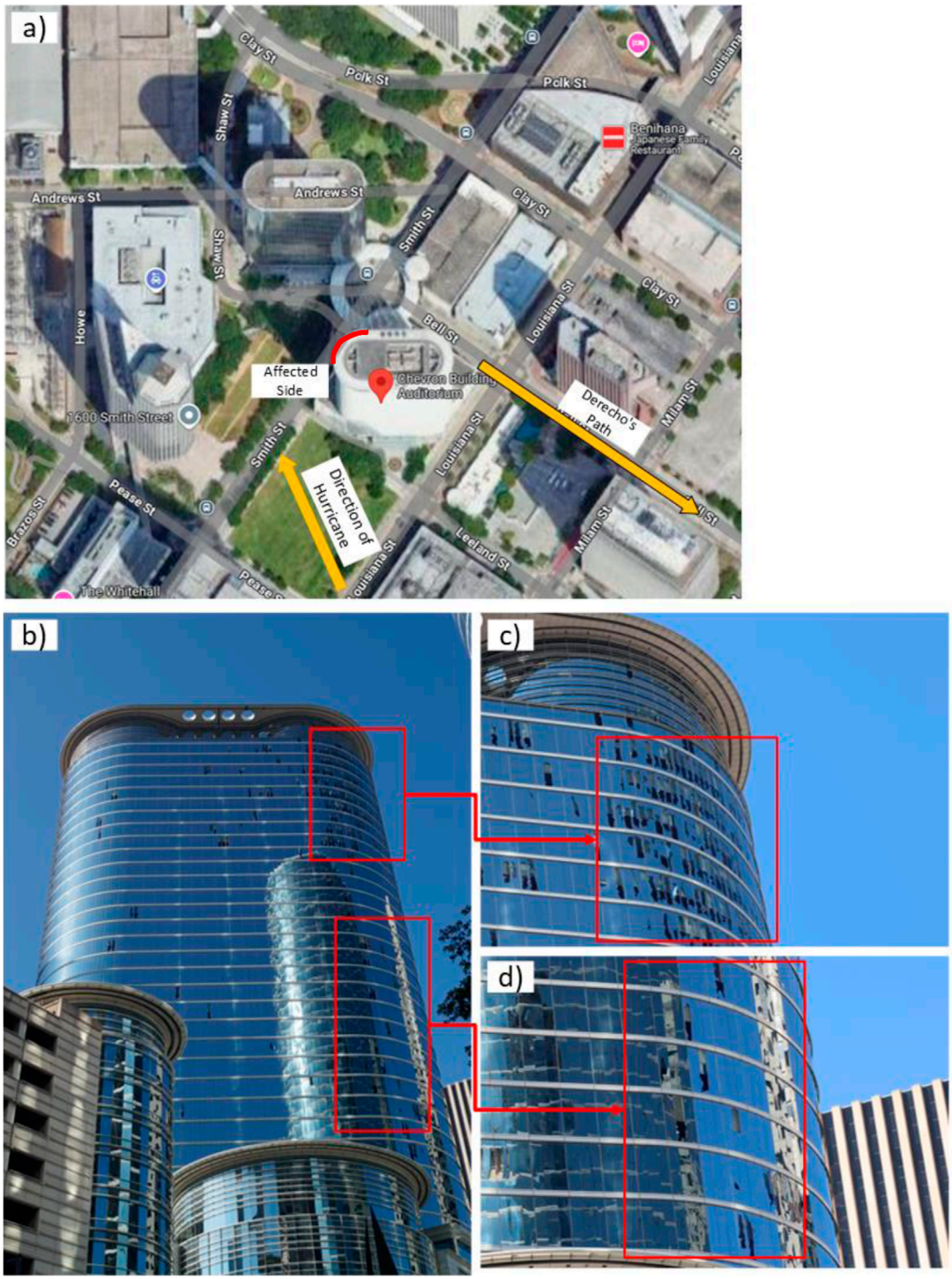

FIGURE 5
Damage sustained by the Chevron Building Auditorium during the derecho, **(A)** damaged side of the building with derecho's and hurricane paths., **(B)** global damage view (Padgett et al., 2024). **(C, D)** localized glass damage (Padgett et al., 2024).

This paper aims to contribute to the efforts of evaluating the field performance of tall buildings façades during extreme wind events, with a focus on hurricanes and downbursts. By connecting case studies of damage observations of tall buildings facades under hurricane and downburst winds to observations from wind tunnel experiments, this paper aims to identify potential gaps that needs further investigation, especially related to the effects of downbursts on tall buildings and propose areas for future investigation. The ultimate goal is to enhance the resilience of tall building facades to extreme wind events, thereby reducing the potential for damage

FIGURE 6
Minor damage sustained by the Chevron Building Auditorium during hurricane Beryl (Kalliontzis et al., 2024).

and associated direct and indirect losses. The remainder of this paper is organized as follows. Section 2 presents the two events under consideration herein, a hurricane and a derecho, for which damage observation is reported. Section 3 focuses on the damage observations during the two events and compares the damage in several tall buildings. Section 4 introduces the wind tunnel testing campaign of tall buildings with some preliminary results that can help understand the observed damage while Section 5 highlights a preliminary comparison between the ASCE provisions for wind loads of façade and the results from the wind tunnel testing.

2 Damage observation

Previous damage observations of tall buildings in Houston after Hurricane Alicia, which took place in 1983, revealed that wind-borne debris, from gravel and roof appurtenances, is the main contributor to façade damage (Williams and Kareem, 2003). This conclusion resulted in some provisions such as banning loose ballast on the roof (Konz, 2009). Kareem, (1986) also recommended studying the effect of new buildings on existing buildings and communicate those effects with owners to enhance existing buildings if the newly added building will have a negative effect. Later in 2008, Hurricane Ike caused façade damage to tall buildings in the same region with wind-borne debris and interference effects being the primary causes of this damage either acting individually or combined (Konz, 2009).

More recently, tall buildings in downtown Houston experienced damage from two subsequent events in 2024: a derecho which took place on May 16 and Hurricane Beryl which made landfall in Texas on July 8th. In the paper, the focus will be directed towards damage observations from those two events. The flow field of those two events is briefly introduced in this section before presenting the damage observations.

2.1 Event 1: houston derecho 2024

Throughout much of May 2024, a powerful heat dome settled over the Caribbean Sea and Gulf of Mexico, leading to scorching temperatures that shattered records across Central America. As the hot air at the dome's northern boundary met cooler, drier air in the U.S., atmospheric instability gave rise to severe thunderstorms in the south-central United States. On May 14, the Storm Prediction Center (SPC) issued a level 2 severe weather alert for parts of Texas, which escalated to level 3 by the morning of May 16, extending toward the Gulf Coasts of Texas and Louisiana. In southeastern Texas and southwestern Louisiana, a northward-moving warm front heightened moisture levels, increasing the potential for storms to intensify along the boundary. By mid-afternoon, a significant mesoscale convective system developed across central and eastern Texas, generating numerous updrafts. As the system advanced southeast, it evolved into a derecho—an extensive, long-lived wind event—striking the Greater Houston area with winds up to 45 m/s and producing three EF1 tornadoes. By early May 17, the storm moved offshore into the Gulf of Mexico, reducing the severe weather threat inland but leaving behind significant damage along the Gulf Coast, including shattered windows, damaged roofs, and numerous downed trees and power lines (National Weather Service, 2024b; Voiland, 2024; Lewis, 2024). A map indicating the progression of the derecho through Houston area is shown in Figure 1. It is noteworthy that the buildings in question were not affected by the tornadoes. Figure 2 shows a map of the location of the studied buildings along with gust speeds recorded at various measurement points from ASOS observation network stations during the derecho (ASOS, 1998). The values indicate a range of 28 m/s to 32 m/s. However, as noted by the reconnaissance team (Kalliontzis et al., 2024), post damage survey reported higher wind speeds reaching 45 m/s in downtown Houston. For example, CoreLogic provided a map of wind speeds that showed values in the range of approximately 36 m/s to 40 m in the location of the buildings (INRIX, 2024).

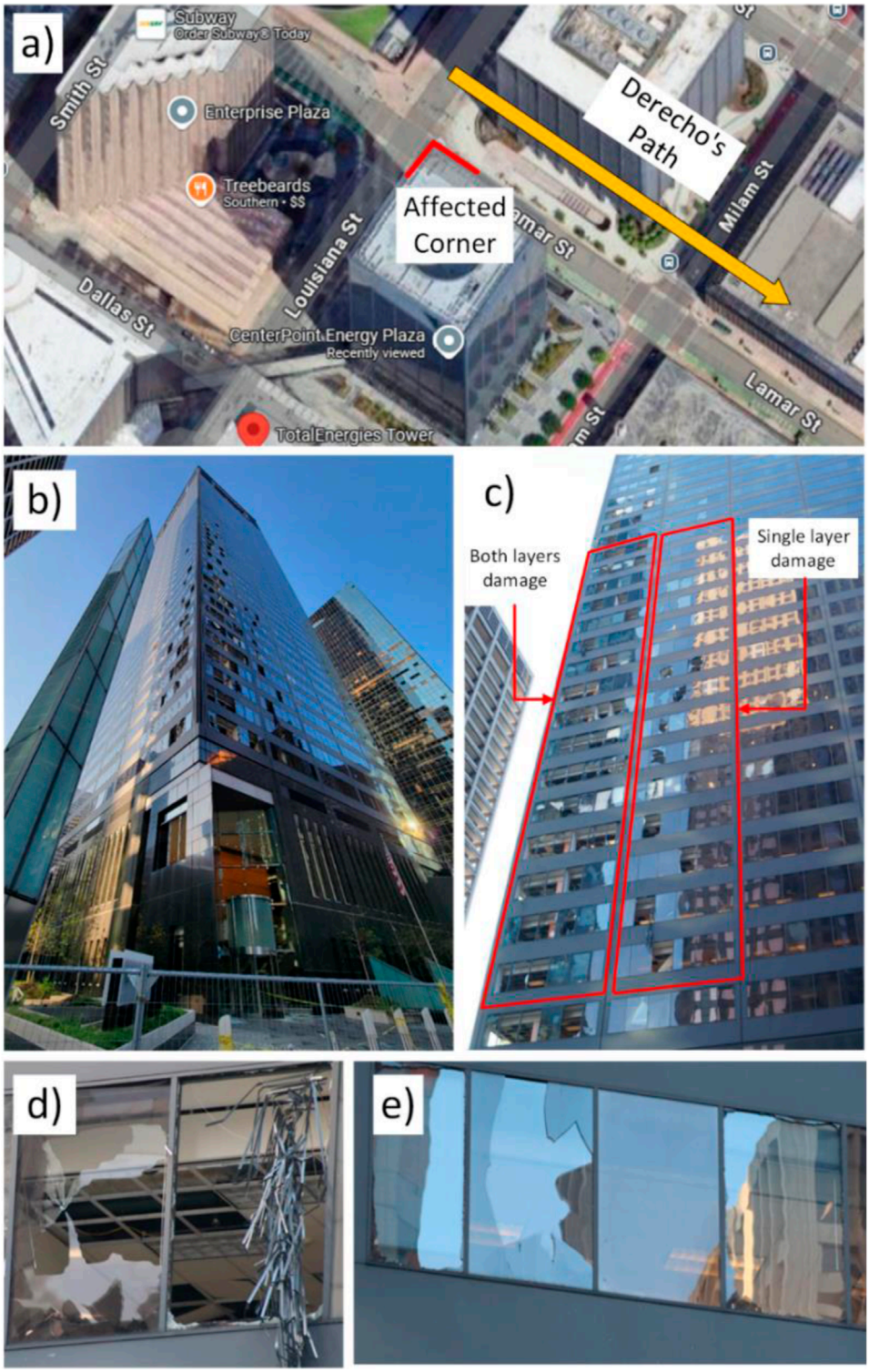

FIGURE 7
Damage sustained by the CenterPoint Energy Plaza, **(A)** corner affected corner with respect to the derecho's path, **(B)** global damage view of the damaged corner, and **(C)** localized damage view, **(D)** damage to both layers of the façade and **(E)** damage to one layer of façade (Padgett et al., 2024).

2.2 Event 2: hurricane beryl 2024

Hurricane Beryl was a significant and devastating storm that struck the Caribbean, the Yucatán Peninsula, and the Gulf Coast of the United States in late June and early July 2024. On 8 July 2024, Hurricane Beryl impacted Houston as a Category 1 hurricane with gust speeds reaching approximately 40 m/s. Marking a historic event, it rapidly intensified becoming the earliest Category

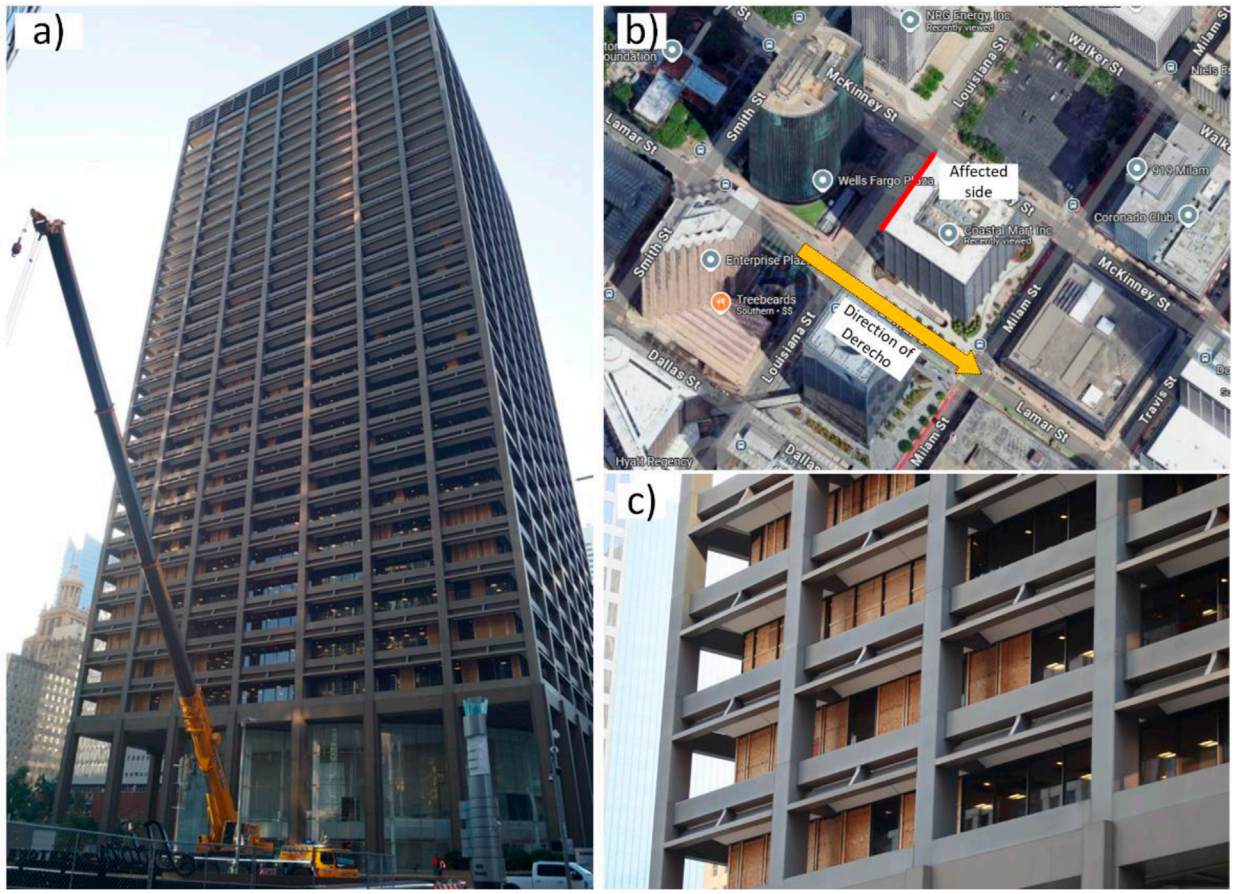

FIGURE 8
Damage sustained by El Paso Energy building, **(A)** global damage view of the damaged side, **(B)** damaged side along with the derecho's path, and **(C)** localized damage view at the corner (Padgett et al., 2024).

5 hurricane ever recorded, reaching maximum sustained winds of 74 m/s. The hurricane originated from a tropical wave off the coast of Africa on 25 June 2024, and rapidly intensified, making its first landfall in Grenada as a high-end Category 4 storm on July 1. Beryl reached its peak strength as a Category 5 hurricane upon entering the Caribbean Sea, but soon weakened due to wind shear. The storm's intensity fluctuated, briefly strengthening back to Category 3 before ultimately making its final landfall in Texas as a Category 1 hurricane on July 8th with sustained winds of 36 m/s. Beryl transitioned to a post-tropical cyclone over Arkansas on July 9 and eventually dissipated over Ontario on July 11 (National Weather Service, 2024a; KHOU 11 Staff, 2024). The track of the storm can be seen in Figure 3. Figure 4 shows a map of the location of the studied buildings along with gust speeds recorded at various measurement points from ASOS observation network stations during hurricane Beryl (ASOS, 1998). The values are showing very narrow range indicating that the wind speeds at the building locations are in this range from 37 m/s to 40 m/s.

3 Tall buildings case studies

This section presents damage observations from the two events. The derecho caused extensive and varied damage to several prominent high-rise buildings in Houston downtown area, such as the Chevron Building Auditorium, Wells Fargo Plaza, Enterprise Plaza, Wedge International Tower, and the Total Energies Tower. These Buildings are supposed to be designed for wind speeds up to 67 m/s (Kalliontzis et al., 2024). However, they were significantly impacted by intense wind forces, urban wind channeling, and wind-borne debris, causing both widespread and localized façade damage across their façades. An assessment of 18 high-rise buildings in the most severely affected downtown areas revealed approximately 3,250 broken windows (Espinoza, 2024). In contrast, during Hurricane Beryl, downtown experienced significantly less glass damage compared to the May 16 derecho. The Downtown Houston Management District noted that 40 buildings exhibited minor structural or facade damage following the hurricane (Miranda, 2024). To provide further context, the following sections will cover case studies of damage, using pictures provided by reconnaissance teams (Padgett et al., 2024; Kalliontzis et al., 2024). Case studies of various buildings are discussed, comparing the observed damages from both events and attempting to identify the underlying reasons for different damage patterns whenever data is available. It should be noted that pictures depicting the damage due to the hurricane might show repairs from the derecho in the form of plywood or sheets. However, the damage from

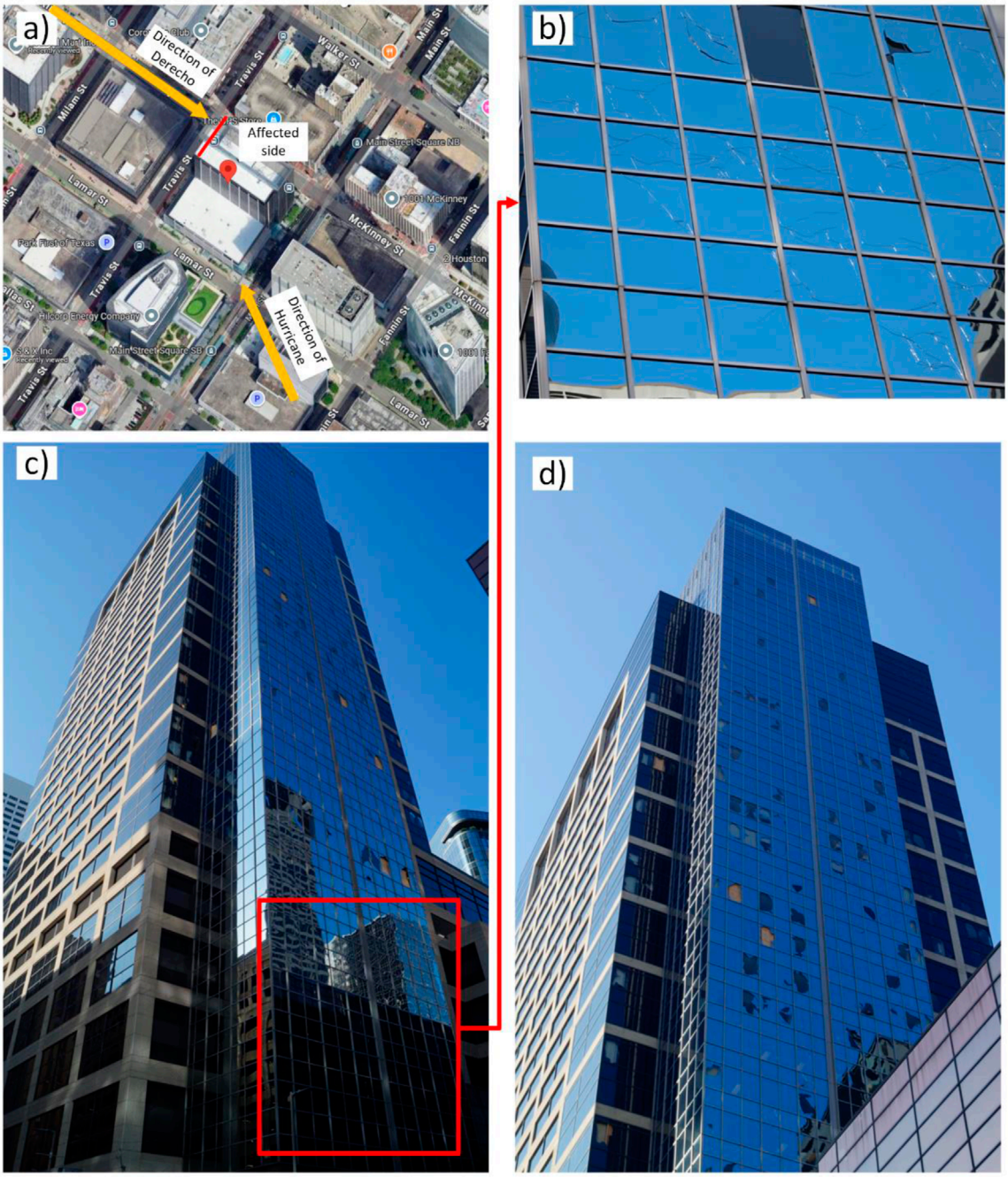

FIGURE 9
Damage sustained by the RRI Energy Plaza building, **(A)** building location with events directions, **(B)** cracked glass, **(C)** global damage view, and **(D)** breakage of façade (Padgett et al., 2024).

the hurricane was not yet repaired during the field survey (Kalliontzis et al., 2024)."

3.1 Chevron building auditorium

This building, located in 1,500 Louisiana St, is a 40-story 182.9 m tall building. The building features a curtain wall façade where the horizontal structural beams support the vertical mullions to which the glass panels are fitted. Despite being a valuable option for construction of curved surfaces, the glass panels add to the lateral stiffness of the building which can cause glass failure in extreme events due to the material's brittleness (Kalliontzis et al., 2024). Similar observations were also reported by (Alawode, et al., 2023) in full-scale testing of single-skin facades where the authors reported that increasing the stiffness of the joints by added vertical protrusions resulted in higher vibration and higher dynamic amplification factors. During the derecho event, the building's cladding system was significantly damaged as shown in Figure 5. Figure 5A highlights the building's location,

FIGURE 10
Damage sustained by the RRI Energy Plaza building during hurricane Beryl.

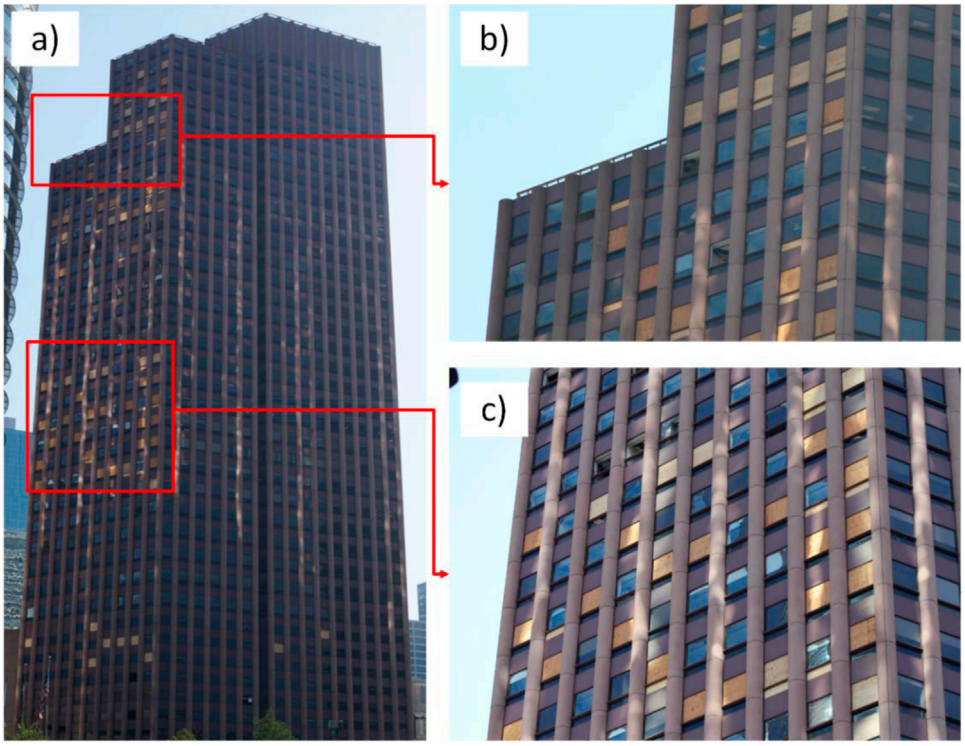

FIGURE 11
Damage sustained by the wedge international tower during the derecho, **(A)** global view of the damage, **(B, C)** detailed views of some damage locations (Padgett et al., 2024).

identifying the damaged side and the direction of the derecho. The intense wind forces caused large and small façade panels to dislodge as shown in Figures 5B–D. Numerous glass windows shattered, raining debris onto the streets below, creating hazardous conditions in the surrounding areas. The damage was predominantly observed on the side facing another tall building, Chevron Corporation Tower, suggesting that the wind channeling effect between the adjacent towers may have amplified the negative pressures (suctions) on the facade. Interestingly, although the Chevron Corporation Tower shares the same oblong shape and orientation and is positioned in front of the Chevron Building Auditorium, it sustained minimal window damage. This discrepancy suggests that the significant damage to Chevron Building Auditorium was likely intensified by channeling effects, particularly as damage was concentrated at

FIGURE 12
Damage sustained by the wedge international tower during hurricane Beryl (Kalliontzis et al., 2024).

higher elevations, reducing the likelihood of wind-borne debris as the primary cause.

During Hurricane Beryl, the building sustained additional but minor impacts, according to company spokesperson Randy Stuart (Miranda, 2024). Figure 6 illustrates the relatively minor impacts observed during hurricane Beryl. It is notable that in both events, damage was concentrated on the curved surfaces of the oblong-shaped buildings, likely due to high suction from flow separation. Similar observation was reported for the same building during hurricane Ike which had wind gusts up to 41 m/s (Konz, 2009). Additionally, inaccurate manufacturing of the curved surface or errors in the installation can cause uneven distribution of the wind loading resulting in concentration of stresses at specific parts of the façade components possibly leading to failures. The building suffered less damage in Hurricane Ike compared to the derecho. The comparatively lower damage from Hurricanes Beryl and Ike, despite comparable gust speeds, underscores, in addition to the importance of interference effects, the need to further study the impact of the different loading mechanism associated with derechos and other related phenomena like thunderstorms as these events produce sudden, intense bursts of wind that can create highly localized stress concentrations on building façades.

3.2 Center point energy plaza

This building, located in 1,111 Louisiana St, is a 53-story 226 m tall building. The building location and sustained damage is shown in Figure 7, with the damaged corner with respect to derecho's path shown in Figure 7A. The building features a double-skin façade system supported by vertical mullions as shown in Figure 7D. The damage to this building during the derecho was mostly concentrated at one corner as can be seen in Figure 7B. This damage may be attributed to the cornering effects in rectangular buildings accompanied by the channeling effects caused by the two tall buildings facing that corner. Both façade layers were damaged in some cases mostly on the corners while some cases had damage to a single layer of the façade mostly away from the corner as depicted in Figure 7C. A detailed view of damage to both layers is shown in Figure 7D opposed to damage in the external layer only in Figure 7E. It is worth mentioning that the configuration of double skin facades, including the layout and the width of the air gap, affects the wind induced pressures and may contribute to the damage of the façade as some configurations have demonstrated higher pressures compared to those for single-skin facades (da Silva and Gomes, 2008; Lou et al., 2012). Therefore, it's recommended to conduct wind tunnel testing for such type of façade to investigate all the design parameters. On the other hand, the building suffered very minor damage during the impact of hurricane Beryl.

3.3 EL paso energy building

This building, located in 1,001 Louisiana St, is a 35-story 153 m tall building. Detailed information about the cladding and building renovation, which was completed in 2012, can be found in (Abendroth L, 2013). The building suffered from considerable damage during the derecho, as shown in Figure 8A, where the damage is concentrated on the side of the building close to another tall building highlighting again the effect of channeling in intensifying the wind pressures. The direction of the derecho along with the damaged side is shown in Figure 8B. When combined with corner effects, most of the damage is concentrated on both corners of the damaged side, similar to CenterPoint Energy Plaza, as can be seen in Figure 8C. It is worth noting that the horizontal and vertical ribs might have affected the local pressure of building façade as these ribs might slightly increase the pressure on the building as noted by several researchers (Cheng et al., 2021). Additionally, the horizontal ribs can significantly affect the location of the stagnation point moving it downward (Liu et al., 2021). This finding aligns with the observation of damage concentrated more on the lower half of the building. However, this preliminary conclusion needs to be investigated more in light of the strong interference effects experienced by the building to study the complex interaction between multiple factors. Although the photos provided by (Kalliontzis et al., 2024) do not offer clear views of the building following hurricane Beryl, the few pictures, where the building was visible, are enough to conclude that the building had minimal damage from the hurricane.

3.4 RRI energy plaza

This building, located in 1,000 Main St, is a 36-story 158 m tall building. The building sustained damage during the derecho as

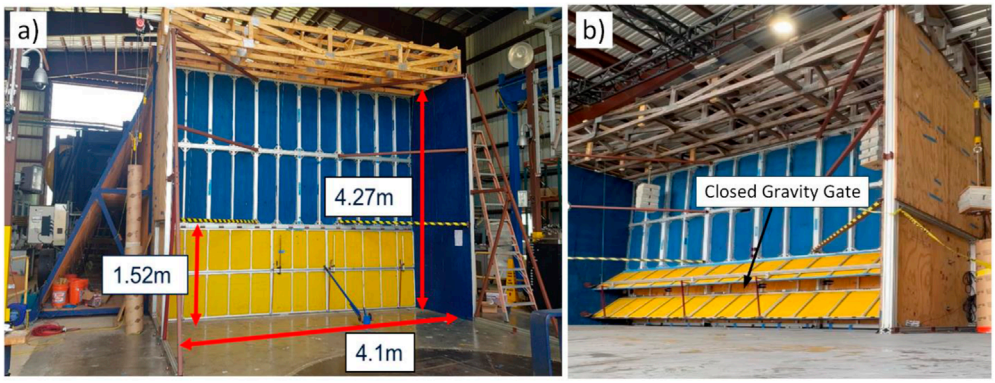

FIGURE 13
WOW downburst simulator attached to the flow management box, **(A)** closed slots, **(B)** open slots with closed gravity gate.

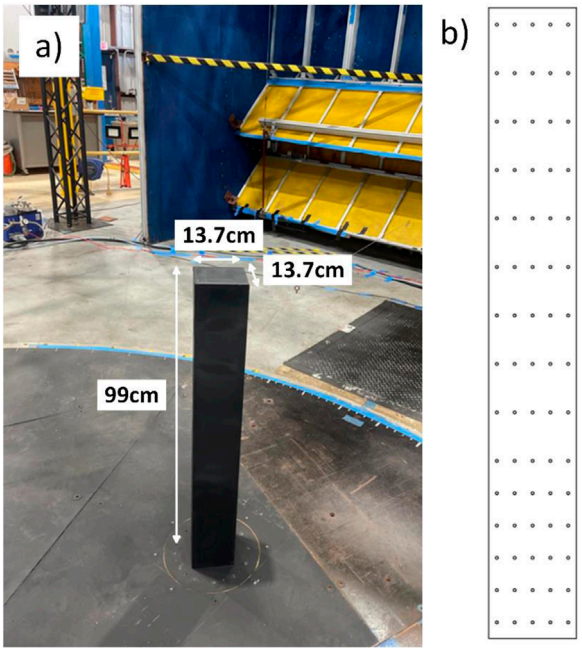

FIGURE 14
Shows **(A)** Tall building model on the WOW turntable, **(B)** Distribution of pressure taps on one surface.

shown in Figure 9, with the building location with respect to the direction of both events shown in Figure 9A. On the lower half of building, less severe damage is observed as shown in Figures 9B, C which indicates only cracking of glass that may be attributed to wind-borne debris since the damage side is the windward wall. Severe damage was concentrated on the upper half of the building as shown in Figure 9D. On the lower half of building, less severe damage is observed as shown in Figure 9B which indicates only cracking of glass that may be attributed to wind-borne debris since the damage side is the windward wall. The same building experienced less damage on the same side during Hurricane Beryl as shown in Figure 10 where only minor cracking in the façade was observed.

3.5 Wedge international tower

This building, located in 1,415 Louisiana St, is a 44-story 168 m tall building. This building, also, suffered considerable damage in the derecho compared to the hurricane. Figure 11 shows the damage in the tower during the derecho indicating widespread breakage of the glass panels compared to minimum damage encountered during the hurricane as shown in Figure 12.

In summary, the damage to tall buildings during the Houston Derecho and Hurricane Beryl highlighted several critical lessons. The event underscored the vulnerability of glass facades in high-rise buildings, with significant damage observed, during the derecho with gust of 45 m/s, despite designed to withstand wind speeds up to 67 m/s as previously mentioned. This highlights the need to reevaluate current design and construction guidelines for façade elements, considering the unique loading characteristics associated with non-hurricane events, such as thunderstorm winds in derechos and downbursts. Additionally, the channeling effects of wind in dense urban areas may significantly alter the flow around tall buildings, further inducing more progressive damage. The abrupt change in wind speeds during transient events may have contributed to the observed damage in façade elements which again motivates the need to study the differences in loading between hurricanes and other transient events such as downbursts. These effects need to be studied in conjunction with the dynamic behavior of the façade system to better understand the interaction between the loading and the system as considered for Atmospheric boundary layer winds in Alawode et al. (2023), Bakhtiari et al. (2024). Additionally, it is recommended for reconnaissance teams to provide more data related to the design of facades to facilitate interpretation of the causes of damage. Similar recommendations were provided by Mayercsik and Bennett (2024), where the authors suggested incorporating facade directionality, and site-specific factors into forensic assessments to pinpoint the causes of failure and distinguish between one-time event and long-term effects. Key

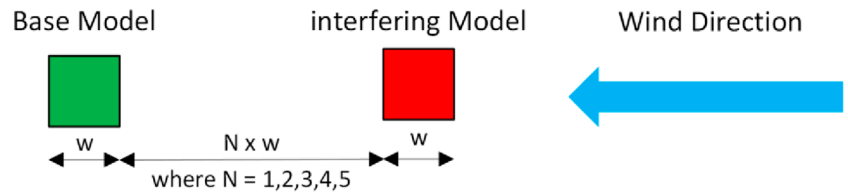

FIGURE 15
Schematic of the locations of interfering models.

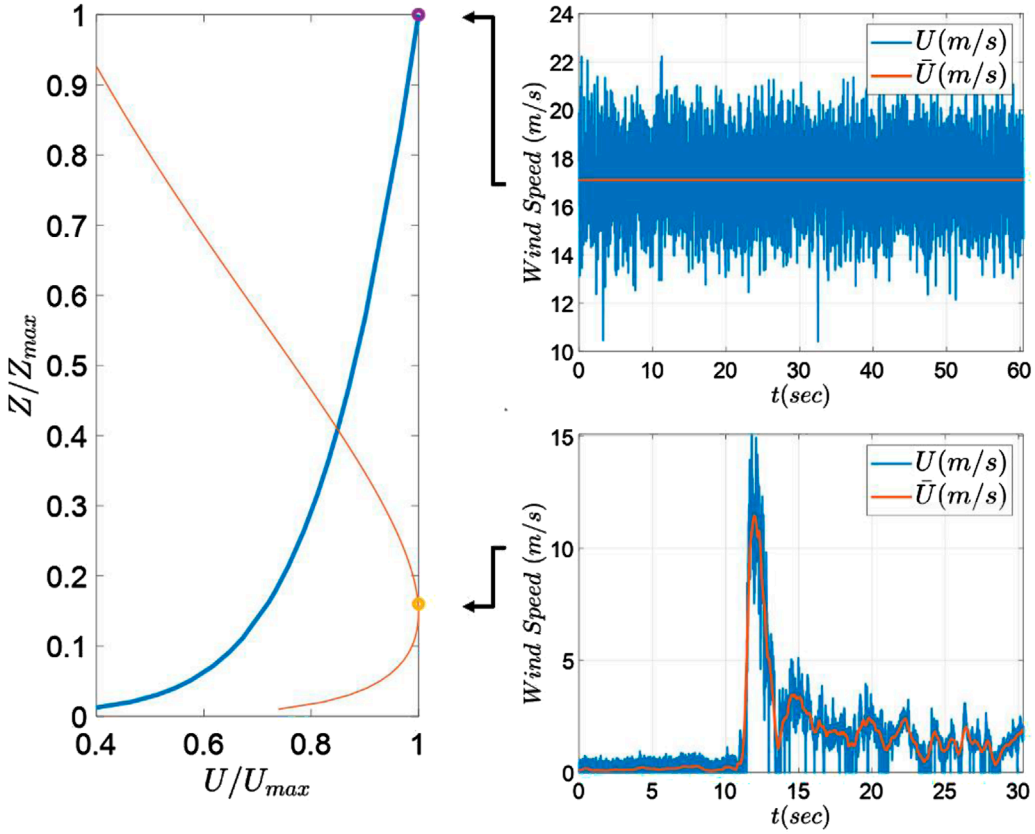

FIGURE 16
Comparison between profiles and time histories of downburst and ABL.

factors include solar exposure, that affect thermal expansion stresses, hail swaths and wind driven rain.

4 Wind tunnel testing

In this section, a series of aerodynamic wind testing of a high-rise building is conducted with preliminary results presented in an attempt to better understand the observed damage during the events in question. The testing was carried out at the US National Science Foundation (NSF) designated facility, the Natural Hazard Engineering Research Infrastructure (NHERI) Wall of Wind Experimental Facility (WOW EF), a large open-jet wind testing facility at Florida International University (FIU). The WOW EF is equipped with a 12-fan system providing 8,400 horsepower, capable of generating wind speeds up to 157 mph (70 m/s), effectively simulating Category 5 hurricane conditions based on the Saffir-Simpson scale. The facility's flow management box, measuring 4.3 m in height, 6.1 m in width, and 9.8 m long after the contraction area, is designed with spires and automated roughness elements to replicate the Atmospheric Boundary Layer (ABL) for various terrains. Additionally, the test section includes an automated turntable to accommodate testing with different wind directions. For further details on the design and features of the facility, refer to (Gan Chowdhury et al., 2017).

Stronger wind areas within the general path of a derecho are primarily caused by downbursts since a typical derecho comprises several downburst clusters, each consisting of numerous smaller downbursts (Lima de Figueiredo et al., 2019; Pryor, 2023). These

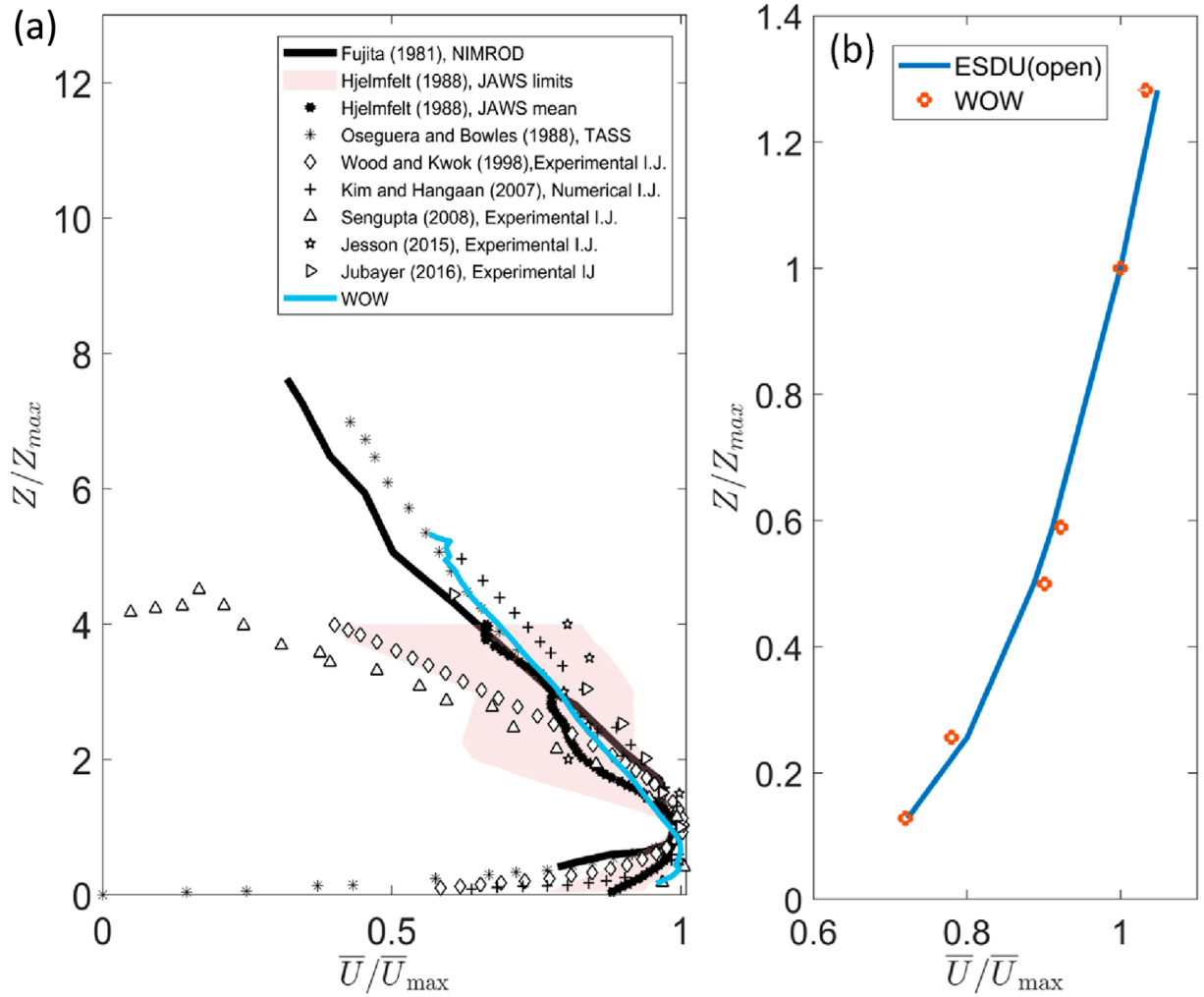

FIGURE 17
Validation of the simulated profiles in **(A)** downburst, **(B)** ABL.

clusters extend almost continuously for at least 250 miles, leading to widespread damage. This contrasts with a single downburst event, which typically results in localized damage. As a result, wind tunnel testing generally focusses on simulating individual downburst events. Despite being well studied under ABL winds, only a few studies have addressed the aerodynamics of tall buildings under downbursts.

Consequently, a downburst simulator was added recently to the WOW EF based on the 2-D wall jet concept (Lin and Savory, 2006; Sengupta and Sarkar, 2008). For downburst experiments, the simulator is attached to the flow management box. The simulator is equipped with two slats which open after pressurizing the gate to allow the flow jet. Then, this opening is closed using a gravity gate after a predetermined time window, representing the desired event duration. More information about the design and validation of the downburst simulator can be found in Mejia et al. (2022). Figure 13A shows the downburst simulator with closed slats while Figure 13B shows the open slats with closed gravity gate.

The conducted testing aims to compare between the aerodynamics of tall buildings under ABL and downburst in an attempt to identify the vulnerability of tall buildings to localized, powerful downburst winds, especially following the damage observed during the Houston derecho.

4.1 Building model and test program

The building model is not intended to be a specific case from the damage observations presented in the previous section but rather a generic case that suits future testing considerations, such as aeroelastic testing which can be beneficial to understanding the effect of building vibration on the performance of the façade (Chen et al., 2023) and also to study the effect of transient events on tall building response (Kwon and Kareem, 2009). The building model is a 1:350 scale of a prototype measuring 48 m × 48 m × 347 m. With scaled dimensions of 13.7 cm × 13.7 cm × 99 cm as shown in Figure 14A, the model is equipped with 300 pressure taps,

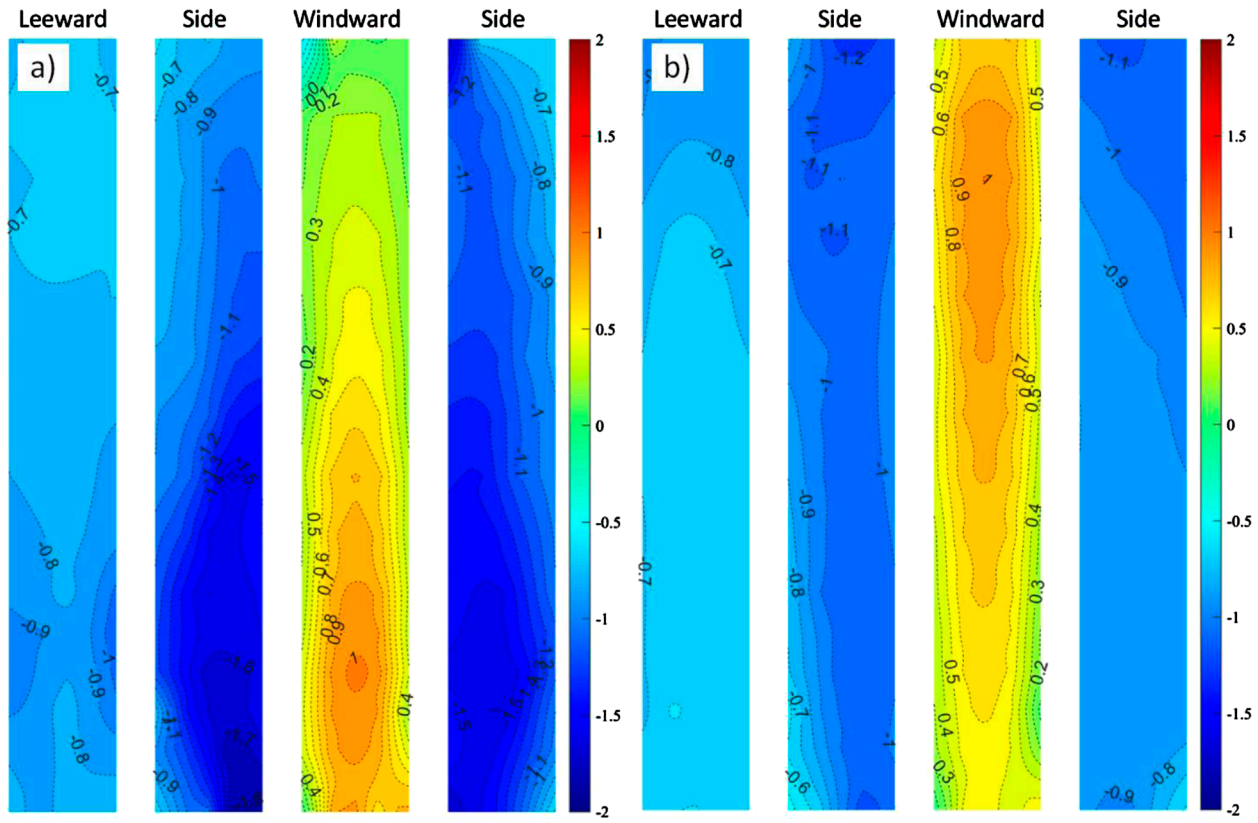

FIGURE 18
Mean pressure coefficient of 0° deg wind direction from **(A)** downburst, **(B)** ABL.

75 taps on each surface, as depicted in Figure 14B, to measure the incident pressure on all surfaces at a sampling rate of 625 Hz using the SCANIVALVE system.

The isolated building will be tested under ABL and downburst for both 0° and 45° wind directions. Interference testing will consider 5 cases where a similar model is located upstream the base model with varying upstream distance. Figure 15 shows a schematic for the location of the interfering building with respect to the base model and wind direction for the five testing cases.

4.2 Comparison of profiles

Figure 16 shows a typical comparison of the wind profiles and time histories for both downbursts and ABL, illustrating the instantaneous and mean wind speeds. In contrast to the ABL time history, which maintains a constant mean wind speed, the downburst time history is non-stationary, characterized by rapid increase, ramp-up, plateau, and decrease, ramp-down, in the wind speed. Therefore, for the downburst case a moving-mean approach is used to describe the time-varying mean. Figure 17 presents a comparison between the WOW downburst profile and various numerical and experimental data, demonstrating a strong match. Likewise, the ABL profile is compared to the ESDU open terrain profile, also showing a good match.

4.3 Data analysis

The pressure coefficient time history is calculated using Equation 1 by normalizing the measured pressure by the maximum mean wind speed which is the maximum moving mean in the case of downburst. Having said that, the mean wind speed for the ABL testing is 17 m/s while the maximum moving mean for the downburst testing is 10 m/s.

$$C_p(t) = \frac{P(t) - P_0}{\frac{1}{2}\rho\overline{U_{max}}^2} \quad (1)$$

where P(t) is the measured pressure, P_0 is the reference static pressure, $\overline{U_{max}}$ is the maximum mean wind speed. Then, the mean pressure coefficient is the mean or maximum moving mean of the calculated time history in ABL and downburst cases, respectively.

4.4 Comparison of mean and RMS pressure coefficient in downburst and ABL

Figure 18 shows a comparison between the mean pressure coefficients resulting from both downburst and ABL simulations for 0° deg wind direction. As depicted, the windward pressure coefficient follows the wind speed profile with stagnation area, corresponding to the highest positive pressure, occurs at higher

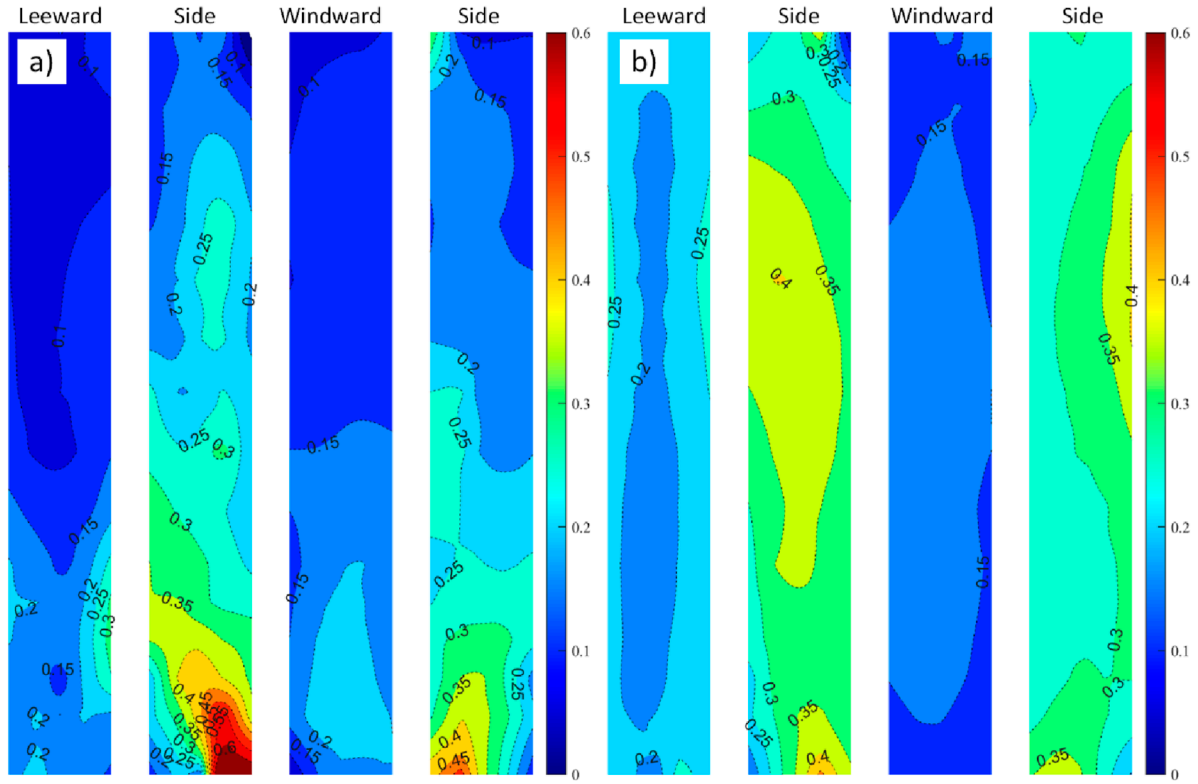

FIGURE 19
RMS pressure coefficient of 0° deg wind direction from **(A)** downburst, **(B)** ABL.

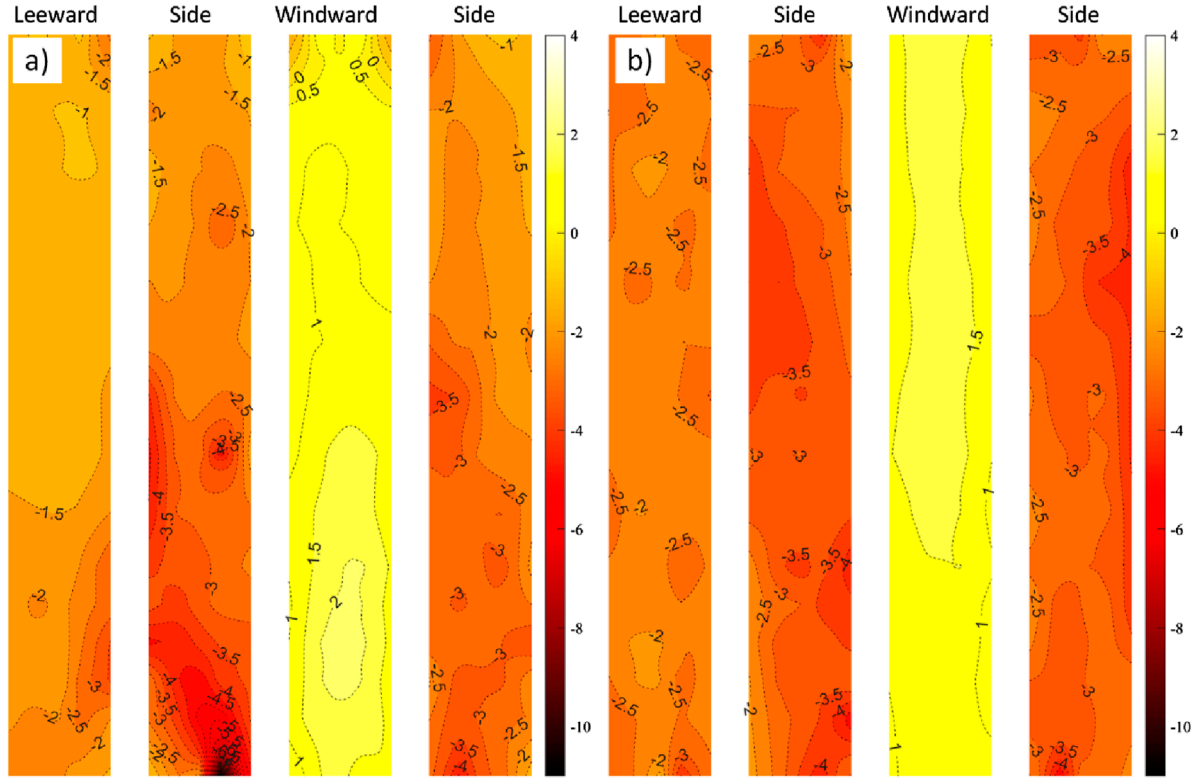

FIGURE 20
Observed peak pressure coefficient of 0° deg wind direction from **(A)** downburst, **(B)** ABL.

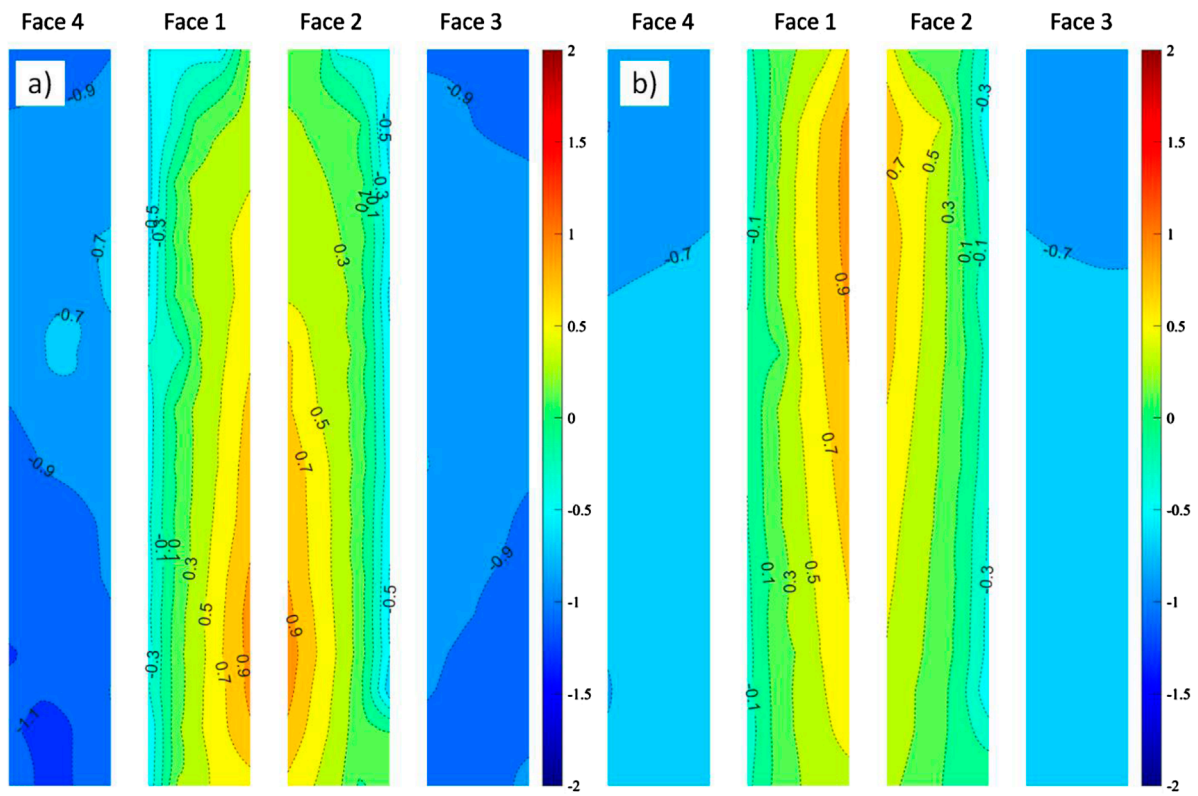

FIGURE 21
Mean pressure coefficient of 45° deg wind direction from **(A)** downburst, **(B)** ABL.

elevation for ABL case while occurring at lower elevations for the downburst case matching the maximum wind speed of the nose-shape profile of the downburst. Despite the location, the maximum values of the pressure coefficient of the windward wall are comparable for both cases.

On the sides, the minimum negative pressure coefficient in the downburst case reaches 1.6 at the base of the leading edge, compared to 1.2 at the middle top in the ABL case which may have contributed to the increased observed damage in the case of the derecho compared to the hurricane especially for the total energies building, given the close range of expected wind gusts from the events as indicated in Sections 2.1, 2.2, which sustained considerable damage on its side wall (Kalliontzis et al., 2024). Additionally, the side pressures exhibit different characteristics. The downburst case has a decreasing magnitude gradient from the base of the leading edge towards the top of the trailing edge, matching the observations of Li et al. (2023), which is different from the typical pressure coefficient contour in the ABL case which shows the maximum negative values near the leading edge at the upper part and base of the side wall (Holmes, 2015). For the downburst case the highest suction in the leeward and side wall occurs at the same height of the max pressure on the windward. The leeward wall, in the ABL case is showing a radial contour plot with the maximum value located at the middle of the top region. In the downburst case, however, the leeward wall is showing different characteristics where the maximum suction is located at the edges at the same height of the stagnation area.

In addition to reporting the mean pressure coefficient, the characteristics of the fluctuating component should be studied to evaluate the turbulent nature of downbursts which affects the potential of inducing damage to tall buildings facades (Zhang et al., 2014). Figure 19 shows a comparison between the Root Mean Square (RMS) pressure coefficients resulting from both downburst and ABL simulations for 0° degree wind direction. In the downburst case, the RMS was calculated for the peak zone of the event which was approximately 3 s. For the windward wall, the RMS pressure coefficients range from approximately 0.09–0.22 in the downburst case, depicting a broader range compared to that observed in the ABL case, which ranges from 0.14 to 0.19. The higher values in the downburst case, especially in the lower half of the building, reflects the variation in the incident turbulence intensity between the two flow types where the turbulence intensity in the downburst case ranges from 0.12 to 0.17 along the height of the model which is higher than the values in the ABL which range from 0.08 to 0.14. On the side walls, the downburst case exhibits generally lower RMS values, except near the lower base close to the leading edge, where the downburst is showing higher values. The lower RMS values in the downburst case suggest that crosswind forces are weaker compared to the ABL case. For the leeward wall, the RMS pressure coefficients are higher at the sides in the ABL case, with values decreasing toward the center. A different pattern is observed in the downburst case where the highest RMS coefficient is located at the base of the leeward wall and decrease upward. Similar to the side walls, the values in the ABL case are higher than the those for

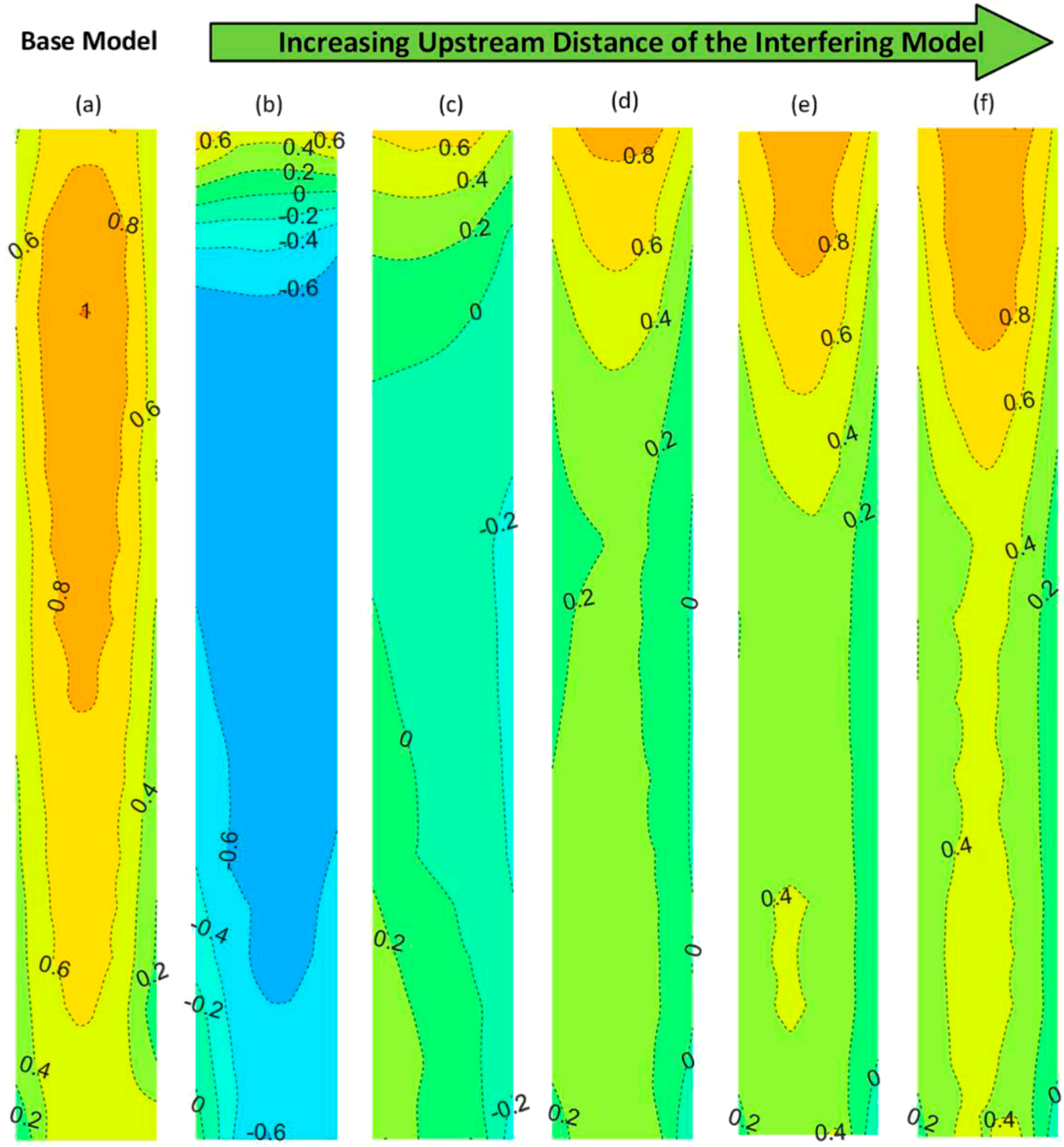

FIGURE 22
Effect of upstream distance on the mean pressure coefficient of the windward wall in the ABL winds for 0 deg wind direction [distance increase from **(A–F)**].

downburst case. Hence, in general, the downburst showed lower RMS values except for the lower half of the windward wall and the base of the side walls. Overall, the values of the RMS pressure coefficient of the downburst case align closely with the results reported by Zhang et al. (2014). Additionally, the observed peak pressure coefficient is shown is Figure 20. The results are showing similar observation as the downburst demonstrates lower observed peaks except for the lower half of the windward wall and the base of the side walls.

For the 45° wind direction, illustrated in Figure 21, positive mean pressure coefficients of 0.9 are observed at the leading edge on the two wind-facing walls, face 1 and face 2, in both the ABL and downburst cases, with pressure decreasing towards the trailing edge. However, the downburst exhibits a steeper gradient of pressure decrease, resulting in higher suction at the trailing edge compared to the ABL case. Similar to the 0° wind direction, on the other two walls (face 4 and face 5), the downburst produces greater suction, reaching a mean negative pressure coefficient of −1.1, compared to −0.7 in the ABL scenario.

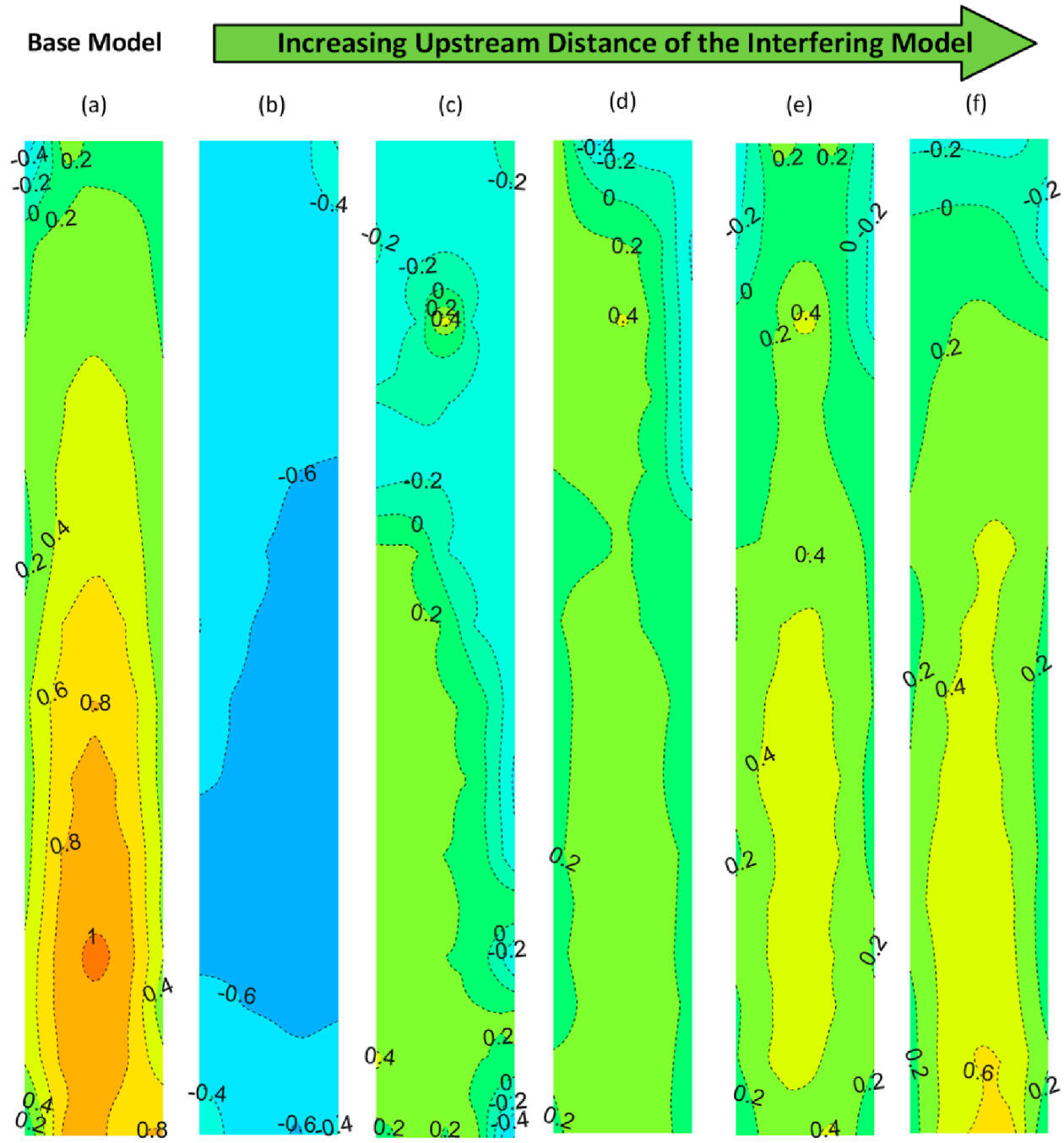

FIGURE 23
Effect of upstream distance on the mean pressure coefficient of the windward wall in the downburst winds for 0 deg wind direction [distance increase from **(A–F)**].

4.5 Comparing interference effects in downburst and ABL

As observed, channelling effects in dense urban environment might have a significant consequence on the wind-induced local pressures and have contributed to the damage observed in Houston during the derecho. This section compares the mean pressure coefficients on the windward wall of the main model with different distances from an upstream interfering building of the same dimensions for both ABL and downburst winds. For ABL wind, Figure 22A shows the ABL-induced mean pressure coefficients on the windward wall for the isolated building while Figures 22B–F shows the mean pressure coefficient with upstream building while increasing its distance. Each case corresponds to increasing the upstream distance by the width of the model as depicted in Figure 15. Figure 22B is when the spacing between both buildings was equal to the width of the building. As shown, at small upstream distance, the windward wall is showing high negative pressure coefficient that reached a value of 0.7 with a bulk area of the windward subjected to this high suction. However, increasing the distance to twice the building width as in

Figure 22C reduced the absolute coefficient to a value of 0.2 in most of the surface area despite having a value that reached 0.6 in very limited zone. This demonstrates that upstream distance dramatically influences pressure coefficients, with the original pattern gradually restored as distance increases since the flow gradually returns to the original state and the pressure coefficient stabilize and returns to the undisturbed case. Similar results were reported by Xie and Gu (2004) where the interference factor, defined as the ratio between the base moment of building with interference effects and the base moment of the isolated building, approaches 1 as the upstream distance increases. Figure 22F shows a very similar pattern, despite lower magnitudes, compared to the base case without interference effects. A similar trend is observed for the downburst case as shown in Figure 23. However, the original pattern and values in the downburst case is taking longer distance to be retrieved than the ABL case. The high suction in the windward wall with close upstream building might have contributed, beside wind-borne debris, to the façade damage of several buildings during the derecho such as the El Paso Energy Building and the CenterPoint Energy Plaza. A separate study should delve more to identify the difference in interference effects between ABL and downburst considering additional interference configurations and studying the effects on all surfaces for both mean and fluctuating components of the pressure coefficient.

5 Conclusion

This study provides critical insights into the impact of extreme wind events on the façades of tall buildings, focusing on the derecho and Hurricane Beryl events that impacted Houston, Texas during 2024. Significant damage was observed on tall buildings in downtown Houston, despite being designed for wind speeds of up to 67 m/s which is higher than the recorded gust wind speed for both events. This damage caused various socio-economic impacts, including direct structural losses, interior damage, traffic disruptions from wind-borne debris, and business interruptions. The findings reveal notable vulnerabilities in tall building façades, particularly related to wind channeling effects in urban environments. Comparing the observations in both events, the damage resulted from the derecho was more severe than that resulted from the hurricane, despite comparable gust speeds. This suggests that the unique loading characteristics of non-hurricane events, such as derechos and downbursts, can have a disproportionate effect on localized areas of building façades. These variations in wind loading are especially critical in regions with mixed climates, where thunderstorm winds may influence design wind speeds and necessitate special provisions.

In the second part of this study, wind tunnel testing was conducted on a tall building under both Atmospheric Boundary Layer (ABL) and downburst wind conditions, with and without upstream interference from nearby buildings. The tests revealed different pressure coefficient patterns corresponding to the difference in wind profiles, with much higher suction on the sides of buildings during downburst events compared to ABL conditions.

Future research should focus on conducting a more detailed analysis of the aerodynamic differences between ABL and downburst winds for tall buildings. Additionally, detailed study of interference effects between closely spaced buildings under both ABL and downburst conditions to identify the difference in those effects. A codification study should also be performed to reassess pressure coefficients for tall building walls compared to building codes. Lastly, further exploration of the vibration response of buildings, specially under downburst events, using aeroelastic testing to study the interaction between building dynamics and transient events characterized by rapid ramp up and ramp down of wind speed which can cause dynamic amplification of the wind-induced forces on the tall buildings. This should be studied with comparison with ABL winds which are considered stationary in general.

By focusing on these areas, future research can contribute to the development of more resilient tall building designs, that might be capable of withstanding the unique challenges posed by both hurricanes and non-hurricane wind events, ultimately enhancing urban safety and reducing economic and social losses.

Data availability statement

The datasets presented in this article are not readily available because Data is not publicly available now. Requests to access the datasets should be directed to aelawady@fiu.edu.

Author contributions

OM: Writing–original draft, Writing–review and editing, Methodology, Formal analysis, Conceptualization. HI: Writing–review and editing, Methodology, Conceptualization. AE: Writing–review and editing, Resources, Funding acquisition, Methodology, Conceptualization. IZ: Writing–review and editing, Methodology. AC: Writing–review and editing, Methodology.

Funding

The author(s) declare that financial support was received for the research, authorship, and/or publication of this article. These tests were conducted at the NHERI Wall of Wind Experimental Facility (NSF Award No. 1520853 and No. 2037899). The authors acknowledge the financial support provided by NSF through "NSF-CMMI Award #2146277: CAREER: Bridging the Global Gap on Understanding Downburst Impacts on Buildings: Field Data-Modeling Research and Education for More Resilient Communities."

Conflict of interest

The authors declare that the research was conducted in the absence of any commercial or financial relationships that could be construed as a potential conflict of interest.

Generative AI statement

The author(s) declare that no Generative AI was used in the creation of this manuscript.

Publisher's note

All claims expressed in this article are solely those of the authors and do not necessarily represent those of their affiliated organizations, or those of the publisher, the editors and the reviewers. Any product that may be evaluated in this article, or claim that may be made by its manufacturer, is not guaranteed or endorsed by the publisher.

References

Abendroth, J. L. (2013). *El Paso Energy – building envelope solutions for 1960s vintage construction*.

Alawode, K. J., Vutukuru, K. S., Elawady, A., Lee, S. J., Chowdhury, A. G., and Lori, G. (2023). Wind-induced vibration and wind-driven rain performance of a full-scale single-skin facade unit with vertical protrusions. *J. Archit. Eng.* 29 (2), 04023003. doi:10.1061/jaeied.aeeng-1393

Asos, A. (1998). "Automated surface observing system: asos user's guide," in *US dept. Of commerce. National oceanic and atmospheric administration: federal aviation administration* (Washington, DC: US Navy: US Dept. of the Air Force). Available at: https://Www.Weather.Gov/Media/Asos/Aum-Toc.Pdf.

Bakhtiari, A., Alawode, K. J., Vutukuru, K. S., Lori, G., Elawady, A., Chowdhury, A. G., et al. (2024). Wind-induced dynamic behavior of single-skin curtain-wall system: a comparative numerical study. *J. Archit. Eng.* 30 (4), 04024032. doi:10.1061/jaeied.aeeng-1725

Butler, K., and Kareem, A. (2012). "Anatomy of glass damage in urban areas during hurricanes," in *Advances in hurricane engineering: learning from our past*, 405–416.

Chen, B., Jiang, L., Zhang, L., Yue, W., Yang, H., and Yu, H. (2023). Wind resistance performance of large-scale glass curtain walls supported by a high-rise building. *Buildings* 13 (3), 636. doi:10.3390/buildings13030636

Cheng, X., Huang, G., Yang, Q., and Zhou, X. (2021). Influence of architectural facades on wind pressures and aerodynamic forces of tall buildings. *J. Struct. Eng.* 147 (1), 04020303. doi:10.1061/(asce)st.1943-541x.0002867

Council on Tall Buildings and Urban Habitat (2023). Year in review: tall trends of 2022: world surpasses 2,000 buildings of 200 meters or greater height. *CTBUH*. 44–51.

Council on Tall Buildings and Urban Habitat (2024). *Year in review: tall trends of 2023: a record-Breaking bear for tall building completions*. The Skyscraper Center.

Cui, W., and Caracoglia, L. (2020). Performance-based wind engineering of tall buildings examining life-cycle downtime and multisource wind damage. *J. Struct. Eng.* 146 (1), 04019179. doi:10.1061/(asce)st.1943-541x.0002479

da Silva, F. M., and Gomes, M. G. (2008). Gap inner pressures in multi-storey double skin facades. *Energy Build.* 40 (8), 1553–1559. doi:10.1016/j.enbuild.2008.02.014

Espinoza, S. G. (2024). Downtown Houston skyscraper window repairs continue after deadly derecho. *Houst. Public Media*. Available at: https://www.houstonpublicmedia.org/articles/news/houston/2024/05/21/488157/downtown-houston-skyscraper-window-repairs-continue-after-deadly-derecho/.

Gan Chowdhury, A., Zisis, I., Irwin, P., Bitsuamlak, G., Pinelli, J.-P., Hajra, B., et al. (2017). Large-scale experimentation using the 12-fan wall of wind to assess and mitigate hurricane wind and rain impacts on buildings and infrastructure systems. *J. Struct. Eng.* 143 (7), 04017053. doi:10.1061/(asce)st.1943-541x.0001785

Holmes, J. D. (2015). *Wind loading of structures*. CRC Press. doi:10.1201/b18029

INRIX (2024). Dallas microburst upends traffic, INRIX IQ shows city's quick recovery. Available at: https://inrix.com/case-studies/dallas-microburst-upends-traffic-inrix-iq-shows-citys-quick-recovery/.

Kalliontzis, D., Rahman, A. U., Khan, W., Kenawy, M., Ghahremani, K., Pham, H., et al. (2024). Joint preliminary virtual reconnaissance report-early access reconnaissance report (PVRR-EARR) field assessment structural team (FAST) lead: field assessment structural team (FAST) Members: Virtual assessment structural team (VAST) section authors: (in order of section authored). Available at: https://www.steer.network.

Kareem, A. (1986). Performance of cladding in hurricane Alicia. *J. Struct. Eng.* 112 (12), 2679–2693. doi:10.1061/(asce)0733-9445(1986)112:12(2679)

Kareem, A., and Bashor, R. (2006). Performance of glass/cladding of high-rise buildings in Hurricane Katrina. *Wind Eng. Newsl. AAWE*, 1–5.

KHOU 11 Staff (2024). Tropical Storm Beryl brings 90+ mph winds, more than a foot of rain in some areas of Houston. Available at: https://www.khou.com/article/weather/hurricane/tropical-storm-beryl-wind-rain/285-4e7cc1e8-ecaa-45c5-a8f7-741d96a9c6cb.

Konz, R. C. (2009). "Cladding performance of high-rise buildings in the Houston CBD during Hurricane Ike," in *Forensic Engineering 2009: Pathology of the built environment*, 739–748.

Krause, K. (2019). *Thousands still without power Monday after powerful storms rake Dallas-Fort Worth*. The Dallas Morning News. Available at: https://www.dallasnews.com/news/weather/2019/06/10/thousands-still-without-power-monday-after-powerful-storms-rake-dallas-fort-worth/.

Kwon, D.-K., and Kareem, A. (2009). Gust-front factor: new Framework for wind load effects on structures. *J. Struct. Eng.* 135 (6), 717–732. doi:10.1061/(ASCE)0733-9445(2009)135:6(717)

Lewis, B. (2024). How Did a derecho form in Houston? City Cast Houston. Available at: https://houston.citycast.fm/explainers/how-did-a-derecho-form-in-houston.

Li, Y., Mason, M. S., Bin, H. Y., and Lo, Y. L. (2023). Aerodynamic characteristics of a high-rise building in a steady thunderstorm outflow-like flow field. *J. Wind Eng. Industrial Aerodynamics* 240, 105501. doi:10.1016/j.jweia.2023.105501

Lima de Figueiredo, E., de Lima Nascimento, E., and Ilha de Oliveira, M. (2019). Analysis of two derecho events in Southern Brazil. *Meteorology Atmos. Phys.* 131, 1171–1190. doi:10.1007/s00703-018-0654-x

Lin, W. E., and Savory, E. (2006). Large-scale quasi-steady modelling of a downburst outflow using a slot jet. *Wind & Struct.* 9 (6), 419–440. doi:10.12989/was.2006.9.6.419

Liu, J., Hui, Y., Yang, Q., and Tamura, Y. (2021). Flow field investigation for aerodynamic effects of surface mounted ribs on square-sectioned high-rise buildings. *J. Wind Eng. Industrial Aerodynamics* 211, 104551. doi:10.1016/j.jweia.2021.104551

Loredo-Souza, A. M., Lima, E. G., Vallis, M. B., Rocha, M. M., Wittwer, A. R., and Oliveira, M. G. K. (2019). Downburst related damages in Brazilian buildings: are they avoidable? *J. Wind Eng. Industrial Aerodynamics* 185, 33–40. doi:10.1016/j.jweia.2018.11.022

Lou, W., Huang, M., Zhang, M., and Lin, N. (2012). Experimental and zonal modeling for wind pressures on double-skin facades of a tall building. *Energy Build.* 54, 179–191. doi:10.1016/j.enbuild.2012.06.025

Malcolm, T. (2024). Louisiana city's hurricane-damaged skyscraper imploded. Available at: https://www.chron.com/news/article/lake-charles-tower-imploded-hurricane-19751079.php.

Mayercsik, N. P., and Bennett, P. J. (2024). Directionality considerations in building facade assessments for distress due to storms and construction defects. *Forensic Eng.* 2024, 948–956. doi:10.1061/9780784485798.097

Mejia, A. D., Elawady, A., Vutukuru, K. S., Chen, D., and Chowdhury, A. G. (2022). Examination of different wall jet and impinging jet concepts to produce large-scale downburst outflow. *Front. Built Environ.* 8, 980617. doi:10.3389/fbuil.2022.980617

Miranda, J. (2024). Downtown Houston hit yet again with more shattered glass. Chron. Available at: https://www.chron.com/news/houston-texas/article/downtown-houston-windows-beryl-19563140.php.

Molina Hutt, C., Almufti, I., Willford, M., and Deierlein, G. (2016). Seismic loss and downtime assessment of existing tall steel-framed buildings and strategies for increased resilience. *J. Struct. Eng.* 142 (8), C4015005. doi:10.1061/(asce)st.1943-541x.0001314

National Weather Service (2024a). Hurricane Beryl 2024. Available at: https://www.weather.gov/lch/2024Beryl.

National Weather Service (2024b). *Tropical event summary*. National Oceanic and Atmospheric Administration. Available at: https://www.weather.gov/hgx/tropicaleventsummary.

NOAA Storm Prediction Center (2024). *Mesoscale discussion 806: severe weather event review for Thursday*. NOAA. Available at: https://www.spc.noaa.gov/exper/archive/event.php?date=20240516.

Padgett, J., Rincon, R., and Tafur, A. (2024). "Reconnaissance of wind damage to buildings in downtown Houston," in *Reconnaissance of wind damage to buildings in downtown Houston* (Texas: DesignSafe-CI).

Pryor, K. L. (2023). "Downburst monitoring and prediction studies," in *Field measurements for Passive environmental Remote Sensing* (Elsevier), 411–429.

Schwartz, T. A., and Gumpertz, S. (2004). The John Hancock tower glass failure-Debunking the Myths.

Sengupta, A., and Sarkar, P. P. (2008). Experimental measurement and numerical simulation of an impinging jet with application to thunderstorm microburst winds. *J. Wind Eng. Industrial Aerodynamics* 96 (3), 345–365. doi:10.1016/j.jweia.2007.09.001

Tamura, Y. (2009). "Wind-induced damage to buildings and disaster risk reduction," in *Proceedings of the APCWE-VII, Taipei, Taiwan*.

Voiland, A. (2024). Derecho darkens Houston. *NASA Earth Obs.* Available at: https://earthobservatory.nasa.gov/images/152843/derecho-darkens-houston.

Williams, T., and Kareem, A. (2003). Performance of building cladding in urban environments under extreme winds. *Proc., 11th Int. Conf. Wind Eng.*

Xie, Z. N., and Gu, M. (2004). Mean interference effects among tall buildings. *Eng. Struct.* 26 (9), 1173–1183. doi:10.1016/j.engstruct.2004.03.007

Zhang, Y., Sarkar, P., and Hu, H. (2014). An experimental study on wind loads acting on a high-rise building model induced by microburst-like winds. *J. Fluids Struct.* 50, 547–564. doi:10.1016/j.jfluidstructs.2014.07.010

frontiers | Frontiers in Built Environment

TYPE Original Research
PUBLISHED 19 March 2025
DOI 10.3389/fbuil.2025.1567729

Check for updates

OPEN ACCESS

EDITED BY
Cheryl Ann Blain,
Naval Research Laboratory, United States

REVIEWED BY
Pedro L. Fernández-Cabán,
Florida A&M University - Florida State University College of Engineering, United States
Simona Bianchi,
Delft University of Technology, Netherlands

*CORRESPONDENCE
Liang Cao,
lic418@lehigh.edu

RECEIVED 28 January 2025
ACCEPTED 26 February 2025
PUBLISHED 19 March 2025

CITATION
Cao L, Marullo TM, Ricles JM, Sause R, Reis C and Saunders J (2025) Recent developments and discoveries in natural hazards mitigation research at the NHERI Lehigh Experimental Facility.
Front. Built Environ. 11:1567729.
doi: 10.3389/fbuil.2025.1567729

COPYRIGHT
© 2025 Cao, Marullo, Ricles, Sause, Reis and Saunders. This is an open-access article distributed under the terms of the Creative Commons Attribution License (CC BY). The use, distribution or reproduction in other forums is permitted, provided the original author(s) and the copyright owner(s) are credited and that the original publication in this journal is cited, in accordance with accepted academic practice. No use, distribution or reproduction is permitted which does not comply with these terms.

Recent developments and discoveries in natural hazards mitigation research at the NHERI Lehigh Experimental Facility

Liang Cao[1]*, Thomas M. Marullo[1], James Michael Ricles[1,2], Richard Sause[1,2], Claudia Reis[1,2] and Joseph Saunders[1]

[1]ATLSS Engineering Research Center, Lehigh University, Bethlehem, PA, United States, [2]Department of Civil and Environmental Engineering, Lehigh University, Bethlehem, PA, United States

Natural hazards, including hurricanes and earthquakes, can escalate into catastrophic societal events due to the destruction of the built environment. To minimize the impact of such hazards on vulnerable communities, civil infrastructure must be designed with performance criteria that prioritize public safety and ensure continuous operation. The National Science Foundation funded Natural Hazards Engineering Research Infrastructure (NHERI) program focuses on advancing the development of resilient infrastructure. The NHERI Lehigh Real-time Multi-directional Simulation Experimental Facility (EF) is one of the facilities within this program. The facility serves as an open-access research hub, offering advanced technologies and engineering tools to develop innovative solutions for natural hazard mitigation. It is uniquely equipped to perform large-scale, multi-directional structural testing in real-time using a cyber-physical simulation technique known as real-time hybrid simulation. This technique enables researchers to model entire systems subjected to dynamic loads at a full scale, allowing for realistic assessments of infrastructure responses to specific hazard scenarios and the development of effective mitigation strategies. This paper explores how cyber-physical simulation has revolutionized research in natural hazards engineering and its influence on engineering practices. It highlights several ongoing projects at the NHERI Lehigh EF aimed at enhancing community resilience in hazard-prone regions. The paper also discusses the planned expansion of the EF, which aims to broaden its focus to include a wider range of natural hazards, and infrastructure systems. This expansion will incorporate both physical and computational resources to enhance the understanding of fluid interactions in combined natural hazards and climate change impacts on coastal and offshore infrastructure. The NHERI Lehigh EF represents a transformative facility that is reshaping natural hazards research and will continue to play a pivotal role in the development of risk management strategies for more resilient communities.

KEYWORDS

large-scale experiments, real-time hybrid simulation, multi-directional, cyber-physical, multi-physics, multi-hazard

1 Introduction

The Natural Hazards Engineering Research Infrastructure (NHERI) Lehigh Experimental Facility (EF), known as the Real-Time Multi-Directional (RTMD) Hybrid Simulation Facility, operates in the Multi-Directional Testing Laboratory at Lehigh University's Advanced Technology for Large Structural Systems (ATLSS) Engineering Research Center. Supported by the NHERI program funded by the National Science Foundation (NSF), the NHERI Lehigh EF provides an open access facility for researchers to use advanced technologies and engineering tools to develop natural hazards mitigation solutions. The facility has a unique portfolio of equipment, instrumentation, infrastructure, testbeds, experimental simulation control protocols, and large-scale simulation and testing capabilities. Various testbeds exist at the NHERI Lehigh EF for researchers to explore civil infrastructure response and develop resilient solutions to enhance infrastructure performance to natural hazards. These include: (1) a lateral load resisting system characterization large-scale testbed; (2) a non-structural component multi-directional dynamic loading large-scale simulator; (3) full-scale damper testbeds; (4) a tsunami debris impact force testbed; (5) soil-foundation structure interaction testbeds; and, the (6) NHERI Lehigh Real-time Cyber-Physical Structural Systems (RCPSS) simulation laboratory.

The NHERI Lehigh EF has the unique ability to conduct large-scale multi-directional structural testing in real-time using a cyber-physical simulation approach, also known as real-time hybrid simulation (RTHS). RTHS integrates the benefits of numerical simulations and physical tests by dividing the structure system into analytical and experimental substructures. In an RTHS, well-understood structural components are modeled numerically in the computer as the analytical substructure, with the remaining components physically modeled using an experimental substructure. The two substructures are coupled in real time by imposing interface displacements and enforcing equilibrium between the substructures. This type of testing and other forms of simulations that can be performed at the NHERI Lehigh EF include: (1) large-scale hybrid simulation (HS) which combines large-scale physical models with computer-based numerical simulations (Lin et al., 2013); (2) large-scale RTHS which is a HS conducted at the actual time scale of the physical models and excitations (Chen et al., 2009; Karavasilis et al., 2011; Chae et al., 2014; Dong et al., 2015); (3) large-scale RTHS with real-time online model updating where some of complex components are physically tested in the laboratory and others are numerically modeled with real-time online model updating (Al-Subaihawi et al., 2022; 2024a); (4) large-scale RTHS with multiple experimental substructures where several experimental specimens are used in a RTHS (Chen and Ricles, 2012; Al-Subaihawi et al., 2020); (5) geographically distributed HS where physical models and/or numerical simulation models are located in different laboratories and connected through the internet (Ricles et al., 2007); (6) geographically distributed RTHS (Kim et al., 2012); (7) quasi-static testing of physical models using predefined force or displacement histories (Zhang and Ricles, 2006; Ricles et al., 2002b; Perez et al., 2013); (8) high-speed testing using servo-controlled hydraulic dynamic actuators at real-time scales to impose predefined force or displacement histories (Ricles et al., 2002a; Chae et al., 2013b); (9) multi-axis RTHS shake table tests with physical models placed on a multi-directional shake table (Villalobos Vega et al., 2022); and (10) multi-physics RTHS with numerical models accounting for soil-structure-interaction or fluid-structure-interaction effects (Al-Subaihawi et al., 2024). The NHERI Lehigh EF enhances the NHERI network by offering complementary testing capabilities to support the diverse experimental needs of the research community. For example, wind pressures measured at a wind tunnel facility (i.e., NHERI Florida International University (Azzi et al., 2020) or the University of Florida Facilities (Catarelli et al., 2020)), wave loads measured at a wave flume (i.e., NHERI Oregon State University Facility (Lomonaco et al., 2020)) can be used for a multi-physics RTHS conducted at the NHERI Lehigh EF. All test results and research data are shared through the NHERI DesignSafe Data Depot Repository (Rathje et al., 2017).

Several experimental research projects have been performed using the equipment and algorithms at the NHERI Lehigh EF, including: (1) multi-directional RTHS of a tall building equipped with nonlinear viscous dampers subjected to earthquake and wind hazards (Al-Subaihawi et al., 2024a); (2) multi-physics RTHS of a tall building with a soil-foundation system modeled using neural networks and subjected to wind hazards (Al-Subaihawi et al., 2024); (3) 3D RTHS using a multi-axis shake table to test floor isolation systems for mitigating detrimental seismic effects on critical building contents (Villalobos Vega et al., 2024); (4) multi-directional cyclic lateral loading tests of self-centering cross-laminated mass timber shear wall sub-assembly (Amer et al., 2024); and, (5) large scale tests of seismic collectors in a steel frame floor system. Discoveries from these projects illustrate the important aspects of large-scale, multi-directional, real-time hybrid testing with multi-physics effects for the development of innovative resilient structural systems that contain new natural hazard mitigation strategies.

The paper is organized into five remaining sections. Section 2 presents an overview of the NHERI Lehigh EF, including the team members and their expertise, equipment, testbeds, real-time integrated control system and testing capabilities. Section 3 presents the protocol for performing real-time cyber-physical simulations at the facility. Section 4 describes recent research projects conducted at the NHERI Lehigh EF and their respective contributions towards creating a more natural-hazards resilient community. A summary and conclusions are given in Section 5.

2 Overview of the NHERI Lehigh EF

This section provides an overview of the NHERI Lehigh EF, including its unique expertise of the staff, equipment, testbeds, real-time control integrated system and testing capabilities. The unique strengths of the facility's equipment, testbeds, control system, and staff expertise enable a wide range of simulations and types of testing. These include: (1) large-scale HS; (2) large-scale RTHS; (3) large-scale RTHS with real-time online model updating; (4) large-scale RTHS with multiple experimental substructures; (5) geographically distributed HS; (6) geographically distributed RTHS; (7) quasi-static testing; (8) dynamic testing; (9) multi-directional RTHS multi-axis shake table tests; and (10) multi-physics RTHS. In addition, multiple simulations and tests can be performed simultaneously,

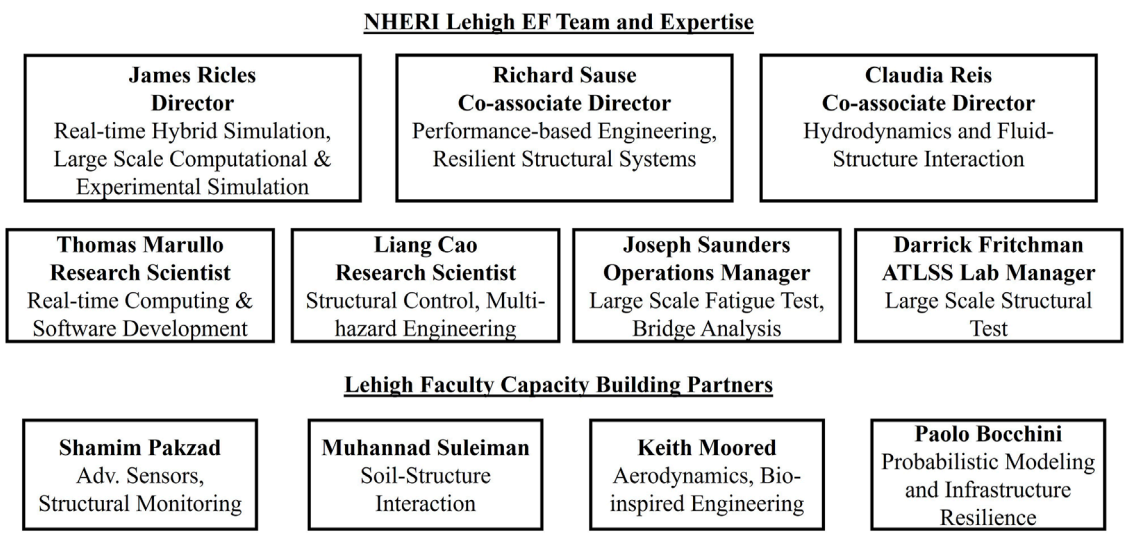

FIGURE 1
NHERI Lehigh EF staff and capacity building council.

allowing numerous users to work concurrently without significant interruption.

2.1 NHERI Lehigh EF team and expertise

The NHERI Lehigh EF is highly dependent on its staff who are dedicated to supporting the operations of the facility. Figure 1 shows the NHERI Lehigh EF staff members and the capacity building advisory council, and lists their main expertise in multidisciplinary and complementary research fields associated with natural hazards engineering.

The ATLSS Engineering Research Center and the NHERI Lehigh EF are led by Dr. James Ricles, who provides overall leadership and accountability for completing the missions of the ATLSS Center and NHERI Lehigh EF. Dr. Richard Sause and Dr. Claudia Reis, associate directors, provide leadership support and technical assistance to the Director, Dr. James Ricles. The expertise of Dr. James Ricles includes RTHS as well as large-scale computational and experimental simulation, while the expertise of Dr. Richard Sause includes performance-based engineering and resilient structural system concepts. Dr. Claudia Reis' expertise includes hyrodynamics and fluid-structure interaction, along with risk mitigation of coastal civil infrastructure. Research scientist Thomas Marullo oversees the facility's IT systems along with the development and implementation of software and algorithms to support testing protocols. Research scientist Dr. Liang Cao supervises the configurations of the experimental protocol, user training, and site improvements. Dr. Joseph Saunders manages the facility's operations and is responsible for the education, communication, and outreach program. Darrick Fritchman manages a team of highly skilled technicians who provide laboratory support for research projects. The skills sets of laboratory technicians include servo-hydraulics, instrumentation, fabrication, and erection of test specimens. The capacity building advisory council of the NHERI Lehigh EF is composed of Lehigh faculty who possess complementary expertise and provide capacity-building advice. Dr. Shamim Pakzad provides technical capacity building advice in the areas of advanced sensors and structural health monitoring. Dr. Muhannad Suleiman provides technical capacity-building advice in soil-structure interaction and geotechnical engineering. Dr. Keith Moored provides technical capacity-building advice in the area of aerodynamics and bio-inspired engineering innovations applied to natural hazards mitigation, while Dr. Paolo Bocchini provides technical capacity-building support in the areas of probabilistic modeling and infrastructure resilience.

The highly skilled multidisciplinary team members, laboratory technicians, and capacity-building advisory council enable the acquisition of high-quality numerical and experimental results through complex simulations and tests performed at the NHERI Lehigh EF.

2.2 NHERI Lehigh EF equipment

The NHERI Lehigh EF is located within the ATLSS Engineering Research Center that has 2,736 m^2 of high-bay laboratory floor space and features a 3D multi-directional reaction wall and strong floor. The NHERI Lehigh EF has a unique portfolio of equipment that enables accurate, large-scale, and multi-directional tests to be readily performed. The natural hazard engineering research community can use these resources to perform various structural experiments under natural hazard effects. In particular, five large-capacity hydraulic actuators manufactured by Servotest Systems are available for large-scale testing. These actuators can achieve a maximum force of 2,300 kN, and a maximum velocity of 1,143 mm/s with a 1,000 mm stroke range. Seven MTS hydraulic actuators are also available for small-scale testing, with a maximum force capacity of 250 kN, a peak velocity of 1,295 mm/s, and a stroke length of 508 mm. The details of the NHERI Lehigh EF equipment portfolio are summarized in (Cao et al., 2020).

2.3 NHERI Lehigh EF testbeds

Various large-scale testbeds are available at the NHERI Lehigh EF. Details of these test beds can be found in (Cao et al., 2020) describing: (1) an 11 m wide by 13.7 m high lateral load resisting system characterization testbed; (2) a 3 m wide by 12 m long non-structural component multi-directional dynamic loading simulator; (3) full-scale damper testbeds with five large-scale dynamic actuators; (4) a tsunami debris impact force testbed; and (5) a soil-foundation-structure interaction testbed with two large-scale soil boxes. These testbeds provide a wide range of large-scale testing capabilities that include quasi-static and dynamic testing in addition to HS. Researchers can use these testbeds to perform multi-directional experimental investigations on large-scale structural components and systems, in addition to non-structural components subjected to extreme natural hazard events that include soil-foundation effects.

2.3.1 NHERI Lehigh real-time cyber-physical structural systems testing laboratory

In addition to large-scale testing capabilities, the NHERI Lehigh EF recently features a 372 m^2 NHERI Lehigh Real-time Cyber-Physical Structural Systems (RCPSS) Testing Laboratory. The laboratory is a multidisciplinary research facility focused on small-scale real-time testing to mitigate the effects of natural hazards on civil infrastructure. It consists of seven new dynamic testbeds, a multi-directional shake table, a dedicated high-speed data acquisition system, a real-time integrated control system that includes a multi-channel digital servo-hydraulic controller. The real-time integrated control system enables real-time dynamic testings to be performed.

The dynamic testbeds in the RCPSS can accommodate a broad range of dynamic characterization and HS natural hazards experiments for researchers to explore structural mitigation solutions. In each testbed, an MTS dynamic servo-hydraulic actuator and test specimen can be placed. A 32 channel high speed data acquisition system and an array of sensors are available to measure displacement, rotation, temperature, acceleration, strain, and force to acquire measured test data.

For example, a setup for testing a next-generation 45 kN capacity semi-active rotary friction damper (Downey et al., 2016) in the RCPSS testing lab is shown in Figure 2A. The test setup consists of an actuator mounted on a foundation beam, with a reaction support (identified as column support) and the rotary friction damper connected to a hydraulic actuator via a roller support. The damper forces applied by the actuator are measured with a load cell, safety relays are incorporated into the test setup to provide safety measures and protection of the test specimens. The testbed has been used to perform various dynamic characterization and RTHS tests (Cao et al., 2024; Coble et al., 2024). The results of these studies show that the rotary friction damper has a dynamic amplification factor of 110, requiring smaller amounts of energy to develop the frictional force compared to conventional friction dampers. This rotary friction damper is therefore a feasible device that can be used to create effective multi-hazard mitigation solutions for reducing damage to civil infrastructure during extreme natural hazard events.

The RCPSS testing laboratory also includes a Real-time Cyber-Physical Structural Systems Multi-directional Shake Table. This shake table has a table platen size of 1829 mm × 1829 mm with a payload of 58 kN at 1 g acceleration. Maximum table motions of ±254 mm in the NS direction and ±177 mm in the EW direction, with a peak velocity of 737 mm/s, can be achieved. It can realistically emulate combined translational and twisting motions that develop in structural systems under extreme 3D wind and earthquake loadings conditions.

Figure 2B shows a photograph of the multi-directional shake table with multi-directional translation and torsional motion applied in the plane. The shake table can be used in different configurations to perform a range of experiments, including real-time multi-axis shake table hybrid simulations, traditional multi-axis shake table testing, or used as a load platen to perform quasi-static and dynamic testing of test specimens.

2.4 NHERI Lehigh EF integrated control system

The NHERI Lehigh EF real-time testing architecture features a real-time integrated control system enabling both real-time and paced control of multi-directional testing. A schematic of the real-time testing architecture is shown in Figure 3. The real-time integrated control system architecture consists of various systems that are linked by Ethernet and SCRAMNet GT communication hardware. SCRAMNet GT is a shared memory fiber optic based network that synchronizes data among a ring of systems thus facilitating experimental protocols and access to data in real time. Synchronization over SCRAMNet GT is enforced by the Servotest Pulsar servo hydraulic controller which has a clock speed of 2048 Hz. The servo hydraulic controller is identified as *RTMDctrl* in Figure 3. The controller operates tunable closed-loop PID control algorithms for each actuator and has I/O controls for managing the hydraulic power system. External control over SCRAMNet GT is enabled and feedback data such as position and force responses from each actuator is written to SCRAMNet GT at the control rate. High fidelity data acquisition is capable through the Pacific Instruments 6,000 series data acquisition system, known as *RTMDdaq*.

The algorithms necessary to execute the experimental protocols are implemented through the Simulation PC workstation, known as *RTMDsim*. The algorithms are tailored specifically for each test and programmed primarily using MATLAB and Simulink. Simulink is used to design a model-in-the-loop system that can interact with the servo hydraulic controller and data acquisition system over SCRAMNet GT. To execute these models, they are compiled and deployed to Speedgoat Real-time Performance Systems, known as *RTMDxPC1* and *RTMDxPC2*. These standalone, robust embedded systems run a unique real-time operating system that is designed to execute compiled Simulink models and interact with various supported hardware typically at a simulation rate of 1,024 Hz. If a simulation requires a large computational model with many degrees of freedom, or there is a need for additional hardware communications such as controlling electric and hydraulic actuators simultaneously, then the executable code is parallelized and placed onto multiple xPC systems, i.e., *RTMDxPC1* and *RTMDxPC2*.

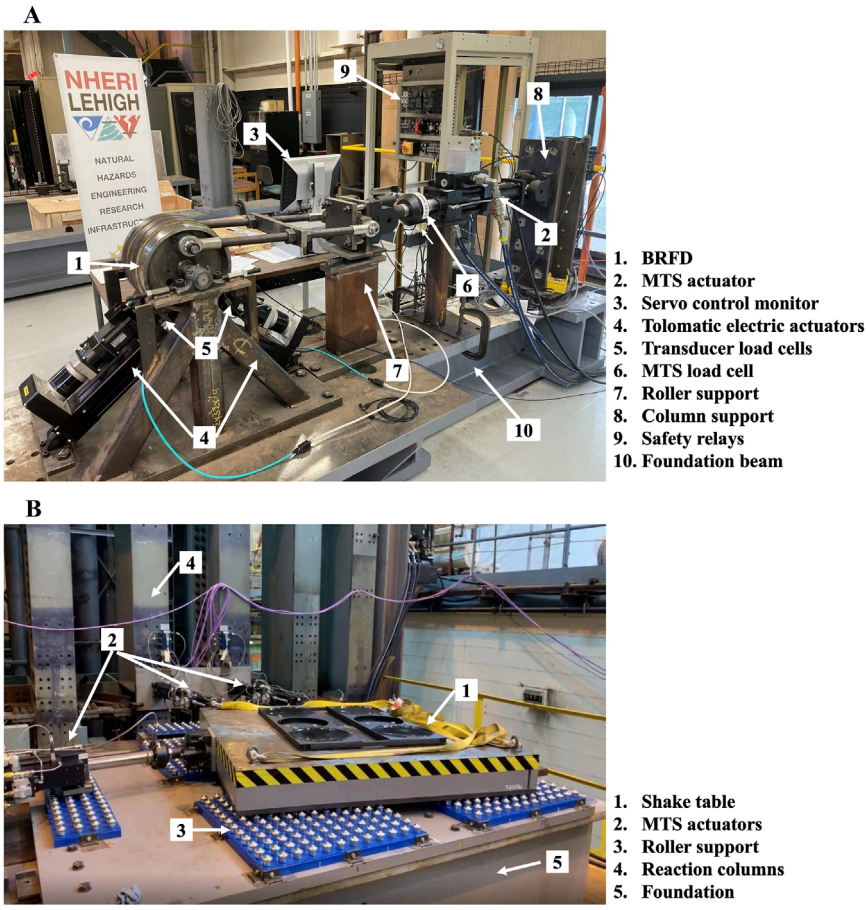

FIGURE 2
NHERI Lehigh RCPSS Testing Laboratory: **(A)** Dynamic test setup of a rotary friction damper; **(B)** Real-time cyber-physical structural systems multi-directional shake table (multi-directional translation and torsional in-plane motion applied).

For models that exceed the capabilities of the xPC computational limit such as large matrix multiplications, the GPU workstation *RTMDcmp* is available for additional high-performance processing. This system is an Intel based i9 CPU and contains an NVIDIA RTX 4000 series GPU along with SCRAMNet GT. Python is the preferred programming architecture executed on this system and is available during real-time simulation. It can also be used for using machine learning to train neural network models and for post processing of test results.

The PC workstation *RTMDcam* is configured with Blue Iris video management software that is capable of configuring, recording and synchronizing web camera video and images along with providing a web interface for users. The PC workstation *RTMDobs* has audio and video capabilities and can be used to observe data, plot feedback signals, and interact with remote users via telepresence software such as Zoom. For RTHS, MATLAB-based software is available to animate the real-time response of a complete system, including the analytical and experimental substructures. Experimental data, metadata and training materials are organized and archived on a Synology dual disk redundancy network attached storage system known as *RTMDdata*. As noted in Figure 3, there is a twin lab known as the RCPSS laboratory with the same real-time integrated control architecture and is directly connected to the RTMD laboratory through SCRAMNet GT and Ethernet. Both laboratories have identical capabilities and allow users to perform experiments simultaneously using multiple testbeds.

3 NHERI Lehigh EF real-time cyber-physical simulation

This section outlines the key approach of the NHERI Lehigh EF, emphasizing real-time cyber-physical simulation, as well as advancements in multi-directional and multi-physics RTHS.

3.1 Overall concept of RTHS

A schematic showing the process for performing an RTHS is given in Figure 4A. The RTHS is governed by the equations of motion, namely:

$$\mathbf{M}\ddot{\mathbf{X}}_{i+1} + \mathbf{C}\dot{\mathbf{X}}_{i+1} + \mathbf{R}^{a}_{i+1} + \mathbf{R}^{e}_{i+1} = \mathbf{F}^{a}_{i+1} \quad (1)$$

where $\ddot{\mathbf{X}}_{i+1}$, $\dot{\mathbf{X}}_{i+1}$, $\mathbf{R}^{a}_{i+1}$ and $\mathbf{R}^{e}_{i+1}$ are the acceleration vector, velocity vector, the restoring force vector of the analytical substructure, and

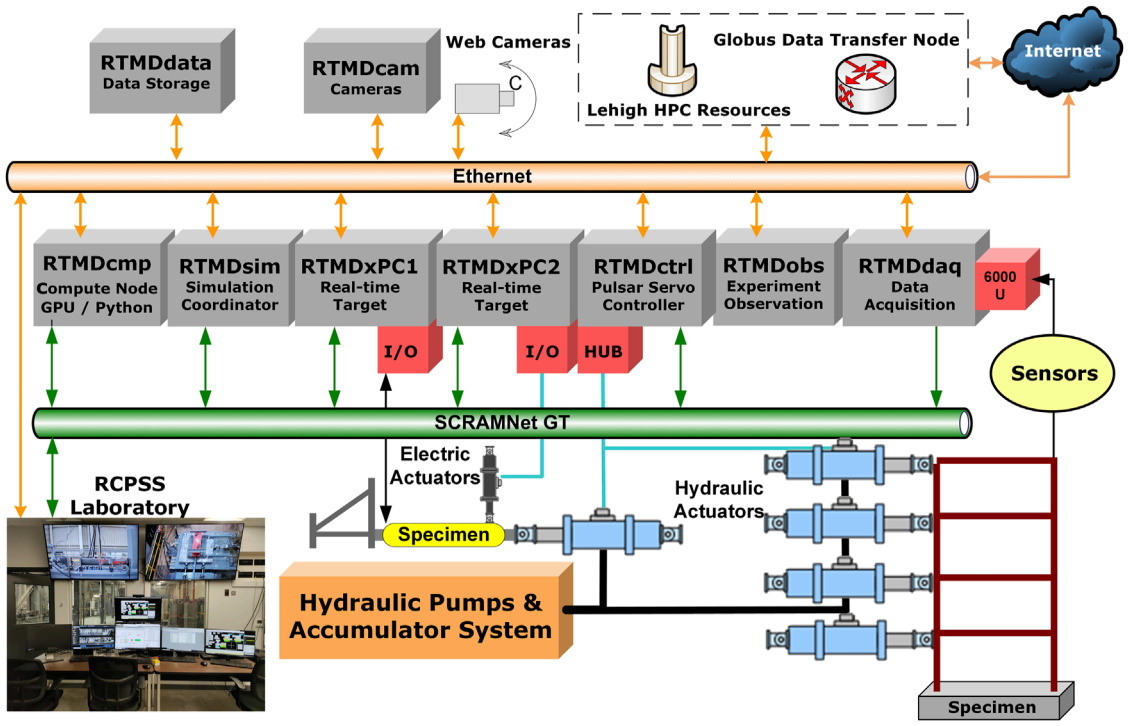

FIGURE 3
NHERI Lehigh RTMD EF real-time testing integrated control system architecture.

the restoring force vector of the experimental substructure of the system at time t_{i+1}, respectively. $\mathbf{F}^a_{i+1}$ in Equation 1 is the excitation force vector (e.g., earthquake or wind loads) at time t_{i+1}, and $\mathbf{M}$ and $\mathbf{C}$ are the analytically defined mass and inherent damping matrices of the system, respectively.

For a given time step t_{i+1}, the RTHS requires explicit integration algorithms to integrate the equations of motion in real time. The NHERI Lehigh EF has developed several explicit model-based dissipative integration algorithms (Al-Subaihawi et al., 2024b; Kolay and Ricles, 2019; Chen and Ricles, 2008; Kolay and Ricles, 2014; Kolay et al., 2015) that are unconditionally stable and therefore well suited for the RTHS. The algorithms are formulated to solve a weighted form of the equations of motion (see (Kolay and Ricles, 2019; Chen and Ricles, 2008; Kolay and Ricles, 2014; Kolay et al., 2015) for details).

Referring to Figure 4A, for an applied loading $\mathbf{F}^a_{i+1}$ the integration algorithm embedded in the simulation coordinator generates command displacements $\mathbf{X}^a_{i+1}$ and $\mathbf{X}^e_{i+1}$ for the analytical and experimental substructures, respectively. $\mathbf{X}^a_{i+1}$ is passed to the analytical substructure, while the command displacement $\mathbf{X}^e_{i+1}$ is imposed on the experimental substructure (e.g., nonlinear viscous dampers) in real-time using servo-hydraulic actuators. An advanced adaptive delay compensation algorithm developed by the NHERI Lehigh EF (Chae et al., 2013a), termed the adaptive time series (ATS) compensator, is used to accurately impose $\mathbf{X}^e_{i+1}$ in real-time to the experimental substructure. The restoring forces $\mathbf{R}^a_{i+1}$ and $\mathbf{R}^e_{i+1}$ are obtained and subsequently used by the simulation coordinator to determine the vector of accelerations $\ddot{\mathbf{X}}_{i+1}$ and complete the integration process for the time step. This process is then repeated for each subsequent time step until the end of the loading history is reached.

3.2 Development for multi-directional RTHS

To conduct RTHS on structures subjected to multi-directional natural hazards, termed multi-directional RTHS, three-dimensional nonlinear models of structural systems are required. The NHERI Lehigh EF staff has developed the MATLAB and Simulink-based finite element program *HyCoM-3D*, (Ricles et al., 2020), for assessing the multi-directional performance of civil infrastructure systems. HyCoM-3D is a three-dimensional (3D) simulation program that is compatible with the xPCs of the real-time integrated control system. The program has nonlinear geometric and material modeling capabilities. It contains a material library for modeling structural steel, reinforced concrete, timber, nonlinear viscous, shape memory alloy, and friction materials. The explicit-formulated element library in HyCoM-3D includes nonlinear truss elements, displacement-based and force-based fiber elements with co-rotational geometric and material nonlinearities, nonlinear geometric elements to model P-Δ effects, nonlinear hysteretic connection elements, nonlinear gap elements, nonlinear panel zone elements, and zero-length elements. Real-time model updating, neural network models, reduced order elements, and multi-point constraint options are also featured in HyCoM-3D. The program has been successfully used to conduct both nonlinear time history analysis and multi-directional RTHS of complex nonlinear

structural systems (Al-Subaihawi et al., 2020; Dong et al., 2018a; Dong et al., 2018b; Kolay et al., 2020; Al-Subaihawi et al., 2020; Villalobos Vega et al., 2022; Al-Subaihawi et al., 2024a; Malik et al., 2025). A kinematic compensation algorithm developed by the NHERI Lehigh EF staff (Mercan et al., 2009) to perform multi-directional RTHS is used to avoid kinematic errors during a test. The algorithm accounts for the nonlinear relationship between the target displacements and the displaced configuration of the test structure and the actuators in determining the actuator command displacement signals.

3.3 Extension to multi-physics RTHS

In nature, the effects of natural hazards on infrastructure systems represent complex multi-physics interactions. In inland locations, these interactions encompass soil-foundation-structure systems while in coastal and offshore regions, the system is subjected to wave-wind-soil-structure interaction effects.

The NHERI Lehigh EF recently implemented a new framework for incorporating soil-foundation-structure interactions (SFSI), enabling realistic simulations of inland systems. The overall concept of multi-physics RTHS is demonstrated using an example of an SFSI system equipped with passive nonlinear viscous dampers subjected to wind loads, as shown in Figure 4B. The structural system is a 40-story steel frame building, with nonlinear passive viscous dampers installed in outrigger trusses to improve its performance under natural hazards. Structural components that include steel frames, associated seismic mass, and inherent damping are numerically modeled using the finite element method, while the soil and foundation beneath the building are modeled using a real-time neural network (NN) model.

The analytical substructure consists of the structure, soil, and foundation models, while the nonlinear viscous dampers are physically modeled in the laboratory as the experimental substructure. Multi-directional earthquake loads are determined from the accelerograms of ground motions. More details are described in Section 4.2. The equations of motion are augmented with the NN model's degrees of freedom and therefore, $\mathbf{R}_{i+1}^{a,\mathrm{NN}}$ is the restoring force of the NN model. $\mathbf{X}_{i+1}^{a}$ for the analytical substructure in time step $i+1$ includes the displacements $\mathbf{X}_{i+1}^{a,\mathrm{FEM}}$ from the finite element model and the displacements $\mathbf{X}_{i+1}^{a,\mathrm{NN}}$ of the NN model, while the analytical substructure's restoring forces at time step $i+1$ consist of the restoring force of the finite element model and the NN model, as shown in Equation 2. Considering the system's degrees of freedom and the associated topography of these vectors,

$$\begin{aligned}\mathbf{X}_{i+1}^{a} &= \mathbf{X}_{i+1}^{a,\mathrm{FEM}} + \mathbf{X}_{i+1}^{a,\mathrm{NN}} \\ \mathbf{R}_{i+1}^{a} &= \mathbf{R}_{i+1}^{a,\mathrm{FEM}} + \mathbf{R}_{i+1}^{a,\mathrm{NN}}\end{aligned} \tag{2}$$

For fluid-soil-structure interactions (FSSI) characteristic of coastal and offshore environments, it is necessary to acknowledge an increased complexity, not only from the physical phenomena, but also because the FSSI system becomes a multi-physics problem. One of the major challenges is to model the behavior of the fluid and the solids in the same domains. Moreover, as they are governed by different laws of physics, it is preferable to use full-scale models to avoid similitude issues. Another challenge is the computational costs deemed necessary to achieve high fidelity numerical solutions realistically reproducing highly nonlinear FSSI phenomena. In addition, there is a lack of field and experimental data of structural compliance within mild to turbulent flows to calibrate and validate the simulation models.

Thus, the NHERI Lehigh EF is developing two complementary approaches to test FSSI of infrastructure subjected to hydraulic loads. The first approach consists of a numerical characterization of the fluid behavior that is imposed on a physical structure or soil-structure system. The numerical models rely on sophisticated numerical schemes capable of modeling two-way fluid-solid interactions. Before their use, these numerical schemes are being subjected to an exhaustive benchmark test using data recorded during experimental campaigns. Given the computational demand inherent to such models, the use of machine learning models, such as the NN models previously adopted to model SFSI, represents a useful tool. In this case, the fluid behavior is numerically computed from the classic fluid model to train the NN model. The trained NN model is then used to impose the fluid loading on the structure, which can be imposed on the experimental structure using as many actuators as needed to account for the multi-degree of freedom nature of the problem.

The second approach is utilizing a wave flume to physically model fluid mechanics in an FSSI RTHS framework. The wave flume will be incorporated into the RTHS framework to complement an existing experimental setup consisting of structural and soil-foundation systems. Complex, multi-physics systems can be modeled by coupling physical setups in Simulink to create a model-in-the-loop system, which is then compiled and deployed to real-time systems. In addition, the wave flume will produce experimental data to calibrate and validate numerical, and machine learning models. Details on the expansion of the NHERI Lehigh EF will be published soon.

4 Developments and discoveries from recent research projects

In this section, five selected example projects performed by researchers that utilized the NHERI Lehigh EF are presented. These example projects leveraged the NHERI Lehigh EF resources to conduct large-scale, multi-directional, and multi-physics experiments. The outcomes and impact of these studies on natural hazards engineering are highlighted, showcasing the benefits of utilizing the NHERI Lehigh EF.

4.1 Multi-directional RTHS of a tall building equipped with nonlinear viscous dampers subjected to natural hazards

The 3D nature of natural hazards requires that 3D structural models be used in order to accurately capture the realistic natural hazard response of the system. The study presented in this subsection introduces a new RTHS framework that overcomes existing challenges in using 3D multi-directional

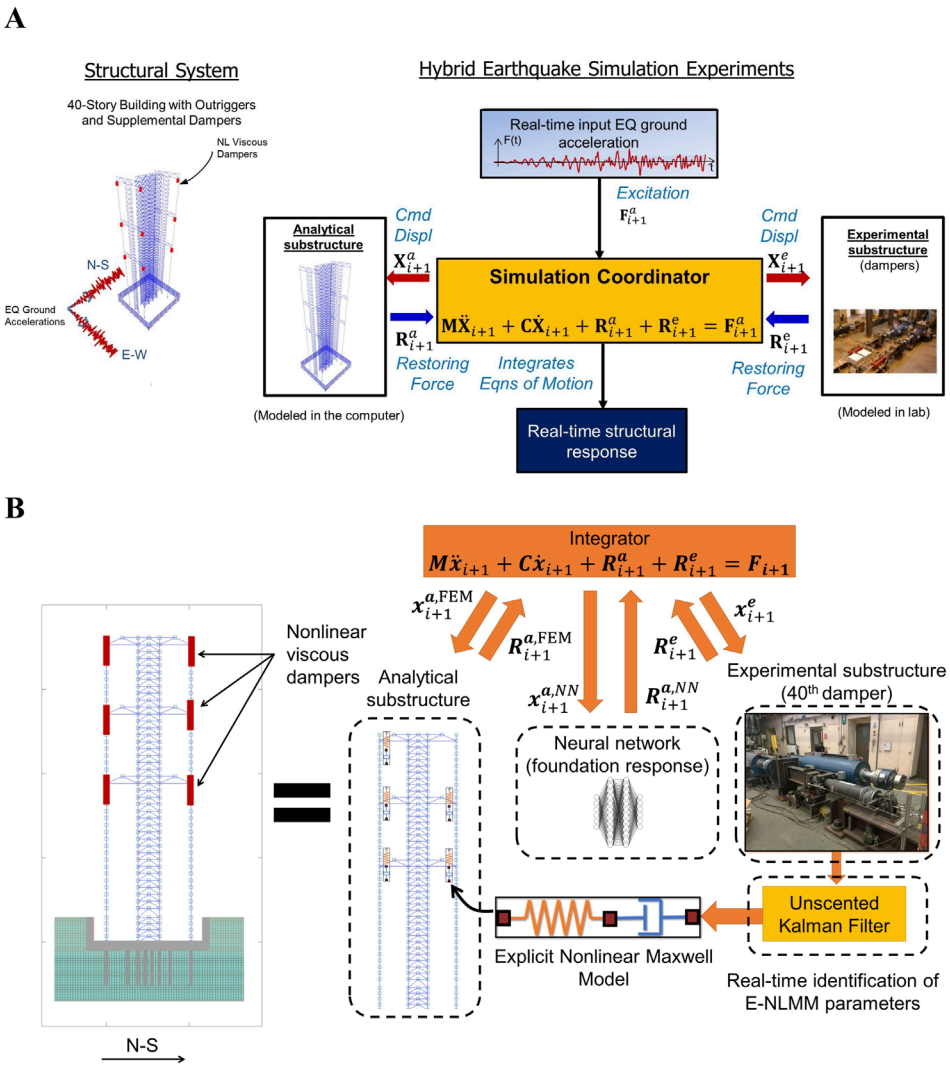

FIGURE 4
(A) Schematic of the RTHS process; **(B)** Multi-physics RTHS example: a 40-story building with soil-structure interaction using neural network (courtesy of Al-Subaihawi et al. (2024)).

RTHS to examine the nonlinear response of tall buildings under multi-hazard excitations. The framework is demonstrated by applying it to a 40-story steel-framed building, where its multi-directional response to earthquake and wind is investigated (Al-Subaihawi et al., 2024a).

4.1.1 40-Story building description

The building is designed by Simpson Gumpertz & Heger Inc. as part of the PEER Tall Building Initiative (Moehle et al., 2011). It is located in Los Angeles, and has a height of 166 m with a 32.6 m by 51.7 m floor plan, as shown in Figures 5A, B. The lateral force resisting system consists of six buckling restrained braced frames (BRBFs) in the North-South and East-West directions with an outrigger system consisting of six outrigger trusses located in the 20^{th}, 30^{th}, and 40^{th} stories at the East and West ends of the building. The building is retrofitted by placing nonlinear viscous dampers (NLVD) between the ends of the outrigger trusses and the perimeter columns of the outrigger, as shown in Figure 5C, as a means to increase the equivalent damping of the building.

4.1.2 Natural hazards description

The earthquake RTHS utilizes the ground motion recorded at the Saratoga Aloha Avenue station during the 1989 Loma Prieta earthquake. This ground motion is scaled to the MCE hazard level, with the uniform hazard curve at the building's location serving as the target response spectrum. The scaling minimizes the error between the geometric mean of the adjusted ground motion and the target response spectrum within the 0.5s–10s period range, using the following error weighting: 10% for 0.5s–3s, 60% for 3s–7s, and 30% for 7s–10s. The final scaling procedure yields a scale factor of 1.98.

A 1/150 scaled aerodynamic model of the building is built and tested in the NHERI FIU Wall of Wind facility to measure the time history data of wind pressure during a simulated wind storm. The wind tunnel model has 336 pressure taps distributed around the

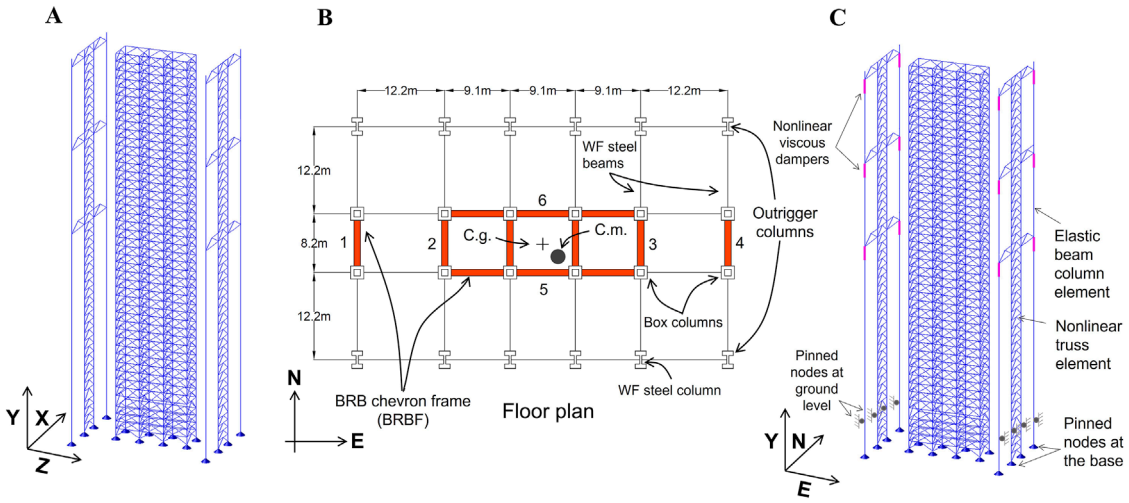

FIGURE 5
Prototype 40-story tall building equipped with a damped outriggers system: **(A)** Isometric view; **(B)** Floor plan; and **(C)** Analytical substructure for multi-directional RTHS (courtesy of Al-Subaihawi et al. (2024a)).

model's surfaces. The wind pressure at each floor level of the building is calculated by linear interpolation of the time history data between pressure taps. The wind storm has a design wind speed of 38 m/s at the equivalent full-scale wind intensity, derived from the 3-s gust wind speed specified in ASCE 7–10 (ASCE, 2010). The wind tunnel tests are conducted with a duration time of 325 s. Lateral wind loads in the east-west and north-south directions and torsional loading normal to the building's floor plan are obtained by multiplying the wind pressure by the tributary areas.

4.1.3 Multi-directional RTHS description

The analytical substructure for the RTHS is developed using HyCoM-3D, and consists of a 3D finite element model of the building with nonlinear viscous dampers. The experimental substructure consists of one full-scale rate-dependent nonlinear viscous damper, with the remaining dampers modeled numerically with online model updating, as explained below. The analytical substructure consists of 1,080 nonlinear truss elements to model the buckling restrained braces and 40 geometric stiffness elements to model the lean-on columns. For the earthquake RTHS an eccentricity of the floor mass of 5% of the building's floor plan dimensions is specified in both horizontal directions to induce torsional loading. To allow the equations of motion to be integrated in real time with an integration time step of 11/1,024 s, a super element is used to model all of the elastic elements of the structure, excluding the outrigger trusses and columns that developed inelastic response under the earthquake load. The use of the super element applied static condensation to the model, reducing the model's number of degrees of freedom from 3,974 to 1,429.

Five nonlinear viscous dampers are placed between each outrigger truss and perimeter column for the earthquake RTHS and three nonlinear viscous dampers for the wind RTHS, leading to a total of 60 and 36 dampers for the earthquake and wind RTHS, respectively. The experimental substructure consisting of one full-scale nonlinear damper has a 600 kN load capacity and a 125 mm stroke. The remaining dampers are modeled analytically using an explicit formulated nonlinear Maxwell model developed by (Al-Subaihawi et al., 2022) and their parameters are updated in real time using an Unscented Kalman Filter.

The unconditionally stable parametrically dissipative MKR-α integration algorithm developed by (Kolay and Ricles, 2019) is used to integrate the weighted equations of motion for the RTHS and the second-order ATS compensator (Chae et al., 2013a) used to compensate for any delay and amplitude error of the servo-hydraulic actuator of the experimental substructure.

4.1.4 Results and outcomes

Figures 6A, B show the time history of the displacement and twist of the building roof under the two natural hazards. The twist under earthquake loading is induced by the 5% eccentricity described previously, while that under wind loading is due to the development of differential pressures that were measured around the perimeter of the building during the wind tunnel testing. The 3D RTHS results demonstrate the essential multi-axis behavior of the structure. For the RTHS earthquake, residual roof displacement and twist caused by the buckling restrained braces' inelastic response are captured in both the North-South and East-West directions. Due to the combined translation and torsional motions of the building, inelastic deformations are observed in the buckling restrained braces over the height of the building. Figures 6C, D shows the ductility demand in the buckling restrained braces of four selected BRBFs over the height of the building in the North-South and East-West directions. Significant differences in the ductility demand of each BRBF are observed due to the torsional effects of building vibration. This outcome illustrates the importance of considering 3D models that include torsional degrees of freedom in order to capture the accurate inelastic response of a structure during a strong earthquake.

For the wind RTHS, while no roof residual displacement and twist are found, the building exhibits a static component of displacement and twist due to the combination of along-wind

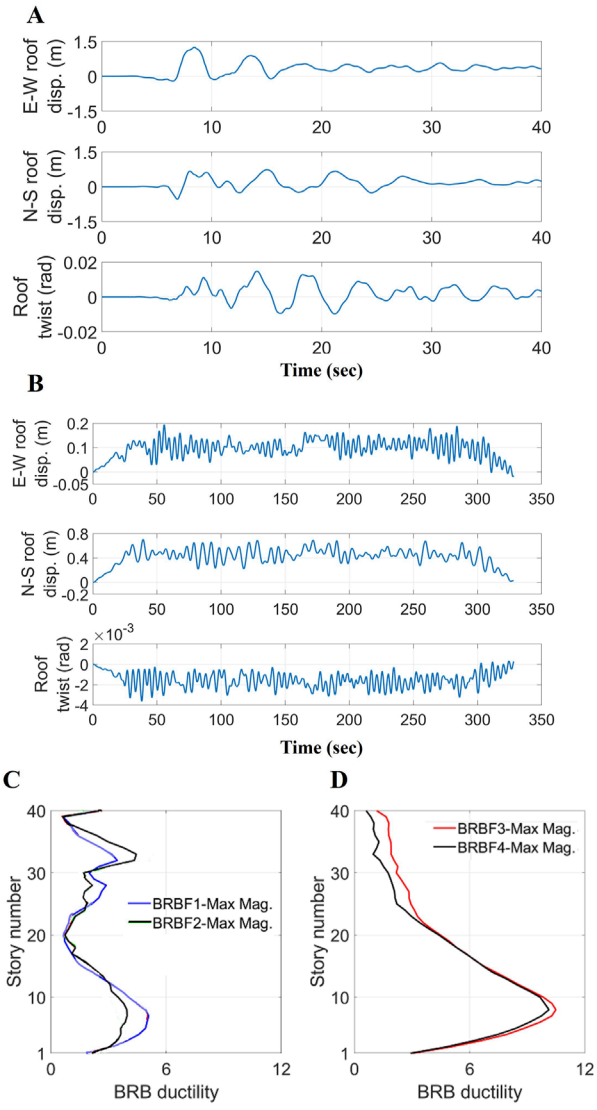

FIGURE 6
Roof displacement time histories: **(A)** Earthquake RTHS; and **(B)** Wind RTHS; Maximum magnitude of BRB ductility over the height of the building: **(C)** N-S direction; and **(D)** E-W direction (courtesy of Al-Subaihawi et al. (2024a)).

and cross-wind effects, as shown in Figure 6B. Consequently, this torsional effect can generate an acceleration increase at the corners of the building. Table 1 compares the peak resultant floor accelerations at the center and corner of the floor plan from selected floors. The acceleration of the corner on the 20^{th} floor has the maximum increase of 47.4% compared to the center of the floor plan. This significant difference demonstrates the importance of a 3D building model in capturing the essential increase in floor acceleration in the corner caused by angular accelerations.

The measured experimental damper response is compared with the numerical damper model response prediction using the updated model parameter values from the online model updating algorithm. The comparison indicates that the Normalized Root Mean Square Errors (NRMSE) for the earthquake and wind RTHS are 1.29% and 2.42%, respectively, indicating an excellent prediction by the

TABLE 1 Peak resultant floor acceleration at the center and corner of floor plan for wind RTHS.

Case	Peak floor acceleration (mg)		
	20th floor	30th floor	40th floor
Center	11.8	19.3	24.1
Corner	17.4	23.0	28.5
Increase (%)	47.4	19.1	18.2

online model updating method. It is also found that the force-deformation hysteric response of the viscous dampers possessed different characteristics under earthquake and wind events, with the wind-induced response exhibiting a static drift due to the static component of the along-wind effect. During the RTHS earthquakes, the dampers developed higher velocities and therefore forces compared to that of the wind RTHS; details can be found in (Al-Subaihawi et al., 2024a).

As noted above, the outcomes from the 3D RTHS illustrate the importance of using 3D models that include torsional degrees of freedom in order to capture the accurate inelastic response of a structure during a strong earthquake and floor accelerations during wind storms. The results from the study provide a practical framework for experimentally investigating the 3D performance of civil structures under multi-natural hazards.

Test results and data (Al Subaihawi et al., 2023a; Al Subaihawi et al., 2023b; Kolay et al., 2023) have been uploaded to the DesignSafe Data Depot Repository and can be downloaded at https://www.designsafe-ci.org/data/browser/public/designsafe.storage.published/PRJ-1439.

4.2 Multi-physics RTHS of a tall building with soil-foundation system using neural networks

To account for soil-structure effects, a piled reinforced concrete raft foundation is designed using a performance-based design approach for the 40-story building described in Section 4.1.1, and is used to perform RTHS. Figure 4B shows the RTHS framework used to model the soil-foundation system. The structure consists of a 2D version of the 40-story building described in Section 4.1, considering a planar model in the plane of the outrigger system in the NS direction. Two parallel nonlinear viscous dampers are placed between the ends of each outrigger truss and the adjacent outrigger column at the 20^{th}, 30^{th}, and the 40th stories. A computationally efficient trained neural network model is used to create a reduced-order real-time model of the soil-foundation system. One experimental nonlinear viscous damper is installed at the end of the 40^{th} story outrigger truss and connected to the outrigger column, where the experimental substructure's restoring force is multiplied by two in order to account for two parallel dampers. The viscous dampers at the remaining five are modeled numerically using the explicit nonlinear Maxwell model developed by (Al-Subaihawi et al., 2022), where the output force of each damper is also multiplied by a factor of two. The numerical damper model

TABLE 2 Multi-physics RTHS test matrix.

Test ID	Test type	No. Of training records	No. Of validation records	Noise injection	ReLU	Target RMSE	Avg actual training RMSE	Avg validation RMSE
1	Multi-physics RTHS	2093	299	Yes	Yes	0.01	0.01	0.008
2	Multi-physics RTHS	455	65	Yes	Yes	0.01	0.02	0.01
3	Multi-physics RTHS	455	65	Yes	Yes	0.05	0.07	0.06
4	Multi-physics RTHS	455	65	No	Yes	0.01	0.01	0.01
5	Multi-physics RTHS	455	65	Yes	No	0.01	0.04	0.03
6	Multi-physics RTHS	2093	299	Yes	Yes	0.01	0.02	0.01
7	RTHS	NA	NA	NA	NA	NA	NA	NA

parameters are updated in real time using the Unscented Kalman Filter. The building, numerical viscous dampers, and soil-foundation system form the analytical substructure. The SFSI response under the wind load described in Section 4.1.2 is used to perform the multi-physics RTHS.

4.2.1 Training and validation of NN model

The NN model for the soil-foundation system contains a block of four long-short-term memory (LSTM) layers in parallel with a rectified linear unit (ReLU). The LSTM block has four hidden layers, with each hidden layer having 75 neurons. To train the NN model, a 2D SFSI model is developed using OpenSees (Mazzoni, 2006). The OpenSees building model contains 717 DOFs and 388 elements while the soil-foundation system model consists of 2,478 DOFs and 2,996 elements. The viscous dampers are modeled using a Kelvin-Voigt model and the damping coefficient is obtained by linearizing the nonlinear viscous damper (Kolay and Ricles, 2018). To generate the training and validation data set, the Opensees model of the SFSI system is subjected to a set of wind load records. The wind loads are obtained by performing wind tunnel tests at the NHERI FIU Wall of Wind facility, where the experimental campaign consisted of 23 different basic wind speeds and 13 different wind directions. The training set for the NN model consists of 2093 records while the validation set consists of 299 records. Noise injection is used in the training set to avoid overfitting of the NN model. NVIDIA Quadro RTX 4000 Graphics Processing Units (GPUs) are used to speed up the training and validation process of the NN model.

The RTHS test matrix is given in Table 2. Test 1 is considered the baseline test, as it contains the largest number of training and validation records. Test 2 investigates the effect of the basic wind speed discretization in the training records. Test 3 stopped the NN model training at a larger value of the target root mean square error (RMSE) during the training process compared to Test 2. Tests 4 and 5 examine the effectiveness of noise injection and the ReLU, respectively, by omitting these effects in the training of the NN model. Test 6 adds a higher amount of noise injection during the training of the NN model. Test 7 is an RTHS where the structure is supported by a rigid base foundation (i.e., no soil-foundation system is included in the RTHS).

4.2.2 Results and outcomes

To assess the accuracy of the NN model, the multi-physics RTHS results of soil-foundation displacement are compared with numerical simulation results from an OpenSees model of only the soil-foundation system. The restoring forces at the interface between the building and foundation from the multi-physics RTHS are used as the inputs for the OpenSees model and the resulting displacements at the ground level are compared to each other. Figure 7 compares the time history of the interface horizontal displacements at the ground level obtained from the OpenSees and the multi-physics RTHS. Tests 4 and 5 are not included since they contain a large level of noise without noise injection training (Test 4) and instability without the ReLU (Test 5). The comparisons show that the NN model can produce a better prediction of soil-foundation-structure interaction effects when trained to a smaller target RMSE value and using a larger number of training sets. Overall, the NN model can precisely predict the dynamics of the nonlinear soil-foundation system and is suitable for performing multi-physics RTHS.

After evaluating the NN model, the multi-physics RTHS results are compared with the RTHS test without SFSI effects (Test 7), as well as with a numerical simulation of the complete system using the OpenSees model. The time histories of roof displacements are shown plotted in Figure 8. The OpenSees numerical simulation results in Figure 8 are labeled *Reference*. The multi-physics RTHS tests with SFSI effects have overall similar results compared with the reference solution, where Test 1 produces the smallest error. The effects of SFSI caused the maximum roof displacement of Test 1 to increase by 60% compared to Test 7 (rigid foundation). The time histories of the experimental damper deformations are also examined (not shown due to lack of space). The damper accumulated 0.04 m of deformation under the applied gravity loading at the beginning of the RTHS of Test 1, while the damper deformed only 0.01 m under gravity loading when the SFSI effects are excluded (Test 7). During the imposed wind loading of the RTHS the maximum damper deformation demand increased up to 90% when considering SFSI effects.

The results of this study validate the proposed multi-physics RTHS framework. Furthermore, the effects of soil-structure

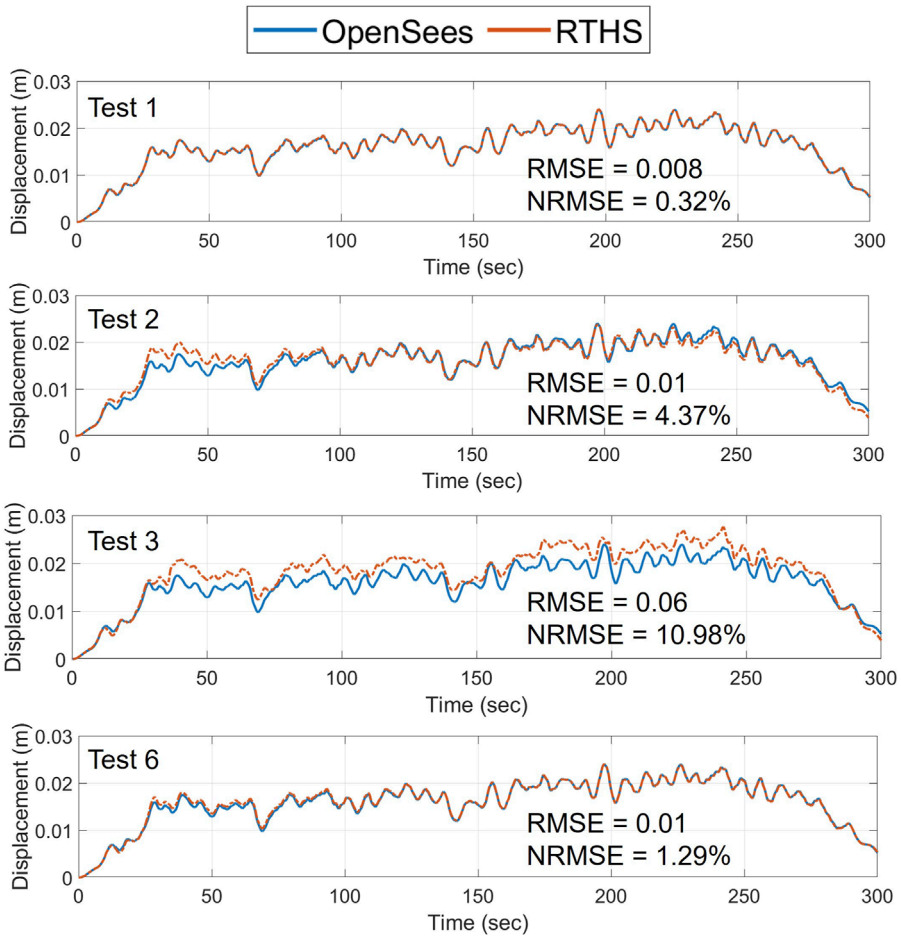

FIGURE 7
Comparison of multi-physics RTHS and OpenSees numerical simulation results of interface horizontal displacements at the ground level (courtesy of Al-Subaihawi et al. (2024)).

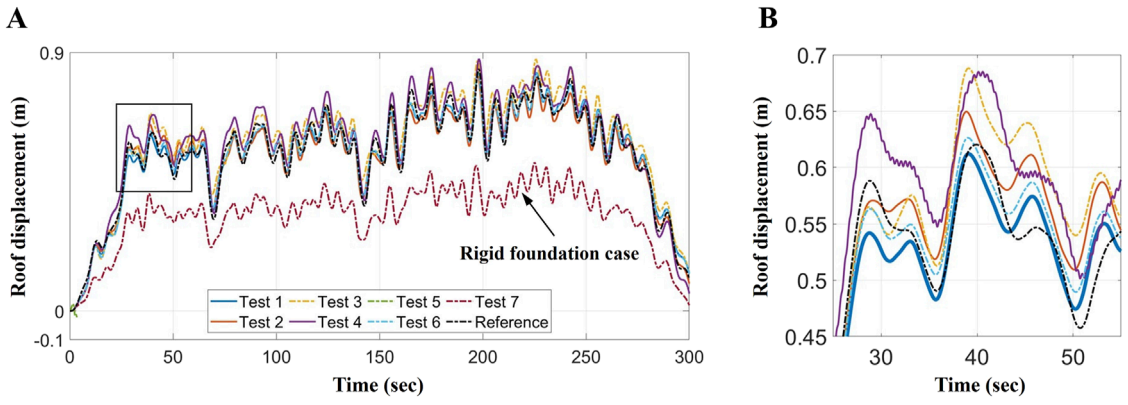

FIGURE 8
Time histories of roof displacements: **(A)** Complete time history; and **(B)** Zoom view (courtesy of Al-Subaihawi et al. (2024)).

interaction are shown to increase the deformation demand on the dampers as well as lateral displacements of the building during a wind storm. By taking into account the effects of soil-foundation-structure interaction, a more realistic structural wind design methodology can be developed, enabling the evaluation of more effective mitigation strategies to be accomplished.

Test results and data (Al Subaihawi et al., 2023a; Al Subaihawi et al., 2023b; Kolay et al., 2023) have been uploaded

to the DesignSafe Data Depot Repository and can be downloaded at https://www.designsafe-ci.org/data/browser/public/designsafe.storage.published/PRJ-1439.

4.3 3D RTHS multi-axis shake table tests of floor isolation systems for mitigating seismic effects on mission-critical building contents

Earthquakes can heavily damage critical building contents and nonstructural equipment, resulting in a significant economic loss. Floor isolation systems (FIS) are a promising retrofitting approach to protect such vital building contents. These systems must be designed and maintained to adequately resist the effects of service and extreme vibrational loads on the building. A new type of rolling pendulum (RP) based FIS has been studied at the NHERI Lehigh EF using the new real-time cyber-physical structural systems multi-directional shake table (Villalobos Vega et al., 2022; Villalobos Vega et al., 2024). The prototype RP-based FIS is a single full-scale OCTO-Base^{TM} isolation system manufactured by WorkSafe^{TM} Technologies. It consists of four RP bearings, where each bearing is composed of two elastomeric coated QuakeCoat^{TM} conical steel plates (affixed to the upper and lower frames of the RP bearing) and a steel ball that rolls between the plates. The test setup of the RP-based FIS is shown in Figure 9A. The bottom frame of the FIS is affixed to the multi-directional shake table. The upper assembly shown in Figure 9B is made up of transfer plates and wide flange sections that represent the tributary weight of the system. Unlike a typical shake table test, the horizontal movement and rotation of the top assembly of the FIS are restricted from developing movement using three restrainers attached to the transfer plate. This unique test setup allows for imposing precise deformations to the FIS during characterization tests. Uniaxial load cells are installed at the end of each restrainer to directly measure the FIS' experimental restoring forces. Each restraint is pinned at both ends to allow vertical movements generated by horizontal displacements as the ball rolls across the surfaces of the conical plates.

4.3.1 Characterization tests

Characterization tests are performed under prescribed displacements to investigate the FIS response when subjected to a variety of multi-directional conditions. Figure 9C plots the normalized shear force and displacement response of the RP-based FIS subjected to uni-directional harmonic displacement inputs with three different maximum speeds of 2 in/s, 20 in/s, and 25 in/s. The normalized shear force is calculated by dividing the measured restoring force from the load cell by the equipment weight on top of the FIS. Results show that higher frequency inputs have a predominant effect on the FIS dynamic response. This can be attributed to higher vertical inertial effects resulting from higher velocities.

4.3.2 3D RTHS multi-axis shake table tests

To evaluate the seismic performance of the RP-based FIS and associated building-FIS interaction, a 3-story steel moment resisting frame (SMRF) building designed for the SAC project (Ohtori et al., 2004) is used for performing RTHS multi-axis shake table tests. The RP-based FIS is assumed to be located on the second floor of the building and a tributary weight of 17.9 kN of the dead load of the server cabinet is installed on top of the FIS. Figure 10 presents the multi-axis RTHS framework used to perform the simulations. The analytical substructure consists of a 3D finite element model of the 3-story SMRF building and a server cabinet. All the beams and columns in the MRFs are modeled using 3D inelastic explicit force-based fiber elements, and the remaining components that include the server cabinet and building gravity system's beams are modeled using 3D elastic elements. An eccentric floor mass and P-Δ effect are included in the building model. The experimental substructure is made up of a single full-scale OCTO-Base^{TM} isolation system. The restoring forces of the experimental substructure $\mathbf{R}^{e}_{i+1}$ are measured using the uniaxial load cells of the restrainers and are fed back to the simulation coordinator, where they are mapped by a kinematic transformation to convert the result from the bearing deformation coordinate system to the global coordinate system of the building. The MKR-α integration algorithm is used along with an enhanced 3^{rd} order version of the Adaptive Time Series (ATS) compensator (Chae et al., 2013a) to achieve accurate control of the servo-hydraulic actuators used to impose the motions to the shake table. The 1994 Northridge earthquake is scaled to the Service-Level Earthquake (SLE) hazard level (50% probability of exceedance in 50 years) for the RTHS multi-axis shake table tests.

4.3.3 Results and outcomes

The absolute (i.e., total) bi-directional accelerations of the second floor of the SMRF are analyzed. It is found that a 68%–82% reduction in equipment acceleration is achieved by isolating the equipment compared to when the equipment is not isolated. The results show that the FIS can effectively isolate sensitive mission-critical equipment under multi-directional ground motions. The 3D RTHS multi-axis shake table test successfully validates the seismic protection performance of 3D RP-based FIS on nonstructural components. The multi-axis motions that include twist acceleration caused by the eccentric mass of the building are found to be important, for they increase the absolute accelerations at locations where the FIS are attached to the floor of the building. Therefore, it is important to account for multi-axis accelerations as done in the study. The results of this study provide a rigorous methodology for assessing the multi-directional seismic performance of FIS's in mission critical buildings that house sensitive equipment.

Test results and data (Harvey et al., 2022) have been uploaded to the DesignSafe Data Depot Repository and can be downloaded at https://www.designsafe-ci.org/data/browser/public/designsafe.storage.published/PRJ-3649.

4.4 Multi-directional cyclic lateral loading tests of self-centering cross-laminated timber shear wall sub-assembly

There has been a growing interest in the use of cross-laminated timber (CLT) for the construction of new building systems. The material is a renewable resource with a reduced carbon footprint compared to conventional construction. CLT panels are constructed

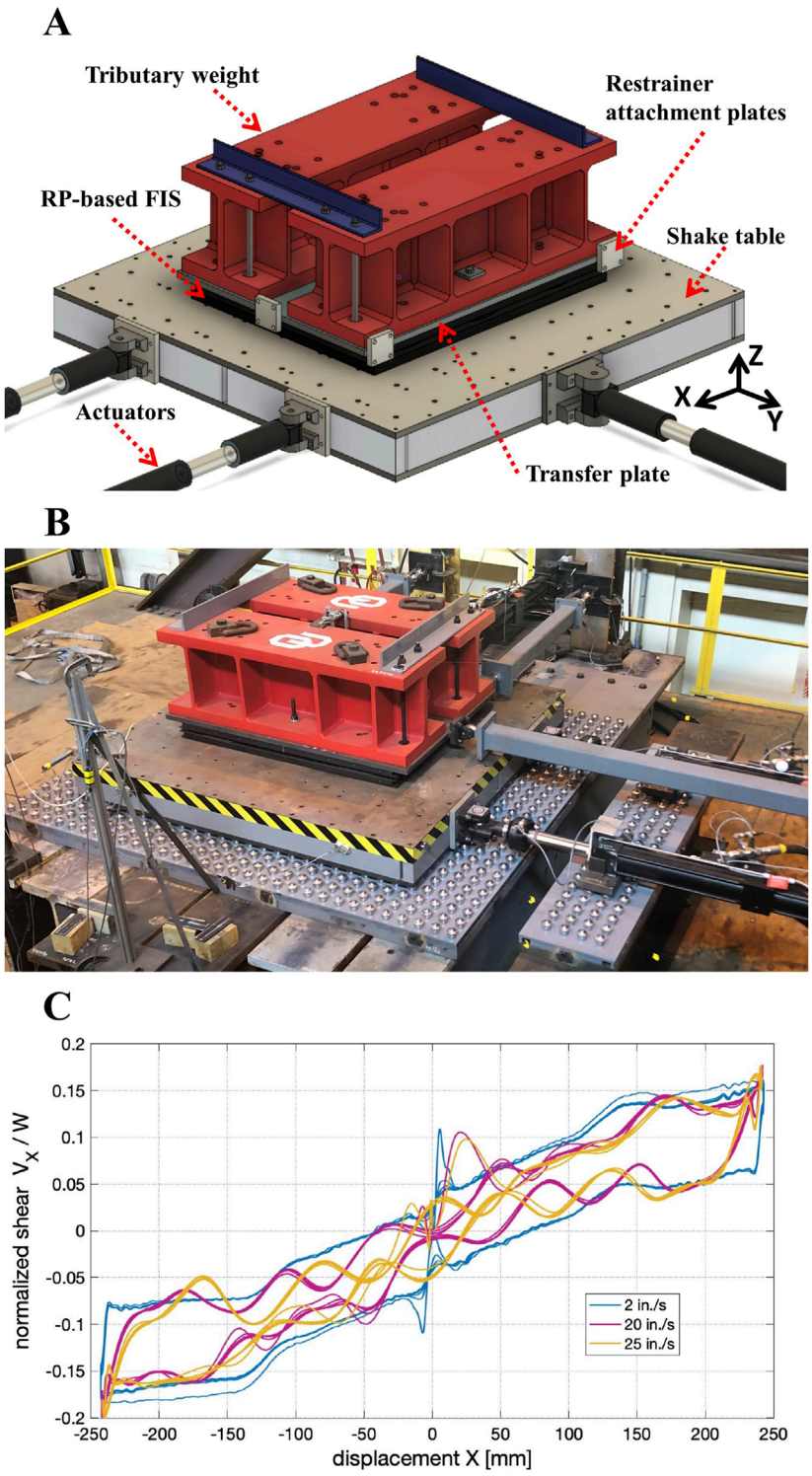

FIGURE 9
(A) Schematic of the RP-based FIS; **(B)** Photograph of the dynamic test setup; **(C)** Normalized shear-displacement of the RP-based FIS response under uni-directional harmonic displacements with maximum speeds of 2 in/s, 20 in/s and 25 in/s (courtesy of Villalobos Vega et al. (2024)).

to create structural elements, where the layers of the timber boards are laminated in an orthogonal pattern and glued together on their wide face. Post-tensioned self-centering CLT structural walls (SC-CLT walls) have been developed where CLT panels are erected vertically and post-tensioning is added. This type of structural element has been recently studied by (Ganey et al., 2017; Pei et al., 2019), where the results demonstrated the potential of the SC-CLT wall to reduce seismic-induced damage in CLT buildings. These prior studies are however limited in scope, where the test specimens are subjected to only unidirectional displacements in the plane of the

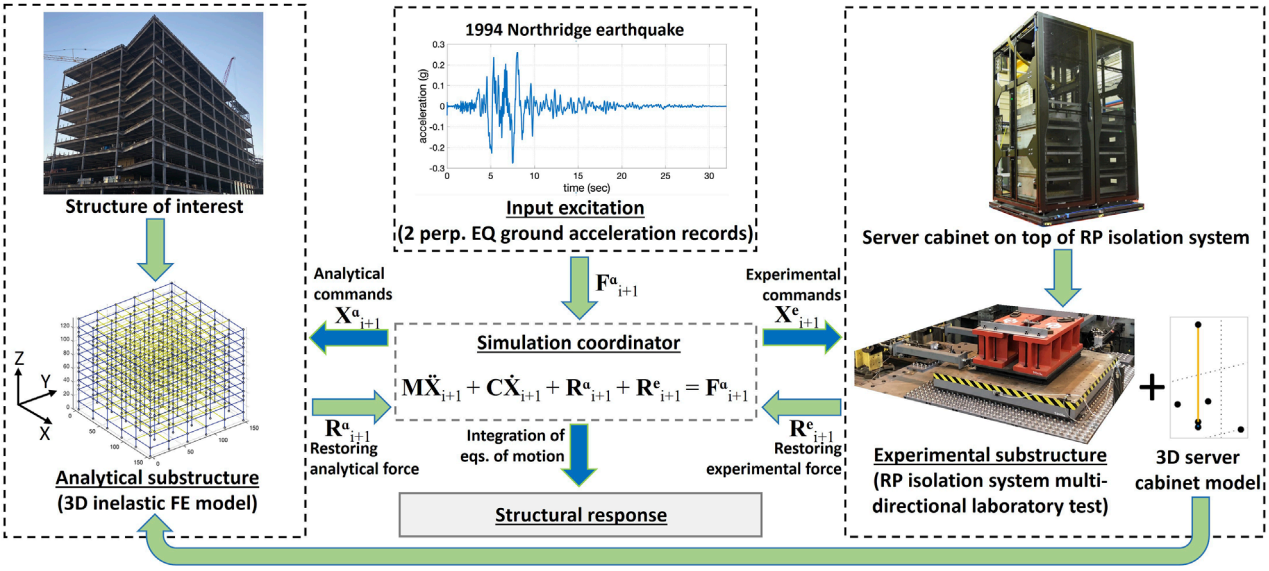

FIGURE 10
Famework for conducting 3D RTHS multi-axis shake table test of structures equipped with RP-based FIS subjected to multi-directional earthquake ground motions (courtesy of Villalobos Vega et al. (2024)).

wall, and neglected the effect of bi-directional earthquake ground motions on the performance of the wall. To study the effect of bi-directional loading on the response of SC-CLT walls, a 0.625-scale subassembly system consisting of a CLT-floor diaphragm-gravity system with an SC-CLT coupled shear wall and collector beams is constructed at the NHERI Lehigh EF and used to perform multi-directional load testing.

4.4.1 SC-CLT wall test setup

Figure 11 shows the 0.625-scale timber test subassembly. The SC-CLT wall is composed of two post-tensioned 5-layer CLT wall panels that are connected with U-shaped flexural plates (UFPs) for energy dissipation. Each CLT wall panel is equipped with a 32 mm-diameter post-pensioned (PT) steel bar. Two glulam collector beams are connected to the SC-CLT wall, one on each side of the wall, to collect and transfer the in-plane (in the direction of the SC-CLT wall) lateral forces from the CLT floor diaphragm through a slotted connection and deliver them to the SC-CLT wall. The out-of-plane bearings are designed to transfer the out-of-plane load from the CLT floor diaphragm to the SC-CLT wall and brace the wall in the out-of-plane direction. Shear keys are placed at the base of each wall to prevent sliding of the wall and to transfer the wall base shear to the foundation. The gravity load system consists of glulam gravity beams and columns with pinned bases. The beam-to-column connections of the gravity load system are designed to accommodate the multi-directional lateral drift of the test sub-assembly. The test fixtures include two actuators placed in-plane to the walls to displace the test sub-assembly through the floor diaphragm. Two out-of-plane actuators are connected to the CLT floor diaphragm to subject the sub-assembly to out-of-plane displacements. Multi-directional displacements of the test sub-assembly are controlled at a structure-physical-node, denoted SPN, which is located in the middle of the SC-CLT wall at the top of the floor diaphragm. All degrees of freedom of the test sub-assembly are associated with the SPN. Continuous real-time feedback from two sets of displacement sensors, attached to the CLT floor diaphragm, are used to measure the displaced position of two measurement-structure nodes (MSN) at the north and south ends of the wall and incorporated into a multidirectional kinematic compensation algorithm (Mercan et al., 2009) to achieve precise actuator control and the target displacements of the SPN.

4.4.2 Multi-directional cyclic lateral loading protocol

The experimental campaign consists of applying predefined unidirectional and multi-directional quasi-static displacement histories to the subassembly, imposing the floor diaphragm to reach a predefined target floor diaphragm story drift, denoted Θ_d^{target}. Θ_d^{target} is defined as the horizontal displacement of the SPN target displacement divided by the height of the floor diaphragm. The in-plane and out-of-plane target floor diaphragm story drifts are denoted by $\Theta_{d,x}^{target}$ and $\Theta_{d,y}^{target}$, respectively. Figures 12A–C illustrate the cyclic lateral loading protocol for the unidirectional and multi-directional tests. In the unidirectional test, increasing amplitude of monotonically applied quasi-static cyclic displacements are imposed on the floor diaphragm, with three cycles of drift applied up to an amplitude of 3% proceeded by two cycles of drift applied up to an amplitude of 6%. In the multi-directional test, a bow-tie-shaped displacement path is used with cycles of increasing amplitude up to a 4% targeted drift in both the in-plane and out-of-plane direction, as shown in Figure 12C.

4.4.3 Results and outcomes

To evaluate lateral response of the SC-CLT wall, four damage states are defined that included: (1) Normal Loading Defect (NLD), which involves minor or cosmetic damage to the CLT wall panel, such as fine compression splits or wrinkling, with no need for repairs; (2) Damage State I (DS_I), a moderate damage

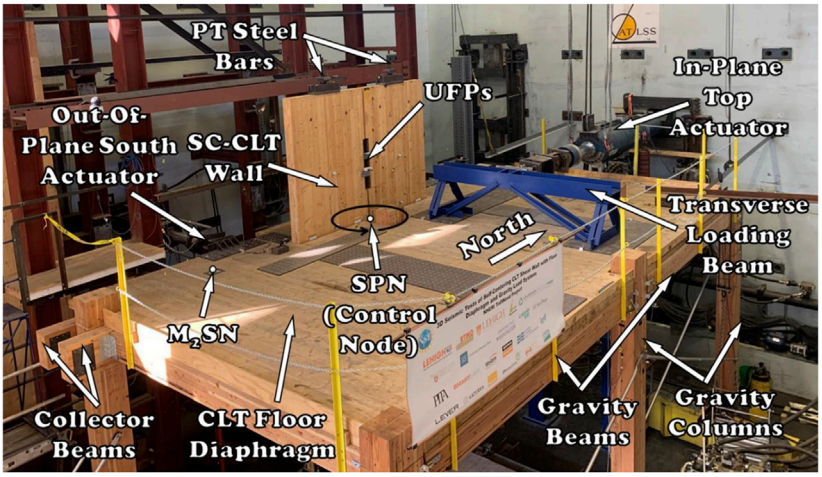

FIGURE 11
Multi-directional test setup of cross-laminated timber self-centering coupled walls-floor diaphragm-gravity system (courtesy of Amer et al. (2024)).

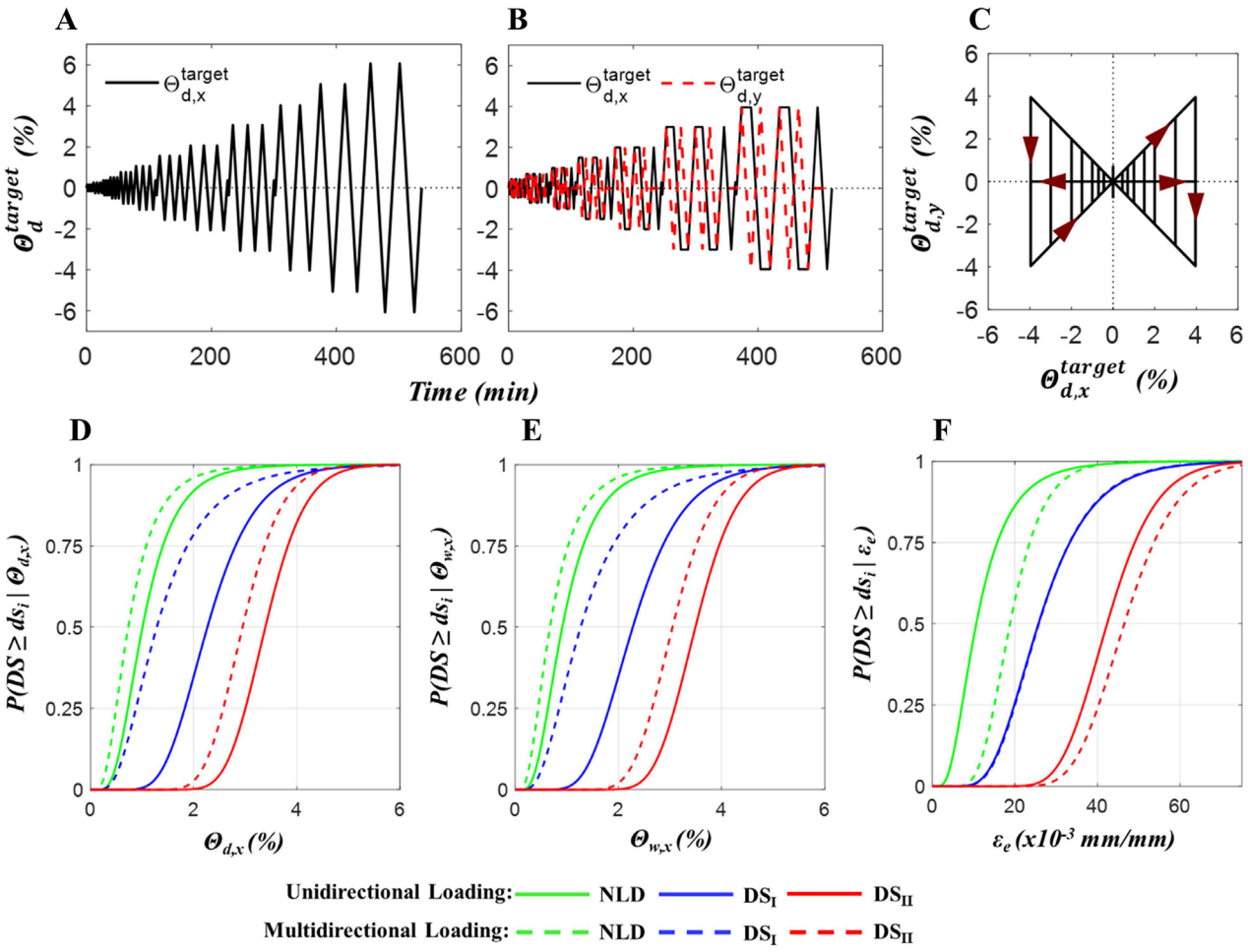

FIGURE 12
Cyclic lateral loading protocol: **(A)** Time history of imposed in-plane floor diaphragm drift under unidirectional test; **(B)** Time history of imposed in-plane and out-of-plane floor diaphragm drift under multi-directional test: and **(C)** Associated multi-directional bow-tie-shaped loading trajectory; Wall component fragility functions conditioned on **(D)** In-plane floor diaphragm story drift ($\Theta_{d,x}$); **(E)** In-plane SC-CLT wall story drift ($\Theta_{w,x}$) and **(F)** The SC-CLT wall panel corner compression strain (ϵ_e) (courtesy of Amer et al. (2024)).

state characterized by the initiation of outer-ply delamination or buckling, corner rounding, or localized corner crushing, requiring simple repair actions; (3) Damage State II (DS_{II}), a significant damage state where excessive outer-ply delamination, buckling, corner rounding, localized corner crushing, end or rolling may occur, necessitating repairs and strengthening of the SC-CLT wall panel; and (4) Damage State III (DS_{III}), where severe damage or a failure state has occurred resulting in a 20% or more reduction of the base shear resistance of the SC-CLT wall panels. The floor diaphragm story drift (Θ_d), SC-CLT wall story drift (Θ_w), wall base shear resistance (V_w), and the SC-CLT wall panel corner compression strain (ϵ_e) are used to quantify the SC-CLT wall damage states.

The in-plane lateral load response of the SC-CLT wall between uni-directional and multi-directional tests are evaluated by (Amer et al., 2024) where the results show that the multi-directional loading generates earlier damage to the SC-CLT wall panel. Figures 12D–F compare the fragility functions of the wall components for the in-plane tests, where the engineering demand parameters (EDP) are $\Theta_{d,x}$, $\Theta_{w,x}$ and ϵ_e associated with the uni-directional and multi-directional tests. The results show that the probability of a CLT wall reaching or exceeding a damage state for a given story drift under multi-directional loading is much greater than that under uni-directional loading conditions. These findings are significant and will have a major impact on the performance-based design of SC-CLT shear walls. The structural components of this type of system are designed to remain damage-free under the design earthquake. The results of the large-scale multi-directional tests will lead to significant changes in design criteria in order to control earthquake-induced damage to SC-CLT walls.

Test results and data (Amer et al., 2023) have been uploaded to the DesignSafe Data Depot Repository and can be downloaded at https://www.designsafe-ci.org/data/browser/public/designsafe.storage.published/PRJ-3850.

4.5 Mixed-mode cyclic loading tests of seismic collector connections for steel-frame buildings

Seismic collectors are critical elements of the seismic force-resisting system that transmit the inertial forces that develop in building floor systems to the primary vertical-plane elements of the seismic force-resisting system. In steel-frame buildings in the U.S., seismic collectors are elements of the floor system specially-designed to carry tension and compression axial forces. Often a line of gravity-load-carrying beams and connections within the floor system are enhanced to serve as a collector. These beams are then designed as beam-columns, and the connections between these beams and the intervening columns in the load path are designed for tension and compression axial forces. Little past research has focused on steel collectors, and the seismic response of these elements is not well established in the literature. The research project scope includes: (1) nonlinear analysis of steel seismic collectors in steel buildings; (2) large-scale testing of steel seismic collector connections at the NHERI Lehigh EF; and (3) shake table testing of a two-story steel-frame structure at the NHERI Earthquake Shake Table Experimental Facility at the University of California, San Diego (Pandey et al., 2022).

4.5.1 Description of steel seismic collector connection loading conditions

The connections within a steel seismic collector, between the collector beams and the columns within the collector force path, may be subjected to tension or compression axial forces, with the largest magnitude forces in the connections closest to the primary vertical-plane element of the seismic force-resisting system (e.g., braced frame). Collector connection types include bolted shear tabs, top-flange-welded (TFW) connections, and all-flange-welded (AFW) connections. Currently, collector connections are designed for the collector axial force and shear from gravity loads, not additional demands due to building lateral drift.

4.5.2 Steel seismic collector connection loading test setup

As shown in Figure 13A, the steel seismic collector connection test setup at the NHERI Lehigh EF includes a test specimen with a single collector connection and the associated collector beam and column (shown in red). The test setup separates the collector beam into two parts, where one part is included in a re-usable test fixture (shown in gray) and the other part is part of the test specimen (shown in red). The reusable test fixture also includes a second column, and together the reusable test fixture and test specimen model two columns and one collector beam in the collector force path. The columns and beams are lying in a horizontal plane to facilitate lateral bracing from the laboratory's strong floor. The bases of the columns provide supports, namely, a roller support at the base of the column in the reusable test fixture (shown in gray) and a pinned support at the base of the column of the test specimen (shown in red). These supports enable the columns to develop axial forces as reactions to shear forces that develop in the collector beam.

As shown in Figure 13B, the unique feature of the steel seismic collector connection test setup is the capability to simultaneously apply a large axial force (up to 4,800 kN) using the loading actuators (painted black, on the left) and impose a rotation of the test specimen column (to simulate the rotation of a column within the collector force path to accommodate the building lateral drift) using the rotation actuators (painted blue on the right), which also provide the main reaction to the applied axial force.

Three loading protocols have been developed for steel seismic collector connection tests: (1) constant column rotation (including the possibility of zero rotation) with applied cyclic axial forces; (2) constant column rotation with applied cyclic axial connection deformations; and (3) simultaneously varying column rotation and axial force to simulate seismic demand histories on collector connections obtained from nonlinear analysis of collectors in a steel-frame building under earthquake loading. Note that test protocol (1), with constant rotation and applied cyclic axial forces, is useful to characterize the initial stiffness and strength of a steel seismic collector connection, and the complete loading history of the test usually involves a series of stages with each stage having a given constant rotation. Test protocol (2), with constant rotation and applied cyclic axial connection deformations, is useful for testing the connection to failure.

4.5.3 Results and outcomes

Three top-flange-welded (TFW) connections and two all-flange-welded (AFW) connections have been tested. The TFW connection

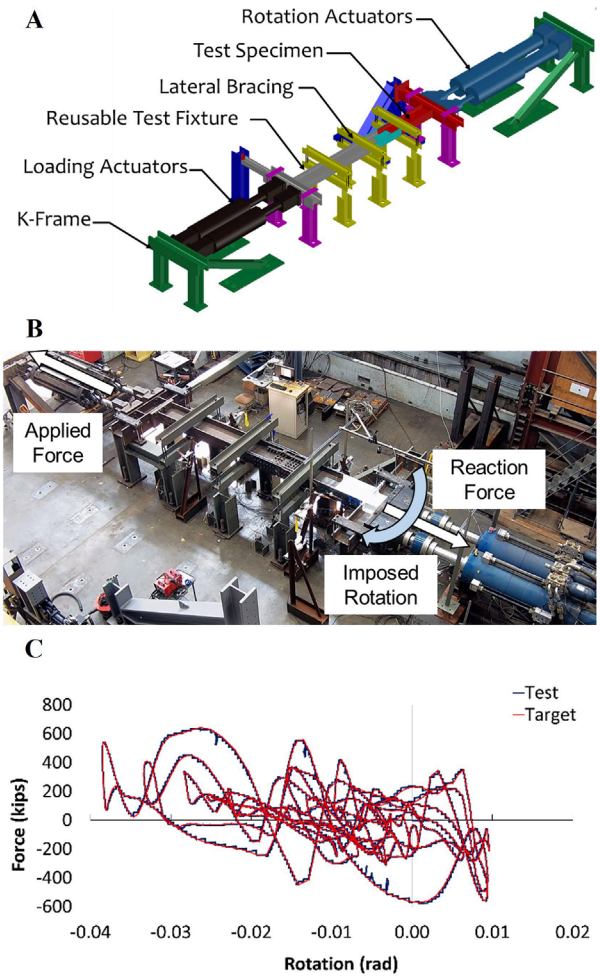

FIGURE 13
(A) Schematic of collector connection test setup; **(B)** Photograph of collector connection; **(C)** Loading protocol with simultaneously applied force and imposed rotation (1 kip = 4.45 kN).

specimens are 0.75 scale and the AFW connection specimens are 0.67 scale. For the TFW specimens, the largest applied force exceeded 4,400 kN. Generally, the TFW connections performed as expected, reaching the expected force capacity. The tests have shown that the imposed column rotation (to simulate the effects of the building lateral drift) can reduce the force capacity.

Figure 13C shows the results from using test protocol (3), simultaneously varying column rotation and axial force to simulate seismic demand histories, in the third TFW specimen test, showing that the loading protocol follows the target imposed rotations and axial forces to fully simulate the seismic demand histories on a steel seismic collector connection.

When complete, the test results will substantially increase the knowledge-base on the seismic response of steel seismic collectors, and recommendations for practical design and fabrication will be made. Project partners include seismic structural engineers, structural steel fabricators, and regulatory organizations.

Upon completion of this study, the results will be uploaded and archived in the DesignSafe Data Depot Repository.

5 Summary and conclusions

The Natural Hazards Engineering Research Infrastructure (NHERI) Lehigh Experimental Facility (EF) is an open-access state-of-art experimental and computational research facility. The unique resources and capabilities of the facility enable novel and impactful natural hazards research to be performed. The unique capabilities include the ability to conduct 3D large-scale multi-directional Real-Time Hybrid Simulation (RTHS) that combine physical experiments with computer-based simulations for evaluating the performance of large-scale components and systems. Several testing protocols are enabled at the facility, including: (1) large-scale HS; (2) large-scale RTHS; (3) large-scale RTHS with real-time online model updating; (4) large-scale RTHS with multiple experimental substructures; (5) geographically distributed HS; (6) geographically distributed real-time hybrid earthquake simulation; (7) quasi-static testing; (8) dynamic testing; (9) multi-directional RTHS multi-axis shake table tests; and (10) multi-physics RTHS. These testing protocols are supported by the facility's unique portfolio of experimental equipment, instrumentation, testbeds, and testing protocols, in addition to the newly developed NHERI Lehigh Real-time Cyber-Physical Structural Systems Testing Laboratory and Real-time Cyber-Physical Structural Systems Multi-directional Shake Table. The NHERI Lehigh EF will continue to enhance its testing capabilities to address a wider range of natural hazards and infrastructure challenges. Planned expansions include a large wave flume for examining fluid-structure interactions in coastal infrastructure and a large-scale soil box for studying soil-structure interactions in onshore and coastal systems exposed to multiple natural hazards.

Several selected example research projects recently performed at the NHERI Lehigh EF are presented. These projects include: (1) development of a framework for multi-directional RTHS of a tall building equipped with nonlinear viscous dampers to enable 3D performance evaluation of the system when subjected to earthquake and wind natural hazards; (2) multi-physics RTHS of a tall building with a soil-foundation system modeled using neural networks to assess the effects on the efficacy of the response modification devices and performance of the structure subjected to wind natural hazards; (3) 3D RTHS multi-axis shake table tests of floor isolation systems to evaluate their effectiveness to mitigate seismic-induced vibrations and damage of critical building contents; (4) multi-directional cyclic lateral loading tests of a self-centering cross-laminated timber shear wall sub-assembly to examine the effects of bi-directional loading on the seismic resiliency of these components in mass timber constructed buildings; and, (5) large-scale tests of seismic collectors in a steel frame floor system to evaluate the performance, and enhance our knowledge of the seismic behavior and design of collector's connections to the lateral force resisting system.

Multi-directional RTHS results on a tall building underscore the importance of 3D models in accurately capturing inelastic responses to natural hazards. Similarly, multi-physics RTHS findings reveal the significant influence of soil-structure interaction on deformation demands in outrigger system dampers. These studies demonstrate that structural responses to natural hazards can vary considerably when multi-directional and multi-physics effects are taken into account.

The successful 3D RTHS multi-axis shake table test validates the seismic protection effectiveness of 3D floor isolation systems for critical equipment, particularly by considering in-plane angular floor accelerations. Experimental results from SC-CLT shear wall tests show that multi-directional loading exacerbates damage, emphasizing the necessity of incorporating such effects into the performance-based design of mass timber systems. Additionally, large-scale seismic collector tests provide key insights into seismic behavior, notably the axial forces induced during inter-story drift and the effects of rotational deformations at the collector-to-lateral force-resisting system connection.

Collectively, these projects highlight the critical role of large-scale 3D testing in enhancing our understanding of structural and non-structural component performance under natural hazards. By utilizing the NHERI Lehigh EF's advanced testing capabilities, researchers can drive innovation in natural hazards engineering through cutting-edge, high-impact studies.

Additional information about the NHERI Lehigh EF can be found at the facility's website at https://lehigh.designsafe-ci.org/facility/overview/. This information includes an overview of the facility, along with the portfolio of equipment and resources, experimental protocols, portfolio of research projects, the facility's education and outreach program, and contact information.

Data availability statement

The original contributions presented in the study are included in the article, further inquiries can be directed to the corresponding authors.

Author contributions

LC: Conceptualization, Data curation, Formal Analysis, Investigation, Methodology, Validation, Writing–original draft, Writing–review and editing. TM: Conceptualization, Data curation, Formal Analysis, Investigation, Software, Validation, Writing–original draft, Writing–review and editing. JR: Conceptualization, Funding acquisition, Investigation, Methodology, Project administration, Supervision, Writing–original draft, Writing–review and editing. RS: Conceptualization, Funding acquisition, Investigation, Methodology, Project administration, Supervision, Writing–original draft, Writing–review and editing. CR: Conceptualization, Funding acquisition, Investigation, Methodology, Project administration, Supervision, Writing–original draft, Writing–review and editing. JS: Funding acquisition, Project administration, Resources, Supervision, Writing–original draft, Writing–review and editing.

Funding

The author(s) declare that financial support was received for the research and/or publication of this article. The research reported in this paper was supported by several grants from the National Science Foundation. This included Award No. CMMI-1663376 *Analysis and Design of a Nonholonomic, Impact-Based, Dual-Mode Vibration Isolator/Absorber System*, Award No. OIA-1929151 *RII Track-4: Quantifying Seismic Resilience of Multi-Functional Floor Isolation Systems through Cyber-Physical Testing*, Award No. CMMI-1943917 *CAREER: Mitigation of Seismic Risk to Critical Building Contents* via *Optimum Nonlinear 3D Isolation*, Award No. CMMI-1463497 *Collaborative Research: Semi-Active Controlled Cladding Panels for Multi-Hazard Resilient Buildings*, Award No. CMMI-1635227 *Collaborative Research: A Resilience-based Seismic Design Methodology for Tall Wood Buildings*, and Award No. CMMI-1662816 *Advancing Knowledge on the Performance of Seismic Collectors in Steel Building Structures*. The research reported in this paper was performed at the NHERI Lehigh Large-Scale Multi-Directional Hybrid Simulation Experimental Facility. Financial support for the operation of the NHERI Lehigh Large-Scale Multi-Directional Hybrid Simulation Experimental Facility was provided by the National Science Foundation under Cooperative Agreement No. CMMI-1520765 and No. CMMI-2037771.

Acknowledgments

The authors are grateful for the financial support of the National Science Foundation and that provided by the Pennsylvania Infrastructure Technology Alliance and Lehigh University.

Conflict of interest

The authors declare that the research was conducted in the absence of any commercial or financial relationships that could be construed as a potential conflict of interest.

Generative AI statement

The author(s) declare that no Generative AI was used in the creation of this manuscript.

Publisher's note

All claims expressed in this article are solely those of the authors and do not necessarily represent those of their affiliated organizations, or those of the publisher, the editors and the reviewers. Any product that may be evaluated in this article, or claim that may be made by its manufacturer, is not guaranteed or endorsed by the publisher.

Author disclaimer

Any opinions, findings, and conclusions expressed in this paper are those of the authors and do not necessarily reflect the views of the National Science Foundation or others acknowledged herein.

References

Al Subaihawi, S., Kolay, C., Marullo, T., Ricles, J., and Quiel, S. (2023a). Assessment of wind-induced vibration mitigation in a tall building with damped outriggers using real-time hybrid simulations. *Designsafe-CI*. doi:10.17603/ds2-mj64-6s83

Al-Subaihawi, S., Kolay, C., Marullo, T., Ricles, J. M., and Quiel, S. E. (2020). Assessment of wind-induced vibration mitigation in a tall building with damped outriggers using real-time hybrid simulations. *Eng. Struct.* 205, 110044. doi:10.1016/j.engstruct.2019.110044

Al Subaihawi, S., Ricles, J., Quiel, S., and Marullo, T. (2023b). Online explicit model updating of nonlinear viscous dampers for real time hybrid simulation. *Designsafe-CI*. doi:10.17603/ds2-pnr0-7476

Al-Subaihawi, S., Ricles, J., Quiel, S., and Marullo, T. (2024a). Development of multi-directional real-time hybrid simulation for tall buildings subject to multi-natural hazards. *Eng. Struct.* 315, 118348. doi:10.1016/j.engstruct.2024.118348

Al-Subaihawi, S., Ricles, J., Quiel, S., Marullo, T., and Malik, F. (2024). Real-time hybrid simulation of structural systems with soil-foundation interaction effects using neural networks. *Earthq. Eng. Struct. Dyn.* 53, 4688–4718. doi:10.1002/eqe.4236

Al-Subaihawi, S., Ricles, J. M., and Quiel, S. E. (2022). Online explicit model updating of nonlinear viscous dampers for real time hybrid simulation. *Soil Dyn. Earthq. Eng.* 154, 107108. doi:10.1016/j.soildyn.2021.107108

Al-Subaihawi, S., Ricles, J. M., Quiel, S. E., and Marullo, T. (2024b). Unconditionally stable central difference dissipative algorithm for multi-directional real-time hybrid simulations of large nonlinear structural systems. *J. Earthq. Eng.* 28, 3256–3290. doi:10.1080/13632469.2024.2333822

Amer, A., Marullo, T., Sause, R., and Ricles, J. (2023). Data for unidirectional and multi-directional cyclic lateral-load testing of self-centering cross-laminated timber shear wall-floor diaphragm sub-assembly. *Designsafe-CI*. doi:10.17603/DS2-DDV9-2235

Amer, A., Sause, R., and Ricles, J. (2024). Experimental response and damage of sc-clt shear walls under multidirectional cyclic lateral loading. *J. Struct. Eng.* 150. doi:10.1061/jsendh.steng-12576

ASCE (2010). *Minimum design loads for buildings and other structures,american socitey of civil engineering*. (Reston, VA: ASCE/SEI 7-10 edition).

Azzi, Z., Matus, M., Elawady, A., Zisis, I., Irwin, P., and Gan Chowdhury, A. (2020). Aeroelastic testing of span-wire traffic signal systems. *Front. Built Environ.* 6. doi:10.3389/fbuil.2020.00111

Cao, L., Malik, F., Al-Subhaihawi, S., Miao, W., Ricles, J., Marullo, T., et al. (2024). "Real time hybrid simulation (rths) of a 2-story building equipped with novel base isolation systems," in World Conference on earthquake Engineering proceedings (WCEE2024), USA, JULY 5, 2024.

Cao, L., Marullo, T., Al-Subaihawi, S., Kolay, C., Amer, A., Ricles, J., et al. (2020). Nheri lehigh experimental facility with large-scale multi-directional hybrid simulation testing capabilities. *Front. Built Environ.* 6. doi:10.3389/fbuil.2020.00107

Catarelli, R. A., Fernández-Cabán, P. L., Phillips, B. M., Bridge, J. A., Masters, F. J., Gurley, K. R., et al. (2020). Automation and new capabilities in the university of Florida nheri boundary layer wind tunnel. *Front. Built Environ.* 6. doi:10.3389/fbuil.2020.558151

Chae, Y., Kazemibidokhti, K., and Ricles, J. M. (2013a). Adaptive time series compensator for delay compensation of servo-hydraulic actuator systems for real-time hybrid simulation. *Earthq. Eng. and Struct. Dyn.* 42, 1697–1715. doi:10.1002/eqe.2294

Chae, Y., Ricles, J. M., and Sause, R. (2013b). Modeling of a large-scale Magneto-Rheological damper for seismic hazard mitigation. Part I: passive mode. *Earthq. Eng. and Struct. Dyn.* 42, 669–685. doi:10.1002/eqe.2237

Chae, Y., Ricles, J. M., and Sause, R. (2014). Large-scale real-time hybrid simulation of a three-story steel frame building with Magneto-Rheological dampers. *Earthq. Eng. and Struct. Dyn.* 43, 1915–1933. doi:10.1002/eqe.2429

Chen, C., and Ricles, J. M. (2008). Development of direct integration algorithms for structural dynamics using discrete control theory. *J. Eng. Mech.* 134, 676–683. doi:10.1061/(asce)0733-9399(2008)134:8(676)

Chen, C., and Ricles, J. M. (2012). Large-scale real-time hybrid simulation involving multiple experimental substructures and adaptive actuator delay compensation. *Earthq. Eng. and Struct. Dyn.* 41, 549–569. doi:10.1002/eqe.1144

Chen, C., Ricles, J. M., Marullo, T. M., and Mercan, O. (2009). Real-time hybrid testing using the unconditionally stable explicit CR integration algorithm. *Earthq. Eng. and Struct. Dyn.* 38, 23–44. doi:10.1002/eqe.838

Coble, D., Cao, L., Downey, A. R., and Ricles, J. M. (2024). Physics-informed machine learning for dry friction and backlash modeling in structural control systems. *Mech. Syst. Signal Process.* 218, 111522. doi:10.1016/j.ymssp.2024.111522

Dong, B., Sause, R., and Ricles, J. (2018a). "Seismic performance of steel MRF structures with nonlinear viscous dampers from real-time hybrid simulations," in *Proceedings of the 9th international conference on behavior of steel structures in seismic areas* (Christchurch, New Zealand: STESSA).

Dong, B., Sause, R., and Ricles, J. M. (2015). Accurate real-time hybrid earthquake simulations on large-scale mdof steel structure with nonlinear viscous dampers. *Earthq. Eng. and Struct. Dyn.* 44, 2035–2055. doi:10.1002/eqe.2572

Dong, B., Sause, R., and Ricles, J. M. (2018b). Seismic response and damage of reduced-strength steel MRF structures with nonlinear viscous dampers. *J. Struct. Eng.* 144, 04018221. doi:10.1061/(asce)st.1943-541x.0002226

Downey, A., Cao, L., Laflamme, S., Taylor, D., and Ricles, J. (2016). High capacity variable friction damper based on band brake technology. *Eng. Struct.* 113, 287–298. doi:10.1016/j.engstruct.2016.01.035

Ganey, R., Berman, J., Akbas, T., Loftus, S., Daniel Dolan, J., Sause, R., et al. (2017). Experimental investigation of self-centering cross-laminated timber walls. *J. Struct. Eng.* 143. doi:10.1061/(asce)st.1943-541x.0001877

Harvey, P., Covarrubias Vargas, B. A., Cao, L., and Ricles, J. (2022). Characterization tests of rolling pendulum isolation bearings with different surface treatments. *Designsafe-CI*. doi:10.17603/DS2-5JE0-5F35

Karavasilis, T. L., Ricles, J. M., Sause, R., and Chen, C. (2011). Experimental evaluation of the seismic performance of steel mrfs with compressed elastomer dampers using large-scale real-time hybrid simulation. *Eng. Struct.* 33, 1859–1869. doi:10.1016/j.engstruct.2011.01.032

Kim, S. J., Christenson, R., Phillips, B., and Spencer, B., Jr (2012). Geographically distributed real-time hybrid simulation of MR dampers for seismic hazard mitigation. *Proc. 20th Analysis Comput. Specialty Conf.*, 382–393. doi:10.1061/9780784412374.034

Kolay, C., Al-Subaihawi, S., Marullo, T., Ricles, J., and Quiel, S. (2020). Multi-hazard real-time hybrid simulation of a tall building with damped outriggers. *Int. J. Lifecycle Perform. Eng.* 4 (1/2/3), 103–132. doi:10.1504/ijlcpe.2020.108937

Kolay, C., Al Subaihawi, S., Marullo, T., Ricles, J., and Quiel, S. (2023). Multi-hazard real-time hybrid simulation of a tall building with damped outriggers. *Designsafe-CI*. doi:10.17603/ds2-pq8k-vq38

Kolay, C., and Ricles, J. M. (2014). Development of a family of unconditionally stable explicit direct integration algorithms with controllable numerical energy dissipation. *Earthq. Eng. and Struct. Dyn.* 43, 1361–1380. doi:10.1002/eqe.2401

Kolay, C., and Ricles, J. M. (2018). Force-based frame element implementation for real-time hybrid simulation using explicit direct integration algorithms. *J. Struct. Eng.* 144. doi:10.1061/(asce)st.1943-541x.0001944

Kolay, C., and Ricles, J. M. (2019). Improved explicit integration algorithms for structural dynamic analysis with unconditional stability and controllable numerical dissipation. *J. Earthq. Eng.* 23, 771–792. doi:10.1080/13632469.2017.1326423

Kolay, C., Ricles, J. M., Marullo, T. M., Mahvashmohammadi, A., and Sause, R. (2015). Implementation and application of the unconditionally stable explicit parametrically dissipative KR-α method for real-time hybrid simulation. *Earthq. Eng. and Struct. Dyn.* 44, 735–755. doi:10.1002/eqe.2484

Lin, Y.-C., Sause, R., and Ricles, J. M. (2013). Seismic performance of steel self-centering, moment-resisting frame: hybrid simulations under design basis earthquake. *J. Struct. Eng.* 139, 1823–1832. doi:10.1061/(asce)st.1943-541x.0000745

Lomonaco, P., Cox, D., Higgins, C., Maddux, T., Bosma, B., Miller, R., et al. (2020). Building resilient coastal communities: the nheri experimental facility for surge, wave, and tsunami hazards. *Front. Built Environ.* 6. doi:10.3389/fbuil.2020.579729

Malik, F. N., Gorini, D. N., Ricles, J. M., and Rahnemoonfar, M. (2025). Multi-physics framework for seismic real-time hybrid simulation of soil-foundation-structural systems. *Eng. Struct. under Rev.*

Mazzoni, S. (2006). *Opensees command language manual*. Pacific Earthquake Engineering Research (PEER) Center.

Mercan, O., Ricles, J. M., Sause, R., and Marullo, T. (2009). Kinematic transformations for planar multi-directional pseudodynamic testing. *Earthq. Eng. and Struct. Dyn.* 38, 1093–1119. doi:10.1002/eqe.886

Moehle, J., Bozorgnia, Y., Jayaram, N., Jones, P., Rahnama, M., Shome, N., et al. (2011). "Case studies of the seismic performance of tall buildings designed by alternative means," in *Report 2011/05, pacific earthquake engineering research center* (Berkeley, California: University of California).

Ohtori, Y., Christenson, R. E., Spencer, B. F., and Dyke, S. J. (2004). Benchmark control problems for seismically excited nonlinear buildings. *J. Eng. Mech.* 130, 366–385. doi:10.1061/(asce)0733-9399(2004)130:4(366)

Pandey, S., Fleischman, R., Sause, R., Ricles, J., and Uang, C.-M. (2022). Behavior of seismic collectors in steel building structures: Proceedings of the 12th National Conference in Earthquake Engineering. Salt Lake City, Utah, USA, June 27-July 1.

Pei, S., van de Lindt, J. W., Barbosa, A. R., Berman, J. W., McDonnell, E., Daniel Dolan, J., et al. (2019). Experimental seismic response of a resilient 2-story mass-timber building with post-tensioned rocking walls. *J. Struct. Eng.* 145. doi:10.1061/(asce)st.1943-541x.0002382

Perez, F. J., Pessiki, S., and Sause, R. (2013). Experimental lateral load response of unbonded post-tensioned precast concrete walls. *ACI Struct. J.* 110. doi:10.14359/51686159

Rathje, E. M., Dawson, C., Padgett, J. E., Pinelli, J.-P., Stanzione, D., Adair, A., et al. (2017). Designsafe: new cyberinfrastructure for natural hazards engineering. *Nat. Hazards Rev.* 18. doi:10.1061/(asce)nh.1527-6996.0000246

Ricles, J., Kolay, C., and Marullo, T. (2020). *HyCoM-3D: a program for multi-hazard nonlinear dynamic analysis and real-time hybrid simulation of 3-D civil infrastructural systems*. Bethlehem, PA: ATLSS Report No. 20-02, Lehigh Unversity.

Ricles, J., Marullo, T., and Roy, S. (2007). *Multiple NEES equipment site soil-structure-foundation distributed hybrid simulations*. Bethlehem, PA: Lehigh Unviersity. *ATLSS Report No. 07-12*.

Ricles, J. M., Fisher, J., Lu, L.-W., and Kaufmann, E. (2002a). Development of improved welded moment connections for earthquake-resistant design. *J. Constr. Steel Res.* 58, 565–604. doi:10.1016/s0143-974x(01)00095-5

Ricles, J. M., Mao, C., Lu, L.-W., and Fisher, J. W. (2002b). Inelastic cyclic testing of welded unreinforced moment connections. *J. Struct. Eng.* 128, 429–440. doi:10.1061/(asce)0733-9445(2002)128:4(429)

Villalobos Vega, E., Harvey, S., Ricles, J., Cao, L., and Burgos, D. T. (2022). "Multi-directional real-time hybrid simulation study of rolling pendulum isolation systems for seismic risk mitigation of critical building contents," in Proceedings of the 12th National Conference in Earthquake Engineering, Salt Lake City, Utah, USA, June 27-July 1.

Villalobos Vega, E., Vanderheiden, E., and Harvey, P. (2024). "The performance of a rolling pendulum isolation system subject to 3d seismic excitation," in Proceedings world conference on earthquake engineering (international association for earthquake engineering), USA, August 2-1998.

Zhang, X., and Ricles, J. M. (2006). Experimental evaluation of reduced beam section connections to deep columns. *J. Struct. Eng.* 132, 346–357. doi:10.1061/(asce)0733-9445(2006)132:3(346)

frontiers | Frontiers in Built Environment

TYPE Review
PUBLISHED 23 April 2025
DOI 10.3389/fbuil.2025.1573390

Check for updates

OPEN ACCESS

EDITED BY
Navid Jafari,
Louisiana State University, United States

REVIEWED BY
Paolo Castaldo,
Polytechnic University of Turin, Italy
Rijalul Fikri,
Syiah Kuala University, Indonesia

*CORRESPONDENCE
John S. McCartney,
mccartney@ucsd.edu

RECEIVED 09 February 2025
ACCEPTED 10 March 2025
PUBLISHED 23 April 2025

CITATION
McCartney JS, Van Den Einde L, Morrison M, Palermo A, Lotfizadeh K, Lai C-T and Conte JP (2025) Multi-degree of freedom shake table testing of large-scale structural and geotechnical systems with NHERI-UCSD LHPOST6.
Front. Built Environ. 11:1573390.
doi: 10.3389/fbuil.2025.1573390

COPYRIGHT
© 2025 McCartney, Van Den Einde, Morrison, Palermo, Lotfizadeh, Lai and Conte. This is an open-access article distributed under the terms of the Creative Commons Attribution License (CC BY). The use, distribution or reproduction in other forums is permitted, provided the original author(s) and the copyright owner(s) are credited and that the original publication in this journal is cited, in accordance with accepted academic practice. No use, distribution or reproduction is permitted which does not comply with these terms.

Multi-degree of freedom shake table testing of large-scale structural and geotechnical systems with NHERI-UCSD LHPOST6

John S. McCartney[1]*, Lelli Van Den Einde[1], Machel Morrison[1], Alessandro Palermo[1], Koorosh Lotfizadeh[1], Chin-Ta Lai[2] and Joel P. Conte[1]

[1]Department of Structural Eng., University of California San Diego, La Jolla, CA, United States, [2]Department of Civil Eng., National Taiwan University, Taipei, Taiwan

This paper focuses on the abilities of the Large High-Performance Outdoor Shake Table (LHPOST6) at UC San Diego to investigate the combined effects of realistic near-field translational and rotational earthquake ground motions applied as dynamic excitation to 3-D and large- or full-scale structural, geotechnical, or soil-foundation-structural systems. The LHPOST6 supports the advancement of innovative materials, manufacturing methods, detailing, earthquake protective systems, seismic retrofit methods, and construction methods, and is a driving force towards improving seismic design codes and standards and developing transformative seismic-resistant concepts. This paper provides: (i) a brief overview of the 6-DOF capabilities of the LHPOST6 facility; (ii) an overview of the research projects conducted so far at the LHPOST6 facility focusing on the performance of the facility, and (iii) new seismic research opportunities enabled by the LHPOST6 to provide data and fragility information on structural and geotechnical systems that can support the full realization of performance- and resilient-based seismic design.

KEYWORDS

shake table testing, structural systems, geotechnical systems, earthquake engineering, retrofits, construction methods, design codes

Introduction

The six-degree-of-freedom (6-DOF) large high-performance outdoor shake table (LHPOST6) at UC San Diego is a shared-use facility enabling the next-generation of seismic testing of large structural, geotechnical, and soil-foundation-structural systems due to its ability to accurately reproduce far- and near-field ground motions. The LHPOST6 was originally conceived as a 6-DOF shake table but was built as single-degree-of freedom (1-DOF) shake table and operated from 2004 to 2019 to perform thirty-four projects as a national shared use equipment facility funded by the US National Science Foundation through the Network for Earthquake Engineering Simulation (NEES) and then the Natural

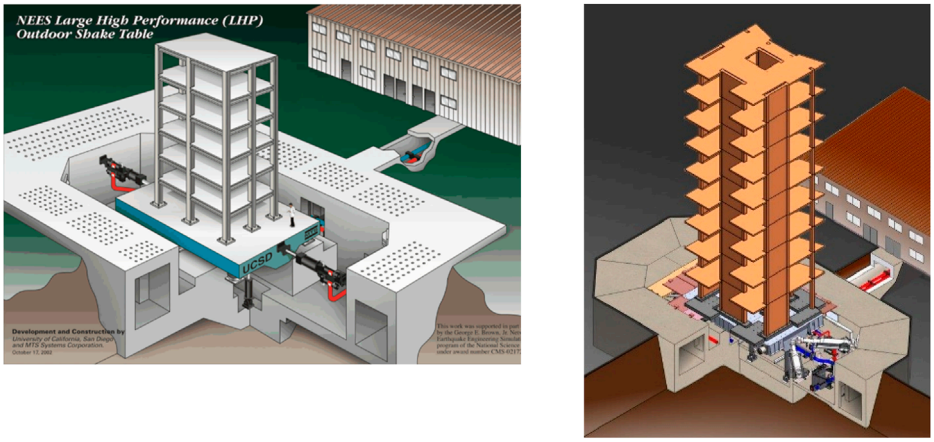

FIGURE 1
Schematics of LHPOST6: **(a)** During operation as a 1-DOF shake table (2004-2019): **(b)** after upgrade to a 6-DOF shake table (2022-present).

Hazard Engineering Research Infrastructure (NHERI, 2025) program. The details of the 34 projects and the upgrade of LHPOST6 to its 6-DOF capabilities were summarized in detail by Van Den Einde et al. (2021). Schematics of the LHPOST6 before and after the upgrade are shown in Figure 1. The LHPOST6 is the largest shake table facility in the US and possesses the largest payload capacity globally, and its 6-DOF capabilities permit investigation of important aspects of the seismic response of 3-D systems to realistic multi-directional input.

The NHERI@UC San Diego Experimental Facility, which hosts and operates the Large High-Performance Outdoor Shake Table (LHPOST6), is rooted in three critical needs for advancing the science, technology, and practice in earthquake disaster mitigation and prevention: (1) Fundamental knowledge for understanding the earthquake system-level behavior of buildings, critical infrastructure, utilities, and geo-structures, from the initiation of damage to the onset of collapse; (2) Experimental data to support the development, calibration, and validation of high-fidelity physics-based computational models that will progressively shift the reliance on physical testing to model-based simulation and address epistemic uncertainties in these models; and (3) Proof of concept testing for novel protective systems and innovative materials which can enhance community protection against earthquakes for either new or existing structures. Since completion of the upgrade in April 2022, four major projects have been performed on the facility which will be summarized in this paper. This paper will also discuss new opportunities to explore the effects of realistic ground motions on structural and geotechnical systems to advance seismic design practice and predictive capabilities for structural, geostructural, and nonstructural systems, leading to improved earthquake safety in the community overall. Indeed, the ability to test full-size structures has made it possible to physically validate the seismic performance of various systems that previously could only be studied at reduced-scale or with computer models.

Need for 6-DOF ground motion capability

The propagation of waves induced by earthquakes produces simultaneous horizontal, vertical and rotational movements of the ground surface. Therefore, the complete characterization of an earthquake ground motion at a given location consists of the three translational (u_x, u_y, u_z) and three rotational (θ_x, θ_y, θ_z) degrees of freedom in a Cartesian coordinate system. Dynamic seismic response analyses of systems for either design or evaluation purposes commonly ignore the rotational components of earthquake ground motions. This has been a widely accepted practice in the earthquake engineering community due to: (1) the lack of recorded rotational ground motions during strong earthquakes and (2) a common assumption in the seismological community that rotational components are small enough to be neglected (Kalkan and Graizer, 2007). Nonetheless, Rosenblueth (1976) discussed the potentially damaging effects of these rotational components on tall buildings, which attracted research interest on the effect of the rotational ground motion components on the seismic behavior of structures (e.g., Ghafory-Ashtiany and Singh, 1986; Zembaty and Boffi, 1994; Trifunac, 2009a; Falamarz-Sheikhabadi, 2014; Falamarz-Sheikhabadi et al., 2016; Falamarz-Sheikhabadi et al., 2017). Moreover, structural failures and damage caused by past earthquakes have been linked to rotational and differential ground motions. For example, the torsional responses of tall buildings during the 1971 San Fernando earthquake were attributed to torsional ground motion (Hart et al., 1975), while rotational and differential ground motions may have caused the collapse of bridges during the 1971 San Fernando, 1978 Miyagi-ken-Oki (Bycroft, 1980), and 1994 Northridge (Trifunac et al., 1996) earthquakes. The high translational accelerations recorded during the February 2011 Christchurch earthquake suggest that rotational motions could have played a significant role in the widespread damage of the area and especially in the central business district consisting of a dense urban setting with closely spaced high-rise buildings (Guidotti, 2012). Numerical studies also indicate

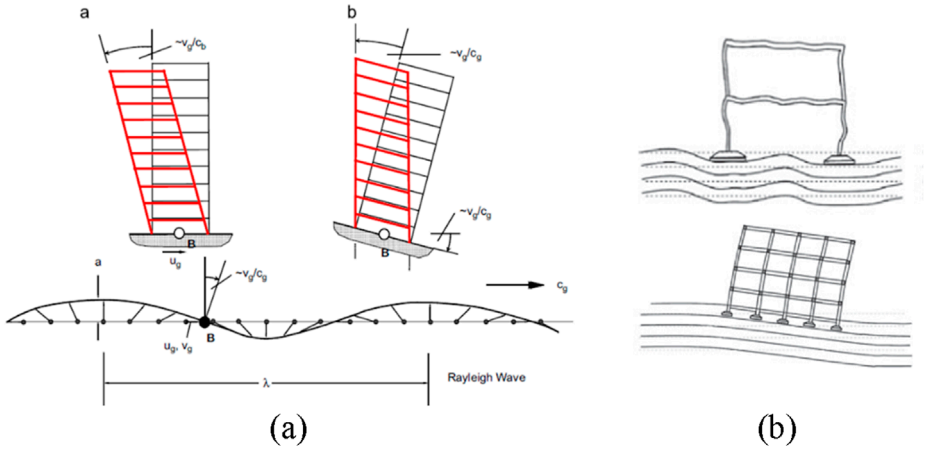

FIGURE 2
(a) Geometric interpretation of how horizontal translation and rocking may contribute to total drift in a simple building during the passage of a Rayleigh wave (from Trifunac, 2009b) and **(b)** response of a building under (top) high- and (bottom) low-frequency content rotational ground motions (from Castellani et al., 2012).

that rotational ground motion components can significantly affect structural response (e.g., Trifunac, 1982; Ghafory-Ashtiany and Singh, 1986; Zembaty and Boffi, 1994; Kalkan and Graizer, 2007; Trifunac, 2009a; 2009b; Jalali and Trifunac, 2009; Castellani et al., 2012; Basu et al., 2015; Falamarz-Sheikhabadi et al., 2017; Bońkowski et al., 2018; Guidotti et al., 2018; Meza Fajardo and Papageorgiou, 2018). It is hypothesized that the significance of this effect is dependent on the magnitude and frequency content of the rotational components as well as the dynamic characteristics of the structure (e.g., Figure 2).

The LHPOST6 will enable the experimental investigation in full 3D and at large- or full-scale of the combined effects of realistic near-field translational and rotational ground motions applied as dynamic excitation to a structural, geotechnical, or soil-foundation-structural system, including the effects of kinematic and inertial soil-structure interaction (SSI), nonlinear soil and structural responses, and soil liquefaction. The data acquired from such landmark tests will enable calibration, validation, and improvement of (mechanics-based, physics-based) analytical and numerical models able to capture the seismic response of civil infrastructure systems, accounting for these realistic and important effects. The LHPOST6 will also be a key experimental facility to deploy, test, and validate sensors to measure rotational components of motion, which may open new frontiers for advanced system and damage identification of structures and structural health monitoring (Trifunac, 2009b).

The 6-DOF capabilities of the LHPOST6 provide new opportunities for studying these different geotechnical applications under realistic 3-D ground motions. As the stiffness and shear strength of soils depend on self-weight, vertical accelerations may lead to changes in soil properties during earthquake shaking, the effects of which are poorly understood in 2-D or 3-D site analyses (Hashash et al., 2010). At some sites, the vertical component of an earthquake motion may exceed the horizontal at short periods (e.g., Bozorgnia et al., 2000; Beresnev et al., 2002; Elgamal and He, 2004). Several element-scale studies have shown that deformations during 2-D horizontal shaking are underestimated when using methods based on unidirectional shaking (e.g., Ishihara and Nagase, 1988; Kammerer et al., 2002; Rutherford and Biscontin, 2013). Pyke et al. (1975) performed 1-g shake table tests on small samples of sand under 3-D motions and observed that while shaking in the vertical direction alone with acceleration amplitudes of less than 1 g did not affect the volumetric contraction of soils, combined vertical and horizontal shaking led to greater settlements than those from horizontal shaking alone.

Capabilities of the LHPOST6

The design of the LHPOST6 was informed using inverse simulation and was then validated using forward simulation. The MTS forward model of the LHPOST6 includes the rigid body dynamics in 6-DOFs of both the platen and a rigid specimen, servovalve and actuator dynamics (with nonlinear flow equations), accumulator banks and line accumulators, and a virtual replica of the MTS 469D controller that has been installed on the LHPOST6. In the forward model, the controller was tuned for the characteristics of the LHPOST6 design using the new 469D Auto-Tuner capability. The tuned closed-loop forward model provides the ability to perform "dry runs" of the LHPOST6 system and thus evaluate, pre-construction, its signal tracking performance capability. The forward model will also allow for offline tuning or pre-tuning based on the test specimen characteristics and will be very useful for safe offline operator training (i.e., shake table simulator). Figures 3a–c compare the target (or desired or reference) and achieved (under bare table condition) translational acceleration, velocity, and displacement time histories of the shake table, respectively, and Figure 3d compares the target and achieved five-percent damped tri-partite (displacement/pseudo-velocity/pseudo-acceleration) linear response spectra for the three translational components of the 1995 Kobe earthquake record. Similar levels of agreement between target and achieved table motions (i.e.,

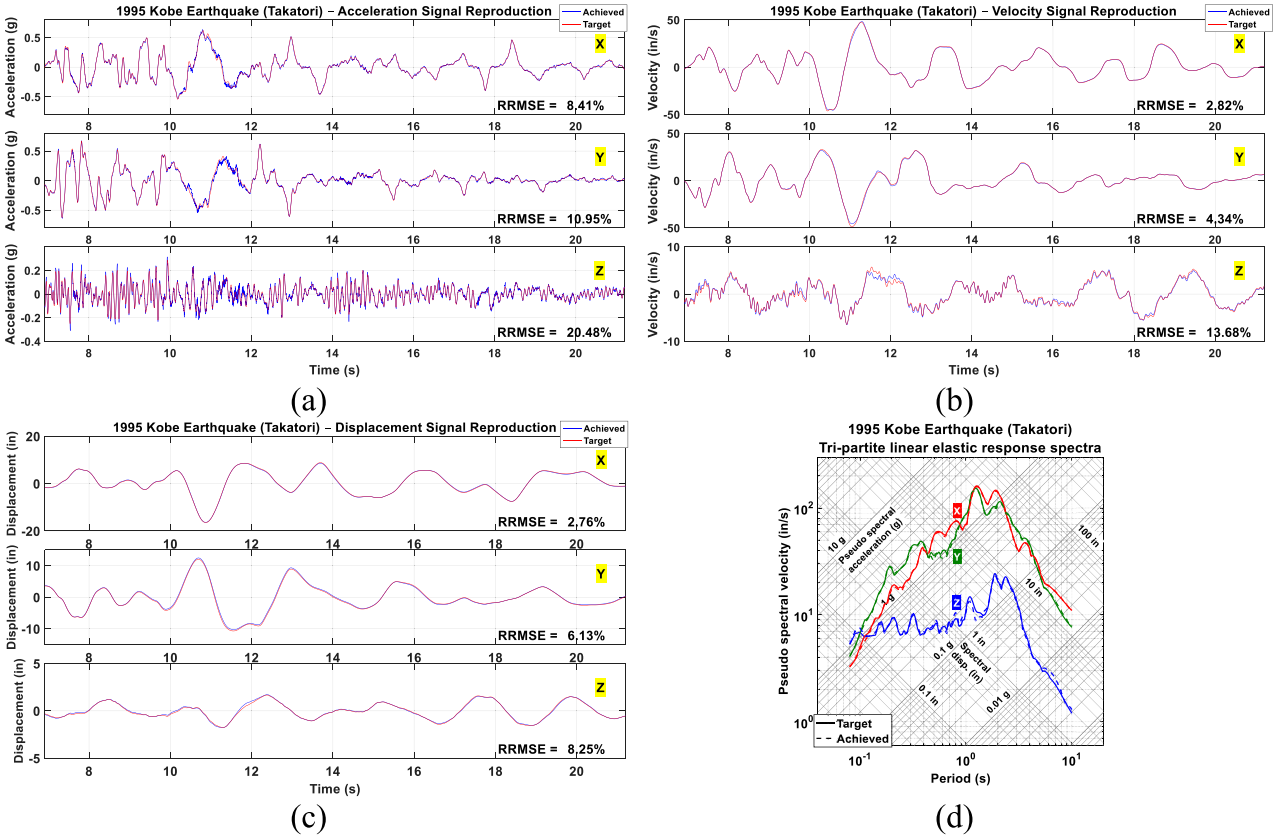

FIGURE 3
Comparison of target and achieved tri-axial 1995 Kobe earthquake record under bare table condition: **(a)** acceleration time histories, **(b)** velocity time-histories, **(c)** displacement time histories, and **(d)** 5% damped tri-partite spectra for linear response.

signal tracking fidelity) were observed for the other strong tri-axial earthquake records considered for the upgrade design.

The comparisons in Figure 3 show a very good signal tracking capability of the LHPOST6. This is especially true for the vertical ground motion component, given the fact that the vertical actuators of the LHPOST6 are single-acting, i.e., these can only push (upwards) and cannot pull (downwards) the platen since they have zero retraction force. The nitrogen-filled hold-down struts pull the platen down but without closed-loop dynamic capabilities. The level of fidelity in signal reproduction for the vertical component and other motion components can also be further improved through the advanced control capabilities built in the MTS 469D controller, such as Adaptive Inverse Control (AIC), Online Iteration (OLI), and Specimen Dynamics Compensation (SDC) as well as the tools available in MTS STEX-Pro. A digital twin of the shake table and hydraulic system has been developed by Lai and Conte (2024), which can be used to simulate the interaction between a specimen on the table and the performance of the LHPOST6. A range of instrumentation including potentiometers, accelerometers, strain gages, load cells, earth pressure cells, and advanced kinemetric sensors are available for deployment on a given project.

Projects performed on the LHPOST6

Modular testbed building

The Modular Testbed Building, or MTB2, was the first specimen tested on the LHPOST6 after the upgrade. Experimental data from this program is available within the DesignSafe Data Depot (Hutchinson et al., 2024), including a detailed technical report (Morano et al., 2024a) and two journal papers (Morano et al., 2024b; 2025). The MTB2 is designed to be a reconfigurable and reusable community shared-use equipment resource. Reuse is accomplished by having a connection scheme that allows yielded members to be replaced, while leaving the rest of the structure in place. This modular design enables low-cost testing of components and subsystems at large to full-scale under simulated dynamic 3D loading. It enables seismic performance verification and acceptance testing of innovative designs, including seismic protective systems, lateral force resisting systems, stairs, nonstructural systems, among others. The MTB2 structure also provides for payload opportunities within the broader community.

The MTB2 reconfiguration allows for different structural configurations. The moment frame configuration consists of a three story (3.7 m/story), two bay (4.9 m/bay) by one bay (6.1 m) frame

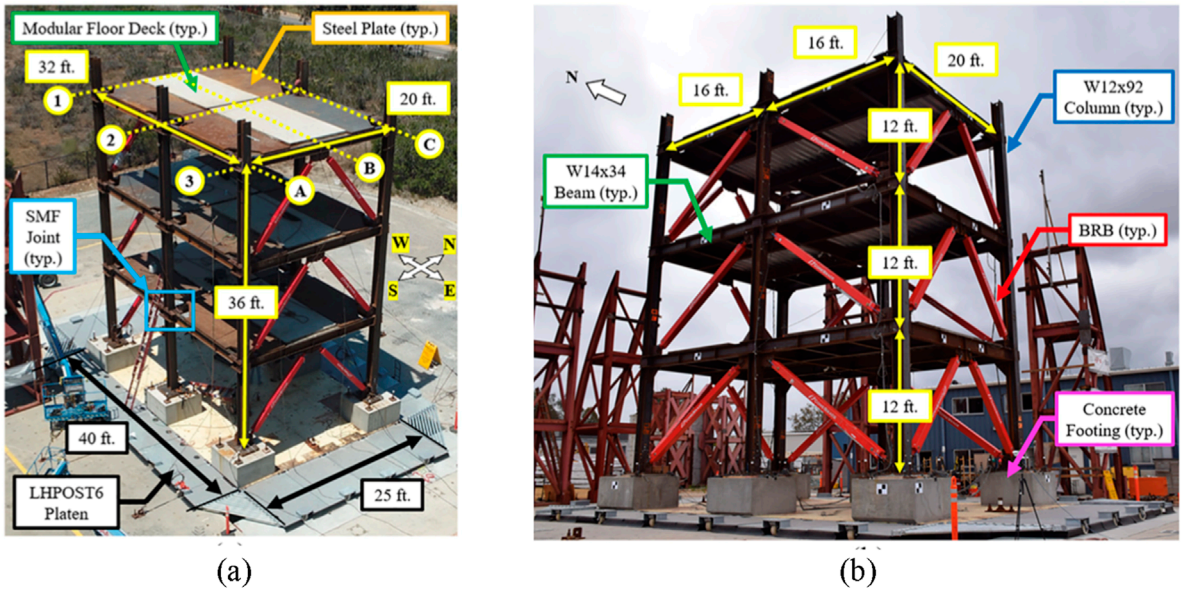

FIGURE 4
Photographs with annotated dimensions of the MTB2 structure (after Morano et al., 2025): **(a)** Moment frame configuration; **(b)** BRB configuration.

structure shown in Figure 4a. The moment frame configuration involves a moment frame with replaceable shear fuse plastic hinges in the longitudinal direction. A second configuration involves three levels of braced frames with buckling restrained braces (BRBs) placed at each story shown in Figure 4b. A third configuration is identical to the second except for the replacement of the BRBs at the first story with moment shear fuses to promote a softer first story. The MTB2 study also capitalized on the staging slab space at LHPOST6, using it as an area for pre-test assembly in one of the configurations to test fit and assembly efficiency. This exercise, while LHPOST6 was completing upgrade, allowed the specimen to be tested and characterized under a variety of low amplitude vibrations (Morano et al., 2024b), prior to its assembly on the shake table.

NHERI TallWood project

With global urbanization trends, the demands for tall residential and mixed-use buildings in the range of 8–20 stories are increasing. One new structural system in this height range is tall mass timber buildings. Granello et al. (2020) provided a review of research, testing and implementation of mass timber in buildings. The vision of the NSF-funded six-university collaborative research NHERI TallWood Project (Pei et al., 2024a) is to develop and validate a resilience-based seismic design methodology for tall wood buildings. During the second year of the NHERI TallWood project, an investigative testing program was completed at the NHERI@UC San Diego shake table facility on a full-scale two-story mass timber building with a resilient cross-laminated timber (CLT) rocking wall lateral system (Pei et al., 2017; 2019). The final capstone shake table test of a full-scale 10-story mass timber building equipped with nonstructural components was performed in 2023 as shown in Figure 5. These tests represented the tallest full-scale building structure ever tested on a shake table yielding unprecedented data which has been reported so far (Pei et al., 2024b) which will help push the boundary of resilient tall wood construction worldwide.

NHERI Converging Design project

The NHERI Converging Design project is an NSF-funded research effort led by Prof. Andre Barbosa from Oregon State University with collaborators from Colorado State University, Stanford University, and Penn State University. The vision of this project is to create a new design paradigm within structural engineering that employs multi-objective optimization to maximize functional recovery while integrating additional sustainable building design principles. This design methodology was validated through shake-table testing of a full-scale six-story mass timber structure at the NHERI@UCSD outdoor facility. This six-story specimen emerged from the previously tested ten-story shake-table specimen from the NHERI TallWood project where the top four stories were deconstructed to leave a six-story specimen to be reconfigured for the NHERI Converging Design project. The six-story structure was then subject to three distinct phases of shake-table testing that include different lateral force resisting systems with details summarized in Figure 6. The first phase of testing featured post-tensioned mass timber self-centering rocking wall lateral force-resisting systems consisting of mass timber wall panels, bounding columns, and U-shaped flexural plates (UFPs) (e.g., Chen et al., 2024) distributed over the height of the building as energy dissipators. The second phase of testing featured buckling-restrained braces (BRBs) as energy dissipators at the base of post-tensioned mass timber rocking walls to serve as the lateral force-resisting system. The third phase of testing featured yield

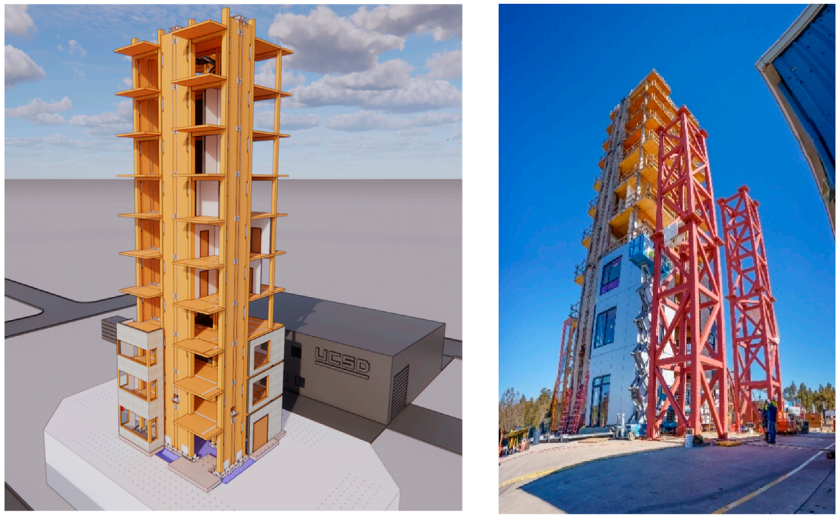

FIGURE 5
TallWood 10 story structure: **(a)** Schematic; **(b)** Photo on the LHPOST6.

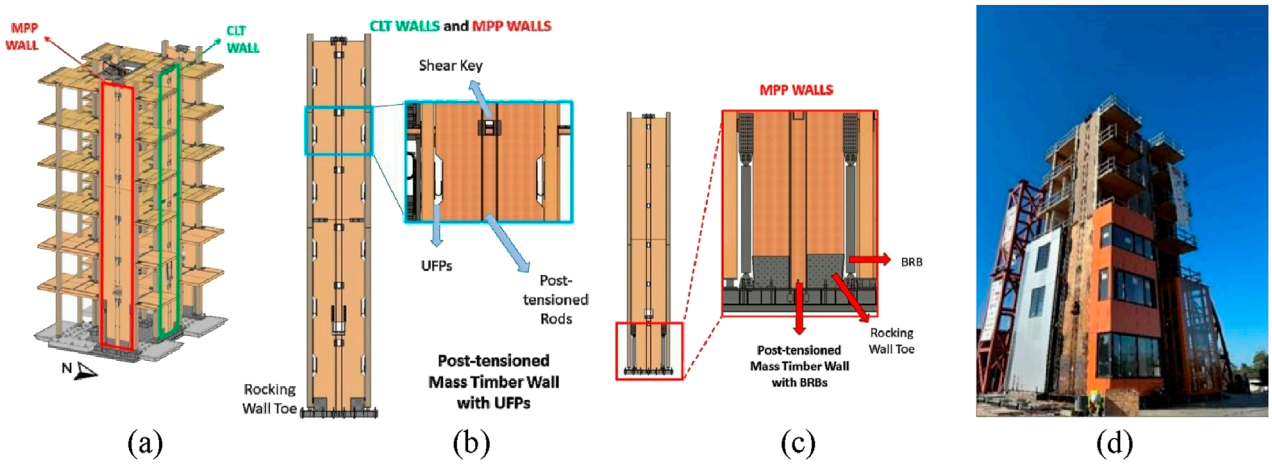

FIGURE 6
NHERI Converging Design 6-story specimen: **(a)** Three-dimensional rendering of the tested specimen with indication of location of different mass timber wall panels, including cross-laminated timber (CLT) and mass ply panels (MPP); **(b)** Main components of the self-centering rocking wall system tested in phase 1; **(c)** Schematics of different components used in the North-south direction in phase 2; **(d)** Picture of phase 1 tested specimen on the LHPOST6.

link brace connections in exploration of hybrid steel mass timber structural system solutions. Data from this project has been archived in DesignSafe (Barbosa et al., 2025) and more information can be found at the NHERI Converging Design Project Website (2025).

Seismic response of spent nuclear fuel casks

In the United States, Spent Nuclear Fuel (SNF) is currently stored onsite at 73 Nuclear Power Plants because a site for a geological repository for permanent SNF has not been identified and permitted. The SNF inventory stored on-site either in pools or dry storage was 84,500 MTU in 2020, with 46% being stored in dry storage with a rate of increase of 3,500 MTUs per year. As the SNF will be stored onsite for longer than expected, the dry storage facilities involving SNF in casks as shown in Figure 7a could experience earthquakes of a different magnitude than the one for which they were originally designed. However, there is little data on the response of SNF inside dry storage systems to seismic loads in the U.S., and the various gaps and nonlinearities between storage containers, canisters, baskets, aggregates, and fuel make it very difficult to evaluate by analytical methods. A 1468 kN generic vertical storage overpack (cask) shown in Figure 7b was tested on

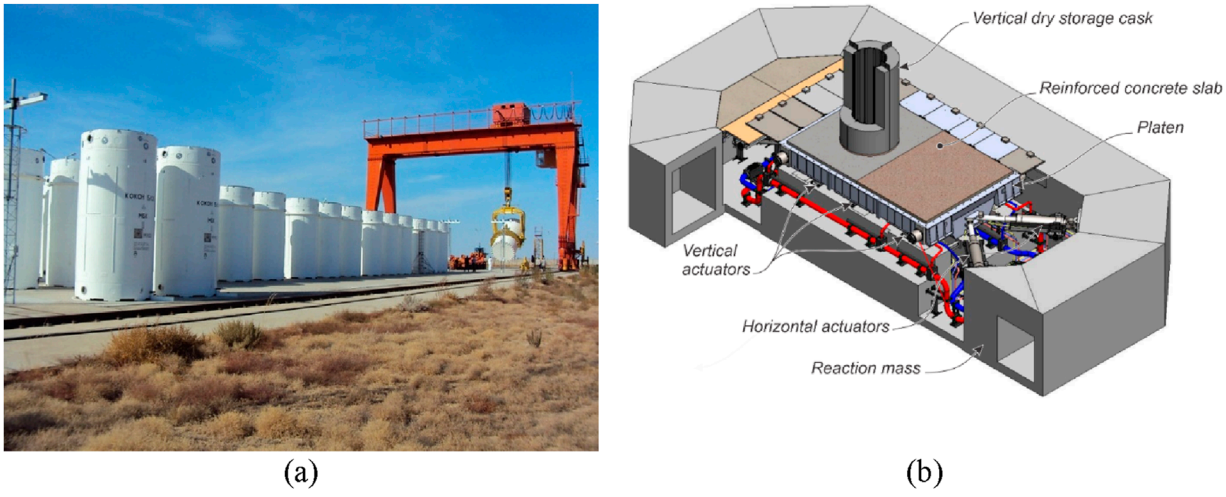

FIGURE 7
Sandia SNF casks: **(a)** Field setting; **(b)** Schematic of test setup on the LHPOST6.

the LHPOST6 in summer 2024. It was equipped with a canister and a fuel basket with a thirty-two fuel assembly capacity. A mix of surrogate fuel assemblies and dummy assemblies filled all basket locations. An eight-inch-thick concrete slab was built on top of the shake table platen to act as the cask's bearing surface. This slab had a surface finish mimicking the one found in real-world conditions. The cask, its components, and content was instrumented with a dense array of sensors consisting of accelerometers strain gauges, pressure indicating films, inclinometers, and displacement transducers. In addition, a series of high-speed, high-resolution cameras were used to monitor the local displacements of the fuel assemblies and the global displacement of the cask. The accelerometers and strain gages were fastened to fuel rods to monitor their dynamic response under generic ground motions representative of hard rock, soft rock, and soil sites in the U.S.

CFS-NHERI capstone test building

As a capstone to the multi-university-industry collaborative CFS-NHERI project, a full-scale 10-story cold-formed steel (CFS)-framed building is currently being constructed on the LHPOST6 and will be tested in Summer 2025 under increasing, multi-directional earthquake motion intensity along with subsequent live fire testing. Coined CFS10 (cfs10.ucsd.edu) the capstone effort follows successful prior system-level 2-story (CFS-NEES) and 6-story (CFS-HUD) structures previously tested on shake tables, the later program at LHPOST prior to its upgrade to 6-DOFs. The CFS10 project is being led by Tara Hutchinson from UC San Diego, Benjamin Schafer from Johns Hopkins University, and Richard Emberley from CalPoly University San Luis Obispo. In addition, collaborations with Thomas Gernay of Johns Hopkins University, Kara Peterman of the University of Massachusetts Amherst, Monica Kohler of Caltech, and Richard Allen of the University of California Berkeley enrich the program.

The CFS-NHERI capstone test building is designed with a height of 31.6 m, exceeding the height limitation of 19.8 m set by the current ASCE 7–22 design standard as shown in Figure 8 (see Singh et al., 2022; 2024; Zhang et al., 2024a; 2024b). The design also advances lateral force resisting system (LFRS) details to provide for the increases in seismic shear and overturning moment demands associated with increases in building height. Data generated will shed light on the impact of architectural exterior and interior finishes, non-designated systems, such as gravity walls or window/door framing. Higher mode effects, which can significantly influence the structural and nonstructural seismic response of tall buildings, will also be studied for the first time for repetitively framed structures. The experiments will provide vital full-scale system-level benchmark test data for a state-of-the-art CFS building under multidirectional seismic input. It will also advance knowledge of the post-earthquake fire performance of mid-rise CFS construction, by incorporating a live fire test sequence following the seismic test phase completion.

Research enabled by the LHPOST6

Importance of large-scale seismic testing of civil infrastructure

The seismic response of structures involves complex physics of heterogeneous materials with highly nonlinear constitutive properties and depends on the boundary/interface conditions, such as the interaction between the structure and the supporting/surrounding soil. There are many open issues regarding how to accurately model these phenomena at the different length and time scales over which the physical processes develop. There are significant knowledge gaps about the seismic response of structures that have been damaged or have partially collapsed and their possible failure modes as identified in the 2011 NRC report (National Research Council, 2011). State-of-the-art nonlinear structural analysis methods are still fairly limited in their ability to model the nonlinear dynamic response of structures, especially when approaching collapse (Deierlein, 2011). Failure is often triggered by localized strain concentrations resulting in

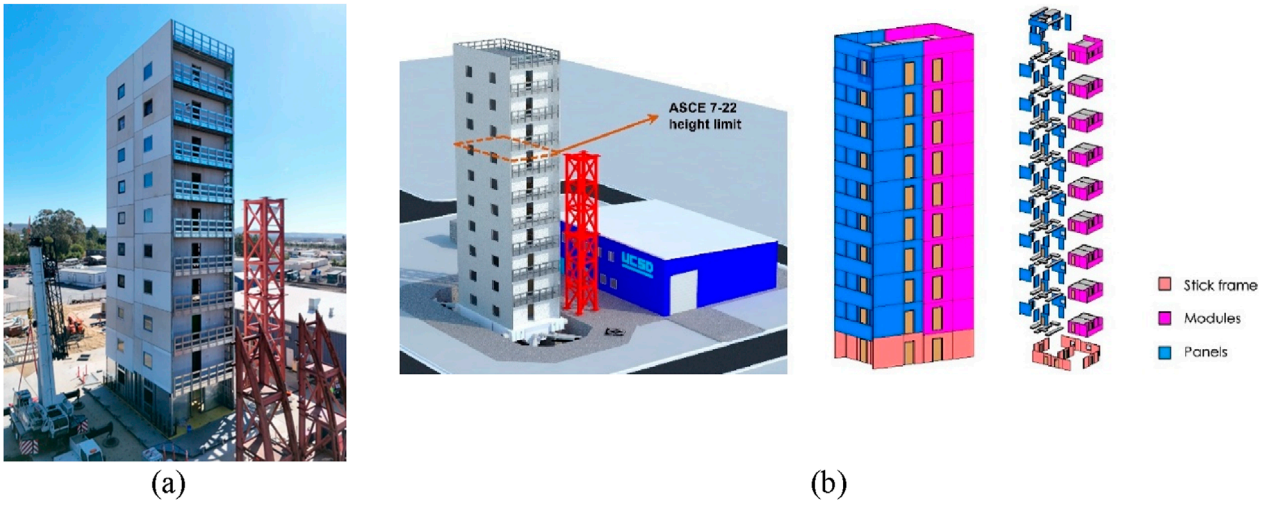

FIGURE 8
CFS-NHERI 10 story structure (at structural height completion, 21 Feb 2025): **(a)** Construction of the CFS-10 structure on the LHPOST6; **(b)** Schematics of the structure and construction methods (by J. Zhang and D. Rivera).

stiffness and strength degradation that is sensitive to loading history. Examples of such behavior include local buckling and fracture in steel (both structural steel and reinforcing steel in concrete), shear failures in reinforced concrete (R/C) columns and walls, and connection or splice failures. While significant experimental research has been performed on individual structural components (e.g., beams, columns, slabs) and subassemblies (e.g., beam-column joints, beam-slab-column joints) at various scales (all the way to full-scale) in the US and other countries, the boundary conditions imposed on these test specimens may not be realistic as compared to their actual boundary conditions within structural systems. The scale of these physical models can also be an issue since some design details, construction materials, and damage and failure mechanisms cannot be accurately reproduced in reduced-scale models. These include the spacing of reinforcement in concrete structures, the size of aggregates in concrete, the quality and properties of welds, and the degree of plastic strain or damage localization, all which affect the ability of a structure to sustain inelastic deformations and the failure mechanisms. Hence, large- or full-scale structural system tests are essential to identifying and overcoming modeling deficiencies and validating these models and design details.

The mechanical behavior of most civil infrastructure systems under extreme earthquake loads is highly nonlinear and complex and varies significantly depending on the structural type and detailing, construction materials, and regional construction practice. Unlike aerospace structures, civil structures cannot be prototyped for mass production or designed to remain within the elastic limit during severe load events. To ensure that structures of different types, system properties and materials have a consistent level of safety and predictable performance in earthquake events, a performance-based design (PBD) approach was extensively developed in the mid-1990s. It is based on a structural reliability framework and enables engineers to design structures and facilities to meet specific performance objectives with quantifiable and acceptable risks of (i) exceeding various damage states, (ii) casualty, (iii) loss of occupancy (downtime), and (iv) economic losses in future earthquakes.

Although the PBD methodology has not been fully implemented in practice, simplified PBD methods have found their way into seismic design codes, such as AASHTO-COPRI 6 (2014), design guidelines like LATBSDC (2020) and assessment guidelines such as ASCE 41 (ASCE, 2017) for the evaluation and retrofit of existing buildings. Notably, the risk-targeted seismic hazard maps that form part of ASCE 7 (ASCE, 2022) rely not only on probabilistic seismic hazard data but also on structural fragility functions to achieve a uniform risk of structural collapse across the US. Furthermore, the recently developed and adopted FEMA 695 Methodology (FEMA, 2009) that quantifies structural performance factors for new structural systems to be designed with ASCE seven is also based on the notion of a uniform and acceptable risk of collapse. It is noteworthy that the development of reliable fragility functions, which are central to PBD, requires relevant experimental data and high-fidelity simulation models that can predict the nonlinear behavior of structural materials, components, and systems under different hazard scenarios. Experimental programs conducted at the LHPOST6 facility provide landmark experimental data at the subsystem and system levels.

It is well established that the extensive damage exhibited by code-compliant conventional buildings during strong earthquake ground motions, while avoiding collapse, has caused a push in earthquake-affected communities in the past 2 decades to use low-damage structural earthquake protective systems. Such systems can sustain significant nonlinear response, large lateral displacements, and damping with practically no damage and maintained operability throughout. Multi-axial large/full-scale shake table tests of building structures are needed to understand their response in 3-D, including the effects of rotational components of earthquake ground motions, and support the development of future design codes. Also, innovative seismic retrofit strategies that will be used and implemented for existing older non-ductile (wood,

masonry, concrete, and steel) buildings should be validated through large-scale shake table system testing to better understand the force redistributions and the overall implications on the system ductility. Limited recent full-scale building shake table tests that incorporate non-structural components and systems, supported by field observations, demonstrate the importance of advancing our understanding and predictive capabilities of nonstructural components and structures (NCSs) in building systems when subjected to multi-directional seismic loading. Full-scale multi-axial shake table tests are needed to support the development of a reliable, unified design methodology for NCSs accounting for multi-directional earthquake excitation. Finally, there is a strong emphasis on the need to develop new sources of energy while preventing or reversing the degradation of the environment (i.e., renewable energy sources). Important examples of the supporting infrastructure are wind turbine farms (onshore and offshore), solar arrays, concrete dams, containment/reactor vessels of nuclear power plants and dry storage casks of spent nuclear fuel, which when built in seismic regions all require better understanding of their seismic response behavior and reliable performance-based assessment and design using experimentally validated high-fidelity computational models.

Understanding inherent damping

Inherent damping (also simply termed intrinsic or elastic damping) is introduced in time-history analyses of the inelastic seismic response of structures to account for damping before the onset of hysteretic response. The pioneering work of Carr (2005) established that the details of the inherent damping model may have significant effects on the calculated inelastic structural response. Several studies have studied inherent damping experimentally (e.g., Takayanagi and Schnobrich, 1979; Otani, 1980; Satake et al., 2003; Rodríguez et al., 2006; Petrini et al., 2008; Moaveni et al., 2010; Papagiannopoulos and Beskos, 2012; Astroza et al., 2016), but the optimal damping model has not been identified. It is also difficult to experimentally separate the inherent and hysteretic damping associated with the inelastic response or soil-structure interaction effects (e.g., Celebi, 1996).

Due to the lack of experimental data, a number of options involving Rayleigh, Caughey (Caughey, 1960; Caughey and O'Kelly, 1965), and modal (Wilson and Penzien, 1972) viscous damping matrices based on initial or tangent (degraded) stiffness properties have been proposed as models (Chrisp 1980, Shing and Mahin, 1987; Bernal, 1994; Carr, 1997; 2005; Hall, 1998; 2006; 2016a; 2017; Ryan and Polanco, 2008; Zareian and Medina, 2010; Jehel et al., 2014; Hardyniec and Charney, 2015; Chopra and McKenna, 2016a; 2016b). Warnings regarding the unintended consequences of these choices and possible remedies have been presented by several authors (Hall, 2006; Charney, 2008; Ryan and Polanco, 2008; Luco and Lanzi, 2019; Anajafi et al., 2020). In recent years, several studies have more closely investigated the problems associated with existing damping models and proposed solutions to overcome some of these problems (Carr et al., 2017; Luco and Lanzi, 2017; Lanzi and Luco, 2018; Chambreuil et al., 2022). The need to better identify the actual inherent damping mechanism(s) suggests the use of harmonic vibration tests (as opposed to seismic simulations) in the vicinity of resonance for excitations close to those leading to instability in the absence of inherent damping (Caughey, 1960; Luco, 2014). Shake table experiments with full 3-DOF or 6-DOF seismic base excitation on large- or full-scale building specimens with and without non-structural components and systems and large-scale bridge sub-structures (e.g., bridge bent) will guide the development and selection of optimum inherent damping models.

Dynamic response of geotechnical soil-foundation-structure systems

The LHPOST6 is ideally suited for experimental investigations of dynamic soil-structure and soil-foundation-structure interaction (Mylonakis and Gazetas, 2000; Gavras et al., 2020; Antonellis et al., 2015; Ebeido et al., 2019; Elsawy et al., 2019; Shahbazi et al., 2020a; Zayed et al., 2020; Zayed et al., 021). For example, the kinematic interaction between a foundation and soil (in the absence of the superstructure) under internal seismic wave excitation leads to translational and rotational components of the foundation input motion. This occurs for embedded foundations for all types of elastic wave excitation and for surface foundations subjected to non-vertically incident seismic waves and to spatially random ground motions. When a superstructure is present, the inertial interaction results in additional rocking components of motion of the foundation and additional torsional components, particularly, when the structure is not symmetrical. Thus, even when it can be assumed that the foundation is sufficiently rigid, the motion of the foundation will have at least 6 DOFs (e.g., (Roesset, 1981; Luco, 1981)). The 6-DOF capabilities of LHPOST6 will enable new types of full-scale dynamic SFSI studies needed to validate analytical or numerical simulations.

Along with the large laminar soil box and the large "rigid" soil box, the LHPOST6 is also ideally suited for experimental studies on the dynamic deformation response of geosynthetic reinforced soil (GRS) retaining walls (El-Emam and Bathurst, 2004; Ling et al., 2005; Ling et al., 2012; Sander et al., 2013; Latha and Santhanakumar 2015; Fox et al., 2015; Zheng et al., 2018a; Zheng et al., 2018b; Zheng et al., 2019a; Zheng et al., 2019b), cantilever retaining walls used in dam spillways (Kim and Elgamal, 2017a), shallow tunnels and buried water reservoirs (Kim et al., 2016; Hushmand et al., 2016a; 2016b; Durante et al., 2022), and slopes or embankments (e.g., Wartman et al., 2005; Nakamura et al., 2011; Sogabe et al., 2013; Yarahuaman and McCartney, 2022). The behavior of shallow buried structures (water reservoirs, tunnels, lifelines, utilities) has been well studied using centrifuge techniques (Hushmand et al., 2016a; 2016b) and large-scale soil-boxes (O'Rourke et al., 2008), but the soil containers on LHPOST6 can accommodate additional instrumentation and better capture system responses. The depth and flexibility of the tunnel structure and the soil compaction techniques were found to have a major effect on the seismic earth pressures in these experiments. Analytical techniques for seismic earth pressure estimation have advanced over time (Davis, 2003; Durante et al., 2022), which require detailed validation from full-scale experiments. The scale of the soil boxes permits dynamic experimental studies on the efficacy of conventional or bio-mediated soil improvement using actual construction techniques (Van Impe, 1989; DeJong et al., 2014) and experimental investigations of geotechnical issues that cannot be studied in laboratory-scale experiments like lateral spread in layered soils (Youd et al., 2002; Zayed et al., 2021), liquefaction of gravelly soils (Hubler et al., 2017), seismic or cyclic response of alternative backfill materials like tire derived aggregates with large particle sizes (Ahn and

Cheng, 2014; McCartney et al., 2017) or expanded polystyrene foam (Trandafir and Bartlett, 2010; Athanasopoulos-Zekkos et al., 2012), seismic settlement of saturated soils (Tokimatsu and Seed, 1987; Bray and Olaya, 2022), and seismic compression of unsaturated soils (Stewart et al., 2004; Ghayoomi et al., 2011a; Ghayoomi et al., 2013a; Rong and McCartney, 2020; 2021).

Seismic testing of geostructures in the centrifuge permits construction of multiple specimens with different configurations to understand the impacts of different geometric variables or design features. Different from seismic testing of geostructures in the centrifuge, testing of geostructures in the large soil boxes on the LHPOST6 permits use of actual construction procedures for compacting soils, consideration of foundation installation effects, consideration of actual ground improvement techniques, and use of actual geosynthetic reinforcements. Accordingly, there are opportunities for collaboration with geotechnical centrifuge facilities to perform multiple simplified parametric-study type experiments in the centrifuge, then consider the effects of full-scale construction features like those permitted in the LHPOST6. Different from centrifuge testing on small-scale models, large-scale testing permits the incorporation of large instrumentation like earth pressure cells and settlement plates (e.g., Keykhosropour et al., 2018; Zheng et al., 2019a; 2019b; Yarahuaman and McCartney, 2022). Use of the large soil boxes available at the LHPOST6 may also help minimize near-field and boundary effects encountered when applying *in-situ* shear wave velocity tomography techniques that may be encountered in centrifuge-scale experiments (Ghayoomi and McCartney, 2011b). Centrifuge testing often uses transparent soil boxes (Ghayoomi et al., 2013b) or even transparent soils (Black, 2015) to visualize soil-structure interaction mechanisms. Accordingly, data obtained from centrifuge and 1-g shake table testing may be complementary.

In many cases, full-scale geostructures can be investigated on the LHPOST6 (e.g., Sander et al., 2013; Fox et al., 2015; Shahbazi et al., 2020a; 2020b). However, in other cases, it may not be possible to test a full-scale geotechnical structure due to the large size of the structure under investigation, such as cut-and-cover tunnels and dam spillways (Kim and Elgamal, 2017a; 2017b; Kim et al., 2016) or deep foundations (Ebeido et al., 2019; Zayed et al., 2020; Zayd et al., 2021). Numerical simulations are often used to extrapolate measurements from reduced-scale tests to large scale tests (e.g., Pereira and Koltuniuk, 2018; Li et al., 2020), but it is more reliable to use scaling relationships to avoid self-weight stress-dependent issues like arching that affect soil-structure interaction. Unlike centrifuge testing where a single scaling factor associated with the g-level can be used to reach geometric similitude, where stresses and strains are the same in a model and prototype, 1 g scale modeling requires a more nuanced approach. Scaling relationships like those developed by Iai (1989) permit extrapolation of measurements from reduced-scale tests to full-scale field conditions by establishing similitude between the model soil layer tested on the shake table and the prototype soil layer in the field. Iai (1989) built upon the work of Rocha (1957) to develop an approach to reach similitude between a reduced scale model and a prototype by considering a geometric scaling factor, a density scaling factor and a strain scaling factor. As the self-weight stresses are lower in a reduced scale 1 g model, the main effect of the scaling approach of Iai (1989) is to reduce the density (and thus stiffness) of the model soil layer so that it has a similar stress strain curve when scaled by the three scale factors. Zheng et al. (2019b) found that it is possible to use only a geometric scaling factor when using a strategically selected relative density that leads to a softer stress-strain response but not a major change in unit weight. Centrifuge modeling can be used to validate the scaling approach of Iai (1989) using the "modeling of models" technique (Ko, 1988). Specifically, models with different length scales (including a prototype at 1 g) can be tested under different g-levels to validate scaling relationships. When studying phenomena like liquefaction, post-liquefaction seismic settlements, seismic compression of unsaturated soils lateral spreading, or the efficacy of soil improvement techniques, scaling may not be necessary for simulating near-surface soil layers having a thickness less than the height of the laminar and rigid soil boxes.

The large soil boxes permit control of the boundary conditions necessary in modeling geostructures, which can have a major effect on the measured seismic response. The large "rigid" soil box permits control of plane strain boundary conditions representative of long geostructures (embankments, slopes, dams). It could also be used to assess soil-structure interaction behavior associated with reinforced concrete retaining wall systems (Castaldo and De Iuliis, 2014). While the rigid back wall boundary condition may not represent those for geostructures in the field, it is straightforward to consider in numerical simulations. The "rigid" soil box at UC San Diego is particularly suitable for tests with 2D shaking (vertical and horizontal shaking in one direction). The large laminar soil box is currently configured for uni-directional horizontal shaking that simulates a flexible shear soil column. While tests with shaking in the vertical and one horizontal direction can be accommodated with the laminar soil box in its current configuration, the laminar container will be upgraded using point-roller bearings for bi-directional horizontal shaking.

Three general types of experimental SSI studies are envisioned using the LHPOST6.

(1) Verification Studies under Tri-axial Excitation: Computational models of the complete soil-foundation-structure system can be used to obtain the total translational and rotational motion of the foundation which would then be applied at the base of the structure placed on the shake table. The resulting response of the structure will be compared with the predictions through numerical simulation to validate both theoretical models and computational methods. Independent of the validation justification, the response of structures to simultaneous translational and rotational base motions is of interest for research intended to represent the free-field ground motion as consisting of both translational and rotational components. This would extend the current design practice of including only translational components (in the absence of SSI) (e.g., Lee and Trifunac, 1985; 1987). Such tests will also open an avenue for blind prediction contests and discussions about the models used to augment knowledge in the community.

(2) Laminar and Rigid Soil Box Studies under Tri-axial Translational Excitation: In these studies, full-scale or scaled models of structures can be supported on soils placed in either the 1D laminar or rigid soil boxes available at the facility. The soil box can be subjected to tri-axial translational base motions to better simulate the seismic input excitation. Such tests could

be used to study the nonlinear response of soils, the response of partially saturated soils, alternative backfill materials, and the nonlinear interaction between foundations, structures, and the soil (e.g., Shahbazi et al., 2020a). The contribution of radiation damping into the soil to the apparent damping in the structure (Cruz and Miranda, 2017) could also be studied using this approach. The effects of coupling through the soil on the seismic response of adjacent structures (i.e., structure-soil-structure interaction), a topic of importance in the urban environment and in farms of storage tanks and wind turbines, could also be investigated through this approach. Liquefaction, seismic-induced settlements and lateral soil spreading in urban areas have accounted for a large percentage of the damage to the built environment in cities stricken by a strong earthquake, such as in the 2010 and 2011 Christchurch earthquake swarm (Bray et al., 2017; Cubrinovski et al., 2014). Liquefaction effects on the seismic response of soil-foundation-structural systems can be studied with the LHPOST6 with one of the two large soil boxes available equipped with a flexible membrane liner to retain the water inside the soil box.

(3) Hybrid Tests: These will be ambitious tests in which the soil will be modeled in the computer and the superstructure on the shake table. The foundation input motion (i.e., the response of the foundation to seismic waves in the absence of the superstructure) and the response of the foundation to the total base inertial forces from the superstructure will be obtained numerically, in real-time. These tests will be used to study the nonlinear seismic response of structures in the presence of soil-structure interaction, including the torsional response of structures.

Advanced and/or innovative earthquake protective systems

Extensive damage in conventional buildings and bridges has caused a push in earthquake-affected communities in the past 2 decades to use low-damage structural earthquake protective systems. Such systems can sustain significant nonlinear response, large lateral displacements and damping with practically no damage and maintained operability throughout. This is a very active research area that includes base isolation, rocking foundations and systems, self-centering systems, inertial force-limiting floor anchorage systems, various types of dampers, buckling-restrained braces, and new materials (e.g., Housner, 1963; Zhang and Makris, 2001; Ozbulut et al., 2011; Clayton et al., 2012; Belleri et al., 2014; Kramer et al., 2016; Tian et al., 2016; Agalianos et al., 2017; Ganey et al., 2017; Moghadam and Konstantinidis, 2017; Silva, 2019).

Many structures have survived strong earthquakes unscathed, courtesy of rocking of the foundation (Housner, 1963). In competent soils not susceptible to liquefaction, rocking can be used as a mechanism to concentrate the nonlinear response and provide energy dissipation in some structures. This aspect has been widely demonstrated in centrifuge, field and 1-g shake table testing (e.g., Chang et al., 2007; Paolucci et al., 2008; Deng and Kutter, 2012; Gelagoti et al., 2012; Anastasopoulos et al., 2013; Liu et al., 2013; Pecker et al., 2014). Antonellis et al. (2015) carried out shake-table testing of two 1:3 scale bride piers with shallow foundations designed to rock. The test specimens were placed inside the large confinement soil box described by Fox et al. (2015), which was partially filled with poorly graded medium sand and water. Because of the uni-directional limitation of the LHPOST at the time, one of the test units was aligned with the direction of the shake table excitation, whereas the other was rotated 30°. While this provided multi-directional input to the specimens, the obvious correlation of the pair of translational input motions was present. This limitation no longer exists with the LHPOST6. The direction of shaking is also critical when studying geosynthetic-reinforced bridge abutments. Zheng et al. (2018a), Zheng et al. (2018b) and Zheng et al. (2019b) performed transverse and longitudinal shaking tests on GRS bridge abutments, respectively, and found a major difference in behavior. However, the geometries of the GRS bridge abutment specimens were different due to the limitations in the size of the UC San Diego Powell Laboratory shake table. Using the LHPOST6, the dynamic behavior of GRS bridge abutments in transverse and longitudinal directions can be evaluated using a single specimen.

To design structural systems for low-damage and reduced inertia forces, Zhang et al. (2018c) conducted shake table testing using the LHPOST on a half-scale four-story building equipped with different types of energy dissipation devices and rocking structural walls. The wall acting in the E-W direction was significantly offset from the floor center of mass to purposely create a strong coupled lateral-torsional response and subject the specimen to complex kinematics. Multi-directional input motion capability would have greatly simplified the specimen design in this research program and facilitated the acquisition of more complete information on the seismic response behavior of this innovative building archetype. Furthermore, these tests would have benefitted from the use of high-resolution piezometric strain gages recorded by the new DAQ system of the LHPOST6 to obtain principal strains in the footings of the bridge piers and rocking walls which experienced large impacts and remained within their quasi-linear range of behavior.

The LHPOST6 will make possible realistic seismic testing of prototype structures equipped with various types of earthquake protective systems at scales which are large enough so that the experimental findings are meaningful for full-scale implementation. For example, testing of a base-isolated structure on the LHPOST6 would account for the variation in axial load on isolation bearings due to multiple components of earthquake ground motion at the base of the structure. Benchmark shake table tests on full-scale rocking structures are needed because the response of such structures depends crucially on their size (e.g., Agalianos et al., 2017). The data from such tests is needed to verify and validate numerical models of rocking structures.

A wide range of promising and/or innovative passive and semi-active seismic response modification devices (SRMDs) must be tested in large- or full-scale structural systems for their ultimate validation and acceptance in real-world structural seismic design. Passive SRMDs include (Housner et al., 1997) metallic yield dampers, friction dampers, viscoelastic dampers (e.g., viscoelastic walls), viscous fluid dampers, tuned mass dampers, tuned liquid dampers, lead extrusion dampers (Parulekar et al., 2004; Soydan et al., 2012), carbon fiber reinforced isolators (Angeli et al., 2013), and shape memory alloys (DesRoches and

Delemont, 2002; Ozbulut et al., 2011). A passive seismic response mitigation strategy based on extremely rapid nonlinear "scattering" of the seismic input energy from low-to high-frequency modes of a structure achieved through a system of strategically placed nonlinear vibration absorbers (termed nonlinear energy sinks) has been investigated numerically and experimentally (on a reduced-scale idealized structural model) shows promising results for practical implementation in civil infrastructure (Luo et al., 2014; Wierschem et al., 2017). Semi-active SRMDs include (Housner et al., 1997) variable-orifice fluid dampers, controllable friction devices, variable stiffness devices, semi-active impact dampers, adjustable tuned liquid dampers, controllable fluid dampers, magneto-rheological dampers (Cha et al., 2013; 2014), and electro-rheological dampers (Spencer et al., 1998).

The LHPOST6 facility will enable the performance validation of full-scale buildings protected with innovative low-cost seismic isolation technologies such as low-cost fiber-reinforced elastomeric isolators (Calabrese et al., 2019). It will also enable the evaluation of the earthquake performance of low-damage rocking-isolated structures, including bridge pier systems (Piras et al., 2022) and buildings with controlled-rocking lateral-force resisting frames subjected to multi-component earthquake base excitation (including rotational components) and validation of high-fidelity models of structural systems equipped with seismic isolation and other structural control devices (e.g., whole-building models). Base isolation for residential construction using geosynthetics or compressible fills like tire derived aggregates is another topic that has been studied with centrifuge modeling and small-scale shake table testing (Yegian and Kadakal, 2004; Tsang, 2008; Hernández et al., 2020; Yarahuaman and McCartney, 2024), but not full-scale testing. Mitigation of seismic pressures on retaining walls using alternative lightweight backfills like EPS or tire derived aggregates that have high damping are topics of interest that have not been explored in full-scale applications (Tsang, 2008; Athanasopoulos-Zekkos et al., 2012).

Retrofit systems/strategies for non-code compliant structures

To promote public welfare and safety by reducing the risk of injury and loss of life that may result from the effects of earthquakes on existing buildings, a number of cities on the west coast (e.g., Los Angeles, San Francisco) have adopted or are in the process of adopting mandatory seismic retrofit ordinances for seismically vulnerable existing buildings that have known deficiencies such as limited ductility, soft story susceptibility, and lack of proper hierarchy of strength in the members and connections. The seismic retrofit strategies that will be used and implemented must be validated through large-scale shake table testing, which serves as the final verification of acceptable performance. The LHPOST6 is well suited to support verification tests of new, innovative retrofit strategies being required by the design community.

Through ATC 78 (Holmes et al., 2017), researchers have been developing a methodology to address the vulnerability of older (pre-1980) nonductile concrete buildings, which represent a significant threat to life safety (Moehle, 2000). By evaluating the likelihood of system collapse, rather than component failures, the approach focuses on assessing existing buildings to find the critical structures without being overly conservative. Other retrofit and repair techniques to improve the seismic performance for soft-story buildings using prestressed concrete jacketing and masonry block techniques have also been tested on shake tables (Bracci et al., 1995). However, there is still a need for research to support the practical and effective application of seismic retrofitting to existing buildings both in the physical implementation of retrofit techniques and methodologies for the numerical evaluation of the performance of retrofitted systems. Other examples of retrofit and repair techniques include: (1) the rehabilitation of reinforced concrete construction using fiber reinforced polymer composites (e.g., Silva and Kanitkar, 2018; Wu and Pantelides, 2019), (2) the use of shape memory alloy on the seismic performance of concrete bridges (Johnson et al., 2008), (3) the use of rocking steel braced frames for the retrofit of seismically deficient steel buildings (Tremblay et al., 2016; Mottier et al., 2018), and (4) the use of various seismic response modification devices such as base isolation, seismic dampers, etc.

Building structures

One of the largest and most diverse areas of research is in low-rise, mid-rise, or high-rise buildings made from a variety of materials such as structural steel, cold-formed steel, reinforced/prestressed/precast concrete, high-performance concrete, wood-frame, cross-laminated (heavy) timber, unreinforced and reinforced masonry, and advanced materials such as Ultra-High Performance Concrete and non-metallic reinforcements. Research topics also include the seismic performance of total building systems, those designed with super columns or outriggers, and special issues such as floor vibration isolation.

Unreinforced Masonry (URM) buildings have suffered severe damage or collapse in past earthquakes. The failures of URM buildings in seismic events have often been characterized by the out-of-plane collapse of the walls (Felice and Giannini, 2001). In addition to other factors, such as the wall aspect ratio and the material properties, the resistance of a URM wall to in-plane seismic forces depends heavily on the gravity load carried by the wall. The gravity load can enhance the shear strength of the bed joints and provide resistance to the overturning moment imposed on the wall. In addition, the resistance of an URM wall to out-of-plane forces relies on arching action, which could be weakened by damage caused by in-plane forces. As a result, bi-axial horizontal ground motions are particularly damaging to an URM building and URM walls subjected to uniaxial in-plane forces tend to exhibit significantly better performance compared with bi-axial loading conditions. Furthermore, the vertical ground acceleration could change the axial load on a wall and thus its in-plane and out-of-plane shear resistance, again affecting the arching mechanism and stability of the wall. The LHPOST6 will enable robust assessment of the seismic safety of URM buildings, development of effective retrofit methods, and improvement of design provisions.

Current seismic design standards for reinforced concrete and masonry wall systems, such as ACI 318-25 (ACI, 2025) and TMS-402-16 (TMS, 2016) are largely based on data obtained from

quasi-static testing of structural components, most of which were conducted with in-plane horizontal loading. While such data are crucial for the development of design and detailing requirements to ensure the ductile behavior of structural members, building performance in an earthquake is also highly dependent on how these components are proportioned, connected, and interact with each other as a system. Without due consideration of the system's behavior in design, the actual seismic response and load-resisting mechanism of a building could differ significantly from what is anticipated by design standards. The uniaxial LHPOST has enabled large-scale structural system tests that have provided the much-needed data to understand the behavior of structural systems as a whole and validate analytical models that can be used to support the development of improved design standards. An important example is the tests on two reinforced masonry wall systems, one system designed according to current codes and the other with a displacement-based method (Mavros et al., 2016; Stavridis et al., 2016). Owing to the strong coupling between the walls and the slabs, both structures exhibited shear-dominated wall behavior, although the code-conforming structure had been designed to avoid this behavior. Despite this, both structures performed satisfactorily under the maximum considered earthquake (MCE). In both cases, the wall systems exhibited a much higher resistance and ductility than what had been observed from shear-dominated walls tested individually under quasi-static loading. This study underscored the importance of considering system behavior in design and providing data to develop and calibrate refined computational models.

The performance of shear-wall systems under bi-axial horizontal seismic actions is not well understood. A planar wall with a rectangular cross-section is designed to carry in-plane seismic forces. However, under multi-axial ground motions, its vertical load-carrying capacity can be significantly jeopardized when it is subjected to a large out-of-plane drift (Tomassetti et al., 2016). Flanged walls are normally designed to resist seismic forces in both horizontal directions, but the bi-axial behavior of flanged walls is not as well studied as that of reinforced concrete columns. The bi-axial behavior of a flanged wall is complicated as in-plane shear cracking or toe crushing in a wall flange could affect the flexural resistance of the wall in the other loading direction. The performance of reinforced masonry archetype buildings under biaxial ground motions have been numerically studied with refined 3D nonlinear computational models that were calibrated with experimental data from uni-directional wall component and system tests (FEMA, 2020; Koutras and Shing, 2021). The numerical results have been used to calibrate simplified simulation models to assess the collapse probability of the building archetypes using the FEMA P695 procedure (FEMA, 2009). Figure 9 also shows the numerical results obtained with the nonlinear computational model of a two-story building. It can be observed that the performance of a building with flanged reinforced masonry walls under bi-axial horizontal ground motions can be significantly worse than that under a uniaxial ground motion. Multi-axial shake table tests are needed to validate such computational models and acquire a better understanding of the behavior of shear walls under earthquake actions. This information is invaluable for developing improved code provisions and assessment methods to enhance the safety and cost-efficiency of reinforced concrete and masonry buildings.

Structural concrete and precast systems have been a prevailing construction material for low, high-rise, and super-tall buildings. However, most research supporting seismic design with structural concrete has been limited to components (e.g., Kurama et al., 1999; Lehman et al., 2004; Naish et al., 2013; Tazarv and Saiid Saiidi, 2016) or reduced-scale models of building systems (e.g., Shahrooz and Moehle, 1987; Rodríguez et al., 1995). In the US, only three landmark building tests were performed at large- or full-scale on a shake table (Schoettler et al., 2009; Belleri et al., 2014; Chen et al., 2016; Zhang et al., 2018c) but under single-axis excitation. Therefore, research is needed on innovative, resilient, seismic-resistant concrete systems under multi-axial seismic base excitation, specifically to validate earthquake protective systems under more realistic conditions and improve modeling and analysis capabilities for component and system behavior. Of particular interest are the use of high strength (or ultra-high performance) materials (reinforcing bars and concrete) and advanced materials (e.g., fiber-reinforced concrete wrapping and non-metal reinforcement) for seismic civil applications, special concrete moment frames, and structural walls, including the combination of dual systems, precast concrete frame, and wall structures, and sustainable reinforced concrete structures utilizing recycled materials. The current building code in the US allows seismic applications of Grade 100 reinforcement only in Special Structural Walls. Insufficient test data was the leading cause for not allowing high-strength reinforcement in Special Moment Frames. Shake-table tests of Special Moment Frames and their interaction with Special Structural Walls (with and without coupling beams) are needed to support their introduction in the building code and to improve methods of analysis, linear and nonlinear, for the design office. There are also important research needs to better understand: (1) the influence of dynamic shear behavior on flexural deformation capacity in RC structural systems, (2) complex dynamic system interactions in the context of realistic multi-component earthquake base excitations to improve our current ability to model system behavior (Panagiotou et al., 2011), and (3) influence of diaphragm connections within the lateral load resisting system, especially if frames are considered.

Of great interest and somewhat neglected in research is the evaluation of the seismic performance of commercial tilt-up buildings. Many such buildings behaved poorly during the 1994 Northridge earthquake (Mitchell et al., 1995), which prompted the need to revisit various diaphragm-to-wall connection methods. Recent research indicates that some of these structures may still be vulnerable to earthquakes (Koliou et al., 2016; Henry and Ingham, 2011). To date, no shake table testing has been conducted on a partial or complete tilt-up structural system. The LHPOST6 will benefit the above research areas by providing the opportunity to conduct large-scale multi-axial shake table tests of complete buildings and structures of complex geometries.

Since the 1994 M6.7 Northridge earthquake, the precast concrete industry has been heavily involved in the research and development of new seismic systems and in developing design methods for building diaphragms (Priestley et al., 1999; Fleischman et al., 2013; Kurama et al., 2018). The speed and quality of construction, durability, and the lower carbon footprint of this industry, compared with the concrete or steel industries, make precast concrete an attractive structural solution for some

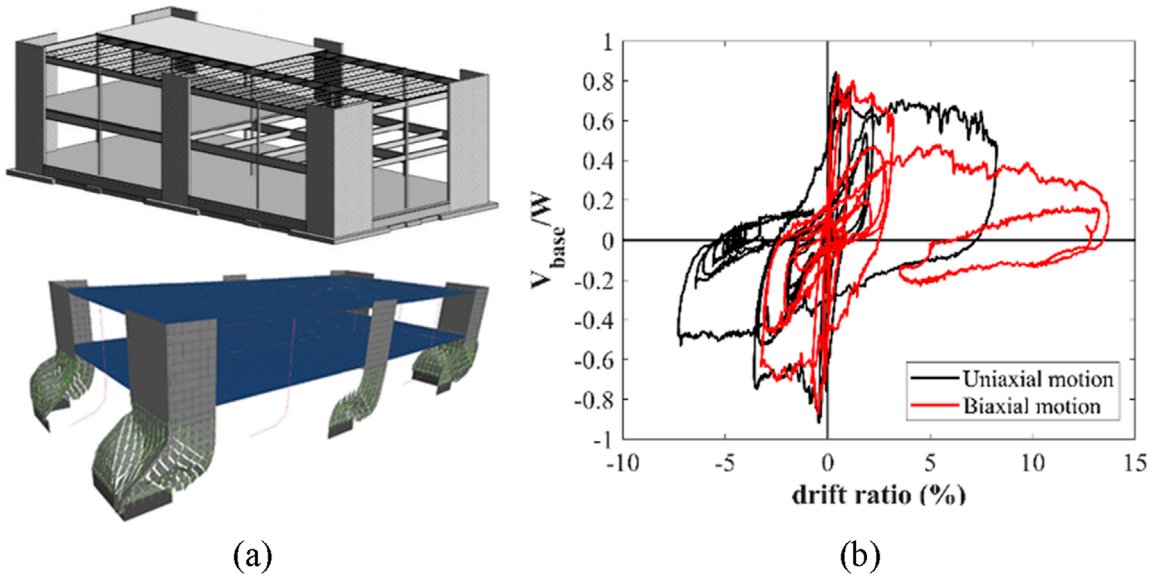

FIGURE 9
(a) FE model assessment of collapse potential of a reinforced masonry building under bi-axial ground motions; **(b)** Response of a two-story reinforced masonry building with flanged walls to uniaxial and biaxial motions (Koutras and Shing, 2021).

building archetypes in the industry. Buckling-restrained braces (BRBs), which originated in Japan as joint venture between the steel and precast concrete industry (Wakabayashi et al., 1973), are one of the most widely used bracing methods in the US for structural steel buildings. Precast frames incorporating reinforced concrete BRBs have significant advantages as these BRBs are precast at the plant and require no special site connections (Oh et al., 2021). Moreover, the precast BRBs can be repaired and replaced at the site should these elements be severely damaged during an earthquake. Research using the LHPOST6 on building systems with precast braced frames has the potential to impact the precast concrete industry.

There has been research on the seismic performance of hot-rolled structural steel and cold-formed steel systems in the areas of structural stability and progressive collapse mitigation, connection behavior, seismic risk, and life-cycle cost quantification (Stojadinović et al., 2000; Khandelwal et al., 2008). However, research is needed to assess interactions in building systems undergoing earthquakes to improve seismic design codes for steel building like AISC 341-16 (AISC, 2016). For example, by competing inelasticity in vertical and horizontal lateral-force resisting systems, overstrength, and system effects derived from the participation of gravity and non-structural framing in lateral response (e.g., Imanpour et al., 2016; Peterman et al., 2016; Cravero et al., 2020). An important area of research that will benefit significantly from the LHPOST6 is the development of innovative low damage seismic resistant steel structures, modeling, and analysis of floor diaphragms, chords, and seismic collectors (Agarwal et al., 2018). The ability to subject a large-scale test specimen of a building or a key portion of a building to a multi-component excitation will be particularly beneficial in the study of the above topics, given their complex and extended geometries and distributed boundary conditions and sensitivity to out-of-plane and vertical excitation. Other research needs are in progressive collapse mitigation, the seismic stability of multi-tiered braced frames under bi-directional shaking, and dynamic collapse evaluation for low-ductility braced frame systems. A critical component of successful large-scale shake table testing is the precise and reliable measurement, synchronization, and storage of numerous sensor channels at a sufficiently high sampling rate. Additionally, efficient data access and organization are essential for real-time visualization and rapid evaluation during a sequence of tests. This aspect helps make decisions on proceeding or pausing the test sequence. The LHPOST6 enables this key aspect of large-scale shake table testing.

An innovative technique for enhancing the seismic performance of steel brace frame and moment frame buildings involves strategically placing seismic fuses in steel frame structures by locally changing the mechanical properties (lowering strength while increasing ductility and toughness) of steel through local exposure to high temperatures followed by slow cooling. The technique lowers seismic force demands on critical elements (promoting economic use of materials), enhances ductility and energy dissipation, and mitigates brittle failures such as connection fractures (Morrison et al., 2015) (Figure 10). With its unique capabilities, the LHPOST6 will provide validation of the benefits this approach provides and will provide knowledge on construction and design methods for applying this technique in new buildings and for retrofit of seismically venerable steel structures.

Nonstructural components and systems (NCSs)

NCSs are generally categorized as elements (e.g., architectural, mechanical, electrical, plumbing, building contents) that facilitate the operation of a building. Importantly, they typically comprise 75%–85% of the construction cost of commercial buildings (Taghavi and Miranda, 2003; FEMA, 2012). NCSs have suffered significant damage, led to appreciable losses, and endangered occupants during

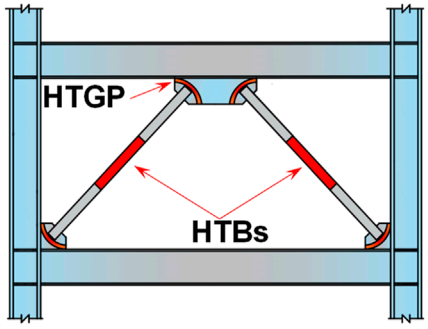

FIGURE 10
Schematic showing local heat-treated regions of brace (HTBs) and gusset plate (HTGPs) intended to enhance seismic performance.

past earthquakes (e.g., Taghavi and Miranda, 2003; FEMA, 2012; Ayres et al., 1973; Steinbrugge and Schader, 1973; Filiatrault et al., 2001; Meneses, 2010; Dhakal et al., 2016). Laudable efforts have been undertaken to develop simplified design procedures to account for the range of practical NCSs configurations (e.g., Asfura and Der Kiureghian, 1986; Burdisso and Singh, 1987a; 1987b; Villaverde, 1997; Bernal, 1999; Pozzi and Der Kiureghian, 2015). The wide range of types, varying mass distribution, and multiple connection locations in a structure have hampered the advancement of a reliable, unified design strategy. Thus, the shortcomings/limitations of modern codes are well-known (e.g., (Filiatrault and Sullivan, 2014; Lim et al., 2017)). The scarceness of full-scale building shake table tests that incorporate NCSs limits our understanding of the seismic response of these NCSs. For example, the landmark NSF-funded Building Nonstructural Components and Systems (BNCS) test program (Pantoli et al., 2016a) incorporated a complete suite of NCSs, including operable egress (stairs and elevators), facades (precast concrete and light-weight cold-formed steel), and interior equipment and architectural support contents (ceiling, HVAC, piping, etc.). This project focused on the "total building" and, in particular, the interactions between components (nonstructural-to-nonstructural and structural-to-nonstructural) and offered new insight into understanding the seismic response of a wide range of NCSs, but the tests were carried out under single-axis ground motions. This test program would have immensely benefited from the capability of the LHPOST6 (Hoehler et al., 2009; Chen et al., 2016; Pantoli et al., 2016a; 2016b). NCSs are by their nature secondary systems; their response depends upon the response of the supporting primary system, in most cases a building. The varying vibratory response of a building under multi-directional input motion will then naturally affect the input motion to the NCSs. Certain systems have been well documented to be particularly susceptible to certain components of ground motion. For example, due to their light weight and hung configurations, the presence of the vertical ground motion component has been shown to greatly affect the response of ceiling subsystems (e.g., Soroushian et al., 2012; Ryan et al., 2016; Wang et al., 2016). Similarly, systems with well delineated weak axes and abrupt bends (often a design feature of a NCS to accommodate necessary layout changes) are vulnerable to failure along these weaker axes (e.g., Ryan et al., 2016). Important to enveloping a building, the wide range of architectural facades have a high degree of variability in their connectivity to the supporting structure, and thus their response to multi-directional input requires understanding (Pantoli et al., 2016c). Limited recent tests (e.g., Pei et al., 2024a), supported by field observations, demonstrate the importance of advancing our understanding and predictive capabilities under multi-directional seismic loading of NCSs in building systems. Full-scale multi-axial shake table tests are needed to advance the development of a reliable, unified design methodology for NCSs accounting for multi-directional earthquake excitation. In this case, full-scale is required due to the difficulty/impossibility to obtain NSCs at a reduced-scale.

Energy structures

There has been a strong emphasis on the need to develop new sources of energy while preventing or reversing the degradation of the environment (i.e., renewable energy sources). Engineering solutions for wind and solar power, nuclear fusion, electrical and hydrological energy are necessary, not only to find cost effective technical solutions for harvesting the energy, but also for designing the infrastructure to support it (National Research Council, 2011).

Research on wind turbine structures has mostly focused on the structural analysis, design and/or assessment of wind turbines primarily against traditional environmental loads rather than extreme natural hazards such as earthquakes, hurricanes and tsunamis. With numerous wind farms being built in seismic regions such as China, the United States, India, Southern Europe and East Asia, more research on the seismic performance of wind structures is needed (Fitzwater and Cornell, 2002; Saranyasoontorn and Manuel, 2006; Burton et al., 2011; Guanche et al., 2013; Katsanos et al., 2016). For this reason, research utilizing the LHPOST6 will provide critical data to improve analysis tools and the seismic design of wind turbines on the dynamic response of these tall and slender structural systems. SSI effects may be considered in scaled systems or using hybrid testing. Areas of research include investigating the performance of newer, larger wind turbines and the effects of multi-directional near-field earthquake base excitations (including rotational components) to develop advanced methodologies to perform multi-hazard risk assessment of wind turbines (Katsanos et al., 2016). A series of full-scale tests of a 22 m high wind turbine with rated power of 65 kW were conducted on the LHPOST (Prowell et al., 2009). The experimentally estimated natural frequencies and mode shapes closely matched those derived from the finite element model developed and calibrated for this specific wind turbine (Prowell et al., 2009).

The performance of Electric Power Supply Systems (EPSSs) is also critical to the seismic resilience of a society (Franchin and Cavalieri, 2015; Sun et al., 2015). The EPPS includes components such as electrical substations, large power transformers, transmission poles/lines. Sun et al. (2015) developed a framework for the probabilistic assessment of the seismic resilience of an EPSS and the community it serves. Research such as this requires accurate data obtained from seismic tests on the LHPOST6 investigating system and component performance. Other researchers (Bosworth et al., 2017) are investigating using computational dynamic analysis methods for the time histories

of electromagnetic reaction forces during short-circuit faults in High-Voltage substation structures.

Solar energy is a safe, clean, renewable energy resource which can replace current fossil fuels for generation of electricity. Many companies have developed solar power systems with structural frames. Testing of solar arrays subjected to wind and seismic forces is necessary to improve product development of solar array support structures and improve industry guidelines for appropriate structural design procedures and requirements for solar energy systems, considering gravity, wind, and seismic effects (Maffei et al., 2014).

The LHPOST6 will also provide a unique facility for the testing of nuclear structures, systems, and components (SSCs). Experimental seismic tests of nuclear SSCs have been performed for decades but often facing limitations on payload and/or multi-directional seismic input. These limitations result in the need for scaled models, or disregarding the vertical earthquake ground motion component, which are significant for rigid-short-period systems such as those in nuclear facilities. Furthermore, the seismic design and qualification of advanced reactors rely heavily on verified and validated numerical models that can capture the interaction between the reactor vessel, the contained fluid and the internal components (Yu et al., 2021). However, very few numerical models have been validated with experimental data. The LHPOST6 will provide critically needed experimental data for the seismic evaluation of next-generation nuclear SSCs and small modular reactors (SMRs), as well as systems and components used for nuclear waste storage and transportation; these data will assist in validating numerical models of these components and systems (Eidelpes et al., 2020; Zargar et al., 2017).

Another energy area requiring seismic testing and validation is hydroelectric dams. Research includes the selection of reasonable safety evaluation earthquakes for design, and the evaluation of structural adequacy of dams and foundations under earthquake loading (Léger, 2007; Hariri-Ardebili and Saouma, 2015). Needed areas of research are in SSI, design and analysis of foundations and abutments, material testing, and strengthening to assure foundation and abutment integrity. Furthermore, research is needed in the development of cost-effective geometry and structural detailing with minimum geometric irregularities and gradual variations in structural stiffness, and the validation of state-of-the-art numerical models of dams based on data obtained from large-scale dynamic testing. The LHPOST6 could be used to conduct scaled-up versions of the shake table experiments conducted on small scale models of concrete gravity dams at Polytechnique Montreal (Tinawi et al., 2000). Fluid-dam interaction could be accommodated on the LHPOST6 using the large soil box as a reservoir.

Bridges

The 1971 San Fernando and 1989 Loma Prieta Earthquakes were a turning point in the seismic design practice of bridges not only for California but for all seismic-prone regions in the United States. The Caltrans seismic retrofit program made large gains in designing retrofit strategies for existing bridge components with known vulnerabilities as well as developing new design strategies (Chai et al., 1991; Xiao et al., 1996; Haroun and Elsanadedy, 2005; Seible et al., 1997). In the 1990s, the feasibility of using advanced composite materials or fiber-reinforced polymers (FRPs) was investigated not only for the rehabilitation of existing structures in the form of seismic retrofit, service load strengthening, and damage repair measures but for new structural systems (Van Den Einde et al., 2003). The use of smart materials such as nitinol shape memory alloy devices for retrofitting bridges continues to be a hot topic (Johnson et al., 2008).

A great challenge in the seismic design of columns that are part of highway interchange systems which may involve complex geometries including curved bridge decks, skewness, etc., is to properly evaluate its response under the combined effects of vertical and bi-directional horizontal excitations. The capabilities of the LHPOST6 will open a new paradigm shift in properly evaluating the seismic response of slender columns and many other complex structures and validating the high-fidelity modeling of nonlinearly responding bridges (Babazadeh et al., 2016), including soil-structure-interaction and liquefaction effects in the case of soils vulnerable to liquefaction (Zhang et al., 2008; Elgamal et al., 2008).

Precast segmental construction methods can ease bridge construction costs by reducing construction time while maintaining quality control. Recent advances in new accelerated bridge construction (ABC) methodologies use precast methods for new bridges or replacing and rehabilitating existing bridges. ABC reduces traffic effects that are often impacted by onsite construction-related activities. While some applications of ABC construction exist in the U.S., regions with moderate to high seismicity require in-depth development, detailing, experimental investigation, and guidelines for suitable connections between the precast members (Mashal and Palermo, 2017; 2019). Shake table testing of prestressed and segmental bridge components and systems have been conducted (Vosooghi and Buckle, 2013; Saiidi and Kavianipour, 2018).

A variety of other bridge-related topics that will benefit from the LHPOST6 are: (1) 3D behavior of precast segmental bridge superstructures for accelerated bridge construction (Nikoukalam and Sideris, 2016), (2) bridges with hybrid sliding-rocking columns (Torres Matos and Rodríguez, 2014; Madhusudhanan and Sideris, 2018), (3) analytical models to predict the static and dynamic nonlinear response of such bridges (Li et al., 2017; Xie et al., 2019), (4) the use of smart materials in bridges (Johnson et al., 2008), (5) high-performance steel highway bridge systems, a field that is steadily growing and offers high strength, excellent fracture toughness, good weldability, and resistance to corrosion, which makes it well-suited for highway bridge applications (Abbas et al., 2015; Ma et al., 2019), and (6) multi-directional dynamic experimental evaluation of bridge superstructure-abutment-substructure interactions for configurations commonly employed in the Central United States.

Structural health monitoring

Condition assessment of structures plays a key role in supporting the decision-making process following natural or artificial hazard or aging events. These events, such as earthquakes, can potentially induce critical damage to civil structures, and subsequent decision-making related to emergency response, inspection, evacuation, and retrofit of structures is of vital importance. Damage initiation and progression cannot always be detected through visual screening

and, therefore, time-consuming, costly, and invasive post-event inspection and evaluation methods are required to detect certain types of damage. Potential impacts of earthquakes as well as other natural and man-made hazards on communities can be reduced through accurate and timely risk mitigation decisions after catastrophic events, which can be supported and facilitated using structural health monitoring (SHM), diagnosis, and prognosis methods to help assess the damage in, and residual strength of, civil structures. Several approaches for SHM of civil structures, and in particular for system identification (SID) and damage identification (DID), have been proposed and studied in the literature for post-earthquake assessment of structural safety. A number of model-free and linear/nonlinear model-based approaches have been proposed in the literature for system and damage identification of civil structures (Catbas and Kijewski-Correa, 2013). Finite element (FE) model updating has emerged as a powerful methodology for structural health monitoring and damage identification of civil structures (Friswell and Mottershead, 1995). Recent years have seen significant developments in the area of nonlinear FE model updating of civil structures by using advanced Bayesian (probabilistic) estimation methods to update a high-fidelity mechanics-based nonlinear FE model of the structure of interest, which can then be interrogated to detect, localize, classify, and assess the damage in the structure at different scales (global and local) (Song et al., 2013; Astroza et al., 2017; Astroza et al., 2019; Roohi et al., 2019).

The high-quality datasets collected from future landmark experiments performed on the LHPOST6 will be invaluable for evaluating vibration-based condition/damage assessment methodologies and resolving the remaining obstacles preventing reliable real-world implementation of such methodologies. Typically, each large- or full-scale specimen tested on the LHPOST6 is subjected to a series of earthquake ground motions of increasing intensity until the brink of collapse. The SHM field will benefit from such high-quality datasets and associated metadata. An algorithm of the wave method for structural health monitoring (SHM) was tested and calibrated using shake table test data of a full-scale, seven-story, reinforced-concrete building slice tested on the LHPOST (Panagiotou et al., 2011). The method is based on monitoring changes in the velocity of waves propagating vertically through the structure, identified by least-squares fit of beam models (Ebrahimian et al., 2017). Data measured on test structures can be used to develop automated system identification and post-earthquake assessment methodologies for instrumented structures subject to complex ground motion effects as structures in the real-world do not have sufficient instrumentation to fully characterize the 6-DOF ground motion effects.

Additive manufacturing (3D printing)

In several other engineering fields, automation has been steadily replacing traditional production methods, dramatically increasing speed, quality of construction, and innovation of design while concurrently reducing cost and waste in a transformative way. Rapid prototyping of 3-dimensional parts (i.e., 3D printing) with cementitious or metallic materials allows geometrically intricate but efficient designs which are today unfeasible to construct using traditional methods (Ma et al., 2018). Recently, this technology has proven its utility at large-scale supporting the construction of elements such as connection nodes in space frame metal structures or even entire buildings and bridges. This research area is still emerging, with most efforts focused on developing the methodologies for rapid and cost-effective 3D prototyping of concrete and metal buildings and bridges at larger scales (Buswell et al., 2007; Le et al., 2012; Lim et al., 2012; Gosselin et al., 2016; Zareiyan and Khoshnevis, 2017; Camacho et al., 2018). However, the mechanical properties of 3D printed materials and the performance of 3D printed structures have not been studied in detail under seismic loading. The use of the LHPOST6 becomes crucial to support the development of large-scale additive manufacturing technologies capable of efficiently producing multifunctional structural elements with enhanced performance (Keating et al., 2017) in both low and high seismicity areas. This development includes the need for standardized testing and quality control, investigating ways to print using multiple materials, and combining additive manufacturing with other processes which rely upon traditional materials or construction techniques.

Liquid storage tanks

Liquid storage tanks (LSTs) are critical structural system elements in the industry. These tanks are used in chemical processes, water, fuel, oil and gas storage and for fermentation of alcoholic beverages, among many uses. Poor seismic performance of LSTs was observed in recent earthquakes in Chile, New Zealand, Italy, and the 2014 South Napa earthquakes (Zareian et al., 2012; Fischer, 2014; Fischer et al., 2016; Brunesi et al., 2015; Yazdanian et al., 2020; Frezzati et al., 2023) and accounted for losses of the order of $7B. The LHPOTS6 is a unique facility where much needed research can be conducted to evaluate, develop high-fidelity models that include the fluid-structure and soil-fluid-structure interaction, and improve the seismic response of storage tanks, with smaller tanks tested at full-scale and large tanks tested at reduced scales, for example, in the range of 1:10 to 1:20.

Other structures

A multitude of topics that do not fit directly into the research areas described above or perhaps span across multiple areas are classified here as "other structures". These include wharves, ports and A-cranes (Roeder et al., 2005; Lemnitzer et al., 2010; Smith-Pardo and Ospina, 2013), water intake towers, airport control towers, deep foundations, and unique military applications such as testing the tailhook gear that fighter jets use to land on aircraft carriers, large-aircraft landing gear, embedded dynamometers and real-time hybrid testing of military hardware. The LPHOST6 will support research on the seismic behavior and design of waterfront structures under multi-directional loading which include earthen, landfill, and wharf structures including material ageing and corrosion

(Andisheh et al., 2016). Research on the LHPOST6 used in combination with a large soil box can complement centrifuge experiments to investigate the seismic performance of levees on different soil conditions (Cappa et al., 2014) to validate computational models. Sideris et al. (2008) conducted shake table tests of steel pallet type tall storage rack structures equipped with advanced base isolation and rocking seismic protection systems. Shake table tests must be performed on much larger rack structures subjected to 3D ground motions which can only be accommodated at the LHPOST6 facility. The tests will require extensive measurements, including horizontal and vertical displacement and acceleration responses at multiple locations, strain measurements at critical locations in beam, column, and bracing members, and relative rotations at the beam to column joints.

Conclusions

The LHPOST6 supports the advancement of innovative materials, manufacturing methods, detailing, earthquake protective systems, seismic retrofit methods, and construction methods, and is a driver towards improving the design codes and standards and developing transformative seismic-resistant concepts. This paper provides an overview of the role of shake table testing with six-degree-of-freedom input motions using the LHPOST6 to provide data and fragility information on structural and geotechnical systems, supporting the advancement of performance-based and resilient-based seismic design.

Author contributions

JM: Writing – original draft. LV: Writing – review and editing. MM: Writing – review and editing. AP: Writing – review and editing. KL: Writing – review and editing. C-TL: Writing – review and editing. JC: Writing – review and editing.

Funding

The author(s) declare that financial support was received for the research and/or publication of this article. The authors are grateful for funding from the US National Science Foundation from award 2227407.

Acknowledgments

The authors are grateful for the support provided by the National Science Foundation (NSF), with Joy Pauschke as Program Director, and by the University of California at San Diego.

Conflict of interest

The authors declare that the research was conducted in the absence of any commercial or financial relationships that could be construed as a potential conflict of interest.

Generative AI statement

The author(s) declare that no Generative AI was used in the creation of this manuscript.

Publisher's note

All claims expressed in this article are solely those of the authors and do not necessarily represent those of their affiliated organizations, or those of the publisher, the editors and the reviewers. Any product that may be evaluated in this article, or claim that may be made by its manufacturer, is not guaranteed or endorsed by the publisher.

References

Abbas, H. H., Kim, B. G., and Sause, R. (2015). "Unconventional high performance steel bridge girder systems," in *Advances in bridge maintenance, safety management, and life-cycle performance, set of book and CD-ROM* (London: CRC Press), 813–814.

ACI (2025). "Building code requirements for structural concrete and commentary,", 318-25. Farmington Hills, MI: ACI.

Agalianos, A., Psychari, A., Vassiliou, M. F., Stojadinovic, B., and Anastasopoulos, I. (2017). Comparative assessment of two rocking isolation techniques for a motorway overpass bridge. *Front. Built Environ.* 3, 47. doi:10.3389/fbuil.2017.00047

Agarwal, A., Lizarraga, D., Beedle, M., Li, C. H., Fleischman, R., Sause, R., et al. (2018). "Investigation of seismic performance of collectors in steel building structures," in *11th national conference on earthquake engineering 2018: integrating science, engineering, and policy, NCEE 2018, 2002-2011* (Oakland, CA: Earthquake Engineering Research Institute).

Ahn, I. S., and Cheng, L. (2014). Tire derived aggregate for retaining wall backfill under earthquake loading. *Constr. Build. Mater.* 57, 105–116. doi:10.1016/j.conbuildmat.2014.01.091

AISC (2016). *Seismic provisions for structural steel buildings (AISC 341-16) and commentary*. Chicago, IL: American Institute of Steel Construction.

Anajafi, H., Medina, R. A., and Santini-Bell, E. (2020). Effects of the improper modeling of viscous damping on the first-mode and higher-mode dominated responses of base-isolated buildings. *Earthq. Eng. and Struct. Dyn.* 49 (1), 51–73. doi:10.1002/eqe.3223

Anastasopoulos, I., Loli, M., Georgarakos, T., and Drosos, V. (2013). Shaking table testing of rocking—isolated bridge pier on sand. *J. Earthq. Eng.* 17 (1), 1–32. doi:10.1080/13632469.2012.705225

Andisheh, K., Scott, A., and Palermo, A. (2016). Seismic behavior of corroded RC bridges: review and research gaps. *Int. J. Corros.* 2016, 1–22. doi:10.1155/2016/3075184

Angeli, P., Russo, G., and Paschini, A. (2013). Carbon fiber-reinforced rectangular isolators with compressible elastomer: analytical solution for compression and bending. *Int. J. Solids Struct.* 50 (22-23), 3519–3527. doi:10.1016/j.ijsolstr.2013.06.016

Antonellis, G., Gavras, A. G., Panagiotou, M., Kutter, B. L., Guerrini, G., Sander, A. C., et al. (2015). Shake table test of large-scale bridge columns supported on rocking shallow foundations. *J. Geotechnical Geoenvironmental Eng.* 141 (5), 04015009. doi:10.1061/(asce)gt.1943-5606.0001284

ASCE (2017). Seismic evaluation and retrofit of existing buildings (ASCE 41-17). *Am. Soc. Civ. Eng.*

ASCE (2022). Minimum design loads and associated criteria for buildings and other structures (ASCE 7-22). *Am. Soc. Civ. Eng.*

Asfura, A., and Der Kiureghian, A. (1986). Floor response spectrum method for seismic analysis of multiply supported secondary systems. *Earthq. Eng. and Struct. Dyn.* 14 (2), 245–265. doi:10.1002/eqe.4290140206

Astroza, R., Alessandri, A., and Conte, J. P. (2019). A dual adaptive filtering approach for nonlinear finite element model updating accounting for modeling uncertainty. *Mech. Syst. Signal Process.* 115, 782–800. doi:10.1016/j.ymssp.2018.06.014

Astroza, R., Ebrahimian, H., Conte, J. P., Restrepo, J. I., and Hutchinson, T. C. (2016). System identification of a full-scale five-story reinforced concrete building tested on the NEES-UCSD shake table. *Struct. Control Health Monit.* 23 (3), 535–559. doi:10.1002/stc.1778

Astroza, R., Ebrahimian, H., Li, Y., and Conte, J. P. (2017). Bayesian nonlinear structural FE model and seismic input identification for damage assessment of civil structures. *Mech. Syst. Signal Process.* 93, 661–687. doi:10.1016/j.ymssp.2017.01.040

Athanasopoulos-Zekkos, A., Lamote, K., and Athanasopoulos, G. A. (2012). Use of EPS geofoam compressible inclusions for reducing the earthquake effects on yielding earth retaining structures. *Soil Dyn. Earthq. Eng.* 41, 59–71. doi:10.1016/j.soildyn.2012.05.004

Ayres, J. M., Sun, T. Y., and Brown, F. R. (1973). "Nonstructural damage to buildings," in *The great Alaska earthquake of 1964. Engineering division of earth sciences* (Washington, DC: National Research Council), 346–456.

Babazadeh, A., Burgueño, R., and Silva, P. F. (2016). Evaluation of the critical plastic region length in slender reinforced concrete bridge columns. *Eng. Struct.* 125, 280–293. doi:10.1016/j.engstruct.2016.07.021

Barbosa, A., Simpson, B., van de Lindt, J., Sinha, A., Field, T., McBain, M., et al. (2025). "Shake table testing program for mass timber and hybrid resilient structures datasets for the NHERI Converging Design project," in *Shake table testing program of 6-story mass timber and hybrid resilient structures (NHERI Converging Design Project)* (Austin, TX: DesignSafe-CI). doi:10.17603/ds2-rh8q-rn95

Basu, D., Whittaker, A. S., and Constantinou, M. C. (2015). Characterizing rotational components of earthquake ground motion using a surface distribution method and response of sample structures. *Eng. Struct.* 99, 685–707. doi:10.1016/j.engstruct.2015.05.029

Belleri, A., Schoettler, M. J., Restrepo, J. I., and Fleischman, R. B. (2014). Dynamic behavior of rocking and hybrid cantilever walls in precast concrete building. *ACI Struc. J.* 111 (3). doi:10.14359/51686778

Beresnev, I. A., Nightengale, A. M., and Silva, W. J. (2002). Properties of vertical ground motions. *Bull. Seismol. Soc. Am.* 92 (8), 3152–3164. doi:10.1785/0120020009

Bernal, D. (1994). Viscous damping in inelastic structural response. *J. Struct. Eng.* 120 (4), 1240–1254. doi:10.1061/(asce)0733-9445(1994)120:4(1240)

Bernal, D. (1999). A dynamic stiffness formulation for the analysis of secondary systems. *Earthq. Eng. and Struct. Dyn.* 28 (11), 1295–1308. doi:10.1002/(sici)1096-9845(199911)28:11<1295::aid-eqe867>3.0.co;2-2

Black, J. A. (2015). Centrifuge modelling with transparent soil and laser aided imaging. *Geotechnical Test. J.* 38 (5), 20140231–20140644. doi:10.1520/gtj20140231

Bońkowski, P. A., Zembaty, Z., and Minch, M. Y. (2018). Time history response analysis of a slender tower under translational-rocking seismic excitations. *Eng. Struct.* 155, 387–393. doi:10.1016/j.engstruct.2017.11.042

Bosworth, M., Steurer, M., Graber, L., Hodgson, I., Sause, R., Tahmasebi, E., et al. (2017). Modeling of reaction forces in high-voltage substation structures. *IEEE Trans. Power Deliv.* 33 (4), 1510–1517. doi:10.1109/tpwrd.2017.2754191

Bozorgnia, Y., Campbell, K. W., and Niazi, M. (2000). Observed spectral characteristics of vertical ground motion recorded during worldwide earthquakes from 1957 to 1995. *Proc. 12th World Conf. Earthq. Eng.* 2671 (4).

Bracci, J. M., Reinhorn, A. M., and Mander, J. B. (1995). Seismic retrofit of reinforced concrete buildings designed for gravity loads: performance of structural model. *Struct. J.* 92 (6), 711–723. doi:10.14359/9665

Bray, J. D., Markham, C. S., and Cubrinovski, M. (2017). Liquefaction assessments at shallow foundation building sites in the Central Business District of Christchurch, New Zealand. *Soil Dyn. Earthq. Eng.* 92, 153–164. doi:10.1016/j.soildyn.2016.09.049

Bray, J. D., and Olaya, F. R. (2022). "Examination of the volumetric strain potential of liquefied soil with a database of laboratory tests," in *Proc. Geo-congress 2022*. Reston, VA: ASCE, 495–505.

Brunesi, E., Nascimbene, R., Pagani, M., and Beilic, D. (2015). Seismic performance of storage steel tanks during the May 2012 Emilia, Italy, earthquakes. *J. Perform. Constr. Facil.* 29 (5), 04014137. doi:10.1061/(asce)cf.1943-5509.0000628

Burdisso, R. A., and Singh, M. P. (1987a). Multiply supported secondary systems part I: response spectrum analysis. *Earthq. Eng. and Struct. Dyn.* 15 (1), 53–72. doi:10.1002/eqe.4290150105

Burdisso, R. A., and Singh, M. P. (1987b). Seismic analysis of multiply supported secondary systems with dynamic interaction effects. *Earthq. Eng. and Struct. Dyn.* 15 (8), 1005–1022. doi:10.1002/eqe.4290150807

Burton, T., Jenkins, N., Sharpe, D., and Bossanyi, E. (2011). "Design loads for horizontal axis wind turbines," in *Wind energy handbook*. 2nd edn. Chichester, UK: John Wiley and Sons, Ltd.

Buswell, R. A., Soar, R. C., Gibb, A. G., and Thorpe, A. (2007). Freeform construction: mega-scale rapid manufacturing for construction. *Automation Constr.* 16 (2), 224–231. doi:10.1016/j.autcon.2006.05.002

Bycroft, G. N. (1980). Soil—foundation interaction and differential ground motions. *Earthq. Eng. and Struct. Dyn.* 8 (5), 397–404. doi:10.1002/eqe.4290080503

Calabrese, A., Losanno, D., Spizzuoco, M., Strano, S., and Terzo, M. (2019). Recycled Rubber Fiber Reinforced Bearings (RR-FRBs) as base isolators for residential buildings in developing countries: the demonstration building of Pasir Badak, Indonesia. *Eng. Struct.* 192, 126–144. doi:10.1016/j.engstruct.2019.04.076

Camacho, D. D., Clayton, P., O'Brien, W. J., Seepersad, C., Juenger, M., Ferron, R., et al. (2018). Applications of additive manufacturing in the construction industry–A forward-looking review. *Automation Constr.* 89, 110–119. doi:10.1016/j.autcon.2017.12.031

Cappa, R., Yniesta, S., Lemnitzer, A., Brandenberg, S. J., and Stewart, J. P. (2014). "Centrifuge experiments to evaluate the seismic performance of levees on peaty soils in the Sacramento-San Joaquin Delta," in *Paper presented at the dam safety conference*. San Diego, CA.

Carr, A. J. (1997). Damping Models for inelastic analyses. *Proc. Asia-Pacific Vib. Conf.* 1, 42–48. doi:10.1007/978-3-031-50631-4_33

Carr, A. J. (2005). "Damping models for time-history structural analyses," in *Proceedings of Asia pacific vibration conference* (Langkawi, Malaysia), 287–293.

Carr, A. J., Puthanpurayil, A. M., Lavan, O., and Dhakal, R. P. (2017). "Damping models for inelastic time history analysis: a proposed modelling approach," in *Proc. 16th world conference in earthquake engineering*. Santiago, 1488.

Castaldo, P., and De Iuliis, M. (2014). Effects of deep excavation on seismic vulnerability of existing reinforced concrete framed structures. *Soil Dyn. Earthq. Eng.* 64, 102–112. doi:10.1016/j.soildyn.2014.05.005

Castellani, A., Stupazzini, M., and Guidotti, R. (2012). Free-field rotations during earthquakes: relevance on buildings. *Earthq. Eng. and Struct. Dyn.* 41 (5), 875–891. doi:10.1002/eqe.1163

Catbas, F. N., and Kijewski-Correa, T. (2013). Structural identification of constructed systems: collective effort toward an integrated approach that reduces barriers to adoption. *J. Struct. Eng.* 139 (10), 1648–1652. doi:10.1061/(asce)st.1943-541x.0000682

Caughey, T. K. (1960). Classical normal modes in damped linear dynamic systems. *ASME J. Appl. Mech.* 27, 269–271. doi:10.1115/1.3643949

Caughey, T. K., and O'Kelly, M. E. (1965). Classical normal modes in damped linear dynamic systems. *ASME J. Appl. Mech.* 32 (3), 583–588. doi:10.1115/1.3643949

Celebi, M. (1996). Comparison of damping in buildings under low-amplitude and strong motions. *J. Wind Eng. Industrial Aerodynamics* 59 (2-3), 309–323. doi:10.1016/0167-6105(96)00014-1

Cha, Y. J., Agrawal, A. K., Friedman, A., Phillips, B., Ahn, R., Dong, B., et al. (2014). Performance validations of semiactive controllers on large-scale moment-resisting frame equipped with 200-kN MR damper using real-time hybrid simulations. *J. Struct. Eng.* 140 (10), 04014066. doi:10.1061/(asce)st.1943-541x.0000982

Cha, Y. J., Zhang, J., Agrawal, A. K., Dong, B., Friedman, A., Dyke, S. J., et al. (2013). Comparative studies of semiactive control strategies for MR dampers: pure simulation and real-time hybrid tests. *J. Struct. Eng.* 139 (7), 1237–1248. doi:10.1061/(asce)st.1943-541x.0000639

Chai, Y. H., Priestley, M. N., and Seible, F. (1991). Seismic retrofit of circular bridge columns for enhanced flexural performance. *Struct. J.* 88 (5), 572–584. doi:10.14359/2759

Chambreuil, C., Giry, C., Ragueneau, F., and Léger, P. (2022). Seismic energy dissipation in reinforced concrete beam: investigating damping formulations. *Eur. J. Environ. Civ. Eng.* 26 (15), 7771–7797. doi:10.1080/19648189.2021.2009380

Chang, B. J., Raychowdhury, P., Hutchinson, T. C., Thomas, J., Gajan, S., and Kutter, B. L. (2007). Evaluation of the seismic performance of combined frame-wall-foundation structural systems through centrifuge testing. *Proc. 4th Int. Conf. Earthq. Geotech. Eng.*

Charney, F. A. (2008). Unintended consequences of modeling damping in structures. *J. Struct. Eng.* 134 (4), 581–592. doi:10.1061/(asce)0733-9445(2008)134:4(581)

Chen, M. C., Pantoli, E., Wang, X., Astroza, R., Ebrahimian, H., Hutchinson, T. C., et al. (2016). Full-scale structural and nonstructural building system performance during earthquakes: Part I–specimen description, test protocol, and structural response. *Earthq. Spectra* 32 (2), 737–770. doi:10.1193/012414eqs016m

Chen, Y., Palermo, A., and Mashal, M. (2024). Finite-element validation of U-shaped flexural plates integrated into a novel brace dissipator. *J. Struct. Eng.* 150 (9). doi:10.1061/jsendh.steng-13167

Chopra, A. K., and McKenna, F. (2016a). Modeling viscous damping in nonlinear response history analysis of buildings for earthquake excitation. *Earthq. Eng. and Struct. Dyn.* 45 (2), 193–211. doi:10.1002/eqe.2622

Chopra, A. K., and McKenna, F. (2016b). Response to John Hall's Discussion (EQE-16-0008) to Chopra and McKenna's paper, 'Modeling viscous damping in nonlinear response history analysis of buildings for earthquake excitation. *Earthq. Eng. and Struct. Dyn.* 45 (13), 2235–2238. doi:10.1002/eqe.2762

Clayton, P. M., Winkley, T. B., Berman, J. W., and Lowes, L. N. (2012). Experimental investigation of self-centering steel plate shear walls. *J. Struc. Eng* 138 (7), 952–960. doi:10.1061/(asce)st.1943-541x.0000531

Cravero, J., Elkady, A., and Lignos, D. G. (2020). Experimental evaluation and numerical modeling of wide-flange steel columns subjected to constant and variable axial load coupled with lateral drift demands. *J. Struct. Eng.* 146 (3), 04019222. doi:10.1061/(asce)st.1943-541x.0002499

Cruz, C., and Miranda, E. (2017). Evaluation of soil-structure interaction effects on the damping ratios of buildings subjected to earthquakes. *Soil Dyn. Earthq. Eng.* 100, 183–195. doi:10.1016/j.soildyn.2017.05.034

Cubrinovski, M., Taylor, M., Henderson, D., Winkley, A., Haskell, J., Bradley, B., et al. (2014). "Key factors in the liquefaction-induced damage to buildings and infrastructure in Christchurch: preliminary findings," in *NZSEE conference*.

Davis, C. A. (2003). "Lateral seismic pressures for design of rigid underground lifeline structures," in *Proc., 6th U.S. Conf. On lifeline earthquake engineering*. Reston, VA: ASCE, 1001–1010.

Deierlein, G. G. (2011). "Earthquake engineering research needs in the planning, design, construction, and operation of buildings," in *Grand challenges in earthquake engineering research*. Washington, DC: The National Academies Press.

DeJong, J. T., Soga, K., Kavazanjian, E., Burns, S., Van Paassen, L. A., Al Qabany, A., et al. (2014). Biogeochemical processes and geotechnical applications: progress, opportunities and challenges. *Géotechnique* 63 (4), 287–301. doi:10.1680/geot.sip13.p.017

Deng, L., and Kutter, B. L. (2012). Characterization of rocking shallow foundations using centrifuge model tests. *Earthq. Eng. and Struct. Dyn.* 41 (5), 1043–1060. doi:10.1002/eqe.1181

DesRoches, R., and Delemont, M. (2002). Seismic retrofit of simply supported bridges using shape memory alloys. *Eng. Struct.* 24 (3), 325–332. doi:10.1016/s0141-0296(01)00098-0

Dhakal, R. P., Pourali, A., Tasligedik, A. S., Yeow, T., Baird, A., MacRae, G., et al. (2016). Seismic performance of non-structural components and contents in buildings: an overview of NZ research. *Earthq. Eng. Eng. Vib.* 15 (1), 1–17. doi:10.1007/s11803-016-0301-9

Durante, M. G., Stewart, J. P., Brandenberg, S. J., and Mylonakis, G. (2022). Simplified solution for seismic earth pressures exerted on flexible walls. *Earthq. Spectra*, 87552930221083326. doi:10.1177/87552930221083326

Ebeido, A., Elgamal, A., Tokimatsu, K., and Abe, A. (2019). Pile and pile-group response to liquefaction-induced lateral spreading in four large-scale shake-table experiments. *J. Geotechnical Geoenvironmental Eng.* 145 (10), 04019080. doi:10.1061/(asce)gt.1943-5606.0002142

Ebrahimian, M., Todorovska, M. I., and Falborski, T. (2017). Wave method for structural health monitoring: testing using full-scale shake table experiment data. *J. Struct. Eng.* 143 (4), 04016217. doi:10.1061/(asce)st.1943-541x.0001712

Eidelpes, E., Ibarra, L. F., and Medina, R. A. (2020). A probabilistic assessment of PWR SNF cladding pinching failure considering potential transportation accident conditions. *Nucl. Eng. Des.* 358, 110423. doi:10.1016/j.nucengdes.2019.110423

El-Emam, M. M., and Bathurst, R. J. (2004). Experimental design, instrumentation and interpretation of reinforced soil wall response using a shaking table. *Int. J. Phys. Model. Geotechnics* 4 (4), 13–32. doi:10.1680/ijpmg.2004.040402

Elgamal, A., and He, L. (2004). Vertical earthquake ground motion records: an overview. *J. Earthq. Eng.* 8 (05), 663–697. doi:10.1080/13632460409350505

Elgamal, A., Yan, L., Yang, Z., and Conte, J. P. (2008). Three-dimensional seismic response of Humboldt Bay bridge-foundation-ground system. *J. Struc. Eng.* 134 (7), 1165–1176. doi:10.1061/(asce)0733-9445(2008)134:7(1165)

Elsawy, M. K., El Naggar, M. H., Cerato, A., and Elgamal, A. (2019). Seismic performance of helical piles in dry sand from large-scale shaking table tests. *Géotechnique* 69, 1071–1085. doi:10.1680/jgeot.18.p.001

Falamarz-Sheikhabadi, M. R. (2014). Simplified relations for the application of rotational components to seismic design codes. *Eng. Struct.* 59, 141–152. doi:10.1016/j.engstruct.2013.10.035

Falamarz-Sheikhabadi, M. R., Zerva, A., and Ghafory-Ashtiany, M. (2016). Mean absolute input energy for in-plane vibrations of multiple-support structures subjected to non-stationary horizontal and rocking components. *Probabilistic Eng. Mech.* 45, 87–101. doi:10.1016/j.probengmech.2016.03.001

Falamarz-Sheikhabadi, M. R., Zerva, A., and Ghafory-Ashtiany, M. (2017). Revised seismic intensity parameters for middle-field horizontal and rocking strong ground motions. *J. Struct. Eng.* 143 (1), 04016155. doi:10.1061/(asce)st.1943-541x.0001646

Felice, G. D., and Giannini, R. (2001). Out-of-plane seismic resistance of masonry walls. *J. Earthq. Eng.* 5 (02), 253–271. doi:10.1080/13632460109350394

FEMA (2009). *Quantification of building seismic performance factors (FEMA P695)*. Washington, DC: Applied Technology Council for the Federal Emergency Management Agency.

FEMA (2012). *Reducing the risks of nonstructural earthquake damage: a practical guide*. Fourth Edition. Washington, DC: FEMA E-74), prepared by the Applied Technology Council for the Federal Emergency Management Agency.

FEMA (2020). Short-period building collapse performance and recommendations for improving seismic design. *FEMA P-2139-3* 3.

Filiatrault, A., and Sullivan, T. (2014). Performance-based seismic design of nonstructural building components: the next frontier of earthquake engineering. *Earthq. Eng. Eng. Vib.* 13 (1), 17–46. doi:10.1007/s11803-014-0238-9

Filiatrault, A., Uang, C. M., Folz, B., Christopoulos, C., and Gatto, K. (2001). *Reconnaissance report of the february 28, 2001 nisqually (Seattle-Olympia) earthquake*. San Diego, La Jolla, CA: University of California.

Fischer, E. (2014). *Learning from earthquakes: 2014 Napa valley earthquake reconnaissance report*. West Lafayette, IN: Lyle School of Civil Engineering, Purdue University e-Pubs. Available online at: https://docs.lib.purdue.edu/cgi/viewcontent.cgi?article=1000&context=civlgradreports.

Fischer, E. C., Liu, J., and Varma, A. H. (2016). Investigation of cylindrical steel tank damage at wineries during earthquakes: lessons learned and mitigation opportunities. *Pract. Periodical Struct. Des. Constr.* 21 (3), 04016004. doi:10.1061/(asce)sc.1943-5576.0000283

Fitzwater, L. M., and Cornell, C. A. (2002). Predicting the long term distribution of extreme loads from limited duration data: comparing full integration and approximate methods. *J. Sol. Energy Eng.* 124 (4), 378–386. doi:10.1115/1.1509768

Fleischman, R. B., Restrepo, J. I., Naito, C. J., Sause, R., Zhang, D., and Schoettler, M. (2013). Integrated analytical and experimental research to develop a new seismic design methodology for precast concrete diaphragms. *J. Struct. Eng.* 139 (7), 1192–1204. doi:10.1061/(asce)st.1943-541x.0000734

Fox, P. J., Sander, A. C., Elgamal, A., Greco, P., Isaacs, D., Stone, M., et al. (2015). Large soil confinement box for seismic performance testing of geo-structures. *Geotechnical Test. J.* 38 (1), 20140034–20140084. doi:10.1520/gtj20140034

Franchin, P., and Cavalieri, F. (2015). Probabilistic assessment of civil infrastructure resilience to earthquakes. *Computer-Aided Civ. Infrastructure Eng.* 30 (7), 583–600. doi:10.1111/mice.12092

Frezzati, M., Loporcaro, G., Buratti, N., Palermo, A., and Walker, A. (2023). Design code review on seismic demand and base detailing criteria: an application to wine tanks in Marlborough. *Front. Built Environ.* 9. doi:10.3389/fbuil.2023.1167237

Friswell, M., and Mottershead, J. E. (1995). "Finite element model updating in structural dynamics,", 38. Springer Science and Business Media.

Ganey, R., Berman, J., Akbas, T., Loftus, S., Daniel Dolan, J., Sause, R., et al. (2017). Experimental investigation of self-centering cross-laminated timber walls. *J. Struct. Eng.* 143 (10), 04017135. doi:10.1061/(asce)st.1943-541x.0001877

Gavras, A. G., Kutter, B. L., Hakhamaneshi, M., Gajan, S., Tsatsis, A., Sharma, K., et al. (2020). Database of rocking shallow foundation performance: dynamic shaking. *Earthq. Spectra* 36 (2), 960–982. doi:10.1177/8755293019891727

Gelagoti, F., Kourkoulis, R., Anastasopoulos, I., and Gazetas, G. (2012). Rocking isolation of low-rise frame structures founded on isolated footings. *Earthq. Eng. and Struct. Dyn.* 41 (7), 1177–1197. doi:10.1002/eqe.1182

Ghafory-Ashtiany, M., and Singh, M. P. (1986). Structural response for six correlated earthquake components. *Earthq. Eng. and Struct. Dyn.* 14 (1), 103–119. doi:10.1002/eqe.4290140108

Ghayoomi, M., Dashti, S., and McCartney, J. S. (2013b). Performance of a transparent Flexible Shear Beam container for geotechnical centrifuge modeling of dynamic problems. *Soil Dyn. Earthq. Eng.* 53, 230–239. doi:10.1016/j.soildyn.2013.07.007

Ghayoomi, M., and McCartney, J. S. (2011b). Measurement of small-strain shear moduli of partially saturated sand during infiltration in a geotechnical centrifuge. *Geotechnical Test. J.* 34 (5), 503–513. doi:10.1520/gtj103608

Ghayoomi, M., McCartney, J. S., and Ko, H.-Y. (2011a). Centrifuge test to assess the seismic compression of partially saturated sand layers. *Geotechnical Test. J.* 34 (4), 321–331. doi:10.1520/gtj103355

Ghayoomi, M., McCartney, J. S., and Ko, H. Y. (2013a). Empirical methodology to estimate seismically induced settlement of partially saturated sand. *J. Geotechnical Geoenvironmental Eng.* 139 (3), 367–376. doi:10.1061/(asce)gt.1943-5606.0000774

Gosselin, C., Duballet, R., Roux, P., Gaudillière, N., Dirrenberger, J., and Morel, P. (2016). Large-scale 3D printing of ultra-high performance concrete - a new processing route for architects and builders. *Mater. and Des.* 100, 102–109. doi:10.1016/j.matdes.2016.03.097

Granello, G., Palermo, A., Pampanin, S., Pei, S., and van de Lindt, J. (2020). Pres-lam buildings: state-of-the-art. *J. Struct. Eng.* 146 (6). doi:10.1061/(asce)st.1943-541x.0002603

Guanche, Y., Guanche, R., Camus, P., Mendez, F. J., and Medina, R. (2013). A multivariate approach to estimate design loads for offshore wind turbines. *Wind Energy* 16, 1091–1106. doi:10.1002/we.1542

Guidotti, R. (2012). "Near-field earthquake ground motion rotations and relevance on civil engineering structures," in *Ph.D. Thesis, Politecnico di Milano, School of Structural, Seismic and Geotechnical Engineering, XXIV Cycle*.

Guidotti, R., Castellani, A., and Stupazzini, M. (2018). Near-field earthquake strong ground motion rotations and their relevance on tall buildings. *Bull. Seismol. Soc. Am.* 108 (3A), 1171–1184. doi:10.1785/0120170140

Hall, J. F. (1998). Seismic response of steel frame buildings to near-source ground motions. *Earthq. Eng. and Struct. Dyn.* 27 (12), 1445–1464. doi:10.1002/(sici)1096-9845(199812)27:12<1445::aid-eqe794>3.0.co;2-c

Hall, J. F. (2006). Problems encountered from the use (or misuse) of Rayleigh damping. *Earthq. Eng. and Struct. Dyn.* 35 (5), 525–545. doi:10.1002/eqe.541

Hall, J. F. (2016a). Discussion of 'Modelling viscous damping in nonlinear response history analysis of buildings for earthquake excitation' by Anil K. Chopra and Frank McKenna. *Earthq. Eng. and Struct. Dyn.* 45 (13), 2229–2233. doi:10.1002/eqe.2761

Hall, J. F. (2017). Discussion on 'an investigation into the effects of damping and nonlinear geometry models in earthquake analysis' by Andrew Hardyniec and Finley Charney. *Earthq. Eng. and Struct. Dyn.* 46 (2), 341–342. doi:10.1002/eqe.2786

Hardyniec, A., and Charney, F. (2015). An investigation into the effects of damping and nonlinear geometry models in earthquake engineering analysis. *Earthq. Eng. and Struct. Dyn.* 44 (15), 2695–2715. doi:10.1002/eqe.2604

Hariri-Ardebili, M. A., and Saouma, V. (2015). Quantitative failure metric for gravity dams. *Earthq. Eng. and Struct. Dyn.* 44 (3), 461–480. doi:10.1002/eqe.2481

Haroun, M. A., and Elsanadedy, H. M. (2005). Fiber-reinforced plastic jackets for ductility enhancement of reinforced concrete bridge columns with poor lap-splice detailing. *J. Bridge Eng.* 10 (6), 749–757. doi:10.1061/(asce)1084-0702(2005)10:6(749)

Hart, G. C., DiJulio Jr, R. M., and Lew, M. (1975). Torsional response of high-rise buildings. *J. Struct. Div.* 101 (2), 397–416. doi:10.1061/jsdeag.0003999

Hashash, Y. M., Phillips, C., and Groholski, D. R. (2010). "Recent advances in non-linear site response analysis," in *5th international conference on recent advances in geotechnical earthquake engineering and soil dynamics*.

Henry, R., and Ingham, J. (2011). Behaviour of tilt-up precast concrete buildings during the 2010/2011 Christchurch earthquakes. *Struct. Concr.* 12 (4), 234–240. doi:10.1002/suco.201100035

Hernández, E., Palermo, A., Granello, G., Chiaro, G., and Banasiak, L. J. (2020). Eco-rubber seismic-isolation foundation systems: a sustainable solution for the New Zealand context. *Struct. Eng. Int.* 30 (2), 180–190. doi:10.1080/10168664.2019.1702487

Hoehler, M. S., Panagiotou, M., Restrepo, J. I., Silva, J. F., Floriani, L., Bourgund, U., et al. (2009). Performance of suspended pipes and their anchorages during shake table testing of a seven-story building. *Earthq. Spectra* 25 (1), 71–91. doi:10.1193/1.3046286

Holmes, W. T., Liel, A. B., Mehrain, M., Moehle, J. P., and Somers, P. (2017). *Seismic evaluation of older concrete frame, frame-wall, and bearing wall buildings for collapse potential*. Redwood City: Retrieved from.

Housner, G., Bergman, L. A., Caughey, T. K., Chassiakos, A. G., Claus, R. O., Masri, S. F., et al. (1997). Structural control: past, present, and future. *J. Eng. Mech.* 123 (9), 897–971. doi:10.1061/(asce)0733-9399(1997)123:9(897)

Housner, G. W. (1963). The behavior of inverted pendulum structures during earthquakes. *Bull. Seismol. Soc. Am.* 53 (2), 403–417. doi:10.1785/bssa0530020403

Hubler, J. F., Athanasopoulos-Zekkos, A., and Zekkos, D. (2017). Monotonic, cyclic, and postcyclic simple shear response of three uniform gravels in constant volume conditions. *J. Geotechnical Geoenvironmental Eng.* 143 (9), 04017043. doi:10.1061/(asce)gt.1943-5606.0001723

Hushmand, A., Dashti, S., Davis, C., Hushmand, B., McCartney, J. S., Hu, J., et al. (2016b). Seismic performance of underground reservoir structures: insight from centrifuge modeling on the influence of backfill soil type and geometry. *J. Geotechnical Geoenvironmental Eng.* 142 (11), 04016058. doi:10.1061/(asce)gt.1943-5606.0001544

Hushmand, A., Dashti, S., Davis, C., McCartney, J. S., and Hushmand, B. (2016a). A centrifuge study of the influence of site response, relative stiffness, and kinematic constraints on the seismic performance of buried reservoir structures. *Soil Dyn. Earthq. Eng.* 88, 427–438. doi:10.1016/j.soildyn.2016.06.011

Hutchinson, T., Pantelides, C., Morano, M., Liu, J., and Diedrich, E. (2024). "Modular testbed building shakedown test program," in *NHERI UC San Diego LHPOST6 modular testbed building (MTB2)* (Austin, TX: DesignSafe-CI). doi:10.17603/ds2-ksqr-nd08

Iai, S. (1989). Similitude for shaking table tests on soil-structure-fluid model in 1g gravitational field. *Soils Found.* 29 (1), 105–118. doi:10.3208/sandf1972.29.105

Imanpour, A., Tremblay, R., Davaran, A., Stoakes, C., and Fahnestock, L. A. (2016). Seismic performance assessment of multitiered steel concentrically braced frames designed in accordance with the 2010 AISC seismic provisions. *J. Struct. Eng.* 142 (12), 04016135. doi:10.1061/(asce)st.1943-541x.0001561

Ishihara, K., and Nagase, H. (1988). Multi-directional irregular loading tests on sand. *Soil Dyn. Earthq. Eng.* 7 (4), 201–212. doi:10.1016/s0267-7261(88)80004-6

Jalali, R. S., and Trifunac, M. D. (2009). Response spectra for near-source, differential, and rotational strong ground motion. *Bull. Seismol. Soc. Am.* 99 (2B), 1404–1415. doi:10.1785/0120080067

Jehel, P., Léger, P., and Ibrahimbegovic, A. (2014). Initial versus tangent stiffness-based Rayleigh damping in inelastic time history seismic analyses. *Earthq. Eng. and Struct. Dyn.* 43 (3), 467–484. doi:10.1002/eqe.2357

Johnson, R., Padgett, J. E., Maragakis, M. E., DesRoches, R., and Saiidi, M. S. (2008). Large scale testing of nitinol shape memory alloy devices for retrofitting of bridges. *Smart Mater. Struct.* 17 (3), 035018. doi:10.1088/0964-1726/17/3/035018

Kalkan, E., and Graizer, V. (2007). Coupled tilt and translational ground motion response spectra. *J. Struct. Eng.* 133 (5), 609–619. doi:10.1061/(asce)0733-9445(2007)133:5(609)

Kammerer, A. M., Pestana, J. M., and Seed, R. B. (2002). "Undrained response of monterey 0/30 sand under multidirectional cyclic simple shear loading conditions," in *Geotechnical engineering report No UCB/GT/02-01*.

Katsanos, E. I., Thöns, S., and Georgakis, C. T. (2016). Wind turbines and seismic hazard: a state-of-the-art review. *Wind Energy* 19 (11), 2113–2133. doi:10.1002/we.1968

Keating, S. J., Leland, J. C., Cai, L., and Oxman, N. (2017). Toward site-specific and self-sufficient robotic fabrication on architectural scales. *Sci. Robotics* 2 (5), eaam8986. doi:10.1126/scirobotics.aam8986

Keykhosropour, L., Lemnitzer, A., Star, L., Marinucci, A., and Keowen, S. (2018). Implementation of soil pressure sensors in large-scale soil-structure interaction studies. *Geotechnical Test. J.* 41 (4), 20170163–20170746. doi:10.1520/gtj20170163

Khandelwal, K., El-Tawil, S., Kunnath, S. K., and Lew, H. S. (2008). Macromodel-based simulation of progressive collapse: steel frame structures. *J. Struct. Eng.* 134 (7), 1070–1078. doi:10.1061/(asce)0733-9445(2008)134:7(1070)

Kim, K., and Elgamal, A. (2017a). "Cut-and-Cover tunnel shake table test program," in *Technical report to the California department of transportation, report No. SSRP-17-09, dept. Of structural engineering*. San Diego, CA: Univ. of California.

Kim, K., and Elgamal, A. (2017b). *Spillway retaining wall shake table test program: soil-structure interaction*. San Diego, CA: Technical Report to the U.S. Bureau of Reclamation, Dept. of Structural Engineering, Univ. of California.

Kim, K., Giacalone, C., Elgamal, A., and Shing, P. B. (2016). Racking response of reinforced concrete cut and cover tunnel (No. CA15-2420; UCSD/SSRP-15-03). *Calif. Dept. Transp.*

Ko, H.-Y. (1988). "Summary of the state-of-the-art in centrifuge model testing," in *Centrifuges in soil mechanics* (London: CRC Press), 11–18.

Koliou, M., Filiatrault, A., Kelly, D. J., and Lawson, J. (2016). Buildings with rigid walls and flexible roof diaphragms. I: evaluation of current US seismic provisions. *J. Struct. Eng.* 142 (3), 04015166. doi:10.1061/(asce)st.1943-541x.0001438

Koutras, A., and Shing, P. B. (2021). Finite element modeling of the seismic response of reinforced masonry wall structures. *Earthq. Eng. Struct. Dyn.* 50, 1125–1146. doi:10.1002/eqe.3388

Kramer, A., Barbosa, A. R., and Sinha, A. (2016). Performance of steel energy dissipators connected to cross-laminated timber wall panels subjected to tension and cyclic loading. *J. Struct. Eng.* 142 (4), E4015013. doi:10.1061/(asce)st.1943-541x.0001410

Kurama, Y., Pessiki, S., Sause, R., and Lu, L. W. (1999). Seismic behavior and design of unbonded post-tensioned precast concrete walls. *PCI J.* 44 (3), 72–89. doi:10.15554/pcij.05011999.72.89

Kurama, Y. C., Sritharan, S., Fleischman, R. B., Restrepo, J. I., Henry, R. S., Cleland, N. M., et al. (2018). Seismic-resistant precast concrete structures: state of the art. *J. Struct. Eng.* 144 (4), 03118001. doi:10.1061/(asce)st.1943-541x.0001972

Lai, C.-T., and Conte, J. P. (2024). Dynamic model of the UC San Diego NHERI six-degree-of-freedom large high performance outdoor shake table. *Earthq. Eng. Struct. Dyn.* 53, 4511–4540. doi:10.1002/eqe.4224

Lanzi, A., and Luco, J. E. (2018). Elastic velocity damping model for inelastic structures. *J. Struct. Eng.* 144 (6), 04018065. doi:10.1061/(asce)st.1943-541x.0002050

Latha, G. M., and Santhanakumar, P. (2015). Seismic response of reduced-scale modular block and rigid faced reinforced walls through shaking table tests. *Geotext. Geomembranes* 43 (4), 307–316. doi:10.1016/j.geotexmem.2015.04.008

Le, T. T., Austin, S. A., Lim, S., Buswell, R. A., Law, R., Gibb, A. G., et al. (2012). Hardened properties of high-performance printing concrete. *Cem. Concr. Res.* 42 (3), 558–566. doi:10.1016/j.cemconres.2011.12.003

Lee, V. W., and Trifunac, M. D. (1985). Torsional accelerograms. *Int. J. Soil Dyn. Earthq. Eng.* 4 (3), 132–139. doi:10.1016/0261-7277(85)90007-5

Lee, V. W., and Trifunac, M. D. (1987). Rocking strong earthquake accelerations. *Soil Dyn. Earthq. Eng.* 6 (2), 75–89. doi:10.1016/0267-7261(87)90017-0

Léger, P. (2007). "Reducing the earthquake induced damage and risk in monumental structures: Experience at École Polytechnique de Montréal for large concrete dams supported by Hydro-Québec and Alcan," in *Extreme man-made and natural hazards in dynamics of structures* (Dordrecht: Springer), 285–309.

Lehman, D., Moehle, J., Mahin, S., Calderone, A., and Henry, L. (2004). Experimental evaluation of the seismic performance of reinforced concrete bridge columns. *J. Struct. Eng.* 130 (6), 869–879. doi:10.1061/(asce)0733-9445(2004)130:6(869)

Lemnitzer, A., Khalili-Tehrani, P., Ahlberg, E. R., Rha, C., Taciroglu, E., Wallace, J. W., et al. (2010). Nonlinear efficiency of bored pile group under lateral loading. *J. geotechnical geoenvironmental Eng.* 136 (12), 1673–1685. doi:10.1061/(asce)gt.1943-5606.0000383

Li, J., Kim, K., and Elgamal, A. (2020). Three-dimensional seismic response of a large embedded structure and induced earth pressure. *J. Geotechnical Geoenvironmental Eng.* 146 (5), 04020025. doi:10.1061/(asce)gt.1943-5606.0002238

Li, S., Zhang, F., Wang, J. Q., Alam, M. S., and Zhang, J. (2017). Seismic responses of super-span cable-stayed bridges induced by ground motions in different sites relative to fault rupture considering soil-structure interaction. *Soil Dyn. Earthq. Eng.* 101, 295–310. doi:10.1016/j.soildyn.2017.07.016

Lim, E., Jiang, L., and Chouw, N. (2017). Dynamic response of a non-structural component with three supports in multi-directional earthquakes. *Eng. Struct.* 150, 143–152. doi:10.1016/j.engstruct.2017.07.028

Lim, S., Buswell, R. A., Le, T. T., Austin, S. A., Gibb, A. G., and Thorpe, T. (2012). Developments in construction-scale additive manufacturing processes. *Automation Constr.* 21, 262–268. doi:10.1016/j.autcon.2011.06.010

Ling, H. I., Leshchinsky, D., Mohri, Y., and Wang, J. P. (2012). Earthquake response of reinforced segmental retaining walls backfilled with substantial percentage of fines. *J. geotechnical geoenvironmental Eng.* 138 (8), 934–944. doi:10.1061/(asce)gt.1943-5606.0000669

Ling, H. I., Mohri, Y., Leshchinsky, D., Burke, C., Matsushima, K., and Liu, H. (2005). Large-scale shaking table tests on modular-block reinforced soil retaining walls. *J. Geotechnical Geoenvironmental Eng.* 131 (4), 465–476. doi:10.1061/(asce)1090-0241(2005)131:4(465)

Liu, W., Hutchinson, T. C., Kutter, B. L., Hakhamaneshi, M., Aschheim, M. A., and Kunnath, S. K. (2013). Demonstration of compatible yielding between soil-foundation and superstructure components. *J. Struct. Eng.* 139 (8), 1408–1420. doi:10.1061/(asce)st.1943-541x.0000637

Luco, J. E. (1981). "Seismic safety margin research program (phase I), project III-Soil-Structure interaction: linear soil-structure interaction," in *Appendix to soil structure interaction: the status of current analysis methods and research, seismic safety margins research program, NUREG/CR-1780, UCRL-53011*. Livermore, CA: Lawrence Livermore National Laboratory.

Luco, J. E. (2014). Effects of soil–structure interaction on seismic base isolation. *Soil Dyn. Earthq. Eng.* 66, 167–177. doi:10.1016/j.soildyn.2014.05.007

Luco, J. E., and Lanzi, A. (2017). Optimal Caughey series representation of classical damping matrices. *Soil Dyn. Earthq. Eng.* 92, 253–265. doi:10.1016/j.soildyn.2016.10.028

Luco, J. E., and Lanzi, A. (2019). Numerical artifacts associated with Rayleigh and modal damping models of inelastic structures with massless coordinates. *Earthq. Eng. and Struct. Dyn.* 48 (13), 1491–1507. doi:10.1002/eqe.3210

Luo, J., Wierschem, N. E., Hubbard, S. A., Fahnestock, L. A., Quinn, D. D., McFarland, D. M., et al. (2014). Large-scale experimental evaluation and numerical simulation of a system of nonlinear energy sinks for seismic mitigation. *Eng. Struct.* 77, 34–48. doi:10.1016/j.engstruct.2014.07.020

Ma, G., Wang, L., and Ju, Y. (2018). State-of-the-art of 3D printing technology of cementitious material—an emerging technique for construction. *Sci. China Technol. Sci.* 61 (4), 475–495. doi:10.1007/s11431-016-9077-7

Ma, H., Sause, R., and Dong, J. (2019). Design of horizontally curved steel bridge girders with tubular flanges. *J. Bridge Eng.* 24 (6), 04019040. doi:10.1061/(asce)be.1943-5592.0001403

Madhusudhanan, S., and Sideris, P. (2018). Capacity spectrum seismic design methodology for bridges with hybrid sliding-rocking columns. *J. Bridge Eng.* 23 (8), 04018052. doi:10.1061/(asce)be.1943-5592.0001248

Maffei, J., Fathali, S., Telleen, K., Ward, R., and Schellenberg, A. (2014). Seismic design of ballasted solar arrays on low-slope roofs. *J. Struct. Eng.* 140 (1), 04013020. doi:10.1061/(asce)st.1943-541x.0000865

Mashal, M., and Palermo, A. (2017). Experimental testing of emulative and post-tensioned earthquake damage resistant technologies for accelerated bridge construction. *Paper# 61, 16th World Conf. Earthq. Eng. 16WCEE 2017, Santiago, Chile, January 9 – 13*.

Mashal, M., and Palermo, A. (2019). Low-damage seismic design for accelerated bridge construction. *J. Bridge Eng.* 24 (7), 04019066. doi:10.1061/(asce)be.1943-5592.0001406

Mavros, M., Ahmadi, F., Shing, P. B., Klingner, R. E., McLean, D., and Stavridis, A. (2016). Shake-table tests of a full-scale two-story shear-dominated reinforced masonry wall structure. *J. Struct. Eng.* 142 (10), 04016078. doi:10.1061/(asce)st.1943-541x.0001528

McCartney, J. S., Ghaaowd, I., Fox, P. J., Sanders, M. J., Thielmann, S. S., and Sander, A. C. (2017). Shearing behavior of tire-derived aggregate with large particle size. II: cyclic simple shear. *J. Geotechnical Geoenvironmental Eng.* 143 (10), 04017079. doi:10.1061/(asce)gt.1943-5606.0001781

Meneses, J. (2010). in *The el mayor cucapah, baja California earthquake April 4, 2010. An EERI learning from earthquakes reconnaissance report, EERI* (Oakland, CA), 114.

Meza Fajardo, K. C., and Papageorgiou, A. S. (2018). Response of tall buildings to base rocking induced by Rayleigh waves. *Earthq. Eng. and Struct. Dyn.* 47 (8), 1755–1773. doi:10.1002/eqe.3040

Mitchell, D., DeVall, R. H., Saatcioglu, M., Simpson, R., Tinawi, R., and Tremblay, R. (1995). Damage to concrete structures due to the 1994 Northridge earthquake. *Can. J. Civ. Eng.* 22 (2), 361–377. doi:10.1139/l95-047

Moaveni, B., He, X., Conte, J. P., and Restrepo, J. I. (2010). Damage identification study of a seven-story full-scale building slice tested on the UCSD-NEES shake table. *Struct. Saf.* 32 (5), 347–356. doi:10.1016/j.strusafe.2010.03.006

Moehle, J. P. (2000). "State of research on seismic retrofit of concrete building structures in the US," in *Proceedings of US-Japan symposium on seismic rehabilitation of concrete structures-state of research and practice*.

Moghadam, S. R., and Konstantinidis, D. (2017). Finite element study of the effect of support rotation on the horizontal behavior of elastomeric bearings. *Compos. Struct.* 163, 474–490. doi:10.1016/j.compstruct.2016.12.013

Morano, M., Hutchinson, T. C., Pantelides, C. P., Liu, J., and Williamson, E. (2024a). "Shake table testing of a full-scale three-story seismically resilient steel-framed building with reconfigurable lateral force resisting systems (modular testbed building: MTB2)," in *La jolla, CA: department of structural engineering*. San Diego: University of California.

Morano, M., Lin, L., Hutchinson, T., Liu, J., Williamson, E., and Pantelides, C. P. (2024b). Modal characterization of a three-story buckling-restrained braced frame steel building by nondestructive field testing. *Earthq. Eng. and Struct. Dyn.* 53, 1705–1726. doi:10.1002/eqe.4077

Morano, M., Liu, J., Williamson, E., Hutchinson, T. C., Pantelides, C., Saxey, B., et al. (2025). Shake table testing of a full-scale three-story seismically resilient steel-framed building with reconfigurable lateral force-resisting systems. *Earthq. Spectra*. doi:10.1177/87552930241301424

Morrison, M., Schweizer, D., and Hassan, T. (2015). An innovative seismic performance enhancement technique for steel building moment resisting connections. *J. Constr. Steel Res.* 109, 34–46. doi:10.1016/j.jcsr.2015.02.010

Mottier, P., Tremblay, R., and Rogers, C. (2018). Seismic retrofit of low-rise steel buildings in Canada using rocking steel braced frames. *Earthq. Eng. and Struct. Dyn.* 47 (2), 333–355. doi:10.1002/eqe.2953

Mylonakis, G., and Gazetas, G. (2000). Seismic soil-structure interaction: beneficial or detrimental? *J. Earthq. Eng.* 4 (3), 277–301. doi:10.1080/13632460009350372

Naish, D., Fry, A., Klemencic, R., and Wallace, J. (2013). Reinforced concrete coupling beams-Part I: testing. *ACI Struct. J.* 110 (6), 1057. doi:10.14359/51686160

Nakamura, T., Sekine, E., and Shirae, Y. (2011). Assessment of aseismic performance of ballasted track with large-scale shaking table tests. *Q. Rep. RTRI* 52 (3), 156–162. doi:10.2219/rtriqr.52.156

National Research Council (2011). *Grand challenges in earthquake engineering research: a community workshop report*. Washington, DC: National Academies Press.

NHERI (2025). NHERI converging design project website. Available online at: https://tallwoodinstitute.org/nheri-converging-design/(Accessed March 3, 2025)

Nikoukalam, M. T., and Sideris, P. (2016). Low-damage posttensioned segmental bridge columns with flexible end joints for seismic accelerated bridge construction. *Transp. Res. Rec.* 2592 (1), 151–161. doi:10.3141/2592-17

Oh, S., Kurama, Y. C., Mohle, J., and Saxey, B. W. (2021). Seismic design and analysis of precast concrete buckling-restrained braced frames. *PCI J.* 66 (5). doi:10.15554/pcij66.5-03

O'Rourke, T. D., Jezerski, J. M., Olson, N. A., Bonneau, A. L., Palmer, M. C., Stewart, H. E., et al. (2008). Geotechnics of pipeline system response to earthquakes. *Geotechnical Earthq. Eng. Soil Dyn.* IV, 1–38. doi:10.1061/40975(318)193

Otani, S. (1980). Nonlinear dynamic analysis of reinforced concrete building structures. *Can. J. Civ. Eng.* 7 (2), 333–344. doi:10.1139/l80-041

Ozbulut, O. E., Hurlebaus, S., and DesRoches, R. (2011). Seismic response control using shape memory alloys: a review. *J. Intelligent Material Syst. Struct.* 22 (14), 1531–1549. doi:10.1177/1045389x11411220

Panagiotou, M., Restrepo, J. I., and Conte, J. P. (2011). Shake-table test of a full-scale 7-story building slice. Phase I: rectangular wall. *J. Struct. Eng.* 137 (6), 691–704. doi:10.1061/(asce)st.1943-541x.0000332

Pantoli, E., Chen, M. C., Hutchinson, T. C., Astroza, R., Conte, J. P., Ebrahimian, H., et al. (2016b). Landmark data set from the building nonstructural components and systems (BNCS) project. *Earthq. Spectra* 32 (2), 1239–1259. doi:10.1193/100614eqs150

Pantoli, E., Chen, M. C., Wang, X., Astroza, R., Ebrahimian, H., Hutchinson, T. C., et al. (2016a). Full-scale structural and nonstructural building system performance during earthquakes: Part II–NCS damage states. *Earthq. Spectra* 32 (2), 771–794. doi:10.1193/012414eqs017m

Pantoli, E., Hutchinson, T. C., McMullin, K. M., Underwood, G. A., and Hildebrand, M. J. (2016c). Seismic-drift-compatible design of architectural precast concrete cladding: tieback connections and corner joints. *PCI J.* 61. doi:10.15554/pcij61.4-03

Paolucci, R., Shirato, M., and Yilmaz, M. T. (2008). Seismic behaviour of shallow foundations: shaking table experiments vs numerical modelling. *Earthq. Eng. and Struct. Dyn.* 37 (4), 577–595. doi:10.1002/eqe.773

Papagiannopoulos, G., and Beskos, D. (2012). Damping identification for building structures subjected to earthquakes: A. *J. Serbian Soc. Comput. Mech.* 6 (1), 129–147.

Parulekar, Y. M., Reddy, G. R., Vaze, K. K., and Kushwaha, H. S. (2004). Lead extrusion dampers for reducing seismic response of coolant channel assembly. *Nucl. Eng. Des.* 227 (2), 175–183. doi:10.1016/j.nucengdes.2003.09.006

Pecker, A., Paolucci, R., Chatzigogos, C., Correia, A. A., and Figini, R. (2014). The role of non-linear dynamic soil-foundation interaction on the seismic response of structures. *Bull. Earthq. Eng.* 12 (3), 1157–1176. doi:10.1007/s10518-013-9457-0

Pei, S., Ryan, K., Berman, J., van de Lindt, J., Pryor, S., Huang, D., et al. (2024b). Shake table test of a resilient full-scale ten-story mass timber building. *DesignSafe-CI*. doi:10.17603/ds2-sxq1-p731

Pei, S., Ryan, K. L., Berman, J. W., van de Lindt, J. W., Pryor, S., Huang, D., et al. (2024a). Shake-table testing of a full-scale 10-story resilient mass timber building. *J. Struct. Eng.* 150 (12), 04024183. doi:10.1061/jsendh.steng-13752

Pei, S., Van de Lindt, J., Barbosa, A., Berman, J. W., McDonnell, E., Dolan, J. D., et al. (2019). Experimental seismic response of a resilient 2-story mass timber building with post-tensioned rocking walls. *J. Struct. Eng.* 145 (11), 04019120. doi:10.1061/(asce)st.1943-541x.0002382

Pei, S., van de Lindt, J. W., Ricles, J., Sause, R., Berman, J., Ryan, K., et al. (2017). "Development and full-scale validation of resilience-based seismic design of tall wood buildings: the NEHRI Tallwood Project," in *Proceedings, 2017 NZSEE conference proceedings. Wellington, NZ: New Zealand society for earthquake engineering*, 1–8.

Pereira, M., and Koltuniuk, R. (2018). Finite element analysis for spillway retaining wall shake table testing program. *USBR Rep.*, 2018–2102.

Peterman, K. D., Stehman, M. J., Madsen, R. L., Buonopane, S. G., Nakata, N., and Schafer, B. W. (2016). Experimental seismic response of a full-scale cold-formed steel-framed building. I: system-level response. *J. Struct. Eng.* 142 (12), 04016127. doi:10.1061/(asce)st.1943-541x.0001577

Petrini, L., Maggi, C., Priestley, M. N., and Calvi, G. M. (2008). Experimental verification of viscous damping modeling for inelastic time history analyzes. *J. Earthq. Eng.* 12 (S1), 125–145. doi:10.1080/13632460801925822

Piras, S., Palermo, A., and Saidi, M. (2022). State-of-the-art of posttensioned rocking bridge substructure systems. *J. Bridge Eng.* 27 (3). doi:10.1061/(asce)be.1943-5592.0001833

Pozzi, M., and Der Kiureghian, A. (2015). Response spectrum analysis for floor acceleration. *Earthq. Eng. and Struct. Dyn.* 44 (12), 2111–2127. doi:10.1002/eqe.2583

Priestley, M. N., Sritharan, S., Conley, J. R., and Pampanin, S. (1999). Preliminary results and conclusions from the PRESSS five-story precast concrete test building. *PCI J.* 44 (6), 42–67. doi:10.15554/pcij.11011999.42.67

Prowell, I., Veletzos, M., Elgamal, A., and Restrepo, J. (2009). Experimental and numerical seismic response of a 65 kW wind turbine. *J. Earthq. Eng.* 13 (8), 1172–1190. doi:10.1080/13632460902898324

Pyke, R. M., Chan, C. K., and Seed, H. B. (1975). Settlement of sands under multidirectional shaking. *J. Geotechnical Eng. Div.* 101 (4), 379–398. doi:10.1061/ajgeb6.0000162

Rocha, M. (1957). The possibility of solving soil mechanics problems by the use of models. *Proc. 4th ICSMFE.* 1, 183–188.

Rodríguez, M. E., Restrepo, J. I., and Blandón, J. J. (2006). Shaking table tests of a four-story miniature steel building—model validation. *Earthq. Spectra* 22 (3), 755–780. doi:10.1193/1.2220575

Rodríguez, M. E., Santiago, S., and Meli, R. (1995). Seismic load tests on two-story waffle–flat-plate structure. *J. Struct. Eng.* 121 (9), 1287–1293. doi:10.1061/(asce)0733-9445(1995)121:9(1287)

Roeder, C. W., Graff, R., Soderstrom, J., and Yoo, J. H. (2005). Seismic performance of pile-wharf connections. *J. Struct. Eng.* 131 (3), 428–437. doi:10.1061/(asce)0733-9445(2005)131:3(428)

Roesset, J. M. (1981). Seismic safety margin research program (phase I), project III-Soil-Structure interaction: a review of soil-structure interaction. Appendix to soil structure interaction: the status of current analysis. *Methods Res. Seismic Saf. Margins Res. Program* 49.

Rong, W., and McCartney, J. S. (2020). Drained seismic compression of unsaturated sand. *J. Geotechnical Geoenvironmental Eng.* 146 (5), 04020029. doi:10.1061/(asce)gt.1943-5606.0002251

Rong, W., and McCartney, J. S. (2021). Undrained seismic compression of unsaturated sand. *J. Geotechnical Geoenvironmental Eng.* 147 (1), 04020145. doi:10.1061/(asce)gt.1943-5606.0002420

Roohi, M., Hernandez, E. M., and Rosowsky, D. (2019). Nonlinear seismic response reconstruction and performance assessment of instrumented wood-frame buildings—validation using NEESWood Capstone full-scale tests. *Struct. Control Health Monit.* 26 (9), e2373. doi:10.1002/stc.2373

Rosenblueth, E. (1976). Tall buildings under five-component earthquakes. *J. Struct. Div.* 102 (2), 455–459. doi:10.1061/jsdeag.0004289

Rutherford, C. J., and Biscontin, G. (2013). Development of a multidirectional simple shear testing device. *Geotechnical Test. J.* 36 (6), 858–866. doi:10.1520/gtj20120173

Ryan, K. L., and Polanco, J. (2008). Problems with Rayleigh damping in base-isolated buildings. *J. Struct. Eng.* 134 (11), 1780–1784. doi:10.1061/(asce)0733-9445(2008)134:11(1780)

Ryan, K. L., Soroushian, S., Maragakis, E. M., Sato, E., Sasaki, T., and Okazaki, T. (2016). Seismic simulation of an integrated ceiling-partition wall-piping system at E-Defense. I: three-dimensional structural response and base isolation. *J. Struct. Eng.* 142 (2), 04015130. doi:10.1061/(asce)st.1943-541x.0001384

Saiidi, M. S., and Kavianipour, F. (2018). "Shake table studies of seismic performance of a segmental bridge pier. Proceedings, special session SS08, new technologies for seismic-resistant bridge columns," in *16th European conference on earthquake engineering*.

Sander, A. C., Fox, P. J., Elgamal, A., Pradel, D. E., Isaacs, D., Stone, M., et al. (2013). Seismic testing program for large-scale MSE retaining walls at UCSD. *Proc. Geo-Congress*, 1188–1195. doi:10.1061/9780784412787.120

Saranyasoontorn, K., and Manuel, L. (2006). Design loads for wind turbines using the environmental contour method. *ASME J. Sol. Energy Eng.* 128, 554–561. doi:10.1115/1.2346700

Satake, N., Suda, K. I., Arakawa, T., Sasaki, A., and Tamura, Y. (2003). Damping evaluation using full-scale data of buildings in Japan. *J. Struct. Eng.* 129 (4), 470–477. doi:10.1061/(asce)0733-9445(2003)129:4(470)

Schoettler, M. J., Belleri, A., Dichuan, Z., Restrepo, J. I., and Fleischman, R. B. (2009). Preliminary results of the shake-table testing for the development of a diaphragm seismic design methodology. *PCI J.* 54 (1), 100–124. doi:10.15554/pcij.01012009.100.124

Seible, F., Priestley, M. N., Hegemier, G. A., and Innamorato, D. (1997). Seismic retrofit of RC columns with continuous carbon fiber jackets. *J. Compos. Constr.* 1 (2), 52–62. doi:10.1061/(asce)1090-0268(1997)1:2(52)

Shahbazi, M., Cerato, A. B., Allred, S., El Naggar, M. H., and Elgamal, A. (2020b). Damping characteristics of full-scale grouped helical piles in dense sands subjected to small and large shaking events. *Can. Geotechnical J.* 57 (6), 801–814. doi:10.1139/cgj-2018-0769

Shahbazi, M., Cerato, A. B., El Naggar, M. H., and Elgamal, A. (2020a). Evaluation of seismic soil–structure interaction of full-scale grouped helical piles in dense sand. *Int. J. Geomechanics* 20 (12), 04020228. doi:10.1061/(asce)gm.1943-5622.0001876

Shahrooz, B. M., and Moehle, J. P. (1987). "Experimental study of seismic response of RC setback buildings," in *Springfield, VA: earthquake engineering research center, college of engineering*. University of California.

Shing, P. S. B., and Mahin, S. A. (1987). Elimination of spurious higher-mode response in pseudodynamic tests. *Earthq. Eng. and Struct. Dyn.* 15 (4), 425–445. doi:10.1002/eqe.4290150403

Sideris, P., Filiatrault, A., Leclerc, M., and Tremblay, R. (2008). "Experimental performance evaluation of inclined shelving for steel pallet type storage racks," in *14th world conference on earthquake engineering* (Beijing, China).

Silva, P. (2019). Collaborative research: self-centering pendulum shear walls in buildings via nonlinear elastic kinematics. *NSF-CMMI 1762170*.

Silva, P., and Kanitkar, R. (2018). "ACI 440.2 R and the new seismic strengthening guidelines using FRP", 327. ACI, Farmington Hills, MI: Special Publication, 20–21.

Singh, A., Hutchinson, T. C., Torabian, S., Schafer, B. W., Peterman, K. D., Padgett, L., et al. (2022). "Structural design narrative of the CFS-NHERI 10-story test building for multi-dimensional shake table testing," in *Proceedings of the cold-formed steel research consortium colloquium 2022*. Baltimore, MD, USA.

Singh, A., Zhang, J., Rivera, D., Eladly, M., Jones, H., Kovac, A., et al. (2024). "CFS-NHERI 10-story building shake table test specimen: design updates," in *Proceedings of the 18th world conference on earthquake engineering (WCEE2024)*. Milan, Italy.

Smith-Pardo, J. P., and Ospina, C. E. (2013). "Special considerations for the seismic analysis and design of piers, wharves and container yards supported on prestressed concrete piles", 295. ACI, Farmington Hills, MI: Special Publication, 1–26.

Sogabe, M., Asanuma, K., Nakamura, T., Kataoka, H., Goto, K., and Tokunaga, M. (2013). Deformation behavior of ballasted track during earthquakes. *Q. Rep. RTRI* 54 (2), 104–111. doi:10.2219/rtriqr.54.104

Song, W., Dyke, S., and Harmon, T. (2013). Application of nonlinear model updating for a reinforced concrete shear wall. *J. Eng. Mech.* 139 (5), 635–649. doi:10.1061/(asce)em.1943-7889.0000519

Soroushian, S., Ryan, K. L., Maragakis, M., Wieser, J., Sasaki, T., Sato, E., et al. (2012). "NEES/E-Defense tests: seismic performance of ceiling/sprinkler piping nonstructural systems in base isolated and fixed base building," in *15th world conference on earthquake engineering (15WCEE)*.

Soydan, C., Gullu, A., Hepbostanci, O. E., Yuksel, E., and Irtem, E. (2012). "Design of a special lead extrusion damper," in *15th world conference on earthquake engineering*.

Spencer, B. F., Yang, G., Carlson, J. D., and Sain, M. K. (1998). Smart dampers for seismic protection of structures: a full-scale study. *Proc. second world Conf. Struct. control* 1, 417–426.

Stavridis, A., Ahmadi, F., Mavros, M., Shing, P. B., Klingner, R. E., and McLean, D. (2016). Shake-table tests of a full-scale three-story reinforced masonry shear wall structure. *J. Struct. Eng.* 142 (10), 04016074. doi:10.1061/(asce)st.1943-541x.0001527

Steinbrugge, K. V., and Schader, E. E. (1973). "Earthquake damage and related statistics in san Fernando, California, earthquake of february 9, 1971,", 1A. Washington DC: National Oceanic and Atmospheric Administration, 709–713.

Stewart, J. P., Smith, P. M., Whang, D. H., and Bray, J. D. (2004). Seismic compression of two compacted earth fills shaken by the 1994 Northridge earthquake. *J. geotechnical geoenvironmental Eng.* 130 (5), 461–476. doi:10.1061/(asce)1090-0241(2004)130:5(461)

Stojadinović, B., Goel, S. C., Lee, K. H., Margarian, A. G., and Choi, J. H. (2000). Parametric tests on unreinforced steel moment connections. *J. Struct. Eng.* 126 (1), 40–49. doi:10.1061/(asce)0733-9445(2000)126:1(40)

Sun, L., Didier, M., Delé, E., and Stojadinovic, B. (2015). "Probabilistic demand and supply resilience model for electric power supply system under seismic hazard," in *Proceedings of the 12th international conference on applications of statistics and probability in civil engineering (ICASP2015)*, 12–15.

Taghavi, S., and Miranda, E. (2003). *Response assessment of nonstructural building elements, PEER report 2003/05*. Berkeley: University of California, 1–96.

Takayanagi, T., and Schnobrich, W. C. (1979). Non-linear analysis of coupled wall systems. *Earthq. Eng. and Struct. Dyn.* 7 (1), 1–22. doi:10.1002/eqe.4290070102

Tazarv, M., and Saiid Saiidi, M. (2016). Low-damage precast columns for accelerated bridge construction in high seismic zones. *J. Bridge Eng.* 21 (3), 04015056. doi:10.1061/(asce)be.1943-5592.0000806

Tian, J., Symans, M. D., Pang, W., Ziaei, E., and van de Lindt, J. W. (2016). Application of energy dissipation devices for seismic protection of soft-story wood-frame buildings in accordance with FEMA guidelines. *J. Struct. Eng.* 142 (4), E4015009. doi:10.1061/(asce)st.1943-541x.0001269

Tinawi, R., Léger, P., Leclerc, M., and Cipolla, G. (2000). Seismic safety of gravity dams: from shake table experiments to numerical analyses. *J. Struct. Eng.* 126 (4), 518–529. doi:10.1061/(asce)0733-9445(2000)126:4(518)

TMS (2016). *Building code requirements for masonry structures*. Longmont, CO: The Masonry Society, 402–416.

Tokimatsu, K., and Seed, H. B. (1987). Evaluation of settlements in sands due to earthquake shaking. *J. geotechnical Eng.* 113 (8), 861–878. doi:10.1061/(asce)0733-9410(1987)113:8(861)

Tomassetti, U., Graziotti, F., Penna, A., and Magenes, G. (2016). "Out-of-plane shaking table tests on URM cavity walls," in *Brick and block masonry*. 1st ed. (London: CRC Press), 10.

Torres Matos, M. A., and Rodríguez, M. E. (2014). Comportamiento sísmico de cimentación tipo candelero para puentes con columnas prefabricadas de concreto reforzado. *Ing. sísmica* (90), 55–87. doi:10.18867/ris.90.14

Trandafir, A. C., and Bartlett, S. F. (2010). "Seismic performance of double EPS geofoam buffer systems," in *Proc. Of fifth international conference on recent advances in geotechnical earthquake engineering and soil dynamics and symposium in honor of professor IM idriss*.

Tremblay, R., Mottier, P., and Rogers, C. (2016). Seismic retrofit of existing low-rise steel buildings in eastern Canada using rocking braced frame system. *Can. J. Civ. Eng.*

Trifunac, M. D. (1982). A note on rotational components of earthquake motions on ground surface for incident body waves. *Int. J. Soil Dyn. Earthq. Eng.* 1 (1), 11–19. doi:10.1016/0261-7277(82)90009-2

Trifunac, M. D. (2009a). The role of strong motion rotations in the response of structures near earthquake faults. *Soil Dyn. Earthq. Eng.* 29 (2), 382–393. doi:10.1016/j.soildyn.2008.04.001

Trifunac, M. D. (2009b). Review: rotations in structural response. *Bull. Seismol. Soc. Am.* 99 (2B), 968–979. doi:10.1785/0120080068

Trifunac, M. D., Todorovska, M. I., and Ivanović, S. S. (1996). Peak velocities and peak surface strains during Northridge, California, earthquake of 17 January 1994. *Soil Dyn. Earthq. Eng.* 15 (5), 301–310. doi:10.1016/0267-7261(96)00004-8

Tsang, H. H. (2008). Seismic isolation by rubber–soil mixtures for developing countries. *Earthq. Eng. and Struct. Dyn.* 37 (2), 283–303. doi:10.1002/eqe.756

Van Den Einde, L., Conte, J. P., Restrepo, J. I., Bustamente, R., Halvorson, M., Hutchinson, T., et al. (2021). NHERI@UC San Diego 6-DOF large high-performance outdoor shake table facility. *Front. Built Environ.* 6, 580333. doi:10.3389/fbuil.2020.580333

Van Den Einde, L., Zhao, L., and Seible, F. (2003). Use of FRP composites in civil structural applications. *Constr. Build. Mater.* 17 (6-7), 389–403. doi:10.1016/s0950-0618(03)00040-0

Van Impe, W. F. (1989). *Soil improvement techniques and their evolution*. Rotterdam: Balkema.

Villaverde, R. (1997). Seismic design of secondary structures: state of the art. *J. Struct. Eng.* 123 (8), 1011–1019. doi:10.1061/(asce)0733-9445(1997)123:8(1011)

Vosooghi, A., and Buckle, I. G. (2013). "Evaluation of the performance of a conventional four-span bridge during shake table tests," in *Center for civil engineering earthquake research department of civil and environmental engineering*. Reno, Nevada: University of Nevada.

Wakabayashi, M., Nakamura, T., Katagihara, A., Yogoyama, H., and Morisono, T. (1973). Experimental study on the elastoplastic behavior of braces enclosed by precast concrete panels under horizontal cyclic loading—parts 1 and 2. *Summ. Tech. Pap. Annu. Meet.* 6, 121–128.

Wang, D., Dai, J., Qu, Z., and Ning, X. (2016). Shake table tests of suspended ceilings to simulate the observed damage in the M s7. 0 Lushan earthquake, China. *Earthq. Eng. Eng. Vib.* 15 (2), 239–249. doi:10.1007/s11803-016-0319-z

Wartman, J., Seed, R. B., and Bray, J. D. (2005). Shaking table modeling of seismically induced deformations in slopes. *J. Geotech. Geoenv. Eng.* 131 (5), 610–622. doi:10.1061/(asce)1090-0241(2005)131:5(610)

Wierschem, N. E., Hubbard, S. A., Luo, J., Fahnestock, L. A., Spencer, B. F., McFarland, D. M., et al. (2017). Response attenuation in a large-scale structure subjected to blast excitation utilizing a system of essentially nonlinear vibration absorbers. *J. Sound Vib.* 389, 52–72. doi:10.1016/j.jsv.2016.11.003

Wilson, E. L., and Penzien, J. (1972). Evaluation of orthogonal damping matrices. *Int. J. Numer. methods Eng.* 4 (1), 5–10. doi:10.1002/nme.1620040103

Wu, R. Y., and Pantelides, C. P. (2019). Seismic experiments and analysis of repaired bridge columns using CFRP donut. *Spec. Publ.* 333, 80–95. doi:10.14359/51720271

Xiao, Y., Priestley, M. N., and Seible, F. (1996). Seismic assessment and retrofit of bridge column footings. *Struct. J.* 93 (1), 79–94. doi:10.14359/9834

Xie, Y., Zhang, J., DesRoches, R., and Padgett, J. E. (2019). Seismic fragilities of single-column highway bridges with rocking column-footing. *Earthq. Eng. and Struct. Dyn.* 48 (7), 843–864. doi:10.1002/eqe.3164

Yarahuaman, A., and McCartney, J. S. (2022). Seismic response of rail embankments. *Proc. GeoCongress 2022. Charlotte. Mar. 20-23. GSP 336*, 300–310. doi:10.1061/9780784484067.031

Yarahuaman, A., and McCartney, J. S. (2024). Full-scale seismic response test on a shallow foundation embedded in tire-derived aggregate for geotechnical seismic isolation. *Soil Dyn. Earthq. Eng.* 177, 108417. doi:10.1016/j.soildyn.2023.108417

Yazdanian, M., Ingham, J. M., Kahanek, C., and Dizhur, D. (2020). Damage to legged wine storage tanks during the 2013 and 2016 New Zealand earthquakes. *J. Constr. Steel Res.* 172, 106226. doi:10.1016/j.jcsr.2020.106226

Yegian, M. K., and Kadakal, U. (2004). Foundation isolation for seismic protection using a smooth synthetic liner. *J. Geotech. Geoenv. Eng* 130 (11), 1121–1130. doi:10.1061/(asce)1090-0241(2004)130:11(1121)

Youd, T. L., Hansen, C. M., and Bartlett, S. F. (2002). Revised multilinear regression equations for prediction of lateral spread displacement. *J. Geotech. Geoenv. Eng.* 128, 1007–1017. doi:10.1061/(asce)1090-0241(2002)128:12(1007)

Yu, C. C., Mir, F. U. H., and Whittaker, A. S. (2021). Validation of numerical models for seismic fluid-structure-interaction analysis of nuclear, safety-related equipment. *Nucl. Eng. Des.* 379, 111179. doi:10.1016/j.nucengdes.2021.111179

Zareian, F., and Medina, R. A. (2010). A practical method for proper modeling of structural damping in inelastic plane structural systems. *Comput. and Struct.* 88 (1-2), 45–53. doi:10.1016/j.compstruc.2009.08.001

Zareian, F., Sampere, C., Sandoval, V., McCormick, D. L., Moehle, J., and Leon, R. (2012). Reconnaissance of the Chilean wine industry affected by the 2010 Chile offshore Maule earthquake. *Earthq. Spectra* 28 (1_Suppl. 1), 503–512. doi:10.1193/1.4000048

Zareiyan, B., and Khoshnevis, B. (2017). Effects of interlocking on interlayer adhesion and strength of structures in 3D printing of concrete. *Automation Constr.* 83, 212–221. doi:10.1016/j.autcon.2017.08.019

Zargar, S., Medina, R. A., and Ibarra, L. (2017). "Effect of pellet-cladding bonding on the vibration of surrogate fuel rods," in *Proceedings of international high-level radioactive waste management (IHLRWM 2017) conference* (Charlotte, NC).

Zayed, M., Ebeido, A., Prabhakaran, A., Kim, K., Qiu, Z., and Elgamal, A. (2020). Shake table testing: a high-resolution vertical accelerometer array for tracking shear wave velocity. *Geotechnical Test. J.* 44 (4), 1097–1118. doi:10.1520/gtj20190066

Zayed, M., Ebeido, A., Prabhakaran, A., Qiu, Z., and Elgamal, A. (2021). Asymmetric input motion for accumulation of lateral ground deformation in laminar container shake table testing. *Can. Geotechnical J.* 58 (2), 210–223. doi:10.1139/cgj-2018-0647

Zembaty, Z., and Boffi, G. (1994). Effect of rotational seismic ground motion on dynamic response of slender towers. *Eur. Earthq. Eng.* 8, 3–11.

Zhang, J., and Makris, N. (2001). Rocking response of free-standing blocks under cycloidal pulses. *J. Eng. Mech.* 127 (5), 473–483. doi:10.1061/(asce)0733-9399(2001)127:5(473)

Zhang, J., Singh, A., Eladly, M., Schafer, B. W., and Hutchinson, T. C. (2024a). "Pre-test numerical modeling of the CFS-NHERI 10-story capstone building," in *Proceedings of the 18th world conference on earthquake engineering (WCEE2024)*. Milan, Italy.

Zhang, J., Singh, A., Eladly, M., Schafer, B. W., and Hutchinson, T. C. (2024b). "Pre-test numerical modeling of the CFS-NHERI 10-story capstone building," in *Proceedings of the 18th world conference on earthquake engineering (WCEE2024)*. Milan, Italy.

Zhang, Y., Conte, J. P., Yang, Z., Elgamal, A., Bielak, J., and Acero, G. (2008). Two-dimensional nonlinear earthquake response analysis of a bridge-foundation-ground system. *Earthq. Spectra* 24 (2), 343–386. doi:10.1193/1.2923925

Zhang, Z., Fleischman, R. B., Restrepo, J. I., Guerrini, G., Nema, A., Zhang, D., et al. (2018c). Shake-table test performance of an inertial force-limiting floor anchorage system. *Earthq. Eng. and Struct. Dyn.* 47 (10), 1987–2011. doi:10.1002/eqe.3047

Zheng, Y., Fox, P. J., Shing, P. B., and McCartney, J. S. (2019a). Physical model tests of half-scale geosynthetic reinforced soil bridge abutments. I: static loading. *J. Geotechnical Geoenvironmental Eng.* 145 (11), 04019094. doi:10.1061/(asce)gt.1943-5606.0002152

Zheng, Y., McCartney, J. S., Shing, P. B., and Fox, P. J. (2018b). Transverse shaking table test of a half-scale geosynthetic reinforced soil bridge abutment. *Geosynth. Int.* 25 (6), 582–598. doi:10.1680/jgein.18.00019

Zheng, Y., McCartney, J. S., Shing, P. B., and Fox, P. J. (2019b). Physical model tests of half-scale geosynthetic reinforced soil bridge abutments. II: dynamic loading. *J. Geotechnical Geoenvironmental Eng.* 145 (11), 04019095. doi:10.1061/(asce)gt.1943-5606.0002158

Zheng, Y., Sander, A. C., Rong, W., Fox, P. J., Shing, P. B., and McCartney, J. S. (2018a). Shaking table test of a half-scale geosynthetic-reinforced soil bridge abutment. *Geotechnical Test. J.* 41 (1), 171–192. doi:10.1520/gtj20160268

frontiers | Frontiers in Built Environment

TYPE Original Research
PUBLISHED 12 June 2025
DOI 10.3389/fbuil.2025.1589067

Check for updates

OPEN ACCESS

EDITED BY
Giuseppe Brando,
G.d'Annunzio University of Chieti and Pescara, Italy

REVIEWED BY
Rui Marques,
University of Minho, Portugal
Julie Paprocki,
University of New Hampshire, United States

*CORRESPONDENCE
Cheryl Ann Blain,
cheryl.a.blain.civ@us.navy.mil

RECEIVED 06 March 2025
ACCEPTED 16 May 2025
PUBLISHED 12 June 2025

CITATION
Blain CA, Ramirez JA, Edge BL, Holmes W, LaChance M, Nelson R, Robertson I and Zehner D (2025) Successful coordination of the distributed network, Natural Hazards Engineering Research Infrastructure. *Front. Built Environ.* 11:1589067. doi: 10.3389/fbuil.2025.1589067

COPYRIGHT
© 2025 Blain, Ramirez, Edge, Holmes, LaChance, Nelson, Robertson and Zehner. This is an open-access article distributed under the terms of the Creative Commons Attribution License (CC BY). The use, distribution or reproduction in other forums is permitted, provided the original author(s) and the copyright owner(s) are credited and that the original publication in this journal is cited, in accordance with accepted academic practice. No use, distribution or reproduction is permitted which does not comply with these terms.

Successful coordination of the distributed network, Natural Hazards Engineering Research Infrastructure

Cheryl Ann Blain[1]*, Julio A. Ramirez[2], Billy L. Edge[3], William Holmes[4], Marti LaChance[2], Robin Nelson[5], Ian Robertson[6] and Dan Zehner[2]

[1]Remote Sensing Division, Naval Research Laboratory, Washington, DC, United States, [2]Lyles School of Civil and Construction Engineering, Purdue University, Lafayette, IN, United States, [3]Department of Civil, Construction, and Environmental Engineering, North Carolina State University, Raleigh, NC, United States, [4]Retired, San Francisco, CA, United States, [5]Department of Biotechnology and Science Engineering, University of Texas at San Antonio, San Antonio, United States, [6]Department of Civil, Environmental and Construction Engineering, University of Hawai'i at Manoa, Honolulu, HI, United States

A Network Coordination Office (NCO) is at the core of the Natural Hazards Engineering Research Infrastructure (NHERI), a national, 12-component, distributed research network, funded by the National Science Foundation (NSF). NHERI is focused on research that both mitigates damage and increases resilience from natural hazards such as hurricanes and other extreme windstorms, storm surge, tsunami waves, and earthquakes. NCO activities engage all facilities within NHERI, uniting the network's four diverse component types comprised of experimental facilities, a cyberinfrastructure for data and computing resources, a center for the creation of modeling and simulation tools, and a repository of equipment, software and support for rapid reconnaissance. Outcomes from NCO governance activities include two network-wide summits, five international partnerships, a central scheduling tool, and a means for external evaluation. The NCO's education and community outreach has established an extremely successful pipeline for engineering education from elementary and secondary educators to undergraduates, graduate students, and early career faculty. The NCO conducts centralized communication activities such as newsletter publication, e-mail announcements, podcasts, and social media engagements that unite the natural hazards research community and amplify NHERI's impact. Led by the NCO, the NHERI Science Plan presents a long-term vision for the natural hazards research community and serves as a roadmap for future high-impact, high-reward, hazards engineering and interdisciplinary research at NHERI facilities. The NCO also promotes technology transfer through education and one-on-one engagement with researchers. Overall, the NCO unifies and strengthens the research network through its variety of initiatives, amplifying the impact of this multifaceted NSF research network and provides a template for the management of large, distributed research networks.

KEYWORDS

NHERI, distributed research network, natural hazards network, research network governance, engineering education pipeline, education and community outreach, extreme events research, natural hazards engineering

Introduction

Since 2015, the NHERI has operated through NSF support as a Mid-Scale Research Infrastructure, where mid-scale is defined as a research infrastructure—including equipment, cyberinfrastructure, large-scale datasets and personnel—whose total project costs are under $20 million. NHERI is a US nationally distributed, 12-component (Figure 1), multi-user facility that provides the natural hazards engineering community with access to research infrastructure. NHERI facilities enable investigators to study damage mitigation from hurricanes and other extreme windstorms, storm surge, tsunami waves, and earthquakes. At the heart of the NHERI is the NCO, and functioning within the NCO are network governance, education and community outreach, centralized communication, science visioning, and research-to-practice initiatives. The governance structure consists of the Council of NHERI awardees, the Network Independent Advisory Committee (NIAC), and the User Forum (UF).

Two funded prototype expansion facilities, NEWRITE and NICHE (indicated by yellow dotted lines in Figure 1), do leverage resources of the NHERI network and most particularly those of the NCO. The NCO engages in promotional communication activities for these upcoming facilities and offers consultation in methods for incorporating technology transfer into their planning. Future research at NICHE is also included in the recent Science Plan (NEWRITE was awarded after the latest Science Plan).

There are, of course, many other natural hazards research institutes located both in the Americas and Europe. Some examples include the US Center for Wind Hazard and Infrastructure Performance (WHIP), funded in 2019 under the NSF Industry-University Cooperative Research Centers Program, focusing on a single hazard, wind; it is a collaborative effort between Texas Tech University and Florida International University with industry partners in insurance and construction. Another network centered at a single university is the University of South Florida's Natural Hazards Network which consists of 50 faculty, cross-cutting university disciplines and also working with industry and policymakers to address causes, mitigation, and response to natural hazards and disasters. In Europe, the Joint Research Centre's European Crisis Management Laboratory adopts a multi-hazard approach as a research, development, and test facility that focuses its efforts toward effective crisis management resulting from threats and natural and man-made hazards. The European Commission is quite supportive of the research infrastructure paradigm. Two examples are 1) ESS, the world's next-generation neutron science facility, a pan-European project with 13 European nations as members, and 2) ELIXIR, a distributed infrastructure for life science information, bringing together scientists from over 240 research institutes spread

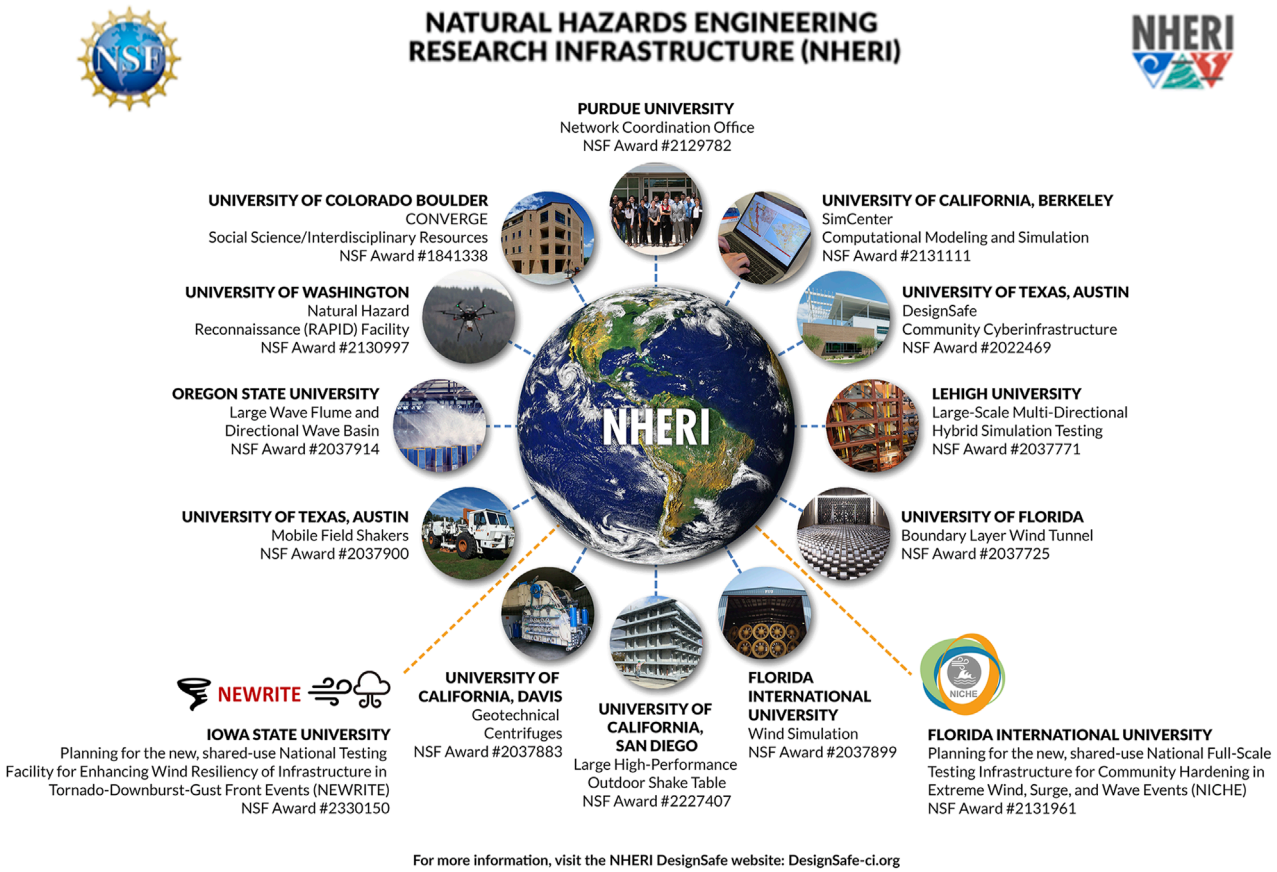

FIGURE 1
The Natural Hazards Engineering Research Infrastructure (October 2024). Twelve distributed, university-based facilities (blue dotted lines) plus two funded prototype expansion facilities, NEWRITE and NICHE (yellow dotted lines).

over 21-member countries and three observer countries. One other research infrastructure is UKCRIC, a multidisciplinary 16-member network of United Kingdom universities connecting research with policy and practice in infrastructure and urban systems. The NHERI NCO has already initiated formal communications with UKCRIC, expecting that we can mutually benefit from our shared experiences in management of a distributed research network, education and outreach, and in the conversion of research into practice. Though there are clearly other networks of research infrastructures, the coordination of these networks is not widely publicized. This work aims to reveal the details of an effective coordination office, the NCO, for a distributed research infrastructure, NHERI.

The leadership and guidance of the NCO has had a profound influence on the success of the network, which is further illustrated by NSF's renewal of the NCO component, announced in August 2024. As the administrative core for the network, the NCO appears at the top of the NHERI wheel in Figure 1. The NCO's role is to lead the organization of network-wide activities such as governance, educational programs, communications, scientific planning, and technology transfer. Indeed, the NCO functions as the network's hub; NCO activities engage all other facilities, uniting the network's diverse components. As "coordination" implies, the NCO team unifies and strengthens the network by guiding, educating, communicating, organizing—and overall amplifying the impact of this multifaceted NSF research network.

The NCO itself is comprised of 15 members, 9 of whom are subject matter experts in various engineering fields that encompass the natural hazards engineering focus of the network. Engineering fields covered include geotechnical, earthquake, tsunami, wind, and coastal as well as the social sciences. These nine experts include a Director of the NCO with the remaining eight persons functioning as the NCO Strategic Committee, which meets bi-weekly to report, discuss, and plan the variety of activities undertaken by the NCO. Additionally, a representative from the User Forum (described under GOVERNANCE) also attends regularly to facilitate communication between the NCO and this governance group. Interaction with another governance group, the Council of NHERI principal investigators, is accomplished through monthly meetings and the NCO director is the convener. The third governance group, the Network Independent Advisory Committee, meets twice a year where the NCO both facilitates and reports at these meetings. Under the same Governance category shown in Figure 2 approximately 5% of the total NCO budget is allocated to support international collaborations in the form of support for participants to attend research collaboration planning meetings, workshops and international conferences. Aside from the Strategic Committee, there is a facility scheduler and operations coordinator whose activities fall under Governance, a communications manager, software engineer, and half-time research assistant who handle the bulk of the Communications effort, and specialists in education and engineering education that focus on the Educational and Outreach aspect of the NCO. Several Strategic Committee members serve in multi-faceted roles overseeing the Education, Communication, Science Planning, and Technology Transfer functions of the NCO. All efforts by NCO personnel are equivalent to the work of 4.5 full-time employees per year. A breakdown of funded personnel by NCO activity is presented in Figure 2. Communications uses the largest portion of the personnel at 46%, while the education and governance

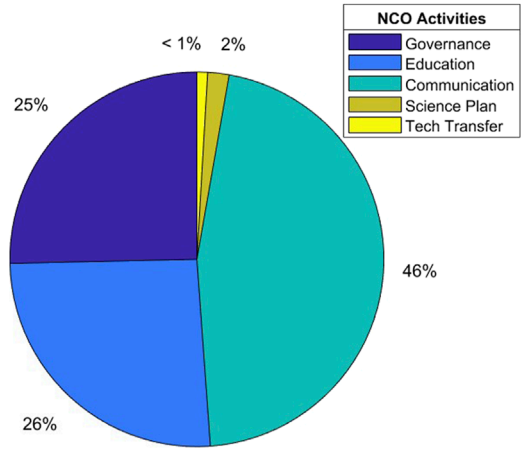

FIGURE 2
NCO personnel breakdown. The NCO activities of governance, education, communication, science planning, and technology transfer shown as a percentage of the total 4.5 full-time employee annual effort of the NCO.

functions consume 26% and 25% of the personnel, respectively, of the NCO effort. The other activities, Science Planning and Technology Transfer rely on partnerships with external volunteers to carry out the mission of these activities.

While personnel costs of the NCO Education effort are incredibly streamlined and efficient, approximately 50% of the total NCO budget is allocated to Education, which is largely to support participants in network-wide activities to strengthen the career development pathway in natural hazards engineering. The NCO subsidizes approximately 30 participants who attend the network's annual Summer Institute for early-career researchers and the 30 undergraduates selected for the network's 10-week Research Experiences for Undergraduates (REU) summer program. These educational activities developed and executed by the NCO have created pathways for emerging natural hazards professionals to experience research opportunities as undergraduates, graduate students, early career faculty, and additionally impacts career promotion and success in obtaining NSF awards.

In addition to NHERI, there is only one other NSF operational Mid-Scale Research Infrastructure that involves multiple, distributed facilities, the National Nanotechnology Coordinated Infrastructure (NNCI). NNCI contains 16 distributed facilities across the nation and a coordinating office at Georgia Tech University; two other mid-scale distributed, multi-awardee networks have been funded by NSF but are in the implementation stage. The NNCI coordination office has a number of similar constructs as the NHERI NCO. For example, NNCI Coordination includes an Executive Committee and an External Advisory Board, analogous to the NCO's NHERI Council and Network Independent Advisory Committee (NIAC), detailed in the "GOVERNANCE" section. While NNCI has Associate Directors overseeing the areas of education and community outreach, computation, and entrepreneurship, the actual implementation of programs and activities seems to occur at a working group level between network participants, a very different construct than that of the NHERI NCO.

While the NHERI network is focused on natural hazards engineering, its successful programs can be emulated and leveraged by other large, distributed research network. This paper elucidates key elements of the NHERI network coordination office, the facility that sustains and advances a nationally distributed network of 12 NSF-funded research facilities at 11 R1 institutions (dotted blue lines in Figure 1). Note, for classification as an R1 (Very High Research Activity) university by the Carnegie Classification of Institutions of Higher Education, a university must spend at least $50 million on research and development annually and award at least 70 doctoral research degrees annually. We will discuss the particulars of NCO network governance, network-wide educational programs and community outreach, network communications, science planning, and research technology transfer. Importantly, we will detail the impact NCO efforts have had on the natural hazards research community. For a list of NCO faculty and staff, visit the NCO website.

Governance

In this section the three governance groups are described, and examples of the positive impact of activities lead by the NCO through these governance groups are provided. With the NHERI network spanning 12 universities (dotted blue lines in Figure 1) and consisting of components that vary widely in their capabilities, the goal of an NCO-supported and coordinated governance is to empower NHERI components into a coherent and collaborative network where the outcome is greater than the sum of the individual component's contributions. The NHERI NCO's charge is to build and engage the natural hazards community, educate and train future researchers and professional engineers, and effectively disseminate information to the NHERI community. Effective governance requires regular engagement from all network principal investigators and feedback from independent external reviews. Successful network governance relieves the individual components from negotiating the network's international partnerships, supports them in establishing independent user satisfaction, and enables transparent user access to the network research laboratories. In the 8 years since its establishment in 2016, the NCO has led NHERI via a governance structure consisting of the Council of NHERI awardees, the Network Independent Advisory Committee (NIAC), and the User Forum (UF). Each of these groups with a specific role is described next.

NHERI Council

It comprises all network principal investigators (PIs) and meets monthly to discuss network-wide events, research initiatives and projects, partnerships, and related items that affect NHERI. The meeting chair rotates through the network PIs. Each of the PIs are nationally recognized in their field, and have significant research and leadership experience managing experimental facilities at R1 universities. The Council provides collective and coordinated leadership for NHERI as a national facility.

Network Independent Advisory Council (NIAC)

The NIAC provides high-level, independent guidance and advice to the NHERI Council. The NIAC is a group of representatives from the broad scientific and engineering communities, composed of practicing engineers, engineering faculty, and representatives from federal agencies such as the Army Corps of Engineers; their successful engagement with NHERI components has resulted in a number of significant accomplishments benefitting the NHERI community broadly, and the users of the components in particular. For example, the NIAC has placed an emphasis in NHERI on 1) ensuring a good balance of fundamental engineering studies and applied or transferable research, 2) interdisciplinary work encompassing the full spectrum of natural hazards research, and 3) eliminating barriers to external use of the experimental facilities.

The NIAC has achieved this through its engagement with all the NHERI components in virtual and in-person individual interviews. For instance, the NIAC had its face-to-face 2023 meeting in San Diego, CA, at the NHERI UCSD facility on May 22–23. The NIAC group toured the recently upgraded LHPOST6 shake table and witnessed 6 different tests of the Tallwood project (Pei et al., 2017). While on-site, the committee also held virtual meetings with 6 NHERI facilities, including the NCO, and held an executive session in preparation for writing its annual report to the NCO and the NHERI network. Two of the NIAC's conclusions are that "both internal and external research is carried out at most [NHERI] facilities and the facilities are fully invested in serving as national resources for large scale testing and research" and that "interviewed sites are receiving good support from the NCO". In 2025, the NIAC conducted its review from Florida International University's Wall of Wind facility during the period 24–25 February.

User Forum (UF)

Members of the NHERI User Forum are elected by the natural hazards community and represent the earthquake, wind, coastal and storm surge, and social science interests. They include nine individuals from universities and government agencies, practitioners and educators. The role of the Forum is to monitor, via annual surveys, user satisfaction of the NHERI facilities. In addition, the User Forum raises awareness about NHERI research and its impact.

The User Forum has led the execution of the annual User Satisfaction Survey and the results are posted on the NHERI platform for cyber-collaboration (DesignSafe-CI) here. For NHERI Y5 (FY 2021) through Y7 (FY 2023), a module was developed specifically to be incorporated in the Exit Survey of researchers at the NHERI facilities, to increase the response rate of the survey. The implementation consisted of a module of questions appended to most experimental facility user surveys beginning on Jan 1; collection occurs throughout the year on a rolling basis. Added to the UF survey were "4 big questions", which are designed to yield a broad-level overview on user satisfaction. Questions featured mixed-response options that captured both qualitative and quantitative data. As in 2022, the user satisfaction subcommittee opted to send the 2023 survey to a targeted population of known

NHERI facility users. Known NHERI facility users were identified with assistance from NHERI facility PIs at NHERI experimental facilities. The User Forum is preparing the FY 2025 User Satisfaction Survey, with plans to include in the survey questions about the NHERI Graduate Student Council. The User Forum meets monthly, including an in-person meeting at the NHERI Summer Institute convened in San Antonio, TX, on June 23, 2023. The approved minutes of the Forum meetings can be found at the User Forum webpage in DesignSafe-CI.

The combined efforts of the Council, NIAC, and User Forum have led to: (i) development of NHERI-wide metrics that illustrate the participation of the user community and the support NHERI provides to its research efforts, and these have been implemented with concurrence from NSF; (ii) dissemination of the impact of NHERI while continuing to build a community of satisfied multi-hazard users, and (iii) execution and publication of the Y-7 User Satisfaction Survey.

Outcomes of collaboration

The effective collaboration of all governance groups, with the leadership of the NHERI NCO, has brought to reality a number of network-wide efforts. In September 2024, NHERI leaders held sessions at the United Nations General Assembly (UNGA 79) Science Summit. Additional efforts have been funded by NSF through award supplemental activities in the annual work plan of the Council. Examples of these activities are the community-driven NHERI Science Plan (Robertson et al., 2023) and two successful community-wide research summit events.

The first Natural Hazards Research Summit took place October 6–7, 2022 at the National Academy of Sciences in Washington, DC. Day one consisted of a town-hall style visioning session in which attendees took deep dives into the research needs and priorities for the profession and the communities we serve. On day two in focused workshops and discussions, summit attendees provided ideas and specific input toward the future of natural hazards engineering research (Bridge et al., 2023). On May 14–15, 2024 at the University of Maryland, a second Natural Hazards Research Summit highlighted findings from the much anticipated NHERI Decadal Visioning Study 2026–2035 (Schneider and Kosters, 2024). In summit talks and concurrent sessions, attendees learned about new and interdisciplinary research underway; a special panel engaged attendees in discussions of technology transfer for natural hazards research projects.

Initiating international partnerships

Such a large research network as NHERI brings the benefits of scale to partnerships with international research organizations for research collaboration, shared-use facilities of mutual benefit, data exchanges, and workforce development contributions aimed at preparing the next-generation of leaders in the field. On behalf of NHERI, the NCO initiates, executes, and maintains formal NSF agreements with leading research organizations in Japan, Taiwan, and Europe for research collaborations in earthquake, wind, and coastal engineering. For current international collaborations, three letters of agreement (LoAs) are listed on the NHERI DesignSafe-CI website (https://designsafe-ci.org/facilities/nco/partnerships/). The first is with the National Research Institute for Earth Science and Disaster Resilience (NIED, nicknamed "E-Defense") in the city of Miki, north of Kobe, Japan. The second is with the National Center for Research on Earthquake Engineering (NCREE) in Taiwan. A third is with the non-profit European Centre for Training and Research in Earthquake Engineering (EUCENTRE) in Pavia, Italy. Since the beginning, the EUCENTRE involvement in over 30 research projects funded by the European Commission has led to the development of fruitful and lasting collaborations with about 300 European partners, including the most important research centers in the field of earthquake engineering and seismology. The latter two partnerships with NCREE and EUCENTRE are currently undergoing renewal.

In January 2024, at a planning meeting hosted by the NHERI UC San Diego facility, an important new phase of the U.S.-Japan earthquake engineering research collaboration began. Following this productive reunion in July 2024, a Memorandum of Cooperation was signed by Japan's National Research Institute for Earth Science and Disaster Resilience (NIED) and Purdue University on behalf of the NSF-funded NHERI Network Coordination Office. The NCO and NHERI firmly believes that collaboration between American and Japanese researchers provides an incredibly strong mechanism for accelerating the pace of discovery and development in engineering that is needed to prevent natural hazards from becoming societal disasters. Specifically, this U.S.-Japan partnership focuses on earthquake engineering with interest on the physical and economic harm that hazards are having on our communities, including cascading effects among multiple hazards. For more than a half century, U.S. and Japanese researchers have a history of smooth and effective collaborations. They began with the NSF-funded George E. Brown Jr. Network of Earthquake Engineering Simulation (NEES) and E-Defense in 2004, and then continued with the NHERI and E-Defense partnership in 2017. Now, we are enthusiastic about our renewed U.S.-Japan collaboration.

The historic NHERI-E-Defense collaboration has led to many landmark shake table tests; the most recent is the large-scale test of a reinforced concrete structure under the Tokyo Metropolitan Resilience Project. Several U.S. researchers participated in this test through payload projects that allowed the evaluation of new data acquisition techniques never before tried in an experiment of this scale. Other tests have led to the implementation of new retrofit techniques and the performance identification of protective technologies. Moreover, data from more than ten large-scale experiments have been made public already in the DesignSafe-CI Data Depot, going back to the predecessor of NHERI, NEES.

Scheduling experiments

The NHERI NCO ensures smooth and transparent access to the network's eight experimental research facilities. To assist researchers planning to use network facilities, the NCO has developed a Facility Scheduling Dashboard tool. With this web-based tool, researchers and the general public can view research projects taking place at NHERI experimental facilities. This centralized approach has a number of benefits to the research community:

- It limits schedule conflicts between researchers
- Researchers outside of the facility's home institution have equal priority
- Small 'payload' projects can identify larger projects to collaborate with
- Stakeholders can see the ongoing value and impact of the NHERI experimental facilities
- All projects are searchable
- Collaboration between researchers is enhanced due to visibility of experimental resources

The scheduler leads to more collaboration between researchers both inside and outside NHERI and maximizes utilization of the shared-use research facilities that comprise NHERI. One project that exemplifies the value of the NCO's centralized scheduling model within NHERI is the University of Florida-led 'Sentinel' instrument development (Phillips et al., 2023). This project was developed in collaboration with multiple NHERI experimental facilities and included field testing, as well as the involvement of NSF's Research Experience for Undergraduates (REU) students.

Education and outreach

Like all NSF awards, NHERI has a broad mandate to educate the next-generation of researchers. Within the NCO, a centralized education and community outreach (ECO) committee is comprised of representatives from each of the NHERI network components and led by the NCO. The ECO Committee ensures vital network-wide input into NHERI's educational programming. The NHERI ECO enables individual research facilities to focus on providing research opportunities centered on their own capabilities. In turn, the NCO ECO group shoulders the work of organizing network-wide educational programs. This includes organizing the annual Research Experiences for Undergraduates (REU) program and the annual NHERI Summer Institute (SI) for Early Career researchers. The ECO handles the task of organizing, managing, and reporting on the success of the NHERI network's educational efforts.

The NHERI ECO collects longitudinal data on these efforts, which have shown outstanding impact on the field of natural hazards engineering, as well as on the researchers and students who have participated in the REU and SI programs. Find the detailed outcomes in Nelson et al. (2025). Specifically, the NHERI ECO has had significant impact in engineering education. One example is NHERI's REU program, which has introduced 166 undergrads to natural hazards research. After the first 7 years of the program, 35% of these undergraduates went on to pursue graduate degrees with 8% already in PhD programs.

The NHERI ECO provides a diverse, connected pathway for academic engineering workforce development. The annual programs train and mentor elementary (ages 5-12) through secondary (ages 13-18), otherwise referred to as Kindergarten through 12th grade or K-12, educators, undergraduates, graduate students, and early career faculty. With a focus on broadening participation, the NHERI ECO encourages diversity in participants and recruits from non-R1 research institutions. NHERI strives to reach students at less elite research institutions where exposure to research opportunities are not commonplace. The NHERI ECO provides training in a wide array of natural hazards research, including geotechnical, wind, coastal, and structural engineering; field investigation; computational programming and analysis; simulation and modeling; and social science disaster studies.

Undergraduate education

The NCO's ECO helps plan logistics for the annual REU internship, in which each NHERI component mentors 2-4 undergraduates for 10 weeks. The students receive hands-on research opportunities at NHERI's world-class facilities as well as the community experience of fellow REU students, graduate student and faculty mentors. The ECO team provides the interconnections for all REU students across sites and ensures that all students have impactful educational outcome experiences. The NCO education team helps guide an inclusive recruitment and selection process and hosts mentorship training activities for site personnel. Throughout the internship experience, the education team holds weekly network-wide virtual activities for career and research skill development and then organizes an in-person research symposium at a selected NHERI site at the conclusion of the program.

Early-career training

The annual NHERI Summer Institute is a 3-day crash course in navigating NSF-funded academia for early career researchers. Participants learn how they may use NHERI facilities and get hands-on practice designing and writing an NSF grant—which often includes K-12 components to help promote broader impacts of the designed research work. K-12 teachers also participate in the Summer Institute. They partner with early career faculty to design effective K-12 lessons plans that guide early-career faculty and can be used in their classrooms.

Graduate student mentorship

The NHERI Graduate Student Council is a new addition to the NHERI community. It was created in October of 2021 and is administered by 19 graduate students on the Executive Committee: 7 officers and 12 Standing Committee Chairs and Vice Chairs. The 600-member Council is run by elected representatives, meets monthly on research topics, and holds an annual research conference. The Council participates in many NHERI activities, including the Summer Institute and NHERI Summits, and also presents NHERI work at related conferences to help broaden the impact of NHERI activities.

The impact of the centralized NHERI ECO is more than significant. Program managers from the National Science Foundation point to NHERI's programming as an example of a well-run educational pathway to STEM careers. Participation in NHERI's educational programs has also furthered the reach of the NHERI brand by engaging students and researchers from every state in the U.S.; the Graduate Student Council reaches international academic partners, as well.

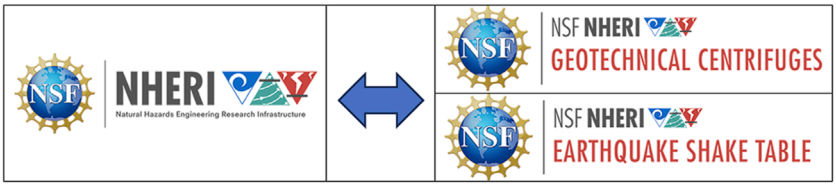

FIGURE 3
The NSF NHERI facility logos are derived from the NHERI logo, giving coherence to our 12-member network. Above see examples from two experimental facilities.

Communications

As part of its community outreach efforts, the NCO provides news and information that engages NHERI researchers and the broader natural hazards community. These centralized communication efforts unite the research community and amplify NHERI's impact, as well as the impact of the U.S. National Science Foundation.

Unifying the community

Since 2016, the NCO communications group has steadily built an audience for natural hazards engineering research. Starting from scratch, the NCO now reaches a broad audience that includes natural hazards researchers, practicing engineers, students from high-school through graduate school—as well as policymakers and people who may use NHERI-derived tools and techniques to mitigate damage. The general public also is interested in learning how NHERI researchers work to mitigate damage from events like hurricanes and storm surge, earthquakes and tsunamis. Ten years ago, very few people knew anything about "natural hazards engineering." Today, NHERI NCO messaging reaches 7,000 email subscribers and 8,500 social media followers. These figures are significant for an NSF-funded research award of its size and funding level.

The NCO publishes a bi-monthly newsletter that broadcasts current NHERI research and educational activities to the natural hazards engineering community. Initially, engagement was low; there was natural resistance to "yet another email." But over time, the NCO has earned the trust of the community. Currently, 40% of newsletter recipients now open and read this bi-monthly publication.

The NCO also distributes actionable email messages, such as invitations to join NHERI workshops and webinars. With centralized email broadcasting, the NCO enables the individual NHERI facilities to leverage the network to reach much larger audiences. For example, the NCO broadcasts customized emails for recruiting participants to NHERI workshops and webinars. On average, 70% of NHERI webinar registrations are the result of the NHERI NCO email broadcasts. In other words, the NHERI NCO communications team directly enables NHERI Network components to fulfill a key NSF mandate to train and educate users.

Another unifying role of NCO communications is maintaining and encouraging use of the network's visual branding standards mandated by NSF. Partnering with DesignSafe, NHERI's cyberinfrastructure component, the NCO maintains a branding toolkit for the NHERI community with NSF-approved logos and other communications tools. Each facility has a logo that reflects the NSF NHERI brand (e.g., Figure 3). Research faculty and staff use their logos in email signatures, on research posters, and in communications about facility events and opportunities. In the next 10 years of the NSF NHERI grant award, the NCO reckons that the NSF NHERI brand will be widely recognized as a key NSF-funded research organization.

Amplifying impact

To reach audiences beyond NHERI, including reporters and the public, the NCO publishes news stories to the NHERI website newsroom on DesignSafe-CI.org, the cyberinfrastructure hub of NHERI. Several other NCO communication activities expand the reach of NHERI. These include the following:

- a bi-monthly podcast called DesignSafe Radio, also published on YouTube, that features NHERI researchers and students;
- a strong social media presence on multiple platforms—including X, LinkedIn, and Facebook—that engages the greater natural hazards community, including government and non-government organizations;
- and a NHERI conference booth, which the NCO deploys at high-level engineering and natural hazards meetings.

NHERI NCO social media accounts tally thousands of followers. On the X platform alone, the @NHERIDesignSafe account has about 2,600 followers and averages 5,500 engagements each month. This reach is amplified by about 15 NHERI-affiliated accounts on X; these include accounts for the ECO Committee, the Graduate Student Council, the User Forum, and the podcast, DesignSafeRadio, as well as accounts associated with each of the NHERI facilities. Content shared on social media includes our news stories, podcast episodes, and a wide variety of events and opportunities initiated by NHERI facilities–such as workshops, research solicitations, and student internships. These engagements on X extend into LinkedIn, where NHERI receives 5,000 to 7,000 impressions each month, with a respectable two-percent engagement rate. Indeed, with its active social media presence, the NCO communications team is making NHERI, the NSF-funded natural hazards research network, a household name in the research community.

Supporting NSF research

At the heart of NCO communications are planned, strategic communications campaigns featuring the research and educational activities of the individual NHERI components. The campaigns consist of news stories, podcasts, and social media posts, all aimed at raising awareness of the ongoing research at an individual NHERI component. There are typically three campaigns ongoing at one time; they are driven by NHERI component priorities to maximize effectiveness. These targeted communications campaigns ensure all NHERI components have opportunities to broadcast specific research and education impact to both the public and the natural hazards community. Because most NSF-funded research awards do not have communications staff or budget, the NCO campaigns provide vital support—and much greater exposure for NHERI experimental facilities and their research.

Publishing NHERI facility research

The NCO tracks the impact made by the researchers who use NHERI facilities and data. Specifically, this translates to journal publications. Since 2014, more than 700 research papers have mentioned or acknowledged the Natural Hazards Engineering Research Infrastructure network, or NHERI. The NCO also coordinates special collections of research papers in the journal, *Frontiers in Built Environment*. This activity enables individual NHERI facilities to ensure high-impact projects taking place at their location can be peer-reviewed and published. Three such collections have taken place:

1. The collection entitled *Natural Hazards Engineering Research Infrastructure (NHERI) 2016–2020: Mitigating the Impact of Natural Hazards on Civil Infrastructure and Communities* is an introduction to NHERI and includes 16 articles. [Chowdhury et al., 2021; https://doi.org/10.3389/978-2-88971-186-4] This collection has experienced 140K topic views, 117K article views, and 117K article downloads.
2. The second collection is entitled *Technology Transfer from the Natural Hazards Engineering Research Infrastructure (NHERI).* It contains 6 articles and highlights examples of technology transfer from NHERI [Blain and Ramirez, 2023; https://doi.org/10.3389/fbuil.2023.1269036]. To date, this collection has 29K topic views, 24K article views, and 3,065 article downloads.
3. The final collection, currently in progress, is entitled *NHERI 2015–2025: A Decade of Discovery in Natural Hazards Engineering*, [https://www.frontiersin.org/research-topics/65402/nheri-2015-2025-a-decade-of-discovery-in-natural-hazards-engineering]. Its soon to be twelve articles that detail key research experiments and discoveries from the NHERI components over the award's 10-year existence.

Given the attention shown to these articles on NHERI facility research, the NCO's strategy to promote network research publications are a success–and a useful NHERI-centric complement to the numerous papers published each year by NHERI researchers.

In summary, the NCO's centralized communications efforts ensure opportunities for all components to engage with the research community and the public, given that individual NHERI components may not have a dedicated mechanism for sharing important news and information. Further, centralized communication reduces duplicative efforts, ensures uniformity in branding, and amplifies individual component activities and accomplishments. With NCO-managed communications, each component relies on NCO communications to "get out the message" on current research and events taking place at their facility.

NHERI's science vision

The NHERI Science Plan, its third edition published in November 2023, presents the long-term vision for the natural hazards research community, which includes NSF and other funding agencies. The Science Plan serves as a roadmap for future high-impact, high-reward, hazards engineering and interdisciplinary research at NHERI facilities. Research directions outlined by the Science Plan are targeted to mitigate damage and reduce casualties from natural hazards while promoting community resilience. The Science Plan can be downloaded from the NHERI DesignSafe Data Depot (Robertson et al., 2023).

The first edition of the Science Plan was published in 2017 based on a compilation of the individual science plans from each of the NHERI facilities. In 2019, the NCO organized an international workshop with participation of researchers from Taiwan, Canada, Japan, Italy and England to guide the development of the second edition of the Science Plan published in 2020. In 2022, another Science Plan workshop was held to develop the third edition of the Science Plan.

The primary objectives of the Science Plan are to:

- Incorporate the width and breadth of experimental capabilities of each NHERI facility, including sample research projects.
- Incorporate perspectives from interdisciplinary science and engineering as well as from social science aspects of hazard mitigation and management through an enhanced focus on interdisciplinarity, equity and inclusion, and collaborations with researchers from the NHERI CONVERGE facility;
- Incorporate input from extreme event reconnaissance and research (EER) networks coordinated by CONVERGE;
- Incorporate publicly available simulation tools developed by the NHERI SimCenter;
- Address the effects of climate change on natural hazards and associated infrastructure impacts;
- Encourage greater engagement of practitioner experience in proposal development, research execution, and implementation of research results;
- Provide a roadmap to assist researchers as they develop their research teams and proposals, perform the research, and shepherd implementation of their research findings into practice; and
- Provide examples of successful transfer of NHERI research findings to practice.

Members of the NCO take editorial responsibility for this key publication. For the third edition, an NCO team organized and formalized input from the nation's natural hazards community.

The team convened a workshop as well as an editorial task group consisting of 17 subject-matter experts that included engineering researchers, social scientists, and practicing engineers. The NCO also coordinated the broad dissemination of the NHERI Science Plan to the natural hazard community through an extensive communications campaign that included workshops, webinars, podcast appearances and video testimonials.

The NHERI Science Plan provides a bold vision for research to support an integrated view of hazard mitigation. It is designed to promote ongoing and meaningful engagement with practice, the leveraging and extension of NHERI components, and the professional development of a broad and diverse range of researchers and practitioners. It builds upon NHERI's prior success while engaging current and likely future trends in advanced methodologies, data, and supporting technologies. The sense of purpose, combined with ethics and ingenuity, are among the research community's greatest assets, so this document is not intended to constrain or limit ideas, but rather to identify high-value research needs and spark the development of meaningful research proposals. The Science Plan is meant to serve as a living document - one that will continue to be reviewed and updated to reflect new funding streams, projects, and challenges as well as new scientific breakthroughs and opportunities for further exploration.

Grand challenges

The Science Plan presents three grand challenges for the natural hazards research community.

- The first is to identify and quantify the characteristics of single, co-occurring, and compounding natural hazards - whether of geophysical and/or atmospheric origin - that have the potential to harm people, damage civil infrastructure, and disrupt communities.
- The second grand challenge is to assess the exposure, vulnerability, and adaptive capacity of civil infrastructure and social systems in areas threatened by natural hazards.
- The third grand challenge is to invest in a diverse hazards workforce and develop the technologies and tools to support the design, construction, retrofit, and operation of equitable, sustainable, and resilient civil infrastructure for the nation.

All three grand challenges are addressed through six, proposed key research questions. Each research question is discussed in detail in the Science Plan, including examples of research that would advance one or more of the grand challenge objectives. Successful implementation of many of the technologies and tools developed by NHERI researchers are highlighted below and in the following section on Research-to-Practice.

Success stories

For examples of high-quality natural hazards engineering research, the Science Plan includes five success stories where innovative research ideas have been investigated using NHERI facilities and transferred into everyday engineering practice. These include three research projects initiated by observations from field reconnaissance after Hurricane Maria in Puerto Rico, Hurricane Michael in the Florida panhandle, and hurricane storm surge effects on coastal fuel storage facilities. The other success stories feature the 10-story NHERI Tallwood building tested on the UC San Diego shake table in 2023, and the field verification of liquefaction mitigation using a microbially induced desaturation improvement technique with the help of the NHERI mobile shaker facility from the University of Texas. The Science Plan also features the success of the Babcock Ranch community in Florida that weathered the effects of Hurricane Ian with minimal disruption, serving as an example of the resilience provided by modern building codes and hazard-resistant residential subdivision planning.

Community engagement

To date, more than 1,000 copies of the Science Plan Third Edition have been downloaded from NHERI DesignSafe-CI.org. Early career researchers in particular are encouraged to cite the Science Plan in their grant proposals. At the annual NCO Summer Institute, early-career researchers are familiarized with the NHERI Science Plan. The NCO shares ways to leverage and cite the Science Plan when writing NSF proposals. Additionally, NCO members regularly speak on the Science Plan and how to use it at network-inclusive NHERI Summit meetings and at NHERI Graduate Student Council events.

Science plan user feedback

Researchers have referenced the NHERI Science Plan in their research proposals and provided valuable feedback on their experience with the Science Plan.

- Elaina Sutley, Associate Professor at the University of Kansas says "I think the Science Plan is really helpful, particularly for newer, more junior researchers. It certainly helped me understand how my research ideas fit into the bigger picture of natural hazards engineering research, and what is seen as important from our research community."
- Petros Sideris, Associate Professor at Texas A&M University says "I cited the NHERI Science Plan in my recently successful proposal. I think it is important to continue emphasizing the need for novel computational simulations informed by physical testing."
- Barbara Simpson, Assistant Professor at Stanford University commented that she cited the NHERI Science Plan in her successful research proposal as "*Thus, the work plan considers the NHERI Science Plan's objective to reduce reliance on experimental data through the development of more detailed numerical simulations and through the shake-table specimen re-use opportunity.*"

Ultimately, this plan is designed to spark new ideas and to facilitate use of the NHERI components and research infrastructure, all with a vision of a more resilient built environment and a

reduction in the harm and suffering caused by geophysical and atmospheric hazards.

Research-to-practice

Focus on technology transfer

A fundamental purpose of natural hazards engineering research is to develop new, sustainable designs and have them adopted into engineering practice, as well as to influence policies that enhance resilience. These engineering improvements may manifest as code changes, software tools, or new building components that can reduce damage from natural hazards. Specifically, these improvements in engineering practice and design strongly support the third grand challenge to extend the research and tool development through transfer of research into practice. For example, the NHERI SimCenter at the University of California has taken significant research findings and incorporated them into open-source numerical tools to characterize significant natural hazards and develop solutions to minimize the effects of those hazards on communities.

In a novel approach to technology transfer, the NHERI NCO appointed and led a Technology Transfer Committee (TTC) to guide and encourage NHERI researchers to envision the transfer of their research findings to practice. The Technology Transfer Committee is comprised of volunteer engineering practitioners and decision-makers who focus on strengthening ties between NHERI researchers and the implementers of NHERI-developed new knowledge. The TTC members are experienced in contributing to the development of design guidelines, technical briefs, building and infrastructure codes and standards, and technical seminars.

Educating the community

The TTC has provided a white paper detailing mechanisms for the implementation of NHERI research results that would facilitate technology transfer (NHERI Technology Transfer Committee, 2020). The TTC also offers free consultation services to researchers. They review NHERI research projects and speak directly to researchers to better understand issues that they face.

To increase awareness of the NHERI program and its research results, the TTC has created a database of the ten years of NSF Awards. This database encourages and facilitates potential implementor's investigations for applicable research results. The database also allows researchers, particularly early-career faculty, to review all NHERI projects and discover colleagues with similar interests.

As noted above, in 2023 the NHERI NCO sponsored a special collection of journal papers on NHERI technology transfer (Blain and Ramirez, 2023) entitled Technology Transfer from the Natural Hazards Engineering Research Infrastructure, NHERI. This collection includes six articles detailing the research-to-practice process associated with several NHERI projects and has had more than 29K total views.

Examples of research-to-practice impacts

High-profile NHERI projects that are resulting in technology transfer include:

- Mass-timber products as resilient material. "A Resilience-based Seismic Design Methodology for Tall Wood Buildings," also known simply as Tallwood, involved several NSF Awards stretching over almost a decade (Pei et al., 2017). The goal was to enable construction of seismically resilient tall buildings using sustainable wood material, known as mass timber systems. The culmination of the collaborations was shake table testing of a full scale 10-story Tallwood structure that included a "rocking wall" seismic resisting system and took place at the University of California San Diego NHERI facility. These successful tests point to future adoption of this new structural system.
- Incorporating building designs into ASCE7 standards. An NSF NHERI RAPID Grant (Sutley et al., 2020) facilitated the collection of valuable field data on damage to low rise buildings, particularly those elevated to avoid flood waters following Hurricane Michael in Florida in 2018. This data plus subsequent experimental wind tunnel testing at the NHERI facility at Florida International University, led to a determination of expected wind pressure loading on the floor undersides of elevated buildings for the first time. Results from this research were incorporated into the ASCE7 national standards for design of such structures, and will result in improved performance in future hurricanes.
- Incorporating wind speed maps into ASCE7 standards. The wide variety of experimental capabilities in the NHERI Network creates opportunities to coordinate and cooperate with other government agencies. Co-occurring funding from the National Institute of Science and Technology (NIST), FEMA, through the Strategic Alliance for Risk Reduction, and an NSF funded NHERI project "Exploring Machine Learning and Atmospheric Simulation to Understand the Role of Geomorphic Complexity in Enhancing Civil Infrastructure Damage During Extreme Wind Events", Masters et al. (2018) enabled characterization of the surface wind field over geometrically scaled models of Puerto Rico and the municipal islands of Vieques and Culebra. In these projects, the wind tunnel at the University of Florida and the DesignSafe cyberinfrastructure at University of Texas, both NHERI facilities, were utilized. Research results led to changes in the ASCE 7 standard wind speed maps for Puerto Rico.
- Influencing policy changes in Texas. Above ground storage tanks are subjected to wind, water, and debris impacts during windstorms, storm surge, and other events. A NHERI project developed probabilistic models of tank performance in severe storms (Bernier, C. and Padgett, J.E., 2020) using the advanced computational resources of the NHERI DesignSafe cyberinfrastructure, filling a major gap in risk assessment. The research helped influence new Texas State legislation on tank safety and is adopted by the U.S. Corps of Engineers when evaluating multi-billion-dollar investments in coastal protection.

The NCO's technology transfer efforts directly assist the National Science Foundation in achieving its goals. In fact, the NCO's Technology Transfer Committee could be viewed as a precursor of the NSF's 2022 new directorate: Directorate of Technology, Innovation, and Partnership, TIP.

Summary and future advances

The Network Coordination Office (NCO) is the core of the Natural Hazards Engineering Research Infrastructure (NHERI), the national, 12-component, distributed network. The multi-faceted role of the NCO includes network governance, education and community outreach, centralized communication, science visioning, and research-to-practice initiatives.

The leadership and guidance provided by NHERI's Network Coordination Office (NCO) fosters unity across the network through the NHERI Council, provides network feedback via external reviews by the Network Independent Advisory Council (NIAC), and gauges user satisfaction through activities of the User Forum. Furthermore, the NCO governance has facilitated coordination of two network-wide Summits in 2022 and 2024, negotiated international partnerships with research groups in Japan, Taiwan, and Europe, maintained a transparent network-wide scheduling tool, and produced multiple evolutions of a decadal science plan for natural hazards engineering research.

The NCO-led centralized education and community outreach (ECO) committee, comprised of representatives from each of the NHERI network components, organizes the annual Research Experiences for Undergraduates (REU) program and the annual NHERI Summer Institute (SI) for Early Career researchers. The NCO also established a unique, self-governing graduate student council as a means of mentorship. NSF recognizes NHERI's NCO educational programming as an example of a well-run educational pathway to STEM careers, including products for K-12 education to the inclusion of undergraduates, graduate students, and early career faculty.

The centralized communication efforts of the NCO unite both NHERI researchers and the natural hazards research community. Bi-monthly NHERI-centric newsletters, podcasts, e-mails, news stories, social media outreach, and publications all amplify the impact of NHERI's research and ensure opportunities for all components to engage with the research community.

The NHERI Science Plan presents a long-term vision for the natural hazards research community. It outlines a roadmap for high-impact, high-reward, hazards engineering and interdisciplinary research at NHERI facilities. Under the NCO's guidance, the Science Plan is designed to promote ongoing and meaningful engagement with practice, the leveraging and extension of NHERI components, and the professional development of a broad and diverse range of researchers and practitioners.

In a novel and effective approach to technology transfer, the NHERI NCO appointed and led a Technology Transfer Committee (TTC), comprised of volunteer engineering practitioners and decision-makers, to guide and encourage NHERI researchers to envision the transfer of their research findings to practice. TTC has shared a white paper on technology transfer detailing various mechanisms for implementation of NHERI research results with the NHERI community. Furthermore, the TTC has created a database covering 10 years of NSF NHERI Awards to encourage and facilitate potential implementor's investigations for applicable research results.

NCO activities engage all facilities within NHERI, uniting the network's diverse components. As "coordination" implies, the NCO team unifies and strengthens the network by guiding, educating, communicating, organizing—and overall amplifying the impact of this multifaceted NSF research network.

The NHERI NCO is presently undergoing a renewal and is prepared to continue guiding the NHERI network from September 2025 through September 2035. Knowing that the number of natural hazards events is ever rising and that new areas of concern within the nation's infrastructure are continually being identified, the need to organize and grow the natural hazards research base is stronger than ever. An expansion of the hazards to include wild urban interface (WUI) fire and inland floods is being considered for future work. There will continue to be a need to support and mentor the next-generation of natural hazards scientists and engineers at early points of their careers. The emphasis of our programs will need to adapt to the use of new technology and climate impact on the resilience of infrastructure to support activities and needs of communities. Moving forward, the NCO plans to continue and enhance ways to leverage international partnerships to continue accelerating findings, establishing new areas of growth, and honing best practices for network coordination. For the NHERI network itself, the future will likely include upgraded and expanded facilities, and the NCO must find ways to closely connect research in its infancy with future building codes and commercial outlets so that the latest new knowledge can translate into specific actions that protect people and property.

Data availability statement

The raw data supporting the conclusions of this article will be made available by the authors, without undue reservation.

Ethics statement

Written informed consent was obtained from the individual(s) for the publication of any potentially identifiable images or data included in this article.

Author contributions

CB: Conceptualization, Writing – original draft, Writing – review and editing. JR: Project administration, Writing – original draft. BE: Writing – original draft. WH: Writing – original draft. ML: Writing – original draft, Writing – review and editing. RN: Writing – original draft. IR: Writing – original draft. DZ: Writing – original draft.

Funding

The author(s) declare that financial support was received for the research and/or publication of this article. The programs and research are based upon work supported by the U.S. National Science Foundation under the Natural Hazards Engineering Research Infrastructure Network Coordination Office Award No. 2129782. Distribution Statement A. Approved for public release: distribution is unlimited.

Conflict of interest

The authors declare that the research was conducted in the absence of any commercial or financial relationships that could be construed as a potential conflict of interest.

Generative AI statement

The author(s) declare that no Generative AI was used in the creation of this manuscript.

Publisher's note

All claims expressed in this article are solely those of the authors and do not necessarily represent those of their affiliated organizations, or those of the publisher, the editors and the reviewers. Any product that may be evaluated in this article, or claim that may be made by its manufacturer, is not guaranteed or endorsed by the publisher.

References

Bernier, C., and Padgett, J. E. (2020). Probabilistic assessment of storage tanks subjected to waterborne debris impacts during storm events. *J. Waterw. Port, Coast. Ocean Eng.* 146 (3). doi:10.1061/(ASCE)WW.1943-5460.0000559

Blain, C. A., and Ramirez, J. A. (2023). Editorial: Technology transfer from the natural hazards engineering research infrastructure (NHERI). *Front. Built Environ. Sec. Earthq. Eng.* 9. doi:10.3389/fbuil.2023.1269036

Bridge, J. A., Cox, D., Kijewski-Correa, T., and Ramirez, J. (2023). "Advances and future needs for collaborative networks for natural hazards and disasters research," in Proceedings ASCE Inspire 2023: Infrastructure Innovation and Adaptation for a Sustainable and Resilient World, Arlington, Virginia, November 16–18, 2023, 217–224. doi:10.1061/9780784485163.026

Chowdhury, A., Conte, J., Masters, F., Ramirez, J., and Ricles, J. (2021). Editorial: natural hazards engineering research infrastructure (NHERI): mitigating the impact of natural hazards on civil infrastructure and communities. *Front. Built Environ. Sec. Earthq. Eng.* 7. doi:10.3389/fbuil.2021.708450

Masters, F. (2018). EAGER: exploring machine learning and atmospheric simulation to understand the role of geomorphic complexity in enhancing civil infrastructure damage during extreme wind events. *EArly-concept Grant Explor. Res. (EAGER) Award, NSF CMMI # 1841979*. Available online at: https://www.nsf.gov/awardsearch/showAward?AWD_ID=1841979&HistoricalAwards=false.

Nelson, R., Vielma, K., and Browning, J. A. (2025). NHERI education and community outreach: longitudinal, educational outcomes of a coordinated, distributed network. *Front. Built Environ. Sec. Earthq. Eng.* 11. doi:10.3389/fbuil.2025.1512507

NHERI Technology Transfer Committee (2020). Mechanisms for implementation for of NHERI research results. Available online at: https://www.designsafe-ci.org/media/filer_public/85/0c/850c36d4-4f89-4ca4-8a50-0bc13c61db4d/mechanisms_for_implementation_of_nheri_research_results_0419_finalr1.pdf.

Pei, S., van de Lindt, J. W., Ricles, J., Sause, R., Berman, J., Ryan, K., et al. (2017). "Development and full-scale validation of resilience-based seismic design of tall wood buildings: the NHERI Tallwood project," in Proceedings of the New Zealand Society for Earthquake Engineering Annual Conference, Wellington, New Zealand, April 27-29.

Phillips, B. M., Masters, F. J., Raubenheimer, B., Olabarrieta, M., Morrison, E. S., Fernández-Cabán, P. L., et al. (2023). "An experimental platform to study wind, hydrodynamic, and biochemical conditions in the littoral zone during extreme coastal storms," in *Frontiers in Ocean Observing: Emerging Technologies for Understanding and Managing a Changing Ocean*. Editor V. Kappel, M. J. Cullen, L. Costello, C. Galgani, A. Gordó-Vilaseca, S. Govindarajan, et al. 36 (Supplement 1), 64–65. doi:10.5670/oceanog.2023.s1.19

Robertson, I., Bobet, A., Edge, B., Holmes, W., Johnson, D., LaChance, M., et al. (2023). *Natural hazards engineering research infrastructure, science plan, multi-hazard research to make a more resilient world*. Third Edition. doi:10.17603/ds2-abbs-0966

Schneider, N., and Kosters, J. (2024). U.S. National science foundation natural hazards engineering research infrastructure (NHERI) decadal visioning study 2026-2035. *DesignSafe-CI*. doi:10.17603/ds2-afza-m544

Sutley, E. J., Vazquez, K., Kim, J. H., Dao, T., Johnston, B., and Hunt, J. (2020). "Performance of manufactured housing during hurricanes irma and michael," *Journal of Performance of Constructed Facilities* 34. doi:10.1061/(ASCE)CF.1943-5509.0001486

frontiers | Frontiers in Built Environment

TYPE Original Research
PUBLISHED 21 July 2025
DOI 10.3389/fbuil.2025.1546616

Check for updates

OPEN ACCESS

EDITED BY
Rebecca Napolitano,
The Pennsylvania State University (PSU),
United States

REVIEWED BY
Ram Krishna Mazumder,
Arcadis, U.S., Inc., United States
Xavier Romão,
University of Porto, Portugal

*CORRESPONDENCE
Mohammad S. Alam,
mohammad.alam@hawaii.edu

RECEIVED 17 December 2024
ACCEPTED 14 May 2025
PUBLISHED 21 July 2025

CITATION
Alam MS, Kijewski-Correa T, Roueche DB, Mosalam KM, Prevatt DO and Robertson I (2025) A unified framework for post-disaster hazard and structural assessment data collection across hazards and infrastructure typologies.
Front. Built Environ. 11:1546616.
doi: 10.3389/fbuil.2025.1546616

COPYRIGHT
© 2025 Alam, Kijewski-Correa, Roueche, Mosalam, Prevatt and Robertson. This is an open-access article distributed under the terms of the Creative Commons Attribution License (CC BY). The use, distribution or reproduction in other forums is permitted, provided the original author(s) and the copyright owner(s) are credited and that the original publication in this journal is cited, in accordance with accepted academic practice. No use, distribution or reproduction is permitted which does not comply with these terms.

A unified framework for post-disaster hazard and structural assessment data collection across hazards and infrastructure typologies

Mohammad S. Alam[1]*, Tracy Kijewski-Correa[2], David B. Roueche[3], Khalid M. Mosalam[4], David O. Prevatt[5] and Ian Robertson[1]

[1]Department of Civil, Environmental, and Construction Engineering, University of Hawaii at Manoa, Honolulu, HI, United States, [2]Department of Civil and Environmental Engineering and Earth Sciences and Keough School of Global Affairs, University of Notre Dame, Notre Dame, IN, United States, [3]Department of Civil and Environmental Engineering, Auburn University, Auburn, AL, United States, [4]Department of Civil and Environmental Engineering, Pacific Earthquake Engineering Research Center, University of California Berkeley, Berkeley, CA, United States, [5]Engineering School of Sustainable Infrastructure and Environment, University of Florida, Gainesville, FL, United States

Post-disaster field observations of the built environment are critical for advancing fundamental research that links hazard data to structural performance, cascading community impacts, and the development of effective mitigation strategies. Yet, data collection efforts remain fragmented across hazard types and infrastructure systems due to varying objectives, methodologies, protocols, and standards among investigators and organizations. To address this, a Unified Assessment Framework has been developed for standardized post-disaster hazard and structural assessment data and metadata collection across multiple natural hazards (earthquake, windstorm, coastal events) and infrastructure typologies. The framework encompasses a tiered performance assessment of infrastructure with increasing rigor and fidelity levels: Basic Assessment (BA), Load Path Assessment (LPA), and Detailed Component Assessment (DCA). The framework has been implemented as an open-access mobile application, the Structural Extreme Events Reconnaissance Network's "StEER Unified App", hosted on Fulcrum, a commercial data collection platform by Spatial Networks Inc. Along with unification of data fields, preliminary mapping rules were developed to map out existing hazard-specific damage rating scales (e.g., wind, surge/flood, rainwater ingress) to the European Macroseismic Scale (EMS-98) compatible unified damage scale, enabling consolidation of global damage ratings into a common data field, facilitating the unification of multiple hazards within a single app. In the mapping process, care was taken to retain the overarching damage level definitions (e.g., slight, moderate, severe damage) while customizing the specific descriptors to reflect hazard-specific damage mechanisms. Two use cases are presented to demonstrate the application of this framework through the StEER Unified App: a supervised pilot after the 2022 Hurricane Ian, Florida and an unsupervised deployment for the 2023 Turkey earthquake sequence. These deployments highlight the framework's flexible and scalable nature, demonstrate the feasibility of standardized

assessments, and offer insights into how data quality is influenced by assessor pre-deployment training and assessment tier, particularly for more complex tasks such as load path evaluation. This work advances the field by providing a scalable, standardized, and hazard-agnostic approach to structural field reconnaissance, enabling more consistent and coordinated data collection across events. The open-access framework and app not only support real-time deployments but also allow integration of legacy datasets into a unified platform—laying the foundation for longitudinal analyses, cross-hazard comparisons, and expanded data reuse within the Natural Hazards Engineering community.

KEYWORDS

damage rating, earthquakes, hurricanes, reconnaissance, StEER, structural assessment, Tsunamis, Tornadoes

1 Introduction

Post-disaster hazard and structural field assessments are essential for advancing both research and practice in natural hazards engineering (e.g., EERI, 1971; NRC, 2007; Delatte, 2008; Wartman et al., 2020; Kijewski-Correa et al., 2018; 2021; 2022). These assessments help correlate hazard characteristics with site-specific load effects, evaluate the performance of civil infrastructure under extreme conditions, and examine the cascading consequences for community resilience. They inform mitigation strategies, guide policy development, and ultimately contribute to more resilient built environments. Over the past several decades, detailed field investigations have been conducted following a wide array of hazard events, including earthquakes, tsunamis, tornadoes, and hurricanes. These investigations—often led by academic teams and interdisciplinary consortia—have yielded valuable insights into structural vulnerability, failure mechanisms, and post-event recovery processes. A summary of representative post-disaster assessments across various hazards is provided in Table 1, illustrating the breadth and depth of these efforts and their contributions to both engineering research and practice.

Despite advances made, data collection efforts remain fragmented across hazard types and infrastructure systems due to varying objectives, methodologies, protocols, and standards among investigators and organizations, limiting cross-event and cross-hazard analysis and comparisons. It is further compounded by the fact that raw field data often exist in cumbersome forms–such as paper notes, unstructured photographic datasets, and materials that lack appropriate metadata or geospatial context. As reconnaissance teams are often assembled on an *ad hoc* basis for each disaster response, standardization of data collection methodologies and data products across different hazard events has been challenging, hindering inter-event analyses (Roueche et al., 2023). As a result, barriers to diverse reuse and knowledge discovery remain, limiting the potential for fully understanding the interactions among hazards, infrastructure, and community resilience across multiple disaster events.

The Structural Extreme Events Reconnaissance (StEER) network was formed in 2018 (Kijewski-Correa et al., 2021) to address these issues and work toward more coordinated and standardized data collection for structural performance assessments under wind, seismic, and coastal hazards. StEER operates within the broader NHERI CONVERGE node (Peek et al., 2020), collaborating with other extreme events research and reconnaissance networks funded by the National Science Foundation. The organization uses Virtual Assessment Structural Teams (VASTs) to gather and contextualize publicly available data, news reports, and social media after major disasters to guide its subsequent field data collection efforts (Level 1 response). Field Assessment Structural Teams (FASTs) then deploy to quickly document the extent of damage over larger geospatial areas using surface-level panoramic (SLP) cameras mounted on vehicles or windshield surveys (Level 2 response). These efforts then direct the efforts of subsequent FASTs visiting target structures to conduct in-depth performance assessments (Level 3 response). StEER leveraged its partnership with Spatial Networks, Inc. to implement these performance assessment protocols in their Fulcrum platform. StEER's initial approach was to digitize the assessment guidelines that had been, to date, established within the natural hazards engineering community (e.g., ATC 20 1989; ATC 45 2004), resulting in the development of a family of hazard- and structural typology-specific mobile apps. While this approach importantly streamlined data acquisition, promoted open data reuse, and moved away from data collection on paper forms, it resulted in multiple mobile apps. Slight variations in the assessment methodology and recorded fields across these established assessment tools, and thereby the apps emulating them, eventually presented obstacles to managing the network's growing collection of data and its use for holistic knowledge discovery across different hazards and events. Moreover, while the data collected in each hazard-specific app is extensive, it still does not encompass the full range of factors likely to influence the structural performance, particularly for multi-hazards or for cascading hazards events (e.g., tsunami following earthquake, hurricane winds and surge, *etc.*). The fragmentation of data across a family of apps with variations in the recorded data fields ultimately impedes efforts to create a comprehensive understanding of built environment performance across different building typologies and hazards. In short, while StEER had greatly advanced swift collection of standardized structural assessments after hazard events, its apps still embodied the fragmentation of the community's assessment methods, limiting the ability to then swiftly draw consistent and meaningful conclusions about how structures respond to diverse

TABLE 1 Representative post-disaster field assessments by hazard type and year.

Hazard type	Notable events	Representative studies
Earthquake	Christchurch (2011) Nepal (2015) Türkiye (2023)	Elwood (2013); Wilkinson et al. (2013); Fikri et al. (2019) Barbosa et al. (2017); Brando et al. (2017) AFAD (2023); Dilsiz et al. (2023); Aktaş et al. (2024)
Tsunami	Indian Ocean (2004) Chile (2010) Japan (2011)	EEFIT (2005); Saatcioglu et al. (2005) EERI (2010); Robertson et al. (2012) EEFIT (2011); Chock et al. (2013); Suppasri et al. (2013)
Tornado	Joplin (2011) Moore (2013) Midwest (2021)	Prevatt et al. (2012a), (b); Roueche and Prevatt (2013) LaFave et al. (2014) Pilkington et al. (2021)
Hurricane	Katrina (2005) Irma (2017) Ian (2022) Helene (2024)	Robertson et al. (2007); Franco et al. (2010) Cox et al. (2019); Tomiczek et al. (2020) Cortes et al. (2022); Prevatt et al. (2022); FEMA (2023) Kyprioti et al. (2024); Alam et al. (2025)

(and potentially multi-hazards cascading and compounding) hazard scenarios.

To address these limitations, this study draws upon the diverse literature on post-disaster structural assessments across multiple hazards to develop a unified tiered structural assessment framework. This framework encompasses requisite hazard, site, structural, and performance assessment data and metadata across different hazards (earthquake, windstorm, coastal) and structure classes. The proposed framework consists of three tiers of performance assessments with increasing rigor and fidelity: basic assessment (BA), load path assessment (LPA), and detailed component assessment (DCA). The framework is implemented as a single, user-friendly open-access mobile application "StEER Unified App" on the Fulcrum platform, facilitating efficient, community-led collection of consistent, high-quality standardized reconnaissance data. The data currently fragmented across StEER's app collection was then mapped to the fields of the new unified app, consolidating all past StEER assessment data into a single backend database to promote diverse reuse and greater knowledge discovery.

This paper is organized into six sections, beginning with this introductory section (Section 1), which discusses the fragmentation of post-disaster data collection efforts across various hazards and infrastructure typologies, highlighting how these fragmented efforts hinder diverse data reuse, knowledge discovery, and the ability to fully understand the interactions between hazards, infrastructure, and community resilience across multiple disaster events. The section then emphasizes the need for developing a unified assessment framework to overcome these barriers and facilitate comprehensive hazard-agnostic assessments. Section 2 provides a detailed literature review of existing post-disaster structural assessment framework and methodologies and how this review informs the development of the unified assessment framework presented in Section 3. Section 4 outlines the implementation of the framework in a mobile application, named StEER Unified App, detailing the app's key features and unification of different assessment attributes across hazards. Section 5 presents two use cases to demonstrate the application of the proposed unified assessment framework *via* the StEER Unified App: a supervised pilot during 2022 Hurricane Ian, Florida and an unsupervised deployment for the 2023 Turkey earthquake sequence and potential learning from those use cases. Finally, Section 6 presents conclusions and recommendations for future improvements.

2 Existing post-disaster structural assessments

Various organizations, including the Earthquake Engineering Research Institute (EERI) Learning from Earthquake (LFE) program, the Army Corps of Engineers (USACE), the National Institute of Standards and Technology (NIST), and the Federal Emergency Management Agency (FEMA) have spearheaded investigations of major earthquakes, tornadoes, and hurricanes in the US. Several field investigation guidance and protocols have emerged from these institutional efforts: (i) for earthquake hazards: ATC 20 (1989); JBDPA (1991); EERI LFE (1996); FEMA 306 (1998); Hughes and Lubkowski (1999); FEMA 352 (2000); CUREE (2010); NZMBIE (2014b); BCH (2019), FEMA (2020) (ii) for wind hazards: ATC 45 (2004); BCH (2019); FEMA (2000); FEMA (2020); and (iii) for coastal hazards: ATC 45 (2004); USACE (2006); NZMBIE (2014a); BCH (2019); FEMA (2020). In parallel, individual research teams have similarly worked to advance field investigations (e.g., for earthquake hazards: Kaminosono et al. (2002); Baggio et al. (2007); Anagnostopoulos and Moretti (2008); Maeda and Matsukawa (2019); Uroš et al. (2020); for wind hazards; Roueche and Prevatt (2013); LaFave et al. (2014); Egnew et al. (2018); and for coastal hazards; Friedland (2009); Franco et al. (2010); Kennedy et al. (2011); Xian et al. (2015); Hatzikyriakou et al. (2016); Tomiczek et al. (2017). These guidelines vary in terms of assessment objectives (e.g., safety, usability, damage, repair, retrofit, *etc.*), assessment fidelity level (e.g., rapid assessment, detailed assessment, engineering assessment, *etc.*), and building typologies (wood, reinforced concrete, steel, masonry, *etc.*) for different hazards, as illustrated in Figure 1.

Notable among these are the Applied Technology Council's (ATC) Procedures for Post-earthquake Safety Evaluation of

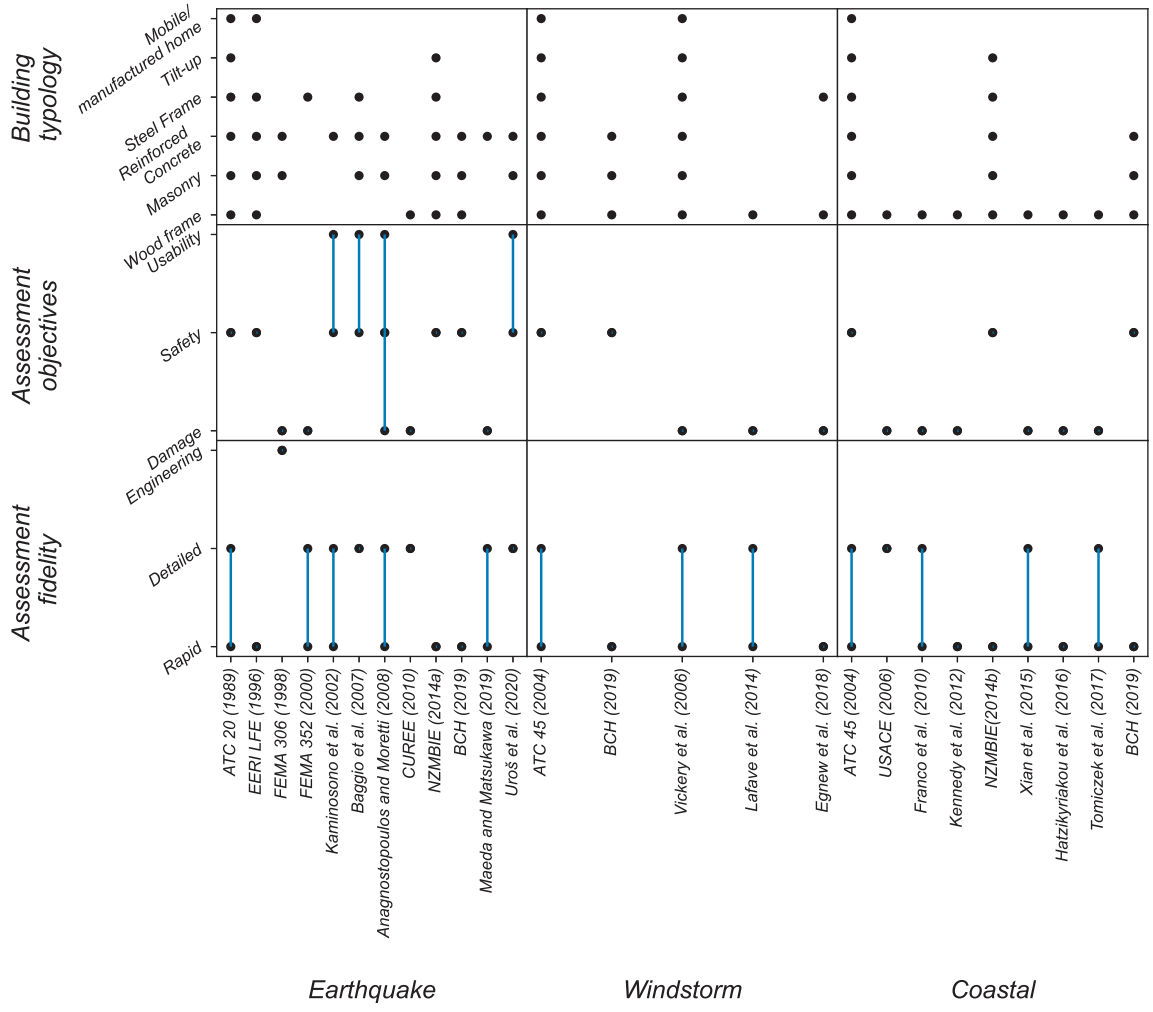

FIGURE 1
Mapping of assessment fidelity, assessment objectives, and building typology in existing post-disaster reconnaissance standards for earthquake, windstorm, and coastal hazards.

Buildings (ATC 20 1989; ATC 20-2 1995; ATC 20-3 1996), which offer guidelines for post-earthquake safety inspections. The first of these guidelines, ATC 20 (1989), serves as a field guide offering clear, structured procedures and forms for inspection and has become a widely adopted standard for post-earthquake field investigation globally. The guideline outlines a three-level assessment methodology with increasing rigor and fidelity, namely, (i) *rapid assessment*: typically completed in under 30 min, focusing primarily on the global performance assessed through inspection of exterior of the building, though interior inspections are recommended for certain special cases; (ii) *detailed assessment*: conducted after a rapid evaluation, this thorough assessment takes several hours and involves a detailed examination of both the interior and exterior with a focus on load path elements; and (iii) engineering assessment: recommended when visual and detailed assessments of load path elements are insufficient to confidently determine the extent of damage; this assessment is performed by licensed structural engineers and may take up to a week or more. The guideline was developed to address the inconsistencies and subjectivity often seen in field evaluations before any formal standard was established. Following ATC20 (1989), similar standards were developed in other countries including Japan (JBDPA, 1991), Canada (BCH, 2019), New Zealand (NZMBIE 2014b; b), and Europe (Baggio et al., 2007). Like ATC 20 (1989), the ATC 45 (2004) field manual was developed to provide comprehensive guidelines for assessing building safety after windstorms and floods, with the goal of determining whether buildings are safe for occupancy or if entry should be restricted or prohibited. The guidelines follow a similar three-level assessment methodology, including rapid, detailed, and engineering evaluations. While the rapid assessment procedures are the same for both wind- and flood-related damage, the detailed assessment requires specific procedures tailored to each hazard type.

The field data gathered varies depending on the assessment objectives and level of fidelity. For example, in *Rapid Assessments*, data collected typically includes general building damage (e.g., collapsed/moved structures, significant leaning, damage to primary structural elements), geotechnical hazards (e.g., foundation scour,

erosion, slope failure), and nonstructural damage and falling hazards (e.g., submerged ME&P system during flooding, chimney, parapet, or other falling hazards). Building performance is then rated on a global damage scale based on visual observations of structural and nonstructural damage and repair costs. Damage scales used to assess overall performance can vary, such as, qualitative scales: a four-point scale: none, slight, moderate to heavy, severe to total (Anagnostopoulos and Moretti, 2008), six-point scale: none, slight, moderate, severe, total, collapse (EERI LFE, 1996), and quantitative scales: five point-scale: none to 100% damage (NZMBIE 2014b; b), seven-point scale: no damage to 100% damage, excluding contents (ATC 20, 1989; ATC 45, 2004).

In *Detailed Assessments*, damage to structural components along the vertical and lateral-load carrying systems (columns, walls, roof framing, roof-to-wall connection, superstructure-to-foundation connection, vertical and horizontal bracing, *etc.*), nonstructural components (e.g., cladding, glazing, ceilings, and MEP systems), and geotechnical hazards (e.g., foundation issues, erosion, slope failures) are evaluated using visual inspection, measurements, and photographs. This process typically involves identifying damage mechanisms (e.g., shear, flexure, axial, sliding, overturning), damage location, damage severity, damage extent, and component behavior (ductile vs brittle) (e.g., EERI LFE, 1996; FEMA 352, 2000; CUREE, 2010; Vickery et al., 2006; Friedland, 2009; Tomiczek et al., 2017; FEMA 2022a). For earthquake assessments, damage severity of components is described both qualitatively and quantitatively, e.g., assessment of concrete structures may consider crack width, crack orientation, spalling, crushing, rebar buckling, as well as measurements of residual drift and ground movement. Component damage severity classifications include a three-point scale: slight, medium to severe, very heavy damage (Baggio et al., 2007), four-point scale: none, slight, moderate to heavy, severe to total (Anagnostopoulos and Moretti, 2008; Uroš et al., 2020), which are adapted and based on a slight variation of the European Macroseismic Scale (EMS-98) (Grünthal, 1998), and a five-point scale: I to V (Maeda and Matsukawa, 2019). For windstorms, damage severity is defined based on building envelope performance, i.e., the percent of building envelope (roof and wall subassemblies) removed or failed during a windstorm (Vickery et al., 2006; FEMA 2022a). For coastal hazards due to hurricanes, damage severity considers both building envelope damage and damage to the structural frame, foundation, and appurtenances due to wind, surge, wave, erosion and scour, and debris impacts using a seven-point scale (none, minor, moderate, severe, very severe, partial collapse, and collapse: Friedland, 2009; DS0 to DS6; Tomiczek et al., 2017).

Some detailed assessments also document the distribution and extent of damage by computing *damage extent indicators* like the damage index (FEMA 352, 2000), residual seismic capacity ratio (Maeda and Matsukawa, 2019), or percentage/number of elements at specific damage levels (Anagnostopoulos and Moretti, 2008; Uroš et al., 2020). These damage extent indicators may involve, *Level-I detailed assessment,* inspecting critical structural components and fracture-susceptible connections of some or all of the moment-frame connections within a story or *Level-II detailed assessment*, inspecting all fracture-susceptible connections in the building if multiple connection fractures and other component damage were observed in the *Level-I detailed assessment* (FEMA 352, 2000). In other cases, damage extent is evaluated by inspecting lateral frame elements of critical stories (Anagnostopoulos and Moretti, 2008; Uroš et al., 2020). For earthquakes, the component-level damage severity and extent results are then mapped to define system-level damage states using residual seismic capacity ratio, which accounts for damage to all structural members in a frame (Maeda and Matsukawa, 2019) or building safety classes (Anagnostopoulos and Moretti, 2008), or usability categories (Baggio et al., 2007; Uroš et al., 2020). For wind and coastal hazards, this component to system-level damage assignment considers the most severe damage state experienced by specific structural components (Vickery et al., 2006; Tomiczek et al., 2017).

In *Engineering Assessments*, building damage is assessed using visual inspection, investigative testing (e.g., nondestructive or intrusive), review of building drawings and design documents, and classification of component damage according to deformation modes and damage severity. These evaluations determine the impact of damage on the building's future performance through hand calculations or numerical simulations of the affected component's force-deformation response. Overall building performance may be linked to specific performance objectives: e.g., immediate occupancy, life safety, collapse prevention (FEMA 306 1998).

As discussed above and illustrated in Figure 1, while clustering of assessment methodologies across hazards is evident based on assessment objectives, fidelity levels, and structural classes, notable similarities exist among these methodologies and the types of data collected—making them largely hazard-agnostic. For instance, in *Rapid Assessments*, it is standard practice to collect basic data on site conditions, infrastructure materials, construction year, geometry, configuration, occupancy, and other metadata to correlate structural performance with site-specific hazards. These assessments evaluate the global performance of a structure primarily through external observations of key performance indicators, such as collapse or partial collapse of the structure, racking damage to primary lateral force-resisting systems, potential falling hazards, foundation failure, and site-specific geotechnical hazards. Similarly, *Detailed Assessments* focus on gathering data related to load path elements (e.g., foundation, columns, walls, beams, beam-column connections, wall-to-roof connections, and roofing systems) and documenting observed damage, though, the level of detail may vary depending on the hazard type—such as focusing on lateral frames for earthquakes *versus* building envelopes for wind events. Furthermore, if the assessment objective extends beyond evaluating damage and loss to assessing the structure's functionality, the collected data—such as building safety, access to stories, tenant safety, and operational status (FEMA 2021)—remains relevant across different hazards, underscoring the hazard-agnostic nature of such assessments.

Recently, FEMA (2020) developed a Preliminary Damage Assessment (PDA) guide to establish a standardized national framework for state, local, tribal, and territorial (SLTT) government officials and FEMA personnel. The guide aims to support the consistent, efficient, and accurate collection, validation, quantification, and documentation of damages through a uniform PDA process, ultimately aiding in requests for federal assistance through a Presidential Disaster Declaration (PDD). The PDA methodology is adaptable to different hazards, utilizing a variety of techniques including self-reporting, door-to-door assessments, windshield surveys, geospatial analysis, remote sensing, and

modeling. This marks a significant shift toward a standardized, hazard-agnostic approach to damage assessment unlike those hazard specific guidelines of ATC 20 (1989) and ACT 45 (2004). However, the PDA methodology focuses solely on preliminary damage assessments over large geographic areas, aiming to identify damage gradients and support decisions regarding federal disaster aid. It does not encompass multi-tiered assessment processes needed for deeper insights, such as correlating infrastructure performance to site-specific hazards, or understanding the complex interactions of factors affecting structural performance under multi-hazard scenarios and thus developing targeted response, recovery, and mitigation measures. Recognizing the need for a holistic, hazard-agnostic, and tiered structural performance assessment methodology, the similarities across existing assessment frameworks and data collection practices are systematically reviewed, documented, and finalized through a consensus-based approach within StEER leadership. Additionally, expert input from multiple hazard disciplines, gathered during the 2018 StEER Cross-Hazard Workshop at the University of California, Berkeley, was instrumental in identifying synergies in structural assessment data for various hazards and structural types, particularly in multi-hazard and cascading hazard contexts. All these efforts helped shape the development of the Unified Assessment Framework, which is discussed in detail in the following section.

3 Overview of StEER's unified assessment framework

Over time, StEER operationalized a number of the existing assessment protocols into its mobile app suite in Fulcrum, generally in response to the sequencing of hazard events. For instance, the first app focused on wind damage to buildings in the US in response to 2017 Hurricane Harvey, adopting HAZUS-style assessments for wood frame residential construction (Vickery et al., 2006), which was quickly followed by a second app after 2017 Hurricane Maria to accommodate concrete and masonry residential construction common to Puerto Rico. The family of apps continued to grow in response to new use cases for unique construction styles and even languages, e.g., English/Creole apps to assess formal and informal construction in Haiti after the 2021 earthquake (Kijewski-Correa et al., 2024). As the prior section illustrates, StEER's experience was not unique; the diversity of real-world performance assessment needs has driven a diversity of assessment protocols and tools in the literature, much like the diversity of custom apps that eventually unfolded in StEER's Fulcrum library. Realizing this approach was both unsustainable and counterproductive to standardizing the assessment process across hazards and structure classes, StEER embarked upon a year-long effort to consolidate its diverse assessment protocols (and Fulcrum Apps) into a single framework.

Figure 2 provides an overview of this Unified Assessment Framework, which comprises three ***data classes***: (1) Unified Assessment, (2) Hazard Survey, and (3) Performance Assessment Survey. These data classes help to organize the framework's data structure by bundling collected data with similar attributes associated with the survey parameters, observed hazards, and the assessed structures, respectively. Within each data class, ***data subclasses*** are defined to further structure the data for improved backend data storage, sorting, discovery, and unification. In the current framework, ***data fields*** describe attributes of surveys, hazards, and structures that are stored within these data subclasses. The data fields can be of various types, including single- or multiple-choice lists, text or numeric input, and media (photo, video, and audio) attachments. Efforts have been made to unify attributes across the three hazard types (earthquake, wind, coastal).

3.1 Unified assessment attributes

In this data class (see Figure 2 inset 1), a generalized data model is developed to organize a comprehensive set of attributes needed for assessments of all possible hazards (earthquake, windstorm, coastal) and structural classes (e.g., buildings, bridges, power infrastructure) so as to call up and populate the necessary sequences of fields for subsequent data classes. The attributes are categorized into several data subclasses: *Application Selection*, *General information and Metadata*, and *Supplemental Media*. Table 2 provides a high-level summary of attributes associated with each subclass. The *Application Selection* subclass encompasses data fields that describe the survey type (hazard survey, infrastructure performance assessment survey), primary and cascading hazard categories, facility category, performance assessment fidelity category, and inspection type (structural, nonstructural, both). These attributes are defined as single-choice selections from a list of data fields. The *General information and Metadata* subclass contains information related to the inspection, such as the inspector's name, affiliation, facility address, sampling method used in facility selection, and the area and elevation being assessed. The *Supplementary Media* subclass includes site photos, videos, and audio gathered by the investigator, as well as asset maps developed by the supporting team to aid in the field investigation. It also incorporates street view and aerial imagery gathered from secondary sources to facilitate the field investigation team's survey efforts. Within the Unified Assessment data class, unification of attributes is achieved at the data class and subclass hierarchy level across hazards (see Table 2).

3.2 Hazard survey attributes

In the Hazard Survey data class (see Figure 2 inset 2), both qualitative and quantitative data is gathered to estimate the hazard intensity at the site being assessed. This data class includes three distinct subclasses: *Earthquake Hazard Survey, Wind Hazard Survey*, and *Coastal Hazard Survey*. Table 3 provides a high-level summary of attributes associated with each hazard survey subclass. The *Earthquake Hazard Survey* subclass encompasses data fields on general earthquake information (e.g., date and time, moment magnitude, location, *etc.*), specific intensity information (e.g., ShakeMap shaking estimate, site peak ground acceleration, site-to-epicenter distance, *etc.*), ground motion recording information, and primary and secondary effects observed at the site. In the *Wind Hazard Survey* subclass, wind hazard intensity indicators such as downed trees, towers, and signposts are used as surrogates to gauge wind hazard intensity in the field. Data collected includes the indicators' geometry, material properties, damage patterns, and

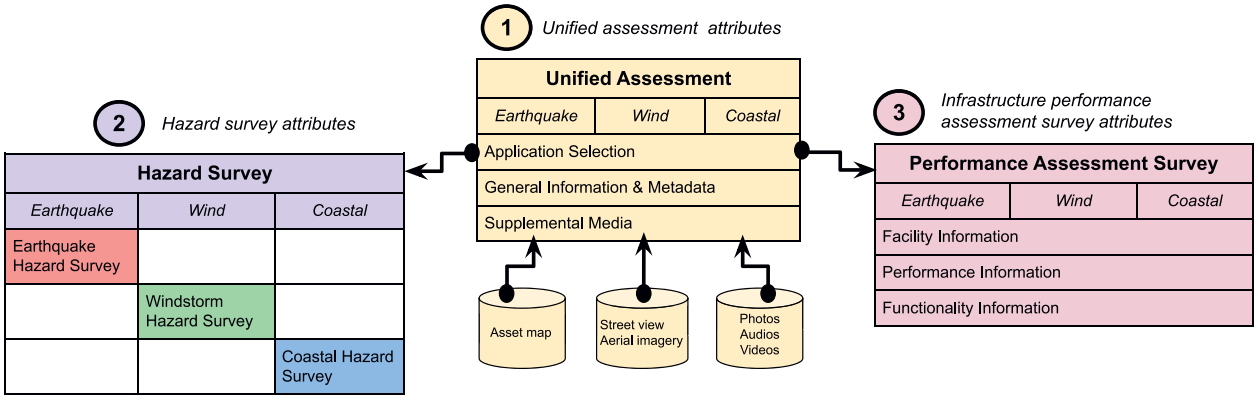

FIGURE 2
Overview of the Unified Assessment Framework illustrating the primary data classes and degree of unification across different hazard types.

TABLE 2 Summary of data subclasses under Unified Assessment data class and associated unification across hazards.

Data subclass	Earthquake	Wind	Coastal
App Selection • Survey category • Primary hazard category • Cascading hazard category • Performance Assessment category • Facility category • Inspection type	x		
General Information • Inspection metadata • Sampling method • Area assessed • Elevation assessed	x		
Supplementary Media • Site media • Secondary media	x		

"x" indicates unification of data subclasses achieved across hazards.

TABLE 3 Summary of data subclasses under Hazard Survey data class and associated unification at individual hazard level.

Data subclass	Earthquake	Wind	Coastal
Earthquake Hazard Information • General earthquake information • Shaking information • Ground motion recording • Primary and secondary hazard at site	x	—	—
Wind Hazard Information • Wind hazard indicators • Wind hazard indicator information	—	x	—
Coastal Hazard Information • Flow intensity measure • Maximum flow depth • Maximum flow velocity • Waves information	—	—	x

"x" indicates unification of data subclasses achieved across hazards.

damage distribution. The *Coastal Hazard Survey* subclass focuses on gathering surge and wave characteristics, such as maximum flow depth, maximum flow velocity, and wave height and period, through various measurement methods, including photo and video evidence, field measurements, post-event modeling, flow surrogate geometry, observed damage, and material properties. In the Hazard Survey data class, unification of attributes is achieved only at the individual hazard survey subclass level, as attributes are unique to each specific hazard (see Table 3).

3.3 Performance assessment survey attributes

In the Performance Assessment Survey data class (see Figure 2 inset 3), information related to the facility and its observed performance and functionality is gathered under three data subclasses: *Facility Information, Performance Information,* and *Functionality Information.* Table 4 provides high-level summary of attributes associated with each subclass and unification of those attributes across hazards. *Facility Information* data is further categorized into site characteristics, facility basic metadata, structural information, and nonstructural information. Site characteristics attributes include site location on slope or beachfront, site soil classification, flood zoning, and terrain classification. These characteristics encompass the range of site conditions potentially affecting structural performance under different hazard conditions, e.g., beachfront properties and properties on slope are vulnerable to earthquakes and in the event of cascading earthquake-tsunami events (Suppasri et al., 2013; Alam, 2024), whereas terrain characteristics influence the structural windstorm performance (Kopp and Fewless, 2014). Facility material, geometry and configuration, construction year, and other relevant metadata

TABLE 4 Summary of data subclasses under Performance Assessment Survey data class and associated unification across hazards.

Data subclass	Earthquake	Wind	Coastal
Facility information • Site characteristics • Facility geometry and other metadata • Structural attributes • Nonstructural attributes		x	
Performance information • Structural performance • Nonstructural performance		x	
Functionality information • Functionality state		x	

known to affect performance under different hazards are collected under Facility Basic Metadata. For buildings, the framework compiles metadata such as the number of stories above and below grade, elevation of the lowest story, mean roof height, vertical (elevation) and horizontal (plan) irregularity, occupancy category, retrofit details, and instrumentation information. Structural information data entails collecting structural systems and components information along the structural load path from foundation to the superstructure. For buildings, this includes structural system classification, structural component information including foundation details, wall subassemblies (framing, anchorage, substrate), fenestration, roof-to-wall attachments, roof subassemblies (framing, cover, secondary water barrier, substrate), soffits, *etc.* For buildings, the structural systems included in the current implementation of the framework are based on the FEMA-310 classification (FEMA 310 1998). This classification represents the structural systems prevalent in the US and is adopted in all HAZUS regional loss modeling methodologies for earthquakes, tsunamis, and hurricanes (FEMA, 2024; FEMA 2022b; FEMA 2022a). Nonstructural information encompasses mechanical, electrical and plumbing (ME&P), interior partitions, and contents.

The *Performance Information* subclass records observed infrastructure performance indicators (e.g., damage, loss, downtime, *etc.*). The level of detailed performance data gathered depends on the infrastructure performance assessment fidelity level. Currently, StEER's field investigation protocols support three increasingly rigorous performance assessments, namely, Basic Assessment (BA), Load Path Assessment (LPA), and Detailed Component Assessment (DCA). Figure 3 depicts the purpose, tradeoffs, use case, and the type of data collected for each of the performance assessment fidelity levels. Note from Figure 3 that the assessments build on one another, e.g., Detailed Component Assessment includes all the fields of the LPA and BA, plus additional fields unique to the DCA.

Finally, *Functionality State* subclass documents the functional recovery state of the structure being assessed. In the current implementation of the framework, the functional recovery state of the building is assessed based on the building safety, story access, tenant safety, and tenant function following the functional recovery methodology outlined in FEMA (2021). Within the Performance Assessment Survey data class, unification of attributes is achieved at the data field level only in a few instances (see Tables 5, 6), with unification across two hazards being more common. Moreover, although not shown herein for brevity, unification of attributes also depends on the performance assessment fidelity level.

In summary, the unified framework adopts a modular design, enabling the collection of hazard-specific observations within a common data architecture. Each hazard type—such as earthquake or windstorm—is supported by tailored data entry fields that align with the physical manifestations and structural consequences unique to that hazard. This design ensures that key performance indicators—such as shear cracking and pounding for earthquakes; roof uplift and cladding loss for windstorms; and inundation depth, scouring, or waterborne debris impacts for tsunamis—are accurately documented. This simplifies the number of apps and databases that must be maintained by organizations like StEER who respond to different hazard classes. As these hazards can occur in a cascading or compound sequence (e.g., tsunami following earthquake, hurricane surge and wave accompanying wind and rain) this avoids users from having to engage multiple hazard-specific apps to document each of these effects on a site. In short, the harmonized data structure of the unified assessment framework is designed to facilitate cross-event and even cross-hazard analysis while preserving the fidelity of hazard-specific insights.

4 App implementation

The Unified Assessment Framework was implemented as a mobile application within the Fulcrum platform, which StEER has used for its Field Assessment Structural Teams (FASTs) since 2017. In addition to being free of charge for humanitarian groups at the time, Fulcrum was selected for its robust offline functionality and flexible cloud syncing, which are critical features in post-disaster environments with limited or intermittent connectivity. Once installed on a mobile device, the app enables surveyors to collect and store observations entirely offline. In the event of complete internet disruption—common after disasters—data is saved locally and automatically synced to the cloud when connectivity is restored. This ensures uninterrupted data collection and reduces the risk of information loss during time-sensitive field operations. In addition to offline capability, and its robust integration with the EsRI suite of services, Fulcrum supports user-level access controls, encrypted data storage, and multiple export formats. These features enhance data security, promote cross-platform compatibility, and support compliance with data protection standards and are downloadable for iOS and Android from all commercial app stores, making the platform well-suited for coordinated, volunteer post-disaster reconnaissance efforts.

Figure 4 illustrates the data flow through the Fulcrum app named as the **StEER Unified App,** designed to be used by FASTs for all future event responses, regardless of the hazard or structure type. The app features nested menus that intelligently display relevant sections and data fields based on the hazard type, assessment class, and infrastructure type under investigation. Information provided in earlier sections of the app will dictate the fields presented to the user in later sections, taking advantage of Fulcrum's embedded logic with conditional if-else statements and logical AND/OR operators. To prepare FAST members for effective use of the app, a

	Basic Assessment (BA)	Load Path Assessment (LPA)	Detailed Component Assessment (DCA)
Purpose	Global performance assessment.	Component-level performance assessment.	Component-level performance assessment with details necessary for advanced analysis.
Data	**Global Performance Information** *Overview damage photos* *Close view damage photos* *Observed Conditions* *Structural damage* *Non-structural damage* *Global damage rating* *Functionality Information*	**Basic Assessment (BA)** + **Component Performance Information** *Geolocation of damaged Critical Load Path Elements (CLPE)* *Damage measure/classes* *Component damage rating*	**Basic Assessment (BA)** + **Load Path Assessment (LPA)** + **Enhanced Component Performance Information** *Specifications (manufacturer, impact rating, etc.)* *Dimensional data* *In-Situ non-destructive measurement, LiDAR scan* *Sample collection for lab testing*
	 Slight *Moderate* 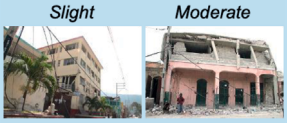 *Severe* *Partial / total collapse*	 *Foundation* *Wall* *Roof* *Column*	 *Soil sample* *Nail size* *Specification* *Nondestructive measurement*
Trade offs	Maximize observations, minimum fidelity.	Fewer observations, more robust damage rating potential.	Limited observations, maximize fidelity.
Use case	Identifying damage gradient, patterns of failure.	Damage quantifications mapped to key rating systems.	Detailed modeling, forensic reconstruction, hindcasting.

FIGURE 3
StEER's increasingly rigorous performance assessment levels: Basic Assessment (BA), Load Path Assessment (LPA), and Detailed Component Assessment (DCA) with summary of purpose, collected data, trade-offs, and use cases.

TABLE 5 Example unification of site characteristics attributes across hazards.

Data fields	Earthquake	Windstorm	Coastal
Site on slope?	x	—	x
Site on beachfront?	x	—	x
Site soil class	x	—	—
Site flood zone	—	—	x
Wind exposure category	—	x	—

comprehensive set of training resources was developed, including a detailed handbook, quick reference sheet (QRS), and instructional videos. These materials were integrated into the pre-deployment briefing—a guidance document containing all relevant information on resources and planning to support FAST operations during active missions. These resources are also publicly available at https://www.steer.network/resources.

As illustrated by Figure 4, the app consists of six major sections: *App Selection, General Information, Supplemental Media, Survey Classes,* and *Record Update Tracking*. The data subclasses and data fields in each section closely follow those described in Section 3, with the addition of the *Record Update Tracking* section. This backend feature is not available to field teams and is intended to document

10.3389/fbuil.2025.1546616

TABLE 6 Example unification of facility basic metadata attributes across hazards.

Data fields	Earthquake	Windstorm	Coastal
Facility material	x		
Construction year	x		
Number of units	x		
Typical story height	x		
Elevation of the lowest floor	x	—	x
Roof shape	—	x	—
Roof slope	—	x	—

the data enrichment and quality control (DEQC) processes engaged by virtual data librarians once field data gathering is complete. Table 7 provides a brief overview of the purpose and type of data collected in each section of the app. In the current version of the app, only Basic Assessment (BA) is available to the users. Work is underway to synthesize and unify relevant fields for two additional assessment levels: LPA and DCA. A complete list of all app fields under each section, along with logic implemented to organize and display relevant sections and fields, is provided in Supplementary File S1. *Unified App: Master Data Sheet.*

Note, while the unified framework has been primarily developed to support coordinated field data collection within the StEER network, it is deliberately designed to be openly accessible and highly adaptable, aiming to facilitate consistent, high-quality data collection across a broad spectrum of users, from individual researchers to multidisciplinary response teams. The framework is readily available to academic, governmental, and professional organizations interested in adopting or customizing it to meet their specific post-disaster assessment needs; its implementation in Fulcrum is available through StEER's account which all members can access. Users can further tailor the framework—such as modifying forms to reflect local construction practices, hazard types, or regulatory requirements—by adapting the data fields in Supplementary File S1. *Unified App: Master Data Sheet* within the platform of their choice or working with a cloned version of the StEER Fulcrum App.

4.1 Special fields: required fields

The data fields in the app are primarily classified into three categories: Required Field (RF), Field Priority (FP), and media attachments. RFs, marked with red asterisks (*), must be completed by field investigators as their responses trigger conditional logic in the app, instructing the display of subsequent sections, data subclasses, and associated fields throughout the app. Refer to the Supplementary File S2. *Unified App: Required Fields* for a complete list of required fields associated with different sections of the app.

The color-coded data subclasses in Figure 4 illustrate the high-level dependencies between different sections and data subclasses in the app. These dependencies are coded as conditional logic using the RF responses in *App Selection* and other sections of the app. See the Supplementary File S1. *Master Data Sheet* for a complete list of all dependencies.

One of the key RFs in the app is the Sampling Method under the *General Information* section. Currently, StEER employs six sampling methods for selecting buildings and other infrastructure for assessment in the field. These sampling methods include: (i) *statistical sampling* where every *N*th building in a cluster or along a route is assessed; (ii) *critical case sampling* selects buildings that meet specific criteria, e.g., instrumented or has targeted performance characteristics; (iii) *cluster-based sampling* where buildings within a defined radius of point are sampled, e.g., within X meters of a ground motion station; (iv) *transect-based sampling* that involves sampling buildings along a path that moves across the hazard intensity gradient; (v) *quota-based sampling* that involves sampling buildings to achieve a representative sample based on characteristics of underlying building inventory; and (vi) *opportunistic sampling,* which involves assessment of structure not included in initial sampling strategy, based upon unique features or performance observed in the field. The recommended sampling method(s) are communicated to the field team through the Field Assessment Structural Team (FAST) Pre-Deployment Briefing.

4.2 Special fields: field priorities

Given the comprehensive and rigorous nature of the unified assessment, it is not efficient or feasible for field investigators to complete every data field on-site. Therefore, the app prioritizes (i) capturing clear photographs of the site and structure from multiple perspectives, (ii) accurately geolocating the assessment, and (iii) populating the field priority (FP) fields. FP fields gather information that is typically discernible only through on-site forensic investigations and may otherwise be impossible for a virtual investigator to gather later. FP data fields are marked as "(Field Priority)" in the app. Refer to the Supplementary File S3. *Unified App: Field Priority Fields* for a complete list of FPs associated with different sections of the app. The majority of the RFs and FPs are single- or multi-choice lists, or text/numeric input fields. Additionally, field investigators are encouraged to note any unusual or unique characteristics of the hazard and structures that might affect their performance under a given hazard, capturing these observations through available free-form notes fields, additional photographs, and sketches. Extra guidance is provided throughout the app using descriptive field titles and text labels for any data fields that are not self-explanatory, helping to clarify the intended purpose of the questions. Figure 5 shows mobile app screenshots highlighting these and other features of the app.

4.3 Special fields: media

The app heavily relies on visual evidence to document site conditions (under the *2. Supplemental Media Attachment*

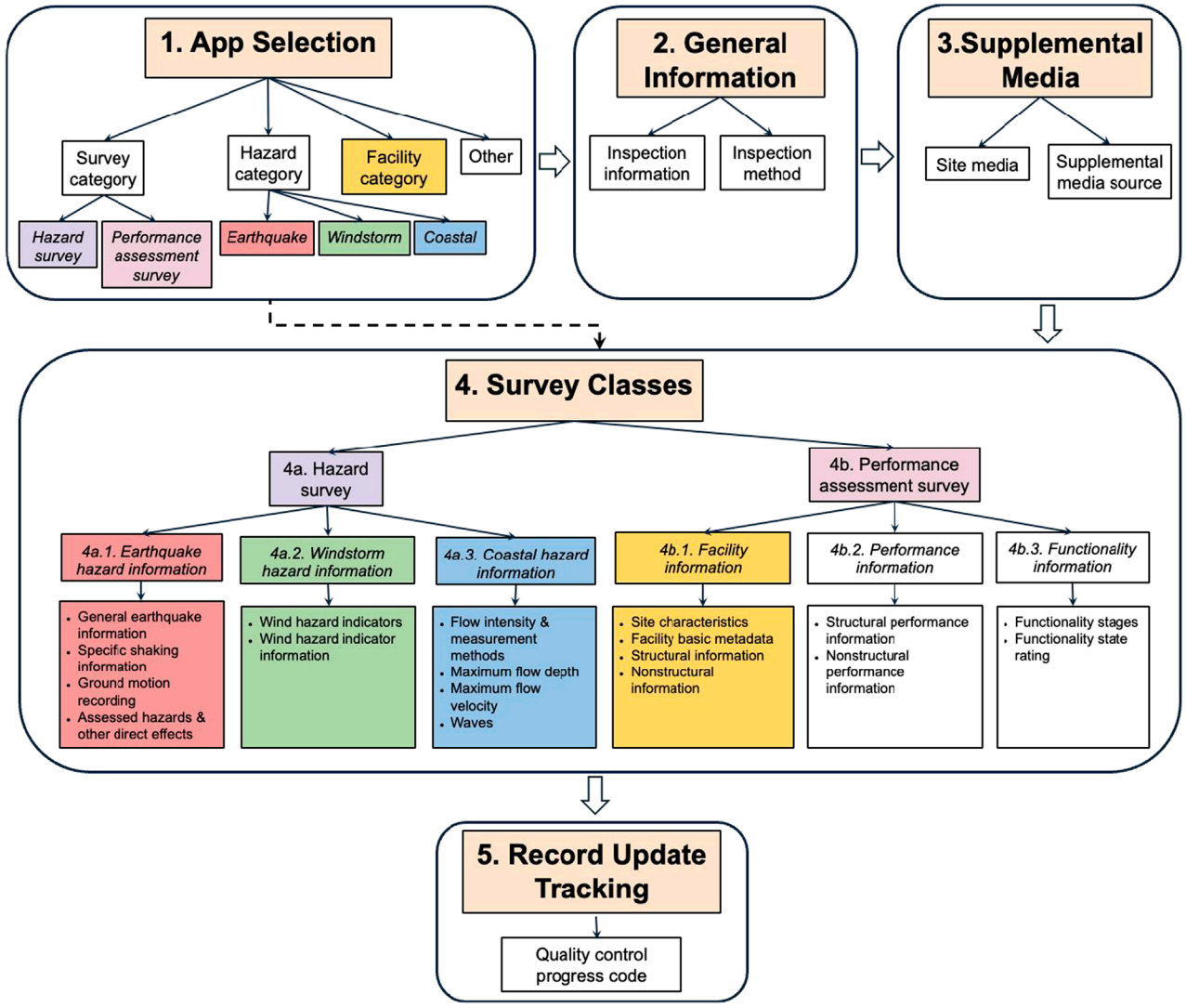

FIGURE 4
Flowchart of the StEER Unified App operationalizing the Unified Assessment Framework in Fulcrum.

section) and infrastructure performance (under the *4b.2 Performance Information* subsection). For documenting site conditions surrounding the structure/site under investigation, field investigators are required to take photos in counterclockwise sequence (1: front, 2: right side, 3: back, and 4: left side) facing away from the structure being investigated. Using the counterclockwise sequence protocol while taking photos ensures documentation consistency, aids in the DEQC process, and aids with detailed numerical modeling at later stages. In the Performance Information subsection, irrespective of the assessment fidelity levels, i.e., BA, LPA, or DCA, visual evidence of structural and nonstructural damage is gathered through (i) *overview photos* - where photos of each accessible face of the structure are taken in counter clockwise direction from a distance sufficient to capture the full elevation; and (ii) *detail photos* - where close-up photos of component damage (e.g., damage to columns, beams, walls, connections) are documented. Field investigators are advised to avoid taking highly zoomed-in pictures that hinder identification of the location of the damage with respect to overall geometry of the structure or component. Additionally, the app includes options for audio dictations and video recordings or free-form note fields to document additional context or observations as needed. To ensure a standardized visual record of the site and structure context, a counterclockwise photo sequence is recommended: (1) front, (2) right, (3) back, (4) left. However, it is recognized that full coverage may not always be feasible due to site constraints, e.g., attached buildings or due to site debris. In such cases, investigators are encouraged to capture as many views as possible (ideally with compass orientation embedded in the photo metadata) and to document inaccessible sides using metadata fields or field notes. This flexible approach ensures adaptability to real-world conditions without compromising the value of a consistent visual record.

In App Selection, users can designate both the primary hazard, and any cascading hazards observed on site, which triggers the app's logic to present fields relevant to both the

TABLE 7 Summary of the purpose and types of data collected in different sections of the app.

1.0	App selection	Desired survey and assessment type, based on hazard and structure.
2.0	General Information	Survey parameters, spatial data.
3.0	Supplemental Media	Media on structure, site.
4.0	Survey Classes	*(adapts based on choices in App Selection)*
	4a. Hazard Survey	Select to document evidence of hazard intensity.
	4a.1 Earthquake Hazard Information	Earthquake source mechanism (magnitude, depth, location), recorded and qualitative shaking information at the site, and other secondary effects.
	4a.2 Windstorm Hazard Information	Windstorm metadata, hazard intensity indicators including trees, towers, signposts metadata and damage observations.
	4a.3 Coastal Hazard Information	Flow condition measurement at site including high water mark (HWM), runup, flow velocity, wave condition.
	4b. Performance Assessment Survey	Select to document evidence of hazard impacts to built environment.
	4b.1 Facility Information	Basic structure information, typology.
	4b.2 Performance Information	*(adapts based on choices in App Selection)*
	Basic Assessment (BA)	Photo documentation, overall conditions, global performance rating.
	Load Path Assessment (LPA)	Documentation and evaluation of critical load path elements.
	Direct Component Assessment (DCA)	Detailed component information, dimensional data, specifications.
	4b.3 Functionality Information	Documents functional recovery/recovery state.
5.0	Record Update Tracking	Notes on quality control, record updating. This is a backend section, not available to the field team.

primary and cascading hazards in subsequent sections and subsections. For example, in a multi-hazard scenario involving a tsunami following an earthquake, selecting Earthquake as the primary hazard and Tsunami as the cascading hazard prompts the app to display facility descriptions relevant to both hazards (e.g., vertical and horizontal irregularity relevant to earthquake damage, and elevation of the lowest horizontal structural member relevant to tsunami exposure) under Subsection *4b.1: Facility Information*. Similarly, under Subsection *4b.2: Performance Information*, the data fields are designed to support both hazard-specific and multi-hazard performance indicators (e.g., soft-story collapse for earthquakes vs debris impact, breakaway wall performance, and floor slab uplift for tsunamis). Users can attribute damage observations to specific hazards by selecting from a predefined list, pairing these observations with geotagged and labeled photos and supplementing them with descriptive notes to provide spatial and contextual clarity. In another scenario, during a coastal hurricane event, users can distinguish between surge and wave damage to lower stories and wind or rain effects on upper stories—capturing the location-specific impacts of multiple hazards within a single structure. Figures MH.1 and MH.2 in Supplementary File S4*: Unified App: Multi-Hazard Fields* showcase screenshots highlighting the multi-hazard (e.g., cascading or/and compounding) documentation capabilities of the StEER Unified App.

4.4 Unified damage rating scale

As discussed in Section 2, numerous qualitative and quantitative damage scales exist, both within individual hazard domains and across different hazards (e.g., Vickery et al., 2006; Baggio et al., 2007; Anagnostopoulos and Moretti, 2008; Friedland, 2009; Tomiczek et al., 2017; Uroš et al., 2020), creating significant challenges for consistent damage assessment. StEER, similar to its hazard-specific mobile apps, has utilized various damage rating scales: (i) for earthquakes–a five-point scale (none, minor, moderate, severe, collapse) by Baggio et al. (2007), (ii) for windstorm: a five-point scale (none, minor, moderate, severe, destroyed) by Vickery et al. (2006), and (iii) for coastal hazard: a seven-point scale (none/very minor, minor, moderate, severe, very severe, partial collapse, collapse) by Friedland and Levitan (2011). The integration of standardized and consistent field damage assessments significantly enhances the accuracy of damage estimates derived from engineering predictions or remote sensing driven proxies, which play a critical role in informing response and recovery decisions, better situational awareness, reoccupation decisions, and the allocation of recovery funding (Loos et al., 2022). In recent years, the earthquake engineering community has made significant strides in developing an International Macroseismic Intensity (IMS) scale, inspired by the EMS-98 scale (Grünthal, 1998), for global adoption (Wald et al., 2024). This scale, which is

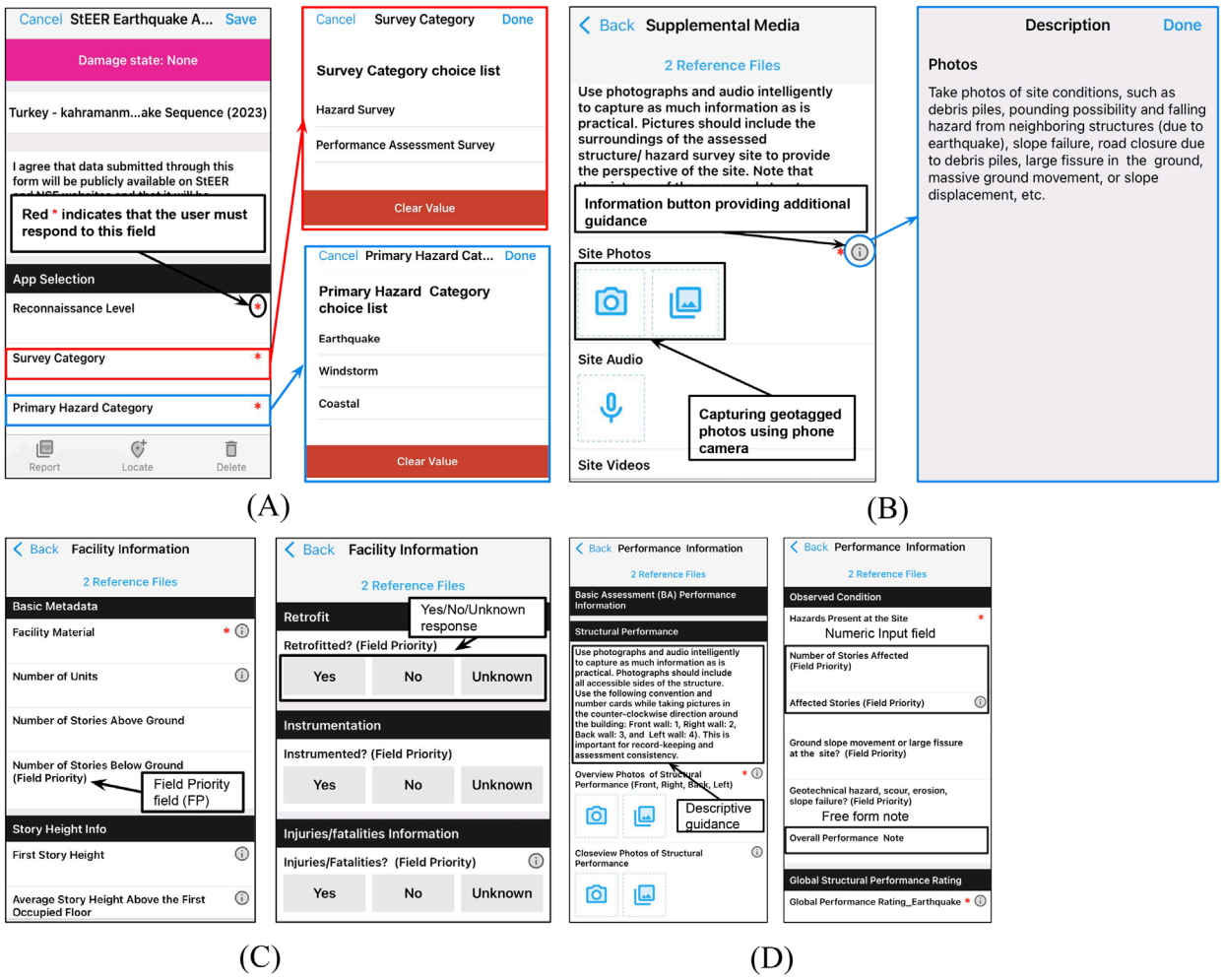

FIGURE 5
Snapshots in iOS highlighting key features of the StEER Unified App **(A)** Required Fields (RF) marked with red asterisks (*) dictates app logic, displaying relevant sections, data subclasses, and fields for hazard- or performance-specific assessments, along with associated choice lists; **(B)** visual evidence collection using geotagged photos taken with the phone camera, with guidance provided *via* the information button (i); **(C)** Field Priority (FP) fields labeled as "Field Priority" and associated single-select responses ("Yes/No/Unknown"); and **(D)** descriptive guidance for capturing visual evidence of structural performance, including both overview and close-up geotagged photos, numeric input fields, and free-form notes for documenting unique hazard characteristics and structural performance.

parameterized by building vulnerability and damage grades, serves as a crucial proxy for instrumented seismic intensity measures. The building vulnerability metrics can be adapted to regional or country-specific building typologies, such as those developed for the U.S. (Hortacsu et al., 2024) and New Zealand (Charleson et al., 2024). Given that instrumented hazard intensity measurements—like wind speed, inundation depth, or flow velocities at specific infrastructure locations during windstorms or coastal events—are often rare and impractical, developing a similar intensity scale to correlate damage with hazard intensity, akin to the IMS, is a logical and valuable step forward. In response to this need, the current version of the StEER Unified App introduces a preliminary mapping rules to map out existing hazard-specific damage rating scales-such as Vickery et al. (2006) for wind and Friedland and Levitan (2011) for coastal hazards to EMS-98-consistent scale. In consolidating damage ratings to a common scale for purposes of unification in the app's data structure, care was taken to retain the overarching level definitions (e.g., slight, moderate, severe damage) while customizing the specific descriptors to reflect hazard-specific damage mechanisms. For example, earthquake-related damage states include descriptors such as "shear cracking" or "wall out-of-plane instability," while wind damage descriptors reference roof loss, wall breach, and debris impact. Each hazard retains its own technical language and damage indicators, and the framework avoids directly transferring seismic descriptors to other hazards. Instead, EMS-98 is used as a conceptual scaffold for a common data structure to promote cross-hazard comparability while preserving hazard-specific relevance and remaining committed to further refinement. Detailed information on this preliminary mapping is provided in the Supplementary File S5: *Quick Reference Sheets: Global Damage Ratings Mapping* and is also available at https://www.steer.network/resources.

It is important to note that this mapping effort of consolidating global damage rating into a common data field was intended solely to support unification of the app's data structure and

not to propose a new damage rating scale or enforce strict equivalencies across hazards. Such harmonization would require rigorous expert consensus. Should such consensus emerge in the future, the app can be readily updated. For now, the initial mapping of wind, surge/flood, and rainwater ingress damage provides a starting point—though admittedly it may not fully reflect the balance between structural and nonstructural impacts for non-seismic hazards, especially when compared to EMS-98's generalized structure. Users are encouraged to consult accompanying guidance documents to interpret the damage ratings within the context of each hazard. This limitation highlights an opportunity for future refinement through the establishment of hazard-specific expert working groups. These groups could enhance the scale by developing more detailed descriptors of structural impacts. For instance, "moderate" flood damage could be better defined by including indicators of structural material degradation—such as corrosion at connections or warping of timber framing—while "moderate" rainwater ingress might include early signs of structural deterioration, like ceiling sag or partial failure of roof sheathing. Such refinements will improve consistency across hazard types and ensure that equivalent damage levels reflect comparable severity in both structural and nonstructural terms.

4.5 Unification of data fields

Table 8 lists the number of data fields in different app sections unified across hazards and structural typologies. In the first three sections, categorized under the Unified Assessment data class (refer to Figure 2), all data fields have been unified, totaling 23 out of 23. This includes seven out of seven fields in *App Selection*, nine out of nine in *General Information*, and seven out of seven in the *Supplemental Media* section. This comprehensive unification is possible because the data fields in these sections are applicable to all hazards, facilitating app branching in subsequent sections for either *Hazard Survey* or *Performance Assessment Survey* classes. In the Survey Classes, unification has been achieved for 110 out of 278 data fields. However, no unification was possible in the *Hazard Survey* section, where the 133 data fields are unique to different hazards. In contrast, the *Performance Assessment Survey* section achieved unification for 110 out of 145 data fields across hazards. As illustrated in Tables 5 and 6, among the remaining 35 data fields in this section, unification across two hazards is more prevalent than no unification at all. In total 133 data fields have been unified out of a total of 301 in the Unified App.

5 Illustrative use case

Two use cases are presented to demonstrate the application of the proposed Unified Assessment Framework *via* the StEER Unified App in Fulcrum: a supervised pilot during 2022 Hurricane Ian, Florida and an unsupervised deployment for the 2023 Turkey earthquake sequence. Hazard-specific apps, StEER Coastal App_v3 for Hurricane Ian and StEER Earthquake App_v2 for Turkey earthquake, were used. Feedback and user experience gathered from these two events contributed to the synthesis and unification of the data fields from these apps into the StEER Unified App_v1, through a consensus-based unification process led by StEER leadership. For Hurricane Ian, a FAST team was deployed by StEER for comprehensive data collection using a mixed methodological approach, which included: (i) rapidly imaging a wider cross-section of impacted regions using surface-level panoramas (SLP), (ii) aerial imaging of the barrier islands using unmanned aerial systems (UAS), (iii) surveying high-water marks (HWMs) and inundation extents across multiple sites, and (iv) conducting performance assessments of damage to buildings and other infrastructure, for which the app was used under the supervision of the first author (who was embedded with the FAST). In contrast, for the Turkey earthquake sequence, StEER did not deploy its own team but instead supported the Earthquake Engineering Field Investigation Team (EEFIT) by providing access to the StEER Earthquake App_v2 and training materials for their team's self-directed structural assessments. The following use cases for these two events highlight the types of data gathered, the completeness of the data, its dependency on pre-deployment training of the app, and the time required to complete assessments of different fidelity levels—specifically, the LPA conducted by StEER FAST *versus* the BA conducted by EEFIT.

5.1 2022 Hurricane Ian

On 28 September 2022, Hurricane Ian made landfall near Cayo Costa, Florida, as a Category 4 hurricane, with peak sustained wind speeds over water estimated at 150 mph and a minimum surface pressure of 940 mb (NHC, 2022). Storm surge inundation measurements reached 7.5 m relative to NAVD88. Despite being a below-design-level wind event, the storm surge impacts were catastrophic, resulting in significant damage to infrastructure and loss of human lives along the densely populated west coast of Florida, particularly in the barrier islands of Fort Myers Beach (FMB), Sanibel, Saint Carlos, Cape Coral, and Bonita Beach (Cortes et al., 2022). Additionally, heavy rainfall led to extensive inland flooding across Florida and into the Carolinas as Ian made a second landfall there on September 30.

In response to Hurricane Ian's impact, StEER activated all the way to Level 3, deploying multiple FASTs in phases to the landfall region (Prevatt et al., 2022). At Level 3, an 18-member team collected data from October 19 to November 4, 2022, which included specialists in aerial and surface imaging, high-water mark (HWM) documentation, and structural assessment, ensuring a diverse skill set for comprehensive data collection. The structural and coastal teams conducted a thorough assessment of 273 buildings and documented 177 HWMs using the StEER Coastal App_v3 (see Figure 6). As shown in Figures 7A, the data collection ensured hazard intensities were documented *via* HWM collocated with performance assessments of affected structures. Figures 7B–E showcase photographs from the HWM assessments and the structural performance assessment of a local post office in FMB. The majority of structural assessments focused on residential buildings (single family 64.7% and multi-family 17.85%), with limited representation of commercial (~7.8%) and critical facilities (~1.8%). The FAST collected extensive data within the Fulcrum app using the LPA option, capturing various attributes such as location, year built, building category, structural systems, details of

TABLE 8 Unification of data fields across hazards and structure typologies.

Sl no.	App sections	Earthquake	Wind	Coastal
1.0	App selection	(7/7)[a]		
2.0	General Information • Inspection information • Inspection method	(9/9) (6/6) (3/3)		
3.0	Supplemental Media • Site media • Supplement source	(7/7) (3/3) (4/4)		
4.0	Survey Classes	(110/278)		
	4a. Hazard Survey	(0/133)		
	4a.1 Earthquake Hazard Information • General earthquake information • Specific shaking information • Ground motion recording • Assessed hazards and other site effects	(0/22) (0/4) (0/3) (0/10) (0/5)		
	4a.2 Windstorm Hazard Information • Wind hazard indicator • Wind hazard indicator information	(0/24) (0/1) (0/23)		
	4a.3 Coastal Hazard Information • Flow intensity and measurement methods • Maximum flow depth • Maximum flow velocity • Waves	(0/87) (0/2) (0/26) (0/56) (0/3)		
	4b. Performance Assessment Survey	(110/145)		
	4b.1 Facility Information • Site characteristics • Facility basic metadata • Structural information • Nonstructural information	(65/89) (1/5) (27/32) (25/37) (12/15)		
	4b.2 Performance Information	(31/42)		
	Basic Assessment (BA) • Structural performance information o Structural performance media o Observed condition o Global structural performance rating • Nonstructural performance information o Architectural component performance (9/9) o ME&P component performance (4/4) o Content performance (3/3) o Loss of nonstructural components (3/3)	(31/42) (12/23) (4/4) (7/18) (1/1) (19/19) (9/9) (4/4) (3/3) (3/3)		
	Load Path Assessment (LPA)	Not adopted in the current version of the app		
	Direct Component Assessment (DCA)	Not adopted in the current version of the app		
	4b.3 Functionality Information • Stage 1: Building safety • Stage 2: Story access • Stage 3: Tenant safety • Stage 4: Tenant function • Functionality State	(14/14) (3/3) (2/2) (2/2) (6/6) (1/1)		

[a](y/x): x indicates total number of fields and y indicates number of unified fields.

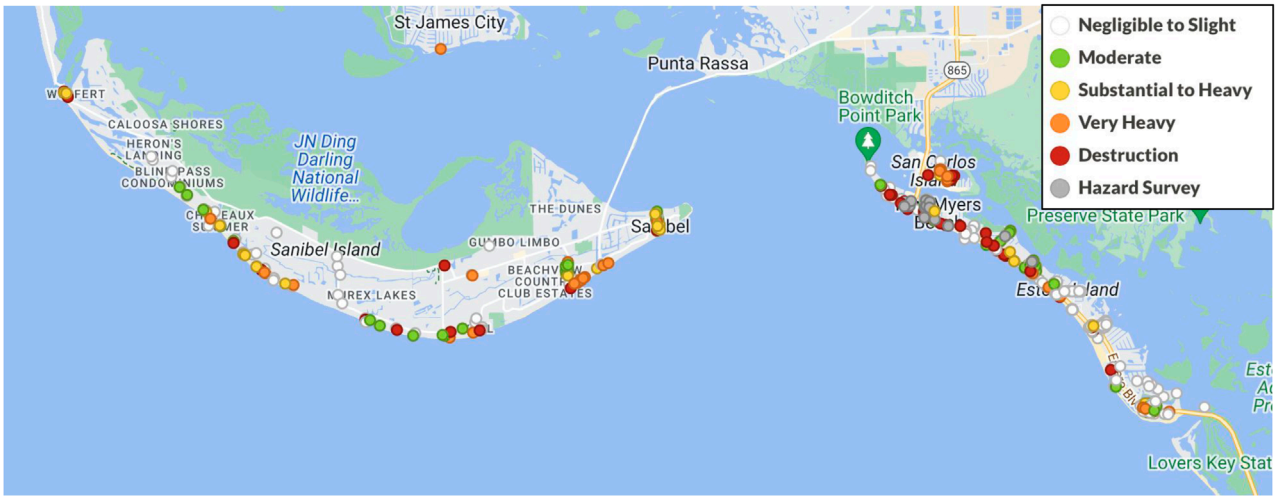

FIGURE 6
Locations of performance assessments and High-Water Mark (HWM) surveys conducted by StEER FAST in Fort Myers Beach and Sanibel Island, Florida, following 2022 Hurricane Ian.

the structural load path, including the presence of breakaway walls and other coastal features, types of loading experienced (hydrostatic, hydrodynamic, debris impact, *etc.*), and observed exterior damage to fenestration, wall cladding, roof cover, and structural systems.

Figure 8A,B represent histograms showing the duration of LPAs and HWMs as assessed by Hurricane Ian FASTs. The mean duration for LPAs is 18.5 min, with a standard deviation of 55.3 min, while HWMs have a mean of 6.5 min and a standard deviation of 17.9 min. In both assessment types, the standard deviation is approximately three times the mean. The LPA assessments involved a larger number of questions compared to HWM assessments, which is reflected in their longer response duration. Figures 8C,D illustrate the completeness of data for two assessment types with increasing fidelity levels, BA and LPA, respectively. Figure 8C shows that for the BA, the mean response rate is 77.9%, with a standard deviation of 18.5%. Notably, two questions—the global damage rating of the structure and the hazard present on-site—achieved a 100% response rate, as they were required fields (RFs) in the app. In contrast, the response rates for field priority fields (FPs) varied between 49% and 97%. The lowest rate, 49%, pertains to the overall damage note, a text input field for additional observations, while the highest rate corresponds to documenting evidence of debris impact on the structure. Other questions related to the number of stories affected and details about affected stories had lower response rates due to the need for access to all floors in multi-story buildings, which the FAST often could not access to. Figure 8D shows that for the LPA, the mean response rate is 47.6%, with a standard deviation of 18.1%. The response rates ranged from 5% to 66%, with the lowest rate corresponding to overall damage notes on lateral load-carrying systems like BA, and the highest related to damage at the connections between the foundation and superstructure. The LPA questionnaire requires considerably more effort, access, and scrutiny to identify damage along load path elements, justifying the lower response rate compared to the BA. Since none of the LPA questions are required fields, no questions reached a 100% response rate. Overall, the differences in data completeness between BA and LPA underscore the varying levels of access, effort, and expertise needed for these different fidelity assessments.

5.2 2023 Turkey earthquake sequence

On 6 February 2023, southeastern Turkey (Türkiye) was devastated by two large-magnitude earthquakes. The first, with a magnitude (Mw) of 7.8 and a focal depth of 17.9 km, occurred along the Eastern Anatolian Fault (USGS 2023a). Nine hours later, a second earthquake of Mw 7.5 and a focal depth of 10 km occurred on the Sürgü-Çardak Fault, located approximately 95 km north-northeast of the initial epicenter (USGS 2023b). The shallow depth of the Mw 7.8 earthquake, combined with a bilateral rupture that extended both southwest and northeast across an area of 100 km by 75 km, impacted 10 provinces in Türkiye—Kahramanmaraş, Gaziantep, Şanlıurfa, Diyarbakır, Adana, Adıyaman, Osmaniye, Hatay, Kilis, and Malatya—which together have a population of approximately 13.5 million people (AFAD, 2023). The seismic activity also affected parts of northwestern Syria. The devastation was particularly severe due to the high population density and the vulnerability of the infrastructure in the impacted areas. As a result of this sequence of earthquakes and aftershocks, around 36,932 buildings partially or completely collapsed, while another 311,000 buildings were severely damaged rendering them unusable in Türkiye (IBC, 2023). In northwest Syria, more than 10,600 buildings were partially/completely collapsed (OCHA, 2023).

Deferring to local engineers to lead the performance assessments, StEER elevated only to a Level 2 response for this event, issuing a joint Preliminary Virtual Reconnaissance Report (PVRR) with the Earthquake Engineering Research Institute (EERI) *Learning From Earthquakes (LFE)* program (Dilsiz et al., 2023). StEER formed a collaboration with other responding groups to hire local contractors to rapidly image the epicentral region using

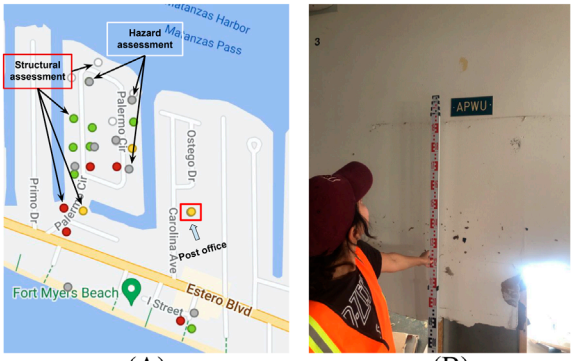

(A)

(B)

4a.3 Coastal Hazard Information	
Assessed Hazard	Flow Conditions
Flow condition measurement method	Photo evidence, Field measurement
Flow intensity measure	Maximum flow depth
Maximum flow depth measure	High-water Mark (HWM)
Measured HWM	
HWM elevation above Datum-1	1.98 m
Datum-1 metadata	Maximum flow elevation from post office floor
HWM elevation above Datum-2	19.02 m
Datum-2 metadata	Geoid, RTK -22.4 m+ 1.4 m floor level + 1.98 m from floor
Processed HWM	
Processed HWM includes	Surge only
Still water elevation above MSL	4.98 m
Still water elevation above NAV88	5.086 m
Flow depth over first floor	1.98 m
Flow depth over grade level	3.38 m
Quality Index	A: Clear debris line, obvious highest debris line, surge level very likely not higher than this elevation (+/- 10 cm)

(C)

(D)

(E)

(F)

(G)

2.General Information	
Address	200 Caroline Ave, Fort Myers Beach, FL
Latitude	26.452476
Longitude	-81.949254
Inspection date	October 19, 2022
Sampling method	Critical case sampling
Area assessed	Exterior and interior both
4b.1 Facility Information	
Site on beach front?	No
Facility Material	Steel, wood, corrugated sheet
Construction year	1977
Number of stories above ground	1
Occupancy category	Post Office
Structural system	Steel braced frame (S2)
Foundation category	Reinforced masonry stem walls
Roof system	Steel cold form
4b.2 Performance Information	
Type of loading experienced	Hydrostatic, Hydrodynamic
Basic Assessment (BA) Information	
Number of stories affected	1
Affected stories	1
Is the facility shielded by other structures from surge and wave action?	Yes
Is there evidence of breakaway wall failure?	No
Is there evidence of any floor-slab uplift?	No
Is there evidence of debris impact or damming on the structure?	No
Is there evidence of surcharge load in floors due to water retention?	No
Overall damage note	Mostly heavy damage to aluminum exterior and fenestration. No collapse but interior totaled.
Global damage rating	Substantial to heavy damage
Load Path Assessment (LPA) Information	
Broken, leaning, or severely degraded moment frames?	No
Broken or severely damaged diaphragm or horizontal bracing?	Yes
Damage or failure of wall-to-floor/wall-to-roof or bracing connections?	Yes
Damaged/ failed connections between superstructure and foundation?	No
Extensive sedimentation around piles, piers, columns, walls, and foundation?	No
Building in zone of suspected slope movement?	No
Damage notes on lateral load carrying system	Damage to connection in horizontal cold form bracing.

(H)

FIGURE 7
Example of hazard and performance assessments for multiple buildings in close proximity from Hurricane Ian field investigation. The figure includes **(A)** a map showing the locations of the assessments, **(B)** a photo of a High-Water Mark (HWM) measurement taken inside a critical case structure (a post office) relative to the floor level, along with **(C)** relevant metadata of the measured and processed HWM recorded in Fulcrum. Additionally, **(D, E)** show overall photos of the damage observed around the same structure, while close-up images **(F, G)** capture damage to load path elements. Lastly, **(H)** shows a sample feature set of data recorded as part of Basic Assessment (BA) and Load Path (LPA) assessments.

SLP camera systems, collecting over 250 km of panoramic imagery hosted on an interactive dashboard to support responding teams. When possible, StEER equipped responding local engineers with the StEER Earthquake App_v2 and technical guidance; chief among these was the Earthquake Engineering Field Investigation Team (EEFIT), who utilized the app to conduct BA of structures. In total, a five-member EEFIT team assessed 322 structures between March 13-17, 2023 (see Figure 9) (Aktaş et al., 2024). Figure 10 shows example assessment conducted to document a Church performance.

Figure 11A displays the histogram of BA duration of EEFIT team during the Turkey earthquake reconnaissance. The mean duration is 6.2 min, and standard deviation is 16.5 min, which is considerably lower than the corresponding statistic for the LPA during 2022 Hurricane Ian. Figure 11B illustrates the completeness of data in the BA. The mean response rate for BA is 37.9%, with a standard deviation of 33.3%. Like the Hurricane Ian response, the required fields (RFs)—specifically the global damage rating of the structure and the hazard present on-site—achieved a 100% response rate. However, the response rates for the remaining field priority fields (FPs) varied between 10.3% and 30.8%. The lowest rate of 10.3% pertains to the affected stories, while the highest rate of 30.8% is associated with whether the building has collapsed or partially collapsed. Overall, the level of data completeness in the unsupervised BA for the Turkey earthquake is much lower compared to that achieved in the supervised LPA assessments during Hurricane Ian. This discrepancy largely reflects the EEFIT team's lack of familiarity with the StEER app's structure during the Turkey response, in contrast to the supervised LPA assessment by the StEER FAST during Hurricane Ian. Additionally, factors such as the need to cover large geographical areas and the nature of the hazard may further contribute to this disparity. Importantly, these findings are not viewed as limitations of the framework itself, but rather as expected outcomes in early-stage, high-pressure field conditions with varying levels of pre-deployment user training and data collection demands, particularly when hybrid (on-site with remote follow-up) assessments are feasible.

Drawing on the feedback and user experience data from the use of hazard-specific apps, as well as data completeness statistics

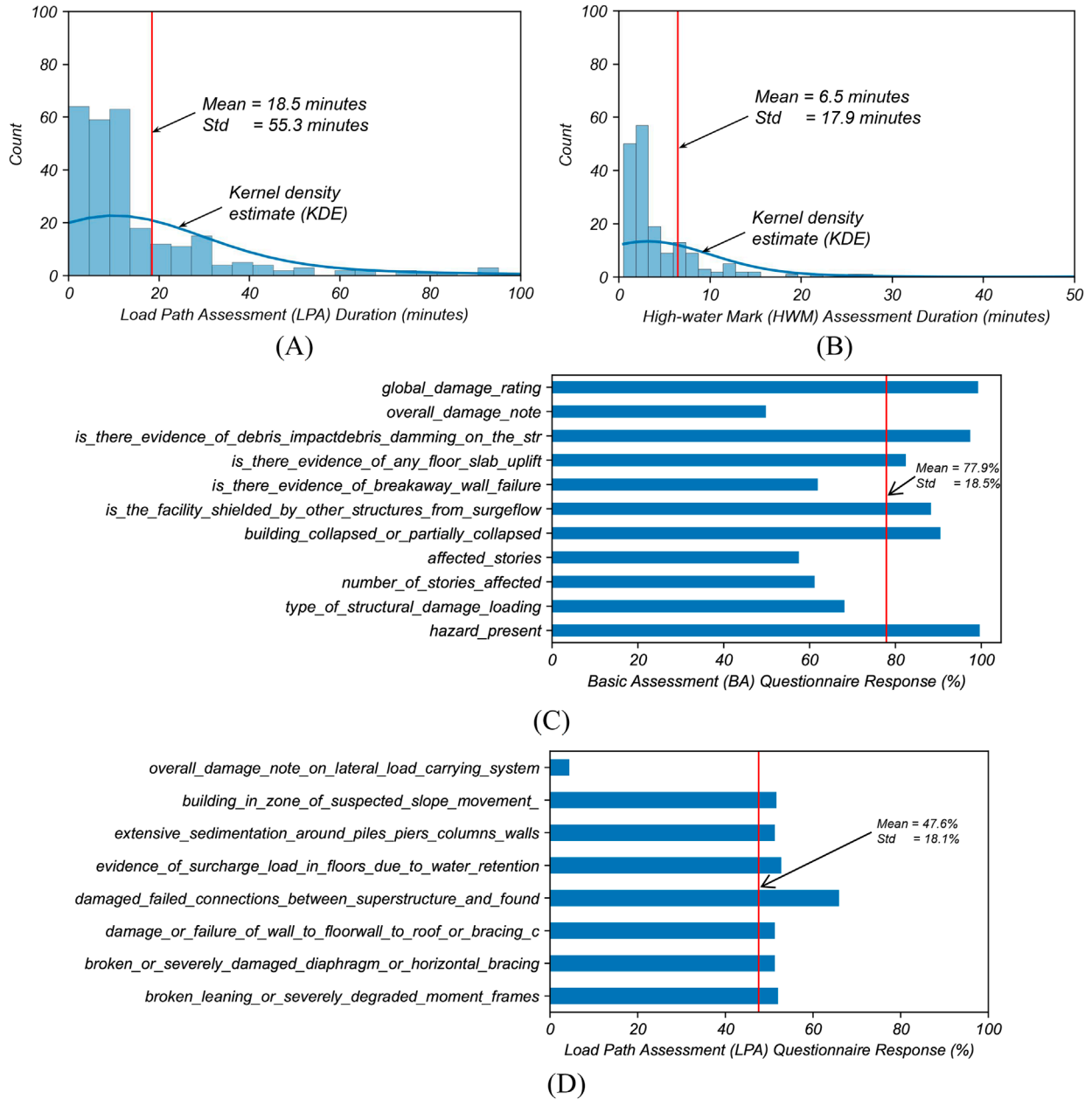

FIGURE 8
Histograms showing the duration of assessments for **(A)** Load Path Assessment (LPA) and **(B)** High-Water Mark (HWM) surveys conducted by the StEER FAST during the 2022 Hurricane Ian deployment. The red vertical lines in these figures represent the mean duration. The completeness of the sample set from questionnaires recorded by the assessment team is shown for **(C)** Basic Assessment (BA) and **(D)** Load Path Assessment (LPA). Note the nested nature of the performance assessment process (see Figure 3), where higher-fidelity assessments, such as LPA, involve completing both BA and LPA questionnaires sequentially.

from the questionnaires in these two use cases, the performance assessment section of the Unified App has been further streamlined. The app logic was refined to prioritize key fields (RFs, FPs, Media), ensuring they are more prominently displayed than other standard fields, thereby enhancing usability. To further support users in navigating the StEER Unified App, a condensed version of the detailed handbook has been created as a quick reference sheet, along with multiple video tutorials for guidance. These refinements to the app interface, targeted onboarding, and improved pre-deployment training are already yielding higher completion rates in more recent deployments. Ongoing efforts will continue to focus on optimizing form usability and streamlining field workflows to maximize data quality without compromising speed or safety.

As demonstrated by the two use cases, the framework's tiered structure affords investigators the flexibility to select the depth of assessment appropriate for their scientific questions and mission constraints. Broad, rapid assessments (BA) are often the preferred modality for large-scale reconnaissance due to time

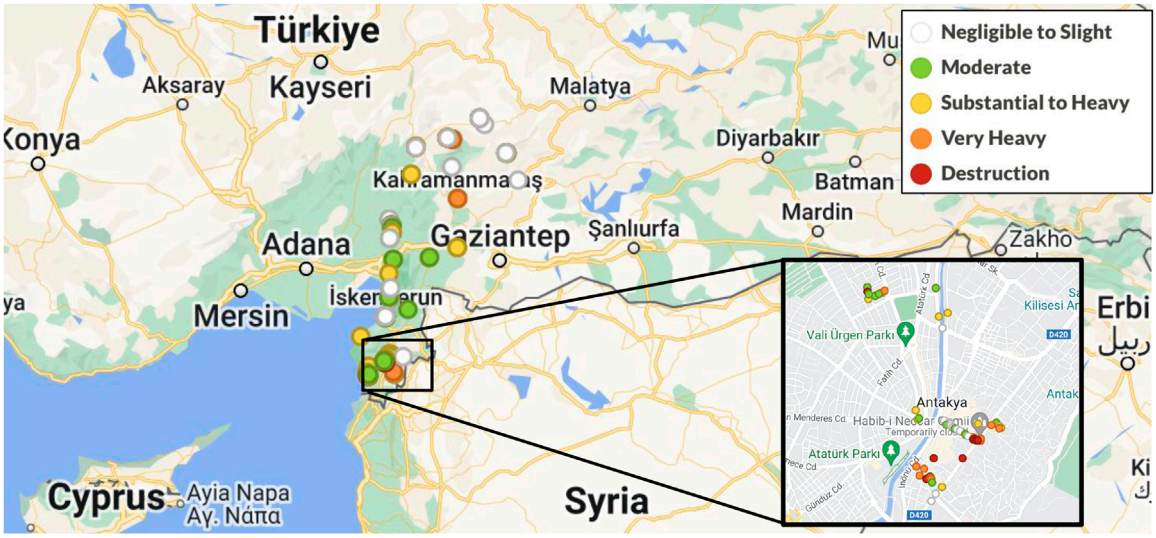

FIGURE 9
Locations of performance assessments conducted by the Earthquake Engineering Field Investigation Team (EEFIT) using the StEER Unified App in the aftermath of the 2023 Turkey earthquake sequence.

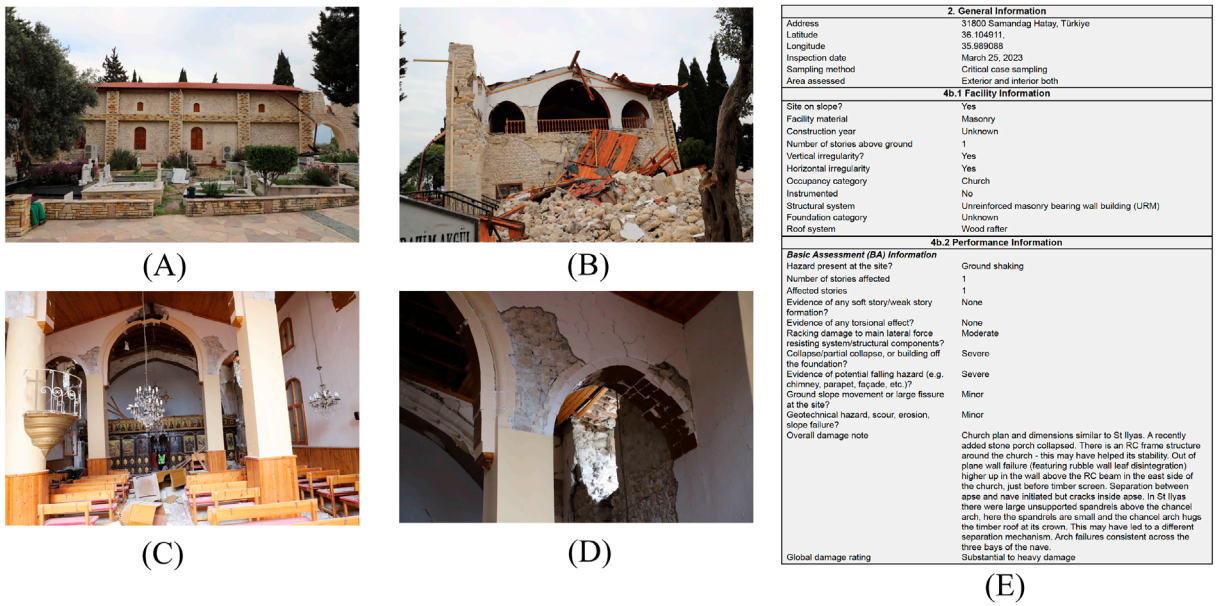

2. General Information	
Address	31800 Samandag Hatay, Türkiye
Latitude	36.104911
Longitude	35.989088
Inspection date	March 25, 2023
Sampling method	Critical case sampling
Area assessed	Exterior and interior both
4b.1 Facility Information	
Site on slope?	Yes
Facility material	Masonry
Construction year	Unknown
Number of stories above ground	1
Vertical irregularity?	Yes
Horizontal irregularity	Yes
Occupancy category	Church
Instrumented	No
Structural system	Unreinforced masonry bearing wall building (URM)
Foundation category	Unknown
Roof system	Wood rafter
4b.2 Performance Information	
Basic Assessment (BA) Information	
Hazard present at the site?	Ground shaking
Number of stories affected	1
Affected stories	1
Evidence of any soft story/weak story formation?	None
Evidence of any torsional effect?	None
Racking damage to main lateral force resisting system/structural components?	Moderate
Collapse/partial collapse, or building off the foundation?	Severe
Evidence of potential falling hazard (e.g. chimney, parapet, façade, etc.)?	Severe
Ground slope movement or large fissure at the site?	Minor
Geotechnical hazard, scour, erosion, slope failure?	Minor
Overall damage note	Church plan and dimensions similar to St Ilyas. A recently added stone porch collapsed. There is an RC frame structure around the church - this may have helped its stability. Out of plane wall failure (featuring rubble wall leaf disintegration) higher up in the wall above the RC beam in the east side of the church, just before timber screen. Separation between apse and nave initiated but cracks inside apse. In St Ilyas there were large unsupported spandrels above the chancel arch, here the spandrels are small and the chancel arch hugs the timber roof at its crown. This may have led to a different separation mechanism. Arch failures consistent across the three bays of the nave.
Global damage rating	Substantial to heavy damage

FIGURE 10
Example of a performance assessment of a church damaged during the 2023 Turkey Earthquake Sequence **(A, B)** show overview photos taken around the church, while **(C, D)** provide close-up views of damage to the arch with **(E)** a sample feature set of data recorded as part of the Basic assessment (BA).

efficiencies; however, the framework still can support detailed, time-intensive follow-up investigations when conditions and resources permit. In such cases, LPA and DCA tiers support more granular documentation of damage, making them especially valuable for case studies focused on specific failure modes, structural systems, or multi-hazard interactions. Though less frequently deployed to date, these higher-resolution tiers offer a robust foundation for targeted investigations and in-depth engineering analysis. As field team training advances and deployment strategies become more modular, broader adoption of LPA and DCA is expected. Elements of the LPA and DCA in previous apps, particularly those tailored to wind and coastal hazards, have already been deployed successfully and supported subsequent forensic analyses (Kijewski-Correa et al., 2022; Marshall et al., 2022; Roueche et al., 2024), lending confidence in the approach, but will require more widespread application across all hazards.

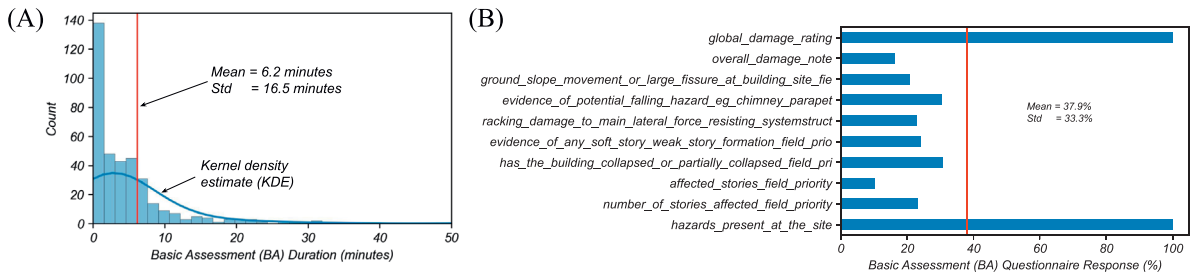

FIGURE 11
Histograms showing **(A)** the duration of Basic Assessments (BA) conducted by the EEFIT team during the 2023 Turkey Earthquake Sequence, and **(B)** the completeness of the sample questionnaire set related to BA.

6 Summary and conclusion

Post disaster structural assessment and hazard data collection efforts remain fragmented across hazard types and infrastructure systems due to varying objectives, methodologies, protocols, and standards among investigators and organizations. This limits our ability to fully understand hazard interactions with the built environment and community resilience across events. To address this barrier to knowledge discovery and diverse data reuse, a hazard-agnostic unified framework has been developed to standardize post-disaster data and metadata collection across multiple natural hazards (earthquake, windstorm, coastal) and infrastructure typologies.

The framework's architecture was shaped through consensus among StEER leadership, guided by a review of existing framework and data collection practices. Input from the 2018 StEER Cross-Hazard Workshop at UC Berkeley further informed its design, highlighting synergies in structural assessment across diverse hazards and structural types, particularly in multi- and cascading hazard contexts. These efforts culminated in the creation of the Unified Assessment Framework. The Framework is structured with three *data classes*: (1) Unified Assessment, (2) Hazard Survey, and (3) Performance Assessment Survey to organize and store the collected data with similar attributes associated with the survey parameters, observed hazards, and the assessed structure, respectively. Within each data class, *data subclasses* are defined to further structure the data for improved backend data storage, sorting, discovery, and unification. Finally, at the lowest level, *data fields* describe attributes of surveys, hazards, and structures that are stored within these data subclasses.

Efforts have been made to unify attributes across the three hazard types (earthquake, windstorm, coastal) to minimize the number of data fields in the framework. Unification of attributes is achieved at the data class and subclass hierarchy level across hazards in the Unified Assessment data class, whereas unification is generally achieved at the data field level, typically across two hazards rather than all three in the Performance Assessment Survey data class. In the Hazard Survey data class, attributes are unique to each specific hazard, so unification is achieved only within individual hazard survey subclasses. The Performance Assessment Survey data class of the framework encompasses a tiered performance assessment approach with increasing rigor and fidelity levels: *Basic Assessment (BA)*, *Load Path Assessment (LPA)*, and *Detailed Component Assessment (DCA),* which enable in-depth analysis of infrastructure performance, correlating infrastructure performance to site-specific hazards, or understanding the complex interactions of factors affecting structural performance under multi-hazard scenarios aiding in the development of targeted response, recovery, and mitigation strategies.

The framework is implemented as an open-access mobile application, the StEER Unified App, hosted on Fulcrum, a commercial form-builder and data collection platform developed by Spatial Networks Inc. The app features nested menus that intelligently display relevant sections and data fields based on the hazard type, assessment class, and infrastructure type under investigation, minimizing the burden on field investigators to input irrelevant data. Along with unification of data fields, preliminary mapping rules were developed to map out existing hazard-specific damage rating scales (e.g., wind, surge/flood rainwater ingress) to the European Macroseismic Scale (EMS-98) compatible unified damage scale. This enabled consolidation of global damage ratings into a common data field, facilitating the unification of multiple hazards within a single app. In consolidating damage ratings to a common scale for the app's data structure, care was taken to retain the overarching level definitions (e.g., slight, moderate, severe damage) while customizing the specific descriptors to reflect hazard-specific damage mechanisms.

To ensure effective use of the app by the StEER Field Assessment Structural Team (FAST) and other users, a comprehensive set of training materials has been developed. These include a detailed handbook, quick reference sheet, and instructional videos. The resources are integrated into the app itself and incorporated into the pre-deployment briefing during active missions. They are also publicly available on the StEER website under the Resources section. Two use cases are presented to demonstrate the application of this Unified Assessment Framework through the StEER Unified App: a supervised pilot during 2022 Hurricane Ian, Florida and an unsupervised deployment for the 2023 Turkey earthquake sequence. Following conclusions are drawn based on the work presented.

- The Unified Assessment Framework provides a foundational step toward harmonizing post-disaster structural reconnaissance across hazards and infrastructure types, resolving long-standing fragmentation in field data collection caused by divergent objectives, protocols, and standards.
- By enabling consistent, high-fidelity data collection across diverse hazard contexts, the framework advances the integration of engineering evidence into resilience-focused

public policy, recovery prioritization, and adaptation planning—making it a critical tool for evidence-based decision-making at local, national, and international levels.

- The framework's implementation through the StEER Unified App open to any member in StEER's Fulcrum account, operationalizes scalable, hazard-agnostic assessment protocols, lowering barriers to participation while improving consistency and completeness of structural damage data collection in the field.
- A tiered performance assessment structure (BA, LPA, DCA) enables flexible deployment of engineering rigor, allowing investigators to pick the assessment most appropriate to the research and response constraints. This approach supports both immediate disaster response and development of intermediate- to long-term targeted response, recovery, and mitigation strategies.
- Initial deployments during Hurricane Ian (2022) and the Türkiye earthquake sequence (2023) demonstrate the feasibility of standardized assessments and offer insights into how data collection is influenced by assessor pre-deployment training and assessment tier, especially in more demanding tasks like load path evaluation.
- The initial mapping of damage states consistent with European Macroseismic Scale (EMS-98) provides consistent data structure to enable compounding and cascading hazard assessments and cross-event comparability. However, refinement is still needed—especially in flood and moisture-related damage domains—to balance structural and non-structural impacts more accurately.
- Future validation efforts can focus on benchmarking LPA and DCA field data against detailed engineering analyses and repair estimates, critical for improving the accuracy of field definitions, damage states, and uncertainty quantification.
- To support reproducibility and interoperability, the framework incorporates a version control system and changelog for all forms and backend schemas, preserving compatibility across datasets and enabling structured updates as knowledge and methods evolve.
- Mapping historical StEER event data into the Unified App and accepting community-contributed data will create a dynamic, growing dataset, establishing a long-term testbed for machine learning models, policy simulations, and resilience research.

Data availability statement

All StEER products, resources and policies are available at www.steer.network; App-based structural assessments of the two use cases presented in this study are available on the StEER Fulcrum account at https://web.fulcrumapp.com; Curated datasets and published reports are available at DesignSafe: https://www.designsafe-ci.org/data/browser/public/ (search keyword StEER).

Author contributions

MA: Conceptualization, Formal Analysis, Investigation, Methodology, Resources, Software, Visualization, Writing – original draft, Writing – review and editing. TK-C: Conceptualization, Funding acquisition, Methodology, Project administration, Resources, Validation, Writing – review and editing, Supervision. DR: Data curation, Funding acquisition, Project administration, Software, Validation, Writing – review and editing. KM: Funding acquisition, Project administration, Validation, Writing – review and editing. DP: Funding acquisition, Project administration, Validation, Writing – review and editing. IR: Funding acquisition, Project administration, Validation, Writing – review and editing.

Funding

The author(s) declare that financial support was received for the research and/or publication of this article. The research presented herein is supported by the National Science Foundation under Grant No. CMMI 2103550.

Acknowledgments

Any opinions, findings, and conclusions or recommendations expressed in this article are those of authors and do not necessarily reflect the views of the National Science Foundation.

Conflict of interest

The authors declare that the research was conducted in the absence of any commercial or financial relationships that could be construed as a potential conflict of interest.

Generative AI statement

The author(s) declare that no Generative AI was used in the creation of this manuscript.

Publisher's note

All claims expressed in this article are solely those of the authors and do not necessarily represent those of their affiliated organizations, or those of the publisher, the editors and the reviewers. Any product that may be evaluated in this article, or claim that may be made by its manufacturer, is not guaranteed or endorsed by the publisher.

Supplementary material

The Supplementary Material for this article can be found online at: https://www.frontiersin.org/articles/10.3389/fbuil.2025.1546616/full#supplementary-material

SUPPLEMENTARY FILE S1
Unified App: Master Data Sheet.

SUPPLEMENTARY FILE S2
Unified App: Required Fields.

SUPPLEMENTARY FILE S3
Unified App: Field Priority Fields.

SUPPLEMENTARY FILE S4
Unified App: Multi-Hazard Fields.

SUPPLEMENTARY FILE S5
Quick Reference Sheets: Global Damage Ratings Mapping.

References

AFAD (2023). Pazarcık (Kahramanmaras MW 7.7) and Elbistan (Kahramanmaras MW 7.6) earthquakes preliminary report. Available online at: https://deprem.afad.gov.tr/assets/pdf/Kahramanmaras%20%20Depremleri_%20On%20Degerlendirme%20Raporu.pdf (Accessed November 10, 2023).

Aktaş, Y. D., So, E., Johnson, C., Dönmez, K., Özden, A. T., Vatteri, A. P., et al. (2024). The Tu¨rkiye earthquake sequence of February 2023: a longitudinal study report by EEFIT. Earthquake Engineering Field Investigation Team (EEFIT). *Institution Struct. Eng. (IStructE)*, 1–330. doi:10.13140/RG.2.2.15906.40641

Alam, B. (2024). "Multi-hazard earthquake-tsunami structural risk assessment framework," in Proceedings of the 18th World Conference on Earthquake Engineering (WCEE2024). International Association of Earthquake Engineering (IAEE). Milan, Italy. June 30–July 5, 2024. 1–12.

Alam, M. S., Pinelli, J. P., Do, T., Wolohan, K., Kijewski-Correa, T., Prevatt, D. O., and Roueche, D. (2025). "StEER: Hurricane Helene early access reconnaissance report (EARR)," in *StEER - Hurricane Helene* (DesignSafe-CI). doi:10.17603/ds2-nqev-2171

Anagnostopoulos, S., and Moretti, M. (2008). Post-earthquake emergency assessment of building damage, safety and usability—Part 1: technical issues. *Soil Dyn. Earthq. Eng.* 28 (3), 223–232. doi:10.1016/j.soildyn.2006.05.007

ATC 20 (1989). *ATC 20, procedure for post-earthquake safety evaluation of buildings*. Redwood City, CA: Applied Technology Council.

ATC 20-2 (1995). *ATC 20-2, addendum to the ATC 20 post-earthquake safety evaluation of buildings*. Redwood City, CA: Applied Technology Council.

ATC 20-3 (1996). *ATC 20-3, case studies in rapid post-earthquake safety evaluation of buildings*. Redwood City, CA: Applied Technology Council.

ATC 45 (2004). *ATC-45: field manual: safety evaluation of buildings after windstorms and floods*. Red Wood City, CA: Applied Technology Council.

Baggio, C., Bernardini, A., Colozza, R., Corazza, L., Della Bella, M., Di Pasquale, G., et al. (2007). *Field manual for post-earthquake damage and safety assessment and short-term countermeasures (AeDES)*. EUR: European Commission—Joint Research Centre—Institute for the Protection and Security of the Citizen, 22868.

Barbosa, A. R., Fahnestock, L. A., Fick, D. R., Gautam, D., Soti, R., Wood, R., et al. (2017). Performance of medium-to-high rise reinforced concrete frame buildings with masonry infill in the 2015 Gorkha, Nepal, earthquake. *Earthq. Spectra* 33 (1_Suppl. l), 197–218. doi:10.1193/051017eqs087m

BCH (2019). *British Columbia post-disaster building assessment framework and recommendations*. BC: BC Housing, Justice Institute of British Columbia. Available online at: https://www.bchousing.org/publications/PDBA-Framework-Recommendations.pdf

Brando, G., Rapone, D., Spacone, E., O'Banion, M. S., Olsen, M. J., Barbosa, A. R., et al. (2017). Damage reconnaissance of unreinforced masonry bearing wall buildings after the 2015 Gorkha, Nepal, earthquake. *Earthq. spectra* 33 (1_Suppl. l), 243–273. doi:10.1193/010817eqs009m

Charleson, A., Goded, T., Wald, D., Lin, S., Beattie, G., Ingham, J., et al. (2024). "Development of a Macroseismic scale for new Zealandd: Aligning with EMS-98 and the developing of IMS," in Proceedings of the 18th World Conference on Earthquake Engineering (WCEE2024). International Association of Earthquake Engineering (IAEE). Milan, Italy. June 30–July 5, 2024. 1–12.

Chock, G., Robertson, I., Kriebel, D., Francis, M., and Nistor, I. (2013). *Tohoku, Japan, earthquake and tsunami of 2011: performance of structures under tsunami loads*. Reston, VA: American Society of Civil Engineers.

Cortes, M., Arora, P., Ceferino, L., Ibrahim, H., Istrati, D., Reed, D., et al. (2022). "StEER: hurricane ian preliminary virtual reconnaissance report (PVRR)," in *StEER - Hurricane Ian*. DesignSafe-CI. doi:10.17603/ds2-kc9k-s242

Cox, D., Arikawa, T., Barbosa, A., Guannel, G., Inazu, D., Kennedy, A., et al. (2019). Hurricanes irma and Maria post-event survey in US Virgin Islands. *Coast. Eng. J.* 61 (2), 121–134. doi:10.1080/21664250.2018.1558920

CUREE (2010). *General guidelines for the assessment and repair of earthquake damage in residential wood frame buildings. CUREE Publication No. EDA-02*. Richmond, CA: Consortium of Universities for Research in Earthquake Engineering CUREE.

Delatte, N. J. (2008). *Beyond failure: forensic case studies for civil engineers*. Reston, VA: ASCE. doi:10.1061/9780784409732

Demir, A., Günay, S., Marinković, M., Dilsiz, A., Bektaş, N., Khalil, Z., et al. (2024). 2022 Düzce, Türkiye earthquake: advances in the past 2 decades, lessons learned, and future projections. *Bull. Earthq. Eng.* 22, 5835–5862. doi:10.1007/s10518-024-01984-z

Dilsiz, A., Gunay, S., Mosalam, K., Prevatt, D., Gerczak, E., Miranda, E., et al. (2023). "StEER: 2023 Mw 7.8 Kahramanmaras, Türkiye earthquake sequence preliminary virtual reconnaissance report (PVRR), in *StEER- February 6, 2023, Kahramanmaras, Türkiye, Mw 7.8 Earthquake*. DesignSafe-CI. doi:10.17603/ds2-7ry2-gv66

EEFIT (2005). *The Indian ocean Tsunami of 26th December 2004. Earthquake engineering field investigation team (EEFIT) report*. London: Thomas Telford.

EEFIT (2011). "The M_W 9.0 Tōhoku earthquake and Tsunami of 11th March 2011," in *Earthquake engineering field investigation team (EEFIT) report*. London: Thomas Telford.

EERI (1971). *Preliminary engineering findings from Los Angeles earthquake of February 9, 1971*. Oakland, CA: Earthquake Engineering Research Institute.

EERI (1996). *Post-earthquake investigation field guide*. Oakland, CA: Earthquake Engineering Research Institute EERILearning from Earthquake Program, Revised in 2000. 2004.

EERI (2010). *The MW 8.8 Chile earthquake of 27 February 2010, EERI special earthquake report*, Oakland, CA: Earthquake Engineering Research Institute EERI Learning from Earthquake Program, 20. June 2010 Newsletter.

Egnew, A. C., Roueche, D. B., and Prevatt, D. O. (2018). Linking building attributes and Tornado vulnerability using a logistic regression model. *Nat. Hazards Rev.* 19 (4), 04018017. doi:10.1061/(asce)nh.1527-6996.0000305

Elwood, K. J. (2013). Performance of concrete buildings in the 22 February 2011 Christchurch earthquake and implications for Canadian codes. *Can. J. Civ. Eng.* 40 (3), 759–776. doi:10.1139/cjce-2011-0564

FEMA (2020). *FEMA preliminary damage assessment guide*. Washington, DC: Federal Emergency Management Agency FEMA. Department of Homeland Security, Department of Homeland Security.

FEMA (2021). *Seismic performance assessment of buildings volume 8 – methodology for assessment of functional recovery time (ATC 138-3)*. Washington, DC: Federal Emergency Management Agency FEMA. Department of Homeland Security, Department of Homeland Security.

FEMA (2022a). *HAZUS hurricane model technical manual: HAZUS 5.1*. Washington, DC: Federal Emergency Management Agency FEMA, Department of Homeland Security, Department of Homeland Security.

FEMA (2022b). *HAZUS tsunami model technical manual: HAZUS 5.1*. Washington, DC: Federal Emergency Management Agency FEMA. Department of Homeland Security, Department of Homeland Security.

FEMA (2023). *Hurricane Ian in Florida. Building performance observations, recommendations, and technical guidance. mitigation assessment team report-FEMA P-2342*. Washington, DC: Department of Homeland Security.

FEMA (2024). *HAZUS earthquake model technical manual: HAZUS 6.1*. Washington, DC: Federal Emergency Management Agency FEMA. Department of Homeland Security, Department of Homeland Security.

FEMA 306 (1998). *Evaluation of Earthquake damaged concrete and masonry wall buildings, basic procedure manual*. Washington, DC: Federal Emergency Management Agency (FEMA). Department of Homeland Security, Department of Homeland Security.

FEMA 310 (1998). *Handbook for the seismic evaluation of buildings*. Washington, DC: Federal Emergency Management Agency FEMA. Department of Homeland Security, Department of Homeland Security.

FEMA 352 (2000). *Recommended post-earthquake evaluation and repair criteria for Welded steel moment-frame buildings*. Washington, DC: Federal Emergency Management Agency (FEMA). Department of Homeland Security.

Fikri, R., Dizhur, D., Walsh, K., and Ingham, J. (2019). Seismic performance of reinforced concrete frame with masonry Infill buildings in the 2010/2011 Canterbury, New Zealand earthquakes. *Bull. Earthq. Eng.* 17, 737–757. doi:10.1007/s10518-018-0476-8

Franco, G., Green, R., Khazai, B., Smyth, A., and Deodatis, G. (2010). Field damage survey of New Orleans Homes in the aftermath of Hurricane Katrina. *Nat. Hazards Rev.* 11 (1), 7–18. doi:10.1061/(asce)1527-6988(2010)11:1(7)

Friedland, C. J. (2009). Residential building damage from hurricane storm surge: proposed methodologies to describe, assess and model building damage. PhD Thesis. Louisiana, USA: Louisiana State University.

Friedland, C. J., and Levitan, M. L. (2011). "Development of a loss-consistent wind and flood damage scale for residential buildings," in In the Proceedings of the Solution to Coastal Disasters Conference, Anchorage, Alaska, June 25–29, 2011, (Reston, VA: American Society of Civil Engineers), 666–677.

Grünthal, G. (1998). "*European Macroseismic scale 1998 EMS-98: Luxembourg, v. 15*," (Cahiers du Centre Européen de Géodynamique et de Séismologie), 99. Available online at: https://www.franceseisme.fr/EMS98_Original_english.pdf

Hatzikyriakou, A., Lin, N., Gong, J., Xian, S., Hu, X., and Kennedy, A. (2016). Component-based vulnerability analysis for residential structures subjected to storm surge impact from Hurricane Sandy. *Nat. Hazards Rev.* 17 (1), 05015005. doi:10.1061/(asce)nh.1527-6996.0000205

Hortacsu, A., Porter, K. A., Osteraas, J., Harris, S. K., Goded, T., Lin, S., et al. (2024). "Development of a Macroseismic intensity scale for the United States: Aligning with EMS-98 and developing IMS," in Proceedings of the 18th World Conference on Earthquake Engineering (WCEE2024). International Association of Earthquake Engineering (IAEE). Milan, Italy. June 30–July 5, 2024. 1–12.

Hughes, R., and Lubkowski, Z. A. (1999). *The survey of earthquake damaged non-engineered structures. A field guide by EEFIT*. London: Earthquake Engineering Field Investigation Team. Institution of Structural Engineers.

IBC (2023). Devastating Earthquakein southern Türkiye and north Syria. International Blue Crescent Relief and development foundation (IBC). Situation Report 30. Available online at: https://reliefweb.int/report/turkiye/devastating-earthquakes-southern-turkiye-and-northern-syria-december-15th-2023-situation-report-30-entr (Accessed November 7, 2024).

JBDPA (1991). *Guideline for post earthquake damage evaluation and rehabilitation*. The Japan Building Disaster Prevention Association JBDPA, Revised in 2001 and 2015. (in Japanese).

Kaminosono, T., Kumazawa, F., and Nakano, Y. (2002). Quick inspection manual for damaged reinforced concrete buildings due to earthquake. Japan: National Institute of Land and Infrastructure Management, Ministry of Land, Infrastructure, and Transport.

Kennedy, A., Rogers, S., Sallenger, A., Gravois, U., Zachry, B., Dosa, M., et al. (2011). Building destruction from waves and surge on the Bolivar Peninsula during Hurricane Ike. *J. Waterw. Port, Coast. Ocean Eng.* 137 (3), 132–141. doi:10.1061/(asce)ww.1943-5460.0000061

Kijewski-Correa, T., Canales, E., Hamburger, R., Lochhead, M., Mbabazi, A., and Presuma, L. (2024). A hybrid model for post-earthquake performance assessments in challenging contexts. *Bull. Earthq. Eng*, 1–24. doi:10.1007/s10518-024-01927-8

Kijewski-Correa, T., Roueche, D., Kennedy, A., Allen, D., Marshall, J., Kaihatu, J., et al. (2022). Impacts of hurricane Dorian on the Bahamas: field observations of hazard intensity and performance of the built environment. *Coast. Eng. J.* 64 (1), 3–23. doi:10.1080/21664250.2021.1958613

Kijewski-Correa, T., Roueche, D. B., Mosalam, K. M., Prevatt, D. O., and Robertson, I. (2021). StEER: a community-centered approach to assessing the performance of the built environment after natural hazard events. *Front. Built Environ.* 7, 636197. doi:10.3389/fbuil.2021.636197

Kijewski-Correa, T. L., Kennedy, A. B., Taflanidis, A. A., and Prevatt, D. O. (2018). Field reconnaissance and overview of the impact of Hurricane Matthew on Haiti's Tiburon Peninsula. *Nat. Hazards* 94, 627–653. doi:10.1007/s11069-018-3410-0

Kopp, G. A., and Fewless, Y. (2014). "Basic hurricane wind principles," in *Engineering investigations of hurricane damage: wind versus water* (Reston, VA: American Society of Civil Engineer ASCE), 1–21.

Kyprioti, A., Yuzbasi, J., Dang, H., Jana, A., Kameshwar, S., Diekmann, A., et al. (2024). "StEER: Hurricane Helene annotated media repository," in *StEER - hurricane Helene* (DesignSafe-CI). doi:10.17603/ds2-mxeh-7712

LaFave, J. M., Gao, Z., Holder, D. E., Kuo, M. J., and Fahnestock, L. A. (2014). Commercial and residential building performance during the May 20, 2013, Tornado in Moore, Oklahoma. *J. Perform. Constr. Facil.* 30 (2), 04014210. doi:10.1061/(asce)cf.1943-5509.0000722

Loos, S., Levitt, J., Tomozawa, K., Baker, J., and Lallemant, D. (2022). Efficacy of damage data integration: a comparative analysis of four major earthquakes. *Nat. Hazards Rev.* 23 (4), 1–18. doi:10.1061/(asce)nh.1527-6996.0000581

Maeda, M., and Matsukawa, K. (2019). An overview of post-earthquake damage and residual capacity evaluation for reinforced concrete buildings in Japan. *Proc. 2019 Pac. Conf. Earthq. Eng. Annu. NZSEE Conf. COMPDYN Proc.* 1, 930–943. doi:10.7712/120119.6969.19228

Marshall, J. D., Roueche, D. B., Berman, J. W., Roberts, J., and Blue, C. (2022). "Forensic investigations into the performance of large-volume, low-rise buildings affected by Hurricane Michael," in Proceedings of the Ninth Congress on Forensic Engineering, Denver, Colorado, November 4–7, 2022. 362–372. doi:10.1061/9780784484548.038

NHC (2022). Hurricane Ian discussion number 25. National hurricane Center Forecast Discussions. Available online at: https://www.nhc.noaa.gov/archive/2022/al09/al092022.discus.025.shtml? (Accessed April 15, 2023).

NRC (2007). *Tools and methods for estimating populations at risk from natural disasters and complex humanitarian crises*. Washington, DC: National Research Council, The National Academies Press.

NZMBIE (2014a). *Field guide: rapid post disaster building usability assessment - flooding*. Wellington: New Zealand Ministry of Business, Innovation and Employment. Available online at: https://www.building.govt.nz/assets/Uploads/managing-buildings/post-emergency-building-assessment/flooding-field-guide-1-1.pdf

NZMBIE (2014b). *Field guide: rapid post disaster building usability assessment-earthquakes*. Wellington: New Zealand Ministry of Business, Innovation and Employment. Available online at: https://www.building.govt.nz/assets/Uploads/managing-buildings/post-emergency-building-assessment/earthquake-field-guide-1-1.pdf

OCHA (2023). Earthquakes: North-west Syria. UN Office of the Coordination of Humanitarian Affairs. Situation Report No. 1. As of 7 March 2023. Available online at: https://reliefweb.int/report/syrian-arab-republic/earthquakes-north-west-syria-situation-report-no-1-7-march-2023.

Peek, L., Tobin, J., Adams, R. M., Wu, H., and Mathews, M. C. (2020). A framework for Convergence research in the hazards and disaster field: the natural hazards engineering research infrastructure CONVERGE facility. *Front. Built Environ.* 6, 110. doi:10.3389/fbuil.2020.00110

Pilkington, S., Roueche, D., Mosalam, K., Gutierrez Soto, M., Alam, M., et al. (2021). "StEER: 10 December 2021 Midwest Tornado outbreak joint preliminary virtual reconnaissance report and early access reconnaissance report (PVRR-EARR)," in *StEER - 10 December 2021 Midwest Tornado Outbreak* (DesignSafe-CI). doi:10.17603/ds2-2b2k-ws96

Prevatt, D., Agdas, D., Faraone, D., Lafontaine, O., Micali, J., Nofal, O., et al. (2022). "StEER: Hurricane ian early access reconnaissance report (EARR)," in *StEER - hurricane ian*. DesignSafe-CI.

Prevatt, D. O., Coulbourne, W., Graettinger, A. J., Pei, S., Gupta, R., and Grau, D. (2012a). *Joplin, Missouri, Tornado of may 22, 2011: structural damage survey and case for Tornado-resilient building codes*. Reston, VA: American Society of Civil Engineers ASCE.

Prevatt, D. O., van de Lindt, J. W., Back, E. W., Graettinger, A. J., Pei, S., Coulbourne, W., et al. (2012b). Making the case for improved structural design: Tornado Outbreaks of 2011. *Leadersh. Manag. Eng.* 12 (4), 254–270. doi:10.1061/(asce)lm.1943-5630.0000192

Robertson, I., Chock, G., and Morla, J. (2012). Structural analysis of selected failures caused by the 27 February 2010 Chile tsunami. *Earthq. Spectra* 28 (1_Suppl. 1), 215–243. doi:10.1193/1.4000035

Robertson, I. N., Riggs, H. R., Yim, S. C., and Young, Y. L. (2007). Lessons from hurricane Katrina storm surge on bridges and buildings. *J. Waterw. Port, Coast. Ocean Eng.* 133 (6), 463–483. doi:10.1061/(asce)0733-950x(2007)133:6(463)

Roueche, D. B., Chen, G., Soto, M. G., Kameshwar, S., Safiey, A., Do, T., et al. (2024). Performance of Hurricane-resistant housing during the 2022 Arabi, Louisiana, Tornado. *J. Struct. Eng.* 150 (5), 04024029. doi:10.1061/JSENDH.STENG-12986

Roueche, D. B., Nakayama, J. O., Kijewski-Correa, T., and Prevatt, D. O. (2023). A unified multi-event windstorm performance testbed for single-family residential buildings. *Nat. Hazards Rev.* 25 (2), 04023060. doi:10.1061/nhrefo.nheng-1796

Roueche, D. B., and Prevatt, D. O. (2013). Residential damage patterns following the 2011 Tuscaloosa, AL and Joplin, MO Tornadoes. *J. Disaster Res.* 8 (6), 1061–1067. doi:10.20965/jdr.2013.p1061

Saatcioglu, M., Ghobarah, A., and Nistor, I. (2005). Effects of the December 26, 2004, Sumatra earthquake and Tsunami on physical infrastructure. *ISET J. Earthq. Technol.* 42 (4), 79–94. doi:10.63898/ODYI3392

Stolle, J., Krautwald, C., Robertson, I., Achiari, H., Mikami, T., Nakamura, R., et al. (2020). Engineering lessons from the 28 September 2018 Indonesian Tsunami: debris loading. *Can. J. Civ. Eng.* 47 (1), 1–12. doi:10.1139/cjce-2019-0049

Suppasri, A., Shuto, N., Imamura, F., Koshimura, S., Mas, E., and Yalciner, A. C. (2013). Lessons learned from the 2011 Great East Japan tSunami: performance of Tsunami countermeasures, coastal buildings, and Tsunami evacuation in Japan. *Pure Appl. Geophys.* 170, 993–1018. doi:10.1007/s00024-012-0511-7

Tomiczek, T., Kennedy, A., Zhang, Y., Owensby, M., Hope, M. E., Lin, N., et al. (2017). Hurricane damage classification methodology and fragility functions derived from Hurricane Sandy's effects in coastal New Jersey. *J. Waterw. Port, Coast. Ocean Eng.* 143 (5), 04017027. doi:10.1061/(asce)ww.1943-5460.0000409

Tomiczek, T., O'Donnell, K., Furman, K., Webbmartin, B., and Scyphers, S. (2020). Rapid damage assessments of Shorelines and structures in the Florida keys after Hurricane Irma. *Nat. Hazards Rev.* 21 (1), 05019006. doi:10.1061/(asce)nh.1527-6996.0000349

Uroš, M., Šavor Novak, M., Atalić, J., Sigmund, Z., Baniček, M., Demšić, M., et al. (2020). Post-earthquake damage assessment of buildings–procedure for conducting building inspections. *Građevinar* 72 (12), 1089–1115. doi:10.14256/JCE.2969.2020

USACE (2006). *Post-event damage survey (PEDS) data requirement white paper, Shore protection assessment*. Vicksburg, Mississippi: U.S. Army Corps of Engineers.

USGS (2023a). *M 7.5 - Elbistan earthquake, Kahramanmaras earthquake sequence*. United States Geological Survey. Available online at: https://earthquake.usgs.gov/earthquakes/eventpage/us6000jlqa/executive (Accessed Auguest 15, 2024).

USGS (2023b). *M 7.8 - Pazarcik earthquake, Kahramanmaras earthquake sequence*. United States Geological Survey. Available online at: https://earthquake.usgs.gov/earthquakes/eventpage/us6000jllz/executive (Accessed Auguest 15, 2024).

Vickery, P. J., Skerlj, P. F., Lin, J., Twisdale Jr, L. A., Young, M. A., and Lavelle, F. M. (2006). HAZUS-MH hurricane model methodology. II: damage and loss estimation. *Nat. Hazards Rev.* 7 (2), 94–103. doi:10.1061/(asce)1527-6988(2006)7:2(94)

Wald, D., Goded, T., Charleson, A., Grünthal, G., Lin, S., Musson, R., et al. (2024). "Developing and implementing an international Macroseismic scale (IMS) for earthquake engineering, earthquake science, and rapid damage assessment," in Proceedings of the 18th world Conference on earthquake engineering. Milan, Italy.

Wartman, J., Berman, J. W., Bostrom, A., Miles, S., Olsen, M., Gurley, K., et al. (2020). Research needs, challenges, and strategic Approaches for natural hazards and disaster reconnaissance. *Front. Built Environ.* 6. doi:10.3389/fbuil.2020.573068

Wilkinson, S., Grant, D., Williams, E., Paganoni, S., Fraser, S., Boon, D., et al. (2013). Observations and implications of damage from the magnitude Mw 6.3 Christchurch, New Zealand earthquake of 22 February 2011. *Bull. Earthq. Eng.* 11, 107–140. doi:10.1007/s10518-012-9384-5

Xian, S., Lin, N., and Hatzikyriakou, A. (2015). Storm surge damage to residential areas: a quantitative analysis for hurricane Sandy in comparison with FEMA flood map. *Nat. Hazards* 79, 1867–1888. doi:10.1007/s11069-015-1937-x

frontiers | Frontiers in Built Environment

TYPE Original Research
PUBLISHED 30 July 2025
DOI 10.3389/fbuil.2025.1594375

Check for updates

OPEN ACCESS

EDITED BY
Jack Cadigan,
Engineer Research and Development Center (ERDC), United States

REVIEWED BY
Andre R. Barbosa,
Oregon State University, United States
Steven Brandt,
Louisiana State University, United States

*CORRESPONDENCE
Ellen M. Rathje,
e.rathje@mail.utexas.edu

RECEIVED 16 March 2025
ACCEPTED 26 May 2025
PUBLISHED 30 July 2025

CITATION
Rathje EM, Kumar K, Esteva M, Brandenberg SJ, Cockerill T, Dawson C, Padgett JE, Pinelli J-P and Stanzione D (2025) A decade of DesignSafe: enabling open science in natural hazards.
Front. Built Environ. 11:1594375.
doi: 10.3389/fbuil.2025.1594375

COPYRIGHT
© 2025 Rathje, Kumar, Esteva, Brandenberg, Cockerill, Dawson, Padgett, Pinelli and Stanzione. This is an open-access article distributed under the terms of the Creative Commons Attribution License (CC BY). The use, distribution or reproduction in other forums is permitted, provided the original author(s) and the copyright owner(s) are credited and that the original publication in this journal is cited, in accordance with accepted academic practice. No use, distribution or reproduction is permitted which does not comply with these terms.

A decade of DesignSafe: enabling open science in natural hazards

Ellen M. Rathje[1]*, Krishna Kumar[1], Maria Esteva[2], Scott J. Brandenberg[3], Tim Cockerill[2], Clint Dawson[4], Jamie E. Padgett[5], Jean-Paul Pinelli[6] and Dan Stanzione[2]

[1]Maseeh Department of Civil, Architectural and Environmental Engineering, University of Texas at Austin, Austin, TX, United States, [2]Texas Advanced Computing Center, University of Texas at Austin, Austin, TX, United States, [3]Civil and Environmental Engineering, University of California at Los Angeles, Los Angeles, CA, United States, [4]Aerospace Engineering and Engineering Mechanics, University of Texas at Austin, Austin, TX, United States, [5]Department of Civil and Environmental Engineering, Rice University, Houston, TX, United States, [6]Department of Mechanical and Civil Engineering, Florida Tech, Melbourne, FL, United States

DesignSafe (www.designsafe-ci.org) is the leading cyberinfrastructure for engineering and social science research related to natural hazards. It provides tools for managing, analyzing, and sharing data, helping researchers study how natural hazards affect both physical infrastructure and communities. DesignSafe connects curated datasets from academic experimental facilities and field reconnaissance teams to researchers focused on data analysis, computation, and numerical simulation. The platform provides researchers with petabyte-scale storage and hundreds of millions of computing hours mediated by intuitive interfaces that lower the bar of entry to advanced computational capabilities. By enabling sophisticated simulations and data-driven workflows previously unattainable with desktop computers or small clusters/servers and enabling streamlined data curation, publication, and dissemination, DesignSafe empowers researchers to accelerate discoveries and helps them amplify the impact of their work.

KEYWORDS

cyberinfrastructure, natural hazards, data, high-performance computing, Jupyter

1 Introduction

Launched in 2015 as part of the Natural Hazards Engineering Research Infrastructure (NHERI), DesignSafe (www.designsafe-ci.org) is the cyberinfrastructure supporting all facets of research related to the impact of natural hazards on the built environment and associated communities. As natural hazards increase in frequency and intensity, so do the data collected and generated by researchers. DesignSafe addresses this explosion of data by providing a cloud-based infrastructure for managing, analyzing, and sharing data, and by providing expanded access to computational resources for performing sophisticated simulations and data analysis. DesignSafe has three core components: the Data Depot repository for data management, curation, and publication; Tools and Applications for cloud-based simulation and analytics; and the Reconnaissance Portal for field research data. Through these integrated components, researchers can accomplish all their data-driven research in a single environment.

DesignSafe focuses on adopting and implementing FAIR (Findable, Accessible, Interoperable, Reusable) data principles. This emphasis on data stewardship led the DesignSafe Data Depot Repository to become a CoreTrustSeal-certified data repository

in 2023, demonstrating its commitment to curating, preserving, and providing access to valuable research data. By providing cloud-based access to high-performance computing (HPC) resources and advanced analysis tools specific to natural hazards research, DesignSafe eliminates traditional computational barriers and enables researchers to tackle previously intractable problems. The integration of data and computation creates new opportunities for discovery, from analyzing massive datasets to performing regional-scale hazard simulations to combining experimental data, field observations, and computational simulation to gain deeper insights into the impacts of natural hazards on physical infrastructure and societal resilience.

DesignSafe helps researchers address a key research question in the NHERI Science Plan: "How can the scientific community more effectively collect and share data and information to enable and foster ethical, collaborative, and transformative research and outcomes?" By creating an integrated platform that supports the full research lifecycle - from data collection and analysis to publication and reuse - DesignSafe promotes a cultural shift toward open science in natural hazards research. It also enables cross-disciplinary collaboration by breaking down traditional silos between experimental, computational, engineering, and social science researchers while enforcing curation best practices and ethical data publication that promote research transparency and reproducibility.

As DesignSafe approaches a decade of operation and almost 10,000 registered users worldwide, its impact extends beyond technological innovation to transforming research practices in the natural hazards community. This paper examines the transformative impact of DesignSafe on natural hazards research from 2015 to 2025, detailing system architecture, platform evolution, community growth, data impact metrics, and case studies across multiple types of hazards and disciplines.

2 DesignSafe architecture

DesignSafe implements a layered architecture that separates core functionality into distinct tiers to enhance maintainability and enable independent scaling of components (Figure 1). At the foundation lies the physical infrastructure provided by the Texas Advanced Computing Center (TACC), consisting of storage systems and high-performance computing clusters such as Frontera, Stampede3, and Lonestar6. This hardware layer supports data-intensive research through large-scale storage and computational capabilities.

The TAPIS API framework (Figure 1) provides the critical interface between the physical infrastructure and the user-facing web portal through a comprehensive RESTful API (Stubbs et al., 2024; 2021; Cardone et al., 2023). TAPIS handles core functionalities, including authentication and authorization across all services, job submission and management on HPC systems, data transfer and management between storage systems, and metadata services for tracking research artifacts. This API-driven architecture enables DesignSafe to integrate new tools and capabilities without disrupting existing services. For example, researchers and developers can leverage TAPIS to access files, submit computational jobs, transfer data, and integrate new applications with existing resources.

The user-facing web portal (Figure 1) represents the top layer, providing intuitive interfaces to access DesignSafe capabilities, such as the Data Depot for data management, curation and publication, Tools and Applications for simulation and analysis, and the Reconnaissance Portal for accessing and contextualizing field research data from natural hazard events. These user interfaces abstract the underlying complexity while maintaining the full power of the infrastructure.

3 Data Depot repository

The Data Depot is the central repository managing more than 1.5 petabytes of research data across private and public workspaces. This repository implements a comprehensive data management strategy that supports users throughout the entire research lifecycle, from initial data collection and curation to analysis and publication.

3.1 Data management

The Data Depot manages data through distinct spaces that serve different phases of research. Individual researchers maintain private storage in My Data, while collaborative research flourishes in My Projects, where more than 3,000 teams have actively developed and shared their work. The commitment to open science manifests itself in its Published section, which hosts almost 1,700 formally curated datasets totaling over 47 million files of publicly accessible research data. The Community Data section enables researchers to store non-curated datasets for less formal sharing needs between colleagues. The Published (NEES) space preserves the research legacy of the previous earthquake-focused cyberinfrastructure (NEEShub, Hacker et al., 2011).

Researchers can easily upload data to the Data Depot through multiple methods, including drag-and-drop file upload, federation with existing cloud data services (e.g., Dropbox, Globus), Secure File Transfer Protocol (SFTP)/Secure Copy Protocol (SCP) for secure transfers, and automated command-line interfaces. The system supports all data formats, accommodating the diverse needs of the natural hazards community. The Data Depot utilizes five specialized data models designed for curating and publishing datasets. These data models provide structured, yet flexible, frameworks for organizing data and other research products such as reports, survey instruments, presentations, and their metadata, ensuring consistent documentation across data derived from different research methods used by the community. The five data models are:

- Experimental Data Model: Supports data from physical experiments, including sensor data, photos, videos, and documentation from the NHERI Experimental Facilities and other laboratories
- Simulation Data Model: Captures computational simulation data, including input files, model configurations, results, and analysis scripts

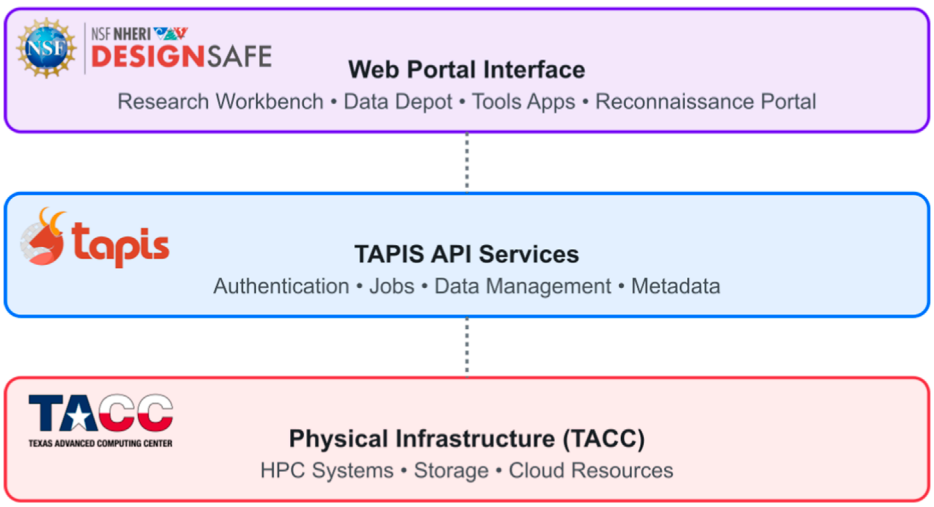

FIGURE 1
DesignSafe system architecture and components: Physical Infrastructure (TACC) providing HPC systems and storage; TAPIS API Services middleware handling authentication and data management; and the Web Portal Interface containing user-facing components for research workflows and data publishing.

- Hybrid Simulation Data Model: Accommodates experiments that combine physical testing with real-time computational simulation
- Field Research Data Model: Handles reconnaissance data collected before, during, and after natural hazard events, including engineering assessments and geoscience observations. This model was adapted to include social science methods such as surveys and interviews collected in the field.
- Other Data Model: Provides flexibility for additional research products such as standalone software, white papers, historical or multi-source data aggregations, and presentations.

Implemented as graphical interfaces (Figure 2), each data model provides a visual map to the key components of each research method listed above. This allows users to organize files in relation to their provenance, understood as the processes by which the data were derived, and in context with the metadata needed for others to understand the published dataset. All data models offer mechanisms for researchers to reference software and other data they reused to create their datasets and the research papers they produce. This creates an ecosystem of data, metadata, software, and publications within and outside the Data Depot, facilitating data reuse, authorship attribution, and research reproducibility.

3.2 Data curation

Like most open-science repositories, the Data Depot offers auto-publication, leaving researchers responsible for releasing quality datasets. In turn, we enable users to publish datasets of enduring value through the infrastructure, the curation interfaces, the enforcement of key data and metadata, and on-boarding and on-demand help.

In the Data Depot, data curation involves the application of the selected data model to organize the uploaded data files within a Project. After upload, the design of the interactive interface enables a progressive approach to data curation, allowing users to assign categories and enter metadata throughout their research process. Projects typically start with minimal metadata during initial data upload, with requirements increasing as they move towards publication. This approach distributes the curation workload across the project timeline rather than concentrating it at the end. The curated dataset is then published, each receiving a Digital Object Identifier (DOI) and appropriate licensing to ensure proper citation and reuse by others.

DesignSafe offers bi-weekly virtual office hours and on-demand assistance from data curators to support the curation and publication processes. Curators also review post-published datasets and suggest amending or versioning to their authors. Another useful resource that helps improve the quality of datasets is the "Leave Feedback" form, which allows reusers of the data to ask questions or make comments about published datasets. The majority of these comments result in improvements to the dataset publication. Over time, this personalized assistance has created stronger trust between DesignSafe staff and the research community, and it has also informed continuous improvements to the curation services and interface.

A unique capability of the DesignSafe Data Depot is that it does not limit the number of files or the size of published datasets. It currently supports individual datasets as large as 26 TB and with millions of files. Other data repositories have size limits on the order of 50–200 GB and file limits of about 100, making them unable to handle many of the datasets created and needed by researchers in natural hazards. In fact, more than 25% of the datasets in the Data Depot are

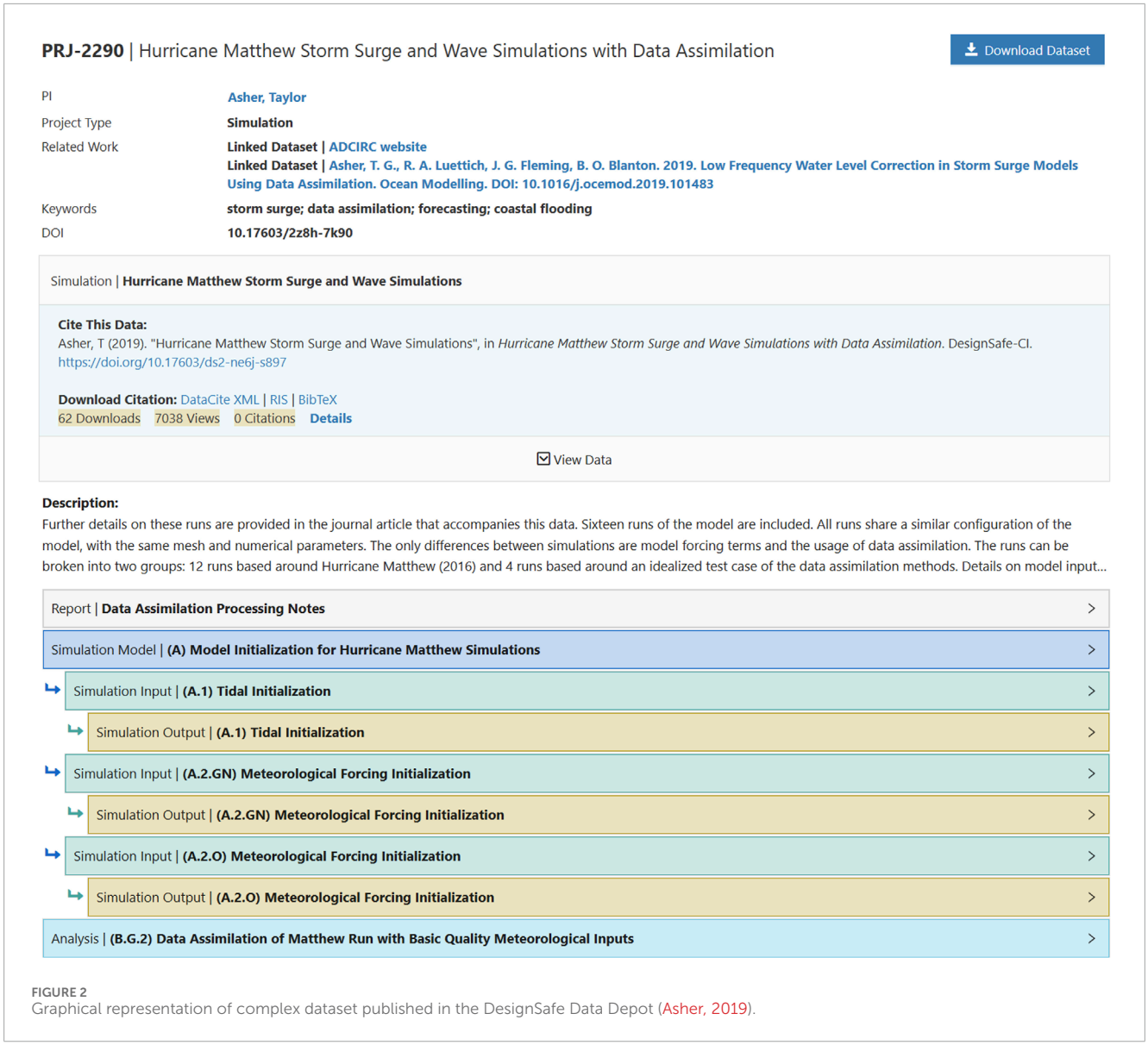

FIGURE 2
Graphical representation of complex dataset published in the DesignSafe Data Depot (Asher, 2019).

larger than 50 GB or have more than 100 files, so it would have been difficult for these researchers to publish their data elsewhere. Furthermore, the graphical representation of the data organization (Figure 2) is particularly useful to navigate these very large and complex datasets.

In January 2023, the Data Depot Repository achieved CoreTrustSeal certification, joining an elite group that represents less than 5% of data repositories worldwide. This certification validates compliance with 16 requirements representing operationalization of the FAIR concepts across organizational infrastructure, digital object management, and technology. Going through the certification process increased the robustness of the Data Depot through enhanced documentation of policies and best practices, the implementation of data integrity and file format identification functionalities, and the use of the Fedora repository software (Payette and Lagoze, 2013) as a connector between the published data and its metadata.

3.3 Publication and usage metrics

As of December 2024, more than 1,700 datasets with assigned DOIs have been published in the DesignSafe Data Depot. We have seen a steady increase in the rate of data publishing (Figure 3a), with almost 400 datasets published in 2024. The published datasets in the first few years were focused predominantly on earthquake hazards, a legacy of the data publishing experience in earthquake engineering during the NEES program. The publishing of datasets associated with hurricanes and other natural hazards quickly accelerated. The current portfolio of published datasets includes a wide range of natural hazards (Figure 3b), with more than half associated with non-earthquake hazards and meaningful percentages associated with inland flooding, tornadoes, landslides, and wildfires. We expect the representation of different hazard types to continue to expand.

To help researchers understand the reach and influence of their data publications, the Data Depot tracks usage metrics compliant with Make Data Count (MDC) standards (Kratz and Strasser,

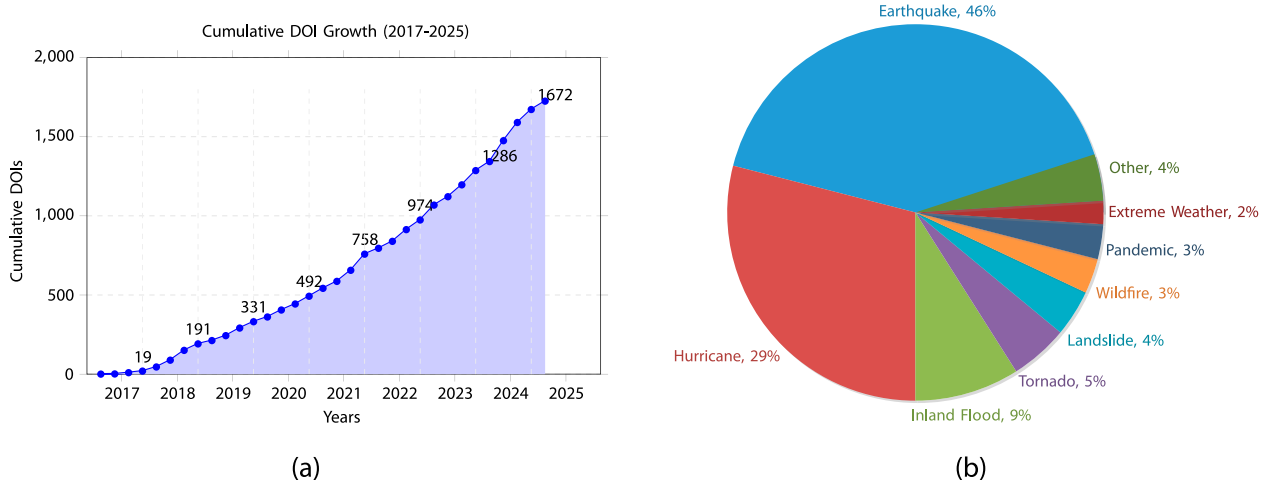

FIGURE 3
Growth in research data accessibility: **(a)** Growth in DOI assignments over time and **(b)** distribution of published datasets by hazard type.

2015). These metrics focus on when and how much users view, copy, preview, and download files and metadata associated with a dataset. They are designed to allow fair usage comparison between small and large datasets. The metrics include Unique Requests, which represent 1-h sessions during which a user previewed, downloaded, or copied files, and Unique Investigations, which represent 1-h sessions during which a user viewed metadata or previewed/downloaded/copied files. DesignSafe adopts the 1-h session definition established by the Make Data Count initiative and Counter Code of Practice, which other major data repositories such as Zenodo also implement to ensure consistent and comparable usage metrics across the research data ecosystem (Make Data Count, 2018). The use of 1-h sessions, rather than individual file downloads, helps normalize usage for datasets of different sizes. We started compiling the MDC metrics in 2022, and since that time published datasets have received more than 55,000 Unique Requests and more than 800,000 Unique Investigations. These metrics are tracked for each DOI and exposed on each published dataset's landing page, allowing to evaluate its impact data over time.

It is difficult to track data use and reuse in the technical literature because the research community is only recently acquiring the habit of properly citing data in their publications. Citing data should be done similarly to citing a paper, with the data citation included in the reference list, and DesignSafe aids researchers by providing the citation language for a dataset on its landing page (Figure 2). Despite these issues, we can quantify the impact of DesignSafe and its data on the natural hazards research community using manual publication counting via Google Alerts and through AI services such as Dimensions.ai. These different mechanisms identified between 1,200 and 1,500 publications that mentioned DesignSafe or DesignSafe datasets. In turn, the impact of these publications on the profession can be quantified by looking at their citations (Figure 4). These publications have been cited more than 12,000 times, and we see rapid growth over time, particularly in the last 4 years, with annual citations increasing from about 1,000 in 2021 to more than 4,500 citations in 2024.

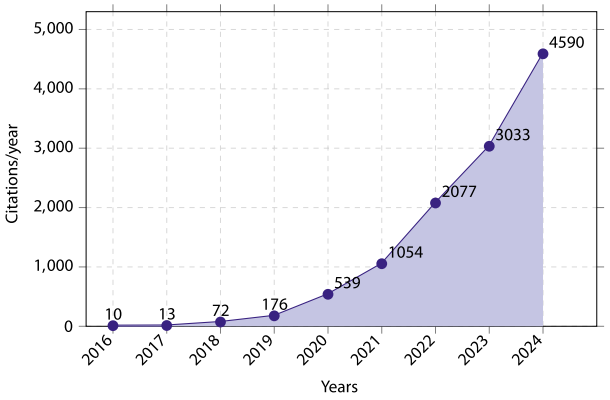

FIGURE 4
Citations of publications that mentioned DesignSafe and DesignSafe datasets, as reported by Dimensions.ai.

DesignSafe also organizes data awareness initiatives to recognize the scientific work involved in creating, curating, and publishing datasets and to demonstrate the science that can be accomplished by reusing data. These initiatives include annual dataset awards (DesignSafe, 2025a), data reuse stories (DesignSafe, 2025b), and "Publish Your Data" events. For instance, recent dataset awards in 2024 highlighted work on "Consistently computed ground motion intensity measures for liquefaction triggering assessment" by Pretell et al. (2023) and "State Hazard Mitigation Plans and Social Vulnerability" by Peek et al. (2024a) and Peek et al. (2024b). Examples of data reuse include the work by Xu et al. (2022) on estimating cascading hazard chains, and the research by Jelínek and Kopačková-Strnadová (2021), which utilized DesignSafe datasets (e.g., Rathje et al., 2017; Massey et al., 2021) for detecting earthquake-triggered landscape changes using Sentinel data. Furthermore, DesignSafe, often in collaboration with partners like CONVERGE, hosts "Publish Your Data" events, such as the

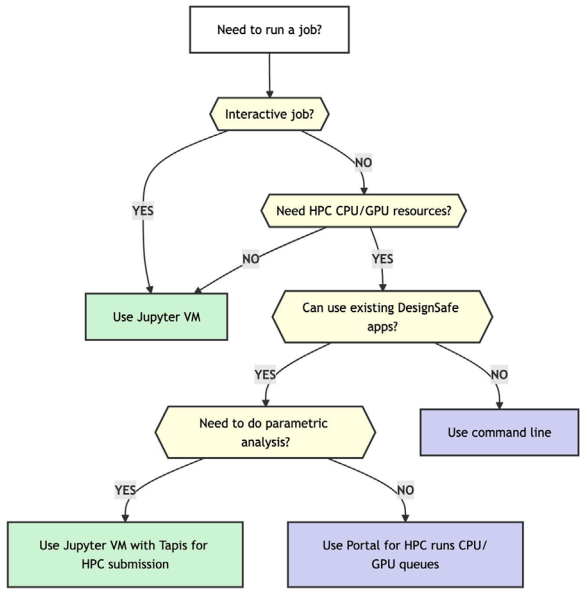

FIGURE 5
Decision flowchart for selecting the appropriate computing environment in DesignSafe based on job requirements.

"Weather Ready Research Instrument and Data Publication Training Session" held in June 2021 (CONVERGE and DesignSafe, 2021), and a series of workshops for social scientists and interdisciplinary researchers in Summer 2020 (CONVERGE and DesignSafe, 2020). As of Spring of 2025, it is possible to search for published field research datasets in the Harvard Dataverse because the Data Depot Repository has a Dataverse sub-collection (DesignSafe, 2025). This integration opens a new venue for disseminating our datasets.

4 Tools and applications

DesignSafe provides researchers access to a comprehensive suite of computational tools running on interactive virtual machines (VMs) and high-performance computing (HPC) resources through its integration with TACC (Stanzione et al., 2020). The platform offers multiple pathways to leverage these resources, following a tiered approach that balances ease of use with customization. Researchers can choose from options ranging from a user-friendly web portal for basic HPC job submission to interactive Jupyter notebooks for data analysis (Pérez and Granger, 2007), all the way to advanced command-line interfaces for orchestrating complex computational workflows. Figure 5 presents a conceptual decision workflow that outlines the options available to users within this computational ecosystem. Researchers with minimal computational requirements and/or interactive needs can utilize the standard Jupyter VM, while those needing HPC resources can leverage existing DesignSafe applications through the web portal interface or build custom Docker containers for specialized workflows (Docker Inc., 2025). This flexible architecture accommodates diverse research needs while maintaining efficient resource utilization.

4.1 TAPIS integration and architecture

In traditional high-performance computing (HPC) environments, researchers can face significant technical barriers. Access requires SSH connections, Linux command-line proficiency, and knowledge of job schedulers like SLURM. This restricts advanced computational resources to those with specialized technical backgrounds, creating a divide between domain scientists and computational capabilities. The DesignSafe TAPIS integration fundamentally transforms this paradigm by creating multiple pathways to utilize computational resources. As illustrated in Figure 6, TAPIS serves as middleware connecting the DesignSafe user-friendly interfaces with the powerful HPC systems at TACC. It manages the complex backend operations—authentication, job scheduling, resource allocation, and file management—while providing several access methods that cater to different technical comfort levels.

DesignSafe offers a multi-tiered approach enabling researchers to begin with simple interfaces and gradually progress to more advanced methods as their skills develop. Beginners can use the web portal's graphical interface to submit HPC jobs through simple forms, while TAPIS automatically handles all file staging and task execution behind the scenes without requiring users to learn command-line operations. Intermediate users can leverage Jupyter Notebooks, which allow Python scripts to call TAPIS commands to orchestrate workflows, masking the SSH-based resource provisioning behind the scenes. Advanced users can fine-tune performance via the command-line interface (CLI) tools, where researchers can inspect and manage TAPIS resources and calls. The resulting democratization of HPC resources has enabled DesignSafe to achieve remarkable throughput—over 60 million core-hours utilized in 2024 alone and almost 400 million core-hours over the last 5 years—demonstrating how effectively TAPIS bridges the gap between natural hazards researchers and computational capabilities.

4.2 Tool integration

The portfolio of simulation tools available in DesignSafe includes widely used applications in natural hazards engineering. ADCIRC (Luettich and Westerink, 2004) enables the modeling of storm surge and coastal circulation, supporting research in hurricane impact prediction and coastal resilience. OpenFOAM (Jasak, 2009) provides CFD capabilities for wind engineering applications, including building aerodynamics and wind load analysis. OpenSees (McKenna, 2011) facilitates structural and geotechnical analysis capabilities for earthquake engineering research. OpenSees also supports hydrodynamic simulations with PFEM (Zhu and Scott, 2014).

DesignSafe works closely with another NHERI component, the Computational Modeling and Simulation Center (SimCenter, Deierlein et al., 2020), to advance the use of simulation in natural hazards research. DesignSafe has deeply integrated the SimCenter computational tools into its infrastructure, providing researchers with streamlined access to advanced natural hazard modeling capabilities. The integration leverages containerized applications that run on the TACC HPC systems

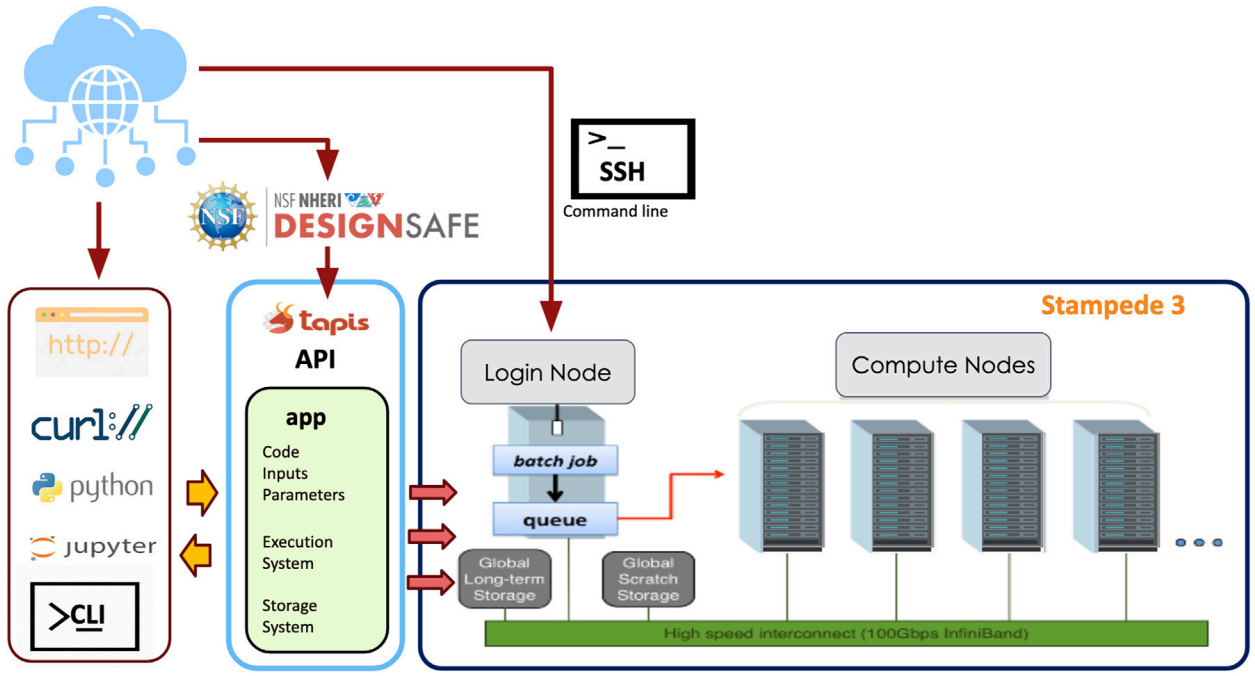

FIGURE 6
TAPIS workflows to access HPC resources. Redrawn based on the original illustration by (Arduino, 2023).

and can be launched directly from the DesignSafe portal. Tools such as quoFEM for uncertainty quantification and R2D for regional-scale hazard assessment use dedicated nodes on the HPC resources for improved performance and throughput. The platform supports web-based interfaces for immediate interaction and batch processing capabilities for larger computational tasks. This integration exemplifies DesignSafe's commitment to providing researchers with comprehensive tools for natural hazards engineering while maintaining ease of use through web-based interfaces.

4.3 Jupyter integration

Jupyter (Pérez and Granger, 2007), an open-source web application for creating interactive computational narratives, has become a cornerstone of the DesignSafe computational ecosystem. Jupyter Notebooks allow researchers to combine live code, equations, visualizations, and explanatory text within a single document, fostering reproducibility, collaboration, and transparency. Within DesignSafe, Jupyter is seamlessly integrated across multiple environments to accommodate diverse computational needs. The Jupyter VM provides an accessible entry point for small-scale analyses and interactive prototyping, enabling users to process experimental data or develop simulation workflows without requiring advanced computational expertise. For larger-scale tasks, DesignSafe offers Jupyter HPC environments, which leverage the TACC HPC clusters to execute parallelized simulations, machine learning workflows, or data-intensive analyses. These environments bridge the gap between user-friendly interfaces and high-performance computing, allowing researchers to scale computations dynamically while maintaining interactive control over their workflows.

4.4 Data access and storage integration

DesignSafe implements a shared data mounting system that provides seamless access to published and shared datasets across its computational environments, including the Jupyter and HPC systems. This architecture enables researchers to access their private data in My Data, collaborative project files in My Projects, and published datasets directly within their computational workflows without requiring separate data transfer steps. A key strength of the DesignSafe Jupyter integration lies in this direct access to the DesignSafe data ecosystem. Researchers can mount data sets from the Data Depot directly into their Jupyter sessions, eliminating manual data transfers and enabling real-time analysis of large datasets within the same environment where simulations are executed. For example, researchers can directly read a published experimental dataset into their Jupyter notebook for analysis or use it as input for simulation runs on HPC systems. Almost 50,000 notebooks have been created in DesignSafe and more than 800 have been published in the Data Depot, many serving as templates for reproducible workflows that are shared and reused across the community. With almost 1,000 active Jupyter users annually, DesignSafe has democratized access to advanced computational resources, empowering researchers to focus on scientific innovation rather than infrastructure management. By embedding Jupyter at the heart of its computational architecture, DesignSafe exemplifies how interactive, cloud-based tools can transform natural hazards research.

4.5 Containerization in DesignSafe

DesignSafe extensively leverages containerization technologies throughout its architecture to create scalable, portable, and reproducible computing environments across diverse resources. For Jupyter services, DesignSafe employs Docker containers orchestrated by Kubernetes (Burns et al., 2016), which provide customizable notebook environments for different analytical needs. This Kubernetes deployment enables elasticity, automatically provisioning more compute and memory for JupyterHub to meet demand. Researchers can select specific notebook containers with libraries and widgets customized to their research workflows.

For high-performance computing environments, DesignSafe transitions to Singularity/Apptainer containers, which are better suited for multi-tenant HPC systems. Containerized applications, including OpenSees Express/Interactive and Jupyter HPC, can be launched directly from the DesignSafe portal and run on TACC HPC systems. This ensures consistent execution across different computing environments, allowing researchers to focus on science rather than software configuration. The TAPIS middleware further enhances this container ecosystem by providing the critical interface between physical infrastructure and user-facing services and transparently managing container deployment, execution, and resource allocation. This comprehensive containerization strategy has proven crucial to DesignSafe's success. It enables the platform to simultaneously support diverse research workflows, maintain software compatibility across heterogeneous systems, and scale resources dynamically in response to community needs.

5 Reconnaissance Portal and tools

The DesignSafe Reconnaissance Portal is a unified platform for discovering and investigating data collected after natural hazard events. This perishable data is collected to document and understand the impact of the event on the built and human environments, and there is an urgency to both collect that data and share it with the broader research community. Through its interactive map interface (Figure 7a), the portal geospatially organizes worldwide reconnaissance data from earthquakes, hurricanes, tsunamis, and other natural hazards, enabling rapid access to event-specific data collected by other NHERI components, such as the NHERI RAPID facility (Berman et al., 2020b) and the CONVERGE extreme events reconnaissance (EER) teams (Peek et al., 2020), as well as relevant data from other sources.

NHERI and CONVERGE EER datasets published in the Data Depot leverage the DesignSafe HazMapper tool (Figure 7b), which allows researchers to visualize and analyze the diverse data types collected, including infrastructure assessments, damage surveys, ground movements, coastal erosion measurements, wind field estimates, and social science surveys. HazMapper supports multiple data formats ranging from geotagged media to LIDAR point clouds and satellite imagery, and recent technical enhancements include improved questionnaire visualization, automated metadata extraction from field instruments, and sophisticated management of overlapping point cloud datasets. Importantly, the HazMapper tool allows researchers to interrogate and analyze these data online without downloading them (Figure 7c).

Importantly, DesignSafe and RAPID not only facilitate the publishing of field data but also facilitate the collection of field data and coordination among field teams during reconnaissance efforts after a natural disaster. Field teams and associated stakeholders use DesignSafe Slack channels to communicate about deployment strategies, damage observations, and preliminary analyses. Once in the field, the teams can synchronize data directly from mobile applications like the RAPID App (RApp) to their DesignSafe projects (Wartman et al., 2021), while integration with Mapillary enables Street View visualization for virtual damage assessment.

The tight coupling of the Reconnaissance Portal with the Data Depot provides researchers with complete access to documentation, metadata, collection protocols, and analysis results for each reconnaissance mission, with proper attribution maintained through DOI-based citations. These features represent another example of how DesignSafe integrates data and tools to create a seamless workflow from data collection to data publication. The Reconnaissance Portal also points to external datasets for each natural hazard event, which provide additional context and information about the impact of the event. Ultimately, the Reconnaissance Portal exemplifies the DesignSafe commitment to enabling data-driven, collaborative research that advances our understanding of natural hazards and community resilience.

6 Growth and impact (2015–2025)

The impact of DesignSafe can be quantified both through detailed metrics, as well as through use cases and user stories that illustrate its influence on research. DesignSafe has experienced substantial growth since its launch in 2015 as the successor to the earthquake-focused cyberinfrastructure, NEEShub (Hacker et al., 2011). This growth demonstrates the increasing adoption of cyberinfrastructure resources by the natural hazards community and the increasing sophistication of research activities performed by the user community.

6.1 Metrics

The user community has grown steadily over the last 10 years, with now almost 10,000 registered users across diverse disciplines. This growth reflects increased adoption of cyberinfrastructure, as well as a broadening of the research community. While NEEShub focused solely on earthquake engineering, DesignSafe supports researchers studying additional hazards, including windstorms, storm surge, tsunamis, and their combined effects, and also supports a user base that spans beyond engineering to include earth science and social sciences.

The impact of DesignSafe becomes particularly evident when examining data storage and usage metrics. The Data Depot has evolved into a comprehensive repository housing over 1.5 petabytes of research data, including both published public data and unpublished private data. Researchers have formally published almost 1,700 datasets, each with a digital object identifier (DOI) enabling proper citation and reuse. The nature of the published datasets has evolved over time, from simple, single-experiment datasets consisting only of sensor data to

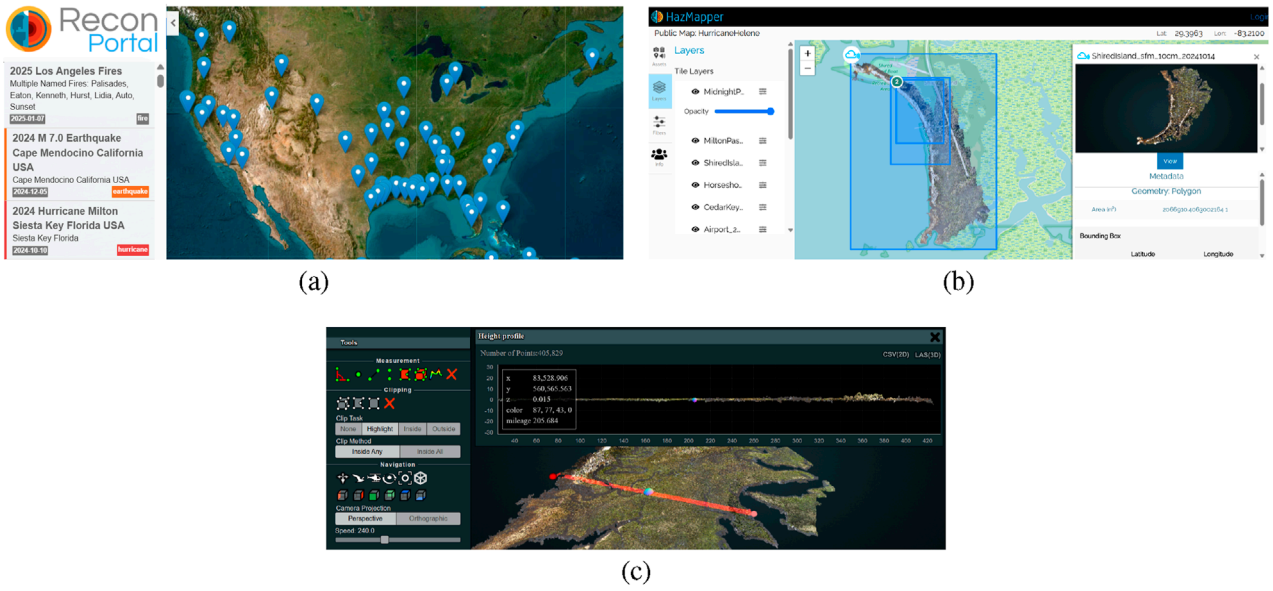

FIGURE 7
The DesignSafe reconnaissance portal: **(a)** Reconnaissance portal showing natural hazard events for which data is available **(b)** HazMapper tool illustrating available data for Hurricanes Helene and Milton (Stark et al., 2025), and **(c)** interrogating the Stark et al. (2025) LIDAR data online in DesignSafe.

complex, multi-disciplinary datasets that capture physical and social responses at a range of scales. The community actively interacts with these published datasets, as demonstrated by over 800,000 1-h sessions in which users viewed metadata or data files since 2022. And publications mentioning DesignSafe have in turn been cited over 12,000 times since 2016, with more than 4,500 citations in 2024. This level of data publishing and data impact represents a significant cultural shift in natural hazards engineering toward open science practices.

Computational usage metrics highlight the role of DesignSafe in enabling sophisticated research workflows. Researchers have utilized more than five million core hours of HPC resources through DesignSafe over the last 5 years. The adoption of Jupyter Notebooks as a primary research tool has been particularly noteworthy, with users creating over 50,000 notebooks for data analysis, visualization, and research workflows. Annually, the Jupyter service attracts 1,000 unique users each year who actively use this cloud-based computational environment.

DesignSafe training and education initiatives drove significant community growth in 2024, engaging 989 researchers through workshops and webinars. These events addressed critical skills from foundational data management to advanced computational methods. Specialized webinar topics—such as Python programming, OpenSees structural analysis, and machine learning applications—consistently attract 50–150 live participants per session, and recordings of the webinars further amplified their reach. The NHERI Computational Academy, which was launched as a joint initiative with the SimCenter, represents a particularly successful engagement model offering extensive hands-on training, tutorials, and hackathon sessions across a four-day program. The Computational Academy has trained more than 150 students since its inception in 2021, evolving its format to better balance instruction with practical application. Tracking the impact of the Computational Academy, participants contributed up to 30 times more to DesignSafe through projects, data publications, and computational resource usage compared to regular users who registered for a DesignSafe account during the same period.

DesignSafe has integrated Slack as a primary communication platform to foster real-time collaboration and knowledge sharing among its user community. The DesignSafe Slack workspace represents a modern evolution from traditional user forums, providing a more dynamic and interactive environment for user support and community engagement. The DesignSafe Slack workspace includes over 4,000 members and actively supports over 100,000 messages and 15,000 file shares per year. The platform organizes discussions through specialized channels that align with different aspects of natural hazards research. These channels include dedicated spaces for specific tools like Jupyter and OpenSees and event-specific channels for particular natural hazard events. These channels become particularly valuable during active natural hazard events, enabling rapid information sharing and coordination among field researchers and data analysts.

6.2 Use cases and user stories

Within its User Guide, DesignSafe provides a collection of comprehensive use case examples that showcase how DesignSafe can be used in natural hazards engineering research. These use cases span multiple disciplines, including earthquake engineering, wind engineering, and storm surge modeling, and feature complete documentation with step-by-step tutorials using Jupyter Notebooks, complete workflows, and examples of research outcomes enabled by DesignSafe. The use cases demonstrate four key capabilities of the platform: (1) seamless integration of large-scale datasets with

interactive analysis tools, (2) efficient execution of complex simulations using high-performance computing resources, (3) advanced data analytics and visualization, and (4) support for uncertainty quantification and machine learning applications. Researchers can access these use cases through the DesignSafe web portal, where they serve as templates for developing similar workflows by others.

There are various user stories that highlight how DesignSafe has influenced research and research practices in the natural hazards community. In 2022, Huang and Swain (2022b) published a paper in Science Advances about the impact of climate change on megafloods in California, and the simulation results that supported this work were published in DesignSafe (Huang and Swain, 2022a). This research was publicized several times over the next few years in media outlets such as the New York Times. As a consequence, the published dataset has seen significant interest with more than 1,100 Unique Investigations over the last 3 years. When asked why they decided to publish their data in DesignSafe, the authors specifically cited the well-designed Data Depot repository, the on-demand curation assistance that was available, and the fact that DesignSafe was focused on reaching researchers with the relevant expertise (i.e., infrastructure, design, risk-assessment) to use their data.

Another example is the impact of DesignSafe on the storm surge research community. The ADCIRC storm surge modeling community runs large models that must be run on HPC platforms, but because these models are so expensive to execute, their use is limited to those researchers with access to HPC resources. DesignSafe has given the broader community access to parallelized versions of ADCIRC that run on the HPC system and are executed easily through the DesignSafe web portal or through TAPIS. Researchers can also utilize the DesignSafe Tools and Applications for end-to-end computing, from data to simulation to data analysis and visualization, all in a cloud-based environment.

Beyond performing simulations, DesignSafe has also facilitated the publishing and reusing storm surge simulation data. Storm surge input data and model output require many GB of storage. After decades of research analyzing historical and synthetic hurricanes and building ever-more complex models, much of the data generated by these studies has been essentially lost. DesignSafe has given the community the ability to reverse this trend, with more than 25 large ADCIRC datasets currently published on DesignSafe. These published datasets have created many avenues for further research in engineering design and ML. Some recent research has used ADCIRC published datasets for improving the accuracy and/or efficiency of storm surge modeling using ML techniques (Pachev et al., 2023a; Cerrone et al., 2025; Rivera-Casillas et al., 2025), and these studies have resulted in their own published datasets (Pachev et al., 2023b; Cerrone et al., 2023; Rivera-Casillas et al., 2024).

Field reconnaissance datasets are crucial for validating community resilience models. By documenting how infrastructure actually performs during natural disasters, these datasets provide real-world data to benchmark simulations and guide evidence-based design standards. For example, the comprehensive structural damage assessments from Hurricane Michael (Roueche et al., 2020; Berman et al., 2020a) documented wind-induced failures and informed updates to wind design provisions. Another example is the detailed geotechnical field observations from the Ridgecrest earthquake sequence (Brandenberg et al., 2019) that captured surface fault rupture, liquefaction, and lifeline performance data essential for identifying potential improvements to earthquake engineering practice. These reconnaissance datasets exemplify how DesignSafe enables the translation of post-disaster observations into actionable knowledge for improving community resilience and informing hazard mitigation policies.

7 Lessons learned from a decade of DesignSafe

The ten-year journey of DesignSafe reveals critical lessons about transforming natural hazards engineering research through cyberinfrastructure. These insights demonstrate how thoughtful platform development and community engagement can fundamentally change research practices while advancing the vision of the NHERI Science Plan.

Perhaps the most important lesson has been the need for a strong collaborative approach between the DesignSafe software developers and the user community of natural hazards researchers. Developing a cyberinfrastructure that will be used by a specific research community must be driven by the needs of that research community, which requires a significant investment of time in understanding research methods and tools used by the community. The development process necessarily is progressive, in which feedback for an initial release is obtained from the community and used to improve the interface for the next release. Over time, strong relationships and trust have been built between the DesignSafe staff and the user community, such that we work together to produce the best interfaces for the user community.

For the Data Depot, the development process has involved evaluation of the interface from the perspective of data publishers as well as data users. Our curation interface and its documentation have evolved as we observed the pain points of users during curation, and we have revised the view of published data to better serve those seeking to reuse data for their research so they can easily understand the published datasets.

The initial data model-based curation and publication design accommodates the different research methods used by our community while maintaining the flexibility to adapt to emerging needs. For example, when social scientists joined NHERI, DesignSafe was able to quickly adapt to support their unique data requirements. This implementation strategy enabled rapid adoption by new user communities while maintaining data quality standards. Additionally, implementing the Fedora repository system provided a robust foundation for long-term preservation of research datasets. The 2023 CoreTrustSeal certification validated this balanced approach, demonstrating that rigorous data stewardship can coexist with researcher-friendly practices.

The computational transformation of DesignSafe reflects the changing nature of research workflows. Early experiences revealed researchers needed interactive access to data and computing resources rather than traditional batch processing. The introduction of Jupyter proved particularly transformative, offering an accessible entry point to advanced computing and support for complex research workflows. As artificial intelligence and machine learning has gained prominence in natural hazards research, DesignSafe adapted by introducing specialized Jupyter environments running on HPC systems that provide essential resources for training

machine learning models. Additionally, collaboration with the SimCenter resulted in their unique simulation tools taking advantage of HPC and lowering the bar to entry for new users. The multi-tiered approach towards computation maintains the accessibility of cloud computing while delivering the computational power needed for advanced research.

Field research support emerged as a prime example of how cyberinfrastructure can bridge traditional disciplinary boundaries. The Reconnaissance Portal and the associated development of specialized tools for field research data demonstrated the importance of incorporating diverse stakeholder needs - from engineering measurements to social science observations. Integration with the RAPID facility and CONVERGE created standardized protocols that enhanced data quality while streamlining data collection efforts. These partnerships showcased how thoughtful collaboration could address complex post-disaster data gathering and analysis challenges.

Looking ahead to the next decade, DesignSafe will continue evolving to meet the changing needs of natural hazards researchers. Future developments will emphasize AI-enhanced data intelligence, extensible research workflows, and deeper integration with HPC resources. These advances will enable new forms of discovery by helping researchers identify patterns across diverse datasets, automate routine tasks, and tackle increasingly complex simulations.

Another significant lesson centers on fostering a cultural change in research practices. The DesignSafe experience revealed that technical capabilities alone do not drive adoption - researchers need comprehensive support through training, documentation, and peer examples. The webinar series evolved into a vital knowledge-sharing channel, regularly attracting hundreds of participants eager to learn about new capabilities and research applications. In-person training events, notably the NHERI Computational Academy, created immersive learning experiences that accelerated the adoption of computational approaches. And the published use case examples provided the peer examples that were templates for how DesignSafe can be used to facilitate research. The introduction of the DesignSafe Slack workspace transformed community interaction, creating a vibrant hub where researchers share knowledge, coordinate activities, and receive real-time support.

These lessons align with broader NHERI objectives by demonstrating how cyberinfrastructure can enable transformative research through adaptable data management, accessible computation, and dynamic community engagement. The evolution of DesignSafe from a specialized earthquake engineering resource that succeeded NEEShub to a comprehensive multi-hazard research environment exemplifies how careful attention to researcher needs can expand the boundaries of scientific investigation. As natural hazards research evolves, these insights provide valuable guidance for developing future cyberinfrastructure initiatives that advance scientific discovery while building resilient communities.

Data availability statement

The datasets presented in this study can be found in online repositories. The names of the repository/repositories and accession number(s) can be found in the reference list of the article.

Author contributions

ER: Writing – original draft. KK: Writing – original draft. ME: Writing – review and editing. SB: Writing – review and editing. TC: Writing – review and editing. CD: Writing – review and editing. JP: Writing – review and editing. J-PP: Writing – review and editing. DS: Writing – review and editing.

Funding

The author(s) declare that financial support was received for the research and/or publication of this article. DesignSafe has been funded by the National Science Foundation (NSF) under Grant Nos. CMMI-2022469 and CMMI-1520817. DesignSafe also leverages the Frontera computing project at the Texas Advanced Computing Center. Frontera is made possible by National Science Foundation award OAC-1818253.

Conflict of interest

The authors declare that the research was conducted in the absence of any commercial or financial relationships that could be construed as a potential conflict of interest.

Generative AI statement

The author(s) declare that no Generative AI was used in the creation of this manuscript.

Publisher's note

All claims expressed in this article are solely those of the authors and do not necessarily represent those of their affiliated organizations, or those of the publisher, the editors and the reviewers. Any product that may be evaluated in this article, or claim that may be made by its manufacturer, is not guaranteed or endorsed by the publisher.

References

Arduino, P. (2023). *Launching HPC jobs with TAPIS*. Personal communication, University of Washington.

Asher, T. (2019). Hurricane Matthew storm surge and wave simulations. DesignSafe-CI. doi:10.17603/ds2-ne6j-s897

Berman, J., Lyda, A., Dafni, J., Yeung, J. S., Grasso, D., Johnson, P., et al. (2020a). RAPID EF team. In *StEER—Hurricane Michael*. DesignSafe-CI. doi:10.17603/DS2-VMQV-RJ36

Berman, J. W., Wartman, J., Olsen, M., Irish, J. L., Miles, S. B., Tanner, T., et al. (2020b). Natural hazards reconnaissance with the NHERI RAPID facility. *Front. Built Environ.* 6, 573067. doi:10.3389/fbuil.2020.573067

Brandenberg, S., Stewart, J., Wang, P., Nweke, C. C., Davis, C. A., Hudson, K., et al. (2019). GEER Association report - Ridgecrest, CA earthquake sequence july 4 and 5, 2019. DesignSafe-CI. doi:10.17603/ds2-vpmv-5b34

Burns, B., Grant, B., Oppenheimer, D., Brewer, E., and Wilkes, J. (2016). Borg, omega, and kubernetes. *Commun. ACM* 59, 50–57. doi:10.1145/2890784

Cardone, R., Padhy, S., Black, S., Stubbs, J., and Cleveland, S. (2023). "A decentralized authorization and security framework for distributed research workflows," in *2023 IEEE 47th annual computers, software, and applications conference (COMPSAC)* (Los Alamitos, CA, USA: IEEE Computer Society), 741–746. doi:10.1109/COMPSAC57700.2023.00102

Cerrone, A., Westerink, L., Dawson, C. N., and Westerink, J. (2023). Improving storm surge forecasts with transformers. DesignSafe-CI. doi:10.17603/DS2-T5MF-3757

Cerrone, A., Westerink, L., Ling, G., Blakely, C., Wirasaet, D., Dawson, C., et al. (2025). Correcting physics-based global tide and storm water level forecasts with the temporal fusion transformer. *Ocean. Model.* 195, 102509. doi:10.1016/j.ocemod.2025.102509

CONVERGE and DesignSafe (2020). Publish your data! events for social scientists and interdisciplinary researchers (series). Series of events held in Summer 2020. Available online at: https://converge.colorado.edu/data/publish-your-data/events-videos/(Accessed May 21, 2025).

CONVERGE and DesignSafe (2021). Publish your data! weather ready research instrument and data publication training session. Event held on June 30, 2021. Available online at: https://converge.colorado.edu/data/publish-your-data/events-videos/ (Accessed May 21, 2025).

Deierlein, G. G., McKenna, F., Zsarnóczay, A., Kijewski-Correa, T., Kareem, A., Elhaddad, W., et al. (2020). A cloud-enabled application framework for simulating regional-scale impacts of natural hazards on the built environment. *Front. Built Environ.* 6, 558706. doi:10.3389/fbuil.2020.558706

DesignSafe (2025). DesignSafe collection on Harvard Dataverse. *Harv. Dataverse*. Available online at: https://dataverse.harvard.edu/dataverse/designsafe (Accessed March 13, 2025).

DesignSafe (2025a). Designsafe dataset awards. Available online at: https://www.designsafe-ci.org/community/dataset-awards/(Accessed May 21, 2025).

DesignSafe (2025b). Impact of data reuse. Available online at: https://www.designsafe-ci.org/use-designsafe/impact-of-data-reuse/(Accessed May 21, 2025).

Docker Inc. (2025). Docker Engine release notes. Version 24.0.5. (Acceesed July 11, 2025).

Hacker, T. J., Eigenmann, R., Bagchi, S., Irfanoglu, A., Pujol, S., Catlin, A., et al. (2011). The neeshub cyberinfrastructure for earthquake engineering. *Comput. Sci. and Eng.* 13, 67–78. doi:10.1109/mcse.2011.70

Huang, X., and Swain, D. (2022a). Arkstorm 2.0: atmospheric simulations depicting extreme storm scenarios capable of producing a California megaflood. DesignSafe-CI. doi:10.17603/ds2-mzgn-cy51

Huang, X., and Swain, D. L. (2022b). Climate change is increasing the risk of a California megaflood. *Sci. Adv.* 8, eabq0995. doi:10.1126/sciadv.abq0995

Jasak, H. (2009). Openfoam: open source cfd in research and industry. *Int. J. Nav. Archit. ocean Eng.* 1, 89–94. doi:10.2478/ijnaoe-2013-0011

Jelének, J., Kopačková-Strnadová, V., Huang, X., Jia, X., Gong, Y., and Zou, Q. (2021). Synergic use of sentinel-1 and sentinel-2 data for automatic detection of earthquake-triggered landscape changes: a case study of the 2016 Kaikoura earthquake (mw 7.8), New Zealand. *Remote Sens.* 13, 879. doi:10.3390/rs13050879

Kratz, J. E., and Strasser, C. (2015). Making data count. *Sci. data* 2, 150039–5. doi:10.1038/sdata.2015.39

Luettich, R. A., and Westerink, J. J. (2004). *Formulation and numerical implementation of the 2D/3D ADCIRC finite element model version 44*, 20. NC, USA: R. Luettich Chapel Hill.

Make Data Count (2018). Make data count: 10 processing rules for underlying reporting data — code of practice for research data. Available online at: https://coprd.countermetrics.org/en/1.0.1/10-processing.html (Accessed May 23, 2025).

Massey, C., Townsend, D., Rosser, B., Morgenstern, R., Jones, K., Lukovic, B., et al. (2021). Version 2.0 of the landslide inventory for the mw 7.8 14 November 2016, Kaikoura earthquake. DesignSafe-CI. doi:10.17603/DS2-1FTV-HM22

McKenna, F. (2011). OpenSees: a framework for earthquake engineering simulation. *Comput. Sci. and Eng.* 13, 58–66. doi:10.1109/mcse.2011.66

Pachev, B., Arora, P., del Castillo-Negrete, C., Valseth, E., and Dawson, C. (2023a). A framework for flexible peak storm surge prediction. *Coast. Eng.* 186, 104406. doi:10.1016/j.coastaleng.2023.104406

Pachev, B., Del-Castillo-Negrete, C., Arora, P., Dawson, C., and Valseth, E. (2023b). Reduced order models for peak storm surge in Texas and Alaska. in *ADCIRC Reduced Order Modeling*, DesignSafe-CI. doi:10.17603/ds2-85j6-k851

Payette, S., and Lagoze, C. (2013). Flexible and extensible digital object and repository architecture (fedora). *arXiv Prepr. arXiv*. doi:10.48550/arXiv.1312.1258

Peek, L., Tobin, J., Adams, R. M., Wu, H., and Mathews, M. C. (2020). A framework for convergence research in the hazards and disaster field: the natural hazards engineering research infrastructure converge facility. *Front. Built Environ.* 6, 110. doi:10.3389/fbuil.2020.00110

Peek, L., Painter, M. A., and Villarreal, M. (2024a). "2016–21 State Hazard Mitigation Plans (SHMPs) and Social Vulnerability Qualitative Data," in *State Hazard Mitigation Plans and Social Vulnerability*. DesignSafe-CI. doi:10.17603/ds2-g8tz-qg93

Peek, L., Painter, M., and Villarreal, M. (2024b). "2016-2021 State Hazard Mitigation Plans (SHMPs) and Social Vulnerability Quantitative Data," in *State Hazard Mitigation Plans and Social Vulnerability*. DesignSafe-CI. doi:10.17603/ds2-sc34-as63

Pérez, F., and Granger, B. E. (2007). IPython: a system for interactive scientific computing. *Comput. Sci. Eng.* 9, 21–29. doi:10.1109/MCSE.2007.53

Pretell, R., Brandenberg, S., and Stewart, J. (2023). Consistently computed ground motion intensity measures for liquefaction triggering assessment. DesignSafe-CI. doi:10.17603/ds2-6vj1-t096

Rathje, E., Wartman, J., Massey, C., and Little, M. (2017). Kaikoura Earthquake Landslide Inventory. DesignSafe-CI. doi:10.17603/DS2508W

Rivera-Casillas, P., Dutta, S., Cai, S., Loveland, M., Nath, K., Shukla, K., et al. (2024). "2D ADCIRC simulation of tidal flow in Shinnecock Inlet, NY parameterized by bottom friction coefficien," in *A neural operator-based emulator for regional shallow water dynamics*. DesignSafe-CI. doi:10.17603/ds2-w533-0n80

Rivera-Casillas, P., Dutta, S., Cai, S., Loveland, M., Nath, K., Shukla, K., et al. (2025). *A neural operator-based emulator for regional shallow water dynamics*. *arXiv Prepr. arXiv*. doi:10.48550/arXiv.2502.14782

Roueche, D., Kijewski-Correa, T., Cleary, J., Gurley, K., Marshall, J., Pinelli, J.-P., et al. (2020). StEER field assessment structural team (FAST). In *StEER—Hurricane Michael*. DesignSafe-CI. doi:10.17603/ds2-5aej-e227

Stanzione, D., West, J., Evans, R. T., Minyard, T., Ghattas, O., and Panda, D. K. (2020). "Frontera: the evolution of leadership computing at the national science foundation," in *Practice and experience in advanced research computing 2020: catch the wave*, 106–111.

Stark, N., Gardner, M., Grilliot, M., Lyda, A., Dedinsky, K., Mueller, J., et al. (2025). NEER/GEER: Hurricanes Helene and Milton dataset. In *Multidisciplinary Pre, During and Post Storm Data Collection*. DesignSafe-CI. doi:10.17603/ds2-m8h3-5802

Stubbs, J., Cardone, R., Packard, M., Jamthe, A., Padhy, S., Terry, S., et al. (2021). Tapis: an api platform for reproducible, distributed computational research. *Adv. Inf. Commun. Proc. 2021 Future Inf. Commun. Conf. (FICC)* 1, 878–900. doi:10.1007/978-3-030-73100-7_61

Stubbs, J., Padhy, S., and Cardone, R. (2024). "Toward smart scheduling in tapis," in *2024 IEEE international conference on big data (BigData)* (IEEE), 4204–4209.

Wartman, J., Berman, J. W., Olsen, M., Irish, J., Gurley, K., Miles, S., et al. (2021). "Capturing geotechnical extreme event performance with the NHERI RAPID," in *Geo-extreme 2021 (ASCE)*, 175–182.

Xu, S., Dimasaka, J., Wald, D. J., and Noh, H. Y. (2022). Seismic multi-hazard and impact estimation via causal inference from satellite imagery. *Nat. Commun.* 13, 7793. doi:10.1038/s41467-022-35418-8

Zhu, M., and Scott, M. H. (2014). Modeling fluid–structure interaction by the particle finite element method in opensees. *Comput. and Struct.* 132, 12–21. doi:10.1016/j.compstruc.2013.11.002

frontiers | Frontiers in Built Environment

TYPE Original Research
PUBLISHED 05 August 2025
DOI 10.3389/fbuil.2025.1590479

Check for updates

OPEN ACCESS

EDITED BY
Rebecca Napolitano,
The Pennsylvania State University (PSU),
United States

REVIEWED BY
Mihaela Kouteva-Guentcheva,
Civil Engineering and Geodesy, Bulgaria
Paulo Providencia,
University of Coimbra, Portugal

*CORRESPONDENCE
Adam Zsarnóczay,
adamzs@stanford.edu

RECEIVED 09 March 2025
ACCEPTED 25 June 2025
PUBLISHED 05 August 2025

CITATION
Zsarnóczay A, Deierlein GG, McKenna F, Schoettler M, Yi S-R, Cetiner B, Satish AB, Zhao J, Bonus J, Melaku AF, Naeimi S, Arduino P, Davidson R, Gorle C, Govindjee S, Kareem A, Kijewski-Correa TL, Lowes LN, Motley M, Spence SMJ, Taciroglu E, Taflanidis AA and DeJong M (2025) An open-source simulation platform to support and foster research collaboration in natural hazards engineering.
Front. Built Environ. 11:1590479.
doi: 10.3389/fbuil.2025.1590479

COPYRIGHT
© 2025 Zsarnóczay, Deierlein, McKenna, Schoettler, Yi, Cetiner, Satish, Zhao, Bonus, Melaku, Naeimi, Arduino, Davidson, Gorle, Govindjee, Kareem, Kijewski-Correa, Lowes, Motley, Spence, Taciroglu, Taflanidis and DeJong. This is an open-access article distributed under the terms of the Creative Commons Attribution License (CC BY). The use, distribution or reproduction in other forums is permitted, provided the original author(s) and the copyright owner(s) are credited and that the original publication in this journal is cited, in accordance with accepted academic practice. No use, distribution or reproduction is permitted which does not comply with these terms.

An open-source simulation platform to support and foster research collaboration in natural hazards engineering

Adam Zsarnóczay[1]*, Gregory G. Deierlein[1], Frank McKenna[2], Matthew Schoettler[2], Sang-Ri Yi[2], Barbaros Cetiner[2], Aakash Bangalore Satish[2], Jinyan Zhao[2], Justin Bonus[2], Abiy F. Melaku[2], Sina Naeimi[2], Pedro Arduino[3], Rachel Davidson[4,5], Catherine Gorle[1], Sanjay Govindjee[2], Ahsan Kareem[6], Tracy L. Kijewski-Correa[6,7], Laura N. Lowes[3], Michael Motley[3], Seymour M. J. Spence[8], Ertugrul Taciroglu[9], Alexandros A. Taflanidis[6] and Matthew DeJong[2]

[1]Department of Civil and Environmental Engineering, Stanford University, Stanford, CA, United States, [2]Department of Civil and Environmental Engineering, University of California, Berkeley, Berkeley, CA, United States, [3]Department of Civil and Environmental Engineering, University of Washington, Seattle, WA, United States, [4]Department of Civil and Environmental Engineering, University of Delaware, Newark, DE, United States, [5]Disaster Research Center, University of Delaware, Newark, DE, United States, [6]Department of Civil and Environmental Engineering and Earth Sciences, University of Notre Dame, Notre Dame, IN, United States, [7]Pulte Institute for Global Development, University of Notre Dame, Notre Dame, IN, United States, [8]Department of Civil and Environmental Engineering, University of Michigan, Ann Arbor, MI, United States, [9]Department of Civil and Environmental Engineering, University of California, Los Angeles, Los Angeles, CA, United States

Computational simulation is a critical tool for assessing the impacts of natural hazards and informing risk mitigation and resilience strategies. The NHERI SimCenter has developed an open-source, modular framework that integrates performance-based engineering methodologies with regional-scale assessments to enable multi-hazard, multi-scale simulations. This paper presents the conceptual foundation and current capabilities of the SimCenter platform, covering hazard characterization, structural response analysis, damage and loss estimation, and recovery modeling. By leveraging high-performance computing, standardized data schemas, and open-source tools, the platform facilitates transparent, reproducible research while bridging local and regional analyses. Key contributions include improved inventory generation, damage simulation, and recovery analysis, with applications extending across multiple hazard domains. The paper also discusses challenges in implementing high-resolution, high-fidelity simulations, advancing multi-hazard assessments, and enhancing accessibility for a broad user base. Looking ahead, expanding hazard models, refining regional-to-local modeling techniques, and fostering community collaboration will be essential for advancing computational simulation in natural hazards engineering. Through continued development, the SimCenter aims to provide researchers and

practitioners with scalable, adaptable tools to enhance disaster risk assessment and resilience planning.

KEYWORDS

computational simulation, natural hazards engineering, regional risk assessment, multi-hazard analysis, recovery analysis

1 Introduction

Natural hazards, including earthquakes, hurricanes, and tsunamis, pose significant risks to communities, infrastructure, and economies worldwide. Understanding and mitigating these risks require advanced computational simulation tools capable of capturing the complexities of hazard events, structural vulnerabilities, and community resilience. Over the past decade, advancements in computational modeling have enabled researchers to develop more sophisticated simulations that inform risk mitigation strategies and disaster recovery efforts. However, to maximize the impact of these tools, there is a critical need for collaboration and shared resources across disciplines.

Recognizing this need, the Natural Hazards Engineering Research Infrastructure (NHERI) was established as a national initiative in the United States to provide a comprehensive research ecosystem supporting the study of natural hazards and their impact on the built environment. As part of this initiative, the NHERI SimCenter has developed a cohesive, open-source platform over the past 9 years. This platform integrates existing research with new software solutions to support next-generation numerical modeling and computational simulation for the broader research community.

In collaboration with natural hazards researchers, the SimCenter designed a flexible, extensible, and scalable computational framework that streamlines complex, probabilistic workflows. This framework integrates diverse numerical models, datasets, and software tools, enabling high-fidelity simulations that account for and quantify uncertainties in inputs and models. Computational efficiency is enhanced through state-of-the-art machine learning approaches, preserving calculation fidelity at a fraction of the computational cost, thus allowing a broad range of researchers to analyze natural hazard impacts on structures, lifelines, and communities. By fostering a collaborative research environment, the SimCenter promotes knowledge generation that informs mitigation efforts, enhances preparedness, and promotes recovery from disasters.

This paper presents the current state of computational simulation research and reviews how the SimCenter's computational platform has evolved to meet research needs and priorities in natural hazards engineering. This paper also highlights areas of rapid development over the past decade and discusses emerging needs and challenges for computational simulation in disaster risk management over the next decade and beyond.

The SimCenter's framework and models draw from extensive past research, notably performance-based earthquake engineering (PBEE) methodologies from the Pacific Earthquake Engineering Research (PEER) Center. It also incorporates contributions from other large research centers, including the Multidisciplinary Center for Earthquake Engineering Research (MCEER), the Mid-America Earthquake (MAE) Center, and the Natural Hazards Center. Additionally, the framework integrates methodologies from major government-funded initiatives for disaster mitigation and response, such as Hazus (FEMA, 2024b), FEMA 273 (FEMA, 1997), and FEMA P-58 (FEMA, 2012). Input from practicing engineers, including SEAOC's VISION 2000 (SEAOC, 1995) and SPUR's Resilient City (SPUR, 2009), and successful technology transfer collaborations between academia and industry have further informed the development of the SimCenter's simulation tools.

Complementary efforts to identify key research gaps and emerging areas have shaped the SimCenter's vision and developments. The NHERI Science Plans (Robertson, et al., 2023; Edge, et al., 2020; Smith et al., 2017) and NHERI Decadal Visioning Study 2026-2035 (Schneider and Kosters, 2024) provide broad insights into community priorities, while the SimCenter's reports on the State of the Art in Computational Simulation (Deierlein and Zsarnóczay, 2021; Deierlein and Zsarnóczay, 2019) have guided development strategies. Additionally, the NHERI Computational Symposia are a critical venue for engaging annually with researchers and practitioners, gathering feedback that informs the SimCenter's research and development priorities.

The SimCenter's mandate has primarily focused on simulating the impacts of hurricanes, earthquakes, and tsunamis. However, the wider open-source modular framework for risk assessment can be extended to multiple hazards, including flood and wildfires, and other aspects of the platform, such as inventory generation, are invaluable beyond natural hazards engineering. While the SimCenter's research engagement has been primarily within the United States—leading to a focus on U.S.-based infrastructure, data, and resources—the platform is inherently adaptable and can be used by research groups worldwide.

This paper primarily focuses on the research and scientific contributions enabled by the SimCenter's software tools and applications. It begins with an overview of the conceptual simulation framework developed over the past 9 years. The following sections explore research areas supported by the simulation platform, including references to related applications of the software in research. The discussion is organized around four broad areas:

1. Inventories of the Built Environment and Communities
2. Natural Hazard Events
3. Asset Modeling and Damage Estimation
4. Losses, Performance, and Recovery

Through its continued efforts, the SimCenter remains committed to advancing computational simulation for natural hazards research, ensuring that the research community has scalable, open-source, and adaptable tools to address the challenges of disaster risk management in the coming decade and beyond.

2 SimCenter framework and simulation platform

The SimCenter Framework for computational simulation in Natural Hazards Engineering is built upon a performance-based engineering methodology, drawing from pioneering research in Performance-Based Earthquake Engineering (PBEE) and risk assessment from the late 1990s and early 2000s (Deierlein et al., 2020). The PBEE approach organizes calculations into a standardized sequence of steps, leveraging a Markovian assumption to systematically decompose the complex problem of seismic loss assessment into smaller, manageable subproblems. This modular structure has facilitated independent yet cohesive advancements across multiple research domains while maintaining the integrity of system-level calculations.

The effectiveness of the PBEE framework has been widely demonstrated in earthquake engineering and its modular organization has, over the past 2 decades, been successfully adapted by performance assessment methodologies under other hazards such as wind and water (e.g., Ouyang and Spence, 2020; Attary et al., 2017; ASCE, 2023) and various infrastructure asset types (e.g., Darestani et al., 2022). Its foundational concepts have led to the development of two widely used but methodologically distinct applications: FEMA P-58, a probabilistic component-based seismic loss assessment method for building-specific evaluation (FEMA, 2012), and HAZUS, a set of regional loss assessment methods for earthquakes (FEMA, 2024b), floods (FEMA, 2024c), hurricanes (FEMA, 2024d), and tsunamis (FEMA, 2024g).

Expanding upon this foundation, the SimCenter has developed a unified and modular computational framework, illustrated in Figure 1, that extends performance-based methodologies beyond individual buildings to regional-scale assessments of the built environment and affected communities. This framework integrates high-resolution simulation models of natural hazard events, infrastructure, and households into a seamless computational workflow that efficiently exchanges information between modules. By preserving complex dependencies throughout the simulation process, the framework ensures that regional-scale analyses are not merely collections of independent evaluations but rather coherent, system-wide representations of disaster impact and resilience.

A key advancement of the SimCenter's framework is its ability to embed local-scale analyses within regional-scale simulations, allowing for detailed assessment of individual assets while maintaining a holistic perspective of broader impacts. This capability bridges traditionally siloed research areas, enhancing the interplay between localized and system-wide evaluations. The resulting framework enhances existing capabilities in five critical areas:

1. Formalize Input Data for Regional Simulations: The framework recognizes the critical role inventory and event information play in regional studies. It includes a formal description of the key variables, including Location (LOC), Asset Information Model (AIM) for inventories, and Intensity Measures (IMs) for events. Through its modular architecture, the framework encourages research on the generation of robust inventories and studies that establish a link between expensive natural hazard event simulation outputs and event IMs (e.g., ground accelerations, wind speeds) corresponding to each asset while accounting for spatial dependencies. Research in these areas can ensure the coherent representation of assets and demands before structural analysis, damage estimation, and loss assessment.
2. Multi-Resolution Model Support: The flexible definitions for structural analysis, damage assessment, and loss estimation accommodate various levels of fidelity and various model resolutions within the same regional simulation. This modularity supports, for example,: (a) the efficient calculation of Loss Measures (LMs) directly from IMs by skipping structural and damage analyses; (b) the use of Engineering Demand Parameters (EDPs) and Damage Measures (DMs) without loss analysis when only response and damage information is needed; and (c) the calculation of damage and losses using detailed, high-fidelity analyses (e.g., finite element, computational fluid dynamics, etc.). The framework's multi-resolution approach fosters benchmarking, calibration, and multi-fidelity studies within a single simulation environment.
3. Generalization Across Hazards: The framework maintains a standardized vocabulary and computational logic across multiple hazard types, fostering interdisciplinary collaboration and enabling multi-hazard simulations. By unifying methodologies across different hazards, the framework enhances interoperability and facilitates the integration of hazard-specific knowledge into a cohesive simulation environment.
4. Adaptability for Diverse Asset Types: Designed for versatility, the framework supports the analysis of various infrastructure assets, including pipelines, electrical transmission towers, and other critical infrastructure. The multi-resolution analysis approach allows for tailored model strategies across different asset classes while ensuring compatibility in response, damage, consequence, and recovery analyses.
5. Regional Recovery Simulation: A key framework enhancement assigns Decision Variable (DV) generation to a regional, systemic recovery analysis step. Unlike traditional PBEE, where loss analyses generated DVs, our framework's loss analyses yield Loss Measures (LMs) limited to direct or immediate losses. This change aligns with recent literature recommending the consistent consideration of systemic effects for regional disaster impact assessments (Koliou et al., 2020). The recovery analysis module is designed to model post-disaster recovery, evaluating the progressive restoration of functionality and repair of infrastructure and communities over time.

Integrating recovery modeling with hazard characterization and inventory development, the framework (Figure 1) offers a comprehensive perspective on disaster resilience—from defining decision Options (OPT) to making decisions based on calculated Decision Variables. These enhancements to the SimCenter's computational framework enable high-fidelity, regionally scalable simulations that support disaster risk reduction and resilience planning.

The SimCenter Framework is the foundation for an implemented simulation platform of versatile applications that can be customized and extended by researchers and practitioners in

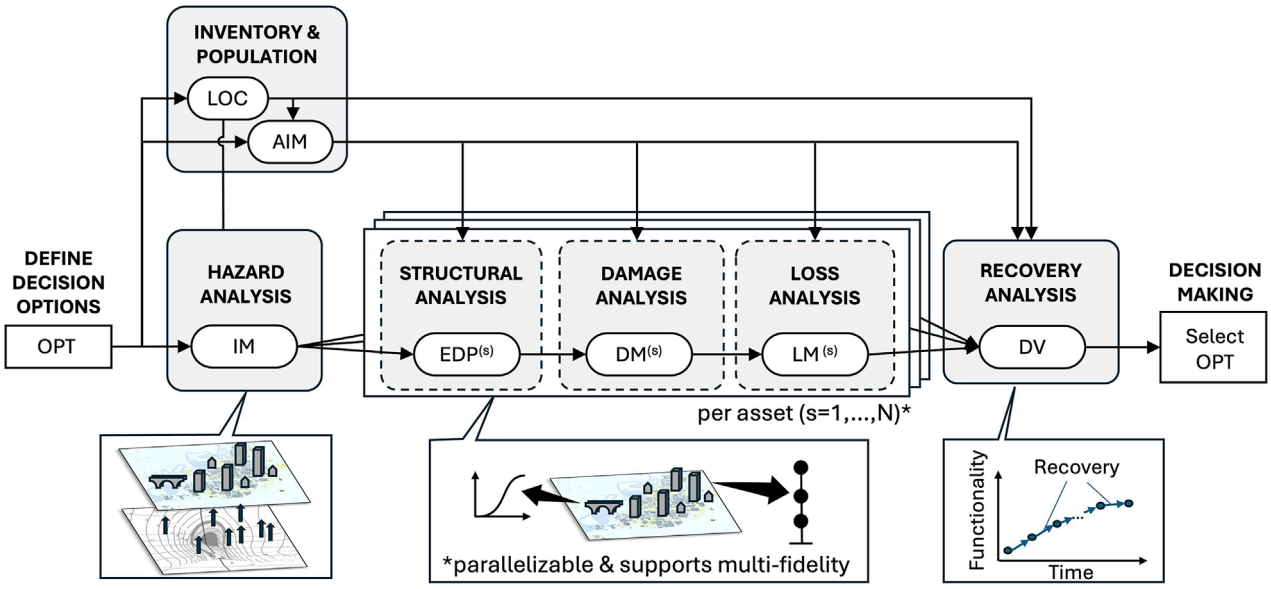

FIGURE 1
SimCenter framework for computational simulation in natural hazards engineering.

natural hazards engineering. We present below the key features of our simulation platform, illustrate the spectrum of supported use cases (Figure 2b) and highlight an example use case (Figure 2c).

The following capabilities are highlighted in Figure 2:

Free and open-source software: SimCenter tools are publicly available in GitHub repositories (NHERI SimCenter, 2025b) and shared with a BSD 3-Clause license, ensuring broad accessibility and extensibility of the tools. Documentation, user guides, and examples housed on dedicated webpages for each tool facilitate platform adoption by researchers and practitioners.

Multiple ways to engage: Six front-end desktop applications provide access to select combinations of computational modules in the framework; each tailored to specific research problems. Figure 3 provides an overview of these applications and describes the types of problems and research questions they are designed to address. The desktop applications (i.e., front end) generate input files for a modular backend engine that performs calculations (Figure 2a). Users can bypass the desktop applications and interact directly with the backend through a command-line interface or custom scripts.

Flexible Workflows: The modular architecture offers researchers diverse modeling options for each simulation step. Standardized interfaces and data schemas enable seamless integration of new or existing applications via wrappers without requiring modifications to the applications. This approach facilitates application contributions, even those with closed-source codes or restrictive open-source licenses.

Democratized High-Performance Computing: SimCenter tools support execution on both local machines and high-performance computing (HPC) clusters, enabling seamless transitions between small-scale test simulations and large-scale research investigations. Through collaboration with DesignSafe (Rathje et al., 2024), another NHERI facility, desktop application users can run simulations on the NSF-supported HPC resources at the Texas Advanced Computing Center.

Public Datasets and Libraries: The SimCenter tools and desktop applications facilitate data collection for setting up simulations by providing built-in interfaces with public datasets, such as building and bridge features from the National Structure and National Bridge Inventories (U.S. Army Corps of Engineers, 2023; FHWA, 2023), ground motion records from the PEER Next-Generation Attenuation database (Ancheta et al., 2014), and experimental wind tunnel test data from the Tokyo Polytechnic University Database (Tokyo Polytechnic University, 2025). Besides these automated approaches, the tools can parse several widely used file formats to facilitate importing event information, such as wind fields of recent hurricane events generated by Applied Research Associates and shared through a partnership between the National Institute for Standards and Technology (NIST) and DesignSafe (Levitan, 2020), or USGS Shakemaps of recent earthquakes (Wald et al., 2003). The SimCenter has also initialized new public libraries, such as the Damage and Loss Model Library (NHERI SimCenter, 2025a) and the CFD Simulation Library (NHERI SimCenter, 2025c), that are seeded with models and data and directly connected with our tools and applications.

Integrated Research Tools: Several commonly used research programs and packages are integrated into the simulation platform, including Dakota (Adams et al., 2020), OpenQuake (Pagani et al., 2014), OpenSHA (Field et al., 2003), OpenSees (McKenna et al., 2000), and OpenFOAM (Jasak, 2009); emerging software tools continue to be added based on user needs, e.g., pyrecodes (Blagojević and Stojadinović, 2025) and REWET (Naeimi and Davidson, 2024). The SimCenter has also developed two standalone research tools to fill important gaps: BRAILS++ for inventory generation

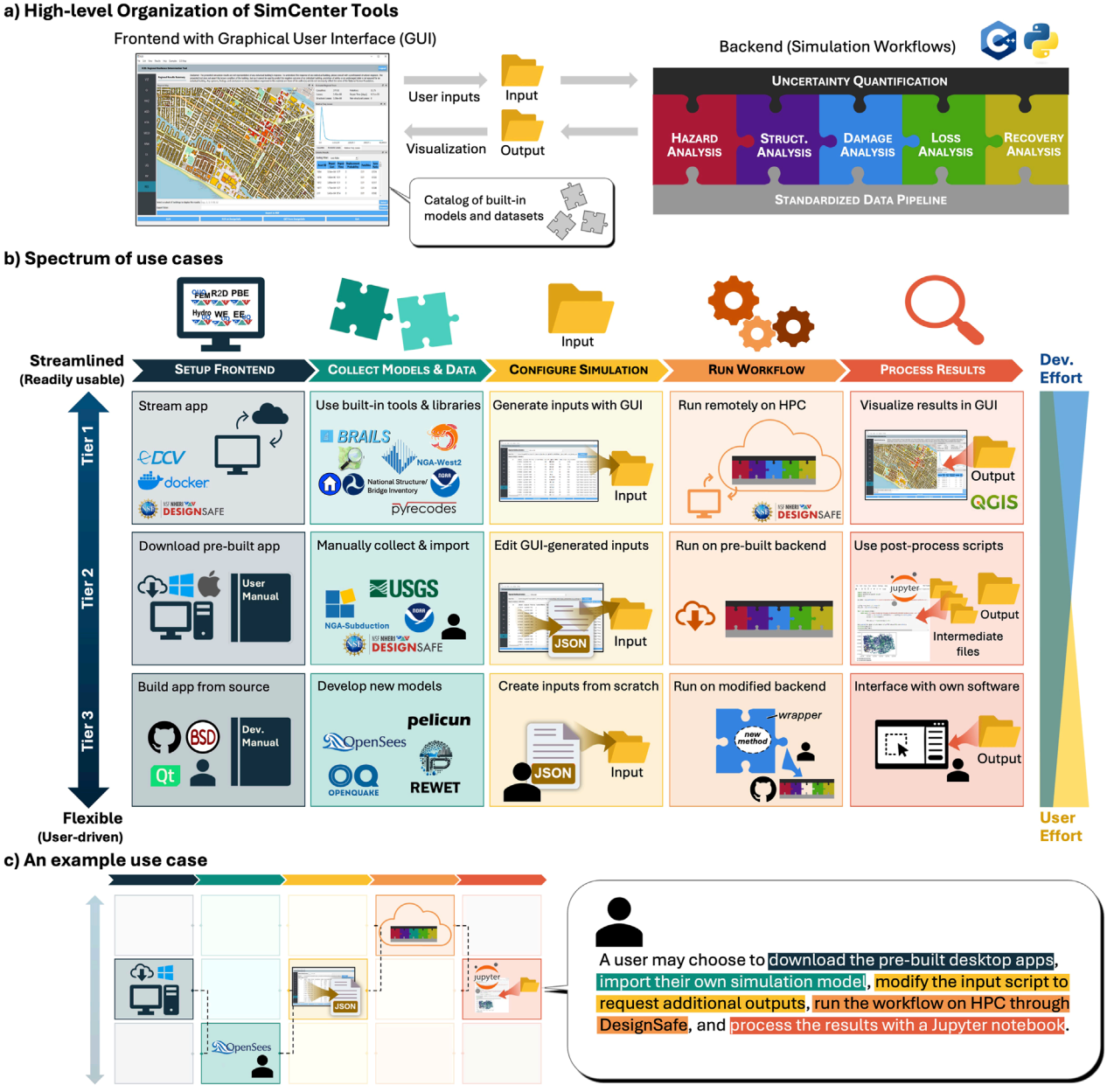

FIGURE 2
Spectrum of user-facing pipelines in the SimCenter computational simulation platform. **(a)** High-level organization of SimCenter tools. **(b)** Spectrum of use cases. **(c)** An example use case.

(Cetiner et al., 2025) and Pelicun for damage and loss assessment (Zsarnoczay et al., 2025a). These research tools are included in Figure 3 and described in detail in Sections 3.1 and 5.3, respectively.

Access to Detailed Outputs: Desktop applications provide summary results for quick, visual interpretation. Further exploration of results is available with all intermediate and final outputs, which are organized in several files using standardized data schemas to support comprehensive post-processing and detailed research analyses.

The SimCenter simulation platform and the applications and tools featured in Figure 3 support the following types of numerical analyses:

Uncertainty Quantification: The architecture of our simulation platform and the interface of each SimCenter tool are designed to encourage and facilitate probabilistic analyses. Every component of our workflows can handle uncertain variables and multiple plausible models to allow consideration and propagation of aleatoric and epistemic uncertainties. quoFEM (McKenna et al., 2025c) operationalizes this foundation and provides state-of-the-art, general-purpose uncertainty quantification features, such as various options for sensitivity analyses and model calibration. Advanced surrogate model training options - with a special focus on stochastic emulation (Zhong et al., 2023; Soize and Ghanem, 2016; Yi and Taflanidis, 2024) and adaptive design of experiments

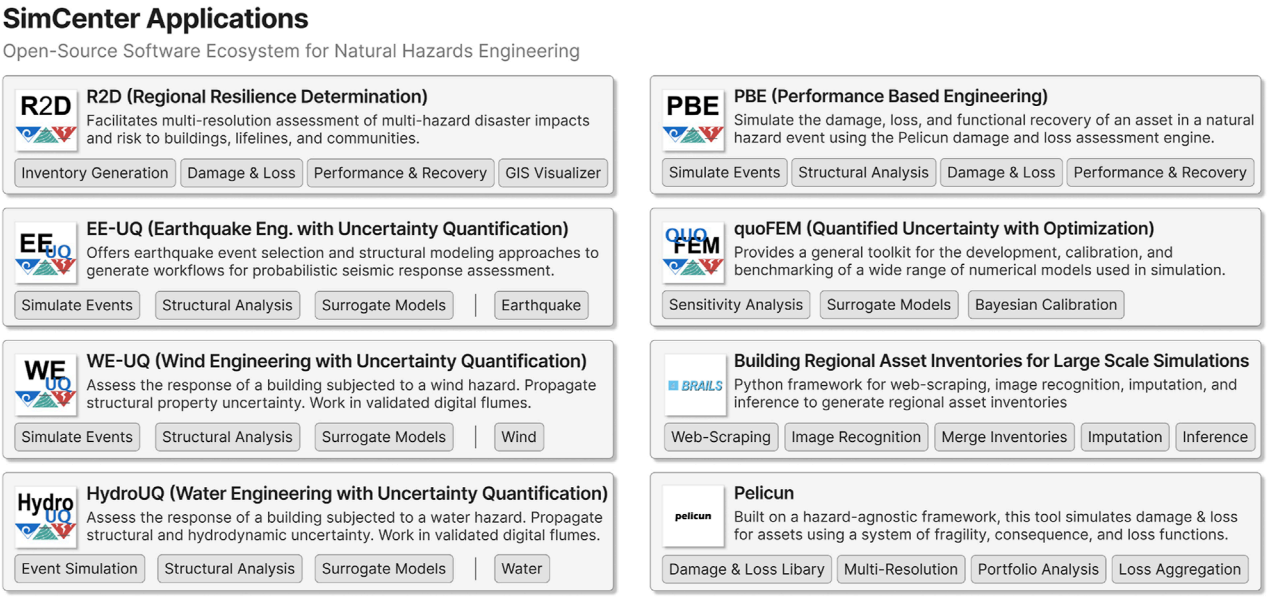

FIGURE 3
SimCenter applications and tools for natural hazards engineering.

techniques (Yi and Taflanidis, 2023) - are available in quoFEM, as well as in the EE-UQ, WE-UQ, and HydroUQ desktop applications. The workflows enabled by PBE and R2D can leverage the trained surrogate models and use the uncertainty propagation capabilities of the simulation platform.

Local-scale Structural Analysis: Simulating the behavior of individual assets in high fidelity is a core feature of our platform. The following desktop applications focus on detailed local-scale simulations for earthquake, wind, and water hazards: EE-UQ (McKenna et al., 2024), WE-UQ (McKenna et al., 2025b), and HydroUQ (Bonus et al., 2025a). These applications connect with the relevant parts of our backend and leverage well-established tools, such as OpenSees and OpenFOAM, for numerical analyses. They also provide supporting features that automate seismic structural design (Guan et al., 2020; Ceballos and Arteta, 2022), help define boundary conditions for fluid dynamic analyses (Mackenzie-Helnwein et al., 2020), and guide users through complex meshing operations. The numerical models can be calibrated to results from NHERI experimental facilities and then used to generate virtual experiments. The common framework allows researchers to directly use the models developed in these local-scale analyses in larger, regional simulations or to calibrate more efficient, idealized models using the high-fidelity results as a reference.

High-Resolution Damage and Loss Assessment: High-resolution damage and loss assessment for individual assets is routinely used in earthquake engineering practice and plays a key role in advancing research on functional recovery simulation. There is interest in adopting these techniques in other hazard areas, especially in wind engineering. SimCenter developed the Pelicun tool (Zsarnoczay et al., 2025a) as a general-purpose damage and loss assessment engine and the PBE desktop application (Zsarnoczay et al., 2025b) to support education and research in high-resolution performance-based engineering. Our Damage and Loss Model Database (NHERI SimCenter, 2025a) collects, organizes, and shares damage and loss model parameters and metadata and makes them available for the workflows managed by the PBE and R2D applications.

Regional-scale Risk Studies: Many of the enhancements the SimCenter Framework provides aim to formalize and facilitate the application of state-of-the-art probabilistic models in regional-scale risk assessment. The local-scale structural analysis capabilities in our backend are complemented by the SimCenter developed module BRAILS++ (Cetiner et al., 2025) that handles the semi-automated creation of inventories. This is further complemented by tools for the automated generation of earthquake and hurricane event scenarios. The backend workflows and these complementary modules are all engaged by our R2D desktop application (McKenna et al., 2025a). This is our most sophisticated tool, integrating the QGIS platform to provide rich geographical visualization capabilities designed to lower the barrier of entry to regional risk studies.

Socioeconomic Impact and Recovery Modeling: The capability of our simulation platform to provide detailed asset, household, and damage information in a standardized format facilitates interfacing with emerging models for socioeconomic impact and the recovery of various infrastructure systems and services. We integrated the pyrecodes framework (Blagojević and Stojadinović, 2025) into our platform to provide a modular system-of-systems approach that is in line with the modularity of other parts of our backend and fosters an environment where many models can be featured and benchmarked to encourage exploration and exchange of ideas. The R2D desktop application provides convenient access to workflows that include functionality and recovery simulations for buildings and lifeline networks, and captures the impact on and behavior of households after a disaster.

By broadening the performance-based applications to support regional-scale modeling, multi-resolution analyses, multi-hazard

applications, and diverse asset types, the SimCenter Framework allows comprehensive and integrated assessments of risk and resilience. Interest in these capabilities is found in a growing base of over 4,200 users, who have leveraged this framework through our desktop applications to execute over 87,000 simulations over the last 6 years. Users are also taking advantage of the flexibility of our applications, accessing Pelicun and BRAILS++ directly from the command line and through online Jupyter notebook environments. The following sections further explore the capabilities of this framework and highlight its applications in advancing the field of natural hazards engineering.

3 Inventories of the Built Environment and Communities

A critical first step in natural hazard risk analysis is characterizing the assets at risk. Understanding key characteristics is essential when modeling structural behavior and vulnerability under different hazards. For instance, assessing earthquake impacts on buildings requires data on building height, plan configuration, structural materials, and structural system type. Similarly, detailed wind and water damage assessments require information on building envelope geometry, finish materials, and openings. Most assessments require information related to details of the design and construction (e.g., lateral strength, load-path integrity, foundation anchorages), which are typically inferred from the year of construction. However, comprehensive datasets providing such granular details are rare, making the creation of regional-scale inventories a significant challenge. Beyond buildings, infrastructure systems such as roads, bridges, pipelines, and power grids require similarly detailed data for high-resolution damage and loss modeling. Additionally, socioeconomic assessments utilize household characteristics in their models, which are often protected and unavailable at the desired resolution.

Traditional catastrophe modeling approaches address data limitations by relying on aggregated asset characteristics to estimate disaster impacts at a city scale (FEMA, 2024b). While valuable, these models often lack the granularity needed for detailed vulnerability assessments or targeted interventions. The SimCenter prioritizes high-resolution studies that simulate the behavior of individual assets within regional-scale analyses, bridging local structural assessments with broader regional evaluations. This approach supports studies on specific asset vulnerabilities and community-level coping capacities.

Compiling such regional-scale inventories, however, remains a formidable task. In the U.S., the National Structure Inventory (NSI) and Hazus building inventory databases (U.S. Army Corps of Engineers, 2023; FEMA, 2024e) provide broad coverage but rely on approximations that limit their suitability for high-resolution modeling. While these resources are notable for their geographical coverage and completeness, many of the building characteristics they contain are inferred using broad approximations (U.S. Army Corps of Engineers, 2023), which lack the accuracy required for higher-resolution simulations (Sanderson and Cox, 2023). Some proprietary datasets offer better accuracy, but their high cost and variable quality pose challenges (Nolte et al., 2023). The SimCenter developed BRAILS++, an open-source Python framework for asset inventory creation, to address this gap by combining open data acquisition with advanced inference methods, democratizing access to high-fidelity regional inventory data.

BRAILS (Wang et al., 2021), an earlier version of BRAILS++, has been widely applied in research to automate the extraction of building attributes. Several studies leveraged BRAILS to generate high-fidelity building inventories for seismic and hurricane risk assessments, enabling large-scale structural classification and vulnerability modeling (Bassman et al., 2022; Kijewski-Correa et al., 2023; Roueche et al., 2022; Yu et al., 2020). Other research incorporated BRAILS into virtual testbeds for community resilience (Enderami et al., 2023) and integrated it with computational fluid dynamics simulations to improve post-hurricane damage assessments (Kim et al., 2024).

BRAILS has contributed to transportation network resilience modeling (Virtucio et al., 2024). It has also supported 3D urban modeling and energy efficiency initiatives by automating building identification for energy retrofits (Liu et al., 2024; Shen et al., 2024). Across these studies, BRAILS consistently enhances large-scale data acquisition, enabling more accurate, scalable, and automated analyses in disaster risk management and urban resilience planning. The tool also inspires research in building inventory generation, as demonstrated by Gouveia et al. (2024) and Pan et al. (2024).

3.1 The BRAILS++ framework

The BRAILS++ framework significantly advances regional-scale studies by bridging gaps in public datasets and enabling high-resolution modeling, which, in turn, supports more accurate disaster risk assessment and resilience planning (Du et al., 2023). As shown in Figure 4, BRAILS++ provides modular workflows for generating inventories by integrating diverse data sources, including public datasets, features extracted from imagery, and ruleset-based inference models. In BRAILS++, an asset inventory consists of geographically referenced points, line-strings, or polygons, each annotated with key attributes. To build these inventories, the data scrapers in BRAILS++ interact with web servers in an automated manner and directly retrieve asset information from public datasets to create an inventory blueprint suitable as a starting point for regional-scale analysis.

Key datasets accessed through BRAILS++ include FEMA's USA Structures (FEMA, 2022), Microsoft Footprints (Microsoft, 2022), Overture Maps (Overture Maps Foundation, 2023), OpenStreetMap (OpenStreetMap contributors, 2017), the U.S. Army Corps of Engineer's NSI, TIGER/Line roadway data (U.S. Census Bureau, 2024), FHWA's National Bridge and Tunnel Inventories (FHWA, 2023; FHWA, 2024), ASCE REST services for design loads (ASCE, 2025), and HIFLD infrastructure data (U.S. Department of Homeland Security, 2024). SimCenter holds annual workshops on incorporating local datasets (e.g., tax assessor and permit data) into regional-scale hazard assessment studies, and BRAILS++ provides utilities for processing such custom datasets. Despite their value, these datasets often contain incomplete or inconsistent information, requiring further enhancement to address the corresponding uncertainties in these high-resolution inventories. BRAILS++ incorporates methods for handling missing data and enhancing the available datasets through modules that

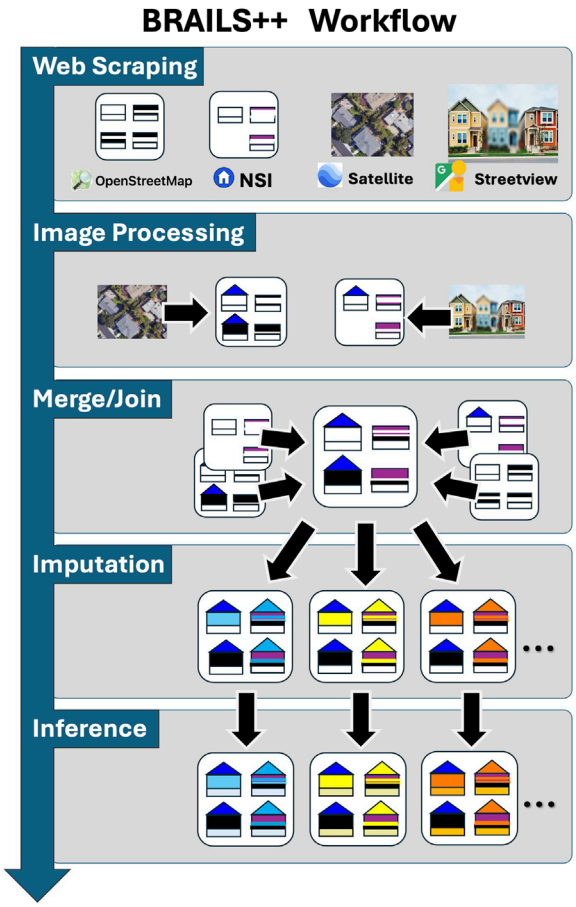

FIGURE 4
Illustration of a workflow for generating a building inventory using various BRAILS++ modules.

enable: 1) feature extraction from images; 2) inventory merging; 3) statistical imputation; and 4) data inference.

1. Feature Extraction from Images: Publicly available imagery from Google Street View (Anguelov et al., 2010), Mapillary (Mapillary contributors, 2020), and NHERI RAPID reconnaissance missions (Berman et al., 2020) can help provide up-to-date asset details. BRAILS++ employs neural networks and vision-language models to extract features such as roof type, material, and construction details. Additionally, advanced models enhance inventory completeness by capturing more complex dimensional data such as roof height and pitch, window areas, and first-floor elevation. Each model is documented to provide information about the dataset it was trained on and its performance in verification tests. We also provide guidance for applying transfer learning techniques to adjust pre-trained models to a new geographic context, if needed.
2. Inventory Merging: BRAILS++ enables merging datasets to resolve discrepancies and consolidate asset information. This process accounts for spatial inconsistencies (e.g., misaligned footprints and parcel boundaries) and integrates metadata from multiple sources to create a unified inventory. Standardized merging techniques establish correspondence between geometries and prioritize data sources based on their reliability. The resulting dataset contains unique assets, each with a specific geographic reference and integrated metadata from the combined data sources.
3. Imputation to Complete Data: Since inventories are often incomplete, BRAILS++ employs statistical imputation methods to fill the gaps and generate complete datasets. Techniques such as K-Nearest Neighbors imputation are available to estimate missing values based on spatial and structural similarities (e.g., using information from adjacent buildings with the same structural system and construction year). Each imputation technique provides several plausible values for the missing features based on the available data, supporting the creation of several plausible inventory realizations (also termed "possible worlds"). These allow researchers to capture and propagate inventory uncertainties through probabilistic regional simulations.
4. Inference to Add Features: Some critical asset attributes, such as roof-to-wall connections for wind vulnerability assessments, are rarely documented and typically missing for all assets in available datasets. BRAILS++ inference engines rely on rule-based and probabilistic models to estimate these missing attributes. For instance, building codes applicable at the time of construction can be used to infer typical connection details (Kijewski-Correa et al., 2022). Existing inference modules build on such code-based assignments and the rules recommended in the Hazus Inventory Manual (FEMA, 2024f) to add features necessary for regional simulations following the Hazus earthquake and hurricane methodologies. Ongoing expansions of this module aim to cover additional hazard models and methods.

3.2 SimCenter testbeds

The SimCenter has been maintaining testbeds to inform the prioritization of development tasks through firsthand experience with the challenges involved in real-world regional simulations. These testbeds also serve as environments for evaluating inventory generation models and provide benchmarking opportunities for high-fidelity simulations. Our first-generation testbeds in the San Francisco Bay Area, CA, Atlantic County, NJ, and Lake Charles, LA (Figure 5) are documented online (NHERI SimCenter, 2025d), including references to online repositories that archive the corresponding datasets. A new second generation of testbeds is under development, focusing on complex infrastructure systems and multi-hazard problems. Based on available inventory data, historical hazard events, and stakeholder interest, the San Francisco and Lake Charles testbeds will be updated, and Fort Myers, FL, will be developed as a new location.

The SimCenter developed a standardized data schema for asset inventories to facilitate the sharing and re-use of such data. Regular updates to testbed inventories provide high-quality datasets for research investigations, supporting studies on community resilience (Enderami et al., 2022; 2023) and regional risk assessments (Bassman et al., 2022; Kijewski-Correa et al., 2023). Researchers

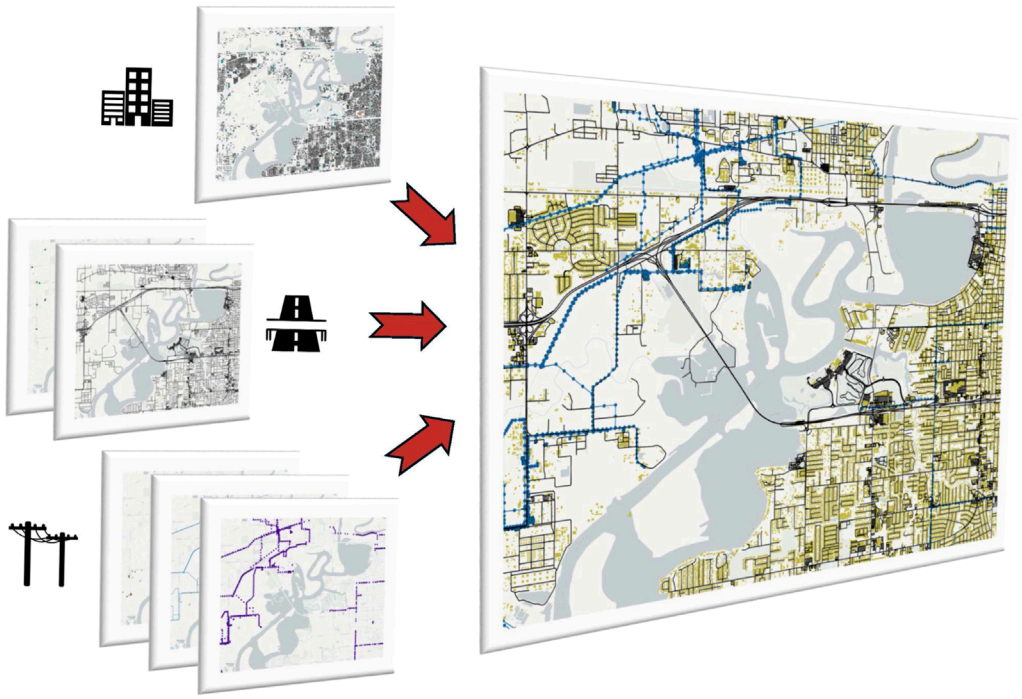

FIGURE 5
The process of creating the building, transportation, and power infrastructure inventories for Lake Charles, LA. Each tile details specific asset attributes or components, while the rightmost tile presents an overview of the assembled inventory.

have used testbeds to evaluate damage inference models (Sheibani and Ou, 2020; Wang et al., 2024b) and optimize post-earthquake reconnaissance and recovery planning (Cheraghi et al., 2024; Wang et al., 2024b). They also serve as a platform to study the impact of infrastructure interdependencies (You et al., 2023a) and resource constraints on resilience (Blagojevic and Stojadinovic, 2022), while enabling assessment of advanced structural systems at the regional scale (You et al., 2023b).

4 Natural hazard events

Hazard analysis quantifies the likelihood and severity of natural hazard scenarios. The SimCenter extends the concept of an Intensity Measure (IM) from the PBEE framework to any measure describing hazard severity at a given location. An IM can be a scalar, such as peak 1-s spectral acceleration, or a vector, such as a spectral acceleration time history. High-resolution local analyses often require complete time histories provided as such vector IMs, which are essential for capturing time-evolving effects and cascading damages.

A regional event in the SimCenter framework is defined by an IM field—a continuous random field discretized geographically using a grid and probabilistically with IM samples at each grid point (Figure 6). These samples are correlated across locations and IM types, preserving essential dependencies for robust regional risk assessment. The SimCenter has developed a GeoJSON-based data schema to store these IM fields. This hazard-agnostic schema enables multi-event simulations, such as combined wind and storm surge in hurricanes, and facilitates multi-hazard and climate adaptation studies.

Computationally intensive simulations, such as regional earthquake rupture and subsurface wave propagation (McCallen et al., 2021; Frankel et al., 2018), large-scale ocean wave propagation and tropical storm surge models (Berger and LeVeque, 2023; Vijayan et al., 2023), and weather simulations (Skamarock et al., 2008) all require highly specialized modeling expertise and computational resources that fall outside the purview of the SimCenter, but are pertinent to enabling regional-scale risk studies.

The SimCenter offers interfaces to integrate outputs from established external models directly into its framework, avoiding the need to support or deploy third-party software. These interfaces enable users to seamlessly map high-fidelity simulation data—from sources like USGS ShakeMaps (Wald et al., 2003), SW4 and M9 simulated ground motions (Petersson et al., 2023; Sjögreen and Petersson, 2012; Frankel et al., 2018), ADCIRC (Luettich et al., 1992) storm surge outputs, and ARA wind maps (Levitan, 2020)—into our GeoJSON format, facilitating interoperability and data re-use. Users can also extend the platform by contributing interfaces for other external data schemas.

4.1 Computationally efficient hazard event simulations

Researchers often prefer the flexibility to choose the hazard scenarios for their study rather than using state-of-the-art,

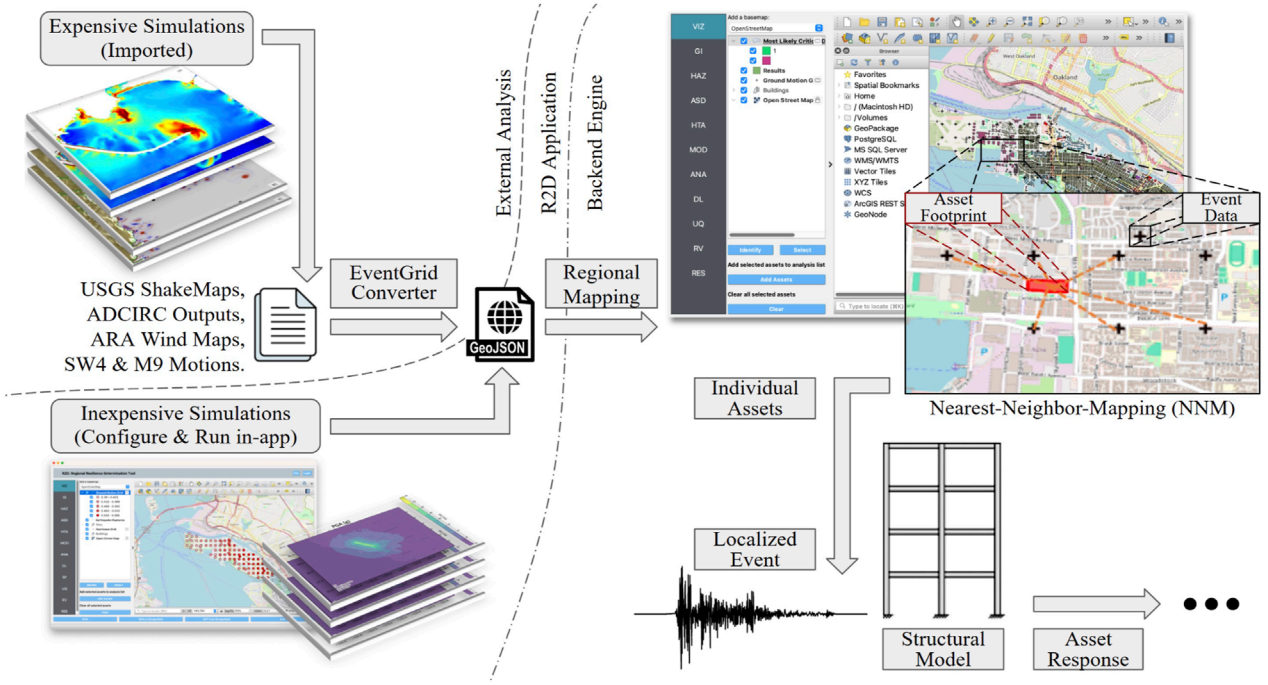

FIGURE 6
Overview of Hazard Analysis capabilities in SimCenter's simulation platform (Illustrative examples of expensive simulations based on Lynett et al., 2017).

computationally expensive simulations of pre-defined scenarios. To support these needs, the SimCenter provides efficient, idealized event models that balance accuracy with usability. These tools lower the barrier to entry by reducing computational demands and required domain expertise while maintaining scientific rigor.

The SimCenter's R2D desktop application includes the following tools for this purpose:.

- The Earthquake Event Simulation Tool interfaces with existing, well-established solutions, such as OpenQuake (Pagani et al., 2014), OpenSHA (Field et al., 2003), and the PEER NGA ground motion database (Ancheta et al., 2014). Its user interface provides a step-by-step approach to generating earthquake event intensity measures (Figure 7a). It facilitates selecting ruptures from earthquake rupture forecast results, choosing models for ground motion attenuation, spatial correlation, and secondary hazards, including landslides and liquefaction. An optional last step automatically selects and scales a set of ground motion records from the PEER NGA database to match calculated intensity measure fields.
- The Hurricane Wind Simulation Tool provides recent historical hurricane track data taken from the IBTrACS database (Knapp et al., 2010; Gahtan et al., 2024) and uses a probabilistic hurricane simulation method contributed to our framework by Snaiki and Wu (2017a), Snaiki and Wu (2017b) to simulate the time-evolving wind field as the hurricane moves along its track (Figure 7b). Users can also input custom hurricane tracks and terrain roughness through CSV and GeoJSON files.

4.2 Regional hazard mapping

Regional hazard event grids often do not align with asset locations, requiring an additional mapping step, referred to as Regional Mapping in Figure 6. The mapping process is event-specific, as some events provide only scalar IM values at mesh points, while others offer vectors of time series. For vector IMs, the underlying approximations used to derive coarse-mesh results introduce challenges in generalizing a mapping approach across all regional hazard event grids.

The SimCenter provides several mapping solutions and is working with researchers to address this challenge:

Nearest Neighbor Mapping (NNM): For scalar IM fields (and as a simplified approach for vector IMs), the SimCenter provides the NNM tool, which efficiently maps regional event data onto large asset inventories. This method utilizes distance-based interpolation for scalar IMs and iterative probabilistic sampling for time histories. The approach approximates a multi-IM field as a smooth hypersurface between grid points, preserving spatial correlations in the IM field.

Physics-Based Multi-Scale Hazard Event Integration: The SimCenter is actively integrating existing multi-scale hazard event simulation approaches. These approaches are useful when the output of the large-scale event simulation is lacking both the spatial and temporal resolution needed to perform robust response simulations for each asset in the region. The approaches taken are hazard-specific:

- Earthquake Simulations: Regional earthquake simulation efforts focus on integrating SimCenter tools with physics-based ground motion databases developed for seismically

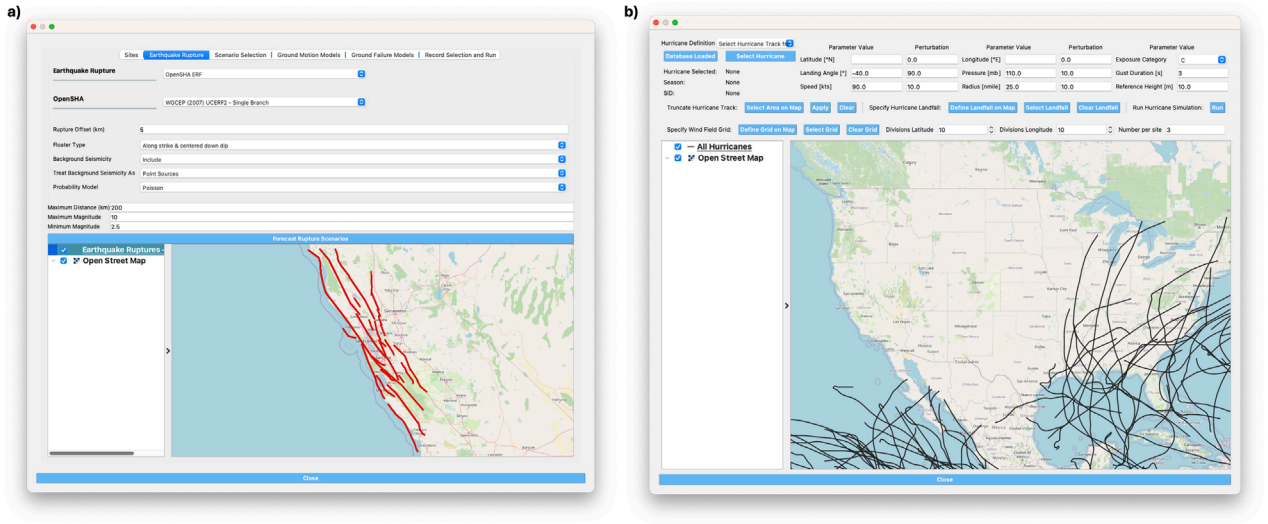

FIGURE 7
Earthquake Event Simulation (left) and Hurricane Event Simulation (right) tools support efficient simulation of intensity measure fields for user-defined scenarios.

active regions in the United States and beyond. These databases leverage simulations based on finite-element methods (e.g., Hercules; Taborda et al., 2010), finite-difference methods (e.g., SW4; Petersson et al., 2023), and broadband (Green's function) approaches (e.g., Shaker Maker, SCEC-BBP; Abell et al., 2022; Maechling et al., 2015). To support applications at locations between grid points, SimCenter tools are being connected to APIs such as M9 (Frankel et al., 2018), Hercules Turkey (Zhang et al., 2021), and EQSIM (McCallen et al., 2021), which enable the retrieval of simulated ground motions at arbitrary locations. In parallel, domain reduction methods (DRM) (Bielak et al., 2003; Yoshimura et al., 2003) are being used to bridge large-scale regional wave propagation models with detailed local site-scale analyses. These efforts enable seamless integration of macro-scale seismic simulations with local geological modeling near critical assets, enhancing the fidelity of the simulations by incorporating higher frequencies, complex 3D soil conditions, and nonlinear soil-structure interaction effects (Pakzad et al., 2024; Zhang et al., 2019).

- Wind Engineering: Multi-scale wind engineering simulations will be facilitated by a new development in SimCenter applications that enables the interfacing of high-resolution local modeling applications with a global weather model. Similar to methods used for earthquakes, this approach interpolates between coarse grid points and incorporates higher frequency content. This allows for the utilization of real weather information as boundary conditions to drive high-fidelity local analyses of wind flow (Huang et al., 2024).
- Coastal Engineering: The SimCenter is exploring interfaces for ADCIRC simulations (Luettich et al., 1992) that integrate auxiliary software such as SWAN (2024) and STWAVE (Massey et al., 2011). This will enable coupling with sub-city-scale Boussinesq models, capturing refined coastal inundation, nonlinear wave interactions, and debris dynamics with increased fidelity (Renteria and Lynett, 2024).

Asset Incorporation in Large-Scale Hazard Simulations: Embedding regional assets directly into large-scale hazard simulations can eliminate the regional mapping step. This requires modifying workflows to extract Engineering Demand Parameters (EDPs) from larger-scale event-asset interactions, rather than from independent asset-specific calculations. For example, while a local-scale soil-structure interaction (SSI) model typically provides asset-specific results (e.g., floor accelerations for a single building), a city-wide SSI model (e.g., Wang et al., 2024a) or a computational fluid dynamics simulation of city-wide wind flow (e.g., Gu et al., 2023) shifts these analyses to the regional level, generating a joint EDP field. While these approaches enable high-resolution regional-scale analyses, they currently demand specialized expertise and significant computational resources due to the fine mesh required for local asset-scale hazard characterization. The SimCenter supports these methodologies by streamlining workflows and integrating outputs from large-scale physics-based simulations.

5 Asset Modeling and Damage Estimation

Given a probabilistic asset inventory and the probabilistic event IMs at each asset's location, the next step is to determine how the assets respond to the demands induced by the event and to quantify the resulting damage (Figure 1). This process leverages extensive past research in earthquake, wind, and coastal engineering and integrates well-established computational tools, such as OpenSees (McKenna et al., 2000) and OpenFOAM (Jasak, 2009). SimCenter supports the robust modeling of response and damage through contributions in the following four areas: (i) Calibration, Validation

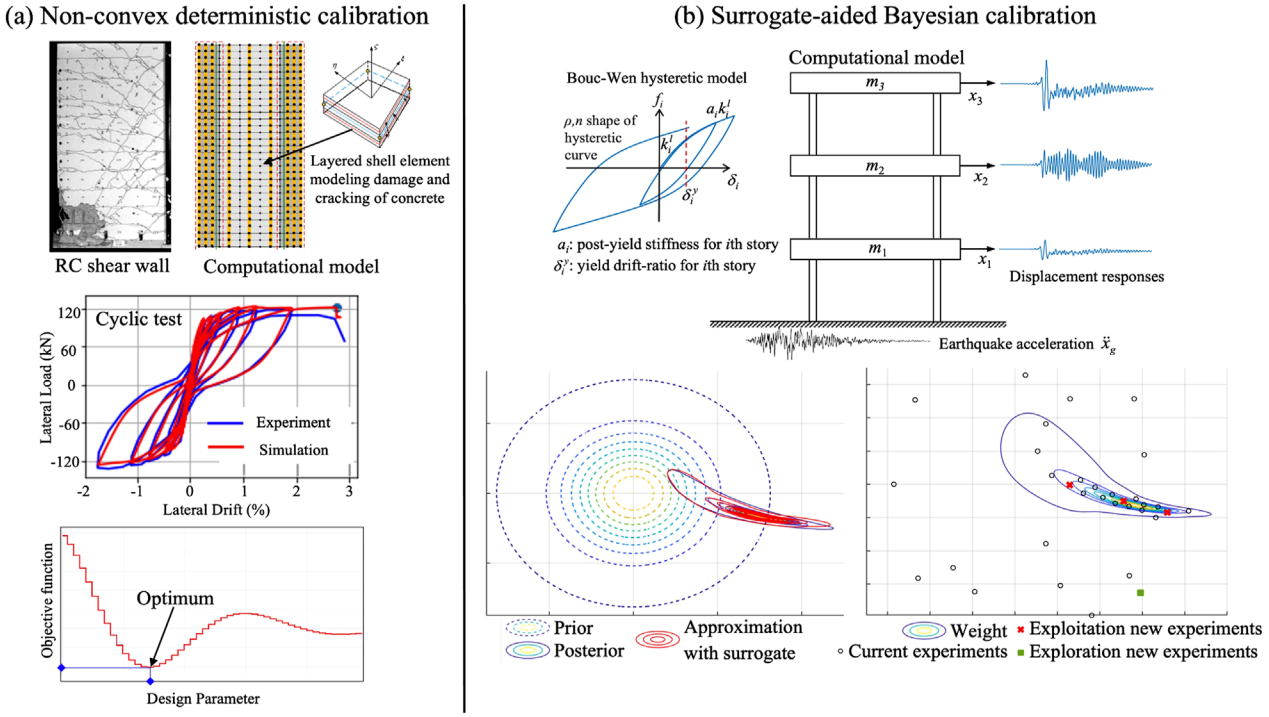

FIGURE 8
Examples of challenging calibration problems facilitated by the quoFEM desktop application. **(a)** Non-convex, deterministic calibration. **(b)** Surrogate-aided Bayesian calibration.

and Model Development; (ii) Structural Analysis with Automated Workflows; (iii) Damage Analysis with Pelicun; and (iv) Model and Simulation Databases.

5.1 Calibration, validation, and model development

Before conducting simulations for large asset portfolios, it is essential to establish confidence in one's ability to make accurate predictions. Reliable simulation outcomes depend on ensuring that the numerical models can capture real-world behavior. Building such confidence requires a combination of experimental testing and computational modeling, as these activities are complementary in refining numerical methods and increasing confidence in predicted responses. Many features in the quoFEM application are specifically designed to strengthen the connection between these activities, enabling researchers to utilize experimental data for robust model calibration (Figure 8). quoFEM provides a convenient interface to both deterministic and probabilistic calibration techniques from the Dakota optimization and uncertainty quantification tool (Adams et al., 2020). For deterministic calibration, it includes gradient-based methods tailored for solving nonlinear least-squares minimization problems (Dennis et al., 1981; Meza et al., 2007), as well as gradient-free approaches for handling non-smooth, non-convex problems (Gray and Kolda, 2006).

Deterministic methods alone cannot fully capture uncertainties in calibrating model parameters. Bayesian calibration provides a probabilistic framework for quantifying uncertainty (Beck and Katafygiotis, 1998; Vrugt et al., 2009; Ching and Chen, 2007; Wu et al., 2018; Kurumbhati et al., 2024). However, for complex models with multiple parameters, Bayesian calibration can become computationally prohibitive. To reduce the computational cost associated with Bayesian calibration of detailed models, we have developed a hybrid approach that integrates surrogate-assisted sampling within a sequential Monte Carlo framework (Taflanidis et al., 2025). Gaussian process regression is used as the surrogate model, iteratively refined by selecting training points that best inform the approximation of the target posterior density. Convergence is evaluated by comparing posterior approximations across successive iterations, and if unmet, the surrogate is further refined using an adaptive design of experiments with a weighted acquisition function that balances exploitation and exploration for improved efficiency and robustness. The method is illustrated in Figure 8b.

Beyond calibration, quoFEM provides capabilities for global sensitivity analysis methods (Weirs et al., 2012; Adams et al., 2020; Hu and Mahadevan, 2019; Jung and Taflanidis, 2023) to support critical evaluation of existing models and the identification of their most impactful inputs and parameters. Through these capabilities, we aim to support the broader research community in developing validated, uncertainty-aware predictive models. quoFEM has been used for sensitivity analysis to assess OpenSees seismic models (Yi et al., 2022), sediment transport dynamics (Feehan et al., 2023), and RC column behavior (Güngör et al., 2023). Bayesian calibration applications include refining the

PM4Sand liquefaction model (Satish et al., 2022) and estimating LVL panel properties via vibration-based methods (Opazo-Vega et al., 2025). Researchers have also leveraged quoFEM for uncertainty propagation inprobabilistic assessments, such as modeling uncertainties in force-limiting connections (Astudillo et al., 2023), RC wall fractures (Navarro Carranza et al., 2025), and seismic risk of bridge towers (Taslimi and Petrone, 2024). It has also supported probabilistic evaluations of hydrodynamic forces on bridges (Pervaiz, 2022) and mechanical properties of geopolymer composites (Artyk et al., 2024).

The advanced uncertainty quantification techniques supported by our local-scale applications (i.e., EE-UQ, WE-UQ, and HydroUQ) facilitate the creation of high-quality numerical models that can capture and faithfully reproduce the complex structural behaviors experienced when assets in the built environment are pushed near and beyond their capacity by extreme events.

We foster strong collaboration between simulation and testing, especially in wind and coastal engineering, through the development of validated digital models of experimental laboratories to facilitate running virtual experiments. These validated digital models form the basis for future experimental facility digital twin initiatives–a highly complex but promising endeavor. The numerical simulations are either performed ahead of the laboratory tests, e.g., to aid in design-of-experiments or to participate in a blind study, or they are performed afterward, i.e., calibrated to the test data, to generate additional, complementary results. The WE-UQ and HydroUQ applications allow users to create such virtual experiments for wind tunnels and wave flumes. These tools support streamlined workflows for multiple experimental facilities, including the Wall of Wind Experimental Facility at Florida International University, the Boundary Layer Wind Tunnel Facility at the University of Florida, the Wind Tunnel Facility at Tokyo Polytechnic University, the Large Wave Flume and Directional Wave Basin at Oregon State University's Hinsdale Wave Research Lab (Bonus, 2023; Lewis et al., 2023), and the Tsunami Wave Basin at Waseda University (Bonus et al., 2025b). The digital flume models, within a SimCenter workflow, include: (i) the modifiable geometric layout of the facilities with sensor placements pre-set to replicate prior experimental works; (ii) automation of most of the setup for boundary conditions and meshing in typical use-cases; (iii) deployment and execution of the corresponding computational fluid dynamics simulations on a remote HPC cluster: and (iv) the post-processing and visualization of the results locally.

Numerical results for a digital wave flume or wind tunnel are typically validated against stochastic sets of experiments (Figure 9). Thresholds for validation are defined by meeting appropriate error metric thresholds that support the hypothesis that dominant phenomena studied within the facility for a given hazard are numerically resolved. Error metrics are most often based on simple time-series comparisons, e.g., root-mean-square error (RMSE), or scalar comparison, e.g., percent difference of maximum values, for a set of field quantities. These include velocity, acceleration, and pressure in fluid flow, and additional measurements of displacement for wave and debris hazards (e.g., free-surface displacement, debris displacement). Quantities are measured at a finite sampling rate for multiple locations throughout the physical facility, which the pre-validated digital wave flumes and wind tunnels aim to replicate for select experiment sets. Internal multi-model validation of digital wave flumes has been demonstrated through several examples. The high performance Celeris wave solver (Tavakkol and Lynett, 2020; (Renteria and Lynett, 2025; Renteria et al., 2025) and the ClaymoreUW Material Point Method (MPM) (Wang et al., 2020; Bonus, 2023; Bonus and Arduino, 2025) event modules within HydroUQ can reproduce pertinent aspects of experiments at Oregon State Univeristy's Large Wave Flume and Directional Wave Basin (Park et al., 2021; Mascarenas, 2022; Koh et al., 2025). Additionally, external multi-model validation of digital wave flumes is ongoing. A recent comparative analysis paper (Bonus et al., 2025b) thoroughly validated HydroUQ's MPM digital wave flume module against external results from the Finite Volume Method (FVM) in STAR-CCM+ and Smoothed Particle Hydrodynamics (SPH) in DualSPHysics, with pertinent data in DesignSafe (Bonus, 2025). It found that our open-source digital wave flume features state-of-the-art capabilities for tsunami debris studies in Waseda University's Tsunami Wave Basin, relative to contemporary numerical approaches for modeling stochastic experiments (Goseberg et al., 2016). Further, our digital wave flume demonstrated superior strong- and weak-scaling on DesignSafe's high-performance computing systems, which are made available within our downloadable desktop applications.

5.2 Structural analysis with Automated Workflows

Our work advances the use of established computational workflows by automating data exchange between tools and eliminating the need for manual intervention (Figure 10). This automation significantly improves the scalability of local-scale workflows, enabling the sophisticated analysis of large building portfolios in regional studies. Well-defined interfaces that specify inputs and outputs clearly for each module allow analysts to choose from a variety of options for each step and tailor workflows to the asset type and investigated problem. This is particularly important in performing computations at the regional scale, as it allows for different levels of fidelity:

1. High-Fidelity simulations are at one end of the computational spectrum, where a local-scale workflow is used for each asset, including vector IMs and a detailed structural model in a nonlinear response analysis. This approach leverages the shared simulation platform between local- and regional-scale analyses. The feasibility of such calculations was demonstrated in our study using the San Francisco Bay Area testbed, where 1.8 million buildings were analyzed, each with a finite element model and multiple nonlinear analyses to propagate structural and event uncertainties (Deierlein et al., 2020).
2. Moderate-Fidelity simulations typically sacrifice fidelity to reduce the amount of required building information and to increase computational efficiency. Simple models, such as the capacity spectrum for earthquakes (FEMA, 2024b) and pressure coefficients under wind loading (ASCE, 2022), can approximate EDPs for large inventories without the need for high-performance computing.
3. Surrogate-Aided simulations use pre-trained surrogate models to characterize the response, or even damage and losses, for

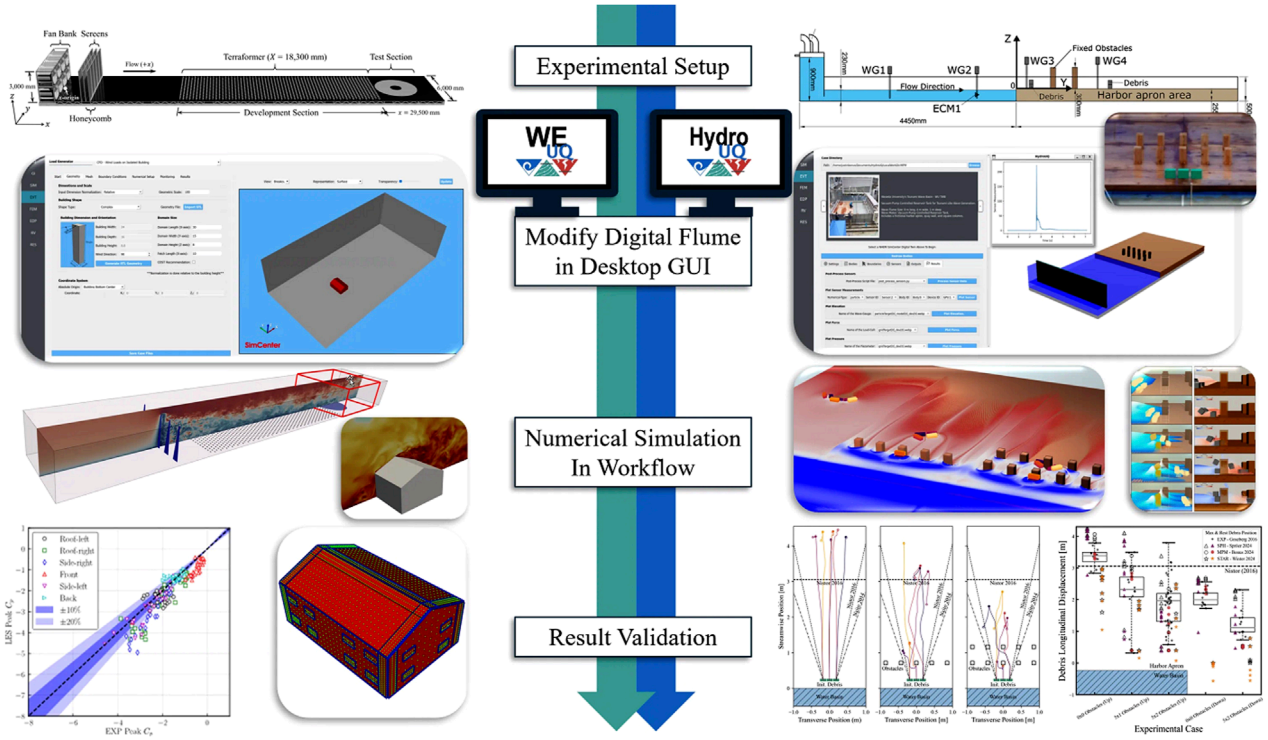

FIGURE 9
Virtual experiment workflows paralleled in the WE-UQ and HydroUQ desktop application for the University of Florida Wind Tunnel and the Waseda University Tsunami Wave Basin (Goseberg et al., 2016; Bonus, 2025; Bonus, 2025), respectively.

assets. Surrogate modeling has become a widely used approach in natural hazards engineering over the last decade. It leverages advances in machine learning and recognizes the substantial benefits of replacing expensive physics-based models with approximate, data-driven ones that are trained to reproduce the expensive models' input-output relationships. Such surrogates can be trained in either the quoFEM application, which provides general-purpose training capabilities, or using one of our local-scale desktop applications (i.e., EE-UQ, WE-UQ, HydroUQ). Surrogate models can provide various levels of fidelity depending on the quality of training data, the type of surrogating used, and how well the training data covers the application domain. In an optimal scenario, surrogates can approach the fidelity of detailed numerical models.

4. Zero-Fidelity approaches to structural analysis do not simulate structural response and directly assess damage and losses using the event IMs.
5. Multi-Fidelity simulations, applicable only in regional studies, employ high-fidelity models for a subset of assets and more efficient options for others. Figure 11 illustrates our vision for a streamlined interface in the platform, allowing users to assign inventory assets to various modeling approaches, thereby optimizing simulation fidelity. We envision models being automatically imported from shared libraries (Section 5.4) or supplied by the user. This approach poses research questions regarding the optimal distribution of computational resources to maximize the fidelity of Decision Variables in regional simulations. As multi-fidelity approaches gain adoption, the natural hazards engineering community will gradually learn more about the needs and opportunities for improving local-scale analyses, potentially influencing experimental research, driving new numerical model developments, and spurring surrogate modeling studies.

5.3 Damage Analysis with Pelicun

The vulnerability of an asset is typically characterized by the likelihood of it being damaged. Component damages can be simulated directly in expensive numerical models that capture detailed material behavior and progressive failure of components (e.g., Galvis et al., 2022; Terashima et al., 2018). Such high-fidelity simulations are often challenging to perform even for individual assets due to the lack of information about important structural details required to define key model parameters. Considering and propagating the corresponding substantial uncertainty in model parameters renders simulations prohibitively expensive for most projects. The SimCenter simulation platform can support such expensive analyses when researchers wrap their simulations with interfaces to align with the input and output data specifications of the structural response simulation module. The continuous scalar damage outputs can be treated as EDPs and, if needed to be compatible with subsequent calculations of consequences and recovery, they can be mapped into Damage States (DS) in the Pelicun damage and loss simulation engine introduced below.

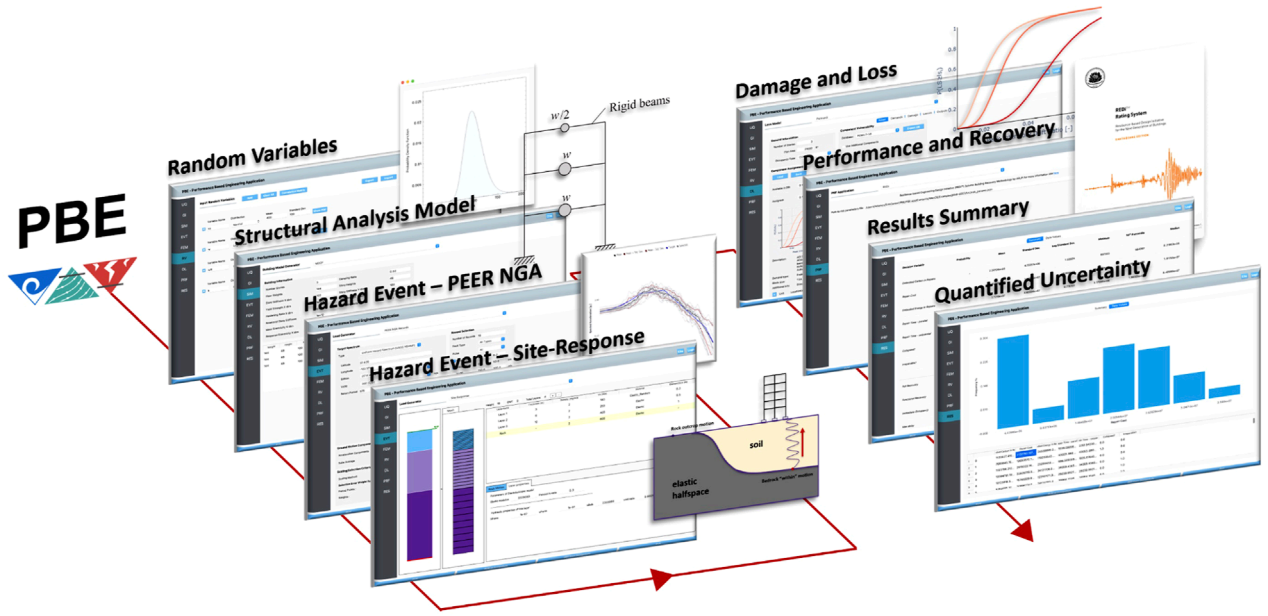

FIGURE 10
Illustrative example of a complex earthquake engineering workflow from the PBE desktop application.

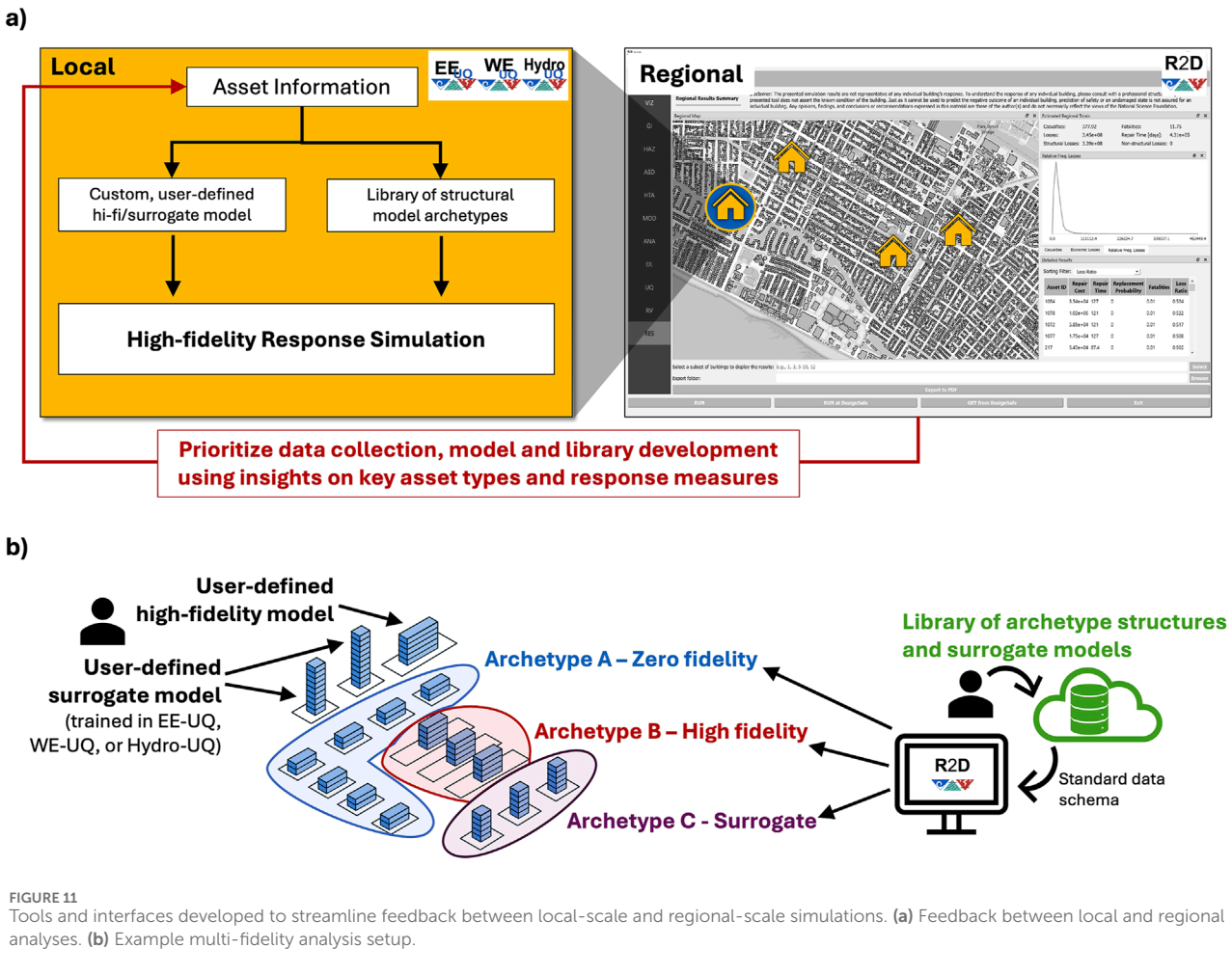

FIGURE 11
Tools and interfaces developed to streamline feedback between local-scale and regional-scale simulations. **(a)** Feedback between local and regional analyses. **(b)** Example multi-fidelity analysis setup.

Researchers often use the concept of fragility functions as a scalable approach to balance data availability and fidelity in damage simulation. A fragility function is a probabilistic description of the demand severity that triggers a limit-state exceedance in a component, subassembly, or entire asset. Rather than simulating the mechanics of damage directly, fragility functions recognize a few important damage states and allow rapid evaluation of the likelihood of each at a given demand. As shown in Figure 1, the SimCenter aims to streamline these calculations through a Damage Analysis module that uses EDPs from the structural response or direct-damage simulations described earlier and classifies damages into a few damage states that are passed as DMs to the following Loss and Recovery Analysis modules.

Damage Analysis needs to characterize and propagate all important sources of uncertainty in demands (i.e., joint distribution of EDPs) and component characteristics (i.e., component quantities and fragilities) to be able to capture the low-probability, high-consequence outcomes with sufficiently high fidelity. This uncertainty quantification often requires a larger sample size than what is feasible to generate directly through traditional numerical simulation of structural behavior. Hence, probabilistic EDP models are fit to raw EDP results and they are used to generate a large EDP sample for subsequent calculations. High-resolution approaches in recent literature introduce further complexity to consider correlations between component capacities (Baker et al., 2024), model cascading damages (i.e., damage to one component triggers damage in another) (Hamburger et al., 2025), recognize changes in demands due to structural and nonstructural damage (Ouyang and Spence, 2019), and simulate the entire time history of damages to capture the behavior of components sensitive to load history (Ouyang and Spence, 2020; Abdelhady et al., 2022).

Existing damage simulation tools typically focus on single methodologies, with many being proprietary and closed-source (e.g., Verisk, 2025; HBRisk, 2025; ATC, 2018; FEMA, 2024a), preventing researchers from benchmarking or improving them. The few open exceptions often focus on low-resolution, aggregate assessments for large-scale studies (e.g., Pagani et al., 2014). Recognizing significant synergies among existing methodologies, we developed a unifying approach that integrates popular damage and loss assessment techniques. Building on the FEMA P-58 methodology, we generalized it across hazards, assets, and resolutions (Zsarnoczay and Deierlein, 2020). These developments are implemented in the Pelicun engine (Zsarnoczay et al., 2025a), which handles damage and loss assessment for both local-scale and regional-scale simulations within the SimCenter backend. Pelicun is instrumental in supporting the diverse structural, damage, and loss assessment workflows shown in Figure 12 within the SimCenter framework (Figure 1).

Pelicun has been widely adopted for regional risk and resilience assessments across seismic and hurricane hazards, enabling high-resolution modeling of damage and losses (Dahal et al., 2025; Zhang et al., 2023; Kijewski-Correa et al., 2023; Khajwal and Noshadravan, 2024). Researchers have leveraged its flexibility in functional recovery analysis for diverse structural systems, including hybrid frames, steel moment frames, and isolated buildings (Rahgozar and Alam, 2023; Galvis et al., 2023; Blowes et al., 2023; AlHamaydeh et al., 2023). Its probabilistic framework has supported sensitivity studies on loss and recovery estimates (Kourehpaz et al., 2025; Banihashemi et al., 2024) and informed optimization-based design and decision-making for resilience (Issa et al., 2023; Pampanin et al., 2023; Pham and Becker, 2023). Studies have also applied Pelicun to assess the impact of rupture characteristics on seismic risk (Payyappilly et al., 2021; 2024) and quantify the benefits of retrofit strategies for vulnerable wood-frame houses (Welch et al., 2020), demonstrating its adaptability in integrating various loss assessment methodologies.

5.4 Model and Simulation Databases

The advent of the George E. Brown Jr, Network for Earthquake Engineering Simulation (Ramirez et al., 2020) established data sharing as the norm and set an example for the hazards research community in data re-use and dissemination, which continues in NHERI. Developing and sharing validated numerical models is essential to continue advancing our understanding of structural vulnerabilities and enhancing the design and retrofit of assets. High-fidelity numerical models of assets are important sources of synthetic reference data to evaluate, calibrate, and improve the efficiency of models to analyze a large number of assets in regional-scale studies. Such efficient approaches include reduced-order models and surrogates, as well as fragility functions for even more streamlined analyses. High-importance and unique, complex structures often lie outside the scope of available high-efficiency models and need to be directly analyzed using specific numerical models in multi-fidelity regional simulations (Figure 11). We believe their organization under shared model libraries will substantially improve our ability to realistically capture the impact of disasters on large metropolitan areas; we are actively building and maintaining libraries of models and data in the following areas:

1. Computational Fluid Dynamics Simulation Library: This repository archives the outputs and model data from high-resolution simulations conducted using WE-UQ, offering benchmark datasets for future research (Melaku and Bitsuamlak, 2024). The stored data for each simulation includes pressure tap locations, time-varying pressure coefficients at these locations, building geometry, and all relevant information related to the simulated wind condition. These datasets are analogous to those obtained from wind tunnel experiments (Ho et al., 2005; Tokyo Polytechnic University, 2025). The primary objective of this effort is to develop a comprehensive aerodynamic database using computational fluid dynamics for various building archetypes and exposures, which later can be queried using specific search criteria, facilitating their integration into uncertainty quantification workflows and the training of surrogate models.
2. Structural Response Model Library: We are curating a library of models for commonly used structural systems in earthquake engineering. These models will be stored with metadata that identifies key limitations, links to relevant publications, and enables researchers to utilize them immediately in our simulation platform. We envision a future extension of this library that includes surrogate models to replace expensive response simulations in regional studies. We are collaborating with researchers who develop such models and aim to establish a standardized schema for storing and sharing surrogates.

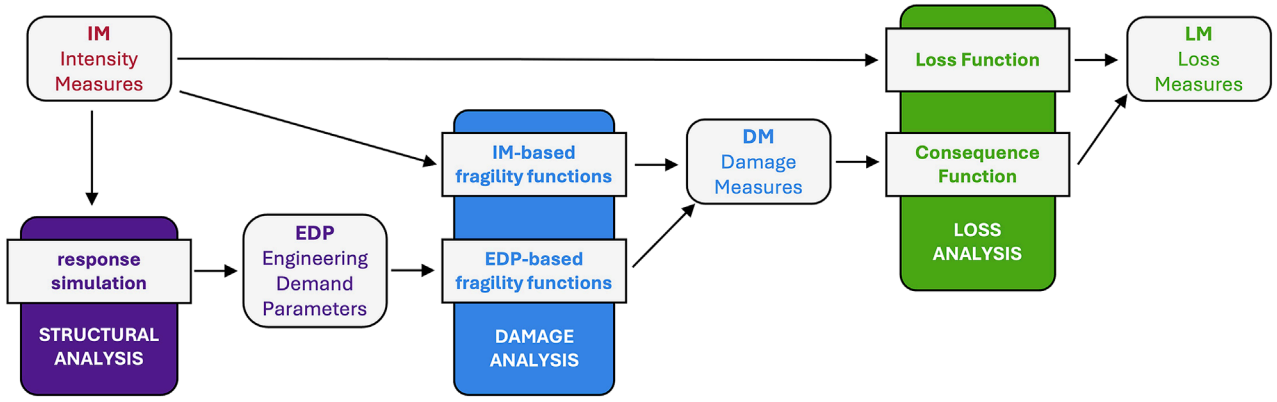

FIGURE 12
Workflow options in the Pelicun engine for damage and loss assessment.

3. Damage and Loss Model Library: The generic data schema for fragility, consequence, and loss functions developed as part of the Pelicun engine described earlier is used in this library to collect and organize a broad range of models required for damage and loss simulations (NHERI SimCenter, 2025a). The library covers seismic, wind, and water hazards, various asset types and resolutions from component-scale to portfolio analysis (e.g., Hamburger et al., 2025; FEMA, 2012; FEMA, 2024d). The models are automatically bundled with Pelicun, but researchers have also leveraged them in studies that do not use Pelicun by directly interfacing with the library (e.g., Klepac et al., 2022).

6 Losses, performance, and recovery

Traditionally, damages and losses have been calculated with methodologies focusing on individual assets, and asset-specific results are used to estimate aggregate metrics in regional-scale studies. In catastrophe modeling, assets in large inventories are classified into a few archetypes, and the analyses are performed using archetype counts across geographic areas, such as census tracts. This approach is efficient because it requires only one assessment per archetype in each area, and it has been successfully used to capture overall trends and high-level consequences (Mitchell-Wallace et al., 2017). Despite these advantages, it is recognized in recent literature that such high-level approaches cannot provide the fidelity required to faithfully capture complex recovery processes of communities or identify opportunities for mitigating critical vulnerabilities in the built environment that have cascading impacts across a city's infrastructure systems and services (Koliou et al., 2020).

The SimCenter leverages the high-resolution inventories and damage information supported by our simulation platform and designed the SimCenter Framework to support the probabilistic simulation of a regional-scale recovery process by regularly evaluating functionality and simulating the restoration of various systems in a region. These systems include buildings, transportation networks, water distribution systems, and electric power systems whose performance is critical for community resilience. Disruptions in road networks can delay emergency response and reconstruction efforts (Hackl et al., 2018), while failures in water and power distribution systems can significantly hinder both short-term coping and long-term recovery (Oikonomou et al., 2021). Interdependencies between these systems present significant challenges in model calibration and recovery simulation (He and Cha, 2018).

The pyrecodes framework (Blagojević and Stojadinović, 2025) is integrated into our platform to simulate recovery and manage infrastructure system models and interdependencies. pyrecodes models a region as a system-of-systems using generic supply-demand relationships, enabling a bottom-up simulation of complex infrastructure interdependencies (Figure 13). It employs an agent-based approach combined with resource-constrained discrete-event simulation to model recovery, evaluating resource allocation and asset restoration over time. In each time step, pyrecodes interfaces with other software to assess system performance and distribute resources. Since the performance of each system can depend on the performance of the others, this distribution step is not trivial. pyrecodes handles the optimization required to converge to an equilibrium in each time step, defining resources available for the restoration of each asset in each system. Regional recovery simulation occurs at the building and infrastructure component level, using recovery models that can range from simple asset-specific restoration curves to complex multi-step, resource-constrained models that account for impeding factors and building component repair. Restoration is tracked by advancing assets to higher functionality states as they recover, a process repeated until full restoration or a time limit is reached. Uncertainties are propagated by running a recovery simulation for each inventory-event-damage realization available from the preceding part of the workflow.

Several research studies have utilized our simulation platform via the R2D desktop application to carry out seismic and hurricane risk assessments (Angeles and Kijewski-Correa, 2022; 2023; Maky et al., 2024; Dahal et al., 2025) and to create network-based methods for assessing infrastructure vulnerability (Li et al., 2025; Oh et al., 2024). The platform also enabled post-disaster recovery modeling and the inclusion of socioeconomic impacts in

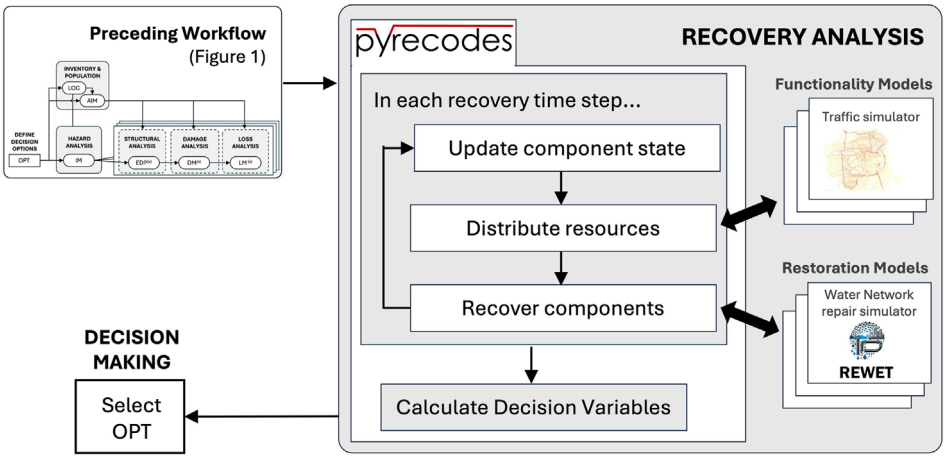

FIGURE 13
Conceptual overview of recovery analysis in the SimCenter Framework using pyrecodes and connected system-specific tools.

regional studies (Wang et al., 2022; Mongold et al., 2024; Byun and Yi, 2024). The following subsections offer more details about the capabilities and opportunities within the SimCenter platform, focusing on risk analysis for buildings, infrastructure networks, and communities.

6.1 Buildings

Disaster impacts on buildings have been traditionally modeled using local-scale workflows even in regional-scale simulations. Such workflows typically yield Loss Measures (LM, see Figures 1, 12) using one of the following two calculation paths:

1) Simulate damage with fragility functions and evaluate the consequences of the resulting damage states using consequence functions. There are several advantages of this approach that enable high-fidelity calculations. Since the same underlying damage state information can be used in consequence functions for various LMs, the considerable partial correlations between LMs due to the underlying damage are directly captured. Utilizing domain experts for the calibration of each type of consequence function supports the development of a robust and comprehensive library. Despite the flexibility of this approach, libraries of functions are typically only prepared to represent consequences at a given location and time. For example, FEMA P-58 functions model losses in a Northern California location in 2011 (FEMA, 2012). If supporting data is available, consequence functions can be scaled in Pelicun to account for alternative conditions in another geographical location (e.g., labor and material costs, contractor availability) or at another point in time (e.g., different relative repair costs due to non-uniform inflation in the construction sector).
2) Calculate LMs directly using event intensity measures as inputs to loss functions. This approach is more efficient because it does not require response and damage simulation. Loss functions are typically calibrated to approximately capture the expected losses for a broadly defined group of building archetypes (Aljawhari et al., 2023). Although the widely used loss functions do not aim to capture the influence of design details and specific vulnerabilities, this is not an inherent limitation of the method. If each loss function is calibrated to a specific, detailed building configuration, a large set of functions can provide high-fidelity loss information for a building with various types of potential vulnerabilities (Welch and Deierlein, 2020). However, it is typically not feasible to prepare a comprehensive set of such high-fidelity loss functions for general-purpose regional simulation.

Pelicun, SimCenter's damage and loss simulation engine introduced in the previous section, supports both of these calculation paths, and our Damage and Loss Model Library includes consequence and loss functions for commonly used calculation methodologies such as Hazus and FEMA P-58. Although these models focus on immediate, direct loss of monetary value (also referred to as repair cost, loss ratio, and even as monetary damage ratio in the literature), they also support the calculation of repair time and injury LMs.

The distinction between the time to repair damage in a building (i.e., reconstruction time) and the time it takes for a building to recover after an earthquake was already recognized by the original Hazus Earthquake Methodology. Recovery typically includes pre-repair delays, often termed 'irrational components' or 'impeding factors' (Comerio, 2006). Modeling these delays and the gradual recovery of building functionality has been an active research area in recent years. The SimCenter promotes functional recovery simulation efforts by supporting the open-source release of ARUP's REDi methodology (Almufti and Willford, 2013) and integrating it into the PBE application. TREADS (Molina Hutt et al., 2022), another functional recovery simulation method, uses the Pelicun engine for damage and direct loss inputs. We are also contributing to the development of a Python version of the ATC 138 methodology (Cook et al., 2022), and aim to integrate it into our platform.

Considering each building in isolation is acceptable for direct losses, but it leads to unrealistic results when considering

impeding factors and other systemic effects that are often correlated between buildings in the same geographical region. Our regional simulation workflow allows the pyrecodes tool to leverage damage and direct loss information from individual building analyses and directly simulate the availability and distribution of resources needed for repair financing, engineering design, permitting, and construction. This allows a shared recovery simulation for buildings by enhancing existing functional recovery simulation frameworks, as shown through the example of F-Rec (Terzic et al., 2021) by Blagojević et al. (2023).

6.2 Transportation networks

Transportation networks play a crucial role in post-disaster recovery; limited transportation access can significantly hinder repair and recovery efforts across infrastructure systems and building inventories. Therefore, to assess potential disruptions to community-wide recovery, it is essential to evaluate both the functionality of individual transportation infrastructure assets—based on their damage states from prior analyses—and the overall performance of the transportation network. To do so, an agent-based residual demand model for city-scale traffic analysis (Zhao et al., 2019) is integrated into our simulation platform, enabling the assessment of regional travel behavior following a natural hazard event. The origin-destination (OD) matrix is an essential component for such traffic simulations, and we are participating in the development of an automated method to estimate a post-event OD matrix based on the changes in the number of households in each locality due to damage to residential buildings. The restoration of transportation assets is modeled either using restoration curves from the Hazus Earthquake Methodology or with the F-Rec + iRe-CoDeS framework through pyrecodes. More complex restoration models will be integrated in the future.

6.3 Potable water networks

Water transfer and distribution networks serve potable water to households, industries, and other critical infrastructures (e.g., healthcare and food facilities) and enable post-event fire-fighting efforts. Limited potable water can critically affect households' ability to shelter in place and disrupt the functioning of key facilities such as those needing water for firefighting (Arango et al., 2025; Davidson et al., 2023). Evaluating water access, however, involves more than establishing a direct connection between a water source and a target location. It requires hydraulic simulations that integrate detailed network characteristics such as flow, pressure, and component constraints.

REWET is an open-source tool developed by Naeimi and Davidson (2024) to streamline damage modeling and recovery of water distribution networks. REWET can simulate the functionality of a damaged network using WNTR (Klise et al., 2020) and the industry-standard EPANET solver (Rossman, 2000) to facilitate a fast, reliable and verified hydraulic simulation with flexible hydraulic leak-damage modeling. The R2D application can import

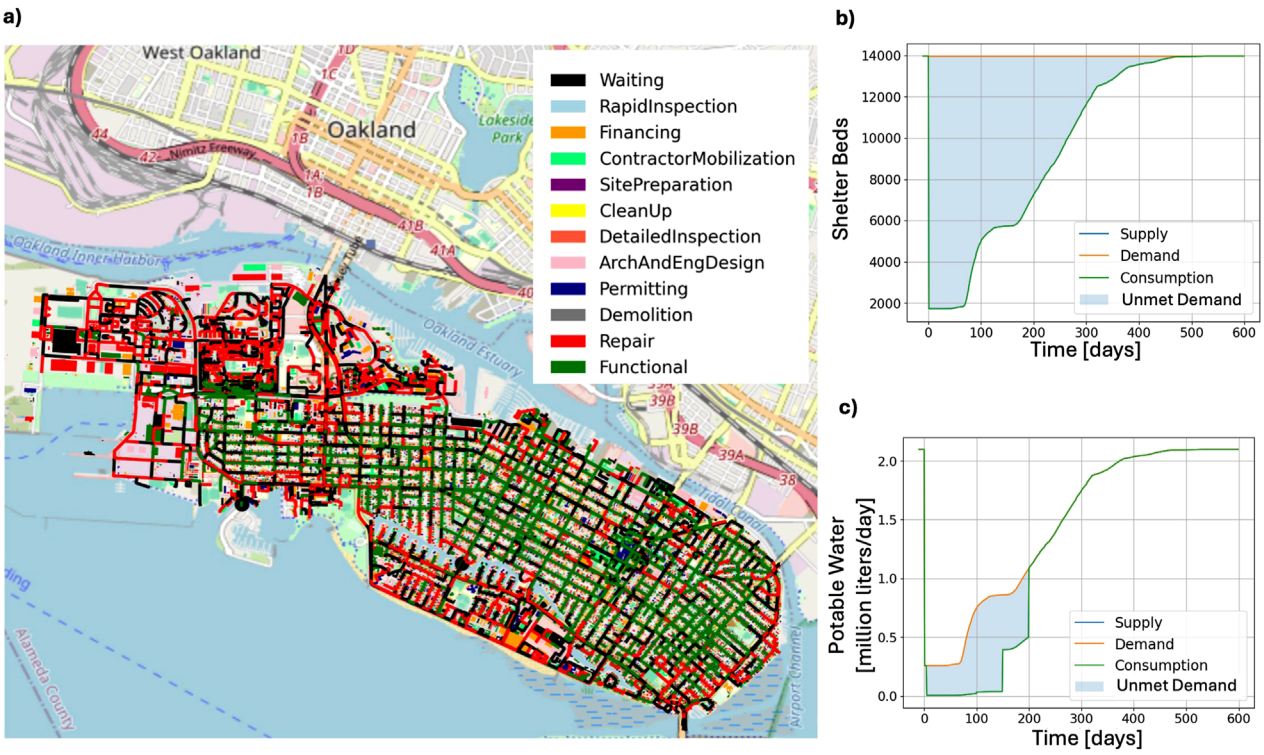

FIGURE 14
Recovery of housing units providing shelter in part of the San Francisco testbed, considering lifeline and building damages. **(a)** Recovery state of assets 2 months after an earthquake. **(b)** Recovery of shelter beds. **(c)** Recovery of potable water utility.

the widely used EPANET input schema to define the characteristics of assets in the network. For recovery, REWET uses a generalized restoration plan structure that enables users to define recovery effort parameters—such as jobs (including their duration and effects on network elements), damage groups, and repair crews (including their initial locations, capabilities, and priorities). Simulating the pipe repair process is challenging due to the need to model damage discovery (i.e., damaged pipes are usually buried, and the damage may not be discovered if the pipes are dry). REWET uses a rule-based damage discovery method for buried pipes that considers the amount of leaking water at each damage location from the hydraulic simulation outputs. The detailed, explicit simulation of hydraulic performance and recovery in REWET provides robust estimates of water availability for researchers studying post-disaster recovery.

6.4 Electric power networks

Electric power not only serves business and household consumers but is also critical for the function of other infrastructure, such as potable water, communication, healthcare, and transportation (He and Cha, 2018). In recent years, the increasing dependency on electric power is being addressed by backup sources, e.g., backup generators for water pumps, hospitals, and communication towers, and solar panels and batteries for households (Cheng et al., 2024). However, the availability, reliability, and longevity of such solutions is highly heterogeneous (Ceferino et al., 2020; Ceferino and Lin, 2023). Similar to potable water disruptions, households can partially adapt to the lack of electric power service (Chakalian et al., 2018; Davidson et al., 2023), but the lack of service has a significant socio-economic impact (Bhattacharyya et al., 2021). Thus, the system performance and post-disaster recovery of electrical power networks are important components of the overall recovery and social and economic impact assessment for a natural hazard event.

Hazus (FEMA, 2024b), for instance, uses a simple recovery method based on time and initial damage to estimate the percentage of power consumers served in the area by a given substation. This efficient methodology is available in our simulation platform and allows users to address the problem at an aggregate level. More sophisticated approaches account for the redistribution of power, considering the redundancy of the power network. Cheng et al. (2024) proposed a Direct Current (DC) model using a connectivity optimization method. Ma et al. (2022) developed a framework for probabilistic simulation of power transmission networks using MATPOWER (Zimmerman et al., 2011) to solve an alternating current optimal power flow model. This latter approach provides more realistic results than a DC model, but requires more information about the network. The SimCenter is exploring the integration of such approaches while also facilitating the collection of the required input data for these calculations.

6.5 Communities

Modeling community impacts and recovery quantitatively requires human behavior and decision-making models that describe how households respond to the shock of the hazard event and subsequent challenges posed by the scarcity of resources and their unmet needs (Lindell and Prater, 2003; Comerio, 1997). The post-disaster experience of households is primarily dictated by the functionality of their housing units, which is dependent on many factors beyond structural performance. These additional factors include the availability of utilities as well as the timing and extent of financial and other support that can facilitate the recovery process (Peacock et al., 2006). For households that need to leave their homes, the availability of temporary shelter through public services and informal connections is critical in avoiding permanent displacement (Johnson, 2007; Levine et al., 2007).

The SimCenter simulation platform has provided damage information for research studies focusing on socioeconomic impacts and community resilience. The high-resolution building inventories and corresponding damage estimates enabled novel, agent-based approaches to capture the behavior of communities through emerging patterns from relatively simple household-scale agents (Costa et al., 2021; Alisjahbana et al., 2022). Besides studying the impact of disasters on the built environment, we also aim to support studies that focus on households. When focusing on the built environment, a researcher can simulate how the number of housing units where residents can shelter in place changes over time (Figure 14). Conversely, studying households could require information on how many times households need to move while coping with the disaster until they can rebuild their home. We aim to support research in this area through the integration of the household dislocation model by Sutley and Hamideh (2017), and the Adaptive Regional Input-Output model for the local economy based on the work of Hallegatte (2013). The streamlined interface provided by pyrecodes facilitates the expansion of the list of supported models and allows members of the research community to contribute without in-depth familiarity with our backend architecture.

7 Concluding remarks

Computational simulation has become an essential tool in natural hazards engineering, enabling researchers to assess risk, evaluate mitigation strategies, and model disaster recovery processes with increasing accuracy. The NHERI SimCenter has contributed to this advancement by developing an open-source, modular framework that integrates high-fidelity simulations with high-resolution regional-scale assessments. Developed over the past decade, the platform provides tools that support collaboration across disciplines, leverage publicly available datasets, and integrate widely used modeling software to enhance the study of natural hazards. Testbeds demonstrate these capabilities and provide an environment for exploration and research discovery. The substantial impact of the SimCenter on research is illustrated in this paper by citing over 50 studies where SimCenter tools or testbeds were instrumental in achieving research objectives.

This paper has outlined the conceptual framework of the SimCenter simulation platform, enabling those studies, and illustrated its applications in hazard characterization, built environment modeling, structural response simulation, damage and loss estimation, and recovery modeling. The modular nature of the framework ensures flexibility and extensibility, allowing researchers to incorporate new methodologies and data sources

as the field evolves. The SimCenter simulation platform currently has capabilities to address the impacts of earthquakes, hurricanes (wind and storm surge), and tsunamis, and the modular framework is readily extensible to other hazards such as wildfires, flooding, and compound events. As new challenges emerge in disaster risk management and resilience planning, continued collaboration and innovation in computational modeling will be essential for advancing the field and improving community resilience to natural hazards.

Data availability statement

Publicly available datasets were analyzed in this study. This data can be found here: https://github.com/NHERI-SimCenter.

Author contributions

AZ: Writing – original draft, Writing – review and editing. GD: Writing – original draft, Writing – review and editing. FM: Writing – original draft, Writing – review and editing. MS: Writing – original draft, Writing – review and editing. S-RY: Writing – original draft, Writing – review and editing. BC: Writing – original draft, Writing – review and editing. AS: Writing – original draft, Writing – review and editing. JZ: Writing – original draft, Writing – review and editing. JB: Writing – original draft, Writing – review and editing. AM: Writing – original draft, Writing – review and editing. SN: Writing – original draft, Writing – review and editing. PA: Writing – review and editing. RD: Writing – review and editing. CG: Writing – review and editing. SG: Writing – review and editing. AK: Writing – review and editing. TK-C: Writing – review and editing. LL: Writing – review and editing. MM: Writing – review and editing. SS: Writing – review and editing. ET: Writing – review and editing. AT: Writing – review and editing. MD: Writing – review and editing.

Funding

The author(s) declare that financial support was received for the research and/or publication of this article. The SimCenter was financially supported by the National Science Foundation under Grants CMMI-1612843 and 2131111. Any opinions, findings, and conclusions or recommendations expressed in this material are those of the authors and do not necessarily reflect the views of the National Science Foundation.

Acknowledgments

We would like to acknowledge the substantial value added to our simulation platform through collaboration with many faculty, post-doctoral researchers, students, and staff over the past 9 years, as well as facilities and institutions within and beyond NHERI and other federal and private sector partners.

Conflict of interest

The authors declare that the research was conducted in the absence of any commercial or financial relationships that could be construed as a potential conflict of interest.

The author(s) declared that they were an editorial board member of Frontiers, at the time of submission. This had no impact on the peer review process and the final decision.

Generative AI statement

The author(s) declare that no Generative AI was used in the creation of this manuscript.

Publisher's note

All claims expressed in this article are solely those of the authors and do not necessarily represent those of their affiliated organizations, or those of the publisher, the editors and the reviewers. Any product that may be evaluated in this article, or claim that may be made by its manufacturer, is not guaranteed or endorsed by the publisher.

References

Abdelhady, A. U., Spence, S. M. J., and McCormick, J. (2022). Risk and fragility assessment of residential wooden buildings subject to hurricane winds. *Struct. Saf.* 94, 102137. doi:10.1016/j.strusafe.2021.102137

Abell, J. A., Crempien, J. G. F., and Recabarren, M. (2022). ShakerMaker: a framework that simplifies the simulation of seismic ground-motions. *SoftwareX* 17, 100911. doi:10.1016/j.softx.2021.100911

Adams, B. M., Bohnhoff, W. J., Dalbey, K. R., Ebeida, M. S., Eddy, J. P., Eldred, M. S., et al. (2020). Dakota, a multilevel parallel object-oriented framework for design optimization, parameter estimation, uncertainty quantification, and sensitivity analysis: version 6.12 user's manual. Sandia National Laboratories, *Tech. Rep*.

AlHamaydeh, M., Maky, A., and ElKafrawy, M. (2023). Probabilistic incremental dynamic analysis for seismic isolation systems through integration with the NHERI-SimCenter performance-based engineering application. *Buildings* 13 (6), 1413. doi:10.3390/buildings13061413

Alisjahbana, I., Moura-Cook, A., Costa, R., and Kiremidjian, A. (2022). An agent-based financing model for post-earthquake housing recovery: quantifying recovery inequalities across income groups. *Earthq. Spectra* 38 (2), 1254–1282. doi:10.1177/87552930211064319

Aljawhari, K., Gentile, R., and Galasso, C. (2023). Simulation-based consequence models of seismic direct loss and repair time for archetype reinforced concrete frames. *Soil Dyn. Earthq. Eng.* 172, 107979. doi:10.1016/j.soildyn.2023.107979

Almufti, I., and Willford, M. (2013). "Resilience-based earthquake design initiative (REDi^{TM}) rating system,". San Francisco, CA.

Ancheta, T. D., Darragh, R. B., Stewart, J. P., Seyhan, E., Silva, W. J., Chiou, B. S. J., et al. (2014). NGA-West2 database. *Earthq. Spectra* 30 (3), 989–1005. doi:10.1193/070913eqs197m

Angeles, K., and Kijewski-Correa, T. (2022). Data-driven framework for automated simulation of wind and windborne debris effects for hurricane regional loss estimation. *J. Wind Eng. Industrial Aerodynamics* 230, 105167. doi:10.1016/j.jweia.2022.105167

Angeles, K., and Kijewski-Correa, T. (2023). Advancing parcel-level hurricane regional loss assessments using open data and the regional resilience determination tool. *Int. J. Disaster Risk Reduct.* 95, 103818. doi:10.1016/j.ijdrr.2023.103818

Anguelov, D., Dulong, C., Filip, D., Frueh, C., Lafon, S., Lyon, R., et al. (2010). Google street view: capturing the world at street level. *Computer* 43, 32–38. doi:10.1109/MC.2010.170

Arango, T., Baker, M., and Bogel-Burroughs, N. (2025). 'Completely dry': how Los Angeles firefighters ran out of water. *N. Y. Times*.

Artyk, Z., Kuan, Y., Zhang, D., Shon, C. S., Ogwumeh, C. M., and Kim, J. (2024). Development of engineered geopolymer composites containing low-activity fly ashes and ground granulated blast furnace slags with hybrid fibers. *Constr. Build. Mater.* 422, 135760. doi:10.1016/j.conbuildmat.2024.135760

ASCE (2022). *ASCE/SEI 7-22: minimum design loads and associated criteria for buildings and other structures*. *Am. Soc. Civ. Eng.* Reston, VA.

ASCE (2023). Prestandard for performance-based wind design, 1. Reston, VA: American Society of Civil Engineers. doi:10.1061/9780784484739

ASCE (2025). ASCE hazard tool. Available online at: https://ascehazardtool.org (Accessed February 26, 2025).

Astudillo, B., Rivera, D., Duke, J., Simpson, B., Fahnestock, L. A., Sause, R., et al. (2023). Modeling uncertainty of specimens employing spines and force-limiting connections tested at E-defense shake table. *Earthq. Eng. and Struct. Dyn.* 52 (14), 4638–4659. doi:10.1002/eqe.3976

ATC (2018). *PACT*: *performance assessment calculation tool - version 3.1.2*. Redwood, CA: Applied Technology Council. Available online at: https://femap58.atcouncil.org/pact (Accessed March 6, 2025).

Attary, N., Unnikrishnan, V. U., van de Lindt, J. W., Cox, D. T., and Barbosa, A. R. (2017). Performance-Based Tsunami Engineering methodology for risk assessment of structures. *Eng. Struct.* 141, 676–686. doi:10.1016/j.engstruct.2017.03.071

Baker, J. W., Almeter, E., Cook, D., Liel, A. B., and Haselton, C. (2024). A model for partially dependent component damage fragilities in seismic risk analysis. *Earthq. Spectra* 40, 1 609–628. doi:10.1177/87552930231205790

Banihashemi, M., Miliziano, A., Zsarnóczay, Á., Wiebe, L., and Filiatrault, A. (2024). Consequences of consequence models: the impact of economies of scale on seismic loss estimates. *Earthq. Spectra* 40 (2), 1396–1424. doi:10.1177/87552930231220001

Bassman, T., Zsarnóczay, A., Saw, J., Wang, S., and Deierlein, G. (2022). "High-fidelity testbed development for regional risk assessment in alameda, California," in *12th national conference on earthquake engineering*. Available online at: https://simcenter.designsafe-ci.org/media/filer_public/d6/72/d67210e9-5149-41a1-bc40-f2c7d1852cc4/bassman_12ncee_alameda_final.pdf.

Beck, J. L., and Katafygiotis, L. S. (1998). Updating models and their uncertainties. I: Bayesian statistical framework. *J. Eng. Mech.* 124 (4), 455–461. doi:10.1061/(ASCE)0733-9399(1998)124:4(455)

Berger, M. J., and LeVeque, R. J. (2023). *Towards adaptive simulations of dispersive tsunami propagation from an asteroid impact, International Congress of Mathematicians*. Berlin, Germany: EMS Press, 5056–5071.

Berman, J. W., Wartman, J., Olsen, M., Irish, J. L., Miles, S. B., Tanner, T., et al. (2020). Natural hazards reconnaissance with the NHERI RAPID facility. *Front. Built Environ.* 6. doi:10.3389/fbuil.2020.573067

Bhattacharyya, A., Yoon, S., and Hastak, M. (2021). Economic impact assessment of severe weather–induced power outages in the US. *J. Infrastruct. Syst.* 27 (4), 04021038. doi:10.1061/(ASCE)IS.1943-555X.0000648

Bielak, J., Loukakis, K., Hisada, Y., and Yoshimura, C. (2003). Domain reduction method for three-dimensional earthquake modeling in localized regions, Part I: theory. *Bull. Seismol. Soc. Am.* 93, 817–824. doi:10.1785/0120010251

Blagojevic, N., and Stojadinovic, B. (2022). A demand-supply framework for evaluating the effect of resource and service constraints on community disaster resilience. *Resilient Cities Struct.* 1 (1), 13–32. doi:10.1016/j.rcns.2022.03.001

Blagojević, N., and Stojadinović, B. (2025). pyrecodes: an open-source library for regional recovery simulation and disaster resilience assessment of the built environment (v0.2.0). *Zenodo*. doi:10.5281/zenodo.14774265

Blagojević, N., Terzić, V., and Stojadinović, B. (2023). F-RecN+ iRe-CoDeS: computational framework for regional recovery simulation using advanced building recovery models. *Eng. Struct.* 288, 116156. doi:10.1016/j.engstruct.2023.116156

Blowes, K., Kourehpaz, P., and Molina Hutt, C. (2023). Risk-targeted seismic evaluation of functional recovery performance in buildings. *Earthq. Eng. Struct. Dyn.* 52 (13), 4245–4264. doi:10.1002/eqe.3984

Bonus, J. (2023). *Evaluation of fluid-driven debris impacts in a high-performance multi-GPU material point method*. Washington: University of. Available online at: https://www.ncbi.nlm.nih.gov/pubmed/2915819774.

Bonus, J. (2025). Tsunami debris motion and loads in a scaled port setting: comparative analysis data for the material point method. *Designsafe-CI*. doi:10.17603/DS2-TFJT-0N76

Bonus, J., and Arduino, P. (2025). *ClaymoreUW*. Geneva, Switzerland: Zenodo. doi:10.5281/zenodo.15128706

Bonus, J., McKenna, F., Lewis, N., Harish, A. B., and Arduino, P. (2025a). NHERI-SimCenter/HydroUQ: version 4.1.0 zenodo. doi:10.5281/zenodo.15319477

Bonus, J., Spröer, F., Winter, A., Arduino, P., Krautwald, C., Motley, M., et al. (2025b). Tsunami debris motion and loads in a scaled port setting: comparative analysis of three state-of-the-art numerical methods against experiments. *Coast. Eng.* 197, 104672. doi:10.1016/j.coastaleng.2024.104672

Byun, J. E., and Yi, S. (2024). Anti-price-gouging law is neither good nor bad in itself: a proposal of narrative numeric method for transdisciplinary social discourses. *npj Nat. Hazards* 1 (1), 4. doi:10.1038/s44304-024-00005-y

Ceballos, V., and Arteta, C. (2022). *RC-FIAP - reinforced concrete frame inelastic analysis platform - version 1.0*. Geneva, Switzerland: Zenodo. doi:10.5281/zenodo.6501833

Ceferino, L., and Lin, N. (2023). Hurricane risk of solar generation in the United States. *Nat. Hazards Rev.* 24 (4), 04023029. doi:10.1061/NHREFO.NHENG-1764

Ceferino, L., Liu, C., Alisjahbana, I., Patel, S., Kiremidjian, A., and Rajagopal, R. (2020). "Disaster resilience of distributed energy resources," in *The 17th world conference on earthquake engineering*.

Cetiner, B., McKenna, F., Yi, S., Wang, B., and Manousakis, I. V. (2025). *BRAILS++*. Geneva, Switzerland: Zenodo. doi:10.5281/zenodo.15610729

Chakalian, P., Kurtz, L., and Hondula, D. (2018). "Understanding vulnerability and adaptive capacity to large-scale power failure in the United States - natural hazards center quick response research report series, report 275," in *Natural hazards center*. Boulder, CO: University of Colorado.

Cheng, B., Nozick, L., Dobson, I., Davidson, R., Obiang, D., Dias, J., et al. (2024). Quantifying the earthquake risk to the electric power transmission system in Los Angeles at the census tract level. *IEEE Access* 12, 126019–126032. doi:10.1109/ACCESS.2024.3408797

Cheraghi, A., Wang, Y., Markovic, N., and Ou, G. (2024). Efficient post-earthquake reconnaissance planning using adaptive batch-mode active learning. *Adv. Eng. Inf.* 60, 102414. doi:10.1016/j.aei.2024.102414

Ching, J., and Chen, Y.-C. (2007). Transitional Markov chain Monte Carlo method for Bayesian model updating, model class selection, and model averaging. *J. Eng. Mech.* 133 (7), 816–832. doi:10.1061/(ASCE)0733-9399(2007)133:7(816)

Comerio, M. C. (1997). Housing issues after disasters. *J. Contingencies Crisis Manag.* 5 (3), 166–178. doi:10.1111/1468-5973.00052

Comerio, M. C. (2006). Estimating downtime in loss modeling. *Earthq. Spectra* 22 (2), 349–365. doi:10.1193/1.2191017

Cook, D. T., Liel, A. B., Haselton, C. B., and Koliou, M. (2022). A framework for operationalizing the assessment of post-earthquake functional recovery of buildings. *Earthq. Spectra* 38 (3), 1972–2007. doi:10.1177/87552930221081538

Costa, R., Haukaas, T., and Chang, S. E. (2021). Agent-based model for post-earthquake housing recovery. *Earthq. Spectra* 37 (1), 46–72. doi:10.1177/8755293020944175

Dahal, L., Burton, H., and Zhong, K. (2025). High-fidelity high-resolution regional seismic risk and resilience assessment of large building inventories. *Earthq. Eng. Struct. Dyn.* 54, 1376–1396. doi:10.1002/eqe.4313

Darestani, Y. M., Jeddi, A. B., and Shafieezadeh, A. (2022). "Hurricane fragility assessment of power transmission towers for a new set of performance-based limit states," in *Engineering for extremes. Springer tracts in Civil engineering*. Editors M. G. Stewart, and D. V. Rosowsky (Cham: Springer). Available online at: https://doi-org.stanford.idm.oclc.org/10.1007/978-3-030-85018-0_8.

Davidson, R. A., Kendra, J., Starbird, K., Nozick, L. K., Ewing, B., and Leon-Corwin, M. (2023). Typology of household adaptations to infrastructure system service interruptions. *Int. J. Disaster Risk Reduct.* 97, 103974. doi:10.1016/j.ijdrr.2023.103974

Deierlein, G. G., McKenna, F., Zsarnóczay, A., Kijewski-Correa, T., Kareem, A., Elhaddad, W., et al. (2020). A cloud-enabled application framework for simulating regional-scale impacts of natural hazards on the built environment. *Front. Built Environ.* 6, 558706. doi:10.3389/fbuil.2020.558706

Deierlein, G. G., and Zsarnóczay, A. (2019). *State of the art in computational simulation for natural hazards engineering* (Geneva, Switzerland: Zenodo). doi:10.5281/zenodo.2579582

Deierlein, G. G., and Zsarnóczay, A. (2021). *State of the art in computational simulation for natural hazards engineering* -. Second Edition (Geneva, Switzerland: Zenodo). doi:10.5281/zenodo.4558106

Dennis, J. E., Gay, D. M., and Welsch, R. E. (1981). Algorithm 573: NL2SOL—an adaptive nonlinear least-squares algorithm [E4]. *ACM Trans. Math. Softw.* 7 (3), 369–383. doi:10.1145/355958.355966

Du, A., Wang, X., Xie, Y., and Dong, Y. (2023). Regional seismic risk and resilience assessment: methodological development, applicability, and future research needs – an earthquake engineering perspective. *Reliab. Eng. and Syst. Saf.* 233, 109104. doi:10.1016/j.ress.2023.109104

Edge, B., Ramirez, J., Peek, L., Bobet, A., Holmes, W., Robertson, I., et al. (2020). "Natural hazards engineering research infrastructure, 5-year science plan, multi-hazard research to make a more resilient world, doi:10.17603/ds2-4s85-mc54

Enderami, S. A., Mazumder, R. K., Dumler, M., and Sutley, E. J. (2022). Virtual testbeds for community resilience analysis: state-of-the-art review, consensus study,

and recommendations. *Nat. Hazards Rev.* 23 (4), 03122001. doi:10.1061/(asce)nh.1527-6996.0000582

Enderami, S. A., Sutley, E. J., Mazumder, R. K., and Dumler, M. (2023). Virtual testbeds for community resilience analysis: step-by-step development procedure and future orientation. *Resilient Cities Struct.* 2, 42–56. doi:10.1016/j.rcns.2023.07.002

Feehan, S. A., McCoy, S. W., Scheingross, J. S., and Gardner, M. H. (2023). Quantifying variability of incipient-motion thresholds in gravel-bedded rivers using a grain-scale force-balance model. *J. Geophys. Res. Earth Surf.* 128 (9), e2023JF007162. doi:10.1029/2023jf007162

FEMA (1997). *Fema 273: NEHRP guidelines for the seismic rehabilitation of buildings*. Washington, DC: Federal Emergency Management Agency.

FEMA (2012). *Fema P-58-1: seismic performance assessment of buildings, Volume 1 - methodology*. Washington, DC: Federal Emergency Management Agency.

FEMA (2022). USA structures. Available online at: https://gis-fema.hub.arcgis.com/pages/usa-structures (Accessed February 26, 2025).

FEMA (2024a). *Hazus 7.0 user guide*. Washington, DC: Federal Emergency Management Agency. Available online at: https://www.fema.gov/sites/default/files/documents/fema_hazus_7_user_guide.pdf (Accessed: March 6, 2025).

FEMA (2024b). *Hazus earthquake model technical manual - Hazus 6.1*. Washington, DC: Federal Emergency Management Agency. Available online at: https://www.fema.gov/sites/default/files/documents/fema_hazus-earthquake-model-technical-manual-6-1.pdf.

FEMA (2024c). *Hazus flood model technical manual - Hazus 6.1*. Washington, DC: Federal Emergency Management Agency. Available online at: https://www.fema.gov/sites/default/files/documents/fema_hazus-flood-model-technical-manual-6-1.pdf.

FEMA (2024d). *Hazus hurricane model technical manual - Hazus 6.1*. Washington, DC: Federal Emergency Management Agency. Available online at: https://www.fema.gov/sites/default/files/documents/Hazus_6.1_Hurricane_Model_Technical_Manual.pdf.

FEMA (2024e). *Hazus inventory national database*. Washington, DC: Federal Emergency Management Agency. Available online at: https://tools.hazards.fema.gov/hazus/maps/data/NationalDB/HazusInventoryNationalData.zip (Accessed March 6, 2025).

FEMA (2024f). *Hazus inventory technical manual*. Washington, DC: Federal Emergency Management Agency. Available online at: https://www.fema.gov/sites/default/files/documents/fema_hazus-inventory-technical-manual-6.1.pdf.

FEMA (2024g). *Hazus tsunami model technical manual - Hazus 6.1*. Washington, DC: Federal Emergency Management Agency. Available online at: https://www.fema.gov/sites/default/files/documents/Hazus_6.1_Tsunami_Model_Technical_Manual.pdf.

FHWA (2023). National bridge inventory. Available online at: https://www.fhwa.dot.gov/bridge/nbi.cfm (Accessed February 26, 2025).

FHWA (2024). National tunnel inventory. Available online at: https://www.fhwa.dot.gov/bridge/inspection/tunnel/inventory.cfm (Accessed February 26, 2025).

Field, E. H., Jordan, T. H., and Cornell, C. A. (2003). OpenSHA: a developing community-modeling environment for seismic hazard analysis. *Seismol. Res. Lett.* 74 (4), 406–419. doi:10.1785/gssrl.74.4.406

Frankel, A., Wirth, E., Marafi, N., Vidale, J., and Stephenson, W. (2018). Broadband synthetic seismograms for magnitude 9 earthquakes on the Cascadia megathrust based on 3D simulations and stochastic synthetics, Part 1: methodology and overall results. *Bull. Seismol. Soc. Am.* 108 (5A), 2347–2369. doi:10.1785/0120180034

Gahtan, J., Knapp, K. R., Schreck, C. J., Diamond, H. J., Kossin, J. P., and Kruk, M. C. (2024). *International best track archive for climate stewardship (IBTrACS) project, version 4r00*. Asheville, NC: NOAA National Centers for Environmental Information. doi:10.25921/82ty-9e16

Galvis, F. A., Deierlein, G. G., Issa, O., Zsarnoczay, A., Molina Hutt, C., and Baker, J. W. (2023). "Functional recovery assessment of tall buildings with pre-northridge welded steel moment frames," in *Canadian conference - pacific conference on earthquake engineering*.

Galvis, F. A., Deierlein, G. G., Molina Hutt, C., and Baker, J. W. (2022). "High-fidelity modeling of fracture-critical welded steel beam-to-column connections and their impact on earthquake stability of tall buildings," in *Proc. Annual stability conference structural reliability council*. Denver, CO.

Goseberg, N., Stolle, J., Nistor, I., and Shibayama, T. (2016). Experimental analysis of debris motion due the obstruction from fixed obstacles in tsunami-like flow conditions. *Coast. Eng.* 118, 35–49. doi:10.1016/j.coastaleng.2016.08.012

Gouveia, F., Silva, V., Lopes, J., Moreira, R. S., Torres, J. M., and Guerreiro, S. (2024). Automated identification of building features with deep learning for risk analysis. *Discov. Appl. Sci.* 6 (9), 466. doi:10.1007/s42452024060702

Gray, G. A., and Kolda, T. G. (2006). Algorithm 856: APPSPACK 4.0: asynchronous parallel pattern search for derivative-free optimization. *ACM Trans. Math. Softw.* 32 (3), 485–507. doi:10.1145/1163641.1163647

Gu, D., Kareem, A., Lu, X., and Cheng, Q. (2023). A computational framework for the simulation of wind effects on buildings in a cityscape. *J. Wind Eng. Industrial Aerodynamics* 234, 105347–45. doi:10.1016/j.jweia.2023.105347

Guan, X., Burton, H., and Sabol, T. (2020). Python-based computational platform to automate seismic design, nonlinear structural model construction and analysis of steel moment resisting frames. *Eng. Struct.* 224, 111199. doi:10.1016/j.engstruct.2020.111199

Güngör, B., Hasanoğlu, S., Çalım, F., Muderrisoglu, Z., and Dindar, A. A. (2023). "Constitutive model characterization of the RC columns using energy terms," in *International workshop on energy-based seismic engineering* (Cham: Springer Nature Switzerland), 258–268.

Hackl, J., Lam, J. C., Heitzler, M., Adey, B. T., and Hurni, L. (2018). Estimating network related risks: a methodology and an application in the transport sector. *Nat. Hazards Earth Syst. Sci.* 18, 2273–2293. doi:10.5194/nhess-18-2273-2018

Hallegatte, S. (2013). Modeling the role of inventories and heterogeneity in the assessment of the economic costs of natural disasters. *Risk Anal.* 34 (1), 152–167. doi:10.1111/risa.12090

Hamburger, R., Zsarnoczay, A., Tackie-Otoo, N. O., Kijewski-Correa, T., Davidson, R. A., and Spence, S. M. J. (2025). Unifying the current state of the art in hurricane wind risk simulations: a systematic review. *ASCE J. Struct. Eng.* 151, 8. doi:10.1061/JSENDH.STENG-14590

HBRisk (2025). SP3: seismic performance prediction platform. *Haselt. Bak. Risk Group*. Available online at: https://sp3risk.com/ (Accessed March 6, 2025).

He, X., and Cha, E.-J. (2018). Modeling the damage and recovery of interdependent critical infrastructure systems from natural hazards. *Reliab. Eng. and Syst. Saf.* 177, 162–175. doi:10.1016/j.ress.2018.04.029

Ho, T. E., Surry, D., Morrish, D., and Kopp, G. A. (2005). The UWO contribution to the NIST aerodynamic database for wind loads on low buildings: Part 1. Archiving format and basic aerodynamic data. *J. Wind Eng. Industrial Aerodynamics* 93 (1), 1–30. doi:10.1016/j.jweia.2004.07.006

Hu, Z., and Mahadevan, S. (2019). Probability models for data-driven global sensitivity analysis. *Reliab. Eng. and Syst. Saf.* 187, 40–57. doi:10.1016/j.ress.2018.12.003

Huang, M., Liao, S., Lou, W., Lin, W., and Kareem, A. (2024). Multi-scale simulation of typhoon wind field at building scale utilizing mesoscale model with nested large eddy simulation. *J. Wind Eng. Industrial Aerodynamics* 249, 105733. doi:10.1016/j.jweia.2024.105733

Issa, O., Silva-Lopez, R., Baker, J. W., and Burton, H. V. (2023). Machine-learning-based optimization framework to support recovery-based design. *Earthq. Eng. Struct. Dyn.* 52 (11), 3256–3280. doi:10.1002/eqe.3860

Jasak, H. (2009). OpenFOAM: open source CFD in research and industry. *Int. J. Nav. Archit. Ocean Eng.* 1 (2), 89–94. doi:10.2478/IJNAOE-2013-0011

Johnson, C. (2007). Strategic planning for post-disaster temporary housing. *Disasters* 31 (4), 435–458. doi:10.1111/j.1467-7717.2007.01018.x

Jung, W., and Taflanidis, A. A. (2023). Efficient global sensitivity analysis for high-dimensional outputs combining data-driven probability models and dimensionality reduction. *Reliab. Eng. and Syst. Saf.* 231, 108805. doi:10.1016/j.ress.2022.108805

Khajwal, A. B., and Noshadravan, A. (2024). Enhancing post-hurricane regional loss assessment with crowdsourcing: a probabilistic inference approach. *Int. J. Disaster Risk Reduct.* 107, 104456. doi:10.1016/j.ijdrr.2024.104456

Kijewski-Correa, T., Cetiner, B., Zhong, K., Wang, C., Zsarnoczay, A., Guo, Y., et al. (2023). Validation of an augmented parcel approach for hurricane regional loss assessments. *Nat. Hazards Rev.* 24, 04023022. doi:10.1061/NHREFO.NHENG-1649

Kijewski-Correa, T., Cetiner, B., Zhong, K., Wang, C., Zsarnóczay, A., Lochhead, M., et al. (2022). SimCenter hurricane testbed: atlantic county, NJ. *Designsafe-CI*. doi:10.17603/DS2-83CA-R890

Kim, S., Ding, F., and Spence, S. M. J. (2024). AI-enabled damage estimation of hurricane-impacted residential communities through CFD simulations and stratified sampling. *J. Wind Eng. Industrial Aerodynamics* 251, 105806. doi:10.1016/j.jweia.2024.105806

Klepac, S., Subgranon, A., and Olabarrieta, M. (2022). A case study and parametric analysis of predicting hurricane-induced building damage using data-driven machine learning approach. *Front. Built Environ.* 8, 1015804. doi:10.3389/fbuil.2022.1015804

Klise, K. A., Hart, D. B., Bynum, M., Hogge, J., Haxton, T., Murray, R., et al. (2020). *Water network tool for resilience (WNTR) user manual*. Washington, DC: U.S. EPA Office of Research and Development.

Knapp, K. R., Kruk, M. C., Levinson, D. H., Diamond, H. J., and Neumann, C. J. (2010). The international best track archive for climate stewardship (IBTrACS) unifying tropical cyclone data. *Bull. Am. Meteorological Soc.* 91 (3), 363–376. doi:10.1175/2009bams2755.1

Koh, M. J., Park, H., Jayasekara, J. R., Kameshwar, S., Doyle, K., Cox, D., et al. (2025). Experimental study on tsunami-driven debris damming loads on columns of an elevated coastal structure. *Coast. Eng.*, 196, 104656. doi:10.1016/j.coastaleng.2024.104656

Koliou, M., van de Lindt, J. W., McAllister, T. P., Ellingwood, B. R., Dillard, M., and Cutler, H. (2020). State of the research in community resilience: progress and challenges. *Sustain. Resilient Infrastructure* 5 (3), 131–151. doi:10.1080/23789689.2017.1418547

Kourehpaz, P., Molina Hutt, C., and Zsarnóczay, A. (2025). Impact of parameter selection on seismic loss and recovery time estimates: a variance-based sensitivity analysis. *Earthq. Spectra* 0 (0). doi:10.1177/87552930241307624

Kurumbhati, M. M., Ramancha, M. K., Aakash, B. S., Conte, J. P., and Lotfizadeh, K. H. (2024). Hierarchical Bayesian modeling for calibration and uncertainty quantification of constitutive material models: application to a uniaxial steel material model. *Eng. Struct.* 318, 118409. doi:10.1016/j.engstruct.2024.118409

Levine, J. N., Esnard, A.-M., and Sapat, A. (2007). Population displacement and housing dilemmas due to catastrophic disasters. *J. Plan. Literature* 22 (1), 3–15. doi:10.1177/0885412207302277

Levitan, M. (2020). NIST/ARA hurricane laura rapid response windfield estimate - windfield release 3. DesignSafe data depot. Available online at: https://www.designsafe-ci.org/data/browser/tapis/designsafe.storage.community/%2FRecon%20Portal%2F2020%20Hurricane%20Laura%20Cameron%20Louisiana%20USA%2FNIST%20ARA%20Rapid%20Reponse%20Windfield%20Estimate (Accessed March 5, 2025).

Lewis, N. S., Winter, A. O., Bonus, J., Motley, M. R., Eberhard, M. O., Arduino, P., et al. (2023). Open-source simulation of strongly-coupled fluid-structure interaction between non-conformal interfaces. *Front. Built Environ.* 9. doi:10.3389/fbuil.2023.1120518

Li, P., Wang, Z., Zhao, B., Becker, T., and Soga, K. (2025). Surrogate modeling for identifying critical bridges in traffic networks under earthquake conditions. *Transp. Res. Part D Transp. Environ.* 138, 104512. doi:10.1016/j.trd.2024.104512

Lindell, M. K., and Prater, C. S. (2003). Assessing community impacts of natural disasters. *Nat. Hazards Rev.* 4 (4), 176–185. doi:10.1061/(asce)1527-6988(2003)4:4(176)

Liu, H., Hellín, C. J., Tayebi, A., Delgado, C., and Gómez, J. (2024). 3D reconstruction of geometries for urban areas supported by computer vision or procedural generations. *Mathematics* 12, 3331. doi:10.3390/math12213331

Luettich, R. A., Jr., Westerink, J. J., and Scheffner, N. W. (1992). ADCIRC: an advanced three-dimensional circulation model for shelves, coasts, and estuaries. *Rep. 1. Theory Methodol. ADCIRC-2DDI ADCIRC-3DL*. Available online at: https://apps.dtic.mil/sti/pdfs/ADA261608.pdf.

Lynett, P. J., Gately, K., Wilson, R., Montoya, L., Arcas, D., Aytore, B., et al. (2017). Inter-model analysis of tsunami-induced coastal currents. *Ocean. Model.* 114, 14–32. doi:10.1016/j.ocemod.2017.04.003

Ma, L., Christou, V., and Bocchini, P. (2022). Framework for probabilistic simulation of power transmission network performance under hurricanes. *Reliab. Eng. and Syst. Saf.* 217, 108072. doi:10.1016/j.ress.2021.108072

Mackenzie-Helnwein, P., Wan, J., and McKenna, F. (2020). *NHERI-SimCenter/TurbulenceInflowTool*. Geneva, Switzerland: Zenodo. doi:10.5281/zenodo.3988635

Maechling, P. J., Silva, F., Callaghan, S., and Jordan, T. H. (2015). SCEC broadband platform: system architecture and software implementation. *Seismol. Res. Lett.* 86 (1), 27–38. doi:10.1785/0220140125

Maky, A. M., AlHamaydeh, M., and Saleh, M. (2024). GIS-based regional seismic risk assessment for dubai, UAE, using NHERI SimCenter R2D application. *Buildings* 14 (5), 1277. doi:10.3390/buildings14051277

Mapillary contributors (2020). Mapillary. Available online at: https://www.mapillary.com/ (Accessed February 26, 2025).

Mascarenas, D. (2022). *Experimental evaluation of loads from inundation-driven debris fields*. Seattle, WA: University of Washington. Available online at: http://hdl.handle.net/1773/48874.

Massey, T. C., Anderson, M. E., McKee Smith, J., Gomez, J., and Jones, R. (2011). *STWAVE: steady-state spectral wave model - users's manual version 6.0, US army Corps of engineers*. Vicksburg, MS: Engineer Research and Development Center.

McCallen, D., Petersson, A., Rodgers, A., Pitarka, A., Miah, M., Petrone, F., et al. (2021). EQSIM—a multidisciplinary framework for fault-to-structure earthquake simulations on exascale computers part I: computational models and workflow. *Earthq. Spectra* 37 (2), 707–735. doi:10.1177/8755293020970982

McKenna, F., Fenves, G. L., and Scott, M. H. (2000). "Open system for earthquake engineering simulation," in *Pacific earthquake engineering research center*. UC Berkeley, CA.

McKenna, F., Gavrilovic, S., Zhao, J., Zhong, K., Zsarnoczay, A., Cetiner, B., et al. (2025a). *NHERI-SimCenter/R2DTool: version 5.4.0 (v5.4.0)*. Geneva, Switzerland: Zenodo. doi:10.5281/zenodo.15446356

McKenna, F., Melaku, A. F., Ding, F., Wan, J., Mackenzie-Helnwein, P., Gardner, M., et al. (2025b). *NHERI-SimCenter/WE-UQ: version 4.3.0 (v4.3.0)*. Geneva, Switzerland: Zenodo. doi:10.5281/zenodo.15420438

McKenna, F., Yi, S., Satish, A. B., Zsarnoczay, A., Gardner, M., and Elhaddad, W. (2025c). *NHERI-SimCenter/quoFEM: version 4.1.0 (v4.1.0)*. Geneva, Switzerland: Zenodo. doi:10.5281/zenodo.14583957

McKenna, F., Zhong, K., Gardner, M., Zsarnoczay, A., Yi, S., Satish, A. B., et al. (2024). *NHERI-SimCenter/EE-UQ*. Geneva, Switzerland: Zenodo. doi:10.5281/zenodo.13865428

Melaku, A. F., and Bitsuamlak, G. T. (2024). Prospect of LES for predicting wind loads and responses of tall buildings: a validation study. *J. Wind Eng. Industrial Aerodynamics* 244, 105613. doi:10.1016/j.jweia.2023.105613

Meza, J. C., Oliva, R. A., Hough, P. D., and Williams, P. J. (2007). OPT++: an object-oriented toolkit for nonlinear optimization. *ACM Trans. Math. Softw.* doi:10.1145/1236463.1236467

Microsoft (2022). Microsoft global building footprints. Available online at: https://github.com/microsoft/GlobalMLBuildingFootprints (Accessed February 26, 2025).

Mitchell-Wallace, K., Jones, M., Hillier, J. K., and Foote, M. (2017). *Natural catastrophe risk management and modelling: a practitioner's guide*. Wiley.

Molina Hutt, C., Vahanvaty, T., and Kourehpaz, P. (2022). An analytical framework to assess earthquake induced downtime and model recovery of buildings. *Earthq. Spectra* 38 (2), 1283–1320. doi:10.1177/87552930211060856

Mongold, E., Costa, R., Zsarnóczay, Á., and Baker, J. W. (2024). Modeling post-disaster recovery: accounting for rental and multi-family housing. *Earthq. Spectra* 40 (2), 1353–1375. doi:10.1177/87552930231222769

Naeimi, S., and Davidson, R. A. (2024). REWET: a tool to model system functioning and restoration of damaged water supply systems. *J. Infrastruct. Syst.* 30 (4), 04024024. doi:10.1061/JITSE4.ISENG-2427

Navarro Carranza, J. M., Deierlein, G. G., and Zhong, K. (2025). Simulation of longitudinal reinforcing steel bar fracture in reinforced concrete walls. *Bull. Earthq. Eng.* 23 (1), 517–551. doi:10.1007/s10518-024-02078-6

NHERI SimCenter (2025a). Damage and loss model library - online documentation. Available online at: https://nheri-simcenter.github.io/DamageAndLossModelLibrary/([Accessed March 5, 2025).

NHERI SimCenter (2025b). GitHub repositories for NHERI SimCenter tools and applications Available online at: https://github.com/NHERI-SimCenter [Accessed: March 5, 2025]

NHERI SimCenter (2025c). SimCenter DB-ES database. Available online at: https://www.designsafe-ci.org/data/browser/tapis/designsafe.storage.community/SimCenter/Datasets/DB-ES (Accessed February 26, 2025).

NHERI SimCenter (2025d). SimCenter testbeds – online documentation. Available online at: https://simcenter.designsafe-ci.org/products/testbeds/([Accessed March 5, 2025).

Nolte, C., Boyle, K. J., Chaudhry, A. M., Clapp, C., Guignet, D., Hennighausen, H., et al. (2023). Data practices for studying the impacts of environmental amenities and hazards with nationwide property data. *Land Econ.* 100 (1), 200–221. doi:10.3368/le.100.1.102122-0090R

Oh, S., Yi, S., and Wang, Z. (2024). Long-range Ising model for regional-scale seismic risk analysis. *Earthq. Eng. and Struct. Dyn.* 53 (12), 3904–3923. doi:10.1002/eqe.4198

Oikonomou, K., Mongird, K., Rice, J., and Homer, J. S. (2021). Resilience of interdependent water and power systems: a literature review and conceptual modeling framework. *Water* 13 (20), 2846. doi:10.3390/w13202846

Opazo-Vega, A., Jara-Cisterna, A., Benedetti, F., and Nuñez-Decap, M. (2025). Estimation of the orthotropic elastic properties of reinforced LVL panels through vibration-based model updating techniques. *Wood Sci. Technol.* 59, 26. Article 26. doi:10.1007/s00226-024-01627-1

OpenStreetMap contributors (2017). Planet dump. Available online at: https://www.openstreetmap.org (Accessed February 26, 2025).

Ouyang, Z., and Spence, S. M. J. (2019). A performance-based damage estimation framework for the building envelope of wind-excited engineered structures. *J. Wind Eng. Industrial Aerodynamics* 186, 139–154. doi:10.1016/j.jweia.2019.01.001

Ouyang, Z., and Spence, S. M. J. (2020). A performance-based wind engineering framework for envelope systems of engineered buildings subject to directional wind and rain hazards. *J. Struct. Eng.* 146 (5), 04020049. doi:10.1061/(ASCE)ST.1943-541X.0002568

Overture Maps Foundation (2023). Overture maps. Available online at: https://overturemaps.org (Accessed February 26, 2025).

Pagani, M., Monelli, D., Weatherill, G., Danciu, L., Crowley, H., Silva, V., et al. (2014). OpenQuake engine: an open hazard (and risk) software for the global earthquake model. *Seismol. Res. Lett.* 85 (3), 692–702. doi:10.1785/0220130087

Pakzad, A., Arduino, P., Zhang, W., and Taciroglu, E. (2024). "Workflow for high-fidelity dynamic analysis of structures with pile foundation," in *Proceedings of the 17th pan-American conference on soil mechanics and geotechnical engineering (XVII PCSMGE), and 2nd Latin-American regional conference of the international association for engineering geology and the environment (IAEG), La serena Chile*.

Pampanin, S., Bianchi, S., and Ciurlanti, J. (2023). Raising the bar in seismic design: cost-benefit analysis of alternative design methodologies and earthquake-resistant technologies. *Bull. Earthq. Eng.* 21, p2723–p2757. doi:10.1007/s10518-023-01625-x

Pan, F., Jeon, S., Wang, B., Mckenna, F., and Yu, S. X. (2024). "Zero-shot building attribute extraction from large-scale vision and language models," in *Proceedings of the IEEE/CVF winter conference on applications of computer vision*, 8647–8656.

Park, H., Koh, M.-J., Cox, D. T., Alam, M. S., and Shin, S. (2021). Experimental study of debris transport driven by a tsunami-like wave: application for non-uniform density groups and obstacles. *Coast. Eng.*, 166, 103867. doi:10.1016/j.coastaleng.2021.103867

Payyappilly, L. J., Karthik Reddy, K. S. K., and Somala, S. N. (2021). Impact of directivity on seismic risk assessment: rupture distance, component and propagation length. *Asian J. Civ. Eng.* 22, 1361–1375. doi:10.1007/s42107-021-00388-7

Payyappilly, L. J., Karthik Reddy, K. S. K., and Somala, S. N. (2024). Influence of rupture velocity on risk assessment of concrete moment frames: supershear vs. subshear ruptures. *Structures* 60, 105895. doi:10.1016/j.istruc.2024.105895

Peacock, W. G., Dash, N., and Zhang, Y. (2006). "Sheltering and housing recovery following disaster," in *Handbook of disaster research*, 258–274.

Pervaiz, F. (2022). *Numerical simulation of hydrodynamic forces on riverine and coastal bridges subjected to extreme weather events doctoral dissertation*. Arlington, TX: The University of Texas at Arlington.

Petersson, N., Sjogreen, A., Houjun, T. B., and Pankajakshan, R. (2023). *geodynamics/sw4: SW4, version 3.0*. Geneva, Switzerland: Zenodo. doi:10.5281/zenodo.8322590

Pham, H. G., and Becker, T. C. (2023). "Inverse design of isolated structures using predicted FEMA P-58 decision variables," in *Life-cycle of structures and infrastructure systems*. 1st Edition (Boca Raton, FL: CRC Press).

Rahgozar, N., and Alam, M. S. (2023). Functional recovery evaluation of hybrid self-centering piston-based braced frames. *Earthq. Eng. Struct. Dyn.* 53 (2), 867–893. doi:10.1002/eqe.4042

Ramirez, J., Anagnos, T., Hacker, T., Rathje, E., Browning, J., Eberhard, M., et al. (2020). *2004-2014 A decade of earthquake engineering research*. DesignSafe-CI. doi:10.17603/ds2-gp23-b207

Rathje, E., Dawson, C., Padgett, J. E., Pinelli, J.-P., Stanzione, D., Adair, A., et al. (2024). Nearshore bathymetry inversion using a physics-informed neural network approach leveraging the Celeris solver, AGU24

Renteria, W., and Lynett, P. (2025). Nearshore bathymetry inversion using a physics-informed neural network approach leveraging the celeris solver. *ESS Open Archive*. doi:10.22541/essoar.174129307.73050322/v1

Renteria, W., Lynett, P., Bonus, J., Mccann, M., and Ebrahimi, B. (2025). CelerisAi: a nearshore wave modeling framework for integrated AI applications. doi:10.22541/essoar.174129311.11936719/v1

Robertson, I., Bobet, A., Edge, B., Holmes, W., Johnson, D., LaChance, M., et al. (2023). Natural hazards engineering research infrastructure, science plan, multi-hazard research to make a more resilient world, doi:10.17603/ds2-abbs-0966

Rossman, L. (2000). *EPANET 2 users manual*. Cincinnati, OH: U.S. Environmental Protection Agency.

Roueche, D. B., Nakayama, J. O., Cetiner, B. M., Kameshwar, S., and Kijewski-Correa, T. (2022). "Hybrid framework for post-hazard building performance assessments with application to hurricanes," in *14th americas conference on wind engineering*. Available online at: https://par.nsf.gov/biblio/10451223.

Sanderson, D., and Cox, D. (2023). Comparison of national and local building inventories for damage and loss modeling of seismic and tsunami hazards: from parcel- to city-scale. *Int. J. Disaster Risk Reduct.* 93, 103755. doi:10.1016/j.ijdrr.2023.103755

Satish, A. B., Yi, S., Nair, A. S., and Arduino, P. (2022). "Probabilistic calibration and prediction of seismic soil liquefaction using quoFEM," in *Conference on performance-based design in earthquake. Geotechnical engineering* (Cham: Springer International Publishing), 1700–1707.

Schneider, N., and Kosters, J. (2024). U.S. National science foundation natural hazards engineering research infrastructure (NHERI) decadal visioning study 2026-2035. doi:10.17603/ds2-afza-m544

SEAOC (1995). *Vision 2000: performance based seismic engineering of buildings*. Sacramento, CA: Structural Engineers Association of California.

Sheibani, M., and Ou, G. (2020). The development of Gaussian process regression for effective regional post-earthquake building damage inference. *Computer-Aided Civ. Infrastructure Eng.* 36 (3), 264–288. doi:10.1111/mice.12630

Shen, H., Ho-Von, L., King, T., Verrier-Paquette, F., Wang, R., Goldman, G., et al. (2024). "Developing a building identification tool to support mass deep energy retrofits," in *112th ACSA annual meeting proceedings, disruptors on the Edge*. Available online at: https://www.acsa-arch.org/chapter/developing-a-building-identification-tool-to-support-mass-deep-energy-retrofits/.

Sjögreen, B., and Petersson, N. A. (2012). A fourth order accurate finite difference scheme for the elastic wave equation in second order formulation. *J. Sci. Comput.* 52 (1), 17–48. doi:10.1007/s10915-011-9531-1

Skamarock, W. C., Klemp, J. B., Dudhia, J., Gill, D. O., Barker, D. M., Duda, M. G., et al. (2008). *A description of the advanced research WRF version 3*. Boulder, CO: NCAR Technical Note NCAR/TN-556+STR.

Smith, T., Holmes, W., and Edge, B. (2017). Natural hazards engineering research infrastructure, five-year science plan, multi-hazard research to make a more resilient world, First Edition. doi:10.17603/ds2-hsrg-1880

Snaiki, R., and Wu, T. (2017a). Modeling tropical cyclone boundary layer: height-resolving pressure and wind fields. *J. Wind Eng. Industrial aerodynamics* 170, 18–27. doi:10.1016/j.jweia.2017.08.005

Snaiki, R., and Wu, T. (2017b). A linear height-resolving wind field model for tropical cyclone boundary layer. *J. Wind Eng. Industrial Aerodynamics* 171, 248–260. doi:10.1016/j.jweia.2017.10.008

Soize, C., and Ghanem, R. (2016). Data-driven probability concentration and sampling on manifold. *J. Comput. Phys.* 321, 242–258. doi:10.1016/j.jcp.2016.05.044

SPUR (2009). The Resilient City - creating a new framework for disaster planning. Available online at: https://www.spur.org/featured-project/resilient-city (Accessed March 5, 2025).

Sutley, E. J., and Hamideh, S. (2017). An interdisciplinary system dynamics model for post-disaster housing recovery. *Sustain. Resilient Infrastructure* 3 (3), 109–127. doi:10.1080/23789689.2017.1364561

SWAN (2024). "Scientific and Technical documentation - version 41.51". Delft, Neatherlands: *Environ. Fluid Mech. Sect.*

Taborda, R., López, J., Karaoglu, H., Urbanic, J., and Bielak, J. (2010). Speeding up finite element wave propagation for large-scale earthquake simulations. *Parallel Data Lab*.

Taflanidis, A. A., Aakash, B. S., Yi, S., and Conte, J. P. (2025). Surrogate-aided Bayesian calibration with adaptive learning strategies. *Mech. Syst. Signal Process.* doi:10.1016/j.ymssp.2025.113014

Taslimi, A., and Petrone, F. (2024). "Uncertainty quantification in the seismic risk assessment of bridge towers near the hayward fault," in *Proc. 18th world conference on earthquake engineering*. Milan, Italy.

Tavakkol, S., and Lynett, P. (2020). Celeris Base: an interactive and immersive Boussinesq-type nearshore wave simulation software. *Comput. Phys. Commun.* 248, 106966. doi:10.1016/j.cpc.2019.106966

Terashima, M., Deierlein, G. G., and Kanvinde, A. (2018). "Computational simulation of ductile fracture in buckling restrained braces,". *Proc Eleventh U.S. Natl. Conf. Earthq. Eng.*

Terzic, V., Villanueva, P. K., Saldana, D., and Yoo, D. (2021). "F-rec framework: novel framework for probabilistic evaluation of functional recovery of building systems - PEER report No. 2021/06," in *Pacific earthquake engineering research center*. Berkeley, CA.

Tokyo Polytechnic University (2025). TPU aerodynamic database. Available online at: https://wind.arch.t-kougei.ac.jp/system/eng/contents/code/tpu (Accessed March 6, 2025).

U.S. Army Corps of Engineers (2023). National structure inventory technical documentation. Available online at: https://www.hec.usace.army.mil/confluence/nsi/technicalreferences/2022/technical-documentation (Accessed February 26, 2025).

U.S. Census Bureau (2024). 2024 TIGER/line shapefiles. Available online at: https://www.census.gov/cgi-bin/geo/shapefiles/index.php?year=2024&layergroup=Roads (Accessed February 26, 2025).

U.S. Department of Homeland Security (2024). Homeland infrastructure foundation-level data (HIFLD). Available online at: https://hifld-geoplatform.hub.arcgis.com (Accessed February 26, 2025).

Verisk (2025). *Catastrophe modeling software solutions*. Jersey, NJ: Verisk Inc. Available online at: https://www.verisk.com/solutions/extreme-event-risk/software-solutions/(Accessed: March 6, 2025).

Vijayan, L., Huang, W., Ma, M., Ozguven, E., Ghorbanzadeh, M., Yang, J., et al. (2023). Improving the accuracy of hurricane wave modeling in Gulf of Mexico with dynamically-coupled SWAN and ADCIRC. *Ocean. Eng.* 274, 114044. doi:10.1016/j.oceaneng.2023.114044

Virtucio, M. B., Barbaros, C., Zhao, B., Soga, K., and Taciroglu, E. (2024). A granular framework for modeling the capacity loss and recovery of regional transportation networks under seismic hazards: a case study on the Port of Los Angeles. *Int. J. Disaster Risk Reduct.* 100, 104164. doi:10.1016/j.ijdrr.2023.104164

Vrugt, J. A., ter Braak, C. J. F., Diks, C. G. H., Robinson, B. A., Hyman, J. M., and Higdon, D. (2009). Accelerating Markov chain Monte Carlo simulation by differential evolution with self-adaptive randomized subspace sampling. *Int. J. Nonlinear Sci. Numer. Simul.* 10 (3). doi:10.1515/ijnsns.2009.10.3.273

Wald, D., Wald, L., Wordern, B., and Goltz, J. (2003). *ShakeMap - a tool for earthquake response*. Reston, VA: United States Geological Survey. Available online at: https://pubs.usgs.gov/fs/fs-087-03/FS-087-03-508.pdf.

Wang, C., Costa, R., and Baker, J. W. (2022). Simulating post-disaster temporary housing needs for displaced households and out-of-town contractors. *Earthq. Spectra* 38 (4), 2922–2940. doi:10.1177/87552930221112690

Wang, C., Yu, Q., Law, K. H., McKenna, F., Yu, S. X., Taciroglu, E., et al. (2021). Machine learning-based regional scale intelligent modeling of building information for natural hazard risk management. *Automation Constr.*, 122, p.103474. doi:10.1016/j.autcon.2020.103474

Wang, X., Qiu, Y., Slattery, S. R., Fang, Y., Li, M., Zhu, S.-C., et al. (2020). A massively parallel and scalable multi-GPU material point method. *ACM Trans. Graph.* 39 (4). doi:10.1145/3386569.3392442

Wang, Y., Amirhossein, C., Ou, G., and Markovic, N. (2024a). Post-earthquake building damage assessment: a multi-period inspection routing approach for Gaussian process regression. *Transp. Res. Part E Logist. Transp. Rev.* 186, 103548. doi:10.1016/j.tre.2024.103548

Wang, Y., Yue, Q., Lu, X., Gu, D., Xu, Z., Tian, Y., et al. (2024b). Digital twin approach for enhancing urban resilience: a cycle between virtual space and the real world. *Resilient Cities Struct.* 3 (2), 34–45. doi:10.1016/j.rcns.2024.06.002

Weirs, V. G., Kamm, J. R., Swiler, L. P., Ratto, M., Tarantola, S., Adams, B. M., et al. (2012). Sensitivity analysis techniques applied to a system of hyperbolic conservation laws. *Reliab. Eng. Syst. Saf.* 107, 157–170. doi:10.1016/j.ress.2011.12.008

Welch, D. P., and Deierlein, G. G. (2020). "Qualifying the performance of retrofit of cripple walls and sill anchorage in single-family wood-frame buildings - technical background report for structural analysis and performance assessment PEER report 2020/22," in *Pacific earthquake engineering research center*. Berkeley, CA. Available online at: https://apps.peer.berkeley.edu/publications/peer_reports/reports_2020/2020_22_Welch_TechnicalBackground.pdf (Accessed March 6, 2025).

Welch, D. P., Deierlein, G. G., Reis, E., and Burton, H. V. (2020). "Quantifying the benefit of retrofitting unbraced cripple walls in single-family wood-frame dwellings," in *17th world conference on earthquake engineering*. Japan.

Wu, S., Angelikopoulos, P., Papadimitriou, C., and Koumoutsakos, P. (2018). Bayesian annealed sequential importance sampling: an unbiased version of transitional Markov chain Monte Carlo. *ASCE-ASME J. Risk Uncertain. Eng. Syst. Part B Mech. Eng.* 4 (1), 011008. doi:10.1115/1.4037450

Yi, S., Satish, A. B., Nair, A. S., Arduino, P., Zsarnóczay, A., and McKenna, F. (2022). "Sensitivity analysis and bayesian calibration of OpenSees models using quoFEM," in *Eurasian conference on OpenSees* (Cham: Springer Nature Switzerland), 63–72.

Yi, S., and Taflanidis, A. A. (2023). Computationally efficient adaptive design of experiments for global metamodeling through integrated error approximation and multicriteria search strategies. *J. Eng. Mech.* 149 (8), 04023050. doi:10.1061/jenmdt.emeng-7083

Yi, S., and Taflanidis, A. A. (2024). Stochastic emulation with enhanced partial-and no-replication strategies for seismic response distribution estimation. *Earthq. Eng. and Struct. Dyn.* 53 (7), 2354–2381. doi:10.1002/eqe.4115

Yoshimura, C., Bielak, J., Hisada, Y., and Fernandez, A. (2003). Domain reduction method for three-dimensional earthquake modeling in localized regions, Part II: verification and applications. *Bull. Seismol. Soc. Am.* 93, 825–840. doi:10.1785/0120010252

You, T., Wang, W., and Chen, Y. (2023a). An asynchronous simulation algorithm for post-earthquake functional recovery of interdependent infrastructure systems. *Earthq. Eng. Struct. Dyn.* 53 (2), 529–544. doi:10.1002/eqe.4028

You, T., Wang, W., and Tesfamariam, S. (2023b). Effects of self-centering structural systems on regional seismic resilience. *Eng. Struct.* 274 (1), 115125. doi:10.1016/j.engstruct.2022.115125

Yu, Q., Wang, C., McKenna, F., Yu, S. X., Taciroglu, E., Cetiner, B., et al. (2020). Rapid visual screening of soft story buildings from street view images using deep learning classification. *Earthq. Eng. Eng. Vib.* 19 (4), 827–838. doi:10.1007/s1180302005982

Zhang, W., Chen, P.-Y., Crempien, G. F., Kurtulus, A., Arduino, P., and Taciroglu, E. (2023). Regional-scale seismic fragility, loss, and resilience assessment using physics-based simulated ground motions: an application to Istanbul. *Earthq. Eng. Struct. Dyn.* 52 (6), 1785–1804. doi:10.1002/eqe.3843

Zhang, W., Esmaeilzadeh Seylabi, E., and Taciroglu, E. (2019). An ABAQUS toolbox for soil-structure interaction analysis. *Comput. Geotechnics* 114, 103143. doi:10.1016/j.compgeo.2019.103143

Zhang, W., Restrepo, D., Crempien, J. G. F., Erkmen, B., Taborda, R., Kurtulus, A., et al. (2021). A computational workflow for rupture-to-structural-response simulation and its application to Istanbul. *Earthq. Eng. Struct. Dyn.* 50, 177–196. doi:10.1002/eqe.3377

Zhao, B., Kumar, K., Casey, G., and Soga, K. (2019). "Agent-based model (ABM) for city-scale traffic simulation: a case study on San Francisco," in *International conference on smart infrastructure and construction 2019 (ICSIC) driving data-informed decision-making* (London, United Kingdom: ICE Publishing), 203–212.

Zhong, K., Navarro, J. G., Govindjee, S., and Deierlein, G. G. (2023). Surrogate modeling of structural seismic response using probabilistic learning on manifolds. *Earthq. Eng. and Struct. Dyn.* 52 (8), 2407–2428. doi:10.1002/eqe.3839

Zimmerman, R. D., Murillo-Sanchez, C. E., and Thomas, R. J. (2011). MATPOWER: steady-state operations, planning, and analysis tools for power systems research and education. *IEEE Trans. Power Syst.* 26 (1), 12–19. doi:10.1109/TPWRS.2010.2051168

Zsarnoczay, A., and Deierlein, G. G. (2020). "PELICUN: a computational framework for estimating damage, loss and community resilience," in *17th world conference on earthquake engineering*. Japan.

Zsarnoczay, A., McKenna, F., Yi, S., Satish, A. B., Gardner, M., Wang, C., et al. (2025b). *NHERI-SimCenter/PBE*. Geneva, Switzerland: Zenodo. doi:10.5281/zenodo.15445666

Zsarnoczay, A., Vouvakis Manousakis, I., and Zhao, J. (2025a). *NHERI-SimCenter/pelicun (v3.6.1)*. Geneva, Switzerland: Zenodo. doi:10.5281/zenodo.15447502

frontiers | Frontiers in Built Environment

TYPE Original Research
PUBLISHED 08 August 2025
DOI 10.3389/fbuil.2025.1568832

Check for updates

OPEN ACCESS

EDITED BY
Julio Alfonso Ramirez,
Purdue University, United States

REVIEWED BY
Aritra Banerjee,
South Dakota State University, United States
Guillaume Veylon,
Institut National de recherche pour l'agriculture, l'alimentation et l'environnement (INRAE), France

*CORRESPONDENCE
Jason T. DeJong,
jdejong@ucdavis.edu

RECEIVED 30 January 2025
ACCEPTED 17 June 2025
PUBLISHED 08 August 2025

CITATION
DeJong JT, Wilson DW, Martinez A, Ziotopoulou K, Ham S-M and Boulanger RW (2025) NHERI centrifuge facility: systems-scale hypergravity modeling in engineering and scientific research. *Front. Built Environ.* 11:1568832. doi: 10.3389/fbuil.2025.1568832

COPYRIGHT
© 2025 DeJong, Wilson, Martinez, Ziotopoulou, Ham and Boulanger. This is an open-access article distributed under the terms of the Creative Commons Attribution License (CC BY). The use, distribution or reproduction in other forums is permitted, provided the original author(s) and the copyright owner(s) are credited and that the original publication in this journal is cited, in accordance with accepted academic practice. No use, distribution or reproduction is permitted which does not comply with these terms.

NHERI centrifuge facility: systems-scale hypergravity modeling in engineering and scientific research

Jason T. DeJong[1]*, Daniel W. Wilson[1], Alejandro Martinez[2], Katerina Ziotopoulou[2], Soo-Min Ham[2] and Ross W. Boulanger[2]

[1]Department of Civil and Environmental Engineering, Center for Geotechnical Modeling, University of California, Davis, CA, United States, [2]Department of Civil and Environmental Engineering, University of California, Davis, CA, United States

The Natural Hazards Engineering Research Infrastructure facility at the University of California at Davis (UC Davis) is equipped with 9-m- and 1-m-radius geotechnical centrifuges that provide unique, world-class facilities for scaled modeling of complex systems. This national, open access research facility allows scientific and engineering communities to realize major advances in understanding, predicting, and improving the performance of civil infrastructure and natural systems. Large-scale centrifuge modeling of systems-level problems is particularly effective in advancing fundamental knowledge, upscaling and testing new technologies at the prototype scale, developing engineering analysis and design methods, and validating advanced computational models. The capabilities and unique role of large-scale centrifuge modeling are illustrated through four example research projects. These are followed by a discussion of envisioned future research directions and opportunities on how hypergravity modeling can be used to address natural and anthropogenic-induced loadings on civil infrastructure and natural systems.

KEYWORDS

centrifuge, physical modeling, geotechnical, inverse analyses, natural hazards

1 Introduction

1.1 UC Davis Centrifuge facility

UC Davis has been operating geotechnical centrifuges for 5 decades, with the 1-m centrifuge acquired in 1975 and the 9-m centrifuge installed in 1986. The Center for Geotechnical Modeling (CGM) was established in 1983 to develop and manage the 9-m "National Geotechnical Centrifuge." The CGM continues to operate the centrifuges as a national shared-use facility that is accessible to any researcher requiring hypergravity to execute their research program. The 1-m centrifuge can subject ~50 kg of soil (container ~178 mm deep, ~560 mm long, and ~280 mm wide) to a centrifugal acceleration of 100 g. The 9-m centrifuge can subject ~1,550 kg of soil (container ~686 mm deep, ~1,722 mm long, and ~686 mm wide) to a centrifugal acceleration of 80 g, representing prototype soil depths of up to ~50 m. Both centrifuges are equipped with shaking tables that enable the simulation of earthquake-like ground motions, the designs of which have been replicated at many other facilities. A more detailed discussion on the history of the facility, including the important

developments enabled by the National Science Foundation (NSF) Network for Earthquake Engineering Simulation (NEES) equipment award, is detailed in Boulanger et al. (2020).

The pair of CGM centrifuges are used synergistically to support hypergravity research. The 9-m centrifuge containers enable sensor-dense, detailed, complex models that provide high fidelity measurements of system performance. These large experiments often have more than 120 sensors and require months of effort from the start of model building through test completion. In contrast, the smaller 1-m centrifuge can prove advantageous for parametric exploration of mechanisms where a low sensor count and small model size are appropriate and time efficient. Here, tests can be completed in a few days. Researchers also often choose to perform 1-m tests to refine designs and train personnel for upcoming 9-m tests. To support this synergistic use, the CGM manages the two centrifuges to operate as similarly as possible from sensor inventory to model building and loading protocols and resources.

The systems investigated by researchers and the characteristics of the tests have evolved with time as research interests have diversified and new testing capabilities have been developed. To date, more than 100 separate research projects, with a total funding of more than $100M (2024 USD), have used the CGM, each performing one to dozens of centrifuge tests on the 1-m and/or 9-m centrifuges. The development of servo-hydraulic shaking tables in the 1980s and 1990s and the uniquely large model container size of the 9-m centrifuge allowed making advances in seismic applications, and to this day it remains one of only two centrifuges worldwide able to subject models with over 1,500 kg of soil to seismic motions. Consequently, up until the 2010s the majority of centrifuge research programs at the CGM focused on problems related to geotechnical earthquake engineering, with topics including liquefaction (triggering, lateral spreading, levee/embankment deformations, quay wall deformations), ground improvement (densification, drainage, grouting, soil-cement reinforcements), soil-structure interaction (shallow and deep foundations in soft or liquefiable soils for buildings, bridges, tanks, wharves, quay walls), buried structures (lateral pressures and kinematic demands on basements, culverts, subway tunnels and stations), seismic site response (sands, soft clays, organic soils), mechanically stabilized earth retaining walls, geosynthetic liner systems for waste containment, and water-structure-soil interaction for buried reservoirs. Common test characteristics drove numerous developments, including sand model construction techniques (e.g., Stringer et al., 2014), saturation with viscous fluids (e.g., Stewart et al., 1998), dense sensor arrays (e.g., Wilson et al., 2002), scaling and design of structure models (e.g., Kutter and Wilson, 2006), and scaling of ground motions (e.g., Mason et al., 2010), as well as associated data analysis and interpretation techniques (e.g., Kutter and Balakrishnan, 1998; Wilson and Almond, 2014).

The breadth of research topics being performed at the CGM has recently expanded to address new engineering challenges, shifts in national research priorities, diversification of researcher interests, and the now established efficacy of centrifuge modeling based on successful past projects. This expanding breadth includes offshore foundation systems (wave, wind, and seismic loading of jacket structures, suction caissons, subsea manifolds, anchors; e.g., Litton et al., 2014; Huang et al., 2024), *in-situ* characterization of challenging soils (gravelly soils, intermediate soils, mine tailings, fly ash, interbedded soils; e.g., Carey et al., 2022; Price et al., 2019; Madabhushi et al., 2023; Chen and Martinez, 2025; Khosravi et al., 2022, respectively), and tsunami effects on coastal stability (e.g., Exton et al., 2019). Associated with this diversification of research topics have been corresponding developments in modular hydraulic and electro-mechanical actuation systems, including CPT (Carey et al., 2018) and full-flow *in situ* penetrometers, foundation installation hammers and screw-in techniques (Martinez and O'Hara, 2021); advanced soil preparation techniques for clays, intermediate soils, and gravels (Sturm, 2019); novel embedded and non-contact sensors for measuring soil response and system deformations (e.g., Sinha et al., 2023a); and systems to evaluate the effect of drainage and rewetting on soil response (Chen and Martinez, 2025). Since 2010, the growth of biogeotechnics has led to biomediated (microbially-induced calcite precipitation, microbially-induced desaturation and precipitation; e.g., Darby et al., 2019; San Pablo et al., 2024; Hall et al., 2018) and bioinspired (e.g., snakeskin-inspired piles, tree root-inspired anchors; e.g., O'Hara and Martinez, 2022; 2024; Kim et al., 2024) research projects, which have driven new developments in prototype fabrications using 3D printers, sensors for partially saturated conditions, and model construction protocols with finite improved zones (e.g., Ham et al., 2024b). These experiences have demonstrated that capability development for hypergravity testing is often effectively achieved through the pursuit of new research topics where researchers can "champion" advances in partnership with the CGM.

1.2 Scaled hypergravity modeling

The hypergravity field imposed during a centrifuge test allows for stress similitude between the model and full-scale prototype, such that the response of a scaled centrifuge model to different loadings is representative of the response expected under field-scale conditions. For example, the profile of vertical effective stress in a 0.5-m-high embankment at 100 g is equivalent to the profile of vertical effective stress in a 50-m-tall embankment in the field (i.e., at 1g). Centrifuge modeling offers similarity advantages for physical processes where self-weight body forces are important, including various porous media, fluid, and gas related phenomena (e.g., Taylor, 1995). Scaling laws and equations of similitude have accordingly been developed for a wide range of physical phenomena (e.g., Schofield, 1981; Kutter, 1995; Garnier et al., 2007).

The use of scaled hypergravity modeling creates an accessible research domain that is expansive and arguably provides a larger parameter space to explore than is possible in 1g model space or in the field, as indicated in Figure 1. In this figure the "field space" domain represents the breadth of conditions present in the built and natural environments. The "field data" is a subdomain of the "field space" where the built and natural environment has been observed and the characteristics and behaviors have been captured through quantitative measurements for scientific and engineering purposes. The ability to capture

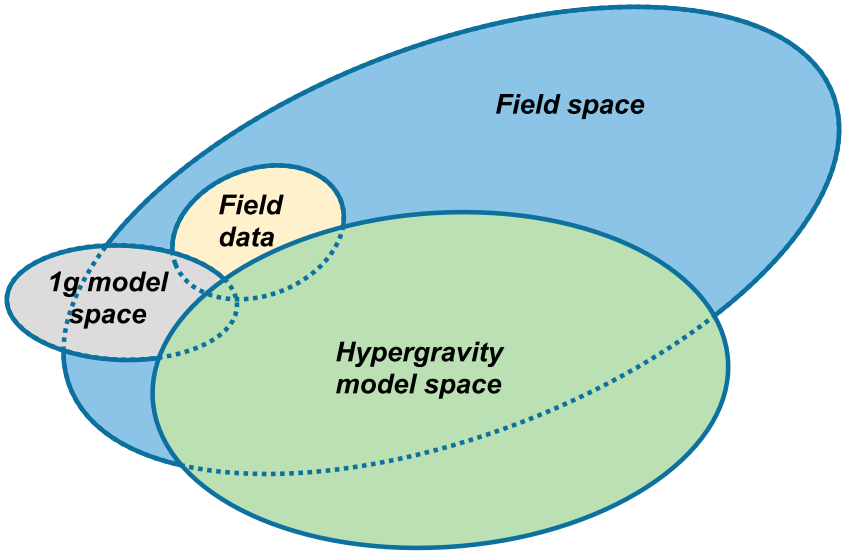

FIGURE 1
Schematic indicating the overlap and interrelationships between the real built and natural environment ("field space"), the subset of real space where data is collected ("field data"), and the accessible domain at 1g ("1g model space") and using hypergravity ("hypergravity model space").

measurements for critical conditions, such as in post-disaster reconnaissance efforts, is limited, as much of the critically valuable information is time-sensitive (perishable) or is not accessible (due to the lack of monitoring systems and limited post-event investigations) (e.g., Bray et al., 2019; Wartman et al., 2020). Simulations of realistic conditions in the lab in "1g model space" for soils and other stress-dependent materials is challenging as soil stiffness, strength, and dilatancy are all directly dependent on the effective confining stress. The domain space where 1g modeling of shallow geotechnical systems may be realistic (i.e., fall within the broader "field space") is relatively small, while scaled modeling of more complex systems in 1g models, such as deep foundations, is realized in a parameter space that exists outside the domain observed in the field for the built environment. Nonetheless, 1g scaled modeling can be used successfully when accounting for how the effective stress profile in the model influences the stress-dilatancy response of sand and the undrained strength profile in clay (e.g., LeBlanc et al., 2010; Bradshaw et al., 2016).

The "hypergravity model space," including the effective use of the scaling relationships, provides the opportunity to more accurately model a larger portion of the domain of full-scale field conditions that exist in the natural and built environments (indicated by large overlap with "field space") and to explore a broad range of conditions that may not exist in the natural environment (i.e., outside the field space). This enables two approaches in the design of a research program. Commonly, the hypergravity environment and scaling laws are used to model field-scale systems with reasonable accuracy, following best practices in applying model scaling laws (e.g., Schofield, 1981; Kutter, 1995; Garnier et al., 2007) and appropriately managing aspects that cannot be scaled exactly. Alternatively, the hypergravity environment allows the gravitational field to be activated as another test variable, where experiments can be designed to ensure that representations of bio-thermo-hydro-chemo-mechanical processes, as often posed in dimensionless groups, have appropriately captured the effect of the gravitational field on the phenomenon being investigated. The former is more often used when researching the built environment, while the latter can be an effective tool for examining fundamental processes. Collectively, this makes the hypergravity environment an effective research tool for advancing knowledge in engineering and science.

1.3 Research approach to experimental design and validation of numerical simulations

Hypergravity experiments can be particularly effective in advancing fundamental knowledge, upscaling and testing new technologies at the system prototype scale, developing engineering analysis and design methods, and validating advanced computational models. Figure 2 illustrates the process through which a hypergravity experiment may be designed and the generated results used to advance analysis and design methods or validate advanced computational models.

Consider a hypothetical full-scale 50-m-high embankment dam with a complex cross-section, a newly identified seismic risk from liquefaction susceptibility of an alluvial foundation deposit, and an extensive proposed seismic remediation scheme (Figure 2a). An engineer performing analyses on this complex section (Figure 2f) may face questions regarding the reasonableness of their analysis due to a lack of physical data for validating their numerical model, especially given limited understanding of fundamental interaction mechanisms for many remediation schemes. To address this, the complex system with its proposed improvements can be acceptably simplified for study by retaining mechanisms critical to seismic system behavior and simplifying features that do not

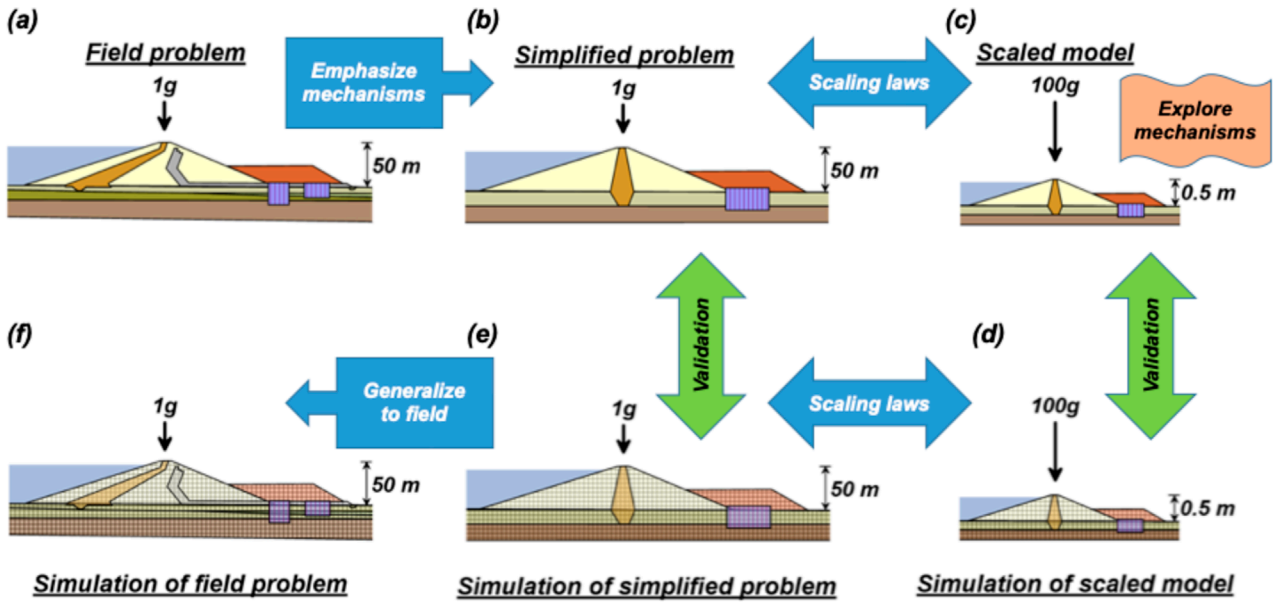

FIGURE 2
Workflow approach from **(a)** the specific field problem, to **(b)** a simplified problem that emphasizes the critical mechanisms, to **(c)** a scaled model that is explored through hypergravity modeling, to simulations of the hypergravity test to validate the numerical simulations at either **(d)** Ng or at **(f)** 1g, and then **(f)** the translation of the validated model to the motivating project field problem.

control the mechanisms being investigated (Figure 2b). A reduced-scale physical model of the simplified problem (Figure 2c) is built following the scaling laws and tested by subjecting it to various seismic loads to explore the critical mechanisms. Scaling laws can then be used to express the observed physical behaviors at real-world (i.e., prototype) scale for easy comparison with field-scale experiences. The engineer can then analyze the simplified problem using design tools to verify that they accurately capture critical behaviors. This comparison can be performed at 1g or Ng (Figures 2e,d, respectively). Comparisons at 1g are easier to compare to real-world systems while comparisons at Ng directly capture the physics and can avoid potential conflicts in scaling laws. Finally, the engineer can generalize their analysis to the field problem, translating their validated understanding and analysis techniques to the specific project of interest (Figure 2f) with confidence.

1.4 Overview of paper

The UC Davis Center for Geotechnical Modeling has been described as a national, open access research facility with the 1-m and 9-m centrifuges. A brief history was presented, and general concepts of hypergravity modeling were introduced. In the remainder of this paper, four examples are used to highlight the breadth of research programs supported by the facility in the past 5 years, including renewable energy systems, pile performance in liquefiable soils, large deformation flow problems, and advancement of biogeotechnical technologies. Finally, envisioned future research directions and opportunities related to natural and anthropogenic-induced loadings on the civil infrastructure and natural systems using the facility are broadly discussed.

2 Research example: renewable energy systems–shared mooring configurations for anchors for offshore wind turbines

The energy harnessed from renewable and sustainable sources, such as solar, wind, and thermal, has increased significantly during the last two decades. About 10% of the energy in the US is now produced from onshore wind (United States Energy Information Administration, 2024). Meanwhile, offshore wind (OW) offers significant potential advantages over onshore. Wind resources are stronger and more consistent offshore, and offshore deployments do not occupy valuable land. In Europe, 28GW of OW energy have been installed as of 2021 (Komusanac et al., 2022), while the US has committed to installing 30GW by 2030 (United States Department of Energy, 2021). Despite its benefits, the cost of OW energy is high compared to other renewable sources due to the cost of installation of the turbines and supporting infrastructure. A key opportunity to improving the cost competitiveness of OW energy is decreasing the cost of the turbine foundations, which can account for 25%–35% of the total construction cost (DNV, 2023).

Approximately 65% of the US' wind resources are in deep water locations where floating offshore wind turbines (FOWTs) are required. In FOWTs, the turbine is maintained in position by subsea anchors and mooring lines. Conventionally, each turbine is connected to three anchors and each anchor is connected to only one turbine. One emerging alternative for reducing the cost of FOWTs is to use a shared mooring configuration where each subsea anchor is shared by three turbines (i.e., each turbine connected to three anchors, each anchor connected to three turbines), as

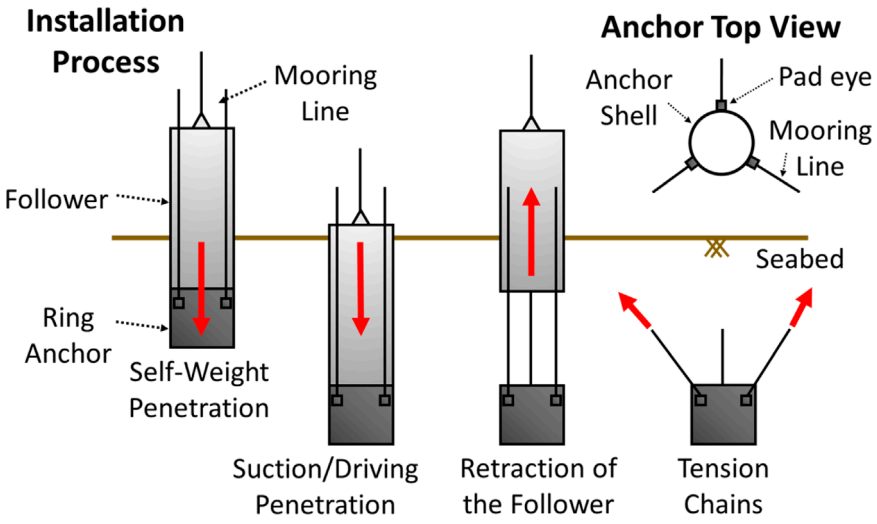

FIGURE 3
Schematic of the installation process and loading of a ring anchor.

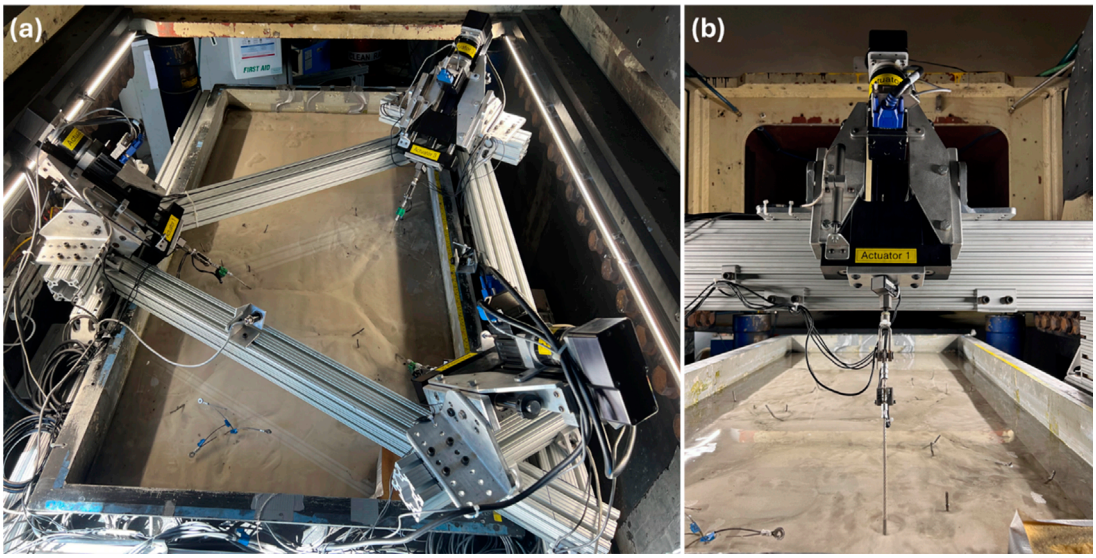

FIGURE 4
Photographs of the actuator system built for load testing **(a)** shared and **(b)** not shared anchors in the 9-m centrifuge.

described in Fontana et al. (2018). Anchor sharing can reduce the number of anchors by up to a factor of three in comparison with the conventional configuration. Meanwhile, a recently developed ring anchor design offers additional potential benefits over common types of FOWT anchors such as driven piles, suction caissons, and plate anchors (Aubeny, 2017), due to its compact size which can simplify shipping and installation logistics, deep embedment which provides a high capacity, and symmetric geometry which is amenable to shared configurations (Lee et al., 2020). Figure 3 depicts the installation process and loading of a shared ring anchor.

Despite the compelling economic and efficiency arguments of shared anchor configurations, research is required because shared anchors are subjected to more complex loading conditions than conventional anchors. Specifically, the individual vertical loads from the three turbines add up, while having multiple turbines connected to a single anchor can lead to changing horizontal load direction which can reduce the soil's strength and stiffness. These complexities are in addition to the cyclic environmental loads from the wind, waves, and tides, which also introduce considerable uncertainty in creating stable designs.

Given the remote location of offshore wind turbines and their very large size, load testing to verify anchor or foundation capacity is in most cases unfeasible. Centrifuge testing provides an opportunity to systematically examine the response of anchor and foundation

systems in conditions that are representative of the field. This enables investigation of the effect of factors such as soil strength and stiffness, embedment depth, and geometry on short- and long-term anchor stability. Centrifuge testing can also be used to verify the behavior of existing and newly developed anchor and foundation technologies, as presented here for the ring anchors. At the UC Davis CGM, equipment has been developed to test subsea anchors in shared and conventional configurations. Specifically, a system capable of applying loads to a buried anchor has been built to perform tests at gravities as high as 70g. This system is composed of three electromechanical actuators that can be controlled in sync to apply representative loads from three individual FOWTs. This system is shown in Figure 4a, showing a buried anchor in a soil deposit being loaded by the three actuators simultaneously. Each actuator can be programmed to produce specific monotonic or cyclic loads. The actuators can apply up to 8 kN in model scale to simulate environmental loads, which is equivalent to 39 MN in prototype scale at 70g. The force and displacement of each line are measured with load cells and linear potentiometers, while the evolution of the line angle is measured with inclinometers. The steel wires connecting the actuators to the buried anchors have a nylon coating to reduce the friction with the soil. This actuator system can also be configured to test anchors in a conventional, non-shared configuration, in which an anchor is loaded by an individual actuator, as shown in Figure 4b.

The loads applied to the anchors during centrifuge load tests were determined using numerical simulations of reference FOWTs and load cases representative of specific locations off the coast of California, as described in detail in Davis (2023) and Coughlan (2024). Monotonic and cyclic load tests have been performed on ring anchors in deposits of sandy and clayey soils. These tests have characterized the effect of parameters including the line angle, out of plane angle, embedment depth, and magnitude of static and cyclic loads on the ultimate capacity and accumulation of displacements of ring anchors. Figure 5a shows the cyclic loads applied to an anchor in a clay deposit under a Service Limit State (SLC) scenario, indicating precise control of the actuators. Figure 5b shows the position of the anchor during application of the loads, showing that as the load out of plane angle (i.e., on the horizontal plane) is changed, the anchor's displacement evolves accordingly. The figure shows the progressive loss of embedment of the anchor, which should be taken into consideration in assessing long-term stability.

Centrifuge testing has been essential in verifying the performance of the novel ring anchor under static loads at varying line angles (Huang et al., 2024; 2025b), and current work is assessing the stability of ring anchors subjected to cyclic loads (Huang et al., 2025a). The satisfactory performance of the ring anchors in centrifuge tests has helped their Technology Readiness Level (TRL) to advance to "field testing in the near future" (i.e., Level 6). Continued developments for testing of offshore wind energy applications in the centrifuge will include expansion of actuator systems to apply different types of loads, assessment of seismic events on anchor and foundation stability using the centrifuges' shake tables, and evaluation of the effect of different installation methods on the response of anchors and foundations.

3 Research example: soil-structure interaction–response of axially loaded piles under post-liquefaction reconsolidation downdrag

Many bridges, critical to transportation infrastructure, are constructed at sites with underlying layers of liquefiable sand. During earthquakes, these sands can liquefy and subsequently reconsolidate, causing significant ground settlement. To prevent excessive bridge settlement and to resist the accompanying downdrag forces on foundation piles, engineers typically extend these piles through the liquefiable layers to reach stronger, deeper soil strata. Determining appropriate pile dimensions presents a challenging optimization problem. Engineers must account for both the bridge's weight and the substantial downdrag forces that develop as settling soil generates downward friction along the pile shaft. This combined loading must be safely transferred to the soil surrounding the pile tip. However, increasing pile diameter to increase load carrying capacity at depth also increases the induced downdrag force by increasing the pile's surface area where the soil liquefies and settles. These increased forces then require longer piles to reach deeper bearing layers, significantly increasing construction costs. This interdependency between pile dimensions and downdrag forces has long been a critical design issue affecting bridge economics.

Research and practice have offered several approaches to analyze pile behavior during and/or after liquefaction (e.g., Boulanger and Brandenberg, 2004; Rollins and Strand, 2007; Fellenius and Siegel, 2008; Hannigan et al., 2016; Muhunthan et al., 2017). The simplest are force-based analyses, which, while straightforward, neglect the displacements of the soil and pile. More sophisticated load-transfer methods (e.g., neutral plane methods) incorporate various factors like skin friction mobilization and modify soil spring properties to account for liquefaction effects, though they fail to capture the problem's dynamic nature. Fully coupled nonlinear dynamic analyses (NDAs) can model the underlying mechanisms but often lack experimental validation. Regardless of the analytical approach chosen, fundamental uncertainties persist regarding three critical aspects: the temporal evolution of excess pore pressure (both generation and dissipation), the reduction and subsequent recovery of shaft friction at the soil-pile interface, and the mechanical response of the pile tip under these conditions. An extensive research program was pursued at the CGM, starting with large-scale dynamic centrifuge model tests and followed by the development and validation of advanced numerical analyses and the development of a design framework that overall advanced the profession's understanding of this problem (Sinha et al., 2023b).

To investigate pile behavior under liquefaction-induced downdrag, Sinha et al. (2021a); Sinha et al. (2021b) performed two comprehensive series of tests using the 9-m centrifuge. The experiments utilized 1/40th-scale models tested at 40 g centrifugal acceleration to accurately simulate full-scale field conditions. The model configurations consisted of heavily instrumented closed-ended aluminum pipe piles, which at prototype scale represented 635-mm-diameter piles. The first test series (Sinha et al., 2021a; 2022a), shown in Figure 6a, examined a simplified soil profile: a liquefiable loose sand layer sandwiched between a low-permeability clay crust above and a dense sand bearing layer below. The second series (Sinha et al., 2021b; Ziotopoulou et al.,

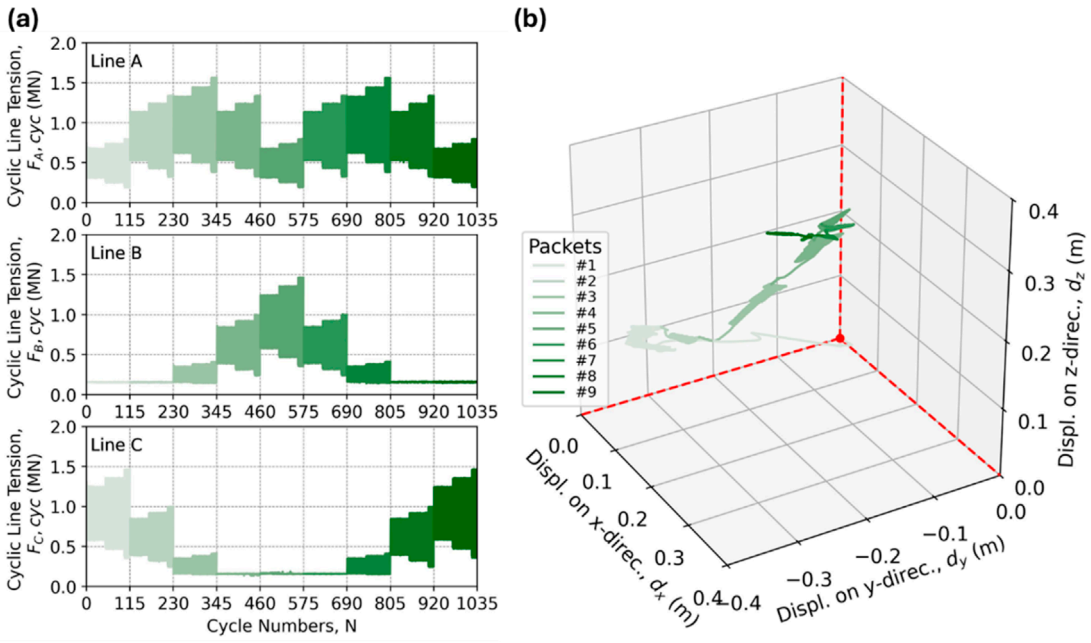

FIGURE 5
Results of a cyclic load test on a shared anchor: **(a)** applied line loads and **(b)** evolution of anchor displacement.

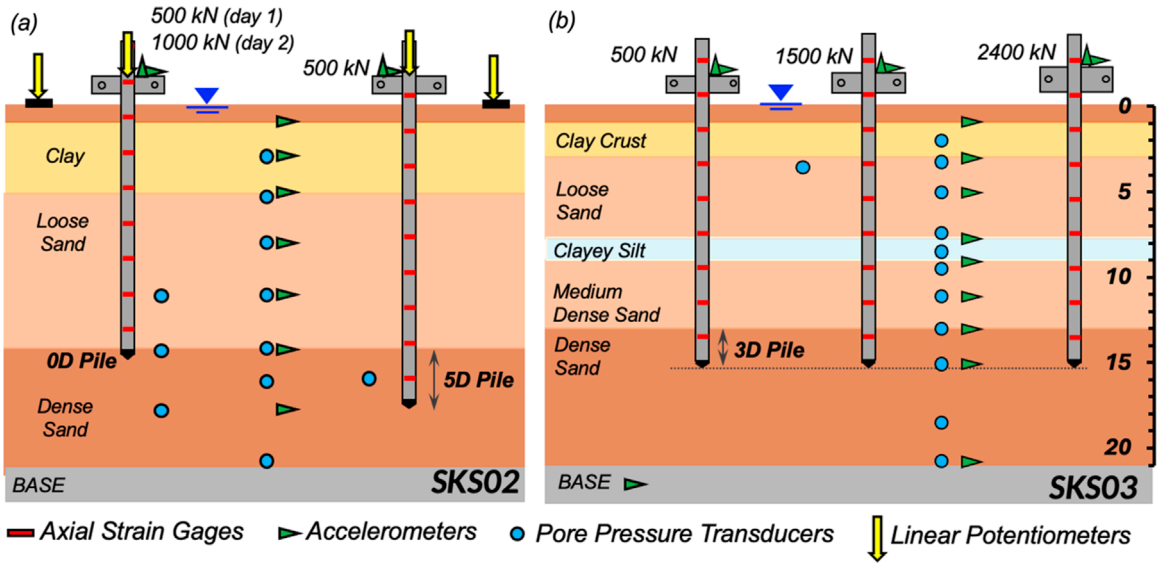

FIGURE 6
Centrifuge model tests **(a)** SKS02 and **(b)** SKS03 including soil layering, instrumentation and instrument locations, and pile properties (embedment depths 0D, 5D, and 3D corresponding to number of pile diameters into the dense sand; and pile head loads defining factors of safety).

2022), shown in Figure 6b, featured more complex soil stratigraphy to better represent typical field conditions. Throughout both series, the loose sand layers were prepared at relative densities between 40% and 45% to simulate highly liquefiable conditions commonly encountered in practice.

The centrifuge model tests were designed to investigate both typical field conditions and extreme scenarios through systematic variation of key parameters. A primary focus was the pile embedment depth into the dense sand layer, which allowed the research team to quantify how end-bearing conditions influenced downdrag load magnitudes and settlement behavior. The piles were also subjected to different levels of static axial load, applied as a lumped mass at the pile head, to assess the role of factor of safety on the pile response. The static factors of safety, defined as the ratio of the ultimate pile capacity to the applied load, spanned from 1.6 to 12.0, the range commonly used in practice. To simulate

seismic conditions, the models were subjected to a sequence of scaled earthquake motions which covered a range of intensities, with peak base accelerations varying from 0.02 g to 0.6 g. The sequential application of multiple shaking events allowed the investigation of how prior seismic history influenced the development of downdrag forces, addressing an important aspect often overlooked in design practice. Between shaking events, sufficient time was allowed for complete soil reconsolidation, confirmed through excess pore pressure measurements from the installed instrumentation.

The centrifuge tests employed state-of-the-art instrumentation to capture high-resolution data on the complex coupled response of the soil-pile system (Sinha et al., 2021c, 2023a, Figure 7). Strain gauge bridges installed at multiple elevations inside the piles provided continuous measurements of axial load distribution. To monitor liquefaction behavior, vertical arrays of pore pressure transducers were densely positioned throughout the soil profile, tracking the generation, dissipation, and redistribution of excess pore pressures during and after seismic events. An innovative aspect of the experimental setup was the implementation of non-contact measurement systems for settlement monitoring. This approach employed laser lines projected onto the model surface and high-contrast markers, with high-speed cameras capturing their movements. Specialized software processed these visual data to yield settlement measurements with sub-millimeter precision. This contactless technique represented a significant advancement over traditional methods, as it allowed highly accurate displacement measurements without introducing sensors that could interfere with the model's dynamic response.

The results illuminated the mechanics of liquefaction-induced downdrag on piles and allowed important conclusions to be drawn regarding how the various processes interact (Sinha et al., 2022a; 2024). Even modest soil settlements, around 1%–2% of the pile diameter, proved sufficient to generate substantial negative skin friction, with significant downdrag loads developing at excess pore pressure ratios well below full liquefaction (i.e., excess pore pressure ratio of 100%) (Figure 8). During seismic events, the generation of excess pore pressures temporarily alleviates these downdrag forces, but the subsequent reconsolidation phase often sees them return to or exceed their pre-shaking magnitudes. Most of the pile settlement occurs during the shaking phase, when the combined loss of shaft and tip capacity leads to significant displacements. The data also demonstrated that pile embedment depth plays a key role in controlling these settlements: piles extending well into the dense sand layer experienced minimal settlement, provided that the tip is not compromised by the generation of excess pore pressures. The latter was observed due to the redistribution of pore pressures from the loose layers (Sinha et al., 2024). Beyond individual pile behavior, the study emphasized the importance of differential settlement between the pile and surrounding soil, particularly for bridge structures where such differences can compromise functionality. These observations culminate in two essential design considerations: the pile's response to inertial loading during shaking with reduced resistance, and the evolution of downdrag loads during post-liquefaction reconsolidation. Additionally, the results suggest that separate serviceability criteria should be established for total and differential settlements to ensure structural functionality.

The experimental data from the centrifuge tests paved the way for the development and validation of an improved load-transfer (neutral plane) numerical modeling procedure for analyzing piles subject to liquefaction-induced downdrag. This was achieved by accounting for changes in the stiffness and capacity of the pile's shaft friction and tip resistance in liquefiable soils. Sinha et al. (2022b) developed a TzQzLiq analysis method, built upon the OpenSees finite element platform (McKenna et al., 2010), which incorporates interface elements to capture the dependence of pile shaft and tip load transfer on the excess pore pressure ratio in the surrounding soil. The TzLiq and QzLiq interface elements utilize extended versions of conventional t-z and Q-z curves that degrade the pile resistances according to a power law function of excess pore pressure ratio. When validated against centrifuge test results, the TzQzLiq analysis accurately reproduced the recorded time histories of axial load distribution and pile head settlement during both shaking and post-shaking reconsolidation phases. Building upon these insights, Sinha et al. (2023b) developed a displacement-based design procedure for piles in liquefiable soils that, unlike the force-based framework in AASHTO (2020), rationally integrates the key mechanisms governing the combined seismic and liquefaction response of piles. The method uses TzQzLiq analysis to generate pile head settlement *versus* length design curves for given earthquake motions by systematically varying pile length while keeping other parameters constant. This allows designers to select pile lengths that satisfy project-specific settlement criteria, potentially realizing economic savings compared to traditional approaches that treat liquefaction as an equivalent consolidation problem without considering shaking-induced settlements and excess pore pressure effects on pile resistances.

Enabled by the well-instrumented test series at the CGM, this body of work marked a significant step forward in the profession's ability to rationally evaluate and design pile foundations to withstand liquefaction-induced downdrag. The high-quality experimental data from the centrifuge tests, obtained using advanced and newly developed instrumentation techniques, provided an unprecedented characterization of the complex soil-pile-interaction mechanisms at play. In addition, the contributions to the development of contactless displacement tracking methods and data processing are poised to enable future work on remaining questions (e.g., pile groups and pile caps, effect of lateral confinement).

4 Research example: large deformation flow problems—runout behavior of waste materials

Mining operations for extracting ore and coal burning for generating electricity produce particulate waste materials that can be harmful to human health and the environment. These materials must be contained in engineered storage facilities that are stable during construction and closure as well as during natural events such as intense rainfall and earthquakes. Large quantities of these waste materials are produced worldwide; the dams containing these materials can reach heights of over 250 m (e.g., Las Tortolas in Chile, Dyncrude in Canada, Pena Negra in Peru). Failures of storage facilities in many countries in the last

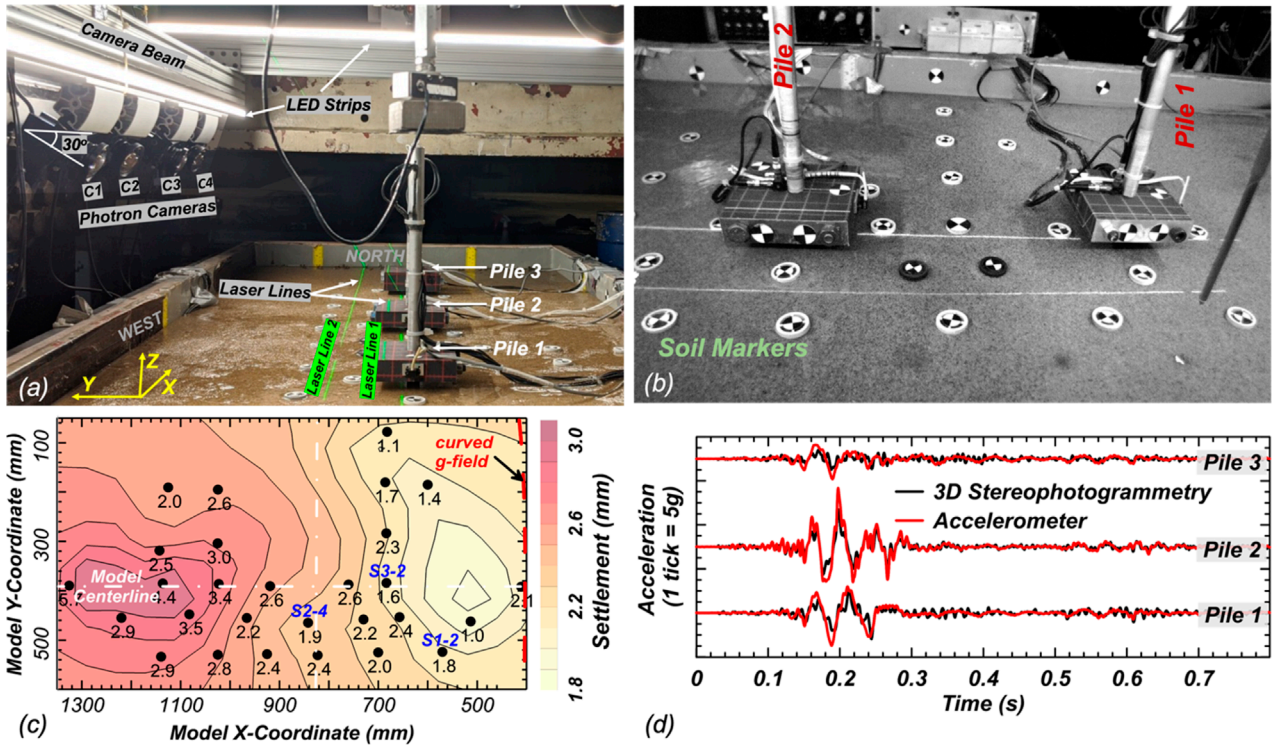

FIGURE 7
Contactless displacement tracking with high-speed cameras, laser lines, and markers in the centrifuge: **(a)** view of centrifuge model test SKS03, **(b)** north section of the model with placed target markers as viewed from camera C2, **(c)** contours of surface settlement after strong shaking event obtained from settlements measured at soil target markers (shown as dots), and **(d)** comparison of acceleration in piles obtained from 3D stereophotogrammetry with measurements from accelerometers for shaking event in SKS03.

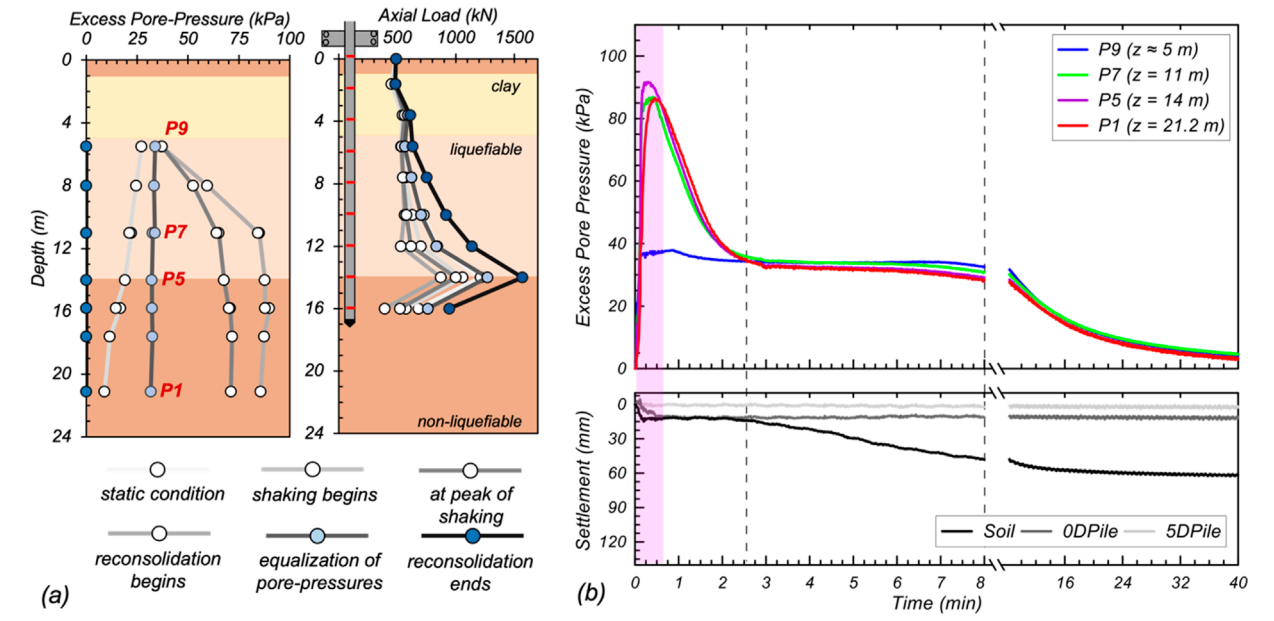

FIGURE 8
Indicative results from centrifuge model test SKS02: **(a)** distributions of excess pore pressures and axial loads along 5D pile at different time instants during and after shaking, and **(b)** time histories of excess pore pressures at pore pressure transducers and settlements of soil and piles.

30 years have resulted in significant life and economic loss and environmental degradation effects (Santamarina et al., 2019). Failure of a containment structure can trigger flow of the waste material downstream for several kilometers, as was the case in Brumadinho (Brazil), Merriespruit (South Africa), Kingston (United States), and Mount Polley (Canada).

The complex behavior of these waste materials combined with changing or unknown geologic and hydraulic conditions complicates the full understanding of the processes leading to initial failure and subsequent runout. Centrifuge testing has emerged as a useful tool for isolating the mechanisms that lead to triggering of failures, such as a rising water table (e.g., Ng et al., 2023) and generation of excess pore pressures in contractive materials (i.e., static liquefaction) (Madabhushi et al., 2023). Such research can isolate processes that govern failure and flow of material to inform the development of constitutive models for material behavior at both small and large deformations. In addition, these centrifuge experiments can be used to calibrate and validate numerical models to subsequently investigate a broader set of conditions numerically (as shown in Figure 2).

Equipment to model large deformation processes in geomaterials was designed, built, and commissioned at the UC Davis CGM between 2018 and 2020. The new equipment enables modeling the runout behavior of waste materials as confinement is rapidly lost at applied accelerations of up to 60 g. The equipment consists of a container in which the waste material is placed, two doors that can be rapidly opened to release the material using a pair of hydraulic actuators, and an interchangeable runout basin. Figure 9a shows a schematic of the main components of the equipment, while Figure 9b details mechanisms that keep the doors closed during centrifuge spin up and then rapidly open the doors to release the material. The material response is monitored using pore pressure transducers and electrical permittivity sensors mounted on the inner side walls of the container, while the evolution of the runout process is measured using high-speed and depth-sensing cameras. This system also allows mounting sensors in the runout basin to elucidate processes such as pore pressure generation and material entrainment or deposition. Additionally, cone penetration tests (CPTs) can be performed in flight to characterize the initial properties of the waste material before the doors are opened. Detailed information of this equipment and sample results are provided in Madabhushi et al. (2022).

Given the significant challenges in obtaining data from a containment facility failure in the field and the uncertainty in the initial geological and hydraulic settings and material properties, centrifuge testing can offer unique datasets to better understand material behavior at high deformations and to guide the continued development of numerical tools to predict systems level behavior. A series of experiments were performed at 60 g to investigate how the susceptibility to flow failure and severity of runout deformations depend on the initial density of waste material, the location of the water table within the material deposit, and the type of waste material (Madabhushi et al., 2023). The results showed that initially loose, saturated deposits, characterized by high void ratios and low CPT penetration resistances, are prone to static liquefaction, leading to rapid failures and large runout distances upon loss of confinement. Figure 10 shows a series of high-speed video frames showing the rapid failure characterized by intense material deformation over a period of about one second. In contrast, denser materials failed in a slope instability mode and exhibited runout distances approximately equal to their initial height. Figure 11 shows data from the depth-sensing cameras on the test on the denser deposit, clearly showing the evolution of the runout process over tens of minutes. These results are being used to help better define the conditions that can lead to failures with large runout distances and to develop procedures for field evaluations based on CPT data.

These waste runout events share characteristics with other processes, such as long runout landslides and debris flows due to precipitation or wildfires (e.g., Kean et al., 2019). The capabilities built at the UC Davis CGM expand on those developed in previous investigations (e.g., Bowman et al., 2010) by enabling modeling a wider range of initial conditions of the material, including the height of the deposit, location of the water table, and density of the material. Future investigations can expand on this work to explore the material response while it runs across the basin by including pore pressure transducers and net pressure sensors. Additionally, the equipment can be modified in the future to consider different initial failure conditions, such as an embankment with a rising water table or a sudden increase in pore pressure within the soil.

5 Research example: upscaling of MICP technology

Biogeotechnics, especially biomediated and bioinspired geotechnical engineering, focuses on improving geotechnical systems through natural pathways. This emerging domain has advanced significantly over the past two decades, establishing itself as one of the most rapidly evolving fields within geotechnics. As the field advances, there is an increasing demand to investigate new engineering techniques at various scales to evaluate their practicality and effectiveness for real-world applications. For example, microbially induced calcium carbonate precipitation (MICP) is a promising novel technology that improves the behavior of sands by enhancing particle-particle contacts, creating surface coatings on particles, and modifying particle angularity (DeJong et al., 2022). Biomediation with MICP depends on calcium carbonate precipitation to create a cemented soil that enhances resistance to liquefaction. While particle- and lab-scale studies have shown significant improvements in reducing liquefaction triggering and its consequences, the transition to practical field applications requires a deeper understanding of system-level response. To address this gap, the synergistic use of the 1-m and 9-m centrifuges at the UC Davis CGM has provided unique opportunities to investigate MICP technology at progressively larger scales, addressing critical challenges in upscaling and implementation. The centrifuges have enabled researchers to examine key factors such as treatment formulation, dynamic response, soil stratigraphy, and soil-structure interaction under realistic stress conditions, providing essential guidance for future field application of these technologies. Six complementary centrifuge studies investigating MICP biomediation described herein highlight the collective contribution of centrifuge technologies toward addressing challenges in

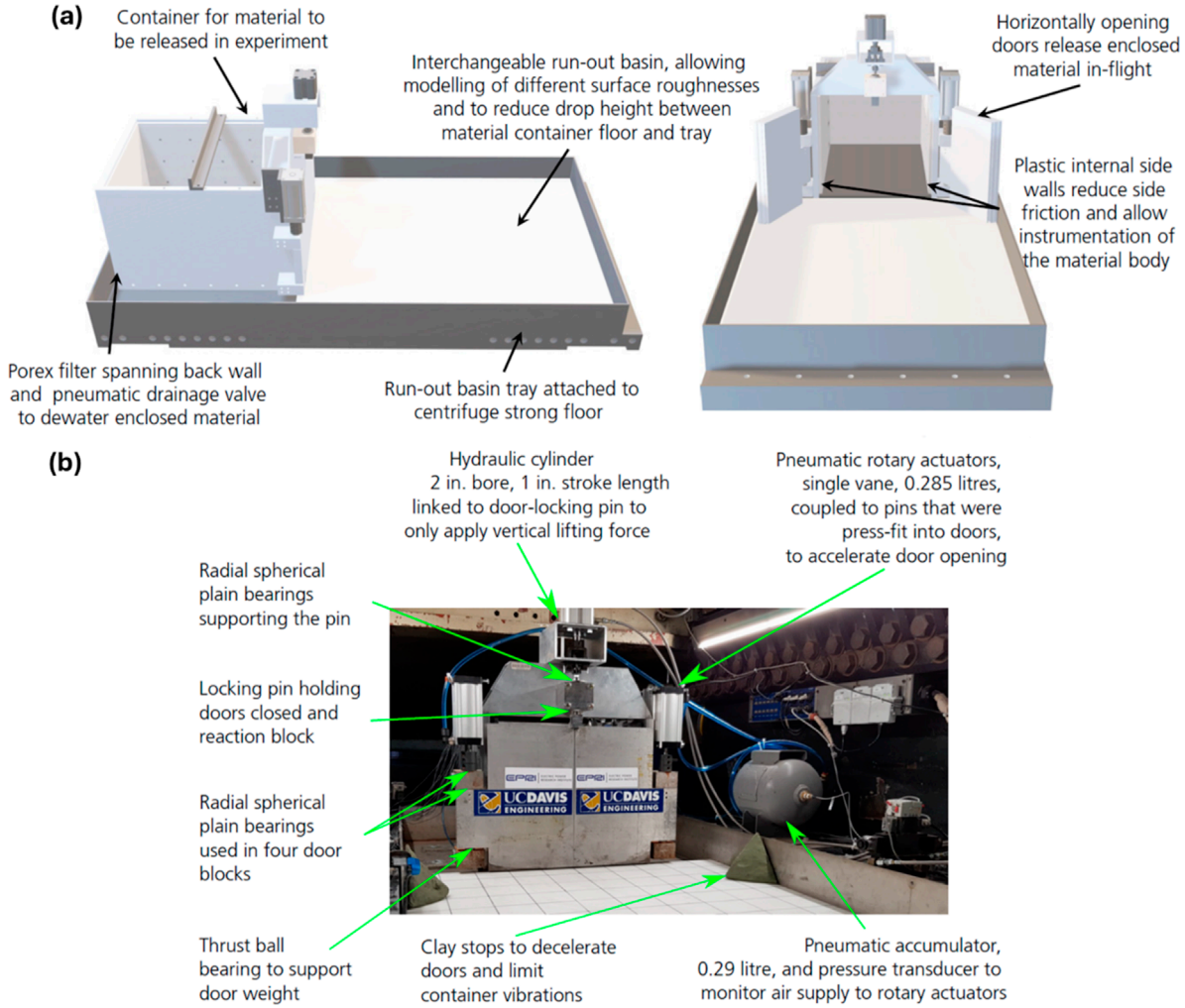

FIGURE 9
(a) Schematic and **(b)** photograph of the container for modeling runout of waste materials for the 9-m centrifuge at the UC Davis CGM.

practical design and implementation of this emerging technology (Figure 12).

The investigation into the use of MICP treatment to mitigate liquefaction triggering and subsequent consequences started with 1-m centrifuge tests. Studies by Montoya et al. (2013) and Darby et al. (2019) used the 1-m centrifuge to systematically investigate the fundamental mechanisms and behavior of MICP treated soils under controlled loading conditions. Simple, small-scale models allowed for efficient testing, making it suitable for exploring fundamental principles, improving model construction protocols, and establishing reliable in-flight characterization methods, such as cone penetration testing and shear wave velocity measurements. These studies marked the first-ever measurements of critical mechanisms, demonstrating that the MICP treatment significantly reduced pore water pressure generation and enhanced cyclic resistance under dynamic loading. Additionally, the degradation of MICP treated soil was analyzed using bender elements, providing valuable insights into how cyclic loading impacts MICP bonding and the effectiveness of MICP treatment after degradation. These initial studies were necessary for building scientific knowledge and guiding the development of larger-scale experiments and practical applications.

Building on insights from the 1-m centrifuge tests, Zamani et al. (2021) upscaled to the 9-m centrifuge to explore more complex geotechnical scenarios including stratified soil profiles and finite treatment zones. The 1-m tests, while effective in understanding fundamental behaviors, had limitations due to the small size of the model container and limited resources available onboard the centrifuge. These limitations included treating the entire container with MICP—a condition not representative of future real-world field applications—and limitations in measurement capabilities, particularly in capturing higher shear strains. The 9-m centrifuge, having enhanced capabilities and a larger physical model size, enabled examining the effect of MICP on finite liquefiable pockets in a stratified soil profile and assessing the performance of simple foundation structures on soils with varying relative densities and MICP treatment.

FIGURE 10
Sequence of failure of a saturated, loose deposit of coal ash tested at 60 g. The images were taken during a time period of about 1 s.

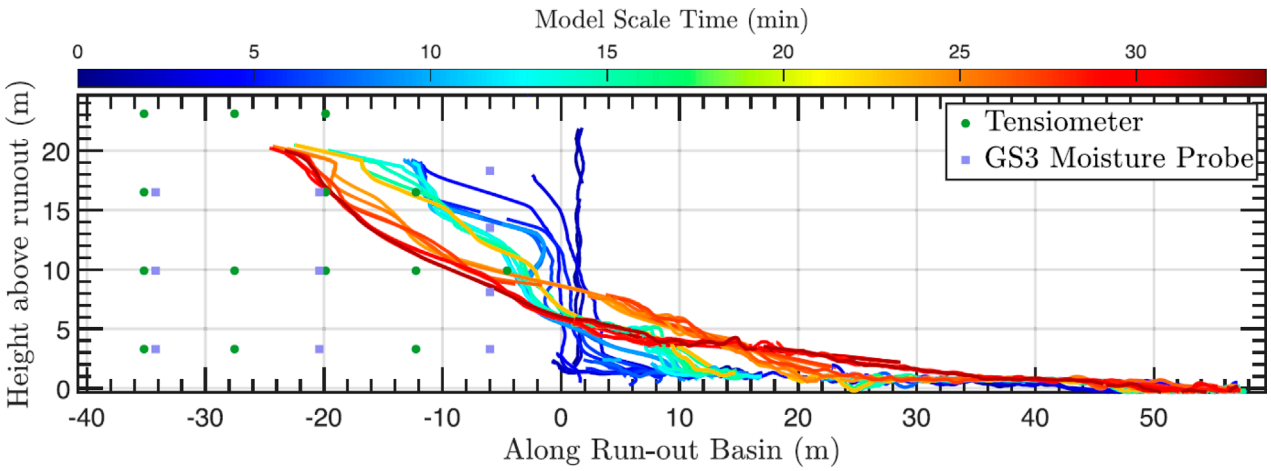

FIGURE 11
Evolution of runout of a deposit of saturated, dense coal ash at 60 g.

Two MICP treated blocks representing finite treatment zones at different depths were implemented to evaluate impact on soil and foundation performance. A new model preparation method was introduced to enable this advanced testing that involved placing precast MICP treated blocks into the centrifuge model (Ham et al., 2024b). The MICP blocks were created in PVC molds and carefully lifted, inverted, and positioned onto the soil model at the target depth using a vacuum lifting system (Figure 13a) before being buried. Instrumentation, including accelerometers, pore pressure transducers, bender elements, and displacement sensors, monitored the responses of the soil and foundations during and after dynamic loading. These experiments provided essential insights into the system-level performance of MICP treatments, revealing their potential to enhance foundation performance by reducing settlement and rotation significantly. A notable advantage of the large-scale test was the ability to facilitate direct comparisons across different treatment strategies within a single experimental setup, ensuring consistency in soil preparation and applied shaking conditions.

While the 9-m centrifuge test provided valuable insights into a complex geotechnical scenario, the complexity of combining varying soil stratigraphy, finite MICP treated zones, and soil structure interaction in one system highlighted a need for additional focused experiments to isolate specific mechanisms. San Pablo et al. (2024) returned to using 1-m centrifuge tests to focus on the fundamental influence of discrete MICP treatment depth in loose soils on liquefaction resistance, especially surface settlement, ground surface acceleration, and MICP degradation. Single discrete MICP treated blocks were created to represent realistic localized treatment zones for each of several soil models. The preparation methodology for the 1-m centrifuge models was similar to that of the 9-m test outlined above (Ham et al., 2024b). The simplified tests explored varying the depth of MICP treatment within a liquefiable soil profile, ranging from untreated to fully and partially treated layers (Figure 13b). The results revealed a base isolation effect from the untreated loose sand below the MICP treated blocks which mitigated accelerations transmitted to the model surface. The isolation tended to balance settlement reduction and reduced dynamic load effects compared to the untreated base case. Fully treated soil layers where MICP treatment extended the full depth of the soil achieved the most significant decrease in settlement but

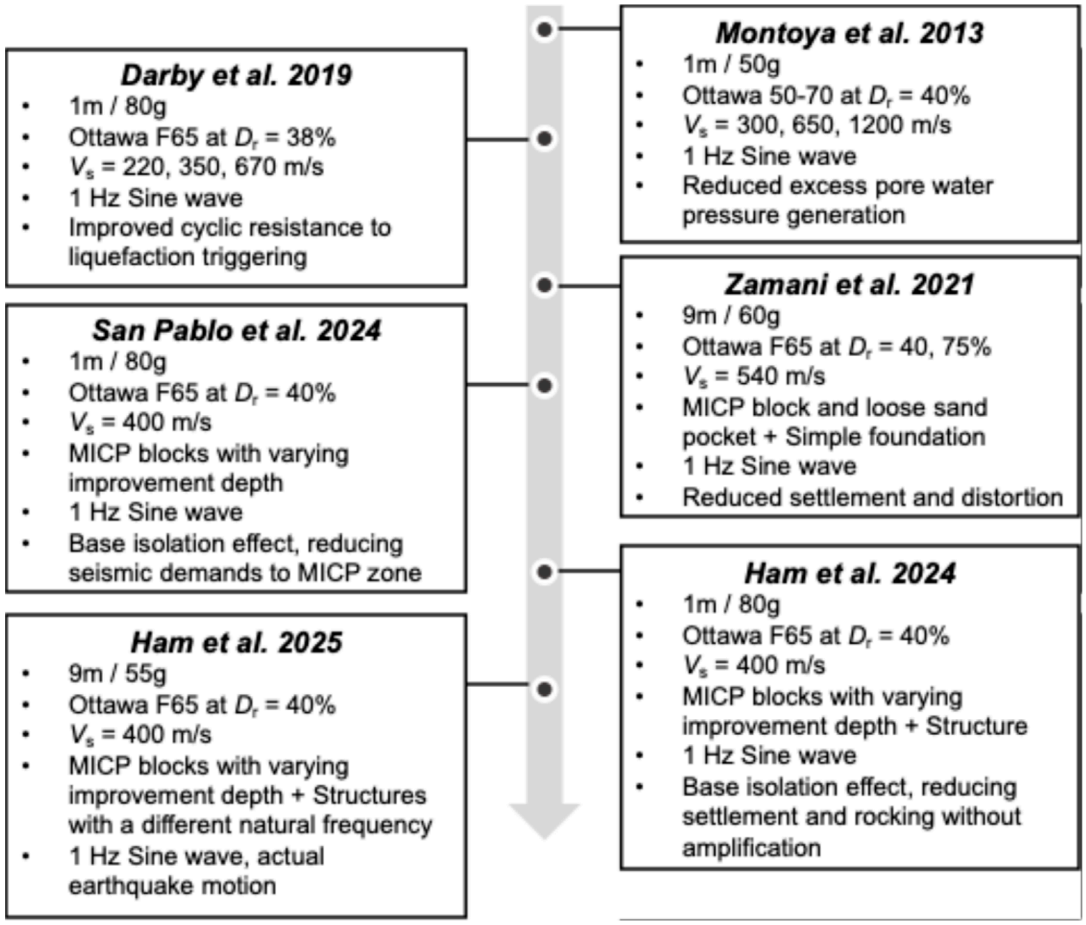

FIGURE 12
Synergistic use of 1-m and 9-m centrifuges to advance MICP ground improvement technology towards the field scale.

transferred higher accelerations to the surface due to increased stiffness. Partially treated layers demonstrated a compromise, with reduced surface accelerations at the cost of slightly increased settlement.

Most recently, researchers have been extending the work of San Pablo et al. (2024) by adding aspects of soil-structure interaction with discrete MICP treated zones using both the 1-m and 9-m centrifuges. Simple tests using single structures on the 1-m centrifuge focused on understanding the balance between increased structural demands from shaking energy transferred through the MICP treated zone with reduced settlement and tilting due to soil stabilization. Ham et al. (2024a) introduced a high-speed camera system on the 1-m centrifuge to monitor structural behavior and soil settlement, addressing the challenge of wire interference in small-scale tests, especially at higher g-levels. A checkerboard-marked structure and soil markers were placed to enable precise tracking of movements using high-speed cameras, as shown in Figure 14a. The results demonstrated that partial improvement of a liquefiable layer with MICP treatment can effectively minimize structural settlement and rocking without amplifying accelerations with the base isolation effect. However, the limitations of using a single structure and input motion highlighted the need for further research to generalize these findings. A subsequent 9-m centrifuge test was performed to explore soil-structure interaction under more realistic conditions. This test included structures with varying natural frequencies to represent a broader range of dynamic behavior. Like the 1-m test, high-speed cameras and 3D photogrammetry were used to monitor structural responses (Figure 14b) (Sinha et al., 2021d). The larger scale of the 9-m centrifuge allowed for a more comprehensive investigation, highlighting the trade-offs between minimizing structural settlement and reducing dynamic accelerations through MICP treatment (Ham et al., 2025).

The synergistic use of the 1-m and 9-m centrifuges supported the progression of biogeotechnical engineering from relatively simple tests to increasingly complex larger-scale system investigations. The 1-m centrifuge facilitated efficient parametric studies and the isolation of critical mechanisms, while the 9-m centrifuge enabled realistic modeling of complex geotechnical scenarios, including varying soil stratigraphy, discrete MICP treated zones, and diverse structural configurations. These studies collectively demonstrate the potential of MICP in balancing structural stability with dynamic response, paving the way for the practical application of this innovative technology in real-world scenarios. Centrifuge testing will continue to bridge the gap between laboratory studies and practical design, advancing MICP treatment to transform

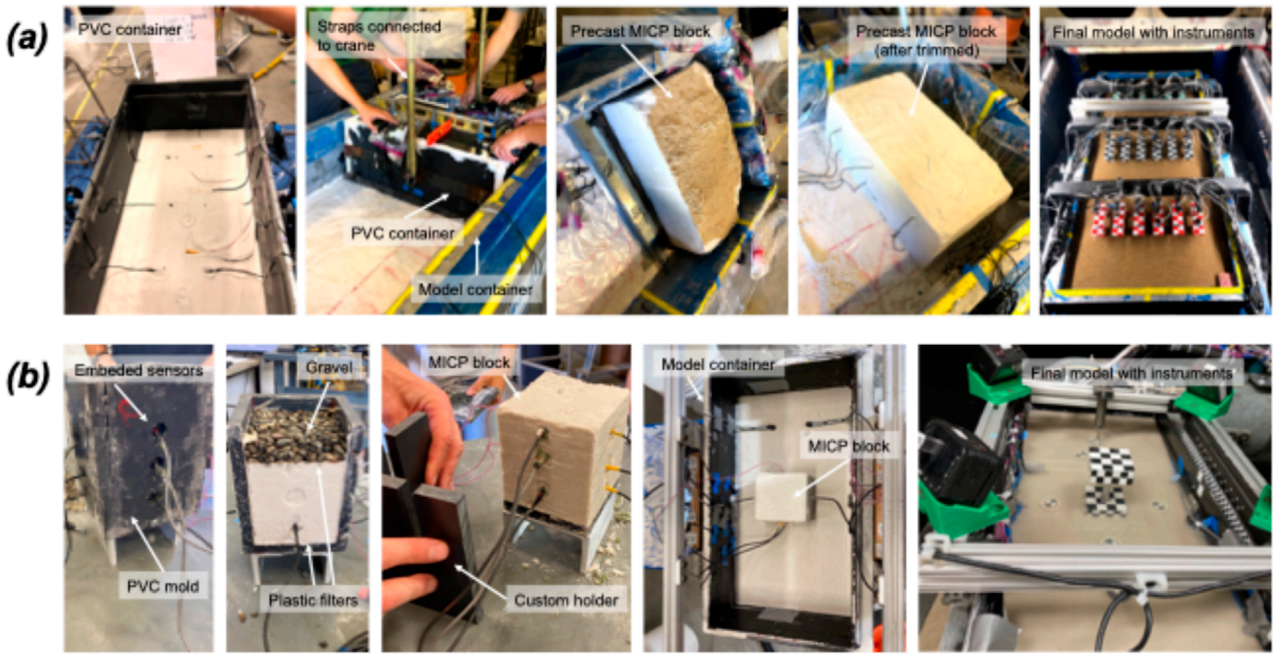

FIGURE 13
Model preparation process with discrete MICP-treated blocks: **(a)** 9-m centrifuge model and **(b)** 1-m centrifuge model.

ground improvement practices and support resilient geotechnical solutions.

6 Future directions and research opportunities

Over the past few decades, hypergravity modeling has transformed the field of geotechnical engineering by enabling researchers to examine system-level performance and the respective underlying mechanisms within a controlled laboratory environment where test conditions can be specified and controlled while remaining realistic. Centrifuge modeling has advanced from a niche research tool to one of the preferred approaches for prototyping new technologies at the system scale, advancing engineering analysis and design methods, and validating advanced computational models (e.g., Travasarou, 2024). This transformation has been enabled by rigorous implementation of research fundamentals and principles (e.g., Schofield, 1981; Kutter, 1995; Garnier et al., 2007), collaboration and sharing of best practices between centrifuge facilities (e.g., the International Journal and the International Conference series of Physical Modelling in Geotechnics, IJPMG and ICPMG), researcher and staff exchanges, coordinated research efforts (e.g., Verification of Liquefaction Analysis by Centrifuge Studies, Arulanandan and Scott, 1993; Liquefaction Experiments and Analysis Project; Manzari et al., 2018), and collective brainstorming and envisioning of the future of hypergravity modeling (e.g., Kutter et al., 2021). The combined experience and knowledge base, combined with the innate attributes of hypergravity scaled physical modeling, position this research approach to extend efficiently and effectively into new science and engineering research topics where existing approaches are deficient.

The role of hypergravity modeling in geotechnical engineering is likely to continue to increase given that the understanding and performance prediction of numerous challenging soils remain (e.g., silts, tailings, volcanics, glauconite, carbonates), geotechnical infrastructure is becoming increasingly larger, more complex, and multi-functional (e.g., Mitchell and Kopmann, 2013), and the impacts of anthropogenic-induced loading conditions are just starting to be considered (Bridges, 2024). This is in addition to numerous seismic-related issues that have yet to be sufficiently resolved (e.g., basin effects), the remaining opportunities in the young field of biogeotechnics, and that capabilities for addressing other issues with hypergravity modeling have yet to be developed (e.g., creation of models with fine depositional variability). Consensus of some of major remaining and upcoming challenges have been detailed in three editions of the NHERI Science Plan (Boulanger et al., 2017; Edge et al., 2020; Robertson et al., 2023), which highlights challenges related to earthquakes, windstorms, and associated hazards, and the NHERI Decadal Vision Plan (Schneider and Kosters, 2024), which highlights impacts of climate change on natural hazards research and use-inspired and translational research. Collectively, the breadth and complexity of challenges that remain in geotechnical engineering is both significant and well-suited to be addressed by hypergravity modeling.

New applications at the CGM are rapidly being developed to enable critical climate related research, where problems like thawing

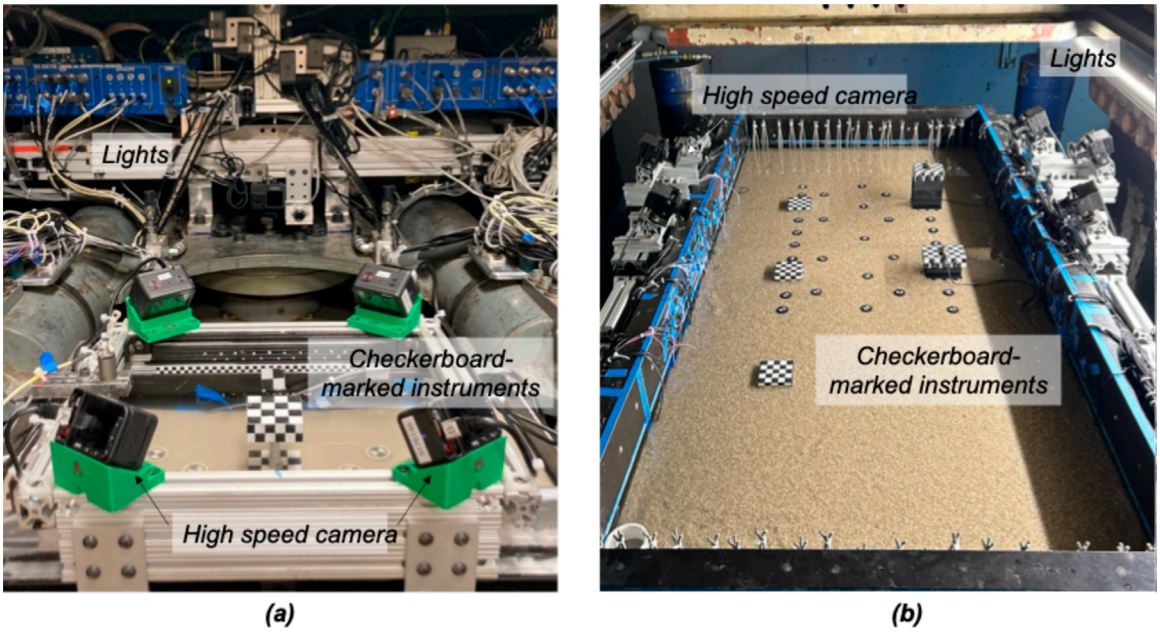

FIGURE 14
Experimental setup with high-speed cameras, structure markers, and soil markers: **(a)** component level model for testing on the 1-m radius centrifuge, and **(b)** system level model for testing on the 9-m radius centrifuge.

permafrost have major impacts on civil infrastructure and a lack of fundamental knowledge affects the ability to predict and thus respond to changes in the Artic and Antarctic. The CGM is seeing considerable investment developing new environmental control capabilities to study these processes. For example, Gardner et al. (2024) is piloting modeling the effects of permafrost thawing and its effect on foundation performance, and the National Science Foundation has made recent NSF awards to Khosravi (CMMI 2400391) and Khosravi (CMMI 2228271) to support the development of a new container for the 9-m centrifuge and supporting infrastructure (e.g., onboard chillers) to actively control cryosphere conditions.

In addition, significant growth opportunities exist more broadly outside the general domain of geotechnical engineering. The role of hypergravity modeling across engineering and science was explored through a recent international workshop. Kutter et al. (2021) assembled a diverse group of scientists and engineers to identify significant opportunities for collaboration between centrifuge experts and researchers in fields where hypergravity techniques are not yet generally accepted or used. Gravity affects many physical quantities including weight, buoyancy, convection, pressure, stress, pressure gradients, and potential energy. These in turn affect secondary quantities such as flow rate, frictional resistance, stability, advection, and consolidation. These secondary quantities play roles in many processes such as the large-scale behavior and stability of granular materials, tectonic structures, combustion and fire, thermal oceanic circulation, and nuclear waste disposal. The ability to adjust gravity can also be a valuable tool by which experiments illuminate microscale phenomena such as crystallization, the stability of liquid bridges between particles, and interactions between gravity forces and interparticle cohesive forces. Opportunities for new hypergravity research thus span a wide range of engineering and scientific disciplines, including many subdisciplines of civil and mechanical engineering, materials science, geosciences, glaciology, artic sciences, oceanography, combustion sciences, and plant physiology.

7 Concluding remarks

The Natural Hazards Engineering Research Infrastructure (NHERI) facility at the University of California at Davis is equipped with 9-m and 1-m radius geotechnical centrifuges that provide unique, world-class facilities for scaled modeling of systems and hypergravity environments. This national, open access research facility allows the scientific and engineering communities to realize major advances in the ability to understand, predict, and improve the performance of civil infrastructure and natural systems. Four research projects were used to illustrate the facility's capabilities and the complementary roles of the 9-m and 1-m centrifuges. The examples included renewable energy systems, pile performance in liquefiable soils, large deformation flow problems, and advancement of biogeotechnical technologies, reflecting the increasing diversity of topics being researched using the CGM facility. A broader discussion of the envisioned future research directions and opportunities using hypergravity modeling was then presented, concluding that there remain significant opportunities within geotechnical engineering, particularly related to natural and anthropogenic-induced loadings, and that the opportunities more broadly in engineering and science are just beginning to be realized and explored.

Data availability statement

The original contributions presented in the study are included in the article/supplementary material, further inquiries can be directed to the corresponding author.

Author contributions

JD: Writing – original draft, Writing – review and editing. DW: Writing – original draft, Writing – review and editing. AM: Writing – original draft, Writing – review and editing. KZ: Writing – original draft, Writing – review and editing. S-MH: Writing – original draft, Writing – review and editing. RB: Writing – review and editing.

Funding

The author(s) declare that financial support was received for the research and/or publication of this article. The National Science Foundation (NSF) has supported the development and operation of the geotechnical centrifuge facilities at UC Davis through the Network for Earthquake Engineering Simulation (NEES) program, award numbers CMS-0086566, CMMI-0402490, and CMMI-0927178, and the Natural Hazards Engineering Research Infrastructure (NHERI) program, award number CMMI 1520581 and 2037883. Additional support for facility development has been provided by Obayashi Corporation, Caltrans, and the University of California at Davis. The four research examples presented herein were supported by the US National Science Foundation (CMMI-1936939 and EEC-1449501), Caltrans (Agreement 65A0688), and the Electric Power Research Institute. Any opinions, findings and conclusions or recommendations expressed in this material are those of the author(s) and do not necessarily reflect those of the above organizations.

Acknowledgments

Contributions to facility developments were provided by past CGM Directors Bruce Kutter, Jim Cheney, and I. M. Idriss as well as all former and current CGM staff and graduate students.

Conflict of interest

The authors declare that the contents of this paper were prepared in the absence of any commercial or financial relationships that could be construed as a potential conflict of interest.

Generative AI statement

The author(s) declare that no Generative AI was used in the creation of this manuscript.

Publisher's note

All claims expressed in this article are solely those of the authors and do not necessarily represent those of their affiliated organizations, or those of the publisher, the editors and the reviewers. Any product that may be evaluated in this article, or claim that may be made by its manufacturer, is not guaranteed or endorsed by the publisher.

References

AASHTO (2020). *AASHTO LRFD bridge design specifications. LRFDUS-9*. Washington, DC: AASHTO.

Arulanandan, K., and Scott, R. F. (1993). Project VELACS—control test results. *ASCE J. Geotechnical Eng.* 119 (8), 1276–1292. doi:10.1061/(ASCE)0733-9410(1993)119:8(1276)

Aubeny, C. (2017). *Geomechanics of marine anchors*. 1st ed. Boca Raton, FL: CRC Press. doi:10.4324/9781351237376

Boulanger, R. W., and Brandenberg, S. J. (2004). "Neutral plane solution for liquefaction-induced down-drag on vertical piles," in *Geotechnical engineering for transportation projects* (Reston, VA: ASCE), 470–478. doi:10.1061/40744(154)32

Boulanger, R. W., Bray, J. D., Deierlein, G. G., Irish, J. L., Lizundia, B., Masters, F. J., et al. (2017). *Natural hazards engineering research infrastructure, 5-year science plan, multi-hazard research to make a more resilient world*. First Edition. DesignSafe-CI. Available online at: https://www.designsafe-ci.org/media/filer_public/20/6f/206f5d4a-5f7d-4ab6-b837-7c5f89c7b251/varwwwdesignsafe-ciorgmediacms_page_media595nheri_science_plan_july_2017.pdf.

Boulanger, R. W., Wilson, D. W., Kutter, B. L., DeJong, J. T., and Bronner, C. E. (2020). NHERI centrifuge facility: large-scale centrifuge modeling in geotechnical research. *Front. Built Environ.* 6. doi:10.3389/fbuil.2020.00121

Bowman, E. T., Laue, J., Imre, B., and Springman, S. M. (2010). Experimental modelling of debris flow behaviour using a geotechnical centrifuge. *Can. Geotechnical J.* 47 (7), 742–762. doi:10.1139/T09-141

Bradshaw, A. S., Giammp, J. R., Gerkus, H., Jalilvand, S., Fanning, J., Nanda, S., et al. (2016). Scaling considerations for 1-g model horizontal plate anchor tests in sand. *ASTM Geotechnical Test. J.* 39 (6), 20160042. doi:10.1520/gtj20160042

Bray, J. D., Frost, J. D., Rathje, E. M., and Garcia, F. E. (2019). Recent advances in geotechnical post-earthquake reconnaissance. *Front. Built Environ.* 5, 5–2019. doi:10.3389/fbuil.2019.00005

Bridges, C. A. (2024). "Climate change inpacts on geotechnical infrastructure," in XVIII European conference on soil mechanics and geotechnical engineering, Lisbon, Portugal, 2838–2841. doi:10.1201/9781003431749-553

Carey, T. J., Chiaradonna, A., Love, N. C., Wilson, D. W., Ziotopoulou, K., Martinez, A., et al. (2022). Effect of soil gradation on embankment response during liquefaction: a centrifuge testing program. *Soil Dyn. Earthq. Eng.* 157, 107221. doi:10.1016/j.soildyn.2022.107221

Carey, T. J., Gavras, A. G., Kutter, B. L., Haigh, S. K., Madabhushi, S. P. G., Okamura, M., et al. (2018). *A new shared miniature cone penetrometer for centrifuge testing*. London, United Kingdom. 293, 298. doi:10.1201/9780429438660-38

Chen, J., and Martinez, A. (2025). A centrifuge modelling setup for dewatering, rewetting, and characterising soil deposits. *Inter. J. Phys. Modell. Geotech.* 25, 86, 101. doi:10.1680/jphmg.24.00027

Coughlan, K. (2024). *Mooring systems for floating offshore wind: mooring design, biocolonisation, and shared anchors*. Amherst, MA: University of Massachusetts. PhD thesis.

Darby, K. M., Hernandez, G. L., DeJong, J. T., Boulanger, R. W., Gomez, M. G., and Wilson, D. W. (2019). Centrifuge model testing of liquefaction mitigation via microbially induced calcite precipitation. *ASCE J. Geotechnical Geoenvironmental Eng.* 145 (10), 04019084. doi:10.1061/(ASCE)GT.1943-5606.0002122

Davis, M. (2023). Loads analysis of fixed-bottom and floating offshore wind structures. MS thesis. Amherst (MA): University of Massachusetts.

DeJong, J. T., Gomez, M. G., San Pablo, A. C. M., Graddy, C. M. R., Nelson, D. C., Lee, M., et al. (2022). "State of the Art: MICP soil improvement and its application to liquefaction hazard mitigation," in Proc. of the 20th ICSMGE-state of the art and invited lectures. Sydney, Australia.

DNV (2023). *Floating wind: turning ambition into action. Tech. report*. Oslo, Norway: DNV.

Edge, B., Ramirez, J., Peek, L., Bobet, A., Holmes, W., Robertson, I., et al. (2020). *Natural hazards engineering research infrastructure, 5-year science plan, multi-hazard research to make a more resilient world, Second Edition*. DesignSafe-CI. doi:10.17603/ds2-4s85-mc54

Exton, M., Harry, S., Kutter, B. L., Mason, H. B., and Yeh, H. (2019). Simulating tsunami inundation and soil response in a large centrifuge. *Sci. Rep.* 9, 11138. doi:10.1038/s41598-019-47512-x

Fellenius, B. H., and Siegel, T. C. (2008). Pile drag load and downdrag in a liquefaction event. *J. Geotech. Geoenviron. Eng.* 134 (9), 1412–1416. doi:10.1061/(ASCE)1090-0241(2008)134:9(1412)

Fontana, C. M., Hallowell, S. T., Arwade, S. R., DeGroot, D. J., Landon, M. E., Aubeny, C. P., et al. (2018). Multiline anchor force dynamics in floating offshore wind turbines. *Wind Energy* 21 (11), 1177–1190. doi:10.1002/we.2222

Gardner, M. H., Khan, H., Buttery, S., Ham, S.-M., DeJong, J. T., and Wilson, D. W. (2024). Hypergravity testing of thawing rates in permafrost. American geophysical union conference, San Francisco, CA, December 12, 2024. Available online at: https://agu.confex.com/agu/agu24/meetingapp.cgi/Paper/1559696.

Garnier, J., Gaudin, C., Springman, S. M., Culligan, P. J., Goodings, D., Konig, D., et al. (2007). Catalogue of scaling laws and similitude questions in geotechnical centrifuge modelling. *Int. J. Phys. Model. Geotech.* 7 (3), 01–23. doi:10.1680/ijpmg.2007.070301

Hall, C. A., Hernandez, G., Darby, K. M., van Paassen, L., Kavazanjian, E., DeJong, J. T., et al. (2018). "Centrifuge model testing of liquefaction mitigation via denitrification-induced desaturation," in Proc., geotechnical earthquake Engineering and soil dynamics V, geotechnical special publication 290. Editors S. J. Brandenberg, and M. T. Manzari (ASCE), 127–137.

Ham, S., San Pablo, A. C. M., Caisapanta, J. L., and DeJong, J. T. (2024a)."Centrifuge modeling of soil-structure interaction with MICP improved soil," Proc., Geo-Congress 2024, Vancouver, BC, February 25-28, 2024, 87–95. doi:10.1061/9780784485330.010

Ham, S., San Pablo, A. C. M., Wilson, D. W., and DeJong, J. T. (2024b). "Development of model preparation procedure for MICP-treated sand in centrifuge tests," in Proc., 5th European Conference on physical Modelling in Geotechnics, Delft, Netherlands, October 2-4, 2-24.

Ham, S. M., Caisapanta, J. L., San Pablo, A. C. M., and DeJong, J. T. (2025). MICP ground improvement design to support structures founded on liquefiable soils. *Biogeotechnics, in review*.

Hannigan, P. J., Rausche, F., Likins, G. E., Robinson, B. R., and Becker, M. L. (2016). *Design and construction of driven pile foundations. FHWA-NHI-16-009*. Woodbury, MN: Federal Highway Administration.

Huang, L., Coughlan, K., Martinez, A., Wilson, D., Aubeny, C., Arwade, S., et al. (2025a). Centrifuge modelling of shared ring anchors for floating wind turbines subjected to cyclic loading in clay. Proc. 5th Int. Sym. Front. Off. Geotech, , Nantes, France, June 9-13, 2025. 6.

Huang, L., Martinez, A., Aubeny, C., Awade, S., DeGroot, D., and Beemer, B. (2025b). Centrifuge modelling of the monotonic capacity of offshore ring anchors in clay. *Geotech. Frontiers*. 290–299. doi:10.1061/9780784486009.030

Huang, L., Martinez, A., Aubeny, C., DeGroot, D., Arwade, S., and Beemer, R. (2024). Centrifuge modeling of the monotonic capacity of offshore ring anchors in sand. *Deep Found. Inst. J.* 18 (1). doi:10.37308/dfijnl.20230915.297

Kean, J. W., Staley, D. M., Lancaster, J. T., Rengers, F. K., Swanson, B. J., Coe, J. A., et al. (2019). Inundation, flow dynamics, and damage in the 9 January 2018 Montecito debris-flow event, California, USA: opportunities and challenges for post-wildfire risk assessment. *Geosphere* 15 (4), 1140–1163. doi:10.1130/GES02048.1

Khosravi, M., DeJong, J. T., Boulanger, R. W., Khosravi, A., Hajialilue-Bonab, M., Sinha, S. K., et al. (2022). Centrifuge tests of cone-penetration test of layered soil. *ASCE J. Geotechnical Geoenvironmental Eng.* 148 (4), 04022002. doi:10.1061/(ASCE)GT.1943-5606.0002716

Kim, Y. A., Burrall, M., Jeon, M. K., DeJong, J. T., Martinez, A., and Kwon, T. H. (2024). Pullout behavior of tree root-inspired anchors: development of root architecture models and centrifuge tests. *Acta Geotech.* 19 (3), 1211–1229. doi:10.1007/s11440-023-02077-y

Komusanac, I., Brindley, G., Fraile, D., and Lizet, R. (2022). *Wind energy in europe: 2021 statistics and the outlook for 2022–2026*. Brussels, Belgium: WindEurope. Available online at: https://windeurope.org/intelligence-platform/product/wind-energy-in-europe-2021-statistics-and-the-outlook-for-2022-2026/.

Kutter, B. L. (1995). Recent advances in centrifuge modeling of seismic shaking. International conferences on recent advances in geotechnical earthquake engineering and soil dynamics, St. Louis, Missouri, April 2-67, 1995, 2.

Kutter, B. L., and Balakrishnan, A. (1998). Dynamic model test data from electronics to knowledge. *International Conference Centrifuge* 98, 931–943. Available online at: https://www.issmge.org/uploads/publications/53/115/P00121.pdf

Kutter, B. L., Fragaszy, R. J., Gaudin, C., Carey, T. J., Chen, Y., De, A., et al. (2021). Frontiers for hypergravity experiments and model tests. UC Davis CGM Rep. UCD/CGM-21/02. Available online at: https://ucdavis.box.com/s/fqs8srl0v0091p417s4c39jyt9lij34c (Accessed December 1, 2024).

Kutter, B. L., and Wilson, D. W. (2006). Physical modelling of dynamic behavior of soil-foundation-superstructure systems. *Int. J. Phys. Model. Goetechnics* 6 (1), 01–12. doi:10.1680/ijpmg.2006.060101

LeBlanc, C., Houlsby, G. T., and Byrne, B. W. (2010). Response of stiff piles in sand to long-term cyclic lateral loading. *Géotechnique* 60 (2), 79–90. doi:10.1680/geot.7.00196

Lee, J., Khan, M., Bello, L., and Aubeny, C. (2020). "Cost analysis of multiline ring anchor system for offshore wind farm," in 45th Annual Conf. on Deep Foundations, October 13-16, 2020.

Litton, R. W., Stringer, M. E., Clukey, E. C., Chen, J.-Y., Kutter, B. L., Wilson, D. W., et al. (2014). *Centrifuge study of offshore platform response to earthquake excitations*. Houston, Texas: Offshore Technology Conference. doi:10.4043/25206-MS*Offshore Technol. Conf.*

Madabhushi, S. S. C., Follett, S. B., O'Hara, K. B., Wilson, D. W., Kutter, B. L., and Martinez, A. (2023). Centrifuge modeling of the run-out behavior of fly ash deposits subjected to a loss of confinement. *Can. Geotech. J.* 61 (3), 375–399. doi:10.1139/cgj-2022-0585

Madabhushi, S. S. C., Martinez, A., Wilson, D. W., and Kutter, B. L. (2022). Design and instrumentation of a novel centrifuge container for fly ash run-out experiments. *Int. J. Phys. Mod. Geotech.* 23 (3), 129–149. doi:10.1680/jphmg.21.00044

Manzari, M. T., El Ghoraiby, M., Kutter, B. L., Zeghal, M., Abdoun, T., Arduino, P., et al. (2018). Liquefaction experiment and analysis projects (LEAP): summary of observations from the planning phase. *Soil Dyn. Earthq. Eng.* 113, 714–743. doi:10.1016/j.soildyn.2017.05.015

Martinez, A., and O'Hara, K. B. (2021). Skin friction directionality in monotonically- and cyclically-loaded bio-inspired piles in sand. *Deep Found. Inst. J.* 15 (1). doi:10.37308/DFIJnl.20200831.222

Mason, H. B., Kutter, B. L., Bray, J. D., Wilson, D. W., and Choy, B. Y. (2010). "Earthquake motion selection and calibration for use in a geotechnical centrifuge," Proc. Int. Conf. Physical Modelling in Goetechnics. Zürich, June 2010, 361–366. doi:10.1201/b10554-56

McKenna, F., Scott, M. H., and Fenves, G. L. (2010). Nonlinear finite element analysis software architecture using object composition. *J. Comput. Civ. Eng.* 24 (1), 95–107. doi:10.1061/(asce)cp.1943-5487.0000002

Mitchell, J. K., and Kopmann, J. (2013). *The future of geotechnical engineering*. Blacksburg, VI, United States: Virginia tech center for geotechnical research and practice, Report #70.

Montoya, B. M., DeJong, J. T., and Boulanger, R. W. (2013). Dynamic response of liquefiable sand improved by microbial-induced calcite precipitation. *Géotechnique* 63 (4), 302–312. doi:10.1680/geot.SIP13.P.019

Muhunthan, B., Vijayathasan, N. V., and Abbasi, B. (2017). *Liquefaction induced downdrag on drilled shafts. WA-RD 865.1*. Pullman, WA: Washington State DOT.

Ng, C. W. W., Crous, P. A., and Jacobsz, S. W. (2023). Centrifuge and numerical modeling of liquefied flow and nonliquefied slide failures of tailings dams. *J. Geotechnical Geoenvironmental Eng.* 149 (9). doi:10.1061/jggefk.gteng-10800

O'Hara, K. B., and Martinez, A. (2022). Load transfer directionality of snakeskin-inspired piles during installation and pullout in sands. *J. Geotech. Geoenv. Eng.* 148 (12). doi:10.1061/(asce)gt.1943-5606.0002929

O'Hara, K. B., and Martinez, A. (2024). Cyclic axial response and stability of snakeskin-inspired piles in sand. *Acta Geotech.* 19 (3), 1139–1158. doi:10.1007/s11440-023-02007-y

Price, A. B., Boulanger, R. W., and DeJong, J. D. (2019). Centrifuge modeling of variable-rate cone penetration in low-plasticity silts. *ASCE J. Geotechnical Geoenvironmental Eng.* 145 (11), 04019098. doi:10.1061/(ASCE)GT.1943-5606.0002145

Robertson, I., Bobet, A., Edge, B., Holmes, W., Johnson, D., LaChance, M., et al. (2023). *Natural hazards engineering research infrastructure, science plan, multi-hazard research to make a more resilient world, Third Edition*. DesignSafe-CI. doi:10.17603/ds2-abbs-0966

Rollins, K. M., and Strand, S. R. (2007). *Liquefaction mitigation using vertical composite drains: full-scale testing for pile applications*. Washington, DC: Transportation Research Board.

San Pablo, A. C. M., DeJong, J. T., and Carey, T. J. (2024). Influence of biocementation treatment extent on dynamic system performance: a centrifuge liquefaction study. *Soil Dyn. Earthq. Eng.* 183, 108792. doi:10.1016/j.soildyn.2024.108792

Santamarina, J. C., Torres-Cruz, L. A., and Bachus, B. S. (2019). Why coal ash and tailings dam disasters occur. *Science* 364 (6440), 526–528. doi:10.1126/science.aax1927

Schneider, N., and Kosters, J. (2024). "U.S. National science foundation natural hazards engineering research infrastructure (NHERI) decadal visioning study 2026–2035," in *U.S. National science foundation natural hazards engineering research infrastructure (NHERI) decadal visioning study 2026–2035*. DesignSafe-CI. doi:10.17603/ds2-afza-m544

Schofield, A. N. (1981). Cambridge geotechnical centrifuge operations. *Geotechnique* 25 (4), 743–761.

Sinha, S. K., Kutter, B. L., Wilson, D. W., Carey, T. J., and Ziotopoulou, K. (2021c). *Use of Photron cameras and TEMA software to measure 3D displacements in centrifuge tests. Report No. UCD/CGM-21/01*. Davis, CA: Center for Geotechnical Modeling, Department of Civil and Environmental Engineering, University of California, 76.

Sinha, S. K., Kutter, B. L., and Ziotopoulou, K. (2023a). Measuring vertical displacement using laser lines and cameras. *Int. J. Phys. Model. Geotechnics* 23 (1), 3–15. doi:10.1680/jphmg.21.00038

Sinha, S. K., Ziotopoulou, K., and Kutter, B. L. (2021a). "SKS02: centrifuge test of liquefaction-induced downdrag in uniform liquefiable deposit," in *DesignSafe-CI PRJ-2828 "Centrifuge testing of liquefaction-induced downdrag on axially loaded piles*. doi:10.17603/ds2-d25m-gg48

Sinha, S. K., Ziotopoulou, K., and Kutter, B. L. (2021b). "SKS03: centrifuge test of liquefaction-induced downdrag in interbedded soil deposits," in *DesignSafe-CI PRJ-2828 "Centrifuge testing of liquefaction-induced downdrag on axially loaded piles*. doi:10.17603/ds2-wjgx-tb78

Sinha, S. K., Ziotopoulou, K., and Kutter, B. L. (2022a). Centrifuge model tests of liquefaction-induced downdrag on piles in uniform liquefiable deposits. *ASCE J Geotech and Geoenv Eng* 148 (7). doi:10.1061/(asce)gt.1943-5606.0002817

Sinha, S. K., Ziotopoulou, K., and Kutter, B. L. (2022b). Numerical modeling of liquefaction-induced downdrag: validation against centrifuge model tests. *ASCE J Geotech and Geoenv Eng* 148 (12). doi:10.1061/(asce)gt.1943-5606.0002930

Sinha, S. K., Ziotopoulou, K., and Kutter, B. L. (2023b). Displacement-based design of axially loaded piles for seismic loading and liquefaction-induced downdrag. *ASCE J Geotech and Geoenv Eng* 149 (9). doi:10.1061/JGGEFK.GTENG-1117

Sinha, S. K., Ziotopoulou, K., and Kutter, B. L. (2024). Effects of excess pore pressure redistribution in liquefiable layers. *ASCE J Geotech and Geoenv Eng* 150 (4). doi:10.1061/jggefk.gteng-11857

Stewart, D. P., Chen, Y.-R., and Kutter, B. L. (1998). Experience with the use of methylcellulose as a viscous pore fluid in centrifuge models. *Geotechnical Test. J. GTJODJ* 21 (4), 365–369. doi:10.1520/gtj11376j

Stringer, M. E., Pedersen, L., Nuss, B. D., and Wilson, D. W. (2014). Design and use of a rotating spiral pluviator for creating large sand models. *ICPMG* 2014. doi:10.1201/b16200-29

Sturm, A. P. (2019). On the liqueaction potential of gravelly soils: characterization, triggering and performance. PhD dissertation. Davis (CA): University of California Davis, 528.

Taylor, R. N. (1995). *Geotechnical centrifuge technology*. London: Blackie Academic and Professional, an imprint of Chapman and Hall.

Travasarou, T. (2024). Geotechnical earthquake engineering in ASCE JGGE: from raising awareness to shaping the state of practice. Geo-Institute ASCE. Available online at: https://www.youtube.com/watch?v=rEKc59GL1Fs (Accessed December 04, 2024).

United States Department of Energy (2021). How were moving to net-zero by 2050. Available online at: https://www.energy.gov/articles/how-were-moving-net-zero-2050 (Accessed January 21, 2025).

United States Energy Information Administration (2024). Where wind power is harnessed - U.S. Energy Information Administration (EIA). Available online at: https://www.eia.gov/energyexplained/wind/where-wind-power-is-harnessed.php (Accessed January 21, 2025).

Wartman, J., Berman, J., Bostrom, A., Miles, S., Olsen, M., Gurley, K., et al. (2020). Research needs, challenges, and strategic approaches for natural hazards and disaster reconnaissance. *Front. Built Environ.* 6, 6–2020. doi:10.3389/fbuil.2020.573068

Wilson, D. W., and Allmond, J. D. (2014). Advancing geotechnical earthquake engineering knowledge through centrifuge modeling. *Phys. Model. Geotechnics*, 125–137. doi:10.1201/b16200-11

Wilson, D. W., and Kutter, B. L. (2002). "Dense instrumentation arrays," in Proc. Int. Conf. On Physical Modelling in Geotechnics 2002, St. Johns, Canada, 10–12 July 2002. Editors P. Guo, R. Phillips, and R. Popescu Lisse, Netherlands: Balkema, pp 131–136.

Zamani, A., Xiao, P., Baumer, T., Carey, T. J., Sawyer, B., DeJong, J. T., et al. (2021). Mitigation of liquefaction triggering and foundation settlement by MICP treatment. *J. Geotech. Geoenviron. Eng.* 147 (10), 04021099. doi:10.1061/(ASCE)GT.1943-5606.0002596

Ziotopoulou, K., Sinha, S. K., and Kutter, B. L. (2022). "Liquefaction-induced downdrag on piles: insights from a centrifuge and numerical modeling program," in *Invited theme paper and lecture. Performance based design IV (PBD-IV) earthquake geotechnical engineering*. Beijing, China: Springer. doi:10.1007/978-3-031-11898-2_40

Frontiers in
Built Environment

Innovations in the engineering of sustainable buildings, cities, and urban spaces

An innovative journal that advances our knowledge of civil engineering. It focuses on the development of sustainable methodologies for the design and management of resilient buildings and infrastructure.

Discover the latest Research Topics

See more →

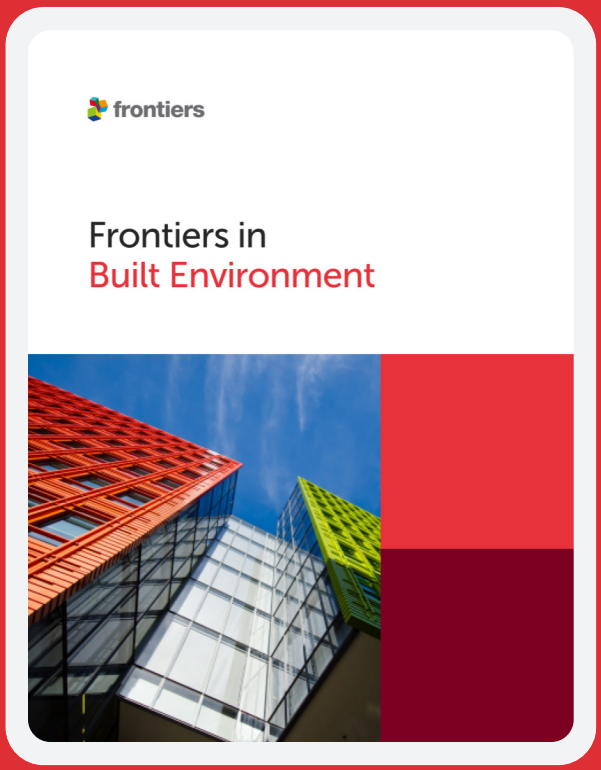

Frontiers

Avenue du Tribunal-Fédéral 34
1005 Lausanne, Switzerland
frontiersin.org

Contact us

+41 (0)21 510 17 00
frontiersin.org/about/contact